

AGARD

ADVISORY GROUP FOR AEROSPACE RESEARCH & DEVELOPMENT

7 RUE ANCELLE, 92200 NEUILLY-SUR-SEINE, FRANCE

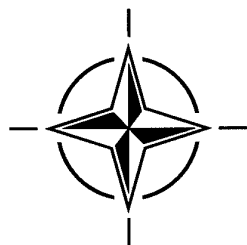
AGARD CONFERENCE PROCEEDINGS 572

Advanced Aero-Engine Concepts and Controls

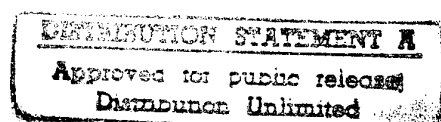
(les Concepts avancés et les commandes des
nouveaux moteurs d'avion)

*Papers presented at the Propulsion and Energetics Panel (PEP) 86th Symposium
held in Seattle, USA, 25-29 September 1995.*

19960730 120



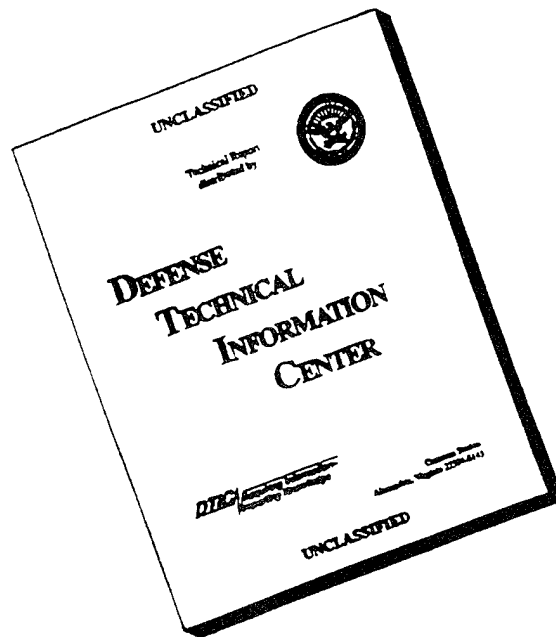
NORTH ATLANTIC TREATY ORGANIZATION



Published June 1996

Distribution and Availability on Back Cover

DISCLAIMER NOTICE



THIS DOCUMENT IS BEST QUALITY AVAILABLE. THE COPY FURNISHED TO DTIC CONTAINED A SIGNIFICANT NUMBER OF PAGES WHICH DO NOT REPRODUCE LEGIBLY.

The Mission of AGARD

According to its Charter, the mission of AGARD is to bring together the leading personalities of the NATO nations in the fields of science and technology relating to aerospace for the following purposes:

- Recommending effective ways for the member nations to use their research and development capabilities for the common benefit of the NATO community;
- Providing scientific and technical advice and assistance to the Military Committee in the field of aerospace research and development (with particular regard to its military application);
- Continuously stimulating advances in the aerospace sciences relevant to strengthening the common defence posture;
- Improving the co-operation among member nations in aerospace research and development;
- Exchange of scientific and technical information;
- Providing assistance to member nations for the purpose of increasing their scientific and technical potential;
- Rendering scientific and technical assistance, as requested, to other NATO bodies and to member nations in connection with research and development problems in the aerospace field.

The highest authority within AGARD is the National Delegates Board consisting of officially appointed senior representatives from each member nation. The mission of AGARD is carried out through the Panels which are composed of experts appointed by the National Delegates, the Consultant and Exchange Programme and the Aerospace Applications Studies Programme. The results of AGARD work are reported to the member nations and the NATO Authorities through the AGARD series of publications of which this is one.

Participation in AGARD activities is by invitation only and is normally limited to citizens of the NATO nations.

The content of this publication has been reproduced
directly from material supplied by AGARD or the authors.

Published June 1996

Copyright © AGARD 1996
All Rights Reserved

ISBN 92-836-0025-8



*Printed by Canada Communication Group
45 Sacré-Cœur Blvd., Hull (Québec), Canada K1A 0S7*

Advanced Aero-Engine Concepts and Controls

(AGARD CP-572)

Executive Summary

Future aircraft will require significant performance gains from the propulsion system to provide better fuel efficiency, longer range and operational flexibility, e.g. multi-role combat aircraft, the HSCT and military transport aircraft. Engines will need to provide excellent performance over a wide range of operating conditions, and improvements in aerodynamics, materials and cooling technology will offer the prospect of significantly improved cycle conditions. The full gains available cannot be realized without further complexity of the cycle, which in turn is dependent upon the combination of control strategies and variable geometry variable flow paths. Although some individual technologies have been reviewed in prior meetings, this has been done in isolation from engine cycle and aircraft requirements. The purpose of the Symposium was to highlight the challenges to the component and system engineers as derived from advanced cycles, with increased flexibility enabled by advanced controls, against a background of future aircraft requirements. Clearly costs of future platforms are a major key, both in acquisition and in operation. By sharing, in the unique AGARD way of free and open discussion, the outlines of potential system requirements, the necessary databases on components can be generated, leading to secure technical decisions being made by industry and governments. Combined with the reduced parts count of future engines and their inherent robustness then the orderly approach to progress can lead to cost effective introduction of new technologies.

The Symposium covered propulsion system advances being considered for a range of flight vehicles, including wing borne combat, with and without vertical landing capabilities, through to transport and tanker engines. Their associated control systems were also addressed. The design, control and actuation considerations of vectoring propulsion nozzles were included, covering single and multi axis vectoring. Dual use technologies were discussed in the areas of similarities such as transport/tanker and civil aircraft engines. In the longer timescale, concepts such as variable cycles and thrust vectoring, will also be feasible in civil applications. The Symposium was targeted to stimulate military and industry by dissemination of quality information and identification of the potential offered by advanced concepts for engines and controls. Research institutes were provided with insight to requirements and would be able to work together towards preparing the data bases for the future.

The Technical Programme was targeted specifically at the areas of engine technologies and demonstrations for improved flexibility, mobility and particularly improved affordability as defined by AASC. No other forum exists for information exchange at this level. ASME, SAE and ISABE are the most general, usually civil technology oriented institutions. It was demonstrated that AGARD offers a unique arena for this topic, thus being consistent with the immediate and long term needs of the NATO Community.

Although significant limitations remain, the Symposium demonstrated that considerable progress has been made since the previous meetings on this subject. The topics covered demonstrated that the principle of integration has been widely accepted. Improvements in the development and application of Computational Fluid Dynamics to the design of aero engines were demonstrated. The importance of both experimental and semi-empirical techniques was emphasized and it was demonstrated that the use of theory and experiment in combination leads to a design tool of high integrity.

Overall the Symposium was very successful, as attested by the high attendance figures and lively discussions. The Technical Evaluator and most of the attendees rated this Symposium as timely and of high quality, having provided relevant information exchange as well as future guidance. Several areas that require emphasis in future research and development programs were identified and an excellent exchange of ideas/experiences occurred.

Les concepts avancés et les commandes des nouveaux moteurs d'avion

(AGARD CP-572)

Synthèse

Les futurs avions militaires devront disposer de systèmes de propulsion dont les performances devront être nettement améliorées afin d'assurer un meilleur rendement du carburant, une distance franchissable plus grande et une meilleure souplesse opérationnelle, par exemple pour les avions de combat multirôle, les HSCT et les avions de transport militaires. Les moteurs devront offrir des performances supérieures dans un large éventail de conditions opérationnelles et les progrès réalisés en aérodynamique, en matériaux et en technologies de refroidissement offriront de nouvelles perspectives pour l'amélioration des cycles moteur. Cependant, la totalité des gains disponibles ne peut être obtenue qu'au prix d'un cycle encore plus complexe, lequel dépend, à son tour, de la combinaison des stratégies de contrôle et de la géométrie variable/trajets d'écoulement variables. Bien que quelques-unes des technologies aient été examinées lors des réunions précédentes, le sujet a été étudié séparément des considérations des cycles moteur et des spécifications des aéronaves. Le symposium a eu pour objet de mettre l'accent sur les défis à relever par les ingénieurs systèmes et les concepteurs de composants compte tenu des cycles moteur avancés et de la souplesse accrue autorisée par les commandes avancées, dans le contexte des spécifications des futurs aéronaves. Il va sans dire que les coûts des plate-formes futures sont l'un des éléments clé du problème, tant du point de vue de l'achat que de l'exploitation. La mise en commun des grandes lignes des spécifications des systèmes potentiels, réalisée par le biais des discussions franches et ouvertes, habituelles au sein de l'AGARD, permettrait la constitution des bases de données pour les composants et conduirait à la prise de décisions techniques sûres de la part de l'industrie et des gouvernements. Une approche bien ordonnée des progrès qui sont à réaliser, qui profiterait du nombre réduit d'organes des futurs moteurs et de leur robustesse intrinsèque, conduirait à l'introduction de nouvelles technologies rentables.

Le symposium a porté sur les futurs systèmes de propulsion, évalués pour une gamme de véhicules aériens, y compris les aéronaves à voilure fixe, avec et sans la possibilité d'atterrissage vertical, jusqu'à et y compris les moteurs d'avions de transport et d'avions-citerne. Les systèmes de commande associés ont également été pris en compte. Les aspects conception, contrôle et commande des tuyères orientables ont été examinés, y compris l'orientation de la poussée monoaxiale et multiaxiale. Les technologies duales ont été discutées dans le contexte des similarités entre les moteurs d'avions militaires/avions-citerne et les moteurs civils. A plus long terme, des concepts tels que le cycle variable et l'orientation de la poussée seraient envisageables pour des applications civiles. Ce symposium a eu pour objet de stimuler les industriels et les militaires par la diffusion d'informations de qualité, et par l'identification du potentiel offert par les concepts avancés des moteurs et des commandes. Pour les instituts de recherche, le symposium a donné un aperçu des caractéristiques requises et la potentialité d'envisager l'élaboration en commun des bases de données pour l'avenir.

Le programme technique a été orienté spécifiquement vers les technologies des moteurs et les démonstrations pour améliorer la souplesse, la mobilité et surtout le coût de possession tel que défini par l'AASC. Il n'existe aucun autre forum tel que celui-ci pour l'échange d'informations à ce niveau. L'ASME, le SAE et l'ISABE sont pour la plupart des organismes plus généralistes orientés vers les technologies civiles. Il a été démontré que l'AGARD offre un forum unique pour discuter d'un tel sujet, ce qui est cohérent avec les besoins immédiats et à long terme de la communauté de l'OTAN.

Bien que des limitations importantes demeurent, ce symposium a confirmé les réels progrès qui avaient été réalisés depuis la dernière réunion sur ce sujet. Les sujets couverts témoignent que le principe d'intégration a été largement accepté. Des améliorations en ce qui concerne le développement et l'application de la dynamique des fluides numérique CFD à la conception des moteurs d'avion ont été démontrées. L'importance des techniques expérimentales et semi-empiriques a été soulignée et il a été démontré que l'utilisation conjointe de la théorie et de l'expérimentation permet de créer des outils de conception de haute intégrité.

Globalement, le symposium a été une réussite, comme en témoignent le nombre élevé de participants et l'animation des débats. L'Évaluateur technique, comme la majorité des participants, a considéré que ce symposium venait à point nommé et qu'il était de haute qualité, puisqu'il a permis un échange d'informations valable et a fourni des directives pour l'avenir. Plusieurs sujets qui mériteraient de faire l'objet de futurs programmes de recherche et développement ont été identifiés lors des échanges d'idées et d'expériences très fructueux.

Contents

	Page
Executive Summary	iii
Synthèse	iv
Recent Publications of PEP	viii
Propulsion and Energetics Panel	x
Theme/Thème	xi
	Reference
Technical Evaluation Report by M.G. Philpot	T
Keynote Address by D.J. Campbell	K
SESSION I: ENGINE RESEARCH AND DEMONSTRATION, REQUIREMENTS AND PROGRAMMES	
The Purpose and Status of IHPTET -- 1995 by R.J. Hill	1
Future Technology Requirements for UK Combat Engines by M.D. Paramour	2
Acquisition et démonstration des technologies pour futurs moteurs militaires — Le programme AMET by J. Dufau	3
SESSION II: AIRCRAFT ENGINE INTEGRATION	
The Impact of Advanced Engine Technology on Combat Aircraft Performance by S.D. Hodder and S.E. Simm	4
Advanced Combat Engines — Tailoring the Thrust to the Critical Flight Regimes by K.R. Garwood, P. Round and G.S. Hodges	5
The STRATO 2C Propulsion System — A New Compound Engine and Control Concept for High Altitude Flying by H. Tönskötter and D. Scheithauer	6
Propulsion Considerations for An Advanced Vertical Take-off & Landing (VTOL) Transport Aircraft by C.M. Norden and J.M. Stricker	7
Powerplants and Lift Systems for ASTOVL Aircraft — The Challenges to an Engine Maker by D.M. Pearson	8
Paper withdrawn	9

SESSION III: PROPULSION SYSTEM AND COMPONENT TECHNOLOGY

Developing Affordable Gas Turbine Engines by C.A. Skira	10
Advanced Small Turbopropulsion Engines by C. Rodgers	11
Preliminary Design and Performance Analysis of a Variable Geometry Recuperative Turboshaft by S. Colantuoni, A. Colella, G. Mainiero, G. Santoriello, L. Cirillo and C. Iossa	12
Variable Cycle Engine Concepts by J.E. Johnson	13
Studies on NOx-Emissions of SST Engine Concepts by F. Deidewig and A. Döpelheuer	14
Analyse des performances d'un superstatoréacteur en fonction des paramètres de combustion (Scramjet Performance Analysis in function of Combustion Process Parameters) by P. Hendrick	15
Combined-Cycle Engines for Hypersonic Applications by F.J. Heitmeir	16
Design and Off-Design Simulation of Highly Integrated Hypersonic Propulsion Systems by Th. Esch, S. Hollmeier and H. Rick	17
Performance Optimization of a Turboramjet Engine for Hypersonic Flight by B. Bareis and W. Braig	18
Application of a System for the Monitoring of Aerodynamic Load and Stall in Multi-Stage Axial Compressors by H. Hönen and H.E. Gallus	19

Paper withdrawn	20
------------------------	-----------

SESSION IV: THRUST VECTORING

Application of Thrust Vectoring to Future Aircraft Design by H. Ross and P. Huber	21
Paper withdrawn	22
Paper withdrawn	23
The F-15 Active Aircraft "The Next Step" by R. Bursey	24
Paper withdrawn	25
Optimization of Actuation and Cooling Systems for Advanced Convergent-Divergent Nozzles of Combat Aircraft by C. Sánchez-Tarifa, M. Rodríguez-Fernández, R. Rebolo, G. Corchero, M. Rodríguez-Martín and I. Ulizar Álvarez	26

SESSION V: ENGINE CONTROL SYSTEMS

An Advanced Control System for Turbofan Engine: Multivariable Control and Fuzzy Logic. (Application to the M88-2 Engine) by A. Garassino and P. Bois	27
--	-----------

Multivariable Control of Military Engines by G.J. Dadd, A.E. Sutton and A.W.M. Greig	28
Système de regulation avancé pour turbomoteur by J.L. Frealle	29
Contribution of Dynamic Engine Simulation to Military Turbofan Control System Design and Development by L. Pierre, J.-P. Duponchel and P. Gérard	30
Paper withdrawn	31
Paper withdrawn	32
Neural Adaptive Control of an Engine Exhaust Nozzle by A. Garassino	33
Adaptive Optimization of Aircraft Engine Performance Using Neural Networks by D.L. Simon and T.W. Long	34
Distributed Architectures for Advanced Engine Control Systems by T.J. Lewis	35
Safety Critical Software Development for Advanced Full Authority Control Systems by F. Tortarolo, G. Crosetti and C. Difilippo	36
Review of Photonic System Development for Propulsion Controls by J.C. Birdsall, C.V. Fields and M. Agnello	37
Modelling of a Fuel Control Unit for Small Gas Turbine Engines Featuring Interacting Electronic Linear Actuators by A.I. Georgantas, T. Krepec and R.M.H. Cheng	38
SESSION VI: INTEGRATED FLIGHT AND PROPULSION CONTROL	
The VAAC Harrier Programme: Flying STOVL with 1-Inceptor Control by G.T. Shanks and F.J. Scorer	39
Integrated Flight and Propulsion Control Simulation Tools for Advanced Aircraft and Propulsion Systems by K.J. Sobanski and I. Khalid	40
Integrated Flight and Propulsion Controls for Advanced Aircraft Configurations by W. Merrill and S. Garg	41
Propulsion Integration Issues for Advanced Fighter Aircraft by M.C. Gridley and S.H. Walker	42
Propulsion Integration Aspects in Advanced Military Aircraft by E. Hienz, L. Illuzzi and P. Herrmann	43

Recent Publications of the Propulsion and Energetics Panel

CONFERENCE PROCEEDINGS (CP)

Interior Ballistics of Guns

AGARD CP 392, January 1986

Advanced Instrumentation for Aero Engine Components

AGARD CP 399, November 1986

Engine Response to Distorted Inflow Conditions

AGARD CP 400, March 1987

Transonic and Supersonic Phenomena in Turbomachines

AGARD CP 401, March 1987

Advanced Technology for Aero Engine Components

AGARD CP 421, September 1987

Combustion and Fuels in Gas Turbine Engines

AGARD CP 422, June 1988

Engine Condition Monitoring — Technology and Experience

AGARD CP 448, October 1988

Application of Advanced Material for Turbomachinery and Rocket Propulsion

AGARD CP 449, March 1989

Combustion Instabilities in Liquid-Fuelled Propulsion Systems

AGARD CP 450, April 1989

Aircraft Fire Safety

AGARD CP 467, October 1989

Unsteady Aerodynamic Phenomena in Turbomachines

AGARD CP 468, February 1990

Secondary Flows in Turbomachines

AGARD CP 469, February 1990

Hypersonic Combined Cycle Propulsion

AGARD CP 479, December 1990

Low Temperature Environment Operations of Turboengines (Design and User's Problems)

AGARD CP 480, May 1991

CFD Techniques for Propulsion Applications

AGARD CP 510, February 1992

Insensitive Munitions

AGARD CP 511, July 1992

Combat Aircraft Noise

AGARD CP 512, April 1992

Airbreathing Propulsion for Missiles and Projectiles

AGARD CP 526, September 1992

Heat Transfer and Cooling in Gas Turbines

AGARD CP 527, February 1993

Fuels and Combustion Technology for Advanced Aircraft Engines

AGARD CP 536, September 1993

Technology Requirements for Small Gas Turbines

AGARD CP 537, March 1994

Erosion, Corrosion and Foreign Object Damage Effects in Gas Turbines

AGARD CP 558, February 1995

Environmental Aspects of Rocket and Gun Propulsion

AGARD CP 559, February 1995

Loss Mechanisms and Unsteady Flows in Turbomachines

AGARD CP 571, January 1996

ADVISORY REPORTS (AR)

Producibility and Cost Studies of Aviation Kerosines (*Results of Working Group 16*)

AGARD AR 227, June 1985

Performance of Rocket Motors with Metallized Propellants (*Results of Working Group 17*)

AGARD AR 230, September 1986

Recommended Practices for Measurement of Gas Path Pressures and Temperatures for Performance Assessment of Aircraft Turbine Engines and Components (*Results of Working Group 19*)

AGARD AR 245, June 1990

The Uniform Engine Test Programme (*Results of Working Group 15*)

AGARD AR 248, February 1990

Test Cases for Computation of Internal Flows in Aero Engine Components (*Results of Working Group 18*)

AGARD AR 275, July 1990

Test Cases for Engine Life Assessment Technology (*Results of Working Group 20*)

AGARD AR 308, September 1992

Terminology and Assessment Methods of Solid Propellant Rocket Exhaust Signatures (*Results of Working Group 21*)

AGARD AR 287, February 1993

Guide to the Measurement of the Transient Performance of Aircraft Turbine Engines and Components (*Results of Working Group 23*)

AGARD AR 320, March 1994

Experimental and Analytical Methods for the Determination of Connected — Pipe Ramjet and Ducted Rocket Internal Performance (*Results of Working Group 22*)

AGARD AR 323, July 1994

Recommended Practices for the Assessment of the Effects of Atmospheric Water Ingestion on the Performance and Operability of Gas Turbine Engines (*Results of Working Group 24*)

AGARD AR 332, September 1995

LECTURE SERIES (LS)

Engine Airframe Integration for Rotorcraft

AGARD LS 148, June 1986

Design Methods Used in Solid Rocket Motors

AGARD LS 150, April 1987

AGARD LS 150 (Revised), April 1988

Blading Design for Axial Turbomachines

AGARD LS 167, June 1989

Comparative Engine Performance Measurements

AGARD LS 169, May 1990

Combustion of Solid Propellants

AGARD LS 180, July 1991

Steady and Transient Performance Prediction of Gas Turbine Engines

AGARD LS 183, May 1992

Rocket Motor Plume Technology

AGARD LS 188, June 1993

Research and Development of Ram/Scramjets and Turboramjets in Russia

AGARD LS 194, December 1993

Turbomachinery Design Using CFD

AGARD LS 195, May 1994

Mathematical Models of Gas Turbine Engines and their Components

AGARD LS 198, December 1994

AGARDOGRAPHS (AG)

Measurement Uncertainty within the Uniform Engine Test Programme

AGARD AG 307, May 1989

Hazard Studies for Solid Propellant Rocket Motors

AGARD AG 316, September 1990

Advanced Methods for Cascade Testing

AGARD AG 328, August 1993

REPORTS (R)

Application of Modified Loss and Deviation Correlations to Transonic Axial Compressors

AGARD R 745, November 1987

Rotorcraft Drivetrain Life Safety and Reliability

AGARD R 775, June 1990

Propulsion and Energetics Panel

Chairman: Prof. Dr. D.K. HENNECKE
Fachgebiet Gasturbinen und Flugantriebe
Technische Hochschule Darmstadt
Petersenstrasse 30,
64287 Darmstadt, Germany

Deputy Chairman: Prof. R.S. FLETCHER
Head of Campus
Cranfield Institute of Technology
Cranfield, Bedford MK43 0AL
United Kingdom

PROGRAMME COMMITTEE

Prof. Dr.-Ing. L. FOTTNER (Chairman)
Universität der Bundeswehr München
Institut für Strahlantriebe
Werner-Heisenberg-Weg 39
D-85577 Neubiberg, Germany

Mr. G. BOBULA
US Army Propulsion Directorate (ARL)
NASA Lewis Research Center MS 77-12
21000 Brookpark Road
Cleveland, OH 44135-3191, USA

Mr. J-F. CHEVALIER
Ingénieur en Chef — Recherches, SNECMA
Centre d'Essais de Villaroche
77550 Moissy Cramayel, France

Prof. Ir. W.B. DE WOLF
National Aerospace Laboratory, P.O. Box 153
8300 AD Emmeloord, Netherlands

Mr. K. GARWOOD
Rolls-Royce Limited
Whittle House
WH23, P.O. Box 3
Filton, Bristol BS12 7QE UK

Prof. R. JACQUES
Ecole Royale Militaire
30 avenue de la Renaissance
1040 Bruxelles, Belgium

Prof. Dr. P. KOTSIPOULOS
Hellenic Air Force Academy
Chair of Propulsion Systems
Dekelia, Attiki, Greece

Prof. C. SANCHEZ-TARIFA
SENER Ingenieria y Sistemas, S.A.
Severo Ochoa, 4, Parque Tecnologia de Madrid
28760 Tres Cantos, Madrid, Spain

Prof. G. TORELLA
Accademia Aeronautica, Direzione Studi
80078 Pozzuoli, Napoli, Italy

Mr. Sinan ULUVAR
Transturk Fren Donanim
Yalova Yolu 12.Km.
16335 Ovaakca/Bursa
Turkey

HOST NATION COORDINATOR

Mr. R.E. HENDERSON

PANEL EXECUTIVE OFFICE

From Europe:
PEP, AGARD-OTAN
7, rue Ancelle
92200 Neuilly sur Seine, France

From US and Canada:
PEP AGARD-NATO
PSC 116
APO AE 09777

Tel: 33 (1) 47 38 57 85 — Telex: 610176 (France)
Telefax: 33 (1) 47 38 57 99/47 38 67 20

Theme

Future aircraft will require significant performance gains from the propulsion system to provide better fuel efficiency, longer range and operational flexibility, e.g. multi-role combat aircraft, the HSCT and military transport aircraft. Engines will need to provide excellent performance over a wide range of operating conditions, and improvements in aerodynamics, materials and cooling technology will offer the prospect of significantly improved cycle conditions. The full gains available can not be realized without further complexity of the cycle, which in turn is dependent upon the combination of control strategies and variable geometry/variable flow paths. The Symposium will cover propulsion system advances being considered for a range of flight vehicles, including wing borne combat, with and without vertical landing capabilities, through to transport and tanker engines. Their associated control systems will also be addressed. The design, control, and actuation considerations of vectoring propulsion nozzles will be included, covering single and multi axis vectoring. Dual use technologies will be discussed in the areas of similarities such as the transport/tanker and the civil aircraft engines. In the longer timescale, concepts such as variable cycles and thrust vectoring, are feasible in the civil applications.

The Symposium is targeted to stimulate Military and Industry by dissemination of quality information and identification of the potential offered by advanced concepts for engines and controls. Research Institutes will have insight to requirements and would perhaps be able to work in collaboration towards preparing the data bases for the future.

Thème

Les systèmes de propulsion des futurs avions militaires devront disposer de performances nettement améliorées afin d'assurer un meilleur rendement du carburant, une distance franchissable plus grande et une meilleure souplesse opérationnelle, par exemple pour les avions de combat polyvalents, les HSCT et les avions de transport militaires. Les moteurs devront offrir des performances exceptionnelles dans un large éventail de conditions opérationnelles. Les progrès qui seront réalisés en aérodynamique, en matériaux et en technologies de refroidissement ouvriront la voie à des cycles moteur considérablement améliorés. Cependant, la totalité des gains réalisables ne peut être obtenue qu'au prix d'un cycle encore plus complexe, lequel dépend, à son tour, de l'association des stratégies de contrôle à la géométrie variable et aux trajets d'écoulement variables. Le symposium portera sur les futurs systèmes de propulsion pour un ensemble de véhicules aériens, y compris les avions de combat, avec et sans la possibilité d'atterrissage vertical et les moteurs d'avions de transport et d'avions-citerne. Les systèmes de commande associés seront également pris en compte. Les aspects conception, contrôle et commande des tuyères orientables seront examinés, y compris l'orientation de la poussée monoaxiale et multiaxiale. Les technologies duales seront discutées dans le contexte des similitudes entre les moteurs d'avions militaires/avions-citerne et les moteurs civils. A plus long terme, des concepts tels que le cycle variable et l'orientation de la poussée seraient envisageables pour des applications civiles.

Ce symposium a pour objet de stimuler l'industrie et les autorités militaires par la diffusion d'informations de qualité, et par l'identification du potentiel offert par les concepts avancés de moteurs et de commandes. Pour les instituts de recherche, le symposium donnera un aperçu des caractéristiques exigées et permettra d'envisager l'élaboration en commun des bases de données pour l'avenir.

TECHNICAL EVALUATION REPORT

by

Dr M G Philpot
Defence Research Agency
Farnborough, Hants GU14 0LS
United Kingdom

1 INTRODUCTION

This symposium was held at a timely moment, especially in the context of military fixed wing combat aircraft applications. Of the 36 papers presented during the conference, 25 were either concerned specifically with fighter engines or discussed technologies which were relevant to such engines. The past five years have seen the intensive development of several combat engines in the thrust/weight ratio =10 class. These include the F119 and F414 engines in the US, the M88 in France and the EJ200 of the 4 nation Eurojet consortium. All are now in full scale development and will enter service within the next few years. As well as offering considerably greater performance capabilities than the previous (1975-1980) generation of engines, these new engines are the first to be designed from the outset with full authority digital electronic control systems (FADECs).

Attention is now turning to the next generation of engines, which will be needed, on both sides of the Atlantic, for combat aircraft projects in the 2010 to 2015 timeframe. The various advanced gas turbine technologies now in the research and preliminary development phase will need to offer still greater performance at lower cost than the current generation. R and D strategies and programmes are dependent on just what operational characteristics will be required, which specific technologies can be brought to maturity in the timescale and how well they will meet perceived service needs. The Symposium has provided a useful contribution to this debate.

Traditionally, advances in gas turbine technology have been driven to a large extent by the need for ever more capable combat aircraft and it is therefore not surprising that this Symposium was heavily biased towards combat engines. However, other applications bring their own distinctive challenges and some of these were also featured. For example, there were 4 papers each on small gas turbine turboshaft engines and propulsion systems for hypersonic vehicles, respectively. These broadened the scope of the meeting and added their own useful lessons.

2 OVERVIEW OF SYMPOSIUM

The Symposium was divided into 6 main sessions, each covering a different topic area, as follows:

- I Engine research and demonstrator programmes (3 papers plus keynote address).
- II Aircraft and engine integration (5 papers).
- III Propulsion systems and component technology (10 papers).
- IV Thrust vectoring and nozzle technology (3 papers).
- V Engine control systems (10 papers).
- VI Integrated flight/Propulsion control (5 papers).

The keynote address, by Mr D G Campbell, Director of NASA Lewis, formed an overview of the NASA role and strategy in the aero-engine field. The NASA focus is now chiefly on advanced technologies for civil aeronautics, with research and development issues for a second generation supersonic transport, both technical and environmental, being a major thrust.

The technical papers came from 8 member countries, broken down as follows:

US	12	Italy	2
Germany	8	Belgium	1
UK	6	Canada	1
France	5	Spain	1

The breakdown in terms of type of organisation was:

Government institutions	13
Industry	18
Academia, etc	5

The relatively high proportion of papers from government departments and research laboratories

and few contributions from academia perhaps reflect the nature of the Symposium theme. Studies of future engine concepts, whether for military aircraft, trans-atmospheric vehicles, or any other applications-oriented purpose, tend to fall outside the normal scope of academic institutions. They are however natural territory for government institutes, relating as they do very largely to government concerns and requirements. It is a healthy sign that the government bodies were strongly represented in the Symposium, presenting their own in-house work as well as outlining the technology demonstration programmes they are sponsoring within their national industries. With industry also strongly represented in the list of papers, the balance of the symposium appeared to be very good.

3 THE TECHNICAL SESSIONS

3.1 Session I: Engine Technology Requirements and Demonstration Programmes (Papers 1 to 3)

This session consisted of three papers, from the US, UK and France respectively. The papers outlined the technical goals and technology acquisition strategies of the three countries for the next generation of military gas turbine engines. All three countries have similar aims. These are to develop the necessary component technologies and demonstrate technology readiness for combat engines in the 15/1 thrust/weight ratio class by the years 2003 to 2005 (with progression to still greater thrust/weight ratios thereafter), while at the same time, maintaining or improving on the life, reliability and maintainability goals set for the current generation of engines. In addition, by seeking improved manufacturing techniques and reduced parts counts, acquisition cost of production engines is to be substantially reduced.

The papers revealed differences in scale of programme and breadth of scope between the three countries, but there was considerable unanimity about key requirements and strategies. These can be summarised as follows:

- a. Historically, costs and technical risks have increased markedly with each succeeding project. To control and reverse this trend it is essential to develop and demonstrate advanced technology well ahead of the specific projects that will exploit it.
- b. Pursuing aggressive technical goals has the potential to lead to big improvements

in engine thrust/weight ratio, providing more capability in significantly smaller and hence less costly engines.

- c. The main key to this is the development of new classes of lightweight materials, combined with innovative design approaches.
- d. The ultimate goal is to maintain and increase the combat superiority of NATO air forces, combined with better engine life and reliability and considerably reduced acquisition costs. Above all else the solutions must be affordable.

3.2 Session II Aircraft/Engine Integration (Papers 4 to 8)

This was a rather more mixed session of 5 papers but all addressing issues related to the selection of powerplant concepts for specific aircraft applications and how powerplant cycle choice or technology level can affect aircraft size and performance. Papers 4 and 5, from the UK Defence Research Agency and from Rolls-Royce, respectively, considered engine/airframe optimisation for conventional combat fighters. A further Rolls-Royce paper (8) considered the particular problems of ASTOVL fighters, while paper 7 from the USAF Wright Laboratory examined the analogous issues for a STOVL jet transport. Paper 6, from IMBG in Germany described a very different technical problem - the design of a powerplant for a very high altitude research aircraft.

The first two papers provided a very useful follow-up to the technology requirements issues discussed in Session I. They gave a good indication of what the advanced technologies cited in that session will offer in terms of aircraft size and performance. At the same time they gave some insight into the complex factors governing cycle choice and engine rating. The incorporation of STOVL capability into a supersonic fighter adds another level of complexity as Paper 8 made clear, not least in terms of mechanical engineering. It was interesting that almost identical mechanical engineering problems emerged from the STOVL transport study (Paper 7). The high altitude aircraft paper addressed a different application, but one with equal technical challenge. It described a novel compound piston engine/gas turbine system, which had been built and successfully flown.

Bringing these different themes together:

- a. Advanced engine technology (high thrust/weight) will bring big improvements to combat aircraft, allowing either considerable reductions in aircraft size for a given mission, or big improvements in mission endurance and point performance for a given size. The goals indicated in Session I are well worthwhile.
- b. To make the most of the advances in technology, cycle selection and engine design point must be carefully matched to application. Otherwise the main benefits will not be achieved at the flight conditions where they are most needed.
- c. Variable cycles can significantly increase the gains - chiefly more high speed capability - but only if accompanied by advanced engine component technologies.
- d. ASTOVL continues to bring major challenges, with complex mechanical engineering and/or gas path configurations needed to achieve the desired aircraft capabilities.
- e. Specialised applications like the high altitude aircraft call for particular design ingenuity and some lateral thinking. But given sufficient imagination it is possible to achieve practical and successful solutions.

3.3 Session III Propulsion Systems and Component Technology (Papers 10 to 19)

Session III covered a broad range of topics but the papers can be grouped into four main areas.

Combining Increased Capability with Affordability (Paper 10)

This paper from the US Wright Laboratory was again a natural follow-up to the technical requirements issues of Session I. It also complemented the first two papers of Session II. Where the latter focused on the aircraft capability gains to be obtained from advanced engine technology, Paper 10 concentrated on the potential for cost reduction. The key conclusion can be summarised as follows:

High thrust/weight ratio engines promise considerable savings in acquisition costs, despite more costly materials and manufacturing routes.

This is because the engines can be made physically smaller and have greatly reduced parts counts.

Cycle Variability and Complex Cycles (Papers 11 to 14)

Two of these four papers described a variety of cycle concepts for small engines, including expendable turbojets, turboshafts and turboramjets for missile applications and recuperative turboshafts for helicopter propulsion. The other two papers focused on the benefits and problems of variable cycle engines. Paper 13 from General Electric was a particularly valuable review of the history of variable cycle research and development at the company, from the 1960s down to the present day. Taking the four papers together:

- a. For mainstream applications variable cycles (or complex fixed cycles) will only be practicable if the mechanical engineering and the gas flow paths remain as simple as possible.
- b. Special applications like very high endurance helicopters, or high altitude drones, may demand different or unusual cycle concepts and the potential of such powerplants is always worth considering.
- c. Many interesting cycle concepts are far from new, but may not have been pursued previously, either for lack of suitable applications, or because the necessary technologies were not available. It is often worth revisiting old concepts in the light of modern technology.

Combined Cycles and Scramjets for Orbital Launchers (Papers 15 to 18)

These four papers described the mathematical modelling and technology requirements assessment of turboramjets and scramjets (supersonic combustion ramjets) for reusable two-stage-to-orbit space launcher vehicles. Three of the papers reported on studies associated with the envisaged Sanger project, carried out under the German government-sponsored Hypersonic Technology Programme. The results and discussion contained in the papers can be summed up in the following way:

- a. Two stage to orbit vehicles using any form of airbreathing propulsion present major technical challenges. The vehicles inevitably have very small payload

fractions and there is very little margin for design error.

- b. The sizing and matching of the system components and the control of the gas path losses require very great care, although advanced cfd is a considerable help.
- c. The temperature environment at M5.0 and above demands very advanced structural materials technologies for the intake and powerplant internals. These technologies are beyond what is currently achievable.

Interest in airbreathing systems for orbital launchers has greatly reduced since these studies were initiated, perhaps because of the costs and technical difficulties. It may well revive but in the shorter term there could be more interest in such powerplants for stratospheric surveillance and weapons vehicles.

Compressor Stall Detection (Paper 19)

This paper could equally have formed part of Session V on engine controls systems. The early detection of incipient compressor stall and its integration into a surge avoidance controller has long been a prized but elusive goal. Paper 19 described a technique based on the measurement of changes in rotating blade wakes at the rear of a 13 stage compressor, as the adjacent blade rows approach stall.

The technique was clearly effective for the particular engine type considered (a land-based gas turbine), but its general applicability is less clear. It would be interesting to see whether it would work for other engine architectures and with the more varied compressor stall phenomena occurring in flight.

3.4 Session IV Thrust Vectoring (Papers 21 to 26)

The greater part of this session addressed a topic of great current and future interest, but one that inspires vigorous debate about its operational utility. Regrettably three of the six papers planned for the session were withdrawn, but Papers 21 and 24 dealt fairly fully with the topic. The former described some of the achievements and results of the Germany/US X31 flight demonstration programme, the main purpose of which was to investigate and prove the handling characteristics and combat manoeuvre techniques of an aircraft

with limited all-axis thrust vectoring. The paper highlighted the ingenious low cost design of the X31 aircraft and the outstanding success of the programme.

Paper 24 described the US F15 'Active' flight demonstrator, which is intended to evaluate other potential attributes of thrust vectoring. These include in particular the use of thrust axis trimming to minimise aircraft drag throughout flight, through an active performance seeking control system. Demonstration of a practicable lightweight vectoring nozzle system was also an important aim.

The third presentation (Paper 26) returned to 'conventional' non-vectoring nozzle systems, the aim reflecting the affordability theme of Session I - reduced weight and cost and increased reliability. It described the nozzle designed for the Eurojet EJ200 engine, in which good performance and effectively 2-parameter operation was achieved with a single actuator, combined with a self-adjusting floating link for the second (exit area) parameter

The key points arising from the session can be summarised as follows:

- a. Practical post stall aircraft operation has clearly been proven and with it a whole new flight manoeuvre regime has been opened up.
- b. Thrust vectoring must be all axis and not just in the pitch plane for fully-controlled post-stall flight. All axis vectoring is equally required in the normal flight regime if it is to be used to reduce or replace conventional flight control surfaces (eg for signature reasons).
- c. All axis thrust vectoring can be achieved with relatively simple nozzle engineering and while there are mass penalties, these need not be great. Integration of vectoring nozzles with the airframe poses problems, but these are being suitably addressed in current programmes.
- d. Big gains in close combat engagements have been demonstrated in limited 1 v 1 trials. An aircraft without thrust vectoring is at a grave disadvantage against one with it. However it needs to be demonstrated that these results can be extended to multiple aircraft engagements and that the advantages of thrust

vectoring will not be nullified by changes in tactics.

- e. In non-vectoring systems, ingenious design and exploitation of advanced non-metallic materials can assure good, wide range performance without sacrificing simplicity and low cost and weight.

3.5 Session V Engine Control Systems (Papers 27 to 38)

This was again a large session of ten papers (two others were withdrawn), covering a range of topics. Broadly the session can be divided into four main areas and as with Session 3 it is convenient to summarise each of these in turn.

Advanced FADECs and Multivariable Controls (Papers 27 to 29)

Two of these papers described research into multivariable controls for fixed wing powerplants, illustrating the benefits by means of simulation results. Paper 29 discussed in general terms the application of Full Authority Digital Electronic Controls (FADECs) to turboshaft engines for helicopters. Among the benefits cited were improved engine response and helicopter handling, with reduced pilot workload. The paper also stressed that costs are particularly important for small engines since FADEC costs tend not to scale with size.

The two multivariable controls papers were united in identifying significant advantages compared with normal monovariable control designs, even for engines which can be controlled quite adequately by the conventional approach. The main benefits are again much improved engine response rates and the ability to control compressor running lines very tightly during transients, thus allowing surge margins to be reduced without loss of safety. Both of these attributes have operational value. The papers indicated that multivariable control design is no more difficult than a monovariable design and can be done in a way that ensures simplicity and good software visibility. Multivariable controls appear likely to become the standard for all future engines that have the requisite number of independent variables. For some applications, eg ASTOVL, they will be essential.

Neural Networks (Papers 33, 34)

Neural network computing concepts have attracted growing interest for engine and aircraft controls

during the past two or three years. These two papers were therefore particularly useful contributions, outlining what neural networks can do and how they might be implemented in a practicable adaptive control FADEC system. The approach allows a mathematical model of the engine to be run in the control computer, "shadowing" and interacting with the real plant.

The potential of the technique is clearly considerable, with performance seeking controls and corrections for engine deterioration being just two of the applications. However, the computational demands are high, especially if the mathematical model is to track transients in real time. The problems of developing the software, accommodating it in a small engine control computer, and validating it, will remain challenging.

Advanced Hardware (Papers 35, 37, 38)

The increasing power and functionality of FADECs bring with them a significant overhead in terms of additional sensors, actuators and cable harnesses. These three papers considered the potential hardware technologies that need to be developed to counter the implicit growth in cost, weight and maintenance burden. Two key technologies were highlighted - distributed architectures and optoelectronics. The latter has the important added advantage of providing much greater immunity from Electromagnetic Interface (EMI). In both cases, by localising much of the sensor signal primary processing to the vicinity of the sensor, transmission to the controller can be reduced to one or two databuses instead of a multiplicity of signal lines. The attractions are considerable.

For distributed electronic architectures, the key to success will be the development of high temperature electronic components. For optoelectronics, sufficiently compact optical sensors and reliable optical connectors, able to withstand the severe environment of an engine-mounted system will be required. The indications are that the necessary technologies are making good progress, although the optical systems in particular need much further development.

Methodology (Papers 30, 36)

Paper 30 from SNECMA in France described that company's approach to real time thermodynamic simulation and engine identification and how these are used in the development and validation of advanced control laws. Paper 36 described the

development of the FADEC software for the Eurojet EJ200 engine. This made a careful and critical analysis of the development process and identified several elements which gave rise to technical problems and/or timescale and cost difficulties. The lessons the authors drew from the analysis are relevant to many other projects. Perhaps the most important technical message can be summarised as follows:

The growth in control and engine health monitoring functions with each succeeding engine project is causing a software explosion, which inevitably poses timescale and cost threats. There is a strong need for improved software writing and checking tools.

3.6 Session VI Flight/Propulsion Controls and Other Integration Issues (Papers 39 to 43)

Although programmed as "Integrated Flight/Propulsion Controls" (IFPCS), this session was rather broader, with two of the five papers addressing powerplant intake/exhaust system issues. The three controls papers were all based on ASTOVL aircraft requirements, but two discussed development methods and tools which would be equally relevant to conventional Take-off/Landing (CTOL) applications.

Paper 39 from the DRA in the UK described Harrier flight experiments with a number of different advanced control laws. The standard Harrier aircraft can be flown perfectly satisfactorily without significant flight/propulsion controls integration. However the paper demonstrated the power of an IFPCS to greatly reduce pilot workload during the take-off, landing and transition segments of flight. The benefits in terms of reduced pilot error and reduced training requirements are clear.

Papers 40 and 41, from PWA and NASA Lewis respectively, described some of the aircraft/engine simulation tools and control design methods being developed in the USA for ASTOVL aircraft. Such aircraft, because they have independent variables to control engine thrust and aircraft pitch/roll altitude in hover and transition, are likely to be virtually unflyable without an IFPCS. The task of developing such systems is complex and the two papers described a number of building blocks and process steps which would be needed to create an effective and practicable methodology.

The final two papers, 42 and 43, discussed the technical problems raised by the intake and

exhaust systems for modern combat aircraft. Wide flight envelope and manoeuvre requirements tend to demand that both intakes and nozzles have variable areas. These add considerably to propulsion system weight and cost and create additional design difficulties for the airframer, especially if low signatures are needed. Paper 42 outlined a number of approaches to these problems currently under investigation in the US. The importance of advanced CFD was stressed, but there was also emphasis on the use of sophisticated aerodynamic techniques such as Coanda effects and wave-rider principles to replace some of the mechanical variables.

To summarise the session:

- a. IFPCS is essential for ASTOVL aircraft and is likely to benefit future helicopters and CTOL aircraft. Advanced flight controls that give good aircraft handling may also reduce the severity of engine transients and thus benefit engine life.
- b. IFPCS development will need to be supported by highly capable simulation tools, some of which have yet to be perfected, and by well-structured, modular controller design methods.
- c. Engine intake and exhaust systems contribute substantially to overall powerplant weight and cost. There is incentive and good scope to develop new, compact and lightweight design concepts.

4 SUMMARY AND CONCLUSIONS

The Symposium covered a fairly broad range of topics within the targeted theme, but was well-focused. Without exception, each paper had something valuable and interesting to say. But, for this Technical Evaluator, perhaps five or six particularly stood out. Papers 4 and 10 provided not only insights but also quantitative trade-offs to show how advanced engine technology should greatly improve aircraft capability on the one hand and reduce costs on the other. Papers 21 and 24 gave considerable encouragement to the cause for the use of thrust vectoring as a combat enhancement technique. Also worthy of special mention were: Paper 13, describing the history of variable cycle engine work at General Electric; and Paper 36, on the software development for the Eurojet EJ200 engine controller. Neither paper presented significant new numerical data, but their analyses of project histories and identification of where and why things went wrong were of great

interest. The ability to learn from the past is an important skill. It was refreshing to have two such presentations.

To sum up the Symposium as a whole the following points can be emphasised:

- a. Advanced engine technology and higher thrust/weight offer real gains in aircraft size, cost and mission/combat capability.
- b. New engine concepts will require sophisticated controls and powerplant/aircraft integration is becoming a major consideration for future projects.
- c. The rapid growth in electronics and computing technology is opening up new horizons for multiple control functions, on-line performance optimisation and engine health monitoring. But software development and validation is becoming ever more challenging and may well become the pacing aspect.
- d. The present decade has become characterised by shrinking budgets, not just for military programmes but also for other high cost areas like space launchers. Real projects are becoming few and further between. It is essential that new technology gives demonstrable value for money. New systems must be affordable.
- e. Complexity generally increases acquisition and maintenance costs and lowers reliability. The gains in aircraft capability achieved by advanced component technologies, variable cycles, etc, are well worth seeking but the right balance must be struck.
- f. The bottom line for all future propulsion technology remains: KEEP IT SIMPLE; MAKE IT AFFORDABLE.

One final point should be made. The Symposium has emphasised the importance of aircraft/propulsion integration - implicitly in the case of overall design concepts, explicitly for controls. Integration aside it is also clear that many of the technical challenges facing the engine controls community are similar to those for aircraft controls. It would be well worth holding a future joint propulsion/aircraft controls symposium, bringing both groups together to pool their experiences. In a similar vein, a joint

propulsion/aircraft design concept symposium would also be of benefit. With technology development on both sides of the Atlantic now moving firmly towards the next engine generation, it would be fruitful to hold these proposed events in perhaps 3 to 5 years time. It is recommended that the PEP consider this in planning the future programme.

ADVANCED AERO-ENGINE CONCEPTS CONTROLS
Keynote Address

Donald J. Campbell
Director
NASA Lewis Research Center
21000 Brookpark Road
Cleveland, Ohio 44135

I am pleased and honored to have been invited to speak to you at this very important symposium. As you all know, the mission of AGARD is to increase the exchange of aerospace technologies throughout the NATO Alliance. The objective is to enable both R&D and military organizations to acquire the same level of knowledge regarding technologies relevant to aerospace systems. AGARD provides a structure which facilitates international collaborative activities in aerospace R&D leading to results that often exceed the research capabilities of individual nations.

The purpose of this symposium is to disseminate information to military, industrial, and research organizations regarding various advanced aeropropulsion system concepts and associated control systems currently under consideration for a wide range of future aircraft. Also, the potential benefits of these advanced concepts will be identified.

Future aircraft will require significantly improved propulsion systems to provide greater fuel efficiency, longer range,

higher performance over a wider range of operating conditions, greater safety, decreased emissions, diminished noise levels, and reduced manufacturing costs. An overall integrated effort is needed to address these technical challenges of developing more competitive aircraft and engines from concept to certification and airline operation.

The Agency I represent is NASA (the National Aeronautics and Space Administration). The first "A" is aeronautics. NASA aeronautics includes aeropropulsion. The propulsion program at NASA is a cross-section of research and development activities that are representative of this Conference Program. By reviewing the NASA program, I hope you see a correlation to the propulsion technology challenges addressed in the next five days at this symposium. Also, NASA propulsion demonstration programs, completed in conjunction with industry, have been the foundation for today's civil aircraft engines.

NASA's role in aeronautics is to develop critical technologies, in collaboration with all our partners, so that industrial organizations can confidently incorporate those technologies in their product

and vehicle development programs. Propulsion technologies are frequently the most difficult and challenging to develop, and they often affect the pace of aircraft system development.

To effectively develop and transfer new technologies, NASA's programs are structured into two synergistic halves. The base research and technology (R&T) program half provides fundamental technologies, in areas such as materials and structures, computational fluid dynamics, instrumentation and controls, and others, which enable the initiation of new system technology programs. The system technology program half is focused on specific vehicle classes and system validation from subsonic to hypersonic.

New concepts, new materials, advanced computational capabilities, and other items are first developed in NASA's base R&T program, which also supports many cooperative programs with industry, international partners, and universities. Attractive new concepts and multidisciplinary technologies developed in the base R&T program are then directly migrated into system technology programs to demonstrate the overall benefits and to address component interactions. For example, ground and flight demonstration programs are often essential to validate

technologies in a system.

NASA, in collaboration with industry, has conducted a variety of such demonstration programs. The following four demonstration programs, done in partnership with General Electric Company, enabled new technologies to be incorporated into the GE-90 engine, which is now in development for the Boeing 777 aircraft. The Experimental Clean Combustor Program demonstrated reduced emissions benefits of dual-annular combustors. The Quiet Clean Shorthaul Experimental Engine Program demonstrated low-noise fans and composite nacelles. The Energy Efficient Engine Program demonstrated a short, durable, high-efficiency, high-pressure-ratio core with a low-emissions combustor. The UnDucted Fan Program demonstrated wide-chord, composite fan technologies.

Another Energy Efficient Engine Program conducted by NASA, in partnership with Pratt & Whitney, demonstrated such things as compressor active clearance control, increased annulus turbines, drum compressor and mini-cavities, improved gaspath seals, more effective cooling system, advanced airfoils, elliptical airfoil leading edges, and wide-chord fan blades. These technologies and concepts are being utilized for the PW-4000 series engines which also are now in development for the Boeing 777 aircraft.

Today's propulsion challenges have changed substantially. Ten years ago, efficiency and performance were the prime concerns in new turbofan

engine development. Now, the global aviation market is demanding lower environmental impact as well. Thus, while efficiency, reliability, and costs are still major concerns, the environmental issues of noise and emissions have taken on a greater urgency and importance. All these critical technology issues are not necessarily synergistic. Therefore, they must be addressed in a balanced manner in the development of future generations of competitive propulsion systems. This balancing, or re-prioritizing of technology development is an important consideration in NASA's programs.

NASA has recently initiated a number of important, new, technology programs. These programs include major propulsion elements that can lead to more environmentally compatible and more efficient aircraft, and high-speed aircraft with greater than current capabilities. The propulsion system is the most critical technology required to achieve the goals of the next generation civil aircraft.

The Advanced Subsonic Technology (AST) Program, a collaborative effort by NASA, U.S. aircraft engine manufacturers, and the Federal Aviation Administration, is developing the technologies to enable a safe, highly productive global air transportation system, which will include a new

generation of environmentally compatible and economical subsonic aircraft. In the area of propulsion, the technologies are being developed to reduce nitrous oxide emissions by 70 percent, reduce direct operating costs by 3 to 10 percent, to improve fuel efficiency by 8 percent, and to reduce engine noise by 6 decibels. These improvements will be dependent on lightweight composite materials and geared engine systems to enable very high bypass ratios, the use of improved metallic disk, blade, and case materials, and the incorporation of improved turbomachinery. Three areas of engine noise reduction being investigated are jet noise, advanced low-noise fan designs, and active control of fan noise. Also, validated turbomachinery aerodynamic and aeroelastic design codes are being developed to reduce the development time and cost of bringing an engine to market.

NASA initiated the High Speed Research (HSR) Program to develop the technology foundation needed by the U.S. aircraft industry to produce a new High Speed Civil Transport (HSCT), in essence a second-generation supersonic transport, which could become a key element for the future international air transportation system. However, significant advances in propulsion and airframe technologies beyond current levels will be required for the HSCT to become a reality. These needed technological advances include a high-efficiency combustor with ultra-low emissions of nitrous oxide; a low-weight nozzle with low noise level; a high-

performance, mixed-compression inlet with adequate stability and acoustic suppression; and a high-efficiency, multiple stage fan with low noise level.

Reducing engine noise essentially requires reduction of the nozzle jet velocity. Achieving this goal is a tradeoff between cycle selection, nozzle noise suppression, and engine sizing. The currently selected HSR engine configuration is a mixed-flow turbofan of moderate bypass ratio. Jet velocity will be reduced with a mixer/ejector nozzle to meet the noise reduction goals.

The economic viability of the HSCT will require an engine with higher performance and lower weight. Advanced, high-temperature materials can contribute to meeting both the environmental and the economic requirements for the engine. The primary materials being developed are ceramic matrix composites for the combustor liner, intermetallic/metal matrix composites for the nozzle, lightweight composites for fan containment, and long-life materials for compressor and turbine disks and turbine blades. Long-term durability is a critical design issue, because the duty cycle of the HSCT engine will be much more demanding than that of current engines. Long life for critical components such as compressors, turbines, and

nozzles exposed to long-duration, high-temperature environments will have to be demonstrated.

In addition to developing new technologies, component designs, and materials for propulsion systems, it is crucial to reduce the time and cost of the development and certification of future aircraft engines, in order to help the aeropropulsion industry. This requires highly advanced computational systems and programs. A prime example is the Numerical Propulsion System Simulation (NPSS) Program. The primary objective of this program is to develop the technologies needed to perform large, computationally intensive system and subsystem simulations of aircraft engines and thereby reduce engine development time and cost by 30 percent. NPSS is being developed in close collaboration with industry to ensure that the software will meet its needs. The approach is to simulate complete engine behavior and thus reduce dramatically the design, test, and redesign iterations needed to meet performance requirements. NPSS captures interdisciplinary and intercomponent coupling effects by means of advanced codes, computing techniques, and paralleled hardware systems. Prototypes demonstrated in NASA's base R&T program have already resulted in savings of 1 year and approximately \$50 million to industry. Current estimates indicate the possibility of even greater savings in the development and certification of a new engine in the future.

To meet the increasing technological challenges with diminishing resources, NASA's technical partnerships in the field of aeropropulsion are gaining momentum. NASA has forged a stronger technical and programmatic relationship with U.S. industry, which has brought increased customer focus and team spirit to our work. Small Disadvantaged Businesses are bringing critical skills and are becoming an increasingly important part of this partnership. NASA is also working more closely with other government agencies, such as the Department of Defense, Department of Commerce, National Institute for Science and Technology, and others, to leverage program resources to meet common needs. Academia is a direct partner in our programs to provide basic research, as well as the scientists and engineers of the future. Historically Black Colleges and Universities are making growing contributions to these efforts and are increasingly important partners. Technical societies provide a critical forum for technology transfer, especially in the fundamental sciences. NASA also works with many international partners to develop a better understanding of fundamental physical processes and to improve aviation safety.

In closing, I want to thank all of you for your time and attention, and I

appreciate having had this opportunity to provide you with an overview of some of NASA's endeavors in the area of aeropropulsion. I expect that all of you will gain very interesting, important, and useful information from this symposium.

The Purpose and Status of IHPTET -- 1995

Richard J. Hill

Chief of Technology, Turbine Engine Division
Aero Propulsion and Power Directorate, Wright Laboratory
1950 Fifth Street, Wright-Patterson AFB, Ohio 45433-7251

1. SUMMARY

IHPTET is the *Integrated High Performance Turbine Engine Technology* program. This paper discusses the purpose (background, goals and applications) and the status of IHPTET through July 1995. IHPTET has finished Phase I and achieved significant success in advancing turbine engine technology levels. The future of IHPTET is bright as work continues into Phase II. Technologies developed in IHPTET are being applied to both new engines and fleet modernization's. IHPTET is the turbine engine technology base and springboard for all future military systems.

2. IHPTET PURPOSE

2.1 Background

IHPTET is a coordinated, three-phase, government and industry, propulsion focused visionary program. Formally initiated in 1988, IHPTET includes virtually all government and industry sponsored propulsion Research and Development (R&D) activities devoted to advancing technology for military turbine engines. The goal of IHPTET is to develop and demonstrate technologies by the turn-of-the-century that, when applied, will double a 1987 level of turbopropulsion capability. The technologies of IHPTET offer significant payoff when applied to any propulsion system.

Under IHPTET there exists one IHPTET government plan and six individual industry plans, coordinated among the Department of Defense (DoD) Military Services -- Army, Navy, Air Force; the Advanced Research Projects Agency (ARPA); and the National Aeronautics and Space Administration (NASA). The structure of the IHPTET program is shown in Figure 1.

As shown in Figure 1, a DoD chaired Steering Committee provides overall IHPTET guidance. The six US turbine engine companies participating in IHPTET form an Industry Panel that advises the Steering Committee on specific issues. These companies are AlliedSignal Engines; Allison Advanced Development Company; General Electric; Pratt and Whitney; Teledyne Ryan Aeronautical; and Williams International. Also reporting to the Steering Committee are seven Component Panels (compressors, combustors, turbines, nozzles, controls, mechanical systems and technology demonstrators) and four Pervasive Technology Panels (materials, computational fluid dynamics (CFD), engine structures, and cost reduction). Each of these panels oversees the technology planning and development in their area. Every panel has membership from each of the government offices.

Each IHPTET technology is funded and developed individually or jointly to the panel plan by one or more of the five IHPTET government organizations. Biannual reviews are held by the Steering Committee where the progress and problems of each technology panel and area are reviewed. Through this steering committee process, IHPTET is successfully meeting each of the technological challenges by readjusting as necessary to changing resource allocations and technical or planning difficulties.

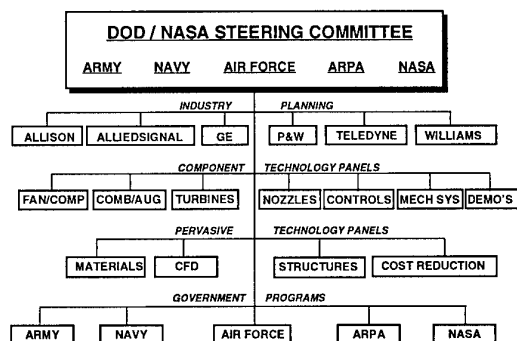
2.2 Goals

Payoffs from IHPTET come from increasing propulsion system performance and affordability with no compromises in system life, reliability or maintainability requirements. To focus the program on these payoffs, IHPTET management established specific goals as a function of time for each of the three aircraft turbine engine classes -- turbofan/jet, turboshaft/prop, and expendable. Shown in Figure 2 are the time phases of IHPTET. The goals of each phase were chosen as having the highest effect in maximizing payoff to military systems. In addition, the three IHPTET phases shown in Figure 2 were created to provide milestones against which to assess progress, and, most importantly, to provide opportunity for transition to current, upgrade, derivative and new engines.

The IHPTET goals for each of the three phases are shown in Table I and are based on a 1987 technology level. The cost goals for the turbofan/jet class of engines were added in February 1995. The goals of IHPTET are "typical" technology goals for each class of engine (*do not interpret them as a combined or specific "engine cycle" description*). Through the

IHPTET Organizational Structure

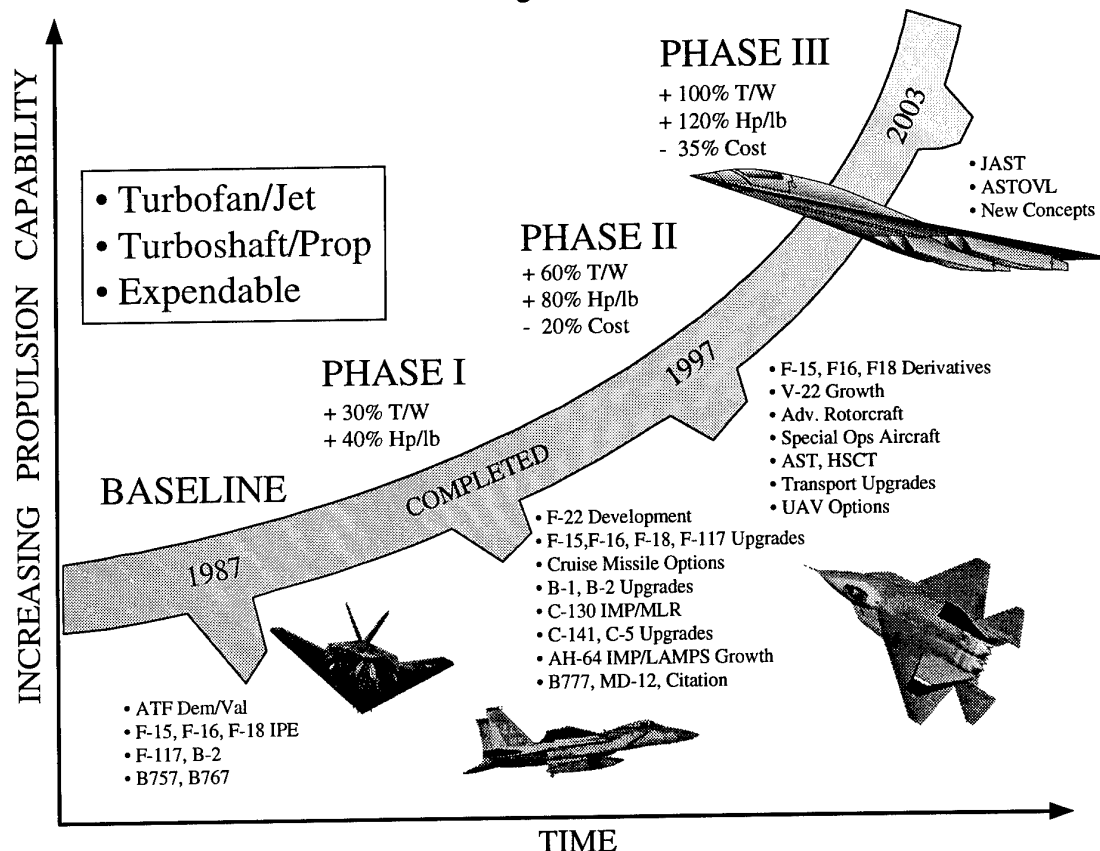
Figure 1

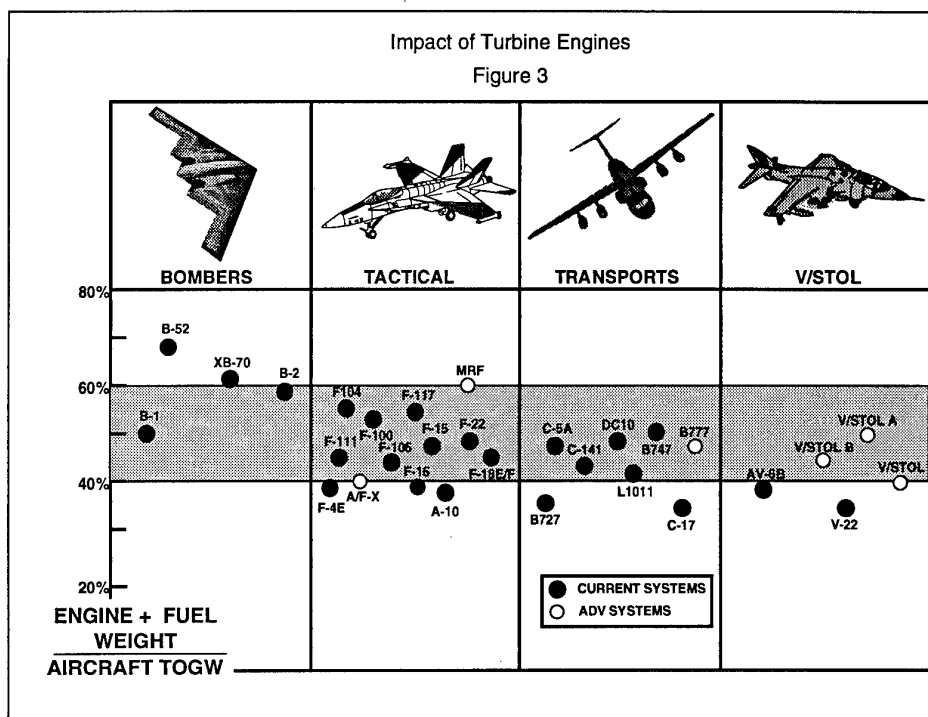


achievement of these goals, IHPTET will provide technology for propulsion systems that are lower cost, lighter weight and easier to maintain than today's systems, yet enable current and future aircraft to fly faster, higher, and with increased maneuverability through a wider flight envelope. This enhanced capability from propulsion technology will produce major payoffs for the field commander. These modernized high performance aircraft will supply the affordable battle field advantage -- low fuel burn allowing longer missions; high thrust-to-weight ratios allowing larger aircraft payloads; low maintenance and support in the field yielding higher sortie rates; and excess specific power during critical flight maneuvers in a wider flight envelope -- the air superiority advantage! The weight significance of propulsion (a major cost indicator) can be seen in Figure 3 for all classes of aircraft -- Bombers, Tactical, Transports, and V/STOL. As shown in Figure 3, the propulsion system weight (engine weight plus fuel weight) typically accounts for between 40% to 60% of the total aircraft takeoff gross weight (TOGW). Any progress in lowering the weight of the engine or decreasing the fuel consumption will have a dramatic impact on the total system weight and size -- the cost drivers. Studies in IHPTET have quantified the weight and size influence on cost for a new engine in a current airframe and a new engine in a new airframe. Using IHPTET Phase II technologies for example, system

studies show a 40% acquisition cost saving for a new engine in a new airframe (new system has an aircraft thrust loading and fuel weight fraction equivalent to the current F-16). Using IHPTET Phase II technology to retrofit a new engine to a current airframe (new, smaller engine at same thrust as current F100-229 engine) shows a 25% acquisition cost saving. Using IHPTET Phase II technologies, individually or in small upgrade packages, for modernization of current propulsion systems show proportionate values of Life Cycle Cost (LCC) savings. In addition to these projected "system application" cost reductions, the IHPTET program has "technology" cost reduction goals of 20% for Phase II and 35% for Phase III. These cost reduction goals were established in February 1995 for the turbofan/jet class of turbine engines. The goal values are for both the acquisition and maintenance aspects of engine costs. Studies are underway to determine equivalent goals for the turboshaft/prop class of engines. Expendable engines had cost goals established in 1988 and are shown in Table I. Considering that the US Government spends approximately \$15 billion per year on aircraft and missile gas turbine propulsion systems, IHPTET's 25% to 40% system's cost savings opportunity, together with the technology cost reduction goals of Phase II and Phase III, amounts to significant financial savings opportunity to major command organizations and future defense budgets!

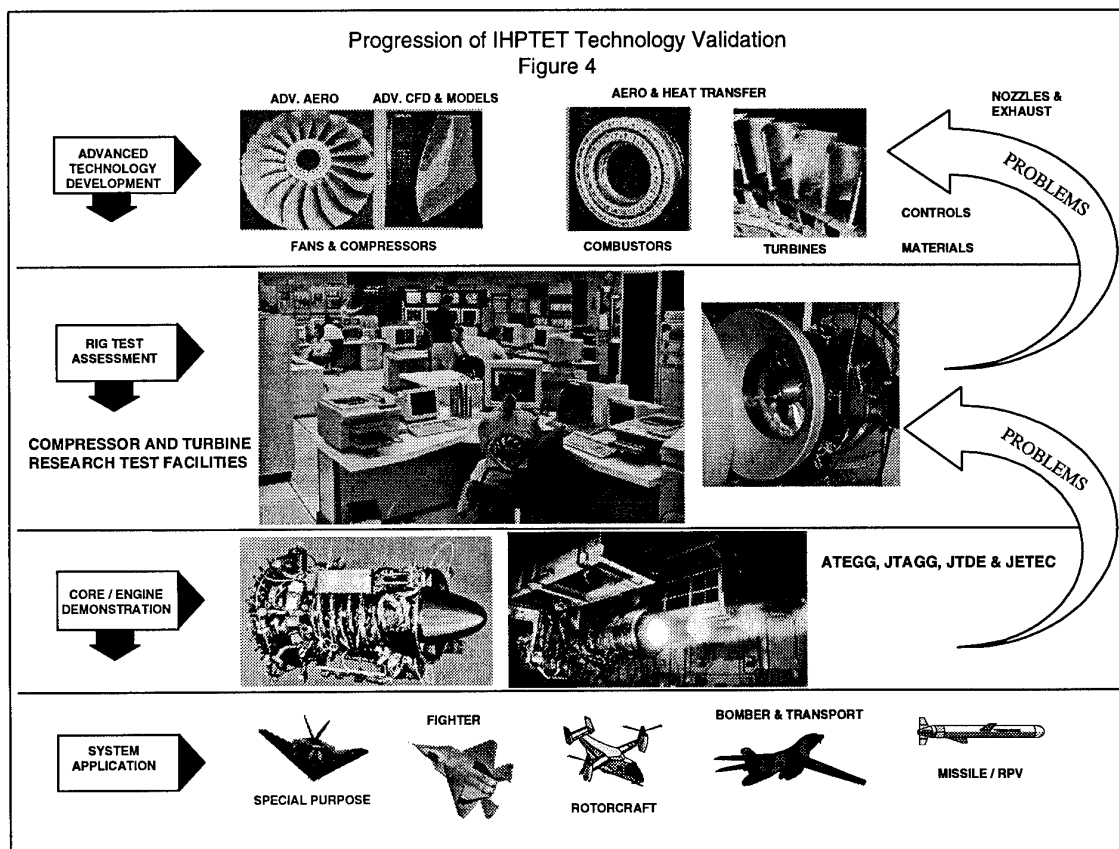
IHPTET Time Phases and Transition Opportunities
Figure 2





Under the IHPTET program, the goals of Table I are not considered to be achieved until the enabling technologies have been assembled and tested under actual engine conditions in an engine demonstrator (core or full engine configuration) -- commonly called

a "Tech Demo." However, some high payoff, low risk technologies have transitioned to current engines early, after successful and substantial rig testing. The normal progression of test validation of IHPTET technologies, however, is shown in Figure 4.



Under IHPTET sponsorship, technologies generally start at the component level. The initial research and development can begin from work sponsored by one of the services, NASA or ARPA or from a contractor's Independent Research and Development (IR&D) program. After having matured to a reasonable level of analytical and sub-scale testing validation, the technology is manufactured and assembled into sub-scale or full scale components for more complete test evaluation in dedicated rigs. The primary IHPTET compressor test facility is the Air Force's Compressor Research Facility (CRF). The CRF became operational in 1984 and can test inlet conditions at ambient temperature from 2 psia to ambient pressure with a core flow of from 15 to 500 pounds mass per second. Instrumentation includes both analog and digital capability with over 1000 channels available. Data can be sent directly across country, in real time, to a contractor's facility in a highly protected format allowing him to view the test data as it is recorded. The facility can run up to 30,000 rpm and evaluate full scale, multi-stage, single spool fans and compressors under realistic operating conditions.

The newest IHPTET test facility, the Turbine Research Facility (TRF), is dedicated to turbine research and also belongs to the Air Force. The TRF can test full scale single and multi-stage turbines at full Reynolds Number, axial Mach Number, Prandtl Number, specific heat ratios, and ratios of gas temperature to blade metal temperature equivalent to conditions of IHPTET turbines. The current test chamber size accommodates turbines from 17 inches to 34 inches diameter and test conditions are achieved in the range of one to five seconds. There are over 500 channels of instrumentation of 12 bit analog-to-digital recording at a rate of 100,000 samples per second. Data includes surface and total pressures and temperatures, rotational speed, torque and surface heat flux. The TRF is the only existing capability that can evaluate both turbine aerodynamic and heat transfer performance of a full scale turbine operating under correctly scaled engine conditions.

The best and most promising technologies that successfully complete testing in rigs like CRF and TRF are continued in the development process to the next level -- Tech Demo testing. In the Tech Demo tests, the technologies of several components are assembled together, first in cores and later into full engines. The purpose of Tech Demo testing is to understand, under actual engine conditions, the synergistic component interaction. If a problem occurs or if testing reveals less than complete understanding of the critical aspects of the technology, the technology is returned to the component level for further research work or additional rig testing. Only well characterized component technologies continue through complete Tech Demo testing. All Tech Demo testing is done with significant amounts of instrumentation. Typically over 1000 pieces of instrumentation are used on a single Tech Demo test with the majority of the testing done at sea level conditions. The major workhorse demonstrators for turbofan/jet engines are the Advanced Turbine Engine Gas Generator (ATEGG)

cores and Joint (Air Force and Navy) Technology Demonstrator Engine (JTDE). For turboshaft/prop engines, the demonstrators are the Joint (Army, Navy and Air Force) Turbine Advanced Gas Generator (JTAGG) cores. Missile engine technology is demonstrated in the Joint (Air Force and Navy) Expendable Turbine Engine Concept (JETEC).

2.3 Applications

The IHPTET program was established during the middle 1980's to be the "technology springboard" for the next century's high performance military turbine engines. The main thrust of IHPTET was focused during this time period on a wide spectrum of new systems, and success in IHPTET would ensure continued US air superiority over any new aggressor system. A second thrust of IHPTET was the systematic spin-off of technology advancements for modernizing the current fleet of aircraft engines. This opportunity occurs primarily at the end of each Tech Demo test.

The major areas of focus for technology application under IHPTET started as, and continues to be, the achievement of affordable growth in the metrics of thrust-to-weight and power-to-weight, lower fuel consumption, decreased (low observable) engine signature, increased repairability, operability and maintainability and decreased acquisition, operation and support costs. In man-rated turbofan/jet propulsion for example, the payoff gained by the achievement of the IHPTET goals is providing the technologies for upgrade and growth F-15 and F-16 aircraft engines (F100 and F110 engine families), as well as provide the technology base for the new F-22 Advanced Tactical Fighter (ATF) engine (F119).

The dismantling of the Warsaw Pact created the need to rethink many of the US military Science and Technology (S&T) plans, including IHPTET. What is reported now by many top command officials is a diminishing need to develop new high performance aircraft to overcome new aggressor advancements and an increasing need to modernize the fleet of current systems. The focus of S&T is now changing to be more evenly split between creating new systems and upgrading existing systems. The new systems, when needed, will be developed in minimum numbers and be replacements for near-obsolete aircraft. They will be based on the best, affordable technology available at key points in the development process. The second focus, that of modernizing the current fleets, will also use the best, affordable technology but will be directed at specific engine components combined to form "upgrade kits." The new US military force structure will rely on a combination of these high quality, technologically advanced systems to cope with regional threats. The major objective of this new trend is to continue a high quality, high readiness force to perform regional operations like Desert Storm at a minimum cost. The Gulf War proved that air superiority is a result of superior training and technologically advanced weapons. Both of which are essential for minimizing casualties and length of conflict. For the new S&T plans, IHPTET remains the

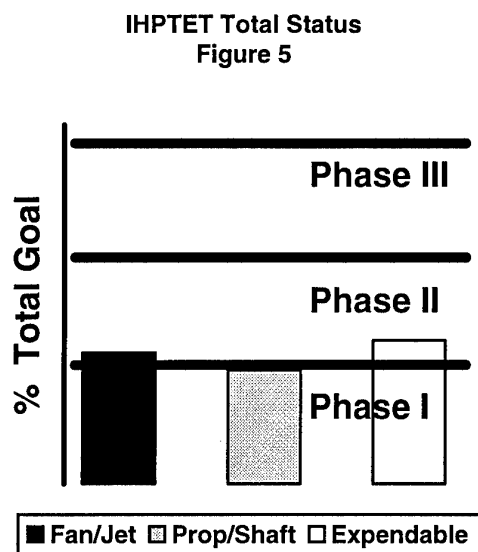
answer for all turbine engines. This is due to the original broad application (non system specific) focus of IHPTET technology planning with many spin-off opportunities to a wide spectrum of aircraft, rotorcraft and missile uses.

The technologies being developed under IHPTET fit naturally this redefined S&T role in meeting the wider DoD objectives. The IHPTET program is providing the foundation for retaining the affordable air superiority advantage sought in the new Air Force strategy of Global Reach - Global Power. The IHPTET plan is to continue to provide enabling technology for affordable upgrades of the existing engines and the technology base for all new engines of the future. The result of this long-term view is that IHPTET will produce the technology to equip the next century peace keeping force with affordable, superior propulsion systems. As defense draw-down continues and weapon system acquisition starts to be based on selective upgrades and new engine low-rate production with a continual insertion of advanced technology, the application of IHPTET technology will increase proportionately.

3. IHPTET PROGRESS

3.1 Status of Goal Achievement

Work has successfully been completed on IHPTET Phase I and work on Phase II is well under way.



As seen in Figure 5, the work on Phase I is complete and Phase II progressing well with completion of the Phase II goals expected in 1997. IHPTET will achieve 100% completion in 2003 and planning has started for the technologies that are beyond the IHPTET plan.

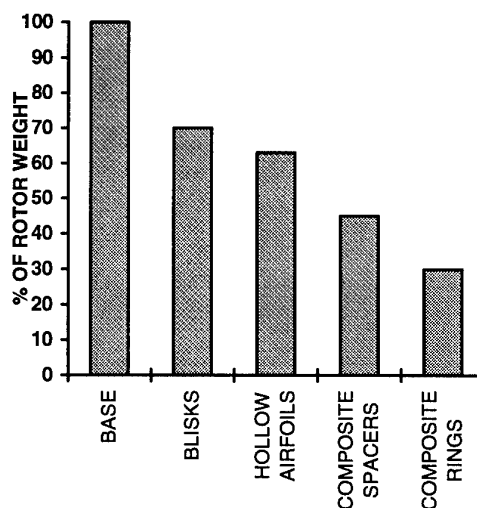
3.2 The Elements of IHPTET

The three main elements of IHPTET are

(1) development and application of advanced aerodynamic and thermodynamic models and theories, (2) development and application of advanced high strength, low density materials (monolithic and composite), and (3) the creation of innovative structural designs that take full advantage of the best of the aerothermodynamics and the advanced

materials. The best combination (different for each company) of these three elements focused on the goals of Table I is the IHPTET "program." Each participant in the IHPTET program has developed innovative designs for each phase of IHPTET based on their "best" IHPTET technology combinations. However, overall there are several IHPTET technologies that are so beneficial, that almost all companies have decided to use them. A good example of one such technology is the technology of silicon carbide fiber reinforced Metal Matrix Composites (MMC) for rotor support structure. The benefits of this technology combined with other innovations for compressor rotor structure can be seen in Figures 6a, b, c and d. These advancements offer, for example, the potential to reduce a compressor rotor's weight 70%. This is accomplished through the application of advanced materials to advanced designs including Integral Blade/Disk Rotors (IBR or BLISK), hollow airfoils and composite spacers (Figure 6c) and ring rotors (Figure 6d). The final Phase III compressor is envisioned to be made entirely of advanced MMC materials and be only made of ring type structure. The primary need for these new materials and innovative designs is centered on the compressor's need for high rotational speeds to take full advantage of the advancements in IHPTET aerodynamics in the blade rows. If the rotor had to be constructed of conventional materials, the design would require full webs and bores on each rotor stage. This would result in a heavy and lengthy rotor. To illustrate this comparison, a compressor rotor was designed to meet the rotational speed requirements of an IHPTET configuration, but constructed from conventional nickel-based alloys. The result of this design effort is shown in Figure 6b as the "Baseline 1987 - All Nickel Compressor." Using this base design, major IHPTET compressor technologies were added, individually, to the design with the progressive reduction of rotor weight as shown in Figure 6a.

Benefits of Innovative Design and Advanced Materials to a Compressor Rotor
Figure 6a



The technologies shown in Figure 6a can be used independently or bundled together to increase the performance attributes of a chosen design application -- new or upgrade component or engine.

Figure 6b
Baseline 1987 - All Nickel Compressor

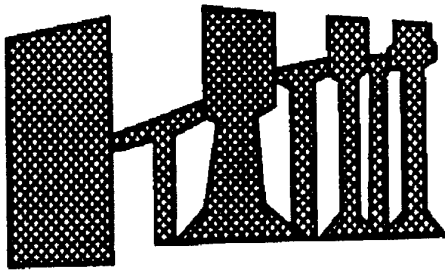


Figure 6c
Addition of Composite Spacers and Blades

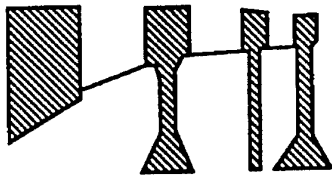


Figure 6d
Addition of MMC Rings to the Rotors

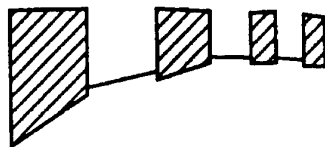
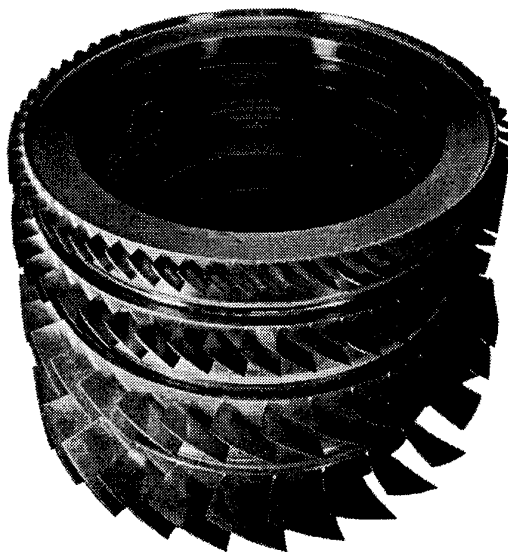


Figure 7
Advanced MMC Reinforced Ring Rotor



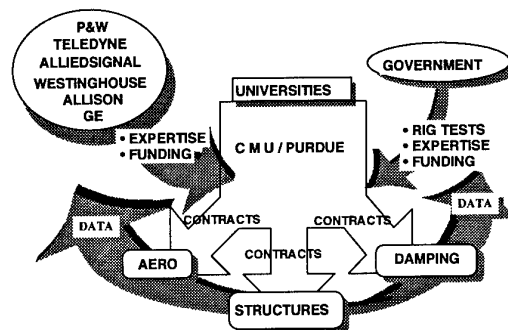
Each of the technologies in Figure 6 has been tested successfully in a Tech Demo. In addition, Figure 7 shows an IHPTET ring rotor that was tested successfully in a recent core engine Tech Demo.

3.3 Affordability – A Reduced Cost Approach

A perceived problem with several IHPTET technologies centers on "affordability." Metal matrix composite material is a prime example. The problem with the MMC class of materials is that they are process sensitive and currently expensive to manufacture, inspect and repair. At best, only a "lean production" of these classes of material will be available for a data base if they remain only applicable to advanced military systems. To address this issue of cost, IHPTET has initiated a major effort to reduce the cost of advanced technologies. The cost reduction goals are as shown in Table I and effort is now underway to achieve these goals. One solution to the cost issue is the broadening of the production base for MMC and Ceramic Matrix Composite (CMC) class materials by broadening the non military market application. The Organic Matrix Composite (OMC) industry is a prime example of how to lower the cost and increase the knowledge base on a new material. This industry created a need for the material system by applying the technology to sports equipment, automotive equipment and home products. With this broadened base for production and broadened demand for the material, the "price came down and the quality went up." IHPTET management is trying to encourage the same success gained by the OMC industry by broadening the need for MMC and CMC material systems. Thus far, some limited success is being achieved with application to racing car components and golf clubs with more commercial applications anticipated in the near future.

IHPTET management is also trying to increase "the affordability" of technologies more globally through the encouragement of teaming and the formation of industry consortia. The intent of these actions is to minimize the cost and maximize the production knowledge of technology through data sharing. The action taken thus far has been the formation of jointly sponsored research consortia and funding teamed contractor Tech Demo testing efforts.

Figure 8
Model of an IHPTET Consortium



The current IHPTET consortia are focused on forced response prediction methods for blades; fiber development for advanced MMC and CMC materials; titanium MMC life prediction; and development of advanced instrumentation concepts and methods. The consortium idea is shown in Figure 8 using the "Forced Response Consortium" as an example. In this example, Carnegie Mellon (CMU) and Purdue Universities are the integrating subcontractors. Each member of the consortium contributes resources at

varying levels (funds, facilities or data) and technical expertise to help meet the consortium goals. In addition, the Government contributes funds, expertise and in some cases, rig testing facilities and test time to the consortium. Contracts are then let to chosen organizations to actually conduct the research and report the findings. The Forced Response Consortium shown in Figure 8 is focused on the establishment of standard industry assessment methods of structural damping and understanding structural response to engine/inlet induced aerodynamic forcing functions. The Materials Consortium, like the Forced Response Consortium, is a jointly funded effort by all six engine companies, DoD, ARPA, and NASA. The objective is to develop affordable high temperature fibers for use as reinforcement in both CMC and MMC material. These will be developed as "industry fibers" -- well understood, documented and ready for reduced cost production use by each of the participants. As shown in Figure 8, the consortium is unique and acts as an impetus for industry to work together on other common IHPTET technology problems resulting in cost benefit and market opportunity to all.

In the area of contractor-teamed Tech Demo testing, significant progress has been achieved. Currently, General Electric and AlliedSignal Propulsion Engines are teamed in JTAGG to develop and share in the technology payoff of the small to medium class of turboprop/shaft engines. This takes the form of testing each company's technologies in several builds of a common JTAGG Tech Demo. A second team, composed of General Electric and Allison Advanced Development Company, is organized to jointly pursue the IHPTET Phase II turbofan/jet goals through government funded ATEGG and JTDE programs.

Considerable synergistic benefit and technology innovation have resulted from these unions. A third team of General Electric, Pratt & Whitney, Allison, and Rolls Royce is working on a joint structural Tech Demo focused on testing advanced intermetallic titanium aluminum compressor blades, innovative turbine cooling designs and reduced engine weight concepts. This program is called the Component And Engine Structural Assessment Research (CAESAR). CAESAR is underway as a successful program as well as business concept. The test of CAESAR will be in October 1996 (core) and July 1997 (engine) and will help reduce the risk of many IHPTET technologies.

3.4 Technology Readiness -- Risk Reduction Through IHPTET Tech Demo Testing

Historically, risk, viewed in terms of level of "readiness," is the reason given for not using advanced technology. In choosing technologies for systems, "better" technology has always been, and remains the enemy of "good enough" technology when budgets are tight. This is due to the manager's dilemma of always having to trade part of the "desired but not critical" capability to meet schedule and budget constraints. Historically, newer and better technology has always had a lower readiness value and higher risk. The same is true for current IHPTET technologies.

Technology readiness is difficult to quantify and understand. However, in IHPTET, a joint industry and

government task is underway to both define criteria for assessing readiness of technology and put in place effort to increase the readiness when a low value is determined. The considerations being used to determining the readiness of IHPTET technology centers on the extent of design and test experience with the new technology; the amount of extension beyond known values for manufacturing and production; and the degree of similarity to known design methods, materials processing and manufacturing. Readiness assessment is judgmental and varies from company to company for the same class of material or application of similar technology advancements. Effort to increase readiness has taken different forms in IHPTET. One such form in the Air Force is the formulation of additional Tech Demo tests for specific technology items. This new effort is termed Advanced Technology Demonstrations (ATDs). These IHPTET programs are short duration, low cost and directed at removing the last remaining risk barriers on a technology -- the ones preventing immediate transition of the technology to a product application. Currently, IHPTET is sponsoring ATDs for the Air Force's F100, F110 and F119 fighter engines. The completion of these ATDs will result in significant performance improvements while producing major life cycle cost savings.

4. THE FUTURE OF IHPTET

4.1 IHPTET "Multi-use"

Today, the American aerospace industry is facing monetary issues of major proportion. Significant profit losses, unsold inventories and declining sales have forced a major restructuring of the aerospace industry. The total US engine production value is down by nearly 1/3 since 1991. Since the IHPTET program represents a major investment by industry (nearly 55% of all money from 1988 through 1996 will come from industry), this problem becomes a significant concern to IHPTET management. The National level approach to this situation is the expansion of "Multi-use" thinking when technology is being developed. Under this idea, technology is developed in such a way that commercial and military application becomes of relative equal importance. Thus, every dollar spent on technology development will energize the commercial economy -- hopefully increasing productivity and availability of new jobs. Such an idea is presented in the Aeronautical Technology Consortium Act of 1993 (Aerotech). IHPTET management will do anything it can do -- without straying from its basic purpose of pursuing high-payoff military goals in aeronautical technology -- to support initiatives like Aerotech.

IHPTET management recognized early that technology modernization and application are key to increased productivity in the aerospace industry. In IHPTET, multi-use has become a significant outlet of the many technologies developed. Numerous IHPTET developed technologies have already transitioned into commercial engines, and over 100 technologies now being developed under IHPTET have potential multi-use application. In total, nearly 80% of IHPTET technologies have commercial spin-off potential to the civil aviation industry, the automotive industry and the industrial ground power generation industry.

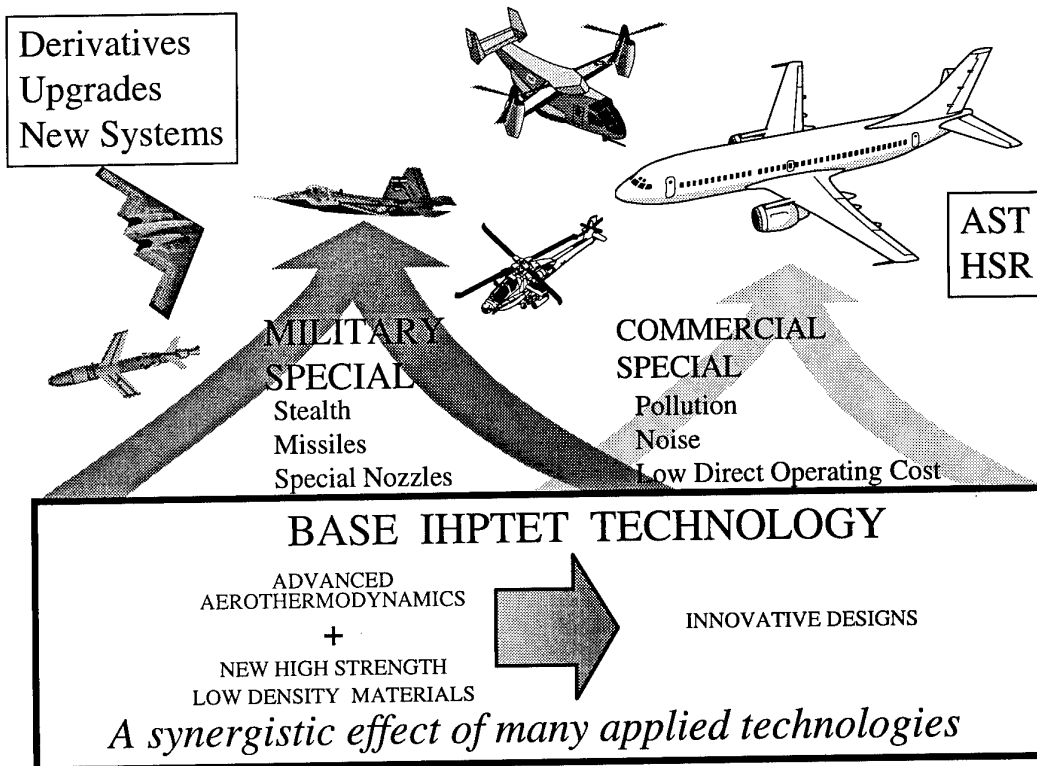
4.2 IHPTET and the New NASA Initiatives

The concept of Multi-use is but one aspect of the new national policy relating to defense reinvestment, diversification, and conversion. This new Congressional policy has inspired new NASA civil air transportation propulsion initiatives -- the Advanced Subsonic Technology (AST) for subsonic commercial aviation (large and "commuter" style aircraft application) and the High Speed Research (HSR) program focused on supersonic transports. IHPTET is a major springboard for these new NASA initiatives as depicted in Figure 9. IHPTET will continue through the nineties working on all advanced technologies for basic military propulsion critical needs and unique features (stealth, expendable engines, and concepts of thrust vectoring for STOVL applications) with NASA pursuing, in addition to their basic IHPTET work, the missing commercial critical technologies (ideas for pollution control, noise suppression, universal fuels, novel regenerative cycles, etc.). The IHPTET spring board for the NASA initiatives will be the more common technologies such as advanced materials, CFD design codes, advanced engine controls and logic, advanced turbine cooling concepts, bearings, seals and structures. Technology success in this common area will be applied to both military propulsion and commercial propulsion needs as necessary. For example, success in advanced

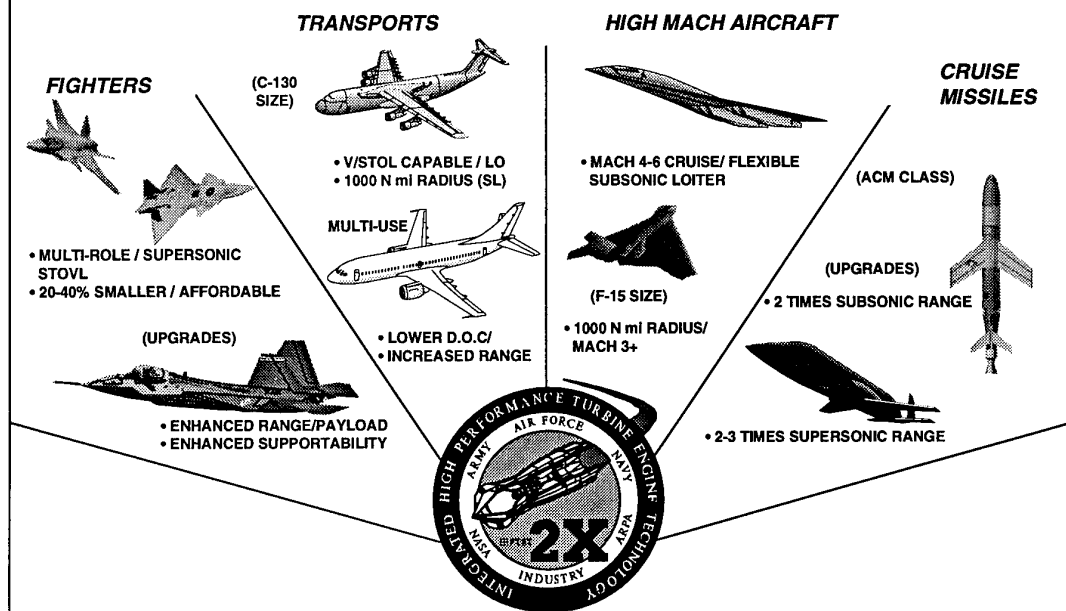
turbine blade cooling technology may be applied in military engines to increase the allowable gas temperature at constant turbine blade life and thereby increase the engine specific thrust. In a commercial application, the technology may be applied to lower the turbine blade bulk temperature at constant gas temperature (constant thrust) and increase the life of the component and thereby decrease the engine's direct operating cost -- same technology but "spent" differently. This concept of wide application for IHPTET technology is shown in Figure 10.

As America approaches the next century and beyond, the programs of IHPTET will provide a strong US propulsion technology base. In 1991 the US aircraft gas turbine engine industry shipped approximately \$22.1 billion of products (split about equally between military and commercial application). Through the IHPTET efforts of DoD and NASA, this high value American industry will continue its dominance of the global aviation market. In addition, through the wide spectrum applicability of IHPTET to many new, growth, and derivative systems, as shown in Figure 10, the US military will continue to achieve affordable national defense -- global reach, global power and global presence.

IHPTET Springboard to US Aviation
Figure 9



IHPTET Potential
Figure 10



IHPTET Goals by Phase
Table I

	PHASE I	PHASE II	PHASE III
TURBOFAN / TURBOJET			
THRUST TO WEIGHT RATIO	+30%	+60%	+100%
COMBUSTOR INLET TEMPERATURE	+100°F	+200°F	+400°F
MAXIMUM TEMPERATURE (TYPICAL)	+300°F	+600°F	+900°F
COST REDUCTION	Consideration	-20%	-35%
TURBOSHAFT / TURBOPROP			
SPECIFIC FUEL CONSUMPTION	-20%	-30%	-40%
POWER TO WEIGHT RATIO	+40%	+80%	+120%
MAXIMUM TEMPERATURE (TYPICAL)	+300°F	+600°F	+1000°F
EXPENDABLE			
SPECIFIC FUEL CONSUMPTION (STRATEGIC)	-20%	-30%	-40%
THRUST TO AIRFLOW RATIO	+35%	+70%	+100%
COST REDUCTION (TACTICAL)	-30%	-45%	-60%
COMBUSTOR INLET TEMPERATURE	1100°F	1200°F	1400°F
MAXIMUM TEMPERATURE (TYPICAL)	+500°F	+900°F	+1400°F

FUTURE TECHNOLOGY REQUIREMENTS FOR UK COMBAT ENGINES

M D Paramour

Procurement Executive, Ministry of Defence
Directorate of Future Systems (Air)
St Giles Court
1 St Giles High Street
London WC2H 8LD
United Kingdom

SUMMARY

The paper reviews the future requirements of the UK Services for combat engines, and discusses the design considerations and technology that will be required to meet them. Emphasis is placed on the need for improved reliability and maintainability and reduced life-cycle costs, as well as improved performance. Current and proposed technology demonstrator programmes, to be undertaken both nationally and in collaboration with other nations, to ensure that the technology will be available, are described.

1. INTRODUCTION

Forecasting the future in military requirements is never easy. It is now more difficult than in the past because of the uncertainty of the exact nature of the threat which may face us in 10 to 20 years time. Some things, however, are certain; aircraft do not last for ever, and will need to be replaced. Moreover, in the light of other demands on government expenditure in advanced countries, the pressure on defence budgets is unlikely to reduce. The challenge which faces us, whether we are suppliers, purchasers or users of defence equipment, is to maintain, and preferably to enhance, our operational capability, using fewer resources in terms of money and people.

This challenge is as difficult in combat aircraft as anywhere else. Since combat aircraft were first produced, their capability has steadily increased, and their unit costs have risen correspondingly. This trend cannot continue for ever if viable force levels are to be maintained. In meeting the aim of increasing capability whilst restraining life cycle costs, engine technology will play a vital part. This paper therefore examines in some detail the requirements for future combat engines, in the light of the need for reduced cost of ownership, as seen by operational requirements and support staff of the Royal Air Force (RAF) and Royal Navy (RN). It goes on to describe some of the technology demonstration work applicable to combat engines which is being supported by the Procurement Executive of the Ministry of Defence - MOD(PE). Finally it draws conclusions about

how the changing operational and financial pressures will affect the technology which may be used in future engines.

2. MILITARY REQUIREMENTS

This section of the paper outlines the main combat aircraft programmes which the UK will require early in the next century and identifies the engine technology which will be needed to meet them; it discusses the tradeoffs that will have to be made to ensure the best compromise between conflicting requirements is made.

2.1 Future Projects

The Royal Navy's requirement is for a Sea Harrier Replacement (SHAR(R)), to fulfil both ground attack and air defence roles. It will be required to operate from the current Invincible class ships, and will therefore need Short Take-Off and Vertical Landing (STOVL) capability. The Royal Navy currently foresee that any replacement of their ships would be at the smaller end of the aircraft carrier range, for which STOVL gives several advantages over CTOL aircraft, e.g. a 20-40% better sortie rate, lower speed on departure, and fewer weather restraints than would otherwise occur with smaller carriers. At take-off the STOVL aircraft requires a high level of installed dry power, but less power in afterburner than a CTOL aircraft.

The RN want an aircraft with better missile capability, and able to carry its weapon load back to the ship. As only one fixed-wing aircraft type will be carried, it must have good multi-role tactical and reasonable fighter performance both beyond visual range and at close quarters. Cost effectiveness considerations indicate moderate supersonic capability and no need for supercruise (otherwise a large and uneconomical engine would be required)

The main programme for the Royal Air Force is a replacement for Harrier and Tornado in their offensive roles. The concept is known as the Future Offensive Aircraft (FOA). At the present time the aircraft is not defined, but the essential requirement is for a long range

ground attack aircraft, as air superiority needs will be met by EF2000. The aircraft must be able to operate in all weathers, day and night, at low and medium level. The aircraft must have engines which provide a good range, a good payload, an appropriate compromise between performance and low observability, and a reasonable self-defence capability. A decision has still to be taken on the need for at least some of the fleet to retain the STOVL characteristics of the Harrier. However, if two new aircraft types are procured, fewer CTOL aircraft will be required, with a consequent effect on their unit production cost. If an Advanced STOVL (ASTOVL) aircraft is required, it would have to be common with the Royal Navy's Sea Harrier replacement, as procurement of two different types would not be affordable.

The RAF still want a twin engined aircraft for FOA, as it is better in terms of intake and weapons bay location. The aircraft must be able to return to base on one engine. The possibility of a contingency rating is being looked at, because of the fuel consumption penalty of engines which are larger than necessary.

The RAF's second requirement will be for upgrades of EF2000 some time in the first 2 decades of the next century. Those technologies which contribute most to its attributes as a fighter, including agility, will be required.

The procurement strategy for these new aircraft is discussed in more detail in Section 3.

2.2 Engine Technology Requirements

The engine technology needed for these future projects may be considered under several general headings, namely performance, environmental issues, reliability and maintainability (R&M), features specific to STOVL, and manufacturing and support technology.

2.2.1 Performance

The main aspects of aircraft performance on which the engine has a significant influence are thrust/weight ratio, agility and fuel consumption. Aircraft thrust/weight is of critical importance, because of the benefits it provides in both combat and take-off performance. The engine thrust/weight ratio contributes directly because of the benefit of a lighter engine, and indirectly because it allows a lighter and smaller airframe to fulfil the same mission. Thrust/weight ratio can be increased through improved cycle and component efficiencies, and higher aerodynamic loadings leading to fewer turbomachinery stages, but as these requirements are to some extent conflicting, the right compromise has to be found. However, there is a limit of about 13:1 using conventional materials. In order to achieve the higher targets described later, significant weight reduction through the use of advanced materials will be needed.

To meet future requirements for agility a high thrust/weight ratio is needed. For some applications the value of thrust vectoring also needs to be further explored. Agility would be less important for an attack aircraft such as FOA than for a future air superiority aircraft. Nevertheless thrust vectoring is of interest in order to reduce trim drag, which would improve range, to improve field performance, and to reduce the size of control surfaces, which improves stealthiness. The Royal Navy likewise are not yet convinced that super-maneuvrability of the aircraft is essential; what matters is weapons system performance, i.e. aircraft plus missile, not aircraft performance alone. A less agile aircraft with a very agile missile at close quarters might defeat a more agile aircraft with a less capable missile.

Thrust vectoring for greater agility would be highly desirable when EF2000 is upgraded. However, studies have shown that the aircraft design must be optimised to take account of thrust vectoring if the potential advantages are to be realised. Significant changes to the current aircraft might therefore be required.

To meet the range requirement both for the Future Offensive Aircraft and Sea Harrier Replacement, improved fuel consumption is important. Better component and cycle efficiencies are obviously desirable, but the need for more radical changes, such as the use of variable cycle engines, must also be considered. Such technology could allow good SFC to be obtained at both low and medium level. However, the extra complexity also raises concerns about cost, weight and reliability. These risks therefore need to be reduced through technology demonstration before such concepts can be adopted, particularly on single engined aircraft, as SHAR(R) is likely to be.

Variable cycle engines would require innovative concepts of engine control, such as multivariable control, to make full use of their potential. Such control concepts likewise must be demonstrated so that their reliability is beyond doubt, and they can be given airworthiness clearance.

Also of importance in improving fuel consumption is a better understanding of engine/airframe interactions. There is little point in spending a large sum of money in extracting the last percentage point of fuel consumption from the basic engine if it is wasted by a poor installation design. Installation design is also important in achieving the best compromise between performance and low observability.

Engine response times are generally adequate, but carefree handling is an essential requirement. Improved control systems should enable engines to operate closer to the surge line, permitting better pressure ratios and efficiencies, without risking handling quality.

2.2.2 Environmental Factors

For military aircraft "good neighbour" considerations are less important than for civil aircraft, but cannot be ignored. Visible emissions such as smoke and oxides of nitrogen are of concern, not just for environmental reasons, but because they contribute to the visible signature of the aircraft. Reducing these emissions, whilst seeking higher turbine temperatures to achieve good fuel consumption and high power/weight ratio, will require advanced combustor designs and design methods. These may include staged combustion, possibly using double annular combustors. Reducing environmental noise will prove difficult. Present practice in the UK is to conduct low flying training where possible in areas where it does not cause annoyance, sometimes overseas. The use of variable cycle engines could help to reduce noise around airfields.

Compared to current engines, the next generation will require the same level of resistance to birds, hailstones, and corrosion, and better resistance to foreign object damage (FOD), sand erosion and battle damage will be required. To improve resistance to FOD, the design of the airframe, the engine and the intake must be considered as a whole. In particular, the position of the intake relative to the ground and the aircraft's wheels is important. The design should be such as to prevent objects entering the intake in the first place and, if they do, to prevent them from entering the engine core. Battle damage resistance is of particular concern, where small arms fire in "over the beach" missions can put the aircraft at risk. The engine must also be capable of continuing to run after sustaining a moderate amount of damage. The Pegasus engine in the Royal Navy's Sea Harrier is able to cope with such "off-design" running, and this quality will be sought in its replacement.

Another major environmental requirement is stealth. Considerations include infra-red (IR), radar, acoustic and visible signatures. Detailed requirements cannot be given in an unclassified paper. For FOA engine requirements will flow from the aircraft concept chosen. For SHAR(R) low IR is important. The trade-off between stealth and other requirements is not yet decided. Clearly engine frontal area, intake and exhaust nozzle design will be major considerations, and the compromise between low IR, low radar cross-section and nozzle vectoring is a question for future decision. It will be necessary to pursue these technologies to determine what is feasible, and thus inform the trade-off process described in paragraph 2.2.6.

2.2.3 Reliability, Maintainability, Durability, Availability

The first three of these "abilities" all contribute to the fourth, availability, which is what the Service user wants. It is a major determinant of operational effectiveness, cost of ownership, and manpower requirements, which in turn are major factors in deciding the fleet size which

can be afforded with diminishing defence budgets.

For the RAF a reliable affordable engine is the predominant requirement. Whilst a high thrust/weight ratio is desirable, a robust engine with lower thrust/weight ratio would be preferable to a delicate unreliable one with a higher ratio. If a variable cycle engine is adopted, reliability issues might lead to a strong preference for a twin engined aircraft. The Royal Navy takes a similar view on reliability. They require longer engine lives and a reduced need for part life overhaul.

To achieve these higher standards, attention needs to be paid to the life of the hot section of the engine, to the robustness of the engine to environmental hazards, as already described, and to the control system and other equipments mounted on it. It is unfortunate that in UK terminology engine equipments are often referred to as "accessories", implying that they are somehow less important than the turbomachinery. This is not so, as our experience shows that, taken together, they are the largest single source of unreliability.

To achieve better hot end life it is important that improvements in combustor and turbine technology are used to improve life as well as performance; there has been a tendency in previous engine developments to go all out for performance and allow the life to be improved at a later stage. This results in an unreliable and short life engine at entry into service, and poor availability later as engines are removed to have modifications embodied. This is a state of affairs which the military operator is no longer willing to accept.

To improve the life of control systems new concepts must be adopted to improve reliability. Less will be done with hydromechanics, and more with electronics. Improved electronic architectures, techniques such as analytical redundancy, distributed processing and improved diagnostics will allow "graceful degradation" rather than sudden failure of the system, greatly reducing the probability of not completing a mission.

Maintainability can be improved by the use of simpler engine concepts, with fewer turbomachinery stages and fewer parts. The advantages of a variable cycle engine for a particular application would also need to offset the likely adverse effect on maintainability arising from its additional complexity. The advanced design techniques and materials required to achieve higher thrust/weight ratios should therefore also improve maintainability. It will, however, be necessary to ensure that components made using such materials can be repaired, unless better reliability can be achieved by long life components with the features needed to achieve repairability, such as joints and fasteners, eliminated, this in itself improving reliability.

It would be worth re-examining the benefits of modular engines. It has been the conventional wisdom for the last twenty years or so that modular engines offer improved maintainability and lower costs. This is because it is possible to exchange modules "on the wing" and get engines back in service quickly. In practice this rarely happens. The Services prefer to change the engine in order to return the aircraft to service, and then return the engine to the depot for repair. It may be the case that the weight of the casings and flanges required for a highly modular engine is a price not worth paying if the maintenance policy adopted does not require such modularity in the first place.

The Royal Navy are seeking 1½ hour engine change times, together with engine installations allowing better removal paths. They also require less routine servicing as they have fewer people available to do it.

Health and Usage monitoring is seen as an important means of improving aircraft availability and reducing costs, as well as increasing safety. Health and Usage Monitoring Systems (HUMS) have been applied in the past in what now seems, with the benefit of hindsight, a somewhat piecemeal manner. Studies recently undertaken, based on the systems already in service, have shown that the greatest benefits can be obtained from HUMS systems fitted to all aircraft in a fleet at entry into service, with a well defined and common interface with the user Service's logistic support system. Attention needs to be concentrated on integrated systems covering the airframe, engine, and possibly weapon and avionics systems.

2.2.4 Features specific to STOVL

The technology requirements for an STOVL engine may be considered in terms of those for the turbomachinery and those for the ASTOVL features. The core engine requirement would be similar to that for a CTOL engine as already described. Those for the STOVL features would depend on the concept which is chosen. At the time of writing, the selection process is getting under way, and the way ahead is not yet clear. The technologies which might be required include lift fans, and their driving mechanisms, lift engines, blocker doors, diverters, variable nozzles, together with their actuation control and sensor systems. Any one of these features in isolation could be achieved at moderate risk, but the combination required for any of the major ASTOVL concepts presents formidable challenges in control and system reliability. If adequate reliability of the system is to be achieved a step change in reliability of individual components will be required, as well as control concepts which will be both technically advanced and amenable to formal validation.

2.2.5 Design, validation, manufacturing and support technology

In seeking to reduce life-cycle costs the UK Services

expect that advanced technology will be used in the design, validation, and support of the engine, as well as being embodied in its hardware. Such technology can provide designs which are right first time, based on hardware which has already been demonstrated, leading to reduced development and validation timescales, and reduced costs. The use of electronic product definition will provide a lower cost linkage with the user's logistic support system through concepts such as CALS. Users are also requiring a closer connection between the manufacturer's design and costing systems, so that more rapid and more accurate estimates can be produced of the costs of new engines, derivatives of existing ones, or modifications.

2.2.6 Trade-offs

In seeking the optimum combination of requirements for a particular aircraft, many trade-offs will have to be made. The UK Services are adamant that they must not all be made in favour of performance, and that reduced life-cycle costs must be an equally important objective. Amongst those that need to be considered are:

engine life cycle cost vs thrust/weight ratio; better turbine technology is required to improve both engine life and thrust to weight ratio, but one of these will be at the expense of the other; moreover, to achieve a very high thrust/weight ratio, advanced and expensive materials are required. The most cost-effective compromise will need to be sought, taking into account performance, the production cost of the engine, and the cost and usage rates of spares.

engine life vs sfc; sfc requires better cycle and component efficiencies, which again match better with higher turbine temperatures,

thrust/weight ratio vs specific fuel consumption; to achieve high thrust weight ratios, turbomachinery with few highly loaded stages is desirable; this also benefits life-cycle cost and durability. But for good efficiency and fuel consumption, more stages and lower stage loading are needed. Maintainability also enters into this trade-off.

These trade-offs will affect engine sizing for the aircraft. The optimum compromise between these conflicting requirements will be determined by analysis of the proposed missions and any need perceived by a Service for performance features such as supercruise. Mission analysis will also be necessary to determine other factors such as bypass ratio, and the trade-off between stealth features and performance. There is also a relationship between stealth and maintainability. Clearly to achieve low observability the engine installation and airframe design must be closely integrated. This must be done in such a way as to retain good access to the engine and

enable it to be removed quickly from the aircraft.

2.2.7 The Key Technologies

It is still too early in the development of our future requirements to be able to generate an engine specification based on a thorough and realistic mission analysis. But we have identified a number of key technologies which need to be demonstrated in order to keep our options open, and to enable us to develop an engine that meets any future specification at low risk. Some of the relationships between these technologies are shown in Figure 1. Progress in acquiring the technology is outlined in Section 4, which describes the UK aero-engine technology demonstration programme.

3. PROCUREMENT STRATEGY

3.1 General Strategy

The job of MOD(PE) is to translate the military requirements into hardware for use by the armed services. The general procurement policy within the UK is to seek best value for money. It is expected that this will usually be best achieved through competition, and the selection of a single Prime Contractor, who will be contractually responsible for ensuring that the needs of the military customer are met. Where competition is not practicable an alternative is collaborative international development. National development by the UK alone will not normally be viable given the likely development cost and production requirements for a major new aircraft system.

3.2 Competitive Procurement

In the UK there is only one indigenous supplier each for combat aircraft and engines. Competition therefore means seeking prime-contractor bids internationally for equipment available off-the-shelf, rather than competition for a development programme. In assessing the bids account would be taken of life-cycle costs rather than just acquisition cost, since cost of ownership is now an important consideration.

However, off-the-shelf systems often require further development to meet the UK specific operational requirements and projects may therefore have an element of collaboration associated with them.

3.3 Collaborative Procurement

Some operational requirements may not easily be met through competition, and new systems will need to be developed. It is unlikely that the UK will develop combat aircraft and their engines in the future on a wholly national basis; they are more likely to be pursued through collaboration. Successful, balanced collaboration requires equitable contributions from the partner nations, but the workshare arrangements should not be allowed to over-ride the achievement of good value for

money. Nevertheless, it is important for the UK to maintain an ability to take on a quality work share.

3.4 Strategy for Sea Harrier Replacement and Future Offensive Aircraft

For SHAR(R) the most likely way ahead is through the American Joint Advanced Strike Technology (JAST) programme. The United Kingdom is negotiating to take part in the ASTOVL element of this programme. This is because no other European nations currently have a requirement for a supersonic ASTOVL aircraft. As a fallback a further development of Sea Harrier would provide a subsonic and therefore less desirable option. If the Royal Navy should decide to return to conventional carriers, possibly in collaboration with other nations, CTOL shipborne aircraft might then be a possibility, but the advantages of ASTOVL would then be lost. The timescale would require a considerable service life extension to the current fleet of both aircraft and ships.

For FOA the way ahead is still being studied. The UK has a good record of collaboration on aircraft such as Tornado and EF2000. Clearly such a collaboration would be a possible route to acquiring FOA. It would, however, be subject to the emergence of a common requirement, and this could take some time. Alternatively, another aircraft arising from the JAST programme might be a possible solution.

4. TECHNOLOGY ACQUISITION

4.1 Strategy

Despite the increasing reliance on the industry to meet our requirements, MOD(PE) retains an interest in ensuring that technology is developed that will meet our future needs. In order to procure competitively, and bearing in mind the risks surrounding new aircraft projects, we do not wish to be dependent on a single supplier, whether based in the United Kingdom or elsewhere. For competitive procurement to be effective we wish to ensure that technology that enables our requirements to be met is available on two shelves, and not just one. We also need to be an 'intelligent customer' and be in a position to assess realistically the opportunities and risks inherent in the technology and equipment we are offered. When collaborative procurement is to be adopted we need to retain in the UK a sound technological base in order to participate effectively.

The lead times for the successful introduction of new engine technology into service are historically long, as shown in Figure 2. Whilst we are looking to industry to employ advanced design techniques which will reduce the time to introduce a new engine, programmes will continue to be high risk, unless the technology they embody has been adequately demonstrated. In order

that any engine development programme might proceed at quantifiable, reduced risk, it is essential that the technology is available when firm operational requirements emerge. Indeed the state of technological development and the risks associated with it are likely to play a significant role in defining the requirements in the first place.

It is these arguments that have sustained the aero-engine technology demonstrator programme within the UK. Funded jointly by the MOD and industry, these programmes aim to acquire the necessary technology to support the needs of future UK aircraft projects, whichever procurement route is finally taken. The funding proportions depend on the extent to which the technology may be applied also to civil or commercial military engines.

It is vital that these programmes should be supported by a comprehensive programme of basic and applied research. The UK MOD uses the Defence Research Agency (DRA) as the principal source of this research. The DRA embraces all the formerly separate UK defence research establishments. It now forms part of the wider Defence Evaluation and Research Agency (DERA), which includes also the UK's Defence Test and Evaluation Organisation. The DRA's research programme is conducted partly in house and partly through extra-mural contracts placed on industry and universities.

The United Kingdom aero-engine technology demonstration programme is entitled 'Rapide' - Reliability and Performance in Demonstrated Durable Engines (Figure 3). Programmes typically consist of four stages:

- component demonstration
- spool demonstration
- whole engine demonstration
- durability demonstration

More than one stage might sometimes be accomplished in a single programme. Earlier papers have described the successful XG40 series of programmes, which supported the technology for the EJ200 engine for Eurofighter 2000. The UK has now embarked on a further series of component demonstrators which will provide the technology for engines for the Future Offensive Aircraft and Sea Harrier Replacement. These programmes were originally aimed at a concept known as Advanced Core Military Engine II (ACME II), which is now being merged into the AMET collaboration with France, described in Section 5 below.

The relationship between the technology demonstration programme and possible future aircraft programmes is shown in Figure 4, and the targets for the various phases of the Rapide strategy are shown in Figure 5. Figure 6

shows how the technology gained from the individual programmes in the 'Rapide' strategy fit together to reduce the risk on FOA. A similar network, using some of the same elements underpins the technology for SHAR(R).

4.2 High Pressure Systems

A new phase of the United Kingdom's long-running High Temperature Demonstrator Unit programme was launched in 1993. This programme, HTDU Phase 5 is contracted with Rolls-Royce, and is aimed principally at improved combustor and HP turbine technology. Amongst the technologies being demonstrated are staged combustion using a double dome combustor, advanced turbine blade cooling concepts, and improved materials. The objective is to achieve turbine entry temperatures in excess of 2100K. These advanced components will be demonstrated in an HP spool based on the EJ200. The programme will also demonstrate 4th and 5th stage compressor bladed disks (blisks) running at the advanced HTDU5 conditions.

4.3 Low Pressure Systems

This technology is being pursued in two stages, a Near Term ACME Technology programme (NTAT) and a Longer term ACME LP systems programme, to be called ACME II(L). NTAT is a component demonstration, also contracted with Rolls-Royce. It is aimed at improved military fans of higher pressure ratio and lower weight, improved LP turbines, a ceramic matrix composite exhaust diffuser, and improvements to the nozzle and reheat systems. This programme will also demonstrate an advanced variable cycle HP compressor.

The objectives for the fan are to achieve as an interim measure a pressure ratio of 5:1 in 3 stages, with more aggressive targets being set for later programmes. Metal matrix composite bladed ring (bling) technology will also feature in this programme. The HP compressor, to be run separately, will be a 6 stage machine of 11.4:1 pressure ratio, including a 1st stage of hybrid design allowing some of the flow to be diverted into the bypass duct. The design style of the LP turbine will be decided following a study of the options which is now being pursued. The number of stages and pressure ratio of the fan and HP compressor which would be used in a future spool or whole engine demonstrator will be decided by means of the study described in Section 5.

Work has been carried out in earlier programmes on ceramic matrix composite components suitable for an exhaust diffuser. NTAT aims to take the work forward by manufacturing and testing a complete unit consisting of a ring of vanes and exhaust cone.

The reheat and jet pipe work will pursue multi-stage fuelling, aimed at improved efficiency and reduced oxides of nitrogen, and advanced composite compo-

nents. Swirl reheat and lightweight reheat liner concepts with low cooling requirements will also be examined.

The later ACME II(L) programme will bring together the component work into an LP system demonstration engine. This will be essentially of EJ200 configuration, and may therefore provide an opportunity to demonstrate advanced components developed by the other EJ200 partner companies.

4.4 Engine Controls

In order to achieve the high level of reliability and integrity, and reduced life-cycle cost sought in future engines advanced control concepts and technology will have to be adopted. Approval has recently been gained for a component demonstrator programme called High Performance Engine Control System (HIPECS). This will be contracted with Rolls-Royce, Lucas Aerospace and Smiths Industries.

The programme will commence with engine system studies, carried out jointly as far as possible, by all 3 contractors. This will be followed by a component demonstration, in which both systems companies will demonstrate an integrated system on a rig. The supplier companies will then compete for a second phase of engine testing. The aims of the programme are firstly to achieve a major improvement in reliability through a system architecture which does more electronically and less with the hydromechanical system. To achieve this aim technologies such as advanced electronic architectures, analytical redundancy, distributed processing and high temperature electronics will be pursued. Secondly, the programme will demonstrate the ability to control advanced engines which include features such as variable thermodynamic cycles and ASTOVL capability. Advanced control techniques such as multi-variable control and actuation technology will be pursued. Preliminary studies on multivariable control have already been carried out successfully.

To achieve high level of reliability, the integrity of the control system software must not be in doubt. In the High Order Language Demonstrator Phase I, contracted with Lucas, the ability to programme the RB199 Digital Electronic Control Unit (DECU) in Ada was demonstrated, and the advantages and disadvantages were compared with the original LUCOLTM assembler language (Ref 1). This work is now being taken forward as part of a wider MOD(PE) initiative on safety-critical software, to find a practical means of adopting formal methods which can be used by the average control engineer.

4.5 Environmental Aspects

There are also programmes to demonstrate improved techniques to enable engines to cope with their operating environments. An example is the Engine Environ-

mental Programme, designed to find ways of designing engines to resist effects such as sand ingestion. A study phase for which contracts were let to Rolls-Royce and AEA Technology Ltd has recently been completed, and a competition is now being held for the demonstration phase.

4.6 Technology Specific to STOVL

The future work on STOVL technology is obviously dependent on the exact nature of the UK's participation in the JAST programme, and it is premature to go into detail of what might be done. Nevertheless, it is important that enabling technology is acquired, and therefore a programme known as STOVL Technology Phase I has been launched. This programme includes work on variable work low pressure turbines, two-dimensional and axi-symmetric vectoring nozzles and STOVL engine control laws, systems and actuation.

4.7 Materials

Achievement of the performance and life-cycle cost objectives for future engines will depend on the successful adoption of advanced materials. Materials development is an integral part of many of the programmes described above, but in addition a number of programmes are going ahead in the UK specifically aimed at advanced materials. Some of these are conducted through research at the Structural Materials Centre of the DRA, and others as part of the 'Rapide' aero-engine technology demonstration programme. Amongst the materials currently being investigated are polymer, ceramic and metal matrix composites, intermetallics, advanced turbine blade and disc alloys, and thermal barrier coatings. In order to introduce these materials into production engines it is not sufficient to show that they can give improvements either in terms of performance or life-cycle costs. Such materials must be thoroughly understood, and their fatigue and lifing characteristics determined, if they are to be used in a manner which is both cost effective and acceptable to military airworthiness authorities.

4.8 Spool Programmes

Many of the component programmes described above will demonstrate technology by running components in engine spools of various kinds. However, in order to integrate the technology the components need to be run together in a single spool. Although the UK had planned to run a high pressure spool in the ACMEII programme, we are now aiming to make this a collaborative programme with France, described in the next section.

5. COLLABORATION WITH FRANCE - THE 'AMET' PROGRAMME

Advanced Military Engine Technology (AMET) is the name given to a collaborative enterprise set up by Rolls-Royce in the UK and SNECMA in France and support-

ted by the UK and French governments. A Memorandum of Understanding on aero-engine technology demonstration was signed by the UK and France in November 1994. The objective of the programme is to run a high pressure core demonstrator at successively higher levels of technology starting in 1997. The component technology will come from UK and French component programmes, the UK ones being described above. A study is now under way to define the demonstrator vehicle and test programme. This is a fully collaborative venture with a joint management committee set up by the two companies, and a joint Steering Committee and project review committee set up by the two governments. The programme is described in more detail in the paper by M Dufau of SNECMA to be given later in the conference.

The UK strategy envisages that a representative engine demonstrator will follow the HP core demonstrator. Although this is currently planned as a UK programme, we would obviously wish to build on the experience gained during the AMET programme, and to undertake the programme as a collaborative venture if this appears to be the best way forward at the time. The possibility of other partners joining the programme would then need to be considered.

6. CONCLUSIONS

In this paper I have tried to show that the UK recognises that further significant advances in aero-engine technology are required if the requirements of future combat aircraft are to be met. In seeking greater operational effectiveness the Services consider all the factors leading to reduced cost of ownership to be as important as performance. These factors will make just as heavy demands on our technical ability as improved performance. Better materials, better design methods and better business methods are all necessary to bring about the improvements we seek.

On earlier engine programmes, development times and costs have exceeded estimates because programmes were started at too high a level of risk. In order to control costs and timescales, it is vital that technology is adequately demonstrated before projects are committed. The UK's 'Rapide' technology demonstration programme is designed to ensure this.

The length of time between major aircraft projects is increasing, but technical development goes on apace. The technical advance between successive generations of aircraft is therefore increasing. The process of technology demonstration needs to be continuous in order to take these advances into future projects at a controlled level of risk and to apply them in updates of current engines. Nevertheless, any future combat aircraft project will be an enormous undertaking, and countries of the size of the UK will continue to find that the option of

developing them in collaboration with other nations is attractive. It therefore makes sense to undertake the technology demonstration collaboratively also, in order to ensure that the best technology which the partner countries can produce can be made available for future projects.

REFERENCES

1. Dolman W C, Ashdown A M and McCallion K J: The Application of Ada and Formal Methods to a Safety-Critical Engine Control System. AGARD Conference Proceedings No 556, Dual Usage in Military and Commercial Technology in Guidance and Control. March 1995.

ACKNOWLEDGEMENTS

The author would like to acknowledge the assistance of many colleagues in the Ministry of Defence, both military and civilian, in the preparation of this paper, and to thank contacts in industry and in the French MOD for their comments.

The views expressed are those of the author, and do not necessarily represent the policy of the Ministry of Defence or Her Majesty's Government.



British Crown Copyright 1995/MOD
Published with the permission of the
Controller of Her Britannic Majesty's
Stationery Office

Paper 2: Discussion

Question from Prof W O'Brien, Virginia Polytechnic Institute, USA

Many (or perhaps most) of the propulsion improvements, which you seek in the UK program are improved system performance, handling, availability and maintenance, for example. What methods are you developing for the assessment of improved component design and technology on the propulsion system performance?

Author's reply

System studies and simulation are undertaken by industry and by the Defence Research Agency. Some of this is done as part of the MOD's applied research programme, which is distinct from the technology demonstration programme I have described. Work is also done by industry using private venture funds. The results of some of this work are described in Papers 5, 28 and 39.

Question from Prof Dr-Ing Kl Broichhausen, MTU, Germany

On one of your vugraphs you showed a close connection between the RAPIDE programme and EJ200/RTM322 demonstrators. Could you explain this strategy more closely?

Author's reply

The targets for propulsion system improvement in the RAPIDE programme take the performances of the EJ200 and RTM322 as the baseline. The principal objectives of RAPIDE are to support future engines. The programme uses spools from current engines, including EJ200 and RTM322, to demonstrate component technologies. These will then be integrated in all-new spools and engines to support future project requirements. The technologies will also be available to up-grade existing engines. The RTM322 and EJ200 were supported by an earlier generation of technology demonstrators in the same way. This experience showed the value of carrying out such programmes.

Acquisition et démonstration des technologies pour futurs moteurs militaires:

Le programme AMET.

Jacques DUFAU

Responsable de Marque Technologies Futures pour Moteurs Militaires
Direction Technique Snecma
Centre de Villaroche
77550 MOISSY CRAMAYEL FRANCE

Introduction

Les nécessités d'un système d'armes performant, au-delà des programmes aéronautiques déjà en cours, parmi lesquels on peut citer l'EUROFIGHTER 2000, le RAFALE, le F22, conduisent à la recherche permanente d'améliorations de chacune des composantes qui font la qualité d'un aéronef :

- la cellule
- les systèmes d'armes
- la motorisation
- l'intégration

Au-delà du simple aspect des performances brutes il convient également de maîtriser le coût de possession (LCC) de ces nouveaux systèmes.

Les progrès que réalisent les motoristes sont habituellement mesurés globalement au travers :

- du rapport Poussée sur Masse du système propulsif
- de la consommation spécifique (au plein gaz et à régimes partiels en croisières supersonique ou subsonique) du turboréacteur
- de discrétion (Signature Electromagnétique Radar et Emissions rayonnant dans le domaine Infra Rouge)
- du coût d'acquisition et d'usage du matériel

Un programme d'amélioration des caractéristiques énoncées ci-dessus a été engagé.

Ce programme est dénommé AMET pour Advanced Military Engine Technology.

Objectifs généraux du programme

Ce programme a pour objet :

- d'identifier les technologies génériques du futur moteur
- d'acquérir ces technologies
- de démontrer ces technologies sur les véhicules d'essais adéquats.

Ces technologies devront pouvoir s'intégrer sur le successeur des moteurs existants. Des objectifs ambitieux ont été assignés à ce programme :

- Augmentation du rapport Poussée sur Masse :
Typiquement les moteurs européens de technologie avancée offrent aujourd'hui un rapport poussée sur masse voisin de 10 daN/kg. Il s'agira au travers du programme AMET de se doter des technologies permettant d'amener le rapport Poussée/Masse du moteur complet, y compris tuyère de propulsion et système de régulation, à des valeurs comprises de l'ordre de 17 à 18.
- Diminution de la consommation des moteurs de 20% sur un ensemble de missions caractéristiques
- Diminution du coût de possession de 30% par augmentation des durées de vie, maintenabilité accrue.

La sélection du meilleur compromis entre les différentes technologies éligibles a été réalisée au travers d'études d'influence des missions potentielles du futur avion de combat sur la configuration moteur requise. Un grand nombre de missions a été considéré, toutes présentant des caractéristiques améliorées par rapport aux missions actuelles (domaine de vol, rayons d'actions, facteurs de charge, capacités d'emports).

Les niveaux de températures et pression moteur ainsi déterminés et les axes de progrès retenus permettent d'envisager des avions de taille raisonnable pour remplir cet éventail de missions. Les technologies et objectifs ont été assignés, pour chaque mission, afin de conduire à l'avion le plus petit accomplissant les conditions fixées.

La figure ci après rappelle l'influence prépondérante du rapport Poussée / Masse et de la consommation spécifique sur la taille d'un avion et par conséquent, en première approximation sur le coût de réalisation d'une mission donnée. L'influence sur la masse est donné ici en considérant que la mission de l'avion reste inchangée, ainsi que ces performances ponctuelles (Longueur de décollage, facteurs de charge dans le domaine de vol et vitesse ascensionnelle max.). La formule aérodynamique de l'avion n'a pas été modifiée. Les courbes présentent les avions de masse minimale permettant de réaliser l'ensemble des contraintes.

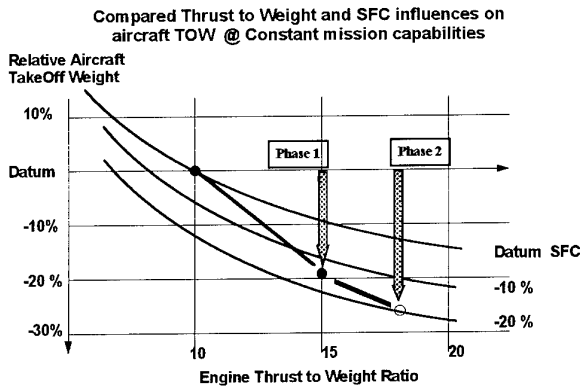


Figure 1: évolution de la masse avion

Trois axes de progrès identifiés permettent d'atteindre les objectifs fixés:

1. Les matériaux métalliques développés présenteront des caractéristiques mécaniques supérieures à celles des alliages existants et offriront une plage de fonctionnement élargie en température. L'utilisation de matériaux composites - à matrice métallique ou intermétallique - réduira la masse des composants.
2. Des technologies novatrices apporteront gains de masse - Anneaux Aubagés Monoblocs (BLING) et Disques Aubagés Monoblocs (Blisks) et amélioration des durées de vie
3. L'augmentation de la charge aérodynamique par étage des composants conduira à la réduction du nombre de parties tournantes .

Les travaux engagés à ce jour, dans le cadre du programme AMET concernent les technologies du corps du corps haute pression. Le programme a été scindé en deux phases :

- AMET Phase 1 : Acquisition et démonstration des technologies permettant de réaliser le corps haute pression d'un moteur dont le rapport Poussée sur Masse serait égal à 15.
- AMET Phase 2 : Acquisition et démonstration des technologies permettant de réaliser un moteur dont le rapport Poussée sur Masse serait égal à 18 .

Evolution du rapport Poussée/Masse moteur complet en fonction des domaines d'acquisition de technologie

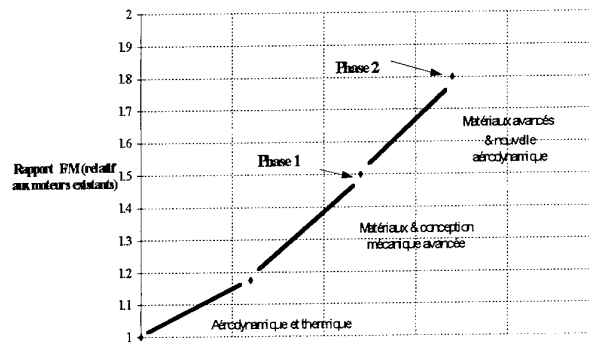


Figure 2 - Technologies et gains apportés

Les travaux dont il sera fait mention dans cet exposé se rapportent à la phase 1 du programme AMET .

La figure ci-après résume les dates clés du programme AMET :

- 1991 : Début du programme
- 1993 : Début de la phase d'acquisition de technologies
- 1995 : Début des travaux préparatoires à la démonstration
- 1997 - 2005 : Démonstration phase 1
- 1998 - 2005 : Acquisition des technologies Phase 2
- 2001 - 2008 : Démonstration des technologies Phase 2

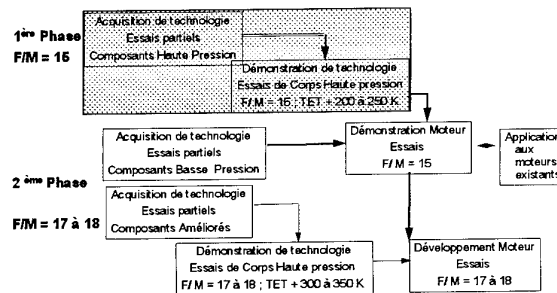


figure 3 - Enchaînement des travaux

Le programme de la phase 1 s'articule autour de 5 étapes principales :

- Etape 1 : Elle consiste en l'évaluation des niveaux technologiques souhaitables et réalisables à l'horizon de la démonstration. Elle est fondée sur l'expérience acquise et les programmes de recherche en cours dans chaque discipline

- Etape 2 : Elle consiste en la sélection d'un ensemble cohérent de technologies et niveaux associés . Ces technologies seront par la suite dénommées génériques.
- Etape 3 : Elle est l'étape d'acquisition des technologies. Elle donne les bases nécessaires à la phase de démonstration.
- Etape 4 : Le corps haute pression servant de véhicule d'intégration et de démonstration des technologies y est défini.
- Etape 5 : Etude, fabrication et essais du corps haute pression défini à l'étape précédente .

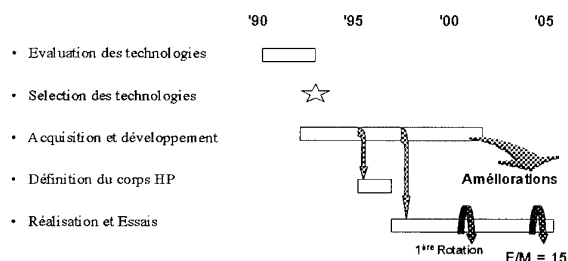


Figure 4 : Planning des étapes de la phase 1

Objectifs techniques du Programme

Démarche

L'architecture et le cycle des moteurs d'avions de combat découlent principalement du type de missions choisies. Ainsi cherchera-t-on de faibles consommations spécifiques pour des avions de pénétration lointaine au travers de forts taux de dilution et de taux de compression élevés. On adaptera le cycle thermodynamique du moteur en vue de réaliser de fortes poussées spécifiques pour des intercepteurs , au moyen de fortes températures de sortie de la chambre de combustion et de faibles taux de dilution.

La cohérence des objectifs techniques AMET a été établie pour couvrir un large éventail de technologies qui soient applicables et validées quel que soit le type d'applications futures auxquelles elles sont destinées.

Ainsi qu'il a été indiqué, des études d'avant-projets ont permis de définir, suivant le type de mission envisageable, les gains potentiels offerts en termes de rapport Poussée sur Masse , Consommation , coût de possession, dans les domaines suivants :

- Aérodynamique des compresseurs
- Aérothermique des turbines
- Combustion et émissions
- Matériaux métalliques et intermétalliques
- Matériaux composites

- Régulation et équipements
- Technologie et architecture générale du moteur

L'accroissement du rapport Poussée / Masse s'obtient par des efforts conjugués d'augmentation de la poussée spécifique, dépendant du choix effectué pour le cycle thermodynamique du moteur et de diminution de la masse spécifique - Masse par unité de débit traversant le moteur - , dépendant principalement du nombre d'étages total de la machine et de la résistance spécifique (σ/ρ) des matériaux utilisés.

L'augmentation de la poussée spécifique est obtenue par élévation de la température et de la pression à l'éjection du moteur . La figure 5 donne un aperçu des gains apportés par un accroissement de la température d'entrée turbine lors d'un fonctionnement au plein gaz sans post-combustion. Elle met en évidence la nécessité d'augmentation de pression dans le canal d'éjection car les niveaux de températures des moteurs se rapprochent du maximum réalisable en utilisant le kérosène comme carburant.

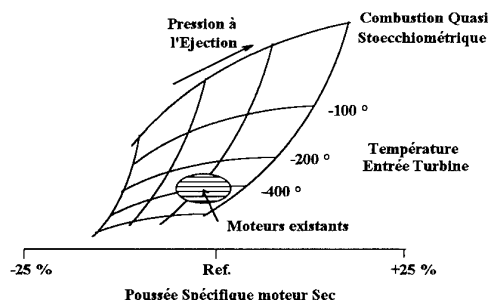


Figure 5. Evolution de la Poussée Spécifique

D'une manière plus générale la technologie du futur corps Haute Pression sera dominée par l'augmentation des températures de fonctionnement .

Outre la recherche de températures d'entrée de turbine haute pression très élevées (T_{41}) il est nécessaire d'augmenter le taux de compression global du moteur dans le but de ne pas favoriser la poussée spécifique au détriment des consommations spécifiques à régimes partiels. Ainsi , dans un diagramme T_{41} - T_{30} (SOT - T_3) - figure 6 - on peut mesurer l'écart séparant les moteurs les plus avancés actuellement et le niveau visé pour le démonstrateur des technologies du corps haute pression

En termes de températures de matériaux d'aubes mobiles de turbine , cette nouvelle étape vers les très hautes températures motive la recherche d'un matériau plus performant que les monocristaux actuels. L'utilisation barrières thermiques à faible conductivité doit être envisagée sur les aubes mobiles aussi bien que sur le distributeur. L'amélioration des propriétés mécaniques du matériau ne doit pas être obtenue par le biais d'une augmentation de sa

densité afin de limiter les contraintes centrifuges et éviter de reporter sur le matériau pour disque l'ensemble des difficultés liées à la conception de la turbine haute pression.

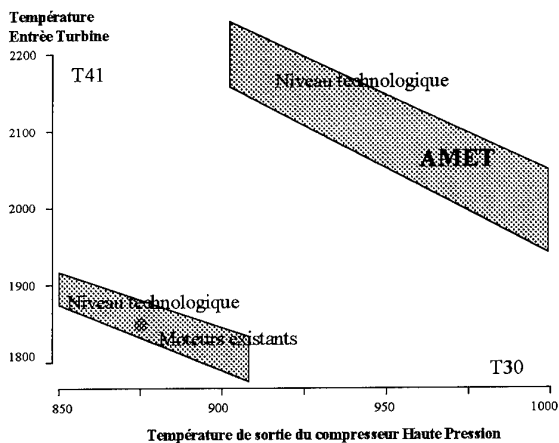


Figure 6 diagramme T41 - T30

La figure 7 donne les gains attendus en température de fonctionnement par rapport à deux matériaux existants. La difficulté réside dans l'augmentation simultanée des caractéristiques sur l'ensemble de la plage de fonctionnement de l'aube.

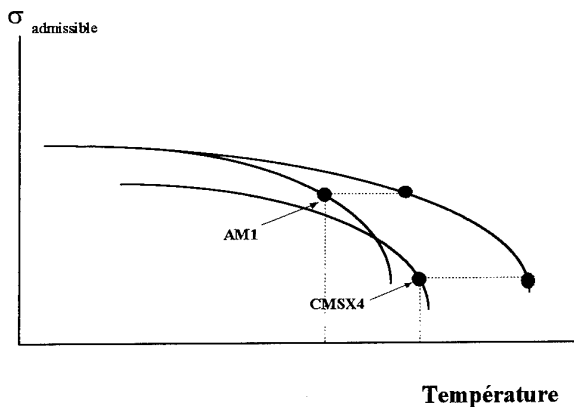


Figure 7 - Extension de la plage de fonctionnement des matériaux monocristallins

Le niveau technologique AMET phase 1 donnera lieu à l'amélioration sensible de l'ensemble des modules du corps haute pression :

- Conception de compresseurs fortement chargés, peu sensibles aux prélèvements et modulations de débit; utilisation sur ceux-ci de matériaux composites avancés.
- Réalisation de fortes températures de combustion au plein gaz et maîtrise des niveaux de signature engendrés
- Acquisition de nouvelles techniques de refroidissement d'aubes de turbine (fixes et

mobile), mise au point de nouveaux matériaux et des moyens de mise en œuvre associés.

Comparés à ceux des moteurs actuels les objectifs de la phase d'acquisition de technologie s'établissent, à l'issue des étapes 1 & 2 aux niveaux ci-après :

Compresseur haute pression

- Augmentation de la charge par étage 30%
- Augmentation de la puissance par étage 40%
- Tolérance à la distorsion et aux modulations de débit

Chambre de combustion

- Augmentation de la richesse Plein gaz 50%
- Réduction des émissions

Turbine haute pression

- Température d'entrée +250 K
- Température métal de l'aubage + 50 K
- Efficacité de refroidissement + 20 %
- Température métal du disque +100 K
- Augmentation de la puissance spécifique +15 %

Le tableau (Figure 8) ci après rassemble les caractéristiques principales communes aux cycles dont sont issus ces objectifs.

$$\begin{aligned} 2000 \text{ Kelvin} &< \text{SOT} < 2200 \text{ Kelvin} \\ 905 \text{ Kelvin} &< T3 < 985 \text{ Kelvin} \\ 0.15 &< \text{BPR} < 1. \end{aligned}$$

Figure 8 : Valeurs caractéristiques de cycle

Les technologies de réalisation associées font largement appel aux nouvelles techniques d'assemblage aubes / disques:

Disques Aubagés monobloc pour les derniers étages compresseur et la turbine haute pression.

Anneaux Aubagés monoblocs en matériaux composites à matrice métallique en ce qui concerne les premiers étages de compresseur haute pression.

Le développement de ces nouvelles technologies sera accompagné d'actions énergiques de maîtrise des coûts, dès la définition et la conception du corps haute pression.

L'organisation du programme

Snecma & Rolls-Royce, soutenus par les Services Officiels Français (STPA/MO) et Britannique (MoD) ont engagé en commun les travaux du programme AMET afin de maîtriser les coûts d'acquisition et de démonstration des technologies.

L'organisation du programme a été conçue de telle sorte que chacune des deux sociétés puisse développer ses compétences technologiques. La collaboration et la mise en commun des résultats permettent d'accélérer l'acquisition des technologies visées. Snecma et Rolls-Royce ont mis en place

une organisation de programme couvrant la phase d'acquisition de technologies et la phase de démonstration. Les principes suivants ont été retenus.

Phase d'acquisition :

Les programmes complémentaires seront mis en place pour couvrir l'ensemble des besoins et des solutions technologiques futures. Les résultats de ces programmes conduisent à la détermination des solutions à démontrer.

Phase de démonstration :

Démonstration conjointe des solutions technologiques retenues.

Objectifs : d'objectifs indépendants à la collaboration

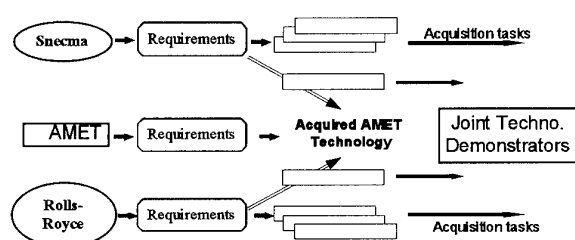


Figure 9 : L'organisation

Les travaux de la phase d'acquisition

Cette partie de l'exposé traitera plus particulièrement des travaux entrepris depuis 1993. Leur contenu est axé sur la réalisation de machines expérimentales dont le niveau technologique permet la réalisation avec un risque acceptable du démonstrateur de technologies. Cette phase, destinée à accroître le savoir faire, couvre les différents aspects techniques de conception, matériaux et procédés. La figure 10 ci après résume dans chaque domaine d'activité les actions engagées et leur date de début. Un certain nombre d'entre elles procèdent néanmoins d'un processus continu et soutenu dans le temps. Cette méthodologie de travail est identique à celle qui a assuré le bon déroulement de la conception à la validation du M88 et actuellement de l'EJ200.

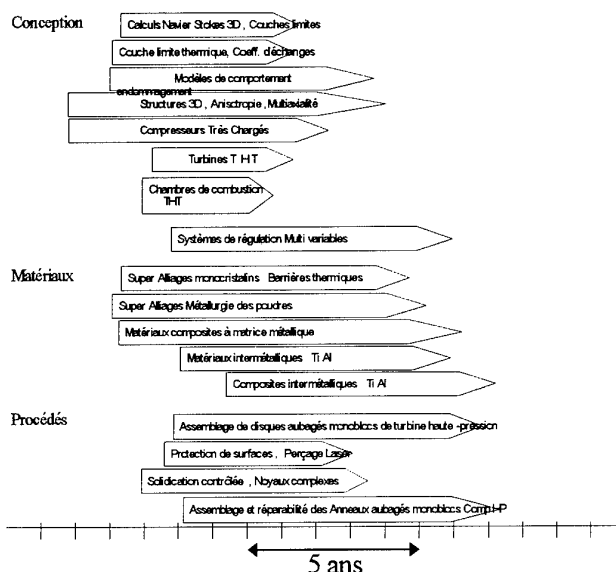


Figure 10 -Synoptique des travaux engagés

La réalisation de chaque module du corps haute pression fait appel à l'intégration des briques élémentaires représentées ci-dessus.

Programme d'acquisition des technologies de compresseur haute pression

Les études de l'Etape 1 ont montré, outre l'intérêt de diminuer le nombre d'étages à taux de compression et vitesse de rotation donnée, l'avantage que pouvait procurer pour un certain éventail de missions, une architecture hybride. Celle-ci caractérise par une double dilution qui s'effectue suivant le type de fonctionnement désiré soit après le compresseur basse pression soit entre deux étages du compresseur haute pression pour augmenter la pression dans le canal secondaire et par voie de conséquence à l'éjection. Une telle architecture permet de décharger la turbine basse pression aux fonctionnements plein gaz en reportant la charge que nécessite l'obtention de fortes pressions d'éjection de la turbine basse pression vers la turbine haute pression. Le fonctionnement avec les deux dilutions ouvertes peut également être envisagé.

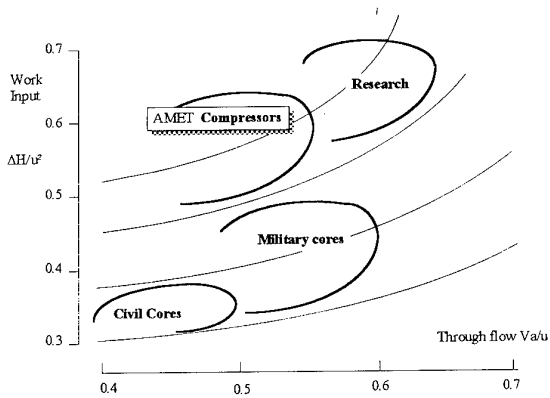


figure 11 - Niveau aérodynamique des compresseurs

Le compresseur haute pression ainsi défini comporte un premier étage relativement comprimé, des étages arrière fortement chargés car opérant à de faibles vitesses d'entraînement. La variation de débit réduit induite par le changement de mode se traduit par la migration importante du point de fonctionnement vers le pompage.

Pour aborder l'ensemble des difficultés générées par des objectifs aussi ambitieux, voir figure 11, deux compresseurs de même taux de compression ont été dessinés. Le premier aura pour objets la démonstration de la faisabilité de charges par étage très élevées sur l'ensemble des étages et l'analyse de l'influence de forts prélèvements inter étages. Le deuxième compresseur, doté des mêmes spécifications de rendement, de marge au pompage et taux de compression est dédié à l'étude de la modulation du débit inter étages. La charge par étage, bien qu'inférieure à celle du premier compresseur, n'en demeure pas moins plus importante que celle des machines actuellement en service.

La conception de ces deux machines au moyen d'outils sophistiqués d'analyse 3D des écoulements a fait appel aux tout derniers progrès réalisés en recherches et en méthodologies de dimensionnement aérodynamique.

De l'analyse réciproque et conjointe de ces deux machines, des résultats d'essais obtenus, Snecma et Rolls-Royce détermineront les spécifications détaillées à appliquer au compresseur du corps haute pression de démonstration.

La réduction du nombre d'étages obtenue grâce aux efforts de conception s'accompagne d'une recherche de réduction de la masse par le choix judicieux de matériaux et des procédés d'élaboration utilisés.

Parmi ceux-ci les matériaux composites à matrice métallique offrent des caractéristiques mécaniques élevées pour une densité plus faible que celle des titanes habituellement utilisés sur premiers étages du compresseur. Le programme de choix du composite entrepris en commun dans le cadre d'un contrat EUCLID sera poursuivi pour aboutir à la démonstration d'un rotor. La réparabilité et la maintenabilité

de l'assemblage d'aubes Titane sur un tambour SiC/Ti fait l'objet d'un programme d'études particulier.

L'élévation de la température de sortie du compresseur haute pression et l'augmentation de la durée de vie recherchée pour diminuer les coûts d'utilisation nécessiteront le développement d'un nouveau matériau pour disques hautes températures. Le choix du matériau sera effectué après démonstration de la faisabilité à un coût raisonnable de blisks (Disques Aubagés Monoblocs) pour les étages de sortie du compresseur HP.

Le gain de masse par rapport aux moteurs existants, à définition aérodynamique identique atteint ainsi 50 % sur le rotor.

Programme d'acquisition des technologies de chambre de combustion

La chambre de combustion de niveau technologique AMET devra pouvoir fonctionner jusqu'à des richesses élevées tout en possédant des caractéristiques de stabilité accrue à bas régimes pour couvrir l'ensemble du domaine de fonctionnement. L'augmentation de la température de sortie de l'ordre de 200 à 300 K par rapport à l'état de l'art actuel, impose d'adapter la technologie de refroidissement aux niveaux de pression, température et richesse des cycles retenus, tout en consacrant une fraction de plus en plus réduite du débit d'air au refroidissement, tendance inévitable si l'on veut atteindre les objectifs fixés.

La maîtrise de la combustion sur une large plage de fonctionnement peut-être atteinte en modulant la richesse en zone primaire. Deux types de technologies sont alors éligibles pour réaliser cet objectif :

- Régulation de la richesse par le débit de carburant injecté. Les chambres obtenues sont du type multi têtes (2 suffisent). Les points d'injection du carburant peuvent être répartis radialement et/ou axialement
- Régulation du débit d'air traversant la zone primaire. Les chambres de combustion obtenues sont alors dites "à géométrie variable".

Les avantages et inconvénients de chaque type, d'ores et déjà connus à des niveaux de températures plus faibles, seront amplifiés dans les conditions thermodynamiques choisies. Ce sont les profils de températures de sortie, l'encombrement et le nombre d'injecteurs pour l'une, la complexité du système de commande et la maîtrise de la vaporisation pour l'autre.

Un programme a été engagé pour comparer les deux concepts aux pressions et températures requis. Il comprend la réalisation d'essais partiels du composant jusqu'au choix de la configuration qui donnera lieu à démonstration. Les travaux ont été répartis entre Snecma et Rolls-Royce.

Ce programme de conception des foyers et des chambres futures s'accompagne d'actions de réduction de masse.

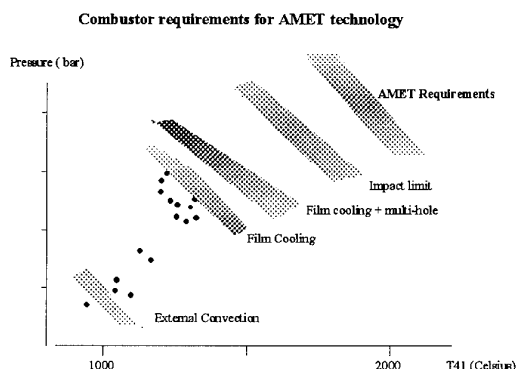


Figure 12 - Objectifs de chambre de combustion

En effet quelle que soit la configuration choisie en final celle-ci nécessitera soit une augmentation du nombre de points d'injection et des circuits d'alimentation correspondants, soit l'ajout d'un système de commande capable de modifier le débit d'air en zone primaire. Les matériaux inter métalliques, de type TiAl, renforcés ou non, participent à l'allègement du module de chambre de combustion. Un programme d'études des procédés de mise en oeuvre de ce matériau a été engagé.

Acquisition des technologies de turbine haute pression

La première difficulté de réalisation de la turbine haute pression est d'ordre thermomécanique. En effet l'augmentation de la température de sortie de la chambre de combustion s'accompagne d'une élévation de la température de l'air de refroidissement pouvant, suivant les cycles, atteindre 100 Kelvin. Dans de telles conditions la tenue thermique et la durée de vie ne peuvent être obtenues que grâce à une augmentation du niveau d'efficacité de refroidissement. Le débit consommé par les aubages devra être minimisé tant pour le distributeur afin de réduire l'élévation de température dans la chambre, que pour la roue pour dégrader le moins possible les performances.

De telles contraintes imposent de développer non seulement de nouvelles technologies de refroidissement d'aubages, mais aussi de nouveaux matériaux ou des dérivés de matériaux existants, adaptés aux niveaux de températures visés. La capacité à fabriquer puis à produire ces nouveaux systèmes de refroidissement doit être démontrée aussi bien en ce qui concerne l'obtention de circuits complexes de type "wall cooling" s'intégrant dans une enveloppe tridimensionnelle, que la maîtrise des barrières thermiques (voir figure 13).

La deuxième difficulté de réalisation est d'ordre aérodynamique. Elle est liée à la volonté de réduire la masse du module de turbine haute pression. En effet celle-ci conçue de manière classique, représente plus de 10% de la masse totale des moteurs. La réduction se réalise par l'effet cumulé du rapprochement de la veine vers l'axe moteur et surtout par la réduction du nombre d'aubes, le disque peut alors être dimensionné pour des contraintes centrifuges moins élevées.

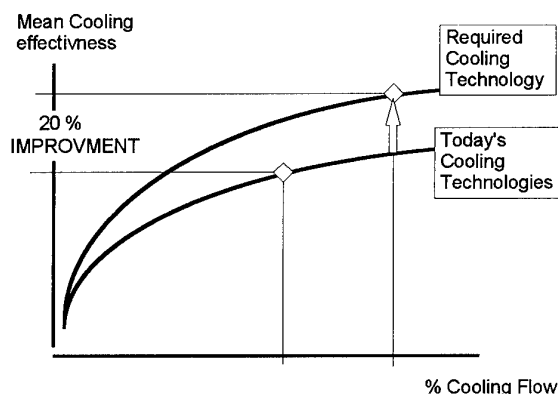


Figure 13 : Efficacité moyenne de refroidissement

La conjugaison de ces deux effets vient augmenter fortement la charge aérodynamique de la turbine. Celle-ci, représentée par $\Delta H/U^2$, est accrue de 10 à 15 % par rapport aux moteurs actuels. De plus la diminution du nombre d'aubes accroît l'effort aérodynamique sur chaque aubage (high lift blades). Dans ces conditions, obtenir un rendement du même ordre que celui des turbines des moteurs existant devient un objectif ambitieux.

Le programme d'acquisition de technologies est organisé autour de trois axes prioritaires et complémentaires :

1. Optimisation de l'aérodynamique d'une turbine fortement chargée et fortement refroidie, caractérisation au banc des performances et choix de conception.
2. Optimisation thermique et vérification sur corps haute pression de l'efficacité de refroidissement et de la durée de vie requises pour les conditions de cycle AMET, des technologies étudiées pour les aubes de turbine haute pression
3. Démonstration de la faisabilité pré industrielle des pièces tridimensionnelles en fonderie, usinage, assemblage et revêtement (barrière thermique) et de la contrôlabilité des pièces réalisées.

Malgré la diminution de la vitesse d'entraînement rendue possible par l'augmentation de la charge aérodynamique du compresseur et de la turbine, les contraintes subies par les aubes mobiles et le disque sont supérieures à celles que peuvent supporter, avec une durée de vie suffisante, les matériaux actuels. Un programme a été mis en place pour élargir le domaine de fonctionnement des monocristaux et des alliages à base Nickel élaborés par métallurgie des poudres. Il est basé sur l'adaptation des compositions et des structures métallographiques des matériaux actuels. L'accent est mis, Rapport Poussée sur Masse oblige, sur l'amélioration des caractéristiques sans augmentation de la densité.

Une autre voie est explorée. Elle réside dans la suppression des pieds d'aubes et des échasses et la réalisation d'un DAM(blink) de turbine haute pression. Sa fabrication est conditionnée par la capacité à réaliser la jonction entre

monocristal et métallurgie des poudres sans que les traitements thermiques spécifiques à chaque matériau ne détériorent les propriétés de l'autre. Le programme d'étude de faisabilité aborde les points suivants :

- Alimentation de la roue.
- Assemblage
- Contrôle et maintenabilité

Le gain attendu est de 30% de masse sur le rotor de turbine haute pression.

Démonstration de technologie

La phase 1 des travaux qui permet la démonstration d'un rapport poussée sur masse de 15 se scinde en trois niveaux technologiques :

- Niveau Technologique 1 : Etablissement d'une référence
- Niveau Technologique 2 : Démonstration des technologies compresseur
- Niveau Technologique 3 : Démonstration des technologies de DAM de turbine haute pression

La durée totale du programme de démonstration est de 8 ans, y compris phase de définition du corps haute pression. Les dates clés s'établissent comme suit :

- fin 2000 : démonstration du niveau technologique de référence
- fin 2001 : démonstration du niveau technologique 2
- fin 2005 : démonstration du niveau technologique 3

Chaque niveau technologique est basé sur l'introduction des technologies procurées par la phase d'acquisition, dès lors qu'elles sont suffisamment matures pour être introduites, sans risque exagéré, sur un corps haute-pression.

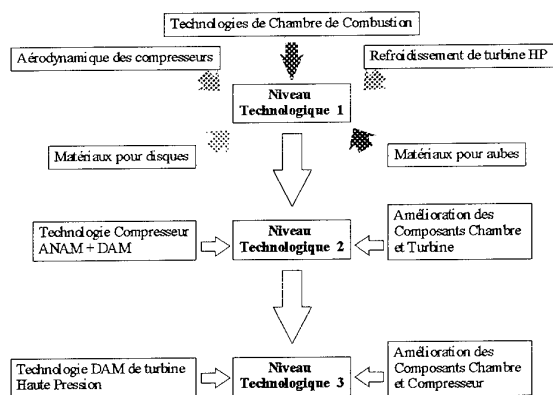


figure 14 - Schéma de démonstration

La phase de démonstration est précédée d'une période initiale de pré définition du corps haute pression dont l'objet est le

choix de la taille adéquate, la sélection des technologies appropriées et des niveaux associés. Cette phase a débuté mi 1995. Son achèvement fournira les informations suffisantes sur le programme de démonstration.

Celui-ci sera conçu de telle sorte que Snecma et Rolls-Royce conservent tous deux, la capacité totale de concevoir et de réaliser un corps haute pression très avancé à l'issue de la phase de démonstration.

Conclusion

AMET est un programme ambitieux de développement des technologies des futurs moteurs militaires. Il apporte, dès la phase d'acquisition de technologies, des gains de performances significatifs sur tous les composants du corps haute pression et, au travers des avancées sur les caractéristiques des matériaux, un allègement du moteur et l'accroissement des durées de vie des parties chaudes.

La maîtrise des coûts de développement des technologies de moteurs d'avions de combat passe aujourd'hui par le travail en coopération. Les travaux entrepris par Snecma et Rolls-Royce dans ce cadre, doteront les deux motoristes de la capacité de concevoir et réaliser le corps haute pression de haute technologie requis par les applications à venir.

Lors de sa mise en service le moteur ainsi conçu offrira des progrès significatifs en termes de rapport Poussée sur Masse ($F/M = +50\%$), de consommation (-20%) et de coût de possession (-30%).

Ce programme aujourd'hui centré sur les technologies de corps haute pression pourra faire l'objet d'une extension aux composants basse pression et arrière corps et conduire à la démonstration d'un moteur complet.

THE IMPACT OF ADVANCED ENGINE TECHNOLOGY ON COMBAT AIRCRAFT PERFORMANCE

S D Hodder
S E Simm
Defence Research Agency
Pyestock
Farnborough, UK
GU14 0LS

SUMMARY

The performance and military effectiveness of combat aircraft depend to a considerable extent on the capabilities of the propulsion system. Advanced engine technologies, and the cycle parameters made possible by them can lead to big improvements in aircraft mass, agility and combat persistence.

This paper examines how advanced engine technology can affect the design and performance of an air-air combat aircraft optimised for typical combat air patrol and intercept missions. The impact of cycle temperatures, component efficiencies, cooling effectiveness and engine thrust/weight ratio are studied independently in order to assess the relative benefits of each aspect of engine technology. Both fixed and variable cycles are considered, enabling the contributions of advanced technology and of cycle variability to be separated.

LIST OF SYMBOLS AND ABBREVIATIONS

ATR	Attained Turn Rate
BME	Basic Mass Empty
BPR	Bypass Ratio
CAP	Combat Air Patrol
HP	High Pressure
LP	Low Pressure
MRAAM	Medium Range Air-Air Missile
MVO	MultiVariate Optimisation
SEP	Specific Excess Power
sfc	Specific Fuel Consumption
SLS	Sea Level Static
SRAAM	Short Range Air-Air Missile
SOT	Stator Outlet Temperature
STR	Sustained Turn Rate
T_1	Inlet total temperature
T_3	Compressor delivery temperature
VCE	Variable Cycle Engine

1. INTRODUCTION

The performance and military effectiveness of combat aircraft depend to a considerable extent on the capabilities of the propulsion system. Advanced engine technologies, and the cycle parameters made possible by them can lead to big improvements in aircraft mass, agility and combat persistence.

Broadly, potential advances in engine technology fall into two categories: aerothermodynamics, and materials and structures. The former encompasses such issues as the aerodynamic design of the turbomachinery, aiming towards higher

efficiencies and higher stage loadings, which can in turn improve the engine thrust/weight ratio (mainly through increasing thrust) and reduce fuel consumption. Other important issues include combustor temperature patterns and cooling techniques, as efforts are made to suppress hot streaks and reduce the required cooling flow.

Materials research is geared mainly towards the development of improved metal alloys offering increased temperature capability, and new lightweight materials such as metal and ceramic matrix composites for hot parts, and polymer composites for the cooler casing components. While metal alloys, metal and ceramic matrix composites potentially offer further increases in temperature capability, the main advantage of the new materials is their much greater strength/weight ratio (allowing, for example, compressor and turbine bladed disks to be reduced to bladed rings). It is the exploitation of these materials to reduce engine weight that will bring the biggest gains in engine thrust/weight ratio.

The aim of this paper is to assess the effects which advanced engine technologies such as these have on the overall performance of an air-air combat aircraft. Engine parameters examined include stator outlet temperature (SOT), compressor delivery temperature (T_3), bypass ratio, cooling effectiveness, component efficiencies and engine rating. In addition, the potential benefits of variable cycle engines are compared to equivalent technology fixed cycles. Since engine mass is dependent largely on materials and engineering technologies rather than the aerothermodynamic factors, it can conveniently be examined as an independent variable.

The aircraft is optimised according to a specified mission and set of point performance requirements. Two air-air missions have been investigated: a Combat Air Patrol and an Intercept mission. Engines are evaluated on the basis of the basic mass empty, mission fuel burn and supercruise capability of the resulting aircraft. The first criterion helps to reduce life cycle costs, while the other two have a direct and strong effect on aircraft range and combat effectiveness. As an alternative measure, the potential gains in aircraft mass empty can be traded for gains in some aspect of

performance, such as combat persistence: this trade-off is also examined here.

2. SCOPE OF ENGINE VARIATIONS

The parametric study encompasses variations in type of cycle, stator outlet temperature, compressor delivery temperature, bypass ratio, component efficiencies and cooling effectiveness. Except in the case where the sensitivity to component performance is examined, polytropic efficiencies have been held constant throughout. Variations in T_1 are therefore equivalent to variations in core pressure ratio. The engine cycles examined are detailed in Table 1.

type of cycle	bypass ratio	SOT (K)	T_3 (K)
fixed	0.4	1850	875, 950, 1025
		2000	875, 950, 1025
		2150	875, 950, 1025
fixed	0.15	1850	875
		2000	950
		2150	1025
fixed	0.8	1850	875
		2000	950
		2150	1025
variable	0.15-0.4	1850	875
		2150	1025
variable	0.4-0.65	1850	875
		2150	1025
fixed (component efficiencies +2%)	0.4	1850	875
fixed (cooling effectiveness +5%)	0.4	1850	875

Table 1 Engine cycles modelled

While SOT and T_1 define engine cycle constraints, the actual performance capability across the flight envelope depends on the flight conditions at which these limits are reached. These are defined here using a temperature rating schedule, as illustrated in Fig 1. The datum rating schedule is typical of modern combat engines, and has been employed for all the engines in Table 1. At sea level static the engine is limited by non-dimensional compressor speed (N/\sqrt{T}). The SOT limit becomes critical as an inlet total temperature (T_1) of around 300K is reached. At a T_1 of 357K (corresponding to a flight Mach number of 1.8 at the 36,000ft), T_1 becomes the overriding constraint. Different rating schedules have also been examined, in which the sea level static SOT has been reduced, so that stator outlet temperature becomes critical at a higher inlet temperature, as also illustrated in Fig 1. This enables compressor non-dimensional speed, and hence also intake airflow, to be maintained up to higher flight Mach numbers. Although rating schedule is not in itself a measure of technology, it is included here to examine how cycle temperatures might influence its choice.

3. METHOD OF ANALYSIS

3.1 Engine synthesis

Steady state engine thrust and fuel flow data have been generated for a complete combat aircraft flight envelope using the DRA engine performance synthesis software. Models of each engine are developed using a number of thermodynamic "blocks", each representing a single thermodynamic process such as compression, combustion or expansion. The blocks are arranged in such a way as to represent the complete engine cycle.

3.1.1 Fixed cycles

The fixed cycle engine is modelled as a two spool mixed turbofan, with a fully variable convergent-divergent nozzle. For reheat operation, a maximum fuel-air ratio of 0.06 has been assumed, with a combustion efficiency of 90%. Dry engine matching is achieved in reheat by assuming a constant equivalent dry nozzle throat area. The mixer is designed at sea level static with a total pressure ratio between the two flows of 1.02, and the mixer areas are then fixed for all off-design points.

3.1.2 Variable cycles

The type of variable cycle engine (VCE) modelled is illustrated in Fig 2. It features two flow splits, forward and aft variable area bypass injectors (in essence variable geometry mixers) and a split fan. The first flow split follows two fan stages, while the second occurs after a further stage. The latter 'T-stage' is assumed here to have a pressure ratio of 1.8, and is powered by the HP turbine.

Variability in the cycle is obtained by controlling the amount of bypass flow passing through each of the two flow splits. When the first bypass ratio is zero, all the bypass flow passes through the T-stage, giving a relatively high total pressure in the bypass duct. This in turn gives a high nozzle pressure ratio, resulting in a high specific thrust. This mode determines the maximum specific thrust available from the engine, and is used at maximum dry power and in reheat, provided no other engine limits prohibit it.

As the engine throttles back, the variable geometry can be employed to maintain intake mass flow at its maximum power value, and hence fan speed is maintained at 100%. Turbine matching is maintained by increasing the first bypass ratio and reducing the second bypass ratio, so that the bypass flow energy falls. The mixer geometry is scheduled to achieve this while maintaining sensible Mach numbers in the two flows. Eventually a part load condition is reached where the second bypass ratio is zero. This point defines the limit of variability, where the engine operates in low specific thrust mode. At lower power settings than this, the engine must throttle back as a

fixed cycle engine, with intake mass flow falling with combustion temperature.

During transition from high to low specific thrust mode, the analysis has assumed the engine to be controlled by maintaining similar total pressures between the bypass and core flows at the aft mixer. This assumption ensures that similar Mach numbers exist in the two mixing flows, thus promoting efficient mixing.

The 1.8 pressure ratio T-stage means that flows of very different total pressure are being mixed in the bypass duct, and there will be an inherent pressure loss associated with this. A datum pressure loss of 10% is assumed, but to examine the sensitivity to this parameter, a 20% loss is also considered.

The way in which the variable cycle engine is rated is shown in Fig 3. At inlet temperatures below 288K, the engine can operate in high specific thrust mode, and undergoes transition as it throttles back to low specific thrust mode. Above 288K inlet temperature, high specific thrust mode cannot be achieved, and the engine must operate in partial transition in order not to exceed the pre-defined SOT limit. At a T_1 of 357K, the engine reaches its limit of variability, and must operate as a fixed cycle for inlet temperatures above this.

3. 2 Aircraft Synthesis

3.2.1 Multivariate Optimisation

The aircraft have been modelled using the DRA MultiVariate Optimisation (MVO) methodology'. This consists of an aircraft outline design synthesis and performance estimation routine, linked to a general code for constrained, non-linear optimisation. MVO allows the major aircraft design parameters (e.g. engine size, wing geometry, fuselage length, etc.) to be optimised, for example in terms of a minimum mass aircraft, whilst meeting a prescribed set of performance requirements. Throughout the optimisation process, a number of design constraints must be observed (e.g. centre of gravity position, sufficient volume for fuel and equipment, etc.), to produce a realistic configuration, but the aircraft is otherwise treated as a 'rubber' airframe containing a 'rubber' engine. Through the use of common design synthesis rules for each configuration, the method allows consistent families of optimised aircraft to be modelled, to meet the given requirements. This approach enables trade-off studies of the effects of design variables, technological advances, and changes in operational requirements to be assessed. For this study, MVO was used to optimise the aircraft in terms of minimum Basic Mass Empty (BME).

3.2.2 Airframe Modelling in MVO

The generic aircraft configurations in the study are all single seat, twin

engined, with conventional swept wing planforms, conventional tailplanes, and twin canted tailfins. The aircraft are stressed to a flight load limit of 9g and maximum design speeds are 800kts at sea level and Mach 2 at altitude (a relatively conventional pitot type intake has been assumed). Mass assumptions for the various engines are discussed in sections 4.1, 4.4 and 4.5. Mass assumptions for the aircraft structure and other systems have been kept constant throughout the study, at current technology levels, in order to highlight the engine effects. No external weapons or fuel tanks are carried; the aircraft have a central weapons bay carrying four medium range air-air missiles (MRAAM), and two outer weapons bays each carrying a single short range air-air missile (SRAAM).

3.2.3 Engine Modelling in MVO

Each engine is defined at given cycle parameters and 73.5 kg/s sea level static mass flow (scale factor 1.0). During the optimisation process, the engine cycle parameters cannot change, but MVO scales the engine up or down in terms of thrust, fuel consumption, mass and geometry, in order to minimise the Basic Mass Empty of the aircraft whilst meeting the performance requirements. Geometry assumptions are the same for all engines.

3.3 Performance Requirements

Two example air-air missions are considered, which place significantly different demands upon the air vehicle: a Combat Air Patrol mission in which the majority of fuel is used at subsonic speeds with the engines throttled back, and an Intercept mission in which the majority of fuel is used in reheat at supersonic speeds. Both missions can be regarded as typical for these roles, but both are arbitrary and have been defined for the purposes of this comparative study only; they do not represent any UK Staff Target or Requirement.

3.3.1 Combat Air Patrol Mission

The combat air patrol mission profile is detailed in Table 2. The weapon load is assumed to be 4 MRAAMs, 2 SRAAMs and a 30mm gun with 150 rounds ammunition.

leg no.	description
1	Engine start, taxi, and take-off
2	Climb in max dry to Mach 0.8/36,000ft
3	Outbound cruise at Mach 0.8/36,000ft to 200nm from base
4	Loiter at Mach 0.7/36,000ft for 60 mins
5	Accelerate in max reheat to Mach 1.6/36,000ft
6	Release all missiles, 1 x 360° 3g turn, Mach 1.6/36,000ft
7	Return cruise at Mach 0.8/36,000ft to overhead base
8	Loiter at Mach 0.4/sea level for 20 mins
9	Land with 5% internal fuel reserves

Table 2 Combat Air Patrol Mission

The point performance specified for the CAP mission is detailed in Table 3. These

requirements are in max reheat, with 4 MRAAMs, 2 SRAAMs, gun and ammunition, and 60% internal fuel.

Parameter	Mach No.	Alt (ft)	Requirement
SEP (m/s)	0.9	36,000	70
SEP (m/s)	1.3	36,000	80
SEP (m/s)	1.6	36,000	100
STR (deg/s)	0.7	sea level	20 (8.5g)*
ATR (deg/s)	0.5	sea level	29 (8.8g)*
Max Mach No.		sea level	1.1
Max Mach No.		36,000	2.0
Take-off ground run(m)			600
Max. approach speed (kts)			150

* Note: Turn rate requirements were also specified at greater heights and speeds, however only the above two influenced the final aircraft designs. The remaining turn rate requirements 'fell-out' in excess of the requirements.

Table 3 Point Performance Requirements

3.3.2 Intercept Mission

The intercept mission profile is given in Table 4. The weapon load is assumed to be the same as for the CAP mission.

leg no.	description
1	Engine start, taxi, and take-off
2	Climb in max reheat to Mach 1.6/36,000ft
3	Outbound dash at Mach 1.6/36,000ft to 175nm from base
4	Release all missiles, 1 x 360° 3g turn, Mach 1.6/36,000ft
5	Return cruise at Mach 0.8/36,000ft to overhead base
6	Loiter at Mach 0.4/sea level for 20 mins
7	Land with 5% internal fuel reserves

Table 4 Intercept Mission

The point performance requirements for this mission are similar to those used for the CAP mission, as detailed in Table 3.

4. STUDY RESULTS

For the majority of the study, aircraft mission and point performance requirements have been kept constant, while the engine cycle parameters and mass have been varied to produce aircraft with differing BME. Aircraft mass however, is not the only measure of effectiveness. Although the aircraft have been 'sized' to meet the same requirements, the study revealed significant differences in 'fall-out' performance between some of the aircraft. In particular, many of the advanced technology engines were found to confer the aircraft with considerable dry thrust 'supercruise' capability. Achieved supercruise Mach number has therefore been used as an additional discriminator

in comparing the different engine technologies.

4.1 Effect of SOT and T_c

Fig 4 shows the effect of cycle temperatures on engine performance in dry power for sea level static conditions. Increasing stator outlet temperature produces more thrust, since more energy is being added to the core flow at combustion. However, the resulting higher jet velocities mean that the propulsive efficiency falls, so specific fuel consumption (sfc) in dry power deteriorates. Increasing T_c at constant SOT results in lower max dry thrust, since the combustor temperature rise is reduced. The effect is most dramatic at low SOT and high T_c , for which the combustor temperature rise is smallest. However, the increased thermal efficiency associated with burning fuel at high pressures means that the sfc in dry power improves. Often it is the metal temperature of the first turbine rotor stage which sets an upper limit on the cycle temperature. Fig 4 includes a typical constant metal temperature line: as SOT increases, T_c (the temperature of the cooling flow) must be reduced to maintain a constant metal temperature. This assumes a fixed amount of cooling flow and constant cooling technology. A change in either of these would shift the position of the line, but would not greatly alter its basic shape. In terms of dry engine performance, Fig 4 demonstrates that at any given metal temperature, there is a strong trade-off between high thrust and good sfc, and a careful balance must be sought between the two. Note that, since all engines are rated in the same way, the trends shown for sea level static conditions will hold true for all flight conditions.

Fig 5 shows the reheat performance at sea level static conditions for the same nine engines. While the effect of cycle temperatures on thrust is the same as for dry power operation, the sfc trend is reversed. As SOT increases sfc improves, because a greater proportion of the fuel is burned with high efficiency in the combustion chamber, rather than during the less efficient afterburning process. Conversely, sfc deteriorates with increasing T_c , since the lower combustor temperature rise means a greater proportion of the fuel is burned in reheat. Hence, in terms of reheat performance for a certain metal temperature limit, it is clearly best to choose a high SOT and low T_c , since these both provide high thrust and low sfc in reheat.

At a scale factor of 1.0, each engine was assumed to have a mass of 1000kg including accessories. The datum engine with SOT/ T_c =1850K/875K is broadly representative of current technology and is assumed to have an uninstalled T/W of 10. If the same mass is assumed for the highest temperature engine with

SOT/ T_3 =2150K/1025K (no allowance being made for the introduction of advanced lightweight materials), then an uninstalled T/W of 11.2 is achieved. All nine engines were run through MVO in turn to produce nine aircraft optimised for the CAP mission and nine aircraft optimised for the Intercept mission.

4.1.1 CAP Mission

The calculated datum aircraft (current technology engine) for the CAP mission is illustrated in Fig 6. The engines are closely spaced at the rear of the aircraft, with the main weapons bay located under the engine intake ducts and the two small weapons bays located outboard of the engine intake ducts. This layout of intake ducts, engines and weapons bays is the same for all the aircraft in the study. The datum aircraft requires an engine scale factor of 1.02, producing a BME of 12,128 kg and requiring 4,854 kg of internal fuel; fuel fraction is 27% of mission take-off mass. The fuel usage breakdown is shown in Fig 7; it is dominated by the CAP loiter and the cruise legs, which together account for 55% of mission fuel. All the CAP aircraft have relatively high wing aspect ratios of between 3 and 3.5 in order to minimise fuel burn during these legs.

Fig 8 compares the BME and fall-out supercruise Mach number of the aircraft with the nine different combinations of engine SOT and T_3 . For all these aircraft, the major requirement driving engine size is the Mach 2 requirement in max reheat at 36,000ft. The primary effect of increasing SOT is to increase the specific thrust of the engine; this has two effects on the aircraft in the CAP mission. Firstly, increasing SOT to 2000K and above, increases supercruise Mach number from 1.13 on the datum aircraft to over Mach 1.4 because of the increases in dry specific thrust. This is significant since it would provide substantial improvements in range, endurance and combat persistence for those missions which require sustained supersonic operation. Secondly it produces BME savings of 2 to 3% at the datum level of T_3 since the increases in reheated specific thrust mean that the point performance requirements can be met with a reduced engine size and consequently a smaller and lighter aircraft.

As already noted, increasing T_3 reduces the specific thrust of the engine but improves its dry specific fuel consumption. At 1850K SOT, the loss of specific thrust with increasing T_3 has an adverse effect, since a larger engine is needed to meet the point performance requirements, and results in a progressively heavier aircraft. However, the increase in specific thrust due to SOT soon outweighs this T_3 effect. In fact, at 2000K and 2150K SOT, increasing T_3 results in further mass savings relative to the datum aircraft. This is

because the improvement in dry sfc with increasing T_3 reduces the fuel required to achieve the mission and results in a smaller and lighter aircraft. However, at every level of SOT, the reduction in dry specific thrust with increasing T_3 results in a slight loss of supercruise. Overall, the largest benefits to aircraft optimised for the CAP mission appear to be gained by increasing both SOT and T_3 simultaneously.

4.1.2 Intercept Mission

The calculated datum aircraft (current technology engine) for the Intercept mission is illustrated in Fig 9. Although the basic layout is the same as the CAP aircraft, the Intercept mission requirements have had a different effect upon aircraft geometry. Wing aspect ratio has reduced, while wing sweep and fuselage length have increased; all three changes help to reduce the supersonic drag of the aircraft. The datum aircraft requires an engine scale factor of 1.03, producing a BME of 12,069 kg and requiring 4,751 kg of internal fuel; fuel fraction is again 27% of mission take-off mass. With virtually the same thrust as the datum CAP aircraft, the lower supersonic drag of the datum Intercept aircraft has resulted in a supercruise Mach number of 1.36. The fuel breakdown for the datum intercept aircraft is shown in Fig 10; it is dominated by the climb/acceleration and supersonic dash legs (all in reheat), which together account for 53% of the mission fuel.

Fig 11 compares the BME and fall-out supercruise Mach number of the aircraft with the nine different combinations of engine SOT and T_3 . For all these aircraft, the major requirement driving engine size is the SEP requirement in max reheat at M1.6/36,000ft. The trends with SOT and T_3 are similar to those found for the CAP mission. However, the BME savings from increasing SOT (6 to 9% at the datum level of T_3) are greater than for the CAP mission. As with the latter, the greater specific thrust of the higher SOT engines allows the performance requirements to be met with a smaller engine. In addition, the improvement in reheated sfc provided by increased SOT means that less fuel is required to achieve the mission, since around 75% of the total fuel is burnt in reheat.

At the datum level of SOT, the adverse effects of increasing T_3 are more severe than for the CAP mission, with a greater loss of supercruise and greater increase in BME. The loss in specific thrust with increasing T_3 means that a larger engine is required to meet the point performance requirements (as on the CAP mission). In addition, increasing T_3 has an adverse effect on reheated sfc, increasing mission fuel burn and hence BME. The increase in specific thrust with SOT, means that at both 2000K and 2150K SOT, the loss of specific thrust with increasing T_3 no longer has an adverse

effect upon engine size. In addition, increasing T_1 has little effect on reheated sfc at the higher levels of SOT. However, the improvement in dry sfc with increasing T_1 causes only small reductions in fuel burn, since the majority of fuel is burnt in reheat. The net result is that increasing T_1 produces only small savings in BME. The loss in supercruise performance is also small. Overall for the Intercept mission, with the emphasis on reheat performance, the benefits from increasing SOT are far greater than those from increasing T_1 .

4.2 Effect of improved component efficiencies and turbine cooling effectiveness

Fig 12 shows sfc loops at sea level static conditions for the datum (1850/875K) engine and the respective effects of raising all turbomachinery component efficiencies by 2%, or increasing turbine cooling effectiveness by 5%. Raising the component efficiencies improves both sfc and maximum reheat thrust by around 4%. Similar improvements could be shown for other low inlet temperature operations, such as the combat air patrol loiter leg (Mach 0.7/36,000ft). At high inlet temperatures (i.e. high Mach number flight conditions), the percentage benefits were found to be approximately half those at sea level static.

Increasing the cooling effectiveness by 5% at a given metal temperature enables the total cooling flow to be reduced by about 30% for the datum engine. Because of the lower cooling flow, the gas temperature at the low pressure turbine exit rises, producing a higher specific thrust cycle. A thrust increase at sea level static of around 3% is shown in Fig 12. However, because more of the flow is entering the combustor, more fuel is required to give the same temperature rise. Hence dry sfc rises by around 1%, while reheat sfc improves by 6% at a given thrust.

The effects on aircraft BME and 'fall-out' supercruise Mach number are illustrated in Figs 8 and 11 for the CAP and Intercept missions respectively. Two points have been added to the plots to show the datum engine with the improved component efficiencies, or with the improved cooling effectiveness. As would be expected, BME is reduced while 'fall-out' supercruise Mach number is increased. The effects of either improvement are broadly equivalent to raising the SOT and T_1 of the datum engine by 100K and 75K respectively (i.e. a metal temperature rise of around 75K at fixed cooling effectiveness). This underlines the powerful gains to be obtained and hence the importance of seeking such improvements in component performance and turbine cooling.

4.3 Effect of rating schedule

Fig 13 shows the effect on net thrust at 36,000ft of changing the rating schedule. With a reduced sea level static SOT, engine airflow is maintained up to higher inlet temperatures, giving more thrust capability at high Mach numbers. However, at Mach numbers lower than about 1.5, less thrust is produced because of the lower cycle temperature. Within this study, being able to achieve the maximum speed requirement of Mach 2 and the SEP requirement at Mach 1.6 (both at 36,000ft) are critical sizing points for the engines, and so re-rating the engine for a lower SOT at sea level static allows these requirements to be met with a smaller engine and consequently a lighter aircraft. Fig 14 shows the effect of rating schedule on aircraft BME and 'fall-out' supercruise Mach number at two levels of engine cycle temperature. Because of the loss of thrust below Mach 1.5 at 36,000ft, re-rating the engines results in a substantial loss of supercruise capability.

We have already seen (Fig 8) that increasing SOT/ T_1 from 1850/875K to 2150/1025K at the datum rating schedule produces around a 5% BME saving on the CAP mission, while the 'fall-out' supercruise Mach number is increased from 1.13 to 1.45. Fig 14 shows that re-rating the engine at high cycle temperatures allows this 'excess' of supercruise performance to be traded for a further mass reduction. For the same supercruise Mach number as the datum aircraft (1.13), re-rating the high temperature engine more than doubles the BME saving, to 11% relative to the datum aircraft.

However, Fig 14 also shows that if the rating schedule becomes too biased towards maximising thrust at high Mach numbers, then the loss of thrust at low Mach numbers means that the low speed point performance requirements become the more critical, causing the required engine size and hence BME to increase again.

4.4 Effect of bypass ratio

As bypass ratio is increased at constant cycle temperatures, the reduction in core flow, and hence also core power, results in a lower specific thrust cycle. Fig 15 shows the effect on max dry power and sfc for three levels of cycle temperature at sea level static conditions. In general, increasing the bypass ratio leads to a considerable improvement in sfc in exchange for a loss of specific thrust. For the most part, the trend is only slightly affected by cycle temperatures. However, at 0.15 bypass ratio, the highest temperature engine suffers a significant increase in sfc, because the ensuing high specific thrust penalises propulsive efficiency. At combat rating (Fig 16), the differences in thrust are less marked, since the higher bypass ratio engines have more unburned air, and so reheat provides a larger boost. The

trend of sfc is reversed in reheat; more fuel is required for afterburning if there is a greater proportion of unburned bypass air, so that sfc increases with bypass ratio.

In modelling engines of different bypass ratios within MVO, the mass assumptions were adjusted to take some account of the different core sizes of the engines (at a given overall mass flow). The changes are shown in Table 5.

Bypass ratio	Engine mass including accessories (kg) at scale factor 1.0	Specific mass (kg/kg/s)
0.15	1100	15.0
0.4	1000	13.6
0.8	920	12.5

Table 5 Engine mass assumptions

The results for the CAP mission, in terms of BME and 'fall-out' supercruise Mach number, are shown in Fig 17. Increasing bypass ratio reduces the fuel used during the mission, since dry power sfc is reduced as well as engine specific mass. Thus, if a minimum mass aircraft is the sole aim, high bypass ratio combined with high SOT/T₁ offers the best solution, albeit at the cost of any effective supercruise capability. Note however, that the return from increasing the cycle temperatures above 2000/950K is relatively small, and might be judged not worth the additional technical difficulty.

However, if there is a requirement for significant supercruise capability then high cycle temperatures combined with a more modest increase in bypass ratio would be preferred. For instance, Fig 17 shows that to achieve a supercruise Mach number of 1.4 with current engine technology, requires a bypass ratio of around 0.2, producing an aircraft BME of around 13,200kg. With SOT/T₁ increased to 2000/950K, the same supercruise performance can be achieved with a bypass ratio of around 0.4, producing a BME saving of around 11% relative to current engine technology. If SOT/T₁ is further increased to 2150/1025K, the same supercruise performance can now be achieved with a bypass ratio of around 0.45, and a BME saving of 14% relative to current engine technology.

The corresponding results for the Intercept mission are shown in Fig 18 and are quite different to those for the CAP mission. Reheat sfc is now a very important factor, for which the lower bypass ratio engines are more suited. However, although reheat sfc improves as bypass ratio is lowered, engine specific mass increases due to the increase in core size. The minimum mass aircraft is now achieved with a bypass ratio of around 0.4 at each of the three temperature levels. Moreover, unlike the

CAP mission, the minimum mass aircraft have considerable supercruise capability at all temperature levels.

4.5 Variable cycles

The datum variable cycle engine has been designed at sea level static with a bypass ratio of 0.15, a maximum stator outlet temperature of 1850K, and a maximum compressor delivery temperature of 875K. Hence this engine produces a similar amount of thrust at sea level static to a fixed cycle engine of the same bypass ratio and temperatures (Fig 19). As the engine throttles back, sfc improves significantly as the bypass ratio increases and specific thrust falls, giving a higher propulsive efficiency. In low specific thrust mode the VCE mimics a fixed cycle engine with bypass ratio 0.4 and a peaked rating schedule, similar to the low specific thrust rating line in Fig 3. The sfc loop does not map onto that of the equivalent fixed cycle engine, but is about 2% higher, primarily due to the bypass duct mixing loss.

Fig 20 shows that the variable cycle engine gives the high thrusts of a low bypass ratio engine at low inlet temperature, together with the high thrusts associated with a peaked rating schedule at high inlet temperature. It can be seen therefore that the advantage of the variable cycle engine relative to a fixed cycle engine with an equivalent sea level static performance is twofold:

- (i) higher thrust at high Mach numbers, and
- (ii) better part load sfc.

The effect of the bypass duct mixing loss was found to be comparatively small. Increasing the loss from 10% to 20% raises sfc by about 0.5% in the high specific thrust mode, and about 1.5% in the low specific thrust mode. Note that the loss only affects a small percentage of the flow when the bypass ratio is 0.15, hence the small effect on sfc. The issue is significant only for those missions where the majority of engine operation is in a low specific thrust mode.

The 0.15 to 0.4 bypass ratio engines were assumed to have a core size similar to that of a 0.15 bypass ratio fixed cycle engine and were assumed to have a mass of 1150kg at a scale factor of 1, allowing a 50kg mass penalty for the mechanical variability. The 0.4 to 0.65 bypass ratio engines were assumed to have a core size similar to that of a 0.4 bypass ratio fixed cycle engine and were assumed to have a mass of 1050kg, using the same mass penalty for cycle variability.

Fig 21 shows the results for the CAP mission, in terms of BME and 'fall-out' supercruise capability. Four VCEs (two levels of cycle temperature and two ranges of bypass ratio) are compared with

the fixed cycle engines at corresponding temperatures and three values of bypass ratio. At current technology levels, the VCEs appear to offer no significant advantages in terms of BME and supercruise performance. At high cycle temperatures both VCEs show BME savings of about 2% relative to a fixed cycle engine providing the same supercruise performance.

Fig 22 shows the equivalent comparisons for the Intercept mission. Here the VCEs show to more advantage, particularly at the higher engine technology. At current technology levels, the 0.4-0.65 bypass ratio VCE offers around a 4% BME saving over the optimum fixed cycle engine, although its supercruise Mach number is only 1.16, compared with 1.38. At high temperatures the 0.15-0.4 bypass ratio VCE offers around a 4% BME saving without loss of supercruise performance.

There are several factors which make the variable cycle more attractive at high temperatures. The most fundamental reason is that for a high stator outlet temperature (and hence high specific thrust), fixed cycle engines have a poor sfc in dry power, giving more incentive to use cycle variability. For such engines, variability gives a bigger percentage improvement in sfc and the highest potential reductions in BME.

In addition, while all the aircraft are sized to meet the same performance requirements, the VCEs give considerably better 'fall-out' point performance at high T_1 flight conditions. This is illustrated by the specific excess power data given in Table 6. Cycle variability gives significant capability where the fixed cycles give little or nothing.

Average 'Fall-out' SEP at M2.0 / 36,000ft	Fixed cycles	Variable cycles (bypass ratio 0.15-0.4)
CAP mission	0	132
Intercept mission	25	158

Table 6 'Fall-out' point performance comparison for fixed and variable cycle engines

4.6 Effect of engine mass reductions

In order to assess independently the effect of engine mass reductions, the datum 0.4 bypass ratio fixed cycle engine was re-run through the CAP mission at two lower masses. The mass of the datum technology engine at a scale factor of 1.0 was reduced from 1000kg to 750kg and then to 500kg. The 25% mass reduction gives an engine T/W=13 whilst the 50% mass reduction gives an engine T/W=19. In reducing the datum engine mass from 1000kg to 750kg, each 1kg reduction in the mass of the propulsion system produced a 2.4kg reduction in BME and a 3.2kg reduction in take-off mass.

Fig 23 plots the results in terms of engine T/W ratio at constant airframe

technology. Increasing engine T/W ratio from 10 to 15 produces about a 15% reduction in both BME and take-off mass, whilst increasing engine T/W from 15 to 20 produces only about a further 6% reduction in both BME and take-off mass.

4.7 Ability of advanced engine technology to improve combat persistence
All the results so far have used engine technology to produce a smaller, lighter aircraft which meets the same mission and point performance requirements. Clearly, there may be demands to use engine technology to produce performance improvements for broadly constant aircraft BME. A number of the advanced technology engines were therefore re-run through MVO but with mission profile requirements increased in key areas.

Fig 24 illustrates the ability of advanced engine technology to increase time on CAP loiter, relative to the datum aircraft for approximately the same BME; all other aspects of the CAP mission profile and point performance requirements are unchanged. For constant BME, increasing engine T/W ratio from 10 to 15 allows time on CAP loiter to be increased from 60 to 108mins.

Alternatively, advanced engine technology might be used to increase time in combat. Fig 25 shows the results for both the CAP and Intercept missions; again, all other aspects of the mission profile and point performance requirements are unchanged. For constant BME, increasing engine T/W ratio from 10 to 15 allows combat time in maximum reheat to be increased from 1.8 minutes to between 6 and 7.8 minutes depending on mission type.

The engines considered represent a considerable jump from current technology, but it can be seen that the potential performance improvements offered by such technology are substantial, allowing the aircraft to nearly double its time on CAP, or to increase its persistence in combat by a factor of three or four.

5. CONCLUSIONS

1. Advanced engine technology in terms of cycle temperatures or efficiencies can produce significant reductions in aircraft mass while meeting a given level of performance. Alternatively, advanced engine technology can be used to provide increased levels of performance for a given aircraft mass. The most influential technologies are dependent on the exact requirements of the mission, in particular upon the proportion of dry and reheat engine operation.
2. Increasing the stator outlet temperature from 1850K to 2000K yields a 2% reduction in BME for a typical CAP mission, and 6% for a representative intercept mission,

together with a substantial rise in maximum supercruise Mach number. Raising SOT by a further 150K raises the above BME improvements by half, showing that the benefits diminish as SOT rises.

3. Increasing T_1 can help to reduce the BME, but only at high values of SOT. Even then it is dependent on the type of mission, only being beneficial where a substantial amount of dry power operation is involved.
4. At a given level of supercruise capability, a higher SOT would allow a higher bypass ratio to be used. For missions involving substantial amounts of dry power operation, this results in further reductions in aircraft mass.
5. Raising each turbomachinery component efficiency by 2% was found to give a BME saving of 2% for the CAP mission and 4% for the Intercept mission. This is equivalent to raising SOT and T_1 by 100K and 75K respectively to 1950K and 950K. Enhancing the turbine cooling effectiveness by 5% was found to give broadly similar results.
6. The choice of rating schedule was shown to be sensitive to the performance requirements. Because of the dominant Mach 2 sizing requirement, biasing the schedule more towards this condition was found to reduce aircraft mass, as long as sufficient thrust capability existed at lower T_1 conditions. On account of this, greater weight reductions were possible at higher cycle temperatures. However, a marked reduction in supercruise capability was also noted.
7. A variable cycle engine is most advantageous where the mission places emphasis on high specific thrust, but where good dry power sfc is also important to give adequate range and endurance on other missions. The largest mass savings have been found to be at high cycle temperatures, since these cycles have the highest specific thrust. The VCE is also advantageous if demanding performance requirements exist at high inlet temperature conditions, such as sustained manoeuvre at Mach 2. However, the cycle is clearly more complex than a fixed geometry cycle, presenting more mechanical problems and having a largely unproven reliability. Any gains in aircraft performance must therefore be weighed against higher development costs and potentially higher maintenance costs.
9. At current levels of airframe technology, increasing engine thrust-to-weight ratio from 10 to 15 provides a BME saving of around 15%. A further increase to 20 only gives an additional 6% improvement.

10. Alternatively, for a constant aircraft BME increasing engine thrust-to-weight ratio from 10 to 15 was shown to increase CAP time from 60 to 108 minutes, or increase combat time from 1.8 to between 6 and 7.8 minutes depending on mission type.

REFERENCES

1. J.A.Kirk, "The use of multivariate analysis to optimise design parameters for extended-range combat aircraft", AIAA 92-4707, September 1992.
2. M.G.Philpot, "Practical considerations in designing the engine cycle", AGARD LS-183, May 1993.

© British Crown Copyright 1995/DERA
Published with the permission of the
controller of Her Britannic Majesty's
Stationery Office.

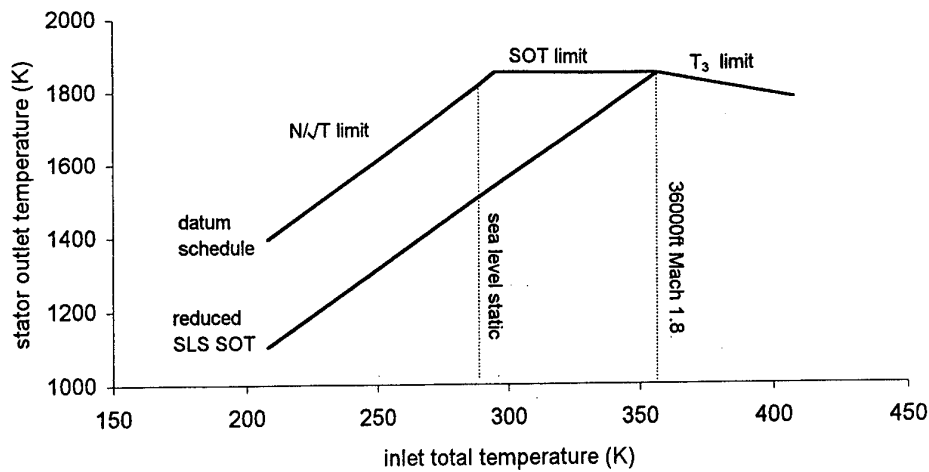


Figure 1 Fixed cycle engine temperature rating schedule

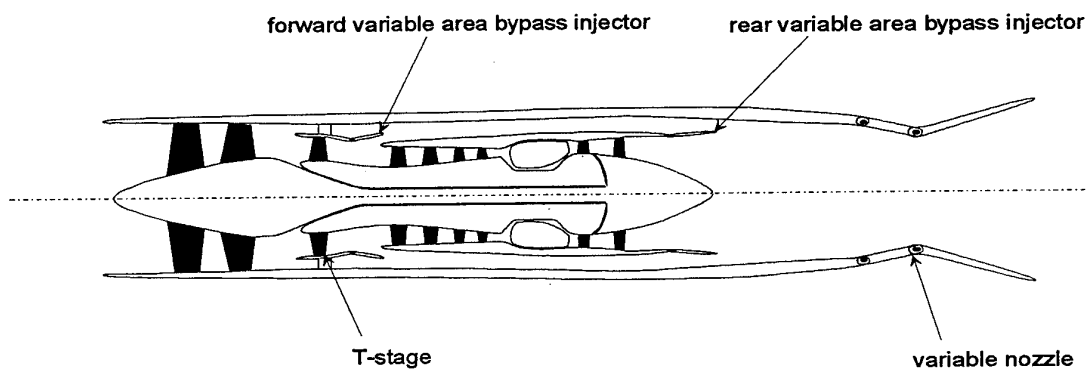


Figure 2 Variable cycle engine

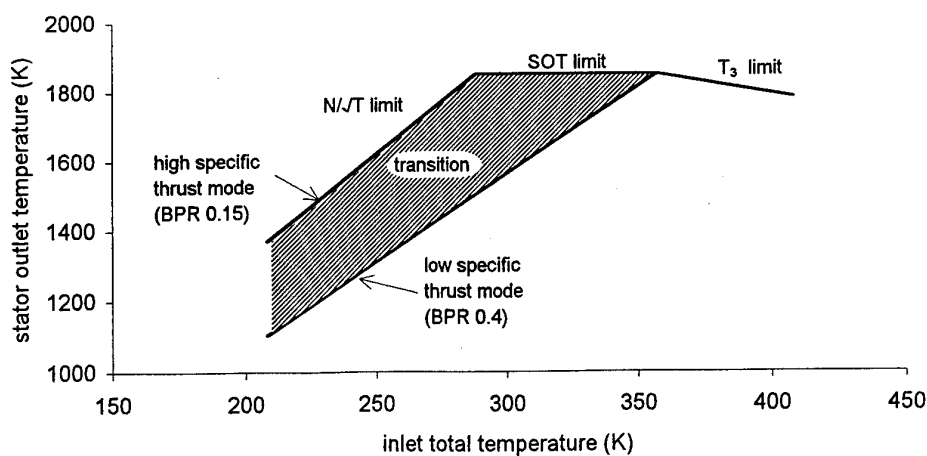


Figure 3 Variable cycle engine temperature rating schedule

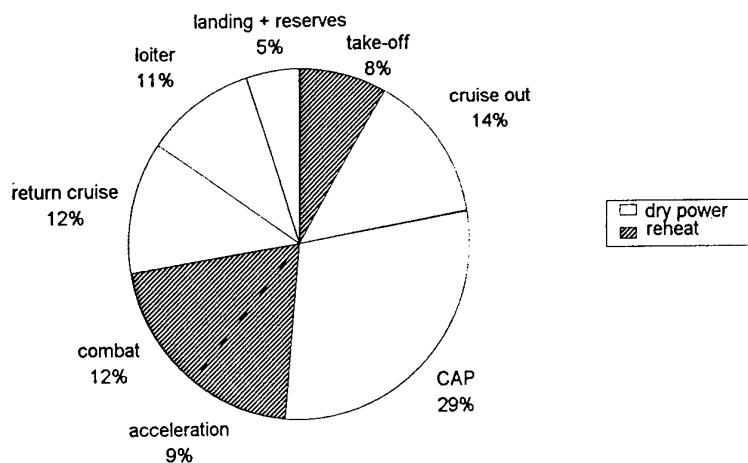


Figure 7 Fuel use on CAP mission

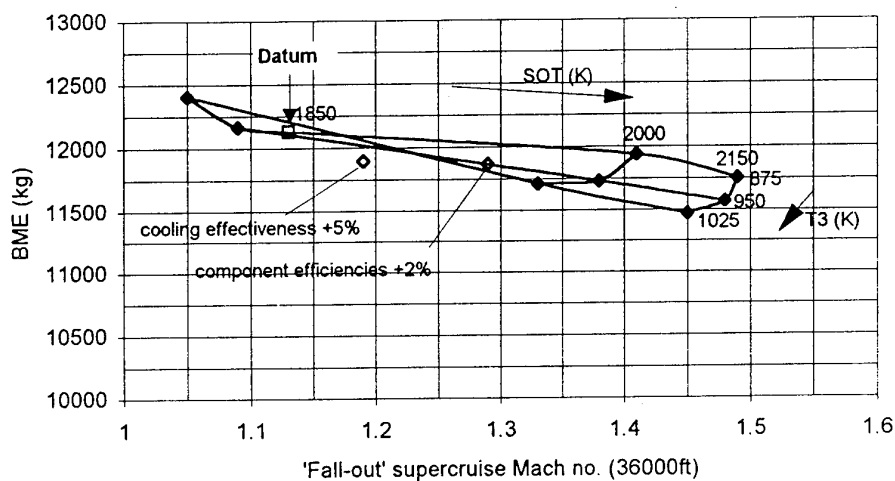


Figure 8 Effect of cycle parameters (CAP mission)

Engine scale factor: 1.03
 Aircraft length (m): 17.4
 Gross wing area (m²): 48.5
 Wing leading edge sweep (deg): 53.3
 Wing aspect ratio: 2.4
 BME (kg): 12,069
 Internal fuel (kg): 4,751

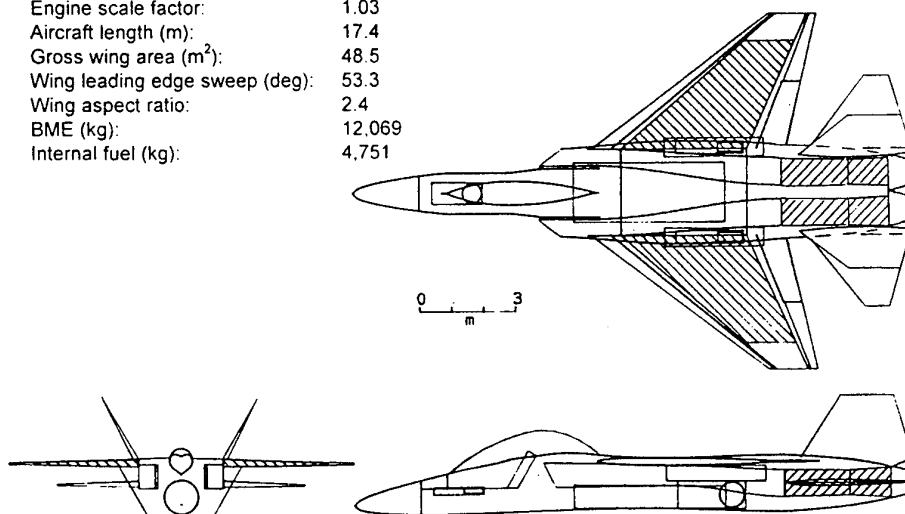


Figure 9 Datum intercept mission aircraft

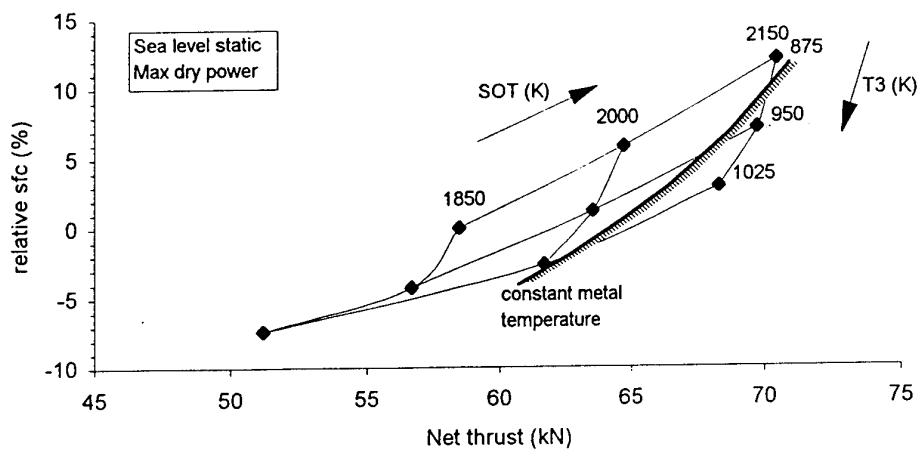


Figure 4 Effect of cycle temperatures on dry engine performance

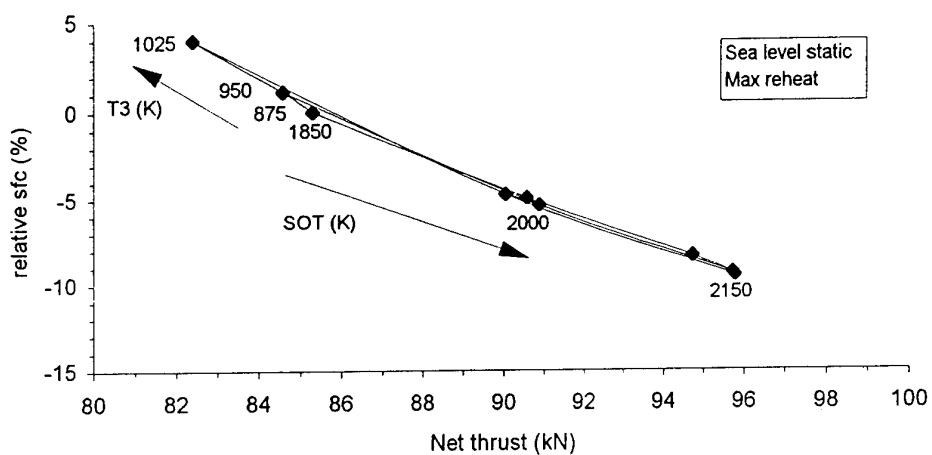


Figure 5 Effect of cycle temperatures on engine performance in reheat

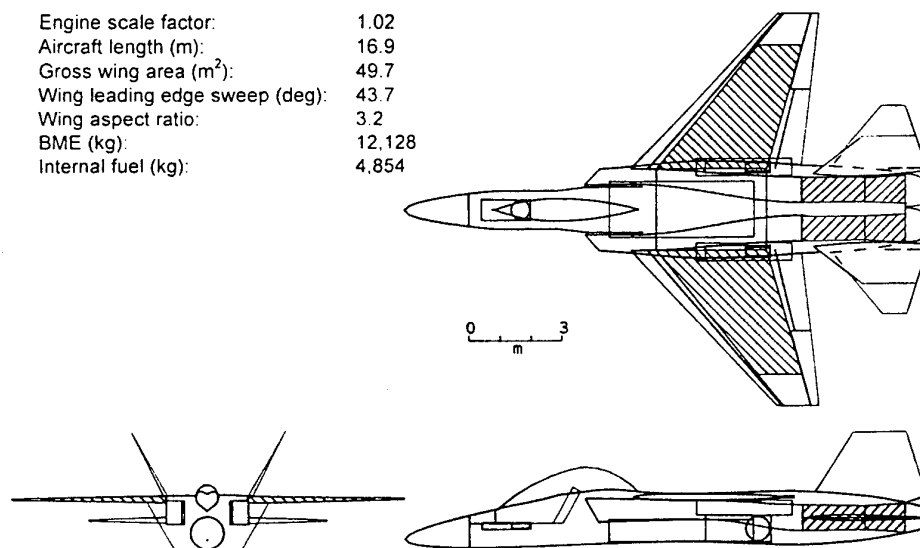


Figure 6 Datum CAP mission aircraft

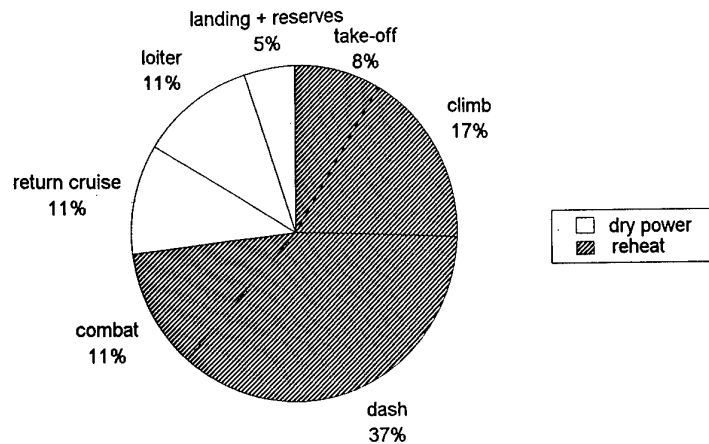


Figure 10 Fuel use on intercept mission

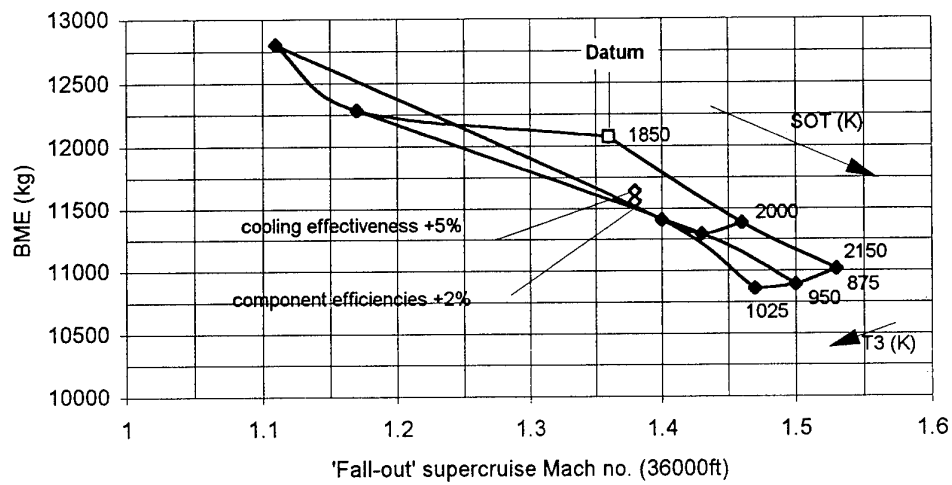


Figure 11 Effect of cycle parameters (Intercept mission)

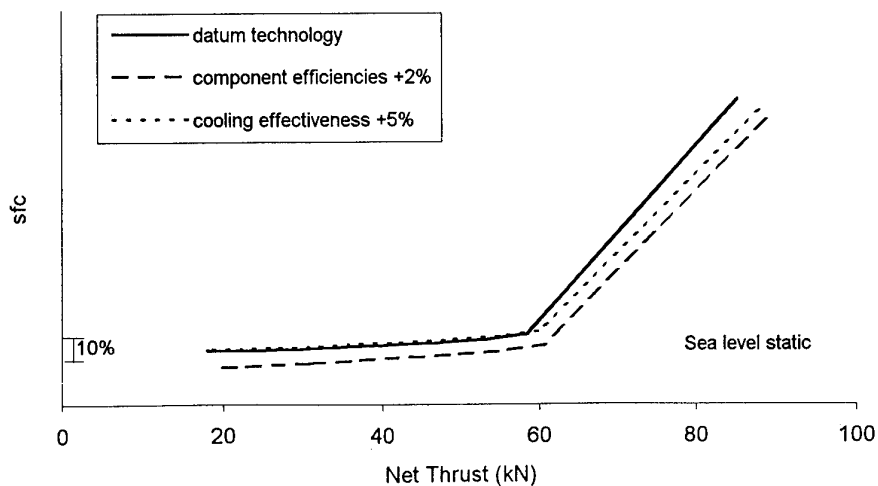


Figure 12 Effect of component efficiencies and cooling effectiveness on engine performance

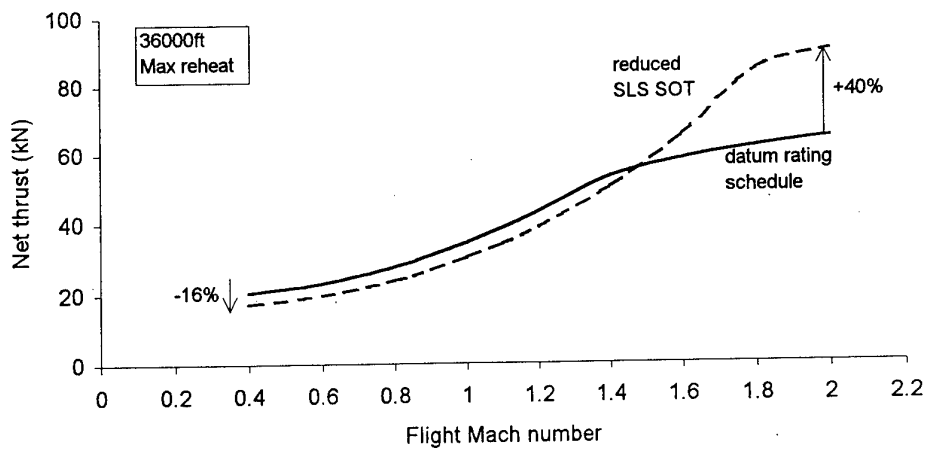


Figure 13 Effect of rating schedule on thrust profile

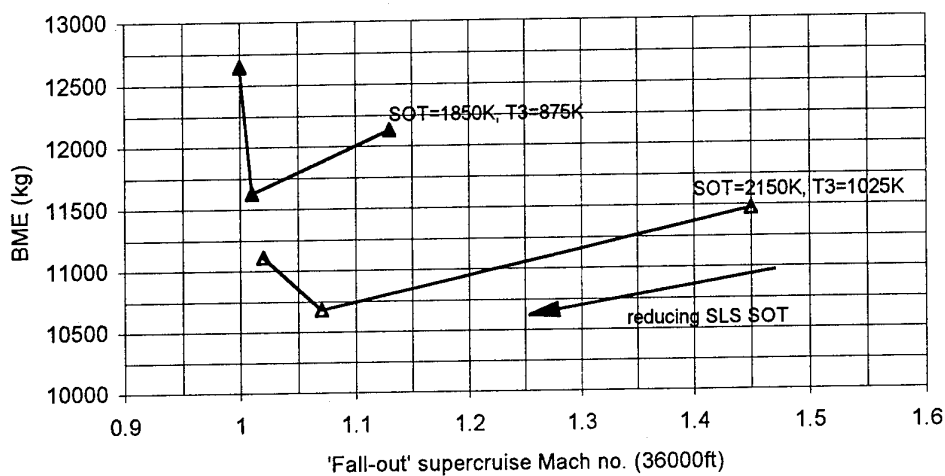


Figure 14 Effect of rating schedule (CAP mission)

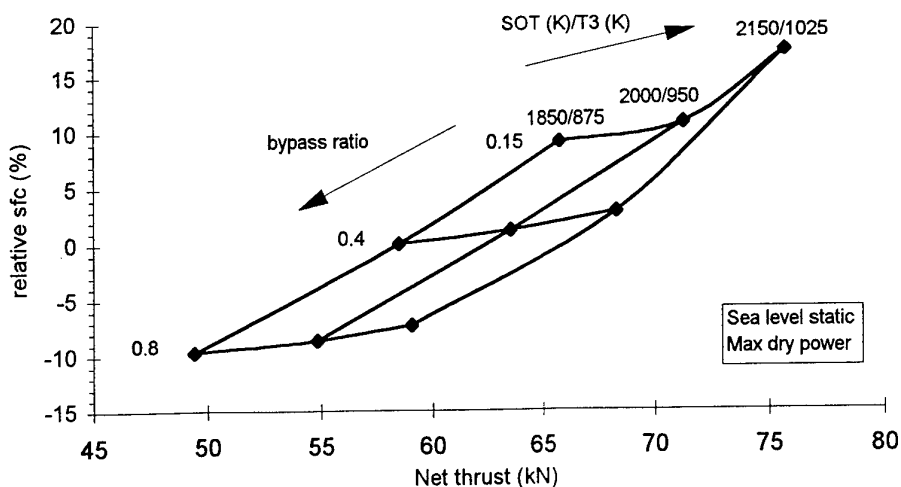


Figure 15 Effect of bypass ratio on dry engine performance

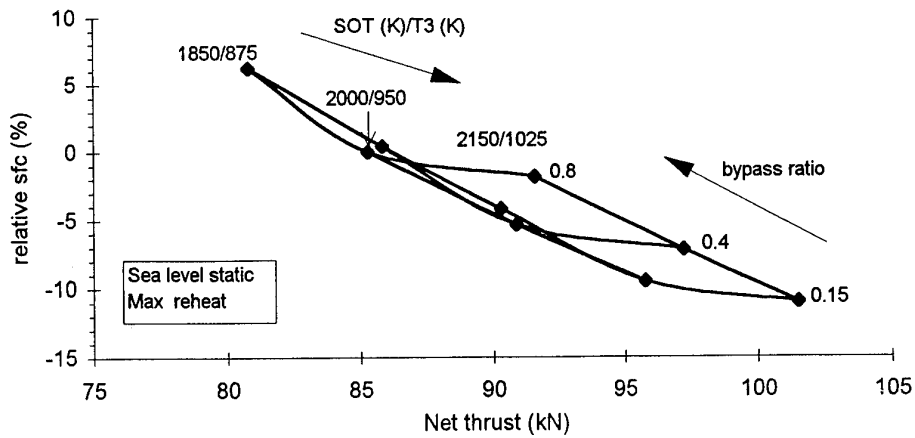


Figure 16 Effect of bypass ratio on reheat engine performance

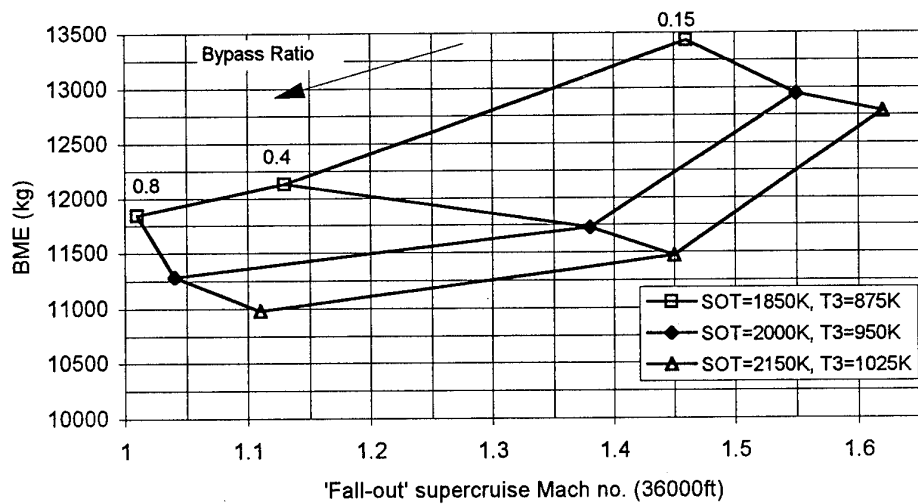


Figure 17 Effect of Bypass Ratio (CAP Mission)

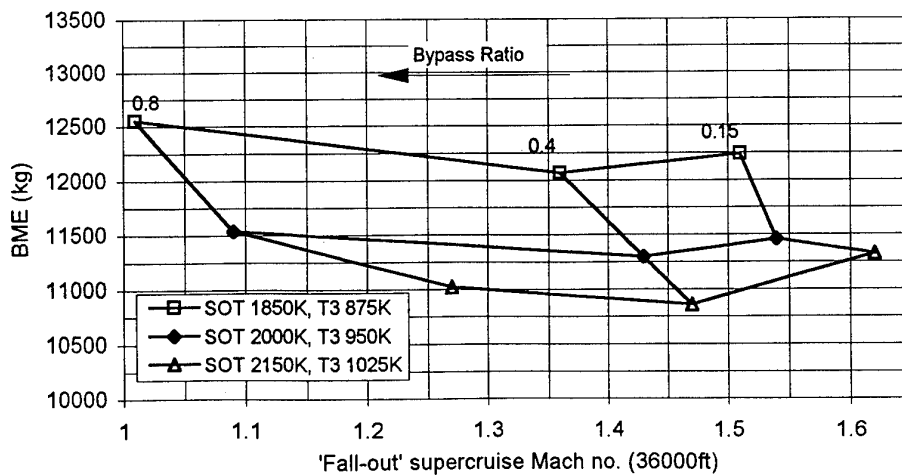


Figure 18 Effect of Bypass Ratio (Intercept Mission)

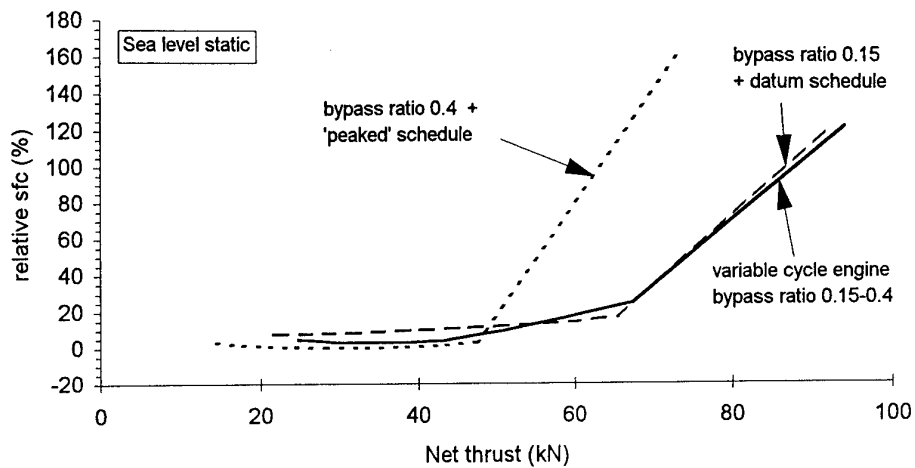


Figure 19 Variable cycle vs Fixed cycle sfc loop

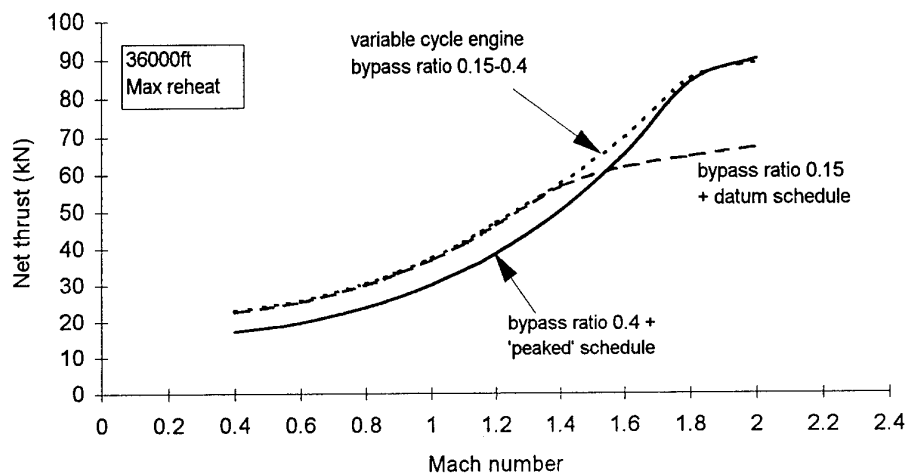


Figure 20 Variable cycle vs Fixed cycle thrust profile

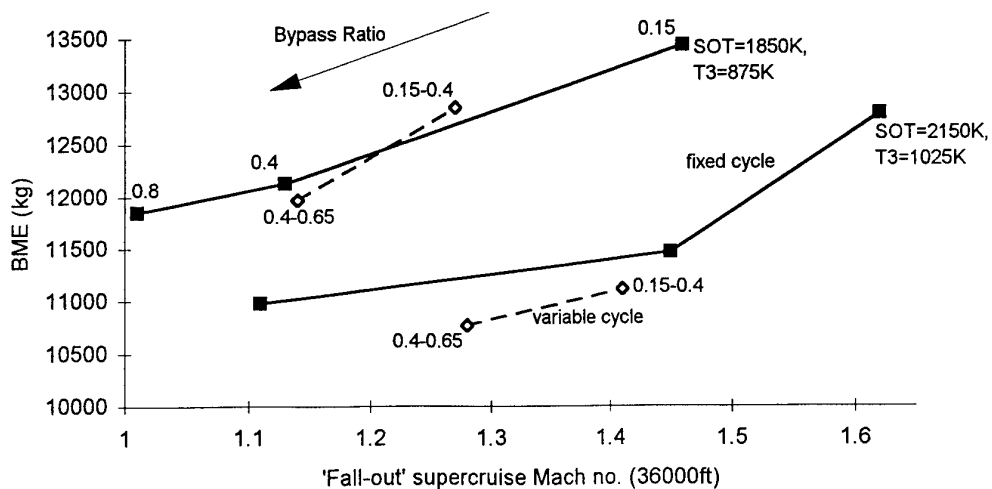


Figure 21 Variable cycle vs Fixed cycle (CAP mission)

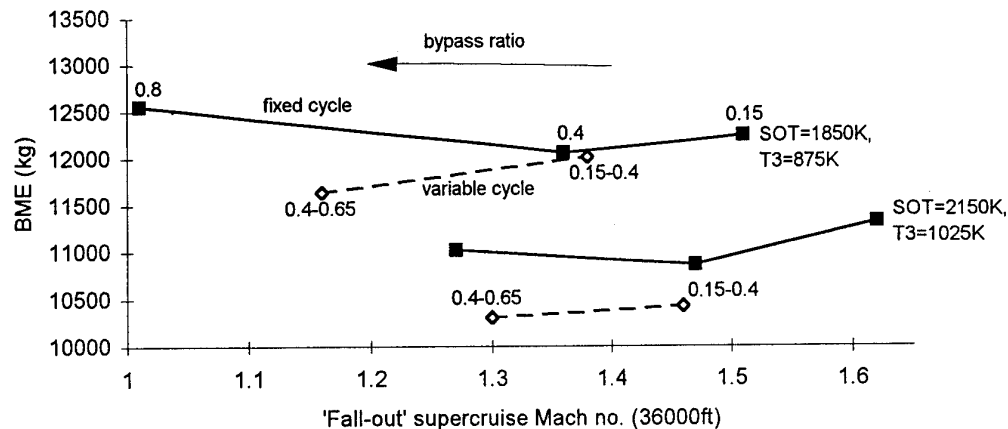


Figure 22 Variable cycle vs fixed cycle (Intercept mission)

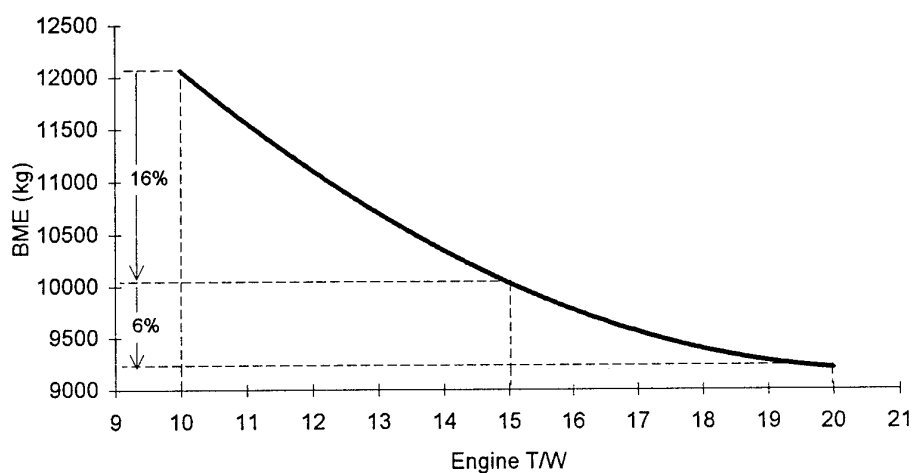


Figure 23 Effect of engine thrust/weight ratio (CAP mission)

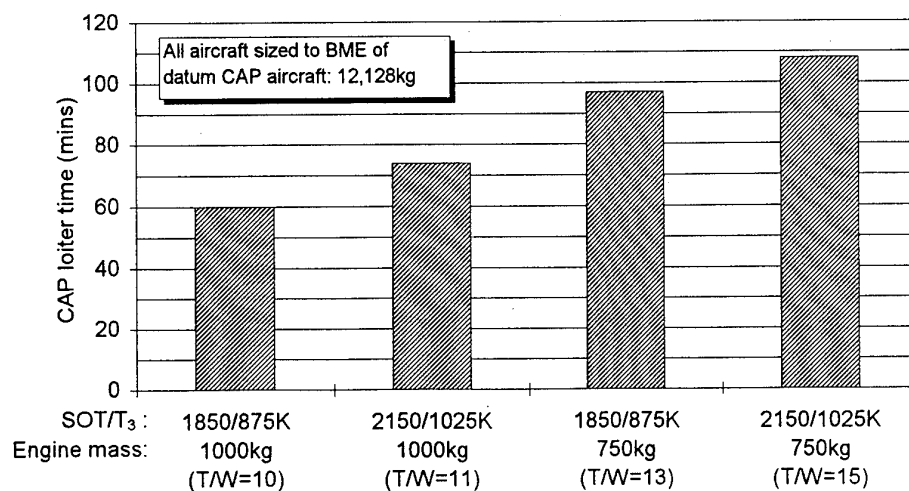


Figure 24 Ability of advanced technology to increase CAP time

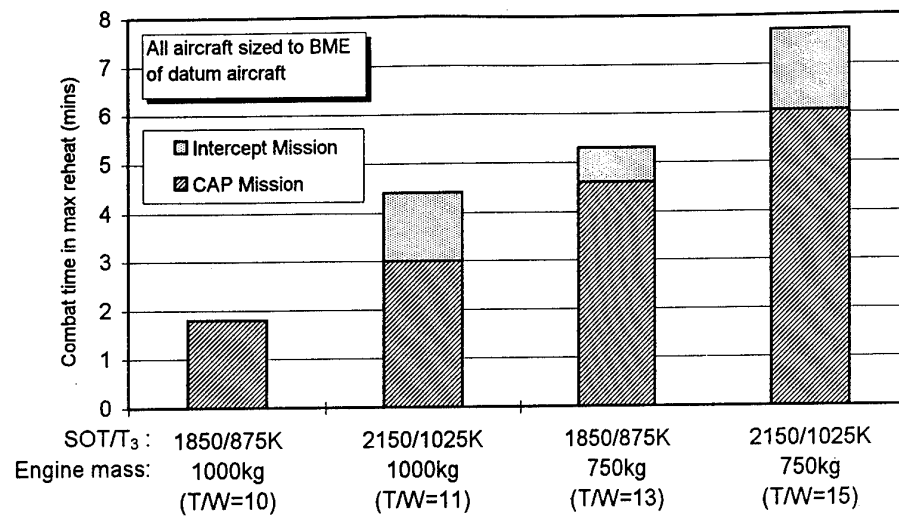


Figure 25 Ability of advanced technology to increase combat time

Paper 4: Discussion

Question from Dr P Pilidis, Cranfield University, UK

At Cranfield we have found that there are some weight penalties associated with variable cycle engines, for example, the need for an extra compressor stage and valves. Please could you comment about the weight issue. Could you also comment quantitatively on the efficiency compromises in the turbomachinery components?

Author's reply

It seems likely that a variable engine will have a greater mass than an equivalent fixed geometry engine having the same thrust. The main reason lies in its complexity - the need for variable mixers and variable compressor stages. An extra stage of compression may be required, although this will depend on the exact split between the LP and HP shafts, and hence on the cycle parameters. In percentage terms, the VCE will probably have a weight penalty in the region of 5% relative to an equivalent fixed geometry engine.

It is difficult to quantify the efficiency compromises of the VCE relative to a fixed geometry engine, since this will depend to some extent on the cycle parameters. However, in general terms the variable cycle engine described here places more work onto the HP shaft. The LP turbine has a reduced loading, and a higher efficiency might be expected here. However, the wider LP turbine diameter may limit the fan tip speed and increase fan loading, giving a lower efficiency. On the HP shaft, efficiencies broadly similar to a fixed cycle engine are expected, although flow distortion behind the T-stage may result in a shortfall of around 1% for the HP compressor.

Question from Dipl-Ing H Ross, DASA, Germany

You have stated that aircraft performance has been kept constant during the scaling process. What procedure has been used for the combat segment - constant time or constant performance such as energy gain or number of turns?

Author's reply

Both the Combat Air Patrol and Intercept missions contain a combat leg which is modelled as a 360°, 3g sustained turn at Mach 1.6/36,000ft; this equates to a fixed turn rate and hence a fixed time, regardless of the particular aircraft. In order to assess the ability of advanced engine technology to improve combat persistence, the number and turns at 3g Mach 1.6/36,000ft were progressively increased until the resulting aircraft had the same mass as the datum. All the optimised aircraft required near maximum reheat thrust to sustain turns at the above condition. The combat persistence results are therefore presented as the time in maximum reheat at Mach 1.6/36,000ft.

Advanced Combat Engines

-Tailoring the Thrust to the Critical Flight Regimes.

by K R Garwood
P Round
G S Hodges

Rolls-Royce plc, P.O. Box 3
Filton, Bristol BS12 7QE
United Kingdom

ABSTRACT

Future combat engines will operate at higher turbine temperatures and overall pressure ratios, which will enable high specific thrusts and good low power specific fuel consumption to be realised. The application of these technologies into aircraft needs to address the weapons platform requirements of agility, range and combat persistence. The influence of engine rating schemes and aircraft performance requirements are discussed with indications that higher specific thrust engines will be required for increased force projection.

INTRODUCTION

The ability of the gas turbine engine to produce thrust is a function of the thermodynamic cycle, and the air density used as the propulsive media. Since the ambient air conditions vary considerably throughout the operating envelope of military combat aircraft, so also will the thrust available. Aircraft drags vary significantly as the flight mach number and load factor changes and the sources change from skin friction and form to wave and lift dependant losses. The imposition of aircraft performance requirements demanding higher agility leads to increased induced drags and hence thrust demand to sustain these manoeuvres at high system energy levels. The engine and aircraft designer need to work closely together such that the aircraft drags incurred in meeting the performance demands and the engine thrusts are matched across the whole flight envelope. Throughout the design process it is necessary to ensure this integration with the vehicle as intake spillage and post engine exit drags can dramatically influence the vehicle performance.

These studies based on a fixed wing, fixed intake aircraft style indicate how the engine designer can influence the way in which the engine develops adequate thrust. It addresses some of the penalties that increased manoeuvrability aircraft incur. The influence of increased range and then combat persistence are also assessed in two typified missions, and the levels of specific thrust for such aircraft indicated.

In order to perform these calculations it is necessary to have an adequate airframe and engine mathematical model with which to estimate mission and in-flight point performance capabilities. Requirements for the aircraft can then be superimposed and the impact on aircraft and engine size assessed.

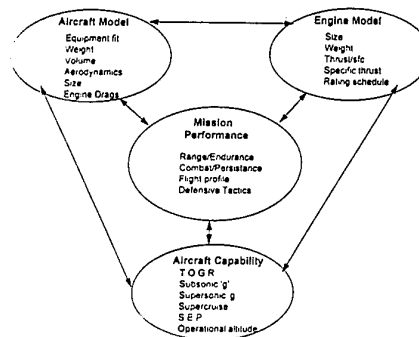


Fig. 1. Interaction between the airframe and engine models, and aircraft capabilities and missions.

In this simplified approach the point performance and combat activities are prescribed. In a real case the levels of combat capability and persistence, both close combat and beyond visual range, would derive from sophisticated 'man in the loop' simulations of candidate solution vehicles, such as Ref (1), as well as probabilistic methods for combat effectiveness.

AIRCRAFT MODEL

In order to generate an airframe model it is necessary to define a reference airframe configuration and technology level, decide the number of engines and crew, and select the avionics and weapons fit. The next most important selection is that of maximum dynamic pressure and design factor which the aircraft will experience. These impact the component structure weight, and hence have a direct influence on the solution airframe size and weight. A fuller description of the airframe packaging process can be found in Ref (2). For all examples used in this paper a twin engined single crew aircraft, canard configuration will be considered, with airframe and avionics technology consistent with entry into service early in the 21st century.

Against the various missions a raft of unconstrained solution aircraft are generated by this process. Fig 2 shows the effect of wing loading and engine scale on the resulting aircraft weights for a combat air patrol mission similar to that identified later. In this particular study, engine thermodynamics and physical properties are for a low by pass ratio reheated turbofan engine.

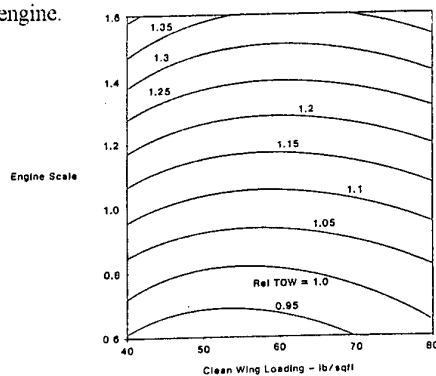


Fig 2 - Unconstrained solutions for typical 'CAP' missions.

At all points in the above figure a solution exists which satisfies the requirements of the study mission, but each has a different balance of point performance capability. As indicated in Fig 1, this aircraft point performance capability is also influential in the final solution aircraft. So, although a mission may not demand a certain capability, the aircraft are configured as capable of that performance.

We can now superimpose some of the constraints into Fig 2 and select the aircraft capability. Fig 3 shows how the two constraints of increasing cruise mach number with dry engine operation, and increasing 'g' capability at altitude lead to demand for increased engine size, and hence by virtue of the requirement for constant mission capability, increased aircraft weight.

For clarity the figure does not indicate other constraints such as attained turn rate which effectively sets the wing loading. The 'best' solution aircraft is one that satisfies the point performance at the lowest aircraft take off weight and generally the smallest engine scale factor, since these factors are indicative of both first and Life Cycle Cost.

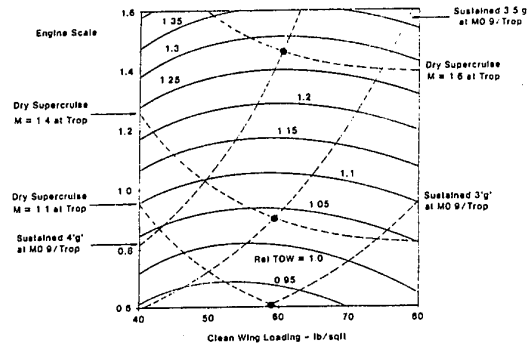


Fig 3 - Influence of aircraft capability on aircraft and engine.

At a wing loading of around 60lb/sq.ft. it can be seen that as the point performance requirement changes for 3 'g' to 4 'g' at the tropopause, so the engine size in the solution aircraft increased by 150% which pushes aircraft weight up by 35%. As a result of providing adequate reheat thrust to satisfy this requirement and generate high manoeuvrability, dry supercruise capability is also enhanced. Whilst the numbers change with wing loading the trend of high agility leading to enhanced supercruise capability remains.

All of the preceding analysis has been done using a singular engine thermodynamic and geometric model which can be scaled for physical size. It is important to determine the influence of engine cycle and rating structure on the resulting aircraft performance.

THE ENGINE MODEL

The engine thermodynamics represents the major activity supported in the engine model. Maximum gas temperatures, in conjunction with maximum component temperatures determine the requirements and viability of cooling. The internal air system necessary to achieve these requirements then influences the power potential of the motor. During the very preliminary stages the utilisation of the engine with the airframe will not have been determined and modifications of the engine cycle will need to be considered in the form of raised cooling or stressing criteria as the utilisation patterns are developed.

With initial cycle conditions established, the component engineers are now capable of assessing the level of efficiencies for each component. Major criterion such as stressing of the turbines, and torque capacity and whirling speeds of the shafts lead quickly to an engine layout. From this the engine envelope (both axial and diametrical) can be determined, including accessory packaging. These data in conjunction with centre of gravity and moments of inertia form the information necessary for the aircraft packaging programs. As may be expected, much of this process is optimised within the computer. This requires that an adequate data base of advanced technology materials and components are readily available; something that is not always the case when dealing with future engines and airframes.

As will be highlighted later, the requirement for component characteristics at off design conditions is soon established. The military engine spends little time at its nominal design point and particularly LP and HP compressor off design efficiency contours are necessary for evaluation of realistic aircraft range or duration calculations. Propulsion nozzle scheduling that alters essentially the LP compressor running line offering the opportunity to track peak fan efficiencies as the speed and mass flow changes, also affects the external drags of the aircraft. Although the engine maker is only responsible for the uninstalled engine, it is essential that the intake and exit drags are correctly and accurately assessed. This is particularly true when engines with differing mass flow variations from sea level static to flight condition are being considered. One of the ways that the engine designer can influence this variation is by changes to the rating system.

ENGINE RATING SYSTEMS

Under ideal thermodynamics a fully rated engine would maintain the same cycle if turbine temperature was proportional to the inlet temperature. However, this situation is not realised, even for a simple turbojet since real gas and component efficiency effects vary throughout the flight envelope. The following need to be considered as variants to the "ideal" non-dimensional thermodynamic engine

- Real gas effects (Cp vs Temperature)
- Reynolds number variations
- Dissociation effects at higher temperature
- Pressure dependency of reheat system

In addition there are normally practical limitations that further prevent maintenance of the ideal non-dimensional thermodynamic engine. These include

- Shaft speed limitations
- Pressure differential limits
- Metal temperature and cooling limits
- Clearance changes influencing component efficiency

All the above combine to make the concept of an engine running at the same cycle regardless of inlet temperature to be a misconception.

Fortunately, the aircraft requirements combine to make the necessity for such an engine also a misconception. Around the flight envelope the absolute thrust requirement will change, and the following are presented as potential thrust sizing conditions.

- Take off ground roll
- Subsonic Rate of Climb
- Subsonic 'g' capability at altitude
- Supersonic 'g' capability
- Supersonic dry engine persistence
- Transonic dry excess power

The above considerations lead to typical rating schedules for combat engines as shown in Fig 4

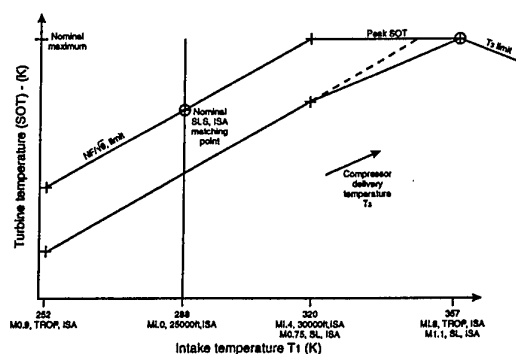


Fig 4 - Typical engine rating system for effects of intake temperature

At low intake temperatures the LP compressor is maintained at maximum aerodynamic speed and both compressor delivery temperature and turbine inlet temperature rise with intake temperature, consistent with maintaining the thermodynamic cycle. At some intake temperature the peak turbine temperature (combustor temperature rise) will be experienced. Further increases in intake temperature lead to a reduction in fan non-dimensional speed and hence intake flow and a smaller reduction in the HP compressor non-dimensional speed. Although the turbomachinery generated cycle pressure ratio is reducing, the effect of increased intake temperature is to increase the compressor delivery temperature.

At some point this compressor delivery temperature will reach a maximum, such that the combustor wall cooling and the HP turbine cooling air supply temperatures are at their maximum. This condition determines the cooling effectiveness targets for the majority of components in the engine. Further increases in intake temperature lead to significant reductions in turbine temperatures as the engine has to be downsped in order to respect compressor delivery temperature. Such down spooling leads to large reductions in engine flow. The flow reduction will of its own lead to power reduction, and can also be the cause of significant intake spill and post-exit exhaust drags.

The engine designer has the relationship of turbine temperature with inlet temperature as a design variable. In order to highlight the effects of variation two examples will be discussed.

Rating for thrust at low intake temperatures

In the first example (Fig. 5) a common core is used to power two different low pressure systems. Both engines are matched to 357K inlet temperature (Mach 1.8 at the Tropopause in an ISA climate). The core compressor pressure ratio, flow and peak turbine temperatures are maintained constant whilst the components within the LP system are designed to accommodate the changes in the $SOT \sim T_1$ schedule. By introducing an arbitrary +170K SOT difference at low inlet temperatures (i.e. rating schedule changed from "A" to "B") the same nominal core can now drive a significantly higher flow and pressure ratio LP compressor. Since the 'B' rating has utilised the maximum SOT by 288K inlet temperature the engine has to be progressively throttled back as intake temperature rises. At the 357K inlet temperature both 'A' and 'B' engines are now operating at the same thermodynamic cycle. However, the 'A' rated engine has only been rejecting flow since 320K inlet, as opposed to the 'B' that has been rejecting flow from 288K inlet. Fig 6 shows this variation for fan performance.

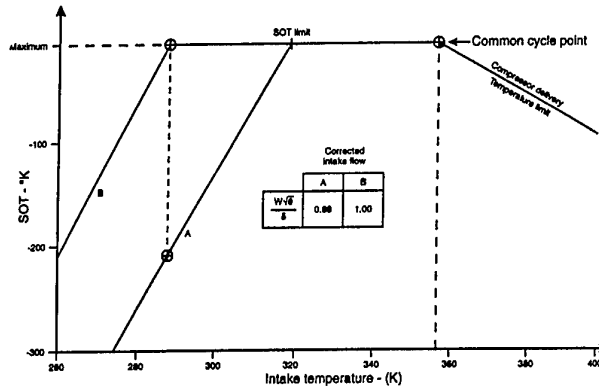


Fig 5 - Changes to engine rating to improve low intake temperature thrust potential.

At 357K inlet the common core will drive the LP compressor at both 'A' and 'B' ratings to the same non-dimensional point of mass flow and pressure ratio (assuming a similar final nozzle schedule, which is a function of the LP component efficiencies). This implies that the net thrust of the engine would be the same at this condition

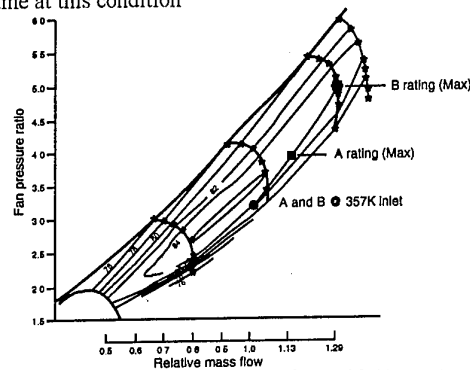


Fig 6 - Fan operating points with 'A' & 'B' rating schedule.

On decreasing intake temperature the common core, scheduled as 'B' will power the LP compressor through the 'A' maximum fan performance to the 'B' maximum fan performance. Approximately 14% more flow can be compressed which directly represents +14% more power. Since the fan pressure ratio is also increased so the specific thrust of the engine is likewise increased, further amplifying the increase in low inlet temperature thrust.

At face value this 'B' rating schedule has all benefits and has no disadvantages. However as Fig 6 indicates the flow variation between 'B' and 'A' rated engines from 288K to 357K intake temperature is more than doubled. Sizing of the intake for the maximum (Low T_1) non-dimensional flow can easily lead to intake spill drags that significantly reduce the full installed thrusts at 357K.

Rating for Improved Cycling Efficiency

In this example an engine that has the same LP compressor map as the above 'B' rating will be utilised. As Fig 7 indicates, the intake temperature at which the peak compressor delivery temperature is reached is reduced from 357K to 320K. The core is also operating at higher temperatures at these T1's, when the throttle is wide open, which must be recognised when engine life is estimated.

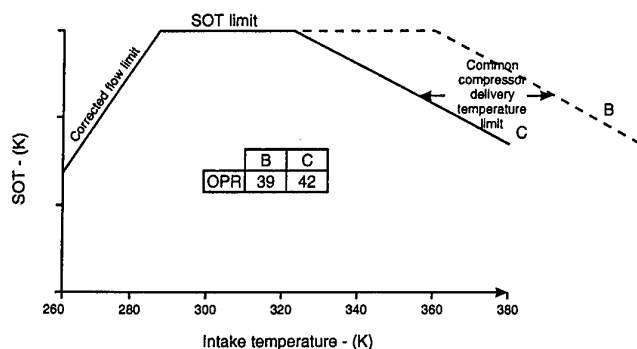


Fig 7 - Engine Rating changes to improve fuel efficiency.

The increased T_3 at lower intake temperatures indicates a higher cycle pressure ratio (42 cf. 39). At the same intake flow sizing this implies smaller rear stage compressor, combustor and HP turbine size. Typically the increased cycle pressure ratio will demand at least one more stage in the core compressor. The resulting change in the thrust/sfc loop at a typical loiter flight condition is given in Fig 8.

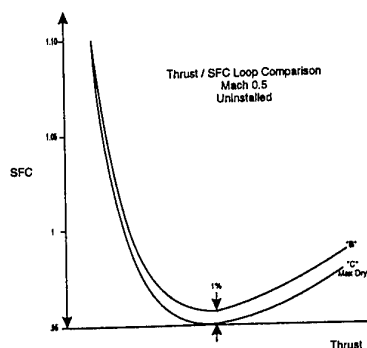


Fig 8 - Thrust~ sfc comparison for 'B' and 'C' rated engines.

A maximum improvement in sfc of 1% is realised in this relatively high specific thrust engine. At low power settings this improvement reduces to an insignificant difference. This area is however of particular importance when considering the degree of

close combat capability to be given to the aircraft, and will be discussed in more detail in a later section.

Rating Comparisons

The above sections have examined some of the thrust and fuel burn differences associated with different ways of rating engines, primarily by scheduling turbine inlet temperature with intake temperature. The table below summarises the relative capabilities at the sea level static, ISA intake temperature of 288K.

Cycle match point at S.L.S. ISA, uninstalled.

Engine Rating	A	B	C
Relative Flow	100	114	114
Fan Pressure Ratio	4.1	5.0	5.0
Overall Pressure Ratio	30	39	42
SOT (K) (@ SLS, ISA)	-170	Max	Max
Peak SOT	<—	Ref	—>
Peak T_3	<—	Ref	—>
Rel. Net Thrust			
Reheat lit	100	123	123
Dry	100	130	130
Rel. s.f.c.			
Reheat lit	100	92	92
Dry	100	106	105
Specific Thrust			
Reheat lit	122	133	133
lb/lb/sec Dry	77	88	88

Of more importance is the thrust potential of these different rating schedules around the flight envelope. Figures 9 and 10 indicate the influence of intake temperature on the capability of these engines to produce thrust. Taking engine rating structure 'A' as the reference, then 'B' rating offers considerably more dry and reheated thrust at all intake temperatures below 320K..

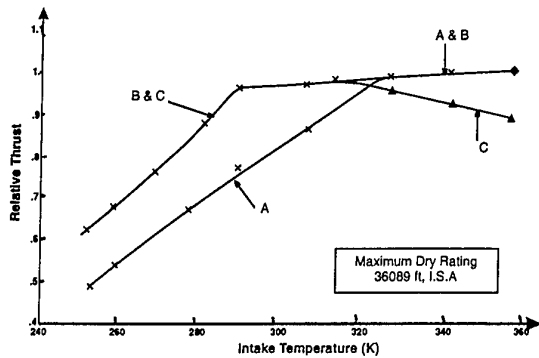


Fig 10 - Comparison of dry engine power availability.

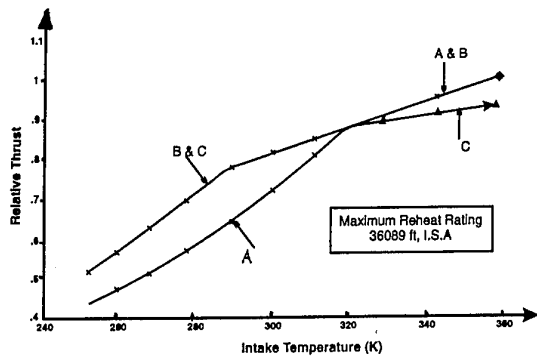


Fig 11 - Comparison of Reheated power availability

By rating engine 'C' with a higher turbomachinery pressure ratio, then the compressor delivery temperature limit (i.e. HP Turbine blade and disc cooling) operates at a lower intake temperature and larger downspooling is required.

Beyond the intake temperature of 320K where the peak compressor delivery temperature is realised, then engine 'C' is throttled back to maintain this limit. By 357K T_1 'C' will have rejected significantly more flow than 'B' and will be generating spill and afterbody drags that are proportionally higher than those of 'B'.

INFLUENCE OF AIRCRAFT MISSION REQUIREMENTS.

In this section the effects of cycle type will be examined against the potential requirements for future combat aircraft. The missions are characterised into two simplified models. The combat air patrol (CAP) mission is characterised by the large amount of fuel consumed at subsonic loiter conditions. Following the cruise out and loiter the aircraft performs a maximum

throttle, fixed duration combat with weapon release. Return to base is made at optimum flight conditions.

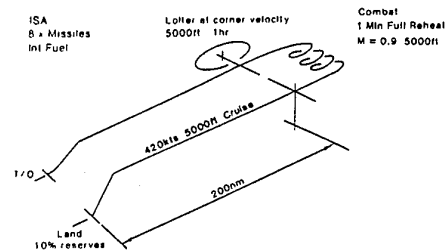


Fig 12 - Typified Combat Air Patrol Mission

The intercept mission utilises high engine powers to maximise time for response. Minimum time to height, a high Mach number approach to the combat zone, followed by a fixed manoeuvre sequence and weapon release at maximum power settings lead to optimum engines with high specific thrusts.

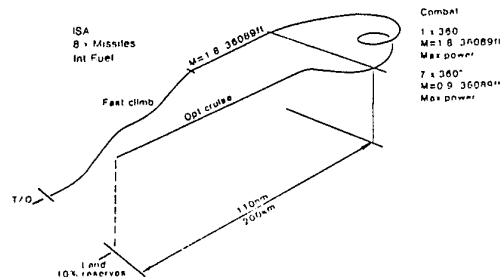


Fig 13 - Typified Intercept Mission

These simplified missions reflect European operation styles and tend to differ from those identified in Reference 3. It is not the purpose of this paper to make comparisons between these operational styles, simply to note that the missions will be scenario and tactically dependant, and a wide variety of these would need to be assessed to determine the optimum characteristics of the airframe and engine combinations.

With the tendency for increased force projection the influence of range and combat persistence need to be assessed. Three engine types, with their inherent performance and geometric characteristics have been modelled in the aircraft packaging and mission modelling system. Levels of aircraft in-flight performance capability have been maintained throughout the study, and turbine temperatures, cooling capability, construction methods and materials are consistent. The three engines types are

1. Similar specific thrusts to today's combat engines - with higher bypass ratio - deriving from increased turbine temperatures and higher cycle pressure ratio.
2. Similar bypass ratio to today's combat engines - with higher dry and reheated specific thrust.
3. Variable cycle engines - representing the highest specific thrust available at the turbine temperatures, but minimising the lower power sfc. penalties associated with higher specific thrust engines.

Engine 1 and 2 are rated at SOT ~T 1 schedule approximately half way between 'A' and 'B'. Engine 3 is rated as indicated in Reference 4.

Increase in radius of action

Figure 14 shows the effects that an additional 100 nautical miles radius of action implies on an aircraft in design.

Taking first the combat air patrol mission. It can be seen that at the datum radius of action the influence of increased specific thrust is to marginally increase the weight of the resulting aircraft, varying from 32000 to 34000lbs. The effect of adopting a mission requirement for an additional +100 nm radius of action is to substantially increase weight from 32000 to 42000lbs, reflecting the additional cruise fuel requirement and the resizing of the aircraft and engine thrust to achieve the mission and maintain the in-flight performance. Again the influence of engine specific thrust is very marginal between 75 and 95, while a slightly more rapid aircraft weight increase follows from 95 to 105.

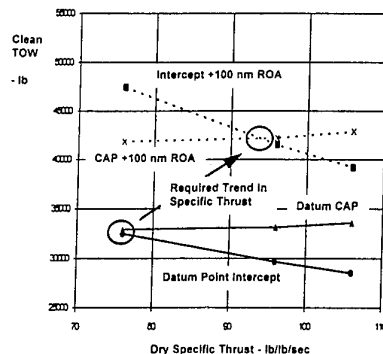


Fig 14 - Effects of increased radius of action.

With the datum Point Interceptor mission the specific thrust increases result in aircraft weight reductions

from 32000 to 28000lbs, in an almost linear relationship. When the radius of action requirements are increased the results are similar, but with an even stronger influence of increased specific thrust reducing the aircraft weight.

Increased combat persistence.

Fig. 15 indicates how the requirement for an additional 2 minutes at combat condition, at the datum R.o.A. influences aircraft weight and preferred specific thrust of the engines. The datum curves are the same as for the R.o.A. changes, with the CAP mission insensitive to specific thrust up to 90 then a small increase in weight as the specific thrust rises to 105. The intercept mission benefits from maximised specific thrust.

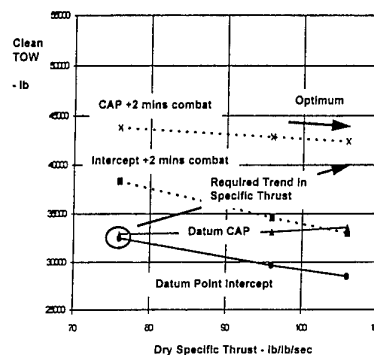


Fig 15 - Effects of increased combat duration.

At the increased combat time both the intercept and the CAP missions benefit from maximisation of specific thrust. This is different from the increased range where there was a small influence against adopting the highest available specific thrust for the CAP mission.

However, if a fighter engine is to satisfy both combat air patrol and intercept roles then further demands for increased power projection and persistence would seem to indicate that an increase in dry specific thrust is beneficial.

INFLUENCE OF INFIGHT PERFORMANCE.

In this section only two engine standards will be considered. They are engines 2 and 3 from the preceding section. Engine 2 represents an engine optimised for the combat air patrol role with a dry specific thrust circa 95 and referred to as FGE (Fixed

Geometry Engine) The other engine, engine 3, is referred to as VCE (Variable Cycle Engine) and represents the interceptor style, where maximisation of specific thrust is most beneficial. Two flight conditions will be considered as indicators of potential combat areas

- 0.9 M. tropopause

-1.8 M. tropopause

These two flight points can be considered as indicative of the subsonic close combat capability and the supersonic beyond visual range/escape capability.

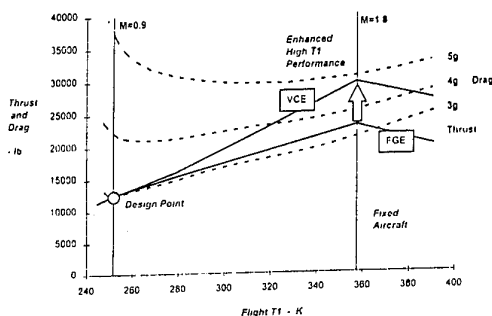


Fig 16 - Aircraft drag and engine thrust availability for varying 'g' capability.

Their relativised thrust requirements are shown in Fig 16. Superimposed on the aircraft thrust requirements are the engine thrust characteristics for both the FGE (engine 2) and the VCE (engine 3). It is apparent that FGE with its SOT-T1 schedule effectively supports the 3G aircraft drag contour whilst the VCE progressively supports higher G capability at increasing inlet temperature (flight mach number).

Subsonic G capability (At 0.9 M tropopause)

As indicated in Fig 16 the thrust requirements for subsonic 'g' capability escalate much faster than at supersonic conditions. An engine designed to provide a 5 'g' capability across the range of T1, demands a rating philosophy which will lead to inefficient operation as T1 rises. The engine will progressively have to be spooled down generating high spillage and afterbody drags as Mach number increased. Clearly if a wholly subsonic aircraft was to be considered then wing loading and aspect ratios could be selected that enabled such a high G and the engine rating scheduled to provide adequate power at this low intake temperature.

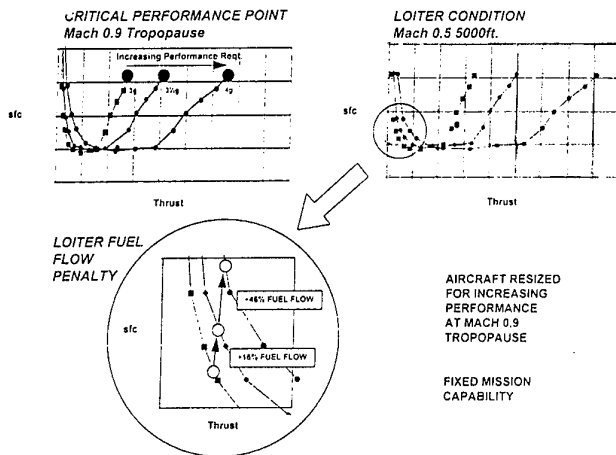


Fig 17 - Effect of increased subsonic 'g' capability on engine operating conditions.

Fig 17 indicates the effect of progressively sizing the aircraft for higher subsonic G capability at 0.9M tropopause. Increases in maximum engine thrust requirements are non linear with a 30% increase from 3 to 3.5 G but a 150% increase to go from 3 to 4 G. Since the engine is at full re-heat power then the thermodynamic cycle (i.e. sfc) is constant although the physical size and thrust of the unit would be changing.

If we now consider the influence that this requirement for high 'g' manoeuvrability imposes on the range potential for the engine/aircraft combination then a typical loiter condition of 0.5M 5000 feet can be used. Firstly it is apparent (from figure 17) that the 1G flight case is not at maximum dry point nor at the bottom of the loop on the sfc curve, but at low throttle settings. With reference to the "3G" engine then the "3.5G" capability incurs a +16% fuel flow increment, and the "4G" aircraft is some 46% worse than the "3G" aircraft. It is for these reasons that the component engineers need to have accurate and reliable off design prediction codes.

The leading engine parameters that relate to the engine operating conditions at this critical and often contractual flight condition are listed below.

Installed Performance at M=0.5, 5000 ft

	Max Dry	Cruise	Cruise	Cruise
		3.0g Sized	3.5g Sized	4.0g Sized
Rel. Thrust	1.00	0.19	0.13	0.09
OPR	35.6	10.53	8.76	7.2
Fan Rc	5.4	2.12	1.87	1.66
SOT (K)	Max	-750	-840	-930
Rel. sfc	1.0	1.08	1.17	1.28

It would appear that the expense and difficulties of equipping an engine with high overall pressure ratio capability have been negated by the demand for high agility. However at these low thrust points it is the proportionally higher OPR relative to today's engines that strongly influences the back of loop sfc. It is for these reasons that the engine designer is exploring flow modulation in the core engine (e.g. Ref 5).

Supersonic G Capability

As indicated in Fig 16 the major maximum thrust differences between FGE and VCE are at the higher inlet temperatures.

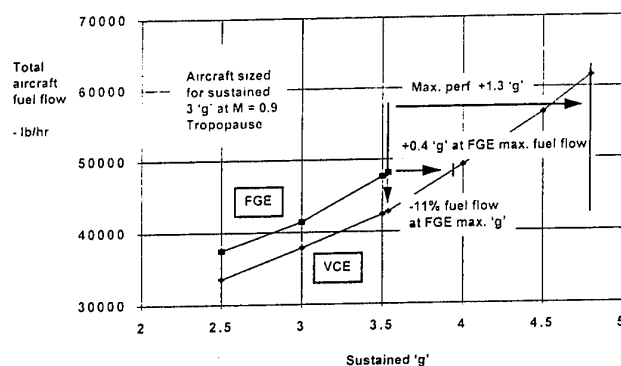


Fig 18 - Influence of increased 'g' capability at supersonic flight conditions.

The above figure shows that the increased performance available from the VCE compared to the FGE can be traded in numerous ways. If the aircraft has a high combat survivability at the lower G capability then the VCE can provide an 11% increase in combat persistence. At the same fuel flow hence combat time an 11% increase in 'g' capability is available, but should escape manoeuvres or other considerations demand then a 36% increase in 'g' capability is on hand at maximum thrust.

DISCUSSION AND CONCLUSIONS.

The engine developer, in conjunction with the airframer, and military operator need to work closely together to ensure that the required and economically achievable weapons platform characteristics are prescribed. The major influence of the engine, once the level of technology within the engine is established (i.e. component efficiency, cycle peak temperatures and structural efficiency) is the rating structure of turbine temperature against intake temperature.

As the capability to operate at higher turbine temperatures is acquired, so the potential of increased specific thrust becomes a greater reality. Due to the increases in cycle pressure ratio the traditional penalties of high specific thrust engines being high on fuel consumption at part power are being overcome. The development of flow modulated cores and variable cycle engines will further alleviate part power fuel consumption deficiencies. Aircraft designed to increase force projection, either by range or combat persistence will benefit by adopting higher specific thrusts than are currently available.

Increases in aircraft 'g' capability, particularly in subsonic, high altitude flight, can lead to a significant penalty of range potential. The 1 'g' throttle setting can be as low as 9% of dry thrust (approx. 6% of total thrust) for an agile aircraft. In such a condition the cycle pressure ratio is well below the thermodynamic optimum, and components, particularly the compression system are well away from their nominal design point. The engine designer needs reliable and realistic off design component characteristics at a very early stage to assess the potential of the engines at such low power conditions. It is becoming the norm that such flight conditions are contractual performance specification points, which only adds to the technology requirement impetus. Aircraft that have high 'g' capability have, as a consequence a higher dry thrust flight envelope which can extend to dry supercruise capability. When such aircraft are used with primarily subsonic operations then the hot section life will be thermal - mechanical fatigue dominated, with significant increase in temperature range from the steady level flight too the maximum throttle condition. If such aircraft are used for supersonic persistence then a creep dominated hot section design will be required.

Supersonic 'g' capability may also be enhanced as a result of subsonic 'g' enhancement. This is subject to the engine rating scheme and the style of engine (i.e. fixed cycle or variable cycle.) Such enhancements can either increase combat persistence at a constrained performance level, or improve capability and energy management during combat.

The preceding comments are pertinent to a vehicle capable of mach two operation. As such the range of intake temperature compromises the engine rating schedule. Vehicles of different flight speeds will have different demands on the engine, although a similar approach to matching the thrust requirements would be pursued.

Acknowledgements

The authors would like to thank their colleagues for their contributions, and to the management for permission to publish. The views expressed are those of the authors and do not indicate commitment by the company.

References

1. Seavers N, et Al
JOUST Air Combat Simulator Facility
DRA 1993
2. Denning R M, Mitchell N A.
Critical Propulsion System Parameters for
future STOVL Combat Aircraft
American Helicopter Society 1986
3. Coons L.
IHPTET Technology mission Pay offs at the
Component level - A look at Phase II
technologies.
Joint Propulsion Conference 1990
4. Garwood K R, Baldwin D R.
The Emerging Requirements for Dual &
Variable Cycle Engines
ISABE Conference 1991
5. Vignon H, Rodellar R, Silet J.
The advantage of variable geometry for
turbine engines at low power.
AGARD CP 421 1987

Paper 5: Discussion

Question from Dipl Ing H Ross, DASA, Germany

Please would you define what you mean by “aircraft agility”?

Author's reply

The term “aircraft agility” as used here is not strictly accurate. Agility is the rate of change of manoeuvre and by prescribing increased ‘g’ levels, the manoeuvrability is increased. However, since it is the engine and not the airframe that is enabling this increased ‘g’ to be achieved, the potential for significantly improved energy management and energy recovery is given to the weapons platform. When considered in terms of the close combat and beyond visual range combat parameters, the effects can be considered as equivalent to improved agility - so long as the airframe has adequate control authority for these flight conditions

The STRATO 2C Propulsion System A New Compound Engine and Control Concept for High Altitude Flying

H. Tönskötter, D. Scheithauer

Industrieanlagen-Betriebsgesellschaft mbH (IABG)
Einsteinstraße 20
D-85521 Ottobrunn
Germany

SUMMARY

The propulsion system of the STRATO 2C High Altitude Long Endurance Aircraft (HALE) is an example for the development of a power plant which is tailored to a special unconventional usage and even though takes advantage of the reliability and low cost of available components as well as the high technology of turbine engines. The disadvantage, a compromise in the optimization of the propulsion system, did not jeopardize the overall design philosophy.

The task of designing a low risk, low cost control system was achieved by

- a conventional certified piston engine control system and
- a new digital control system for matching the turbocharger stages under steady state and transient operating conditions, for cooling flow control and for rotor speed and manifold pressure limitation.

On the basis of the control philosophy for matching the major components emphasis lies on the hardware and software design route.

Besides the design aspects experiences from the development and some results from testing the engine in a high altitude test facility and in a demonstrator aircraft are presented.

1. INTRODUCTION

End of March 1995 GROB*) started flight testing of the STRATO 2C demonstrator aircraft (POC). The STRATO 2C is an all-composite manned High Altitude Long Endurance Aircraft which will be used by the DLR**) to conduct stratospheric research work at altitudes up to 24 km.

Development of the STRATO 2C began in May 1992 and in less than 3 years the aircraft was ready for flight testing. Two flight engines and one test engine have been developed, built and tested during that time. The tests were carried out on ground and in altitude test facilities at simulated altitude conditions of more than 24 km. Some details of the aircraft, the design missions and the propulsion system are described in Ref. 1.

Fig. 1 shows the STRATO 2C and the installation of the compound engines above the wing.

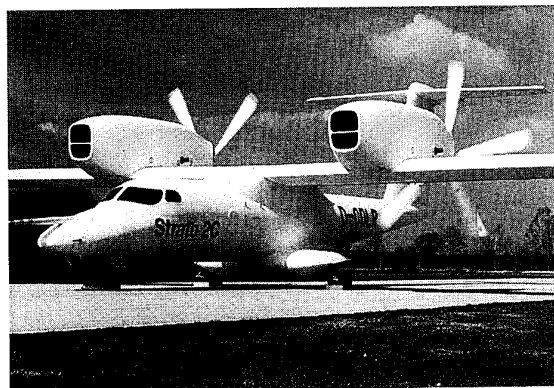


Fig. 1: Installation of the Engines on the STRATO 2C Aircraft

The STRATO 2C, as far as known the biggest all-composite aircraft of the world, has been developed and built by GROB. IABG, subcontractor of GROB, designed and developed the propulsion system and carried out the verification testing. The hardware for the engine was provided by the suppliers shown in Fig. 2.

The STRATO 2C engine is the first piston engine that was operated at altitude conditions of 24 km.

To reduce the risk, the program was divided in a Proof of Concept (POC) and Mission Aircraft (MAC) Phase. The aim of the POC-Phase is to demonstrate that the aircraft and the propulsion system are capable of operating at very high altitudes and that the Mission Aircraft will fulfill the Specification. The minimization of weight and fuel consumption and the demonstration of life and reliability as well as aircraft certification are the major tasks of the Mission Aircraft Phase.

*) BURKHART GROB Luft- und Raumfahrt GmbH & Co KG, 86874 Mattsies

**) Deutsche Forschungsanstalt für Luft- und Raumfahrt e.V., 51147 Köln

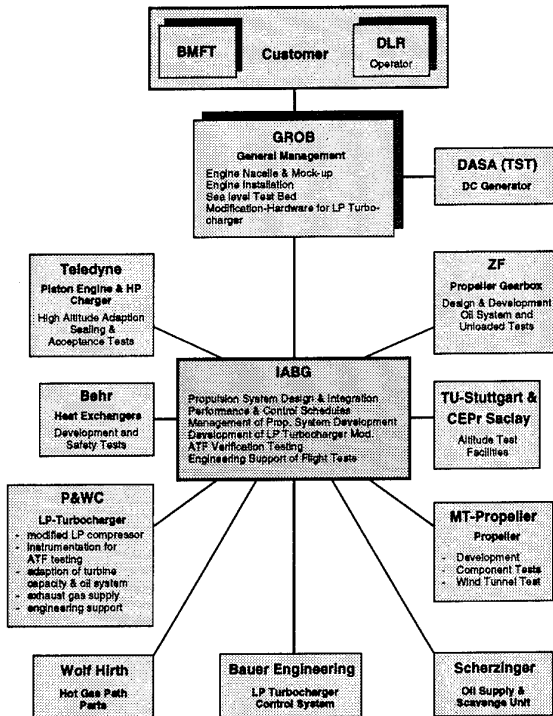


Fig. 2: Organization of the STRATO 2C Propulsion System Development

2. PHILOSOPHY OF PROPULSION SYSTEM DEVELOPMENT

With increasing altitude the necessary technology level for the components of a HALE propulsion system is increasing too. E.g. the turbocharging system of an engine designed for 25 km compared to 20 km features twice the compression pressure ratio, e.g. 48 instead of 24 and twice the flow capacity and the volume of the

heat exchangers is more than two times bigger.

Hence, for the STRATO 2C 24 km engine:

- maximum efficiency of the turbo components,
 - minimum pressure losses in the intercoolers and flow paths,
 - minimum weight,
 - minimum heat rejection
 - and minimum fuel consumption
- are absolutely necessary.

On the other side, the requirement of the customer was to develop and build the engine within 3 years and with total costs of less than 30 million DM.

This ambitious goal was only achievable by:

- Consequent usage of the High Tech and Systems Engineering Know How gained in other civil and military engine development projects.
- Extensive usage of available „High Tech Components“ of other aircraft engines and their adaptation to the HALE application.
- Systems Engineering performed by a small highly motivated team.
- Component development by small or middle sized companies supported by the „High Tech Know How“ of the Systems Engineering Team.
- Limited Documentation.

One example for the use of available „High Tech Components“ is the Pratt & Whitney Canada (P&WC) two-spool gas generator of the PW 127 turboprop engine which was modified for the STRATO 2C LP charger application as shown in Fig. 6.

The advantage was, that the P&WC gas generator is a very reliable proven component which incorporates the state-of-the-art technology in aerodynamics, performance, materials and design and which could be modified and delivered by P&WC within 2 years.

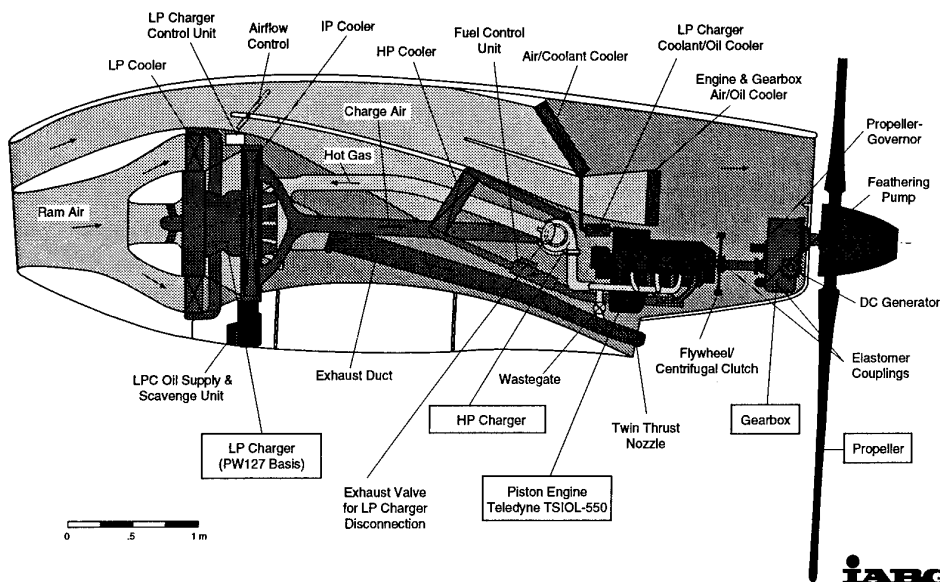


Fig. 3: STRATO 2C Propulsion System (POC)

On the other hand the disadvantage was that the integration of the intercoolers and of the hot gas supply to the turbine could not be fully optimized in terms of performance and weight, that a separate oil supply and scavenge unit had to be developed and that the turbine efficiencies are a little bit lower than possible, as the turbines are not optimized for the operation with changed capacities and switched-off cooling air to the vanes and blades.

The development of a completely new two-spool LP charger with the same technology standard would have been far beyond the cost and time frame of this project.

The limited use of available „Low Tech Components“ was possible for the demonstrator aircraft but is not acceptable for the Mission Aircraft as the contributed penalties in performance and weight are too high. One example is the POC HP Turbocharger which is a standard low cost component for general aviation engines.

3. POC/MAC PROPULSION SYSTEM

The target for the POC engine development was to demonstrate that the MAC engine will provide constant power up to 24 km, can provide up to 40 g/s bleed air for cabin pressurization in the single engine flight case and is reliable controllable during steady state and transient operation within the flight envelope of the aircraft.

Therefore, the minimization of fuel consumption and weight was not the primary target during the development of the POC engine. Fig. 3 shows the propulsion system and the arrangement of the components.

Piston Engine

The power of the Teledyne Continental TSIOL-550-A liquid cooled piston engine was improved by 15 % and the maximum speed was increased from 2700 rpm to 3100 rpm.

For the MAC a Single Engine Emergency Rating of 320 kW at 2700 rpm is desired and an optimization of the engine for the increased speed to reduce fuel consumption and allow lean operation at Max. Cruise Power (300 kW at 3100 rpm) will be carried out. Furthermore, the capacity of the oil sump will be increased from 12 to 20 liters for the Long Endurance Mission (Ref. 1).

The crankcase pressure is controlled by an absolute pressure regulating valve with a back-up pressure relief valve in parallel. The absolute pressure valve had to be developed as no suitable unit was available. To avoid icing at low power/high Mach or windmilling conditions the valves can be electrically heated.

Drive System

The propeller gearbox is driven through a 250 mm long drive shaft, two elastomer couplings and a centrifugal clutch. The clutch was developed by GROB to reduce the risk of too high torsional vibration during starting the engine, as a standard electric starter motor was used. Tests have shown, that for the MAC the centrifugal clutch can be replaced by a much lighter flywheel. The elastomer couplings are automotive

components with a weight of only 0.9 kg per unit (Fig. 4).

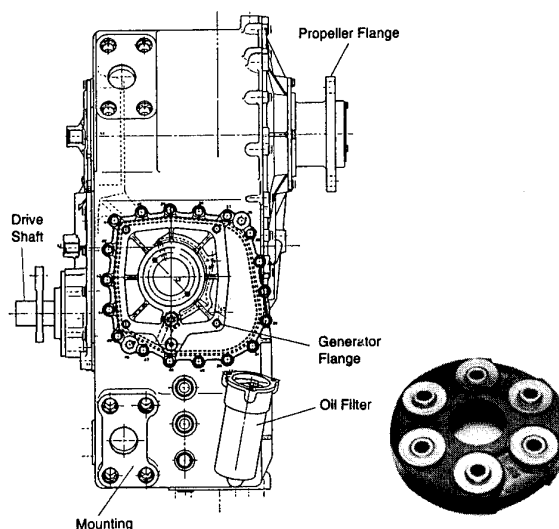


Fig. 4: Propeller Gearbox and Elastomer Coupling

One set of couplings has accumulated up to now under ground and altitude conditions more than 200 running hours without any signs of fatigue.

Propeller and Gearbox

For the POC a low risk propeller was developed with a conventional aluminium hub and five blades made of a wooden spar combined with a composite shell. The blade pitch is controlled hydraulically and a pitch stop in case of hydraulic pressure loss is integrated. Feathering of the non-rotating propeller or in case of a malfunction of the hydraulic control can be carried out by an electric feathering pump.

The 6 m diameter propeller was tested by the manufacturer MT-Propeller in a wind tunnel in Moscow and with the engine during the ground tests at GROB at different speeds and crosswind conditions. Flight testing showed no increased vibration of the blades and the bending load of the propeller shaft due to the downwash of the wing in front of the propeller was as low as expected.

For the MAC new all-composite blades with reduced blades stiffness will be developed to reduce weight and decrease the propeller shaft bending load under crosswind conditions.

The two stage reduction gearbox (Fig. 4) with a gearing ratio of 4.87 was completely new developed and has a dry weight of 63 kg including the integral oil system. Besides the propeller it drives the prop-governor and the alternator.

As no suitable oil cooled generator was available an 11 kW/28 V DC generator with a speed range of 6000 to 16000 rpm at maximum load was developed by DASA (TST).

Furthermore, the gearbox oil is used to drive the LP charger oil unit through an engine mounted hydraulic pump.

HP Turbocharger

A standard Garrett turbocharger was chosen for the POC engine. Only turbine wheel and housing material was changed to MAR-M-247 and HK 30 high temperature material to allow operating the turbocharger at turbine inlet temperatures up to 980°C with installed thermal insulation blankets.

The HP turbine is connected to the piston engine by an Inconel 625 exhaust system (Fig. 5) manufactured by W. Hirth GmbH. It incorporates three spherical bellows from Witzemann to allow engine motion relative to the frame mounted HP charger. Furthermore, the exhaust wastegate for MAP control is integrated.

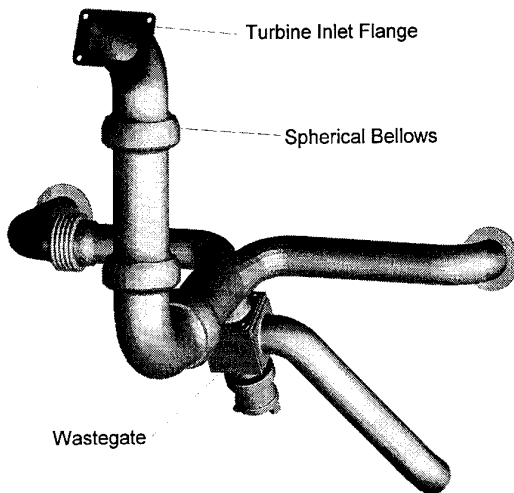


Fig. 5: HP Exhaust System with Spherical Bellows and Wastegate

For the Mission Aircraft a new turbocharger with improved performance and much lower weight is required. Due to the full containment requirement the reduction of the turbine housing wall thickness is limited. Therefore, a ceramic-matrix-composite turbine is considered.

LP Turbocharger

The LP turbocharger is derived from the two-spool gas generator of the P&WC PW 127 turboprop engine by the integration of LP and IP charge air intercoolers and

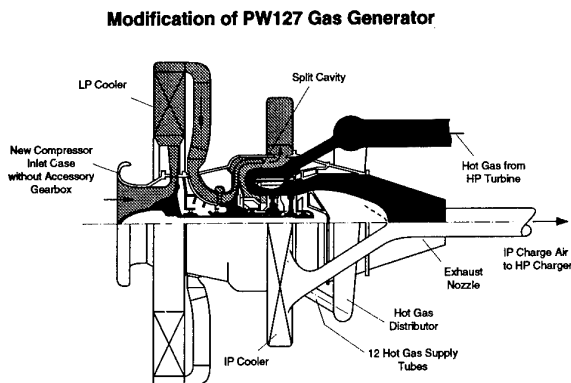


Fig. 6: LP Turbocharger Based on PW127 Gas Generator

by the introduction of an external hot gas supply to the IP turbine (Fig. 6 and Ref. 1).

In the LP charger application the turbines are running at lower speed (IPT 78% and LPT 90%) and lower turbine inlet temperature (850°C). Therefore, the cooling air to the blades and vanes could be switched off. Only the IPT liner and the turbine disks are still cooled.

A small penalty in turbine efficiency had to be accepted, as the turbine blading is not optimized for the operation without cooling air and with reduced capacity.

Furthermore, on the ground and at low altitudes the LP charger has to be disconnected from the piston engine, as the labyrinth seals of the bearing chambers and the turbine disk cooling are not working at very low rotor speeds (low pressure ratio) resulting in oil loss and overheating of the turbine disks. Furthermore, an unacceptable heat soak of the rear LP turbine (LPT) bearing after shutdown would cause bearing life problems.

Disconnection of the LP charger is accomplished by a hot gas bypass valve at HP charger turbine outlet. The task was to develop a valve that provides reliable operation at temperatures above 900°C with zero leakage in the closed position. This was achieved by a flap design with a spherical sealing surface. The flap is operated by an electrical actuator and is spring loaded when it is closed to compensate thermal expansion (Fig. 7).

To reduce the remaining hot gas flow to the LP charger when the valve is open in addition a non-sealing internal flap was introduced which is mechanically linked to the outlet valve (Fig. 7).

Up to now the exhaust valve ran on the test engine for more than 200 hrs without any problem. The valve is operated by the digital charger control system (CCS). It is closed at about 5 km during climb and opened again between 5 and 7 km altitude during descent depending on the power setting of the engine. The impact on manifold pressure and hence on engine power during the transition phase is very low.

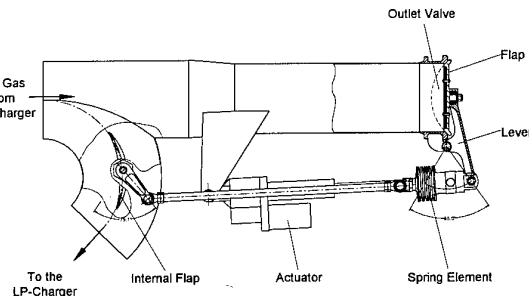


Fig. 7: LP Charger Hot Gas Bypass Valve

On the charge air side no bypass is necessary. When the LP charger is not running the HP charger gets enough air through the LP and IP compressors which are running slowly under windmilling conditions and through the open LP and IP bleed valves.

Engine and Charge Air Cooling System

After each compressor stage the charge air is cooled down to about 0°C by air-to-air coolers. The performance of the coolers was evaluated by measuring the temperature distribution at cooler outlet assuming constant temperature at cooler inlet. The result was that due to the low pressure loss in the cooler the cooler outlet had to be designed carefully to get a homogeneous charge air flow distribution within the cooler.

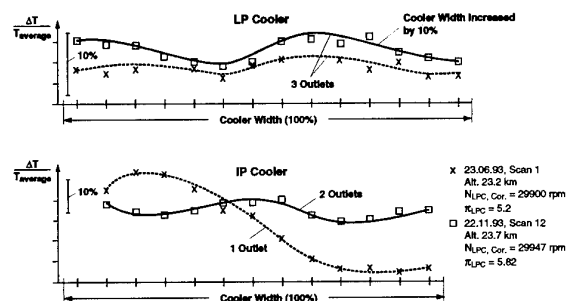


Fig. 8: Charge Air Temperature Distribution at Cooler Exit

Fig. 8 shows the temperature distribution at LP and IP cooler outlet and the improvement by the introduction of a second outlet at the IP cooler exit cover.

The former LP charger air/oil cooler which was mounted on top of the engine coolant cooler was replaced by a coolant/oil cooler (Fig. 3) to avoid blockage of the oil cooler at altitudes below 15 km were the necessary heat rejection to the LPC oil is very low (low LP and IP rotor speeds) and in addition the cooling air is very cold (less than -50°C).

As all heat exchangers had to be sized for the highest altitude (24 km) they are extremely oversized at low altitudes. Without cooling air flow control blockage of the oil coolers and manifold temperatures of -50°C and less would be the result. At very low manifold temperature the fuel/air ratio decreases and turbine inlet temperature at rich mixture setting increases. Furthermore, fuel vapourization and ignition capability become worse. Leaning of the mixture with decreasing manifold temperature is due to the characteristic of the fuel control unit which is a standard Precision Airmotive mechanical unit (RSA-7 and later RSA-10).

Therefore, different cooling airflow control systems have been investigated. Finally, the diffuser inlet flap (Fig. 3) in the front part of the nacelle was chosen due to the following reasons:

- One control device for HP charge air and fluid coolers.
- Lowest complexity and weight.
- Compared to nacelle outlet flaps no additional walls and sealings in the rear part of the nacelle are necessary improving accessibility to the engine.

The cooling airflow flap is controlled by the CCS as a function of altitude, ambient temperature and power setting.

For the mission aircraft the engine and gearbox air/oil coolers will also be replaced by coolant/oil coolers so that only one big air/fluid cooler remains which is easy to control.

The charge air coolers will not be changed as the air-to-air coolers offer the lowest weight and complexity.

Testing showed that a cooling fan for ground operation is not necessary as the propeller generates sufficient cooling air flow through the nacelle and as dissipation of the heat after shutdown is provided by convection.

Engine Frame

For mounting the engine components in the nacelle and attaching the propulsion system to the wing by four mounts an engine frame of thin-walled steal tubes was chosen instead of an integral composite frame due to the following reasons:

- Fire proof design.
- Electrical bonding of the individual engine components.

A finite element model was established taking into account the loads and stiffnesses introduced by the engine components and allowing the calculation of stresses, deformation and relativ movement of the components (Fig. 9).

The engine frame was designed for vertical acceleration of +4.7 g and -2.7 g and a forward acceleration of 6 g in combination with the maximum propeller drive torque and the bending moments under worst crosswind conditions.

For the mission aircraft the frame will be replaced by an all-titanium design, to further reduce weight.

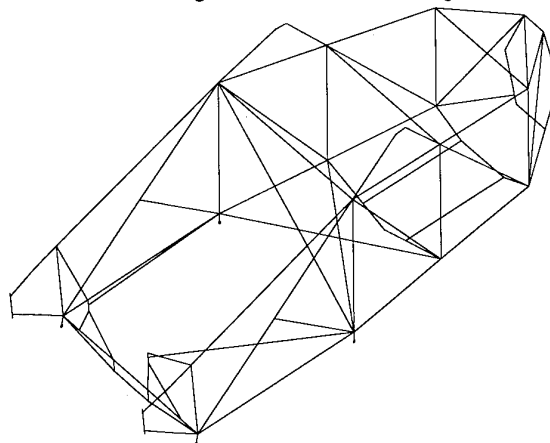


Fig. 9: STRATO 2C Engine Frame FE-Model

4. ENGINE RATING AND PERFORMANCE

ATF and flight testing showed that it is very difficult to control the engine precisely by manifold pressure (MAP) setting as at constant MAP a variation in manifold temperature (MAT) has a high impact on engine torque and power which are the life limiting parameters.

Therefore, during the POC flights the pilots run the

engine in the takeoff and climb phase at constant crankshaft torque. The engine speed is increased from 87% at takeoff to 100 % at high altitude climb to achieve best propeller efficiency. Fig. 10 shows the speed and max. power versus altitude.

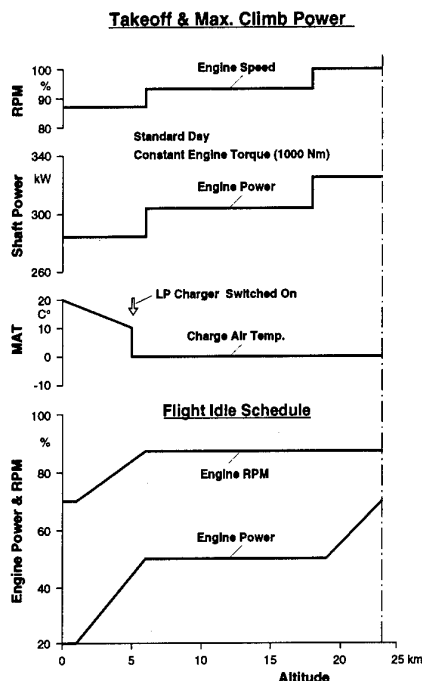


Fig. 10: POC Engine Ratings

For the mission aircraft an automatic (electronic) torque control system is anticipated to replace the hydromechanical MAP control system of the POC engine. In this case the Overboost Control will be replaced by an Overtorque Control.

Flight Idle power setting is limited by:

- Impending compressor/turbine power imbalance if the wastegate flow becomes zero and if e.g. the cabin bleed is increased at the same time.
- Minimum cabin bleed air pressure to ensure the required cabin pressurization.
- Minimum HP compressor surge margin, as increasing throttle losses in the fuel control unit (FCU) at low power settings and engine speed decrease surge margin.

Taking further into account a certain margin for engine component and control tolerance, varying cabin bleed flow and hot day conditions minimum Flight Idle power was limited to 50 % at altitudes between 6 and 19 km increasing to 70 % at 23 km and decreasing to 20 % below 6 km (Fig. 10).

5. ENGINE CONTROL SYSTEM

5.1 FUNCTIONAL REQUIREMENTS AND DESIGN CONSTRAINTS

In general, control of the STRATO 2C propulsion system consisting of a piston engine and three turbocharger stages is a complex task. A variable pressure ratio in the range from 1 to 40 has to be

guaranteed with an appropriate margin to the surge limits of all compressor stages.

The requirement to design a low risk and low cost control system affordable in the scope of the STRATO 2C development programme is somewhat contradictory to the complexity of the task.

No proven solution for the complete engineering problem was available. Well established is only the wastegate control of the single stage turbocharger of general aviation piston engines. To extend this control scheme to a three stage turbocharger was not found to be a realistic low risk perspective. On the other hand incorporation of a wastegate controller for one stage was a measure to reduce the development risk. In particular engine certification is easier if HP turbocharger and piston engine are controlled conventionally at low altitudes e.g. during takeoff and landing when the LP charger is disconnected.

In a second step an appropriate matching of the LP turbocharger with the basic system has to be ensured. This is performed by bleed valves downstream of LP and IP cooler as indicated in Fig. 11. The bleed valves are operated by an electronic control system named Charger Control System (CCS).

Although control of LP and IP bleed are the driving factors for the design of the CCS other more or less important functions are controlled by the CCS as well:

- The LP charger has to be deactivated at low altitudes. The oil supply to the bearings is switched off and the turbines are disconnected via an exhaust valve.
- Cooling air control flaps have to be actuated to keep oil and manifold temperature in the allowable operating range.
- For overspeed and overboost control a HP bleed valve has to be operated.
- Compressor surge has to be detected and the LP bleed valve has to be opened to clear the situation.
- The CCS has to indicate its own and the engine status to the pilot.
- For engine monitoring the CCS has to store the relevant data.
- The CCS has to assist in sampling data for flight test purposes.

The constraints to be considered for the design of the CCS are integrity and the need for a low cost implementation.

The basic integrity requirement of FAR Part 23.1309 is applicable to the CCS. This paragraph requires an extremely remote probability (less than 10^{-9} per flight hour) of catastrophic failure cases. The worst scenario identified for the CCS is that both engines failed and no restart is possible. It could be demonstrated during testing that the CCS has no influence on the restart capability of the engine at low altitudes. Due to this the CCS is no critical equipment. But in agreement with the national airworthiness authority it is classified as essential because cabin pressurization depends on running engines. In conclusion, the following requirements were derived for the CCS:

- Ensure that no single component failure leads to

an engine shutdown and provide a long reaction time to the pilots in case of malfunctions.

- Review the design and design the system thoroughly to avoid common mode failures leading to an engine shutdown.

With respect to the second requirement it has to be said that a software design error may effect both engines nearly simultaneously. Consequently, the software criticality was classified as Level B in accordance with RTCA/DO 178B. Another challenge with respect to integrity are the environmental conditions which the CCS is exposed to.

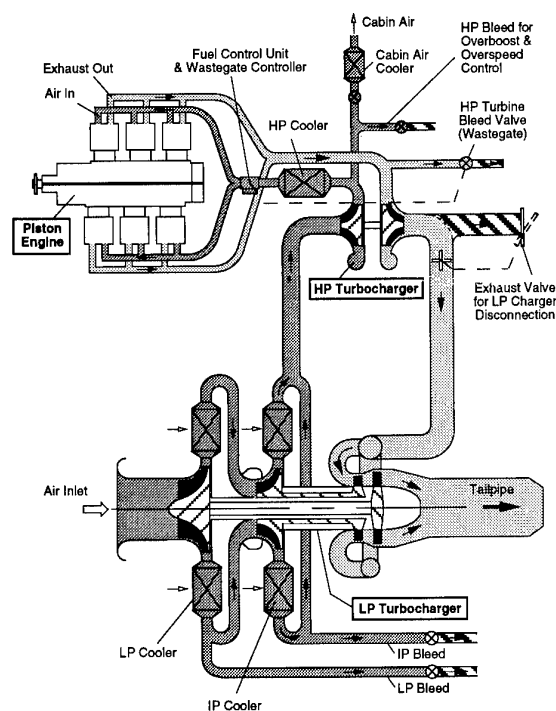


Fig. 11: Turbocharging System and Control

Most of the CCS units are installed in the engine nacelle to save wiring and weight. For example, cooling of the electronics is a more severe engineering problem of high altitude aircrafts compared with other aircrafts. With an ambient pressure of 30 mbar at maximum altitude convection cooling is not very efficient. One solution is the introduction of liquid cooling. Considering effort, weight and costs this was not favoured. Convection cooling was retained instead but power consumption is minimized and the mounting position of the CCS was optimized with regard to the thermal environment.

To achieve a low cost implementation a market survey was performed looking for off-the-shelf equipment. The analysis showed that a modification of existing engine control units was not affordable. Power consumption was too high, adaptation of actuator drives and to some extent also of sensor interfaces were expected, and a major software change to implement the required functionality for the STRATO 2C CCS was necessary. Even with all modifications it was still in doubt whether all requirements could be finally satisfied.

On the other hand a completely new development has a higher risk unless more advanced technology is available. In our case new components originally developed for the automotive industry build up the hardware design basis. High production numbers have led to an optimization of each component and reasonable prices.

5.2 SYSTEM ARCHITECTURE

Fig. 12 shows a schematic block diagram of the CCS. Concerning the essential control functions the CCS is a full duplex system with duplex sensors, duplex processors and for the design driving LP and IP bleed valve control also duplex actuators. This architecture provides at least full fail safe capabilities for the essential control functions. Additional contributions are made for improving the availability of the CCS by in-lane monitoring and reversionary operating modes.

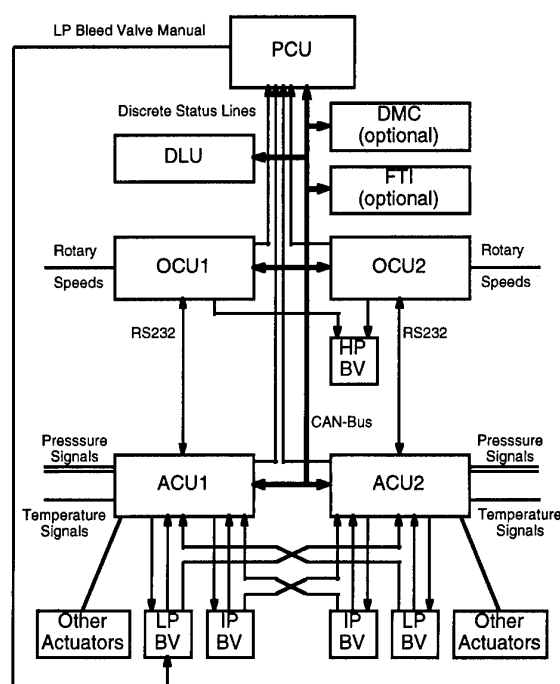


Fig. 12: Schematic Illustration of the Charger Control System (CCS)

Two processing functions are built in each channel. One of them is named Actuator Control Unit (ACU) because it drives all actuators except the HP Bleed Valve which is operated by the Overspeed Control Unit (OCU). ACU and OCU of one lane are assembled in the same housing. Fig. 13 shows a view of the CCS Control Computer housing. The design is modular organized into four layers. One layer is consisting of the ACU processor, the power supply and actuator drives.

The interfaces to all rotary variable differential transducers (RVDTs) for position sensing are built in a separate module. The third module comprises pressure transducers and interfaces for temperature sensors. The fourth layer contains the OCU. No common motherboard is installed. The layers communicate via connectors. No flexible wiring is required.

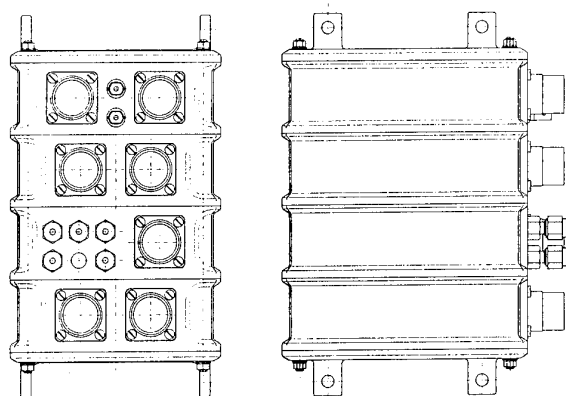


Fig. 13: CCS Control Computer

All four controllers are linked by a serial data bus to exchange sensor values and actuator positions as well as status information. In addition to the ACUs and OCUs the Pilot's Control Unit (PCU) and a Data Logging Unit (DLU) are connected to the data bus. The PCU displays status and warning information to the pilots and serves as input device. The DLU stores the information available on the data bus on a memory card for engine monitoring purposes. Optionally a Flight Test Interface (FTI) and a Diagnosis and Maintenance Computer (DMC) may be connected to the data bus. The DMC has several passive and active operating modes to assist in failure detection and system calibration.

The data bus is an implementation of a CAN-Bus originally developed for automotive applications. CAN is the abbreviation of Controller Area Network. Data on the CAN-Bus is organized in messages. Each message has a unique identifier that determines its priority. No central bus controller is needed to manage arbitration. Special contributions are made regarding data integrity and data consistency over the network. Due to its advantages the CAN-Bus is applied in many areas outside the automotive industry, e. g. as field bus for smaller plants and processes.

Although the data bus is the backbone of processor communication it is still simplex. To implement redundancy in case of data bus failures it was not efficient to make the data bus duplex. Other means were investigated to ensure continuing operation of the CCS and redundancy management in case of data bus failures. For data exchange of ACU and OCU in one lane a computer internal serial data link is incorporated running in parallel to the CAN-Bus. Operation of the bleed valves is still fail safe by cross-channel monitoring.

The positions of all LP and IP bleed valves are crossmonitored by each ACU while the HP bleed valve can only be operated if both OCUs command to open it. One hardwired status signal from each processor fed to the PCU is providing the pilot with rudimentary status information if the data bus has failed.

In case of total CCS failure the pilot can actuate the cooling air control flaps continuously and one LP bleed valve may be opened by pilot switch to allow the engine running during a descent.

From a hardware point of view CAN-bus controllers are cheap compared with proprietary aerospace technology as ARINC busses or the MIL-Bus. For the CCS it is sufficient to use one CAN-Bus controller as the only computing element for each processing function. Bus transmitter and receiver are on chip enhancing simplicity and reliability of the hardware design.

With respect to environmental qualification components for industrial applications have the disadvantage that the specified temperature range is less than for components used for aerospace applications. The lower allowable maximum temperature is acceptable if the ambient temperature is less than the tolerable maximum, heat dissipation inside the box is low and hot spots inside the box are avoided by appropriate constructional measures. Power consumption of each CCS Computer is well below 10 W and copper layers are used to transfer heat to the housing when necessary. Concerning the minimum temperature limit a provision for computer heating can ensure that components are operated in their specified temperature range.

5.3 FUNCTIONAL IMPLEMENTATION

The principles of functional implementation will be explained for the LP and IP bleed valve control and the overboost control.

Because no validated model exists for the dynamics of the whole engine, feedforward control is preferred rather than feedback control. With respect to LP and IP bleed valve control a distinction between steady state and dynamic behaviour is made. For calculation of the steady state position of the valves the ratio of manifold pressure setting and ambient pressure is evaluated.

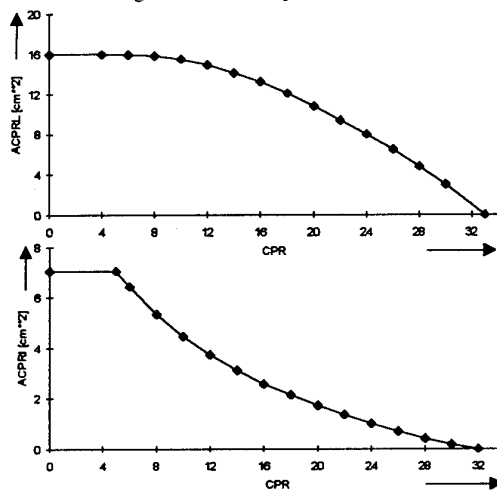


Fig. 14: Control Schedules of LP and IP Bleed Valves (ACPRL, ACPRI) versus Pressure Ratio Setting (CPR)

Fig. 14 shows the control schedule for the LP bleed valve area (ACPRL) and the IP bleed valve area (ACPRI) as a function of the charger pressure ratio setting (CPR). Corrections are computed in dependence of the deviation from the ISA atmosphere, cabin bleed air flow and the rotary speed of the piston engine. The control schedules were initially derived from a steady state computer model of the engine and were refined

during system validation in the altitude test facility.

Dynamic LP and IP bleed valve control is needed to protect the engine against surge when the pilot is reducing power by actuating the power lever. The maximum gradient and the total change of lever position are sensed to compute the additional opening of the valves. The dynamic control value is faded out via second order filters. The mode was designed by a rule of thumb. Surprisingly, the mode worked nearly perfect during tests and only minor adjustments were necessary. The effectiveness of the dynamic LP and IP bleed valve control function can be seen for a fast deceleration in the compressor maps of Fig. 15. No critical reduction of the safety margin from the compressor surge limits exist.

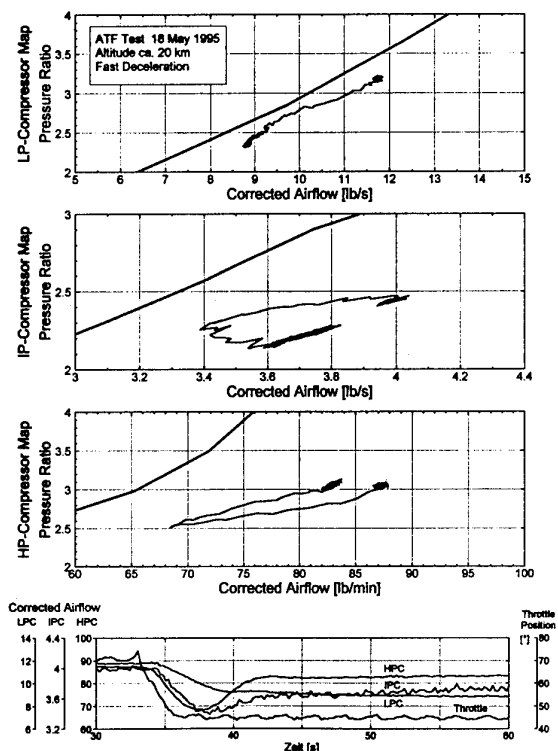


Fig. 15: LP, IP and HP Compressor Behaviour During Fast Deceleration (3 sec) at 20 km with Dynamic LP and IP Bleed Valve Control

For overboost control the function of a mechanical overboost valve usually installed with turbocharged piston engines had to be imitated. The implementation of a mechanical overboost valve was not possible for the STRATO 2C engine. These valves are designed as differential pressure valves. Considering the minimum ambient pressure in the STRATO 2C flight profile compared with ambient pressure at sea level no appropriate differential pressure setting is possible to give full overboost protection in the whole flight envelope. Compared with the mechanical overboost valve some effort is necessary to produce the same effect with a butterfly valve that is used as HP bleed valve. The disadvantage of the overboost valve is the small flow change when the drive is running out of the closed position. To provide a quick reaction the first 10 degrees are passed with maximum possible speed while it is limited afterwards to a reasonable value. When manifold pressure is again lower than the limit

value the HP bleed valve closes. The function was validated with a reduced setting of the manifold pressure limit, see Fig. 16.

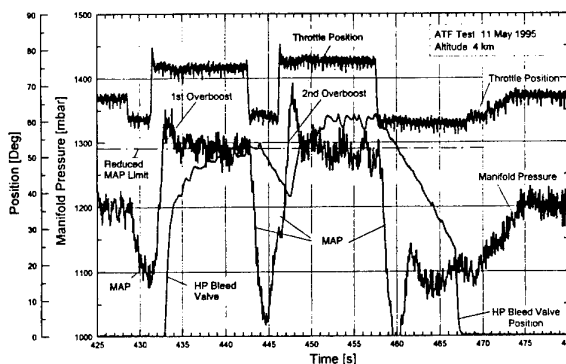


Fig. 16: Overboost Control Test

Special emphasis is laid on the redundancy management of the CCS. All sensor data that contribute to control functions are independently measured in both lanes. The inputs are consolidated by in-lane and cross-channel monitoring. The raw sensor data of the other lane is received via the data bus. A disparity between the values in both lanes lead to actuator freeze of the affected control functions unless the faulty sensor can be isolated by the dedicated in-lane monitor. Although processors are continuously self-tested including the memory a command plane monitor was implemented for the LP and IP bleed valve control function for an immediate failure isolation in case of hardware, e. g. memory failures.

All actuator drives are self-monitored by the processor in control. For LP and IP bleed valve the valve motor will be isolated from the computer by relais in case of failure. If one valve has failed it is therefore blocked in the last valid position. The remaining valve compensates the failure within its physical limits. Because both valves can provide approximately 150 percent of the maximum required bleed rate this compensation may suspend any noticeable effect on engine behaviour. As mentioned before the fail safe characteristics of the LP and IP bleed valve control are still available after loss of the data bus. Both ACUs are operating independently from the other. Because each valve position is measured by each ACU correct operation can be monitored via comparison of both LP respectively IP valve positions.

As the HP bleed valve is a simplex device implementation of the fail safe characteristic differs. If the overboost control function is lost normal operation of the engine is unrestricted despite from the advise to handle the engine gently. Therefore, it is no drawback if the function is only available when both OCUs are in normal operation. One OCU drives the open coil with pulses while the other coil feeds permanently 28 VDC to the closing coil. With this implementation the HP bleed valve can only be opened when the driving OCU is commanding open and the monitoring OCU gives the closing coil free.

Software design of embedded systems often has to be considered a programme risk. For the CCS it was

advantageous that only few people are involved in software development. The requirements according RTCA/DO 178B for Level B software could be implemented with reasonable effort. But the technical risks had to be sorted out satisfactorily to meet the software development standard. The chosen microcontroller can be programmed in C or in assembler. Because the C compiler or any used subset would have been to be validated the code is written in assembler. Strict programming rules and guidelines were established to keep the product maintainable.

5.4 ACCUMULATED EXPERIENCE

The CCS was extensively validated during testing in the altitude test facility. During more than 180 hours in the test chamber and several 100 hours of ground testing including engineering testing by Bauer Engineering, the manufacturer of the CCS hardware and software, the CCS operated well. Some hardware defects were observed, but no problems with the industrial electronic components. The internal temperatures in the CCS Control Computer were always in the specified range of industrial components. A number of changes of control algorithms and schedules were implemented successfully demonstrating the practicability of the chosen software design route.

In the initial flight testing phase some EMC problems with respect to bonding and earthing had been observed. This is not unusual for an all-composite aircraft. After some improvements had been implemented the CCS worked very well.

Some optimizations of the CCS are still outstanding. With the available flight test experience the ergonomic interface may be improved.

Furthermore, monitor thresholds have to be adjusted to offer the best compromise between best failure recognition and suppression of nuisance failure indications. With incorporation of these changes the first software development cycle can be closed successfully.

6. PROPULSION SYSTEM TESTING

Due to the short development time and the cost restrictions engine component tests were limited to LP charger system tests at the altitude test facilities (ATF) of the University of Stuttgart, LP charger oil supply/scavenge unit and ignition system tests in an altitude chamber at IABG and the wind tunnel ground tests of the propeller at Moscow. All other components were tested together with the complete engine.

Two POC flight engines and one ATF test engine have been built and the following tests were carried out:

- | | |
|--|---------|
| • LP Charger System Test at ATF of TU Stuttgart | 60 hrs |
| • Propulsion System Ground Tests incl. 30 hrs Endurance Test at GROB | 50 hrs |
| • Propulsion System ATF Tests at TU Stuttgart | 50 hrs |
| • Propulsion System ATF Tests at CEPr, Saclay | 130 hrs |

- Flight Tests with POC engines at 120 EFH GROB (200 hrs accumulated engine running time)

The 4th of August 1995 the POC aircraft reached an altitude of 18.5 km (60700 ft).

LP Charger Testing

The LP Charger ATF testing was started in May 1993. During these tests the LP charger was operated with external hot gas up to an altitude of 25 km. The test program included:

- Verification of the lubrication system and establishment of the necessary heat rejection to the oil.
- Effectiveness of the labyrinth seals at differential pressures of less than 50 mbar.
- Cooling of the turbine disks and IPT liner.
- Characteristics of the LP and IP compressors at high altitudes and evaluation of the surge line.
- Matching of the compressors with installed intercoolers and their controllability by LP bleed.
- Impact of installation and low Reynolds numbers on heat exchanger efficiency.

All systems behaved as predicted. Only the intercooler performance needed to be increased by 10 to 20%, the hot gas supply to the IP turbine was modified by P&WC to avoid turbine support structure cooling and the air supply to the LP turbine bearing seal was improved.

The tests confirmed that the impact of low Reynolds numbers (high altitude) on centrifugal compressor performance is relatively low and is primarily related to the flow capacity of the LP compressor. The impact on surge margin and efficiency were within measuring tolerance and partially compensated by the impeller clearance reduction.

Some effort had to be spent on minimizing flange and tube connection leakage.

Propulsion System Ground Tests

The ground tests were carried out at GROB with a water brake attached to the propeller gearbox for performance measurements and with the propulsion system installed outside on a rotary tower for propeller and initial endurance tests.

During the tests with installed propeller a vibration survey of all major propulsion components was carried out and the impact of crosswind on propeller blade vibration/flutter and propeller shaft bending moment was measured.

Furthermore, a 30 hrs Endurance Test based on the procedures of the JAR-E-440 (b) (1) was carried out without any problems contributing to the Initial Flight Clearance by the LBA (Luftfahrtbundesamt).

Propulsion System ATF Test

ATF testing of the propulsion system was started in May 1994 at the TU Stuttgart. The first tests were carried out without the propeller gearbox and the water

brake directly connected to the piston engine. Then the tests were continued with the gearbox installed. A flywheel representing the propeller moment of inertia was attached to the gearbox.

After two test campaigns in Stuttgart the ATF testing was continued in France in December 1995 at the Centre D'Essais des Propulseurs (CEPr) at Saclay as the air-cooler of the test facility at Stuttgart had to be replaced and no tests were possible for several months.

The ATF test program covered the following tests at altitudes from zero to 24 km:

1. Piston engine and charger system decoupled on the charge air side with external air supply to the engine and a variable throttle at HP charger exit:

- Verification of the high altitude capability of the piston engine (sealing and crankcase pressurization), of the ignition system and of the fuel control unit (FCU).
- Verification of the matching of the three compressors up to 25 km and adaptation of the LP and IP bleed schedules.
- Function of the LP charger exhaust bypass valve and assessment of the transient behaviour of the turbochargers during the valve opening and closing phase.

2. Piston engine and charger system connected:

- Matching of charger system and piston engine; impact of engine speed and MAP setting on the compressor operating lines versus altitude.
- Fine tuning of the LP and IP bleed schedules.
- Verification of compressor surge margins.
- Adaptation of the cooling air control schedules at ISA and Hot Day conditions and at different engine power settings.
- Impact of varying cabin bleed flow from 0 to 40 g/s (0 to 14 %) on engine power and HPC operating line.
- FCU characteristic (pressure loss and impact of fuel pressure and manifold temperature on the mixture).
- Comparison of the FCU RSA-7 and RSA-10.
- Assessment of the minimum Flight Idle Schedule versus altitude.
- Impact of low and high Flight Mach Numbers on compressor operating lines and engine cooling.
- Dynamic behaviour (acceleration and deceleration of the engine and adaptation of the dynamic bleed control schedules).
- Verification of the overspeed and overboost control capability of the CCS.
- Hot Day conditions.
- Engine Restart after descent with the engine shut off and with the engine driven externally at windmilling speed.
- Pilot Training
- Limited Failure Simulation

It was demonstrated that the turbocharger system and the piston engine are capable of running up to an altitude of 25 km in the decoupled mode.

Furthermore, the POC propulsion system provides constant power up to 23 km with 20 g/s (7 %) cabin bleed.

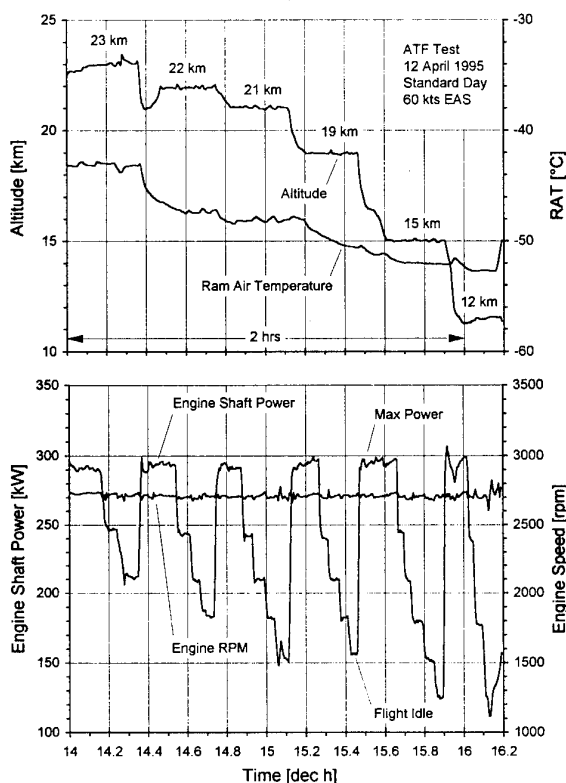


Fig. 17: STRATO 2C Engine Max. and Idle Power at High Altitudes (ATF Test Results)

Above 23 km up to 24 km the power decreases according to the air density decrease. Minimum Flight Idle power was 50 % at 87 % engine speed up to 21 km and 70 % at 23 km.

Fig. 17 shows the power variation from Idle to Max Power at various altitudes up to 23 km. Engine speed was 87 % during this test.

At constant shaft power, turbine inlet temperature (TIT) increases with increasing engine speed whereas the manifold pressure (MAP) shows a minimum at 2900 rpm (94 %) at rich fuel/air ratio. (Fig. 18).

The reason for this characteristic and the high SFC is the POC engine which is not optimized for the higher speeds and which needs to be operated at rich fuel/air ratios. The optimization of the camshaft and air induction system will be carried out for the Mission Aircraft.

The flight Mach number -simulated by increasing ram air pressure at constant ambient pressure- was varied between minimum climb velocity and maximum allowable velocity at Max and Idle Power settings. The impact on the compressor operating lines is low and no compensation is necessary. Only the engine oil cooler becomes too cold at Idle/High - Mach conditions. Therefore, the engine air/oil cooler will be replaced by a coolant/oil cooler for the Mission Aircraft.

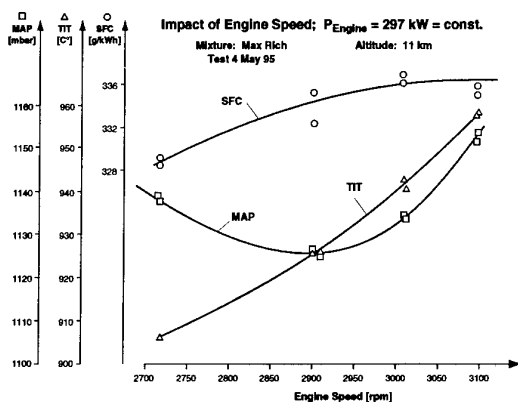


Fig. 18: Impact of Engine Speed on TSIOL-550 Engine Performance

7. CONCLUSIONS

A propulsion system for the 24 km HALE Demonstrator Aircraft STRATO 2C has been developed and tested.

The target for the Mission Aircraft engine: 300 kW engine shaft power at 23.5 km respectively 300 kW equivalent power (shaft + exhaust thrust power) at 24 km was nearly achieved even with the not optimized demonstrator (POC) engine.

In the ATF the POC engine provided 300 kW shaft power with 20 g/s cabin bleed at 23 km and an exhaust thrust as predicted.

It was demonstrated during the ATF and flight tests that the engine and the three-stage turbocharger system are reliable controllable at steady state and transient conditions. The concept of a conventional hydromechanical wastegate controller and a standard fuel control unit combined with a new developed digital turbocharger control unit to reduce risk and cost was validated.

For the Mission Aircraft some weight reduction measures and the optimization of the piston engine - which was investigated but not ordered for the POC engine - to reduce turbine inlet temperature at lean mixture and decrease fuel consumption are defined and will be carried out.

Furthermore, a new HP turbocharger with improved performance and less weight will be developed and an all digital control system with a torque control instead of the MAP control to fully use the potential of the engine without increasing the workload of the pilots has been proposed.

In addition the development of all-composite more flexible propeller blades to reduce weight and decrease crosswind sensitivity is recommended.

With these modifications the performance specified for the MAC engine can be achieved or even exceeded without major risk.

ACKNOWLEDGMENT

The authors would like to thank the DLR (Deutsche Forschungsanstalt für Luft- und Raumfahrt) and the German Ministry for Research and Technology (BMBF) for supporting this projekt.

References

- Ref. 1: H. Tönskötter, „The STRATO 2C Propulsion System, A Low Cost Approach for a High Altitude Long Endurance Aircraft“, AGARD CP 547, May 1993, Paper 17

Paper 6: Discussion

Question from C Rodgers, USA

Was a three spool turbocharger considered in the initial design trade-off studies?

Author's reply

One aspect of the design philosophy for the STRATO 2C compound engine was to have two main propulsion subsystems:

- a. the piston engine system, including the gearbox, propeller and HP turbocharger, which is conventionally controlled and which can operate at low altitudes even if the LP charger failed
- b. the LP charger system with two compressor stages, integrated charge air coolers and its own oil and control system.

To reduce nacelle size and to cover safety aspects, the LP charger had to be installed in front of the wing spar and the piston engine with the HP charger behind it. For this arrangement a three-spool turbocharger even if available would provide no advantage.

Question from Dr P Pilidis, Cranfield University, UK

With the small sized turbomachinery and the high altitude of operation, the engine will be sensitive to component degradation. Can you take any steps to delay the onset of deterioration?

Author's reply

The exhaust system is designed such that even at maximum altitude (the design point), some exhaust gas is bypassing the turbines through the wastegate. This is to compensate for hardware tolerances, deterioration and cabin bleed flow variations.

Question from M B Leroudier, Dassault Aviation, France

Can you elaborate about the weight of the strato engine and the comparison with an equivalent turbofan or turboprop?

Author's reply

An equivalent turbofan/turboprop will provide a worse specific fuel consumption and will also be very large - in the 10000/15000 lb class. The total weight of the strato engine (including nacelle and propeller) is 1050 kg.

Propulsion Considerations For An Advanced Vertical Take-off & Landing (VTOL) Transport Aircraft

Christopher M. Norden & Jeffrey M. Stricker
Aero Propulsion & Power Directorate
Wright Laboratory, 1950 Fifth Street
Wright-Patterson AFB, OH 45433-7251
USA

1.0 SUMMARY

A vertical take-off and landing transport aircraft offers unique challenges to a propulsion system. These challenges are addressed with advanced propulsion technologies. Two types of propulsion configurations are examined - a mechanical driven transmission and a gas driven duct system. A conceptual design analysis for the propulsion components is presented. Furthermore, the benefits of propulsion technology on aircraft system performance are quantified and discussed.

2.0 INTRODUCTION

The objective of this paper is to show the benefits and challenges of advanced propulsion system technologies on a vertical take-off and landing (VTOL) transport aircraft (Figure 1). The propulsive system will meet a demanding set of requirements which address civilian, military, and search and rescue aircraft applications. The study concentrates on two types of propulsion concepts: mechanical and gas driven configurations. Both use turbofans for cruise and lift fans for vertical operations. A conceptual design analysis for the propulsion components will be presented. Unique propulsion design characteristics associated with VTOL aircraft are discussed as well. These include sizing, hover, and operational constraints.

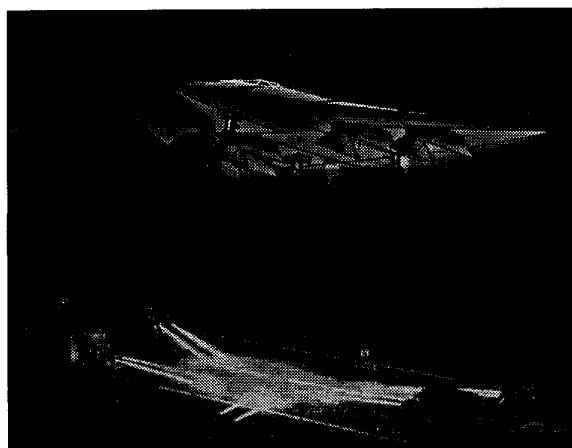


Figure 1 - VTOL Transport Aircraft

Advanced propulsion technologies offer the potential for substantial range increases for both the mechanical and gas driven aircraft. To this end, several propulsion technology levels are assessed in a reference aircraft to show their effect on vehicle range. These include current, mid term (late

1990s), and far term (early 2000s) technology availability dates. It should be emphasized that the vehicle used should not be viewed as the optimum configuration. The airframe serves merely as a platform from which to measure propulsion technology gains. However, realistic aircraft design configurations are defined which satisfy both volume and weight limitations.

3.0 SYSTEM DESIGN REQUIREMENTS

Range, high subsonic speed, and VTOL capability are all highly desired features for this aircraft. Packaging all of these qualities into a propulsion system has proved to be very challenging. An unrefueled radius of 1000 nautical miles (nm) and cruise speed of 0.8 Mach number was selected (Figure 2). A midmission 5 minute hover ability is also desired. The aircraft is envisioned to have a cargo compartment in the size class of the C-130. The payload weight requirement would vary depending on whether the aircraft is used in a conventional or vertical mode. A 10,000 pound maximum payload would be representative of a short takeoff and landing mission and a 4,500 pound payload for a midmission hover type mission.

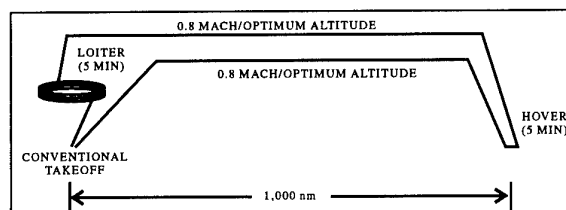


Figure 2 - Mission Profile

VTOL poses a number of additional requirements which tax the propulsion system. These include lift sizing constraints, hover control, and personnel operating conditions beneath the hovering aircraft. To increase the operational safety of the aircraft, a one engine inoperative (OEI) condition was levied on the propulsion system. This means that if the aircraft loses an engine during hover or cruise, it will still be able to either return to its point of departure or to a safe location. The engines must therefore be sized with sufficient thrust margin in order to accommodate such a situation. Environmental conditions for ground personnel operating under the propulsion down-wash during hover is also a consideration. A measure of this capability is exhaust dynamic pressure and disk loading (lift force/exit area). Existing literature and past studies vary on the range of values for an acceptable environment. The XV-5A was a Vertical Short Take-off and Landing (VSTOL) aircraft with a ducted lift fan system

similar in concept to this paper's VTOL designs. It demonstrated an acceptable operating environment during its hover flight tests. Thus it was deemed that the exhaust pressure and diskloading in the VTOL transport be limited to that of the Ryan XV-5A.

The vehicle size and take-off gross weight was also constrained. Military, search, and rescue applications put certain restrictions on aircraft weight and dimensions. This transport was envisioned as a multiple service (Air Force, Navy, and Army) vehicle. It would need to be capable of operating from ships and aircraft carriers. It was found that to operate on an aircraft carrier elevator, the weight should be kept below 90,000 pounds. Furthermore, the aircraft height, wing span, and length were set with the assurance of fitting through the passageways below deck.

4.0 GEAR DRIVEN PROPULSION SYSTEM

The gear driven propulsion system uses a cross linked shaft system to transmit power for both cruise and lift modes of operation. As illustrated in Figure 3, four gas generators are linked to separate cruise and lift fans through a series of shafts and gearboxes. Cross-shafting is used as a safety feature in case an emergency shutdown is necessary on one of the gas generators. The gas generators, lift fans, and cruise fans all run at different speeds in order to optimize their design characteristics. Separate gearboxes are contained within the cruise fans and lift fans to set the proper gear ratios.

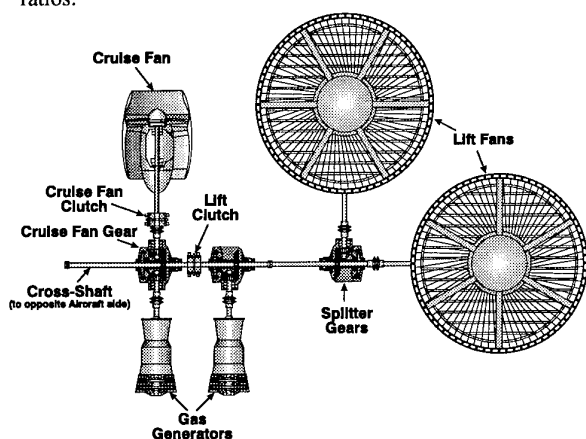


Figure 3 - Mechanically Driven Propulsion System Layout:

Attitude control in hover is a major challenge for any vertical takeoff and landing aircraft. A transport is particularly difficult because of its high gross weight. The gear driven system is designed to run at essentially constant speed during hover to minimize the time lag associated with thrust transients needed for attitude control. Variable inlet guide vanes on the lift fans regulate the power distribution for pitch and roll. This approach is better able to rapidly transfer thrust between the lift fans as opposed to a design which requires varying lift fan speed. Yaw control is achieved by a set of variable louvers in each of the lift fan exhaust streams. These louvers allow the thrust to be vectored. By vectoring thrust on one wing forward and the other aft, the aircraft will rotate along its yaw axis.

Transitioning from cruise to hover or visa versa is a major design consideration for a vertical takeoff and landing

aircraft. Because of the significant difference in power required between the cruise and hover modes, only one of the four gas generators is required for cruise. The gas generator on the opposite side of the aircraft remains running at idle power during cruise for safety reasons. As the pilot approaches a landing site, the aircraft slows to a speed which will allow the lift fan entrance and exit doors to open. The two remaining gas generators are started and accelerate to sufficient shaft speed to approximately match the speed of the other gas generators. At this point, the lift fan clutch can be engaged. The cruise fan clutch is disengaged and the four gas generators accelerate to the required power level to transition into hover. When transitioning from hover to cruise, all four lift fan exit guide vanes are vectored to provide maximum forward thrust. The speed of the aircraft increases beyond the stall speed, at which point the cruise clutch is engaged and the lift fan clutch is disengaged. Although the cruise fans will be windmilling due to the forward velocity of the aircraft, there will be a speed difference between the gas generator and the cruise fan power shaft. This could cause excessive wear on the cruise clutch, so the clutch must be sized to absorb the slip energy during engagement. The two gas generators which are directly linked to the lift fans are shut down, and the doors to the lift fans can now be closed. The aircraft is now ready to accelerate and climb to its desired cruise condition.

4.1 GEAR DRIVEN COMPONENT CHARACTERISTICS

The following sections describe some of the design characteristics associated with the major propulsion components. Both lift and cruise elements of the gear driven system are discussed. As mentioned previously, the hover design condition was assumed to be 4000 ft altitude, 95°F day. The various propulsion components were sized for a 90,000 lbs takeoff gross weight aircraft. At the mid mission hover point, the aircraft weight was approximately 78,000 lbs.

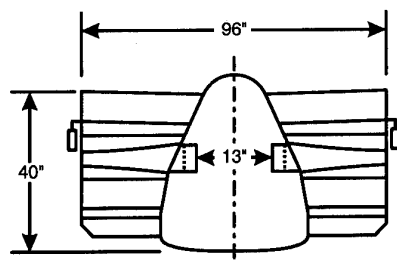
4.1.1 LIFT FAN DESIGN (MECHANICAL)

The lift fans provide the total lift for the transport aircraft when in hover. A significant thrust margin is required for aircraft stability and control. Based on a hover controllability analysis, a 28% thrust margin is needed. Lift fan installation losses are estimated to be 10%. Therefore, the total thrust margin for the lift fan system was 38%.

Because this is a tactical transport vehicle, it is highly desirable for the aircraft to operate from austere locations. It is conceivable that the aircraft will need to operate over concrete, asphalt, sod or broken pavement surfaces. Ground personnel will need to work in close proximity to the aircraft when it is in hover as well. The XV-5A demonstrated a ability to operate within these constraints. Maintaining a disk loading roughly equivalent to the Ryan XV-5A limits the lift fan maximum pressure ratio to 1.2.

Current knowledge of design and manufacturing experience drove the selection of the fan size parameters. The fan blades must be high aspect ratio (3), low hub to tip ratio (0.35), high specific flow (40 lbs/sec-ft²) designs in order to minimize the height and diameter of the lift fan system. It was assumed in

this study that the fan diameter should not exceed 8 ft because of fan blade manufacturing limitations. As a result, four lift fans are required. Each fan produces a maximum uninstalled thrust of 27,000 lbs at the design hover condition. The design characteristics for the lift fan are contained in Figure 4. Flowpath speeds and dimensions remained constant across the various technology levels. The blade material changed from aluminum to organic composite between the mid and far term technology levels to reduce weight. All other materials remained unchanged from the current to far term configurations.



DESIGN CHARACTERISTICS

Pressure Ratio = 1.2 (1.14 Nominal)
 Flow = 1482 lbm/sec
 Tip Speed = 1436 ft/sec; Hub Speed = 636 ft/sec
 RPM = 3417
 Thrust (4000'/95° F Day) = 27,000 lbs
 (19,500 lbs Nominal)
 Horsepower Required = 17,200
 Rh/Rt = 0.35; $W_{a,cr}/AA = 40$ lbs/sec-ft²

MATERIALS

	Current	Mid Term	Far Term
Blade	Aluminum	Aluminum	Composite
Disk	Aluminum	Aluminum	Aluminum
Static Struct	Ti/Comp.	Ti/Comp	Ti/Comp

Figure 4 - Lift Fan Characteristics (Mechanical)

A major challenge in the lift fan design was to come up with a highly responsive way to vector/module thrust. A constant speed design was adopted, with variable inlet guide vanes (IGVs) for thrust modulation. In order to meet controllability requirements, thrust for a given lift fan must be able to be varied from 12,000 lbs minimum to 27,000 lbs maximum, with a nominal thrust of 19,500 lbs. The IGVs are set at -10° closed at the nominal thrust point. The IGVs are closed down to reduce thrust and opened to increase thrust. It is estimated that the IGVs will require a total movement from -35° closed to +15° open to provide the total throttling necessary. It is interesting to note that while the thrust required from a given lift fan may vary substantially, the total thrust, and hence, horsepower, remains constant in hover. As the thrust required increases on one lift fan, its opposing fan decreases by an equivalent amount. As a result, the total horsepower required out of the gas generators is constant. Exit louvers provide thrust vectoring capability for yaw control and transition to cruise. It is estimated that approximately 20° of thrust vectoring is needed, which is well within demonstrated capability for this type louver system. This will provide a maximum forward thrust of 6600 lbs per lift fan, which is believed to be more than enough for transition.

4.1.2 GAS GENERATOR DESIGN (MECHANICAL)

The gas generator must provide power for both cruise and hover and, as such, is a compromise between these two conditions. High specific horsepower (SHP/Airflow) for hover and low cruise thrust specific fuel consumption (fuel flow/thrust) is desired. An added design challenge is the large horsepower discrepancy between cruise and hover. Every effort was made to minimize the number of gas generator units in order to reduce system cost while improving maintainability and supportability. Four gas generators were selected. All four gas generators are required for hover. In order to keep the gas generator running near its optimum condition, only one of the gas generators is needed in cruise.

The cycle used to define the cruise performance was assumed to be a two spool separate flow turbofan, with the gas generator acting as the core. In hover, the low pressure turbine acts as a power turbine for the lift fan system. The current technology gas generator was defined based on an assessment of existing turboshaft engine cycle characteristics. For the two advanced generations, a cycle analysis was performed to determine the desired turbine inlet temperature, overall pressure ratio, and bypass ratio within the constraints of the mid and far term technology levels. Both hover (4000 ft/95°F day) and cruise (0.8Mn/36,098 ft) conditions were examined to define the cycle. The selected cycles are described in Table 1. Note the significant impact the advanced technologies have on both hover shp/airflow and cruise specific fuel consumption.

COMPONENT	CURRENT	MID TERM	FAR TERM
Cruise Fan:			
Pressure Ratio	1.6	1.8	1.8
Efficiency	Base	+1 Count	+2 Counts
Bypass Ratio	5.2	6.6	8
HP Compressor:			
Pressure Ratio	14.3	20	35
Efficiency	Base	+2 Counts	+3.5 Counts
HP Turbine:			
Max Turbine Temp.	2020 F	2600 F	2800 F
Efficiency	Base	+1 Count	+2 Counts
% Cooling	11.3%	14.0%	14.0%
LP/Power Turbine:			
Efficiency	Base	+1 Count	+2 Counts
Overall Performance			
Hover SHP/Wa (SHP/lbm/sec)	132.9	225	271.3
Cruise TSFC (lbm/lbf/hr)	0.647	0.606	0.539

Table 1 - Gas Generator Cycles

The gas generators were sized to deliver 17,200 hp at the hover condition. The advanced technology cycles had smaller gas generators because of the substantial increase in hover shp/airflow. In addition to improvements in the cycle, advanced materials are expected to increase allowable stresses and reduce engine weight. Cross sections of the various gas generators, as well as some pertinent design features, are contained in Table 2. Note the large size advantage associated with the far term technology level.

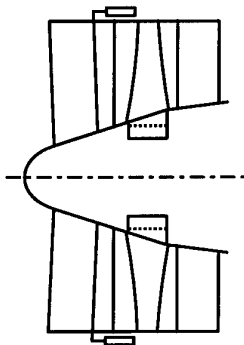
COMPONENT	CURRENT	MID TERM	FAR TERM
HP Compressor:			
Materials	Steel/Ti/Ni Alloy	Ti/Ni Alloy	Ti MMC/Ni Alloy
Stage Count	14	11	9
Corrected Flow (lbs/sec)	137.2	88.3	73.1
Tip Speed (ft/sec)	1105.5	1306	1639
Pressure Ratio	14.3	20	35
Compressor:			
Materials	Ni Alloy	Ni Alloy	Ni Alloy
Space Heat Rate (BTU/(atm-hr-ft ²))	15.0x10	15.0x10	15.0x10
Max Exit Temp. (°F)	2096	2724	2922
HP Turbine:			
Materials	Ni Alloy	Ni Alloy	Ni Alloy
Stage Count	2	2	2
Tip Speed (ft/sec)	1280	1395	1569
AN (in -RPM)	21.1x10	20.9x10	25.3x10
H/ (BTU/lbm)	39.1	40.7	44.1
Max Rotor Inlet Temp. (°F)	2020	2600	2800
LP/Power Turbine:			
Materials	Ni Alloy	Ni Alloy	Ni Alloy
Stage Count	2	2	2
Tip Speed (ft/sec)	1531	1438	1218
AN (in -RPM)	45.6x10	45.4x10	36.3x10
H/ (BTU/lbm)	26.8	36.7	44.1
RPM	8000	10000	10000
Overall:			
Max Diameter (in)	44.1	33.2	28.2
Front Diameter (in)	33.2	25.6	21.1
Length (in)	108	81	65
Design Horsepower (4000/95 °F)	17200	17200	17200

Table 2 - Gas Generator Characteristics

It is desirable to keep the power turbine at as low a wheel speed as possible in order to minimize the gear ratio between the turbine and the lift and cruise fans. However, because the advanced technology gas generators are smaller in size, the corrected turbine work ($\Delta h/\theta$) increases, resulting in a higher aerodynamic stage loading. In order to keep the aerodynamic stage loading at a reasonable level, it was necessary to raise the power turbine wheel speed for the advanced technology generations.

4.1.3 CRUISE FAN DESIGN (MECHANICAL)

The cruise fans deliver the thrust necessary for normal flight. One gas generator provides the required power to the two cruise fans. Since the gas generators for the various generations are sized to a constant hover horsepower output, they provide roughly equivalent power at cruise. As a result, the mid and far term technology cruise fans are similar since they operate at the same pressure ratio. The current technology cruise fan is larger due to current single stage pressure ratio limits. Since the gas generators get smaller for the advanced generations, the bypass ratio increases, resulting in improved cruise specific fuel consumption. Once again, advancements in materials technology will result in higher stress capability and reduced weight. The cruise fan characteristics are summarized in Figure 5.



DESIGN CHARACTERISTICS

	Current	Mid Term	Far Term
Pressure Ratio	1.6	1.8	1.8
Corrected Flow	706 lbs/sec	549 lbs/sec	537 lbs/sec
Tip Speed	1316 ft/sec	1800 ft/sec	1794 ft/sec
Wheel Speed	4964	7696	7765
Materials:			
Statics	Steel/Ti	Ti	Composite
Rotating	Ti	Ti	Ti MMC
Size:			
Length	38.3 in	34.0 in	33.5 in
Diameter	60.7 in	53.6 in	53.0 in

Figure 5 - Cruise Fan Characteristics (Mechanical)

4.1.4 TRANSMISSION SYSTEM DESIGN

The design of the transmission system represents a significant design challenge because of the high horsepower and inherent complexity associated with STOVL aircraft. Existing aircraft gearbox systems are rated up to 6000 shp, with the exception of commercial research propfans, which are in the 10,000 to 12,000 shp class. The aircraft in this analysis required 17,200 shp out of each gas generator. A clutch system is required to transition from hover to cruise and visa versa. Several gearboxes are needed to delivery the power at the appropriate lift and cruise fan speeds. All these constraints result in a transmission system which makes up a significant percentage of both the weight and volume of the aircraft.

The gears can be grouped into three different categories: 1) cruise fan, 2) cross shaft/splitter, and 3) lift fan. The cross shaft/splitter gears link the gas generators to the lift and cruise fans and provide a means to turn the power shafts 90°. They do not reduce the shaft speed. All speed reduction is done in the cruise and lift fan gears. Straight bevel gears with a 20° pressure angle are used throughout the various gear sets. The gears are assumed to be made of steel. The primary design parameters used in this analysis are gear tooth bending stress and pitchline velocity ($2\pi R_{pitch}(RPM)/12$). The design bending stress is 42,000 lbs/in² and pitchline velocity is limited to 35,000 ft/min.

There are a number of additional parts which make up the mechanical drive system. The hollow shafts are made of titanium aluminide with a 4 inch diameter and a 1/8 inch thickness. The bearings are assumed to be ceramic balls with steel races. Each wing contains two clutches, one to engage the cruise fan and the other for the lift fan. Their weights are estimated using a standard empirical design methodology derived from existing clutch data. The lubrication system weight was found using statistical data for existing transmissions. These data indicated that the lubrication system represents roughly 30% of the total transmission weight.

Transmission size and weight were estimated for each technology level on the basis of the above constraints. Unfortunately, little technology is being worked in the field of transmission design. Only minor advancements are anticipated in the foreseeable future. No advanced materials were incorporated in the mid and far term technology levels. Only a slight reduction in weight occurred going from the current to advanced generations because of the component speed differences. The mid and far term technology transmission weights were constant because the various component wheel speeds are roughly equivalent.

4.2 PROPULSION SYSTEM WEIGHTS (MECHANICAL)

A comprehensive analysis was performed to determine the gear driven propulsion system weights for the various generations. The results are summarized in Table 3. Clearly there is a significant reduction in weight with the advanced propulsion technologies. This, combined with the performance advantages of the advanced generations, illustrate the dramatic improvements still left to be achieved in the area of gas turbine engines. The effect this will have on weapon system capability will be quantified in Section 7.

COMPONENT	CURRENT	MID TERM	FAR TERM
Inlets/Nozzles (2)	1944	1598	1322
Cruise Fans (2)	4967	3912	1684
Gas Generators (4)	14347	7243	4773
Transmission	3466	3271	3271
Lift Fans (4)	9026	9026	7052
Lift Fan Misc. (4) (Doors, Louvers, Actuators)	1464	1464	1464
Total Weight (lbs)	35214	26514	19566

Table 3 - Propulsion System Weights Breakdown (Mechanical)

5.0 GAS DRIVEN PROPULSION SYSTEM

For the gas driven system, no suitable way was found to use the gas generators to drive a separate cruise fan. As a result, the gas driven system differs from the gear driven in that the lift and cruise systems are totally independent. In the lift mode, a series of ducts are used to pipe gas generator exhaust air to the lift fan tip turbines. In the cruise mode, separate high bypass turbofans provide thrust. As a result, the cruise engine can be optimized for cruise Specific Fuel Consumption (TSFC). On the negative side, this means that in addition to the four gas generators, an additional two cruise engines are required. Figure 6 illustrates the configurational layout.

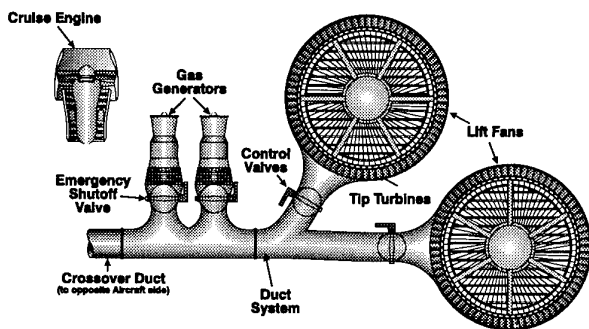


Figure 6 - Gas Driven Propulsion System Layout

As in the gear driven system, gas generator emergency shutdown capability is provided through the use of a crossover duct. In an emergency, it is necessary to isolate the

exhaust gas from the other gas generators to prevent reverse flow through the shutdown gas generator. Therefore, a valve system is required at the exit of each gas generator.

Hover control is done in a similar manner to the gear driven design in that the lift fans operate at constant speed. Lift fan IGVs are used to regulate the power required to each lift fan for pitch and roll control. The power which each tip turbine provides must be regulated in harmony with the fan demanded power, so the control valves should be as closely coupled as possible to the lift fan. Exhaust louvers are used for yaw control.

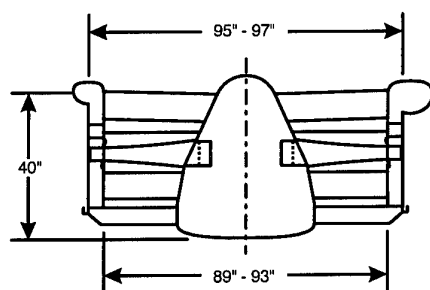
The transition problem is considerably easier for the gas driven system because of the separate cruise and lift systems. When transitioning from cruise to hover, the only constraint is that the aircraft be at sufficiently low speed to open the lift fan doors and start the gas generators. When transitioning from hover to cruise, the two cruise fans must be started in the air. However, this is not considered to be a safety issue since the aircraft hover system is independent of the cruise engines.

5.1 GAS DRIVEN DESIGN COMPONENT CHARACTERISTICS

Many of the gas drive components are similar to the gear system due to the common design constraints. The hover and cruise design conditions remained the same for the gas driven system (4000 ft/95°F day hover, 0.8Mn/36,098 ft cruise). As in the mechanically driven design, the lift system was sized for 27,000 lbs thrust at 4000 ft, 95°F day. The cruise engines were sized to provide 12,000 lbs thrust at sea level static standard day based on conventional takeoff and cruise thrust requirements. The following sections describe the design characteristics associated with the gas drive system.

5.1.1 LIFT FAN DESIGN (GAS)

The four lift fans must provide the total thrust required in hover. The design constraints are the same for the mechanical and gas driven systems. That is, the fan pressure ratio (1.2 maximum) and diameter (8 ft maximum) limits remain the same. The power used to drive the fan is generated at the fan itself using a tip turbine similar in design to the XV-5A. As in the gear driven design, each lift fan is designed to produce 27,000 lbs thrust at the hover condition. However, because the tip turbine exhaust produces thrust, the fan itself can be reduced in size. The net result is that even with the tip turbine, the overall diameter of the lift fan system remains essentially constant. Figure 7 shows the design characteristics for the various generations of the gas driven lift fan system.



DESIGN CHARACTERISTICS

Pressure Ratio = 1.2 (1.14 Nominal)
 Thrust (4000'/95 F Day) = 27,000 lbs
 (19,500 lbs Nominal)
 $R_h/R_t = 0.35$; $W_{a,cor}/A_a = 40$ lbs/sec-ft²

	Current	Mid Term	Far Term
Fan Flow	1273 lbs/sec	1350 lbs/sec	1376 lbs/sec
Turbine Flow	164 lbs/sec	78 lbs/sec	65 lbs/sec
RPM	3485	3384	3352
Material			
Fan Blade	Titanium	Titanium	Composite
Disk	Titanium	Titanium	Ti MMC
Static Structure	Ti/Composite	Ti/Composite	Ti/Composite
Turbine	Nickel Alloy	Nickel Alloy	Nickel Alloy
Size:			
Length	40 in	40 in	40 in
Fan Diameter	89.2 in	91.9 in	92.8 in
Total Diameter	97.2 in	96.2 in	95.4 in

Figure 7 - Lift Fan Characteristics (Gas)

New lift fan materials were required because of the high gas temperature (1330°F for the current up to 1733°F for the far term generation) and high stress environment associated with the tip turbine design. Titanium was used extensively for the various fan components with the tip turbine made of nickel based materials. For the far term configuration, it was opted to use composite fan blades with a titanium metal matrix composite disk (MMC) in order to reduce propulsion system weight.

5.1.2 GAS GENERATOR DESIGN (GAS)

The gas generator for the gas driven system provides high pressure, high temperature exhaust air which is used to drive the lift fan tip turbines. All four of the gas generators are tied together through a series of interconnected ducts. As in the gear driven design, the gas generators are designed to operate at constant speed. Attitude control is achieved by a series of valves which regulate the airflow to the tip turbines. As noted previously, it is important that the valves be close coupled to the lift fans since rapid throttle response is critical.

The gas generator design used for the lift system is identical to that used in the mechanical system except for the removal of the power turbine. Flowpath design and component materials were consistent with the mechanical design, as well. Refer back to Table 2 for a summary of the design characteristics.

A significant challenge to the gas driven system is the duct design. These pipes must transfer high temperature exhaust gases to the tip turbines. Cooling is critical because the ducts are contained within the aircraft wing structure. The ducts are

double walled pipes with exterior wrapped insulation. Purge air is used both within the double walled structure and outside the duct to control the heat transfer to the wing interior. A maximum temperature on the exterior duct wall is estimated to be 400°F. The duct design Mach number is 0.3 based on a compromise between pressure losses and minimized diameter. However, this criteria could not be satisfied for the current generation because the duct size was too large to fit within the wing. Therefore, the current technology duct system was increased to a design Mach number of 0.45. Table 4 compares the duct designs for the various generations.

	CURRENT	MID TERM	FAR TERM
Duct Diameter (ft)	1.87	1.46	1.12
Design Mn	0.45	0.3	0.3
Material	Ti	Ti MMC	Ti MMC
Weight/Foot	16.9	11.8	9.2

Table 4 - Duct Design Characteristics

5.1.3 CRUISE ENGINE DESIGN (GAS)

Cruise power for the gas driven system is provided by two separate flow, high bypass turbofan engines. In the interests of consistency, the cycles used are the same as the mechanical system (see Table 1). The low pressure turbine is directly linked to the fan, so its speed is reduced compared to the power turbine used in the gear driven system. As a result, the low pressure stage count had to be increased to four stages. All other design constraints and materials are consistent with the mechanical design. Since the cruise engines are independent of the lift system, they can be sized to the thrust needed for normal flight. As previously noted, the cruise engine size is set to 12,000 lbs thrust at sea level static in order to provide adequate takeoff performance.

5.2 PROPULSION SYSTEM WEIGHTS (GAS)

As in the mechanically driven system, a comprehensive analysis was performed to determine the gas driven propulsion system weights. The results are summarized in Table 5. Once again, there is a significant propulsion weight savings with the advanced generations. Reduced fuel consumption is a benefit associated with advanced propulsion technology, also. Section 6 will quantify the impact of these improvements on the weapon system. A comparison between the gas and gear driven designs will be discussed as well.

COMPONENT	CURRENT	MID TERM	FAR TERM
Inlets/Nozzles (2)	1916	1550	1442
Cruise Engines (2)	3780	2908	2363
Lift Gas Generators (4)	12280	5914	3936
Ducts & Valves	885	621	481
Lift Fans (4)	9488	9219	7127
Lift Fan Misc. (4) (Doors, Louvers, Actuators)	1464	1464	1464
Scrolls	625	643	649
Total Weight (lbs)	30437	22319	17462

Table 5 - Propulsion System Weights Summary (Gas)

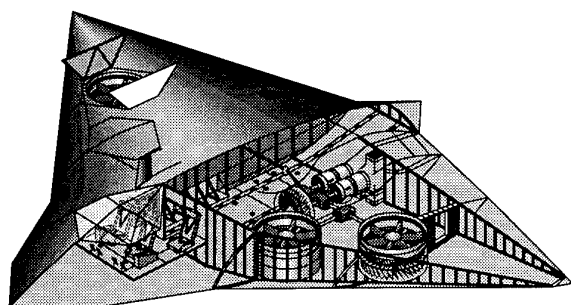
WING	BODY
Area (exposed) = 1170 ft**2	Length = 47.6 ft
Area (wetted) = 3078 ft**2	Width = 11.0 ft
Area (ref) = 1610 ft**2	Depth = 9.4 ft
Sweep (leading edge) = 45 degrees	Fineness Ratio (L/D) = 4.7
Sweep (chord/4) = 35.5 degrees	Wetted Area (Aero) = 1042 ft**2
Aspect Ratio = 3.0	
Taper Ratio = 0.075	
Thickness/Chord = 0.15	
Mean Aero Chord = 28.4 ft	
Span = 69.4 ft	
Wing Loading (max) = 55.89 lb/sq. ft	

Table 6 - Airplane Design Characteristics

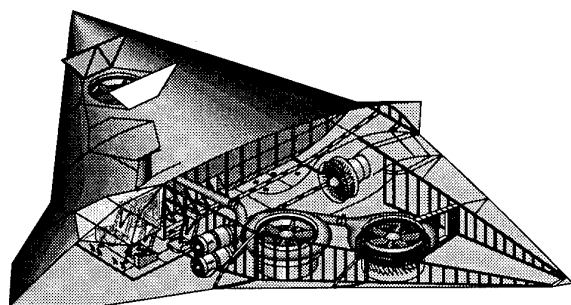
6.0 VEHICLE DESCRIPTION

The objective of the aircraft study is to serve as a platform to assess propulsion configurations and technology tradeoffs. The airframe was deltoid shaped and tailless to minimize drag. Airframe technology, exterior shape and dimensions remained the same for both the mechanical and gas driven configurations. The installed propulsion layouts of the gear and gas driven systems are illustrated in Figure 8. Table 6 displays the airplane design characteristics.

The ability to operate on an aircraft carrier set restrictions on aircraft weight and dimensions. A takeoff gross weight (TOGW) of no more than 90,000 pounds was recommended due to elevator load capacity. Airframe length of 47.6 feet, wing span of 69.4 feet, and height of 9.4 feet were chosen with hanger door bay and elevator dimension limitations in mind. A detailed weights breakdown of the aircraft is shown in Table 7 for each propulsion technology level and drive system. Note that the primary differences in aircraft weights are due to the propulsion systems and fuel. The effects of these differences will be discussed in more detail in the Section 7.



Gear Driven



Gas Driven

Figure 8 - Aircraft Layouts

Component	Technology Level		
	Current	Mid Term	Far Term
Structure			
Wing	5623	5422	5172
Body	12668	12668	12663
Landing Gear	2579	2579	2568
Total Structure	20879	20670	20402
Propulsion			
Main Engines	6911	5510	3006
Starting	99	81	47
Fuel System	799	969	1071
Drive System	19277	11978	9508
Lift Fans (4)	9026	9026	7052
Total Propulsion	36112	27563	20684
Fixed Equipment	14208	14176	14135
Weight Empty	71200	62409	55221
Operating Weight	72256	63498	56340
Payload	4500	4500	4500
Fuel	13244	22002	28560
Gross Weight	90000	90000	89400

Table 7a - Aircraft Weight Breakdown for Gear Driven System

Component	Technology Level		
	Current	Mid Term	Far Term
Structure			
Wing	5525	5270	5392
Body	12668	12650	12604
Landing Gear	2579	2539	2439
Total Structure	20772	20459	20436
Propulsion			
Main Engines	5695	4457	3804
Starting	83	67	58
Fuel System	899	1008	1008
Drive System	152545	8642	6530
Lift Fans (4)	9488	9219	7127
Total Propulsion	31419	23392	18527
Fixed Equipment	14191	14113	13990
Weight Empty	66382	57964	52953
Operating Weight	67424	59038	54027
Payload	4500	4500	4500
Fuel	18076	24387	24403
Gross Weight	90000	87925	82930

Table 7b - Aircraft Weight Breakdown for Gas Driven System

The fuel tanks are located on the outboard side in the wings. Placing fuel tanks near or around the fuselage area was considered but quickly abandoned in favor of passenger safety. Additional unused volume in the aircraft nose was also used for fuel. The volume for fuel was calculated with consideration given to space occupied by the lift fans, flaps, leading edge slats, spars, shafts (gear driven system), and ducts (gas driven system). This yielded a maximum fuel volume availability of 587 ft³ (or 28,600 pounds of fuel) for the gear driven system and 501 ft³ (or 24,400 pounds of fuel) for the gas driven system.

The payload compartment is sized such that it can carry a multipurpose wheeled vehicle (7.1 feet wide by 6.5 feet high) and military pallets. It was found that cargo area dimensions of 7.7 feet wide by 6.5 feet high by 28 feet length accommodates most items of interest for this type of aircraft. This size can fit a 10,000 pound maximum payload of 20 troops and a wheeled vehicle for the short takeoff and landing (no midpoint hover) type mission. Loading and unloading takes place through a rear clam shaped ramp door.

Stability and control of the aircraft is accomplished in two ways. During the cruise mode of operation, conventional flaps and ailerons are used for pitch and rolling maneuvers. Split-flaps are used for yaw control in the absence of a tail (similar to that used on the B-2 bomber). Control during hover utilizes the propulsion force from the lift fans. This is accomplished by variable inlet guide vanes and exhaust louvers in the lift fans.

7.0 PROPULSION SYSTEM TECHNOLOGY IMPACTS ON AIRCRAFT PERFORMANCE

Both the gear and gas driven propulsion systems for each of the three technology levels (current, mid term, and far term) were installed in the aircraft to assess system payoffs. As discussed earlier, the vehicle technology and planform dimensions remained constant for each propulsion technology level. Advanced propulsion technology reduced both the weight and specific fuel consumption of the propulsion

system. Table 8 expresses this in terms of improved aircraft propulsion and fuel weight fractions. Two limits were observed - a takeoff gross weight of 90,000 pounds and the maximum fuel tank volume available in the wings.

	Technology Level		
	Current	Mid Term	Far Term
TOGW (lb)	90000	90000	89400
FUEL FRACTION	14.7%	24.4%	31.9%
PROPULSION FRACTION	40.1%	30.6%	23.1%
STRUCTURAL FRACTION	23.3%	22.9%	22.8%
EQUIPMENT FRACTION	17.0%	17.0%	17.1%
PAYLOAD FRACTION	5.0%	5.0%	5.0%

Table 8a - Gear Driven Propulsions Technology Payoffs

	Technology Level		
	Current	Mid Term	Far Term
TOGW (lb)	90000	87925	82930
FUEL FRACTION	20.1%	27.7%	29.4%
PROPULSION FRACTION	34.9%	26.6%	22.3%
STRUCTURAL FRACTION	23.1%	23.3%	24.6%
EQUIPMENT FRACTION	16.9%	17.3%	18.2%
PAYLOAD FRACTION	5.0%	5.1%	5.4%

Table 8b - Gas Driven Propulsion Technology Payoffs

The range capabilities of both the gear and gas driven systems are illustrated graphically in Figure 9. One can clearly see that technology has a significant effect on increasing range for both types of drive systems. Concentrating first on the gear driven system it was found that range increased by 3.2 times for the mid term, and 5.6 times for the far term compared to current capability. However, the far term technology level is required to achieve the 1,000 nm radius goal. The gas driven system did significantly better than the gear system in the current and mid term technology levels. Furthermore, it reached the goal radius with mid term technology. However, it did not realize its full potential in both the mid term and far term technologies. In fact, the far term gear driven configuration actually performs better. This was because of the reduced wing volume available for fuel in the gas driven system. Even though there was weight margin available, it could not be used because there was no room to put the additional fuel. This is why range increases at a diminished rate for the gas driven advanced technology configurations. Note in Table 8 that the gear driven system also runs into a fuel volume limit for the far term technology.

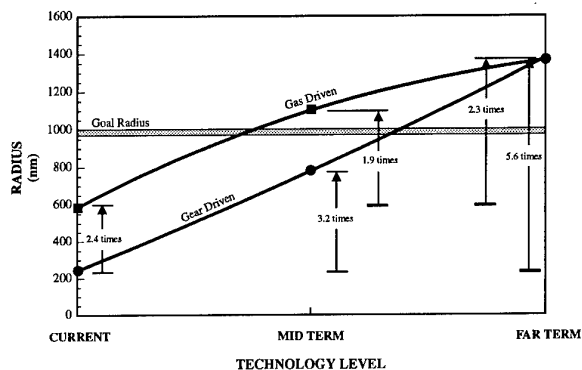


Figure 9 - Propulsion Technology Payoffs

8.0 CONCLUSIONS

Substantial range benefits are realized through advanced propulsion technology. The full potential of these technologies are limited, however, by aircraft weight and fuel volume restrictions. This was particularly obvious for the gas driven system which was not able to take advantage of its propulsion weight savings. The mid term gas driven technology level was still able to achieve the goal radius of 1,000 nm. The gear driven system required far term propulsion technologies to accomplish the mission radius goal.

Future improvements in weight reduction for mechanical power transmissions in aircraft are not anticipated to be significant. This is unfortunate because it limits the payoffs for the mid term gear driven system. There is fuel volume available but is unused due to the TOGW constraint.

The gas driven system does, for the most part, enjoy a clear advantage over the gear driven in terms of range potential. This is largely attributed to separate cruise and hover propulsion systems. The cruise system for the gas driven design could be sized to deliver better cruise specific fuel consumption. In retrospect, a similar design could have been done for the gear system (ie. having a separate cruise gas generator system). Fuel weight would be traded for additional propulsion weight in favor of better cruise fuel consumption. However, the desire to minimize the number of propulsion systems in favor of reduced acquisition cost, supportability, and maintainability was thought to be a more favorable tradeoff. Another area of unique concern with the gas driven system is the leakage danger associated with high pressure and temperature gases flowing through the ducts in close proximity to the fuel tanks. This is a potential safety hazard, especially if the aircraft is exposed to enemy ground fire or combat.

9.0 ACKNOWLEDGEMENTS

The authors wish to thank Mr Micheal Bruggeman for his graphics support. His illustrations in this document have enhanced the understanding of the various propulsion integration challenges as well as provided a more readable document. Special thanks go to the other members of the Integration and Assessment Branch (WL/POTA) as well for their substantial technical input on the performance, control, and integration requirements.

Paper 7: Discussion

Question from M D Paramour, MOD, UK

1. How does the cost-effectiveness of the concepts you have described compare with that of a tilt-rotor aircraft?

2. You stated that an engine failure should not hazard the aircraft, and described how the lift fans would be controlled to achieve this objective. What measures have you taken to ensure that the gas generators can also respond quickly if one of them fails?

Author's reply

1. A cost effectiveness analysis of other configurations such as the tilt-rotor was not accomplished in this study. The selection of a turbofan/lift fan concept was based on maintaining a low observable configuration for military requirements. Furthermore, the primary objective of this study was to assess propulsion technology benefits. Both the aircraft and propulsion configurations served as platforms to accomplish this. The gas generator technologies would show similar benefits in a tilt-rotor configuration.

2. The gas generators were designed with a 200°F overtemperature capability, allowing a quick recovery in the case of an engine failure.

Question from Capt J Tallarovic, Edwards AFB, USA

Ground crew safety was considered when you set the lift fan pressure ratio. Was consideration also given to the thermal environment below the lift fan in the gas driven design (ie, you are blowing hot exhaust gasses on ground crew, will that impact their safety)?

Author's reply

Consideration was given to the thermal environment in the gas driven system. The table below shows the exit conditions of both the fan and tip turbine streams. Note that although the tip turbine exit temperature is high (1388° to 1477°R), its flow is very low in comparison to the large cooler fan flow. The pressures between the two streams are equal. Thus, it was anticipated that the tip turbine temperature would quickly be dissipated.

	<u>CURRENT</u>	<u>NEAR TERM</u>	<u>FAR TERM</u>
<u>TIP TURBINE EXHAUST:</u>			
T(°R)	1388	1579	1477
P(psi)	12.69	12.69	12.69
AIRFLOW(lb/s)	164.	78.	65.
<u>LIFT FAN EXHAUST:</u>			
T(°R)	550	550	550
P(psi)	12.69	12.69	12.69
AIRFLOW(lb/s)	1273	1350	1376

POWERPLANTS AND LIFT SYSTEMS FOR ASTOVL AIRCRAFT - THE CHALLENGES TO AN ENGINE MAKER

David M Pearson

Chief Design Engineer ASTOVL

Rolls-Royce plc, WH 62

P.O. Box 3, Filton, Bristol BS12 7QE, England

1. SUMMARY

This paper discusses the design requirements and major challenges associated with powerplants for the STOVL capable aircraft currently being studied under the Joint Advanced Strike Technology (JAST Program). Challenges specific to four different lift system concepts are described, namely; Direct Lift, Shaft Driven Fan, Gas Driven Fan and Lift plus Lift/Cruise. Generic issues which must be resolved for any of these powerplants, namely; exhaust design, attitude control provision, reliability and affordability, are also discussed. All of the proposed concepts present significant challenges to the engine maker particularly if the powerplant is to be used in a common CTOL/STOVL aircraft as proposed for the JAST program.

2. ABBREVIATIONS

ASTOVL	- Advanced Short Take-Off and Vertical Landing.
CALF	- Common Affordable Light Fighter
CTOL	- Conventional Take-off and Landing
DL	- Direct Lift
HP	- High Pressure
GDLF	- Gas Driven Lift Fan
JAST	- Joint Advanced Strike Technology
LP	- Low Pressure
LSPM	- Large Scale Powered Model
L+LC	- Lift plus Lift/Cruise
SDLF	- Shaft Driven Lift Fan
STOVL	- Short Take-Off and Vertical Landing
USMC	- United States Marine Corps

3. INTRODUCTION

The potential for the gas turbine engine to provide sufficient vertical thrust to lift an aircraft due to its inherently high thrust/weight ratio was recognised over 50 years ago. Indeed it is over 40 years since the first jet lift aircraft took to the air. To date, however, the only Western STOVL fixed wing aircraft to enter service is the Harrier powered by the Rolls-Royce vectored thrust Pegasus Turbofan engine.

The proven capability of the Harrier has transformed the way in which its operators (e.g. Royal Navy, USMC) will conduct a future conflict to such an extent that STOVL is an essential requirement for any new strike aircraft for these services.

Numerous studies have been carried out in the past into enhanced STOVL aircraft, in particular aircraft with supersonic flight capability. Typical of these were the studies of 4 different concepts carried out under the US/UK memorandum of understanding (Ref 1). Such aircraft have been termed Advanced Short Take Off and Vertical Landing (ASTOVL).

Recently, initiatives have been put in place in the United States to reduce the cost of future aircraft procurement programmes by adopting a modular philosophy to provide aircraft to meet the requirements of the US Air Force, US Navy, US Marine Corps and its allies.

This initiative was formerly known as the Common Affordable Lightweight Fighter (CALF) and has now grown into the Joint Advanced Strike Technology (JAST) programme.

The USMC and Royal Navy requirement for a Harrier replacement means that one variant of the JAST airframe must be STOVL capable. Consequently, requirements are being placed upon engine manufactures to define propulsion systems which not only provide both efficient vertical and supersonic thrust but are also readily adaptable between STOVL and CTOL configurations.

Rolls-Royce has been actively involved in all the competing JAST airframe studies, in particular providing STOVL related hardware for large scale powered models and supporting studies of the proposed demonstrator and production weapon systems.

This paper discusses difficult challenges which are faced by the engine maker in realising the powerplant concepts currently being proposed for potential JAST STOVL capable airframes. Generic issues affecting ASTOVL propulsion are also discussed.

4. THRUST REQUIREMENTS

The ASTOVL propulsion system has to fulfil two often conflicting thrust requirements;

- a) Horizontal thrust for high speed forward flight
- b) Vertical thrust for short take-off and landing

The engine design is therefore a difficult balance in order to provide both;

- o a propulsion engine cycle and size which gives the lowest aircraft take-off gross weight for a given flight mission.
- o a lift propulsion system which provides sufficient vertical thrust, and the correct front/rear thrust split for aircraft balance, while not having a significantly adverse effect on aircraft cross-section.

The installed thrust in vertical flight has to match the landing weight of the aircraft (including any bringback weapons/full load) plus allowances for;

- Nozzle turning losses
- Thrust loss due to hot gas re-ingestion (very height dependent)
- Aircraft suckdown effects (very height dependent)
- Thrust margins associated with attitude control
- Thrust margin for arresting descent rate and to abort a landing.

A typical vertical thrust account is shown in Figure 1. Of course, this thrust requirement must be met under the most adverse combination of temperature and altitude at which the aircraft is to operate.

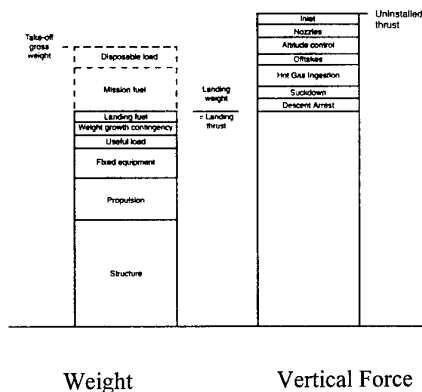


Fig. 1 Vertical Lift Budget

The obvious point of departure for ASTOVL propulsion studies is the extension of the Pegasus concept where engine jet thrust is used directly to produce lift. Rolls-Royce studies have shown that, with the exception of aircraft with a dry supersonic flight requirement, the critical engine sizing point for such a powerplant is the vertical landing case. The direct lift engine therefore has an excess of thrust in the conventional flight mode. While pilots are unlikely to complain about excess performance, it does mean that if the same powerplant is retained for a CTOL only variant of the aircraft, the engine, intake and exhaust would be larger and heavier than necessary. One means of avoiding this problem is to use a different (smaller) LP spool around the same engine core for the CTOL variant but clearly this is at the expense of commonality.

The criticality of an engine sized for vertical thrust is compounded by the fact that with high lift jet energy inherent in future ASTOVL engines, hot gas ingestion levels are increased requiring even higher uninstalled thrust levels.

Alternative powerplant configurations are being studied in order to address the issues described above. The basic principal is to provide a means of augmenting the engine thrust in the vertical mode either by increasing the potential propulsive efficiency of the engine, or incorporating an additional engine purely for producing lift.

To maximise propulsion efficiency in the lift mode (i.e. static or near static entry conditions) the lift system efflux should possess as low a level of energy per unit air mass flow as possible. This objective is also consistent with reducing hot gas ingestion and ground erosion problems and is best achieved by incorporating a relatively low pressure ratio fan system producing thrust in the lift mode only. However, the larger the fan mass flow, the larger the aircraft and therefore compromise between pressure ratio and mass flow is required. Such a fan may be mechanically coupled to the main engine (shaft driven fan). Alternatively, it may be driven by the expansion of high energy gas ducted from the main engine and exhausted through a separate turbine driving the lift fan (gas driven fan). The fan may also, of course, be driven by a separate engine (lift engine)

Schematic layouts of the three lift fan concepts described above are shown in Figure 2. The choice of mounting the lift fan remote from the main engine (typically just behind the aircraft cockpit) allows the main engine to be positioned at the rear of the aircraft and still maintain the vertical thrust centre coincident with the aircraft centre of gravity. This enables an efficient intake to be designed, which can be tailored to reduce radar cross section, and also avoids exhaust impingement on the fuselage during conventional flight. It is also possible to conceive of a direct lift engine which can be sited in the tail of the aircraft with airducted to a forward ventral nozzle to maintain the correct thrust centre. (see Figure 3).

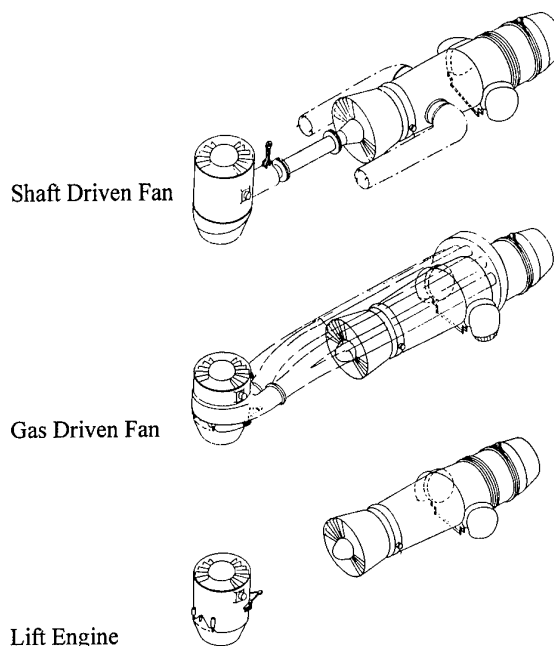


Fig. 2 Remote Fan Concepts

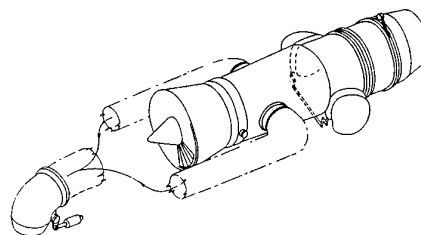


Fig. 3 Direct Lift Concept

The four different types of powerplant described above namely

- o Direct Lift
- o Shaft driven fan
- o Gas driven fan
- o Lift engine plus lift/cruise engine

are all being studied by the various ASTOVL/JAST airframer teams. The next section of this paper deals with the specific challenges associated with each of these systems.

5. CONCEPT SPECIFIC ASTOVL POWERPLANT CHALLENGES

5.1 Direct Lift

A typical direct lift powerplant configuration is shown in Figure 4. The upper half of the picture shows the engine in lift mode, the lower half in flight mode. In flight mode the engine is a conventional low bypass ratio reheated turbofan. On transition to jet borne flight, the rear propulsion nozzle is blocked off and valves opened to allow the engine exhaust to exit through vectoring nozzles.

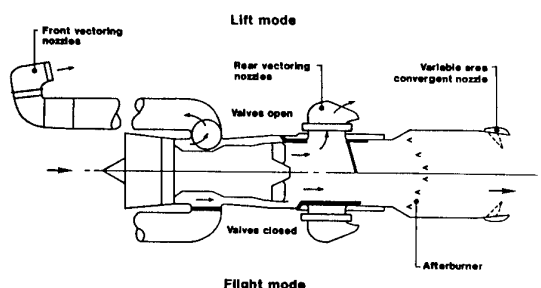


Fig. 4 Direct Lift Engine Operation

In the example shown the bypass and core streams are ducted separately to front and rear nozzles respectively necessitating the use of an additional valve to block the exit from the bypass duct in the lift mode. This unmixed type of engine allows greater flexibility in the choice of fan and core exit pressures in the lift mode and enables the long ducts to the front nozzles to be constructed from lightweight materials due to the relatively low temperature of the fan bypass air. The major disadvantage of the unmixed engine is, however, the exhaust gas temperature from the rear nozzles leading to ground erosion and hot gas ingestion concerns. Direct lift engines with mixed exhaust in the lift mode have therefore been proposed which reverse the advantages and disadvantages described above.

Despite the apparent complexity of Figure 4 the direct lift powerplant is effectively the simplest of the ASTOVL concepts currently proposed and raises no specific mechanical challenges which are not also suffered by the other concepts. The fact that, as described in section 4, the direct lift engine is sized for lift performance does mean however, that lift thrust related challenges such as nozzle/valve pressure losses and particularly powerplant weight reduction are more critical for this concept.

5.2 Shaft Driven Lift Fan

Figure 5 shows an example of a shaft driven fan powerplant concept. On transition from flight to lift mode, a clutch is used to engage a mechanical drive from the LP spool of the engine. Power is transmitted via a shaft through a right-angle gearbox to a vertically oriented fan unit. The exhaust from the core engine is also deflected downwards to form the rear thrust post. In Figure 5 a 2D fully vectoring nozzle is used. This could equally be a block and turn system as shown for the direct lift concept. The relative merits of these systems are described in section 6.



Shaft driven remote fan
(Rear lift vectoring nozzle)

SPV5209

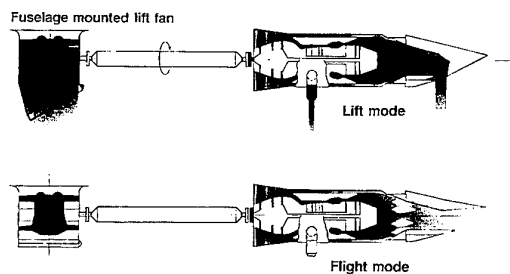


Fig. 5 Shaft Driven Fan

In the lift mode, the engine LP turbine has to produce a significantly higher level of work in order to drive the remote fan. This has a number of effects;

- The core exhaust pressure reduces to a level inconsistent with mixing with the fan bypass stream. A bypass blocker is therefore required and additional nozzles have to be provided for the fan bypass exhaust flow. These nozzles can however, be used to provide additional lift thrust and an effective means of aircraft control, particularly for the roll axis.
- An additional stage of LP turbine will probably be required to deal with the large work output required.
- The LP turbine must be designed to operate efficiently at both low loadings in flight mode and high loadings in lift mode. This may necessitate the use of variable geometry in the turbine, especially the exhaust vane. Lightweight, reliable variable geometry mechanisms are difficult enough to engineer in the cold sections of engines. They represent a major challenge in the hot turbine environment.

The most significant challenges associated with the shaft driven fan are, however, the gearbox and clutch. Levels of power in excess of 15000KW (20 000 BHP) have to be transmitted by these systems for a typical ASTOVL configuration. Engineering a gearbox with sufficient stiffness to reliably transmit such high powers at a weight consistent with use in a combat aircraft requires major advances in this technology compared to current gearboxes such as those used in helicopters, turboprops and civil turbofans.

The problem of heat rejection due to the inevitable friction losses in the gearbox may necessitate the use of air or fuel coolers for the lubrication system.

Advances in clutch technology will also certainly be required. It will be essential to reduce the level of power absorbed by the remote fan during the clutching and de-clutching operations. This will require either a variable fan pitch mechanism or variable inlet guide vanes. Neither of these options is very attractive from a cost, weight and reliability viewpoint but once provided, could be used to augment or provide attitude control in the pitch axis.

5.3. Gas Driven Lift Fan

Figure 6 shows a typical gas driven fan propulsion system. On transition from flight to lift mode, the cruise jet pipe is blocked and valves opened to allow the mixed core and bypass exhaust gasses to be directed to; (a) a pair of rear vectoring nozzles, and (b) ducting leading forward to the remote fan unit.

This remote fan unit includes a hot gas manifold and inner chamber. This system ducts the hot gas to a turbine which mechanically drives the remote fan. The front post thrust is therefore made up of contributions from the fan airflow and the remote turbine exhaust.

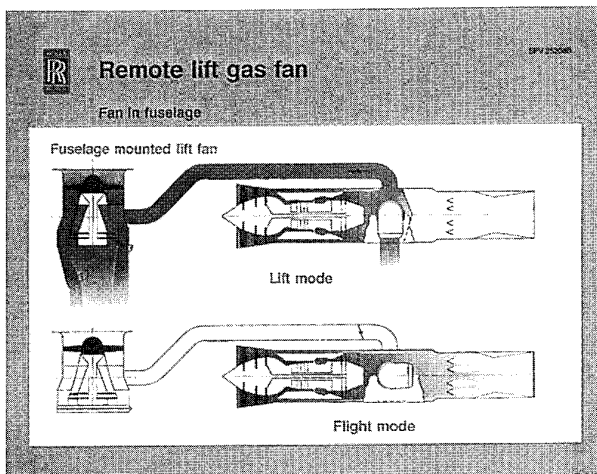


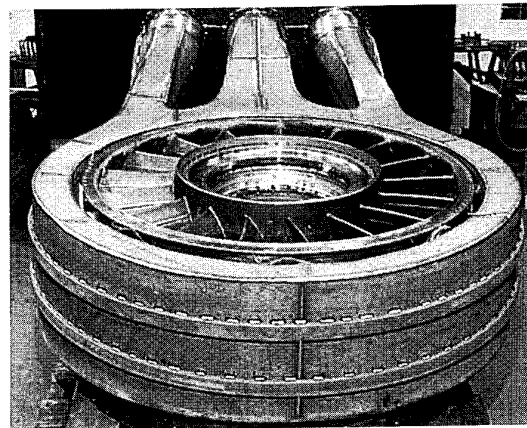
Fig. 6 Gas Driven Fan

The major challenge with this type of powerplant is in the hot gas transfer system, in particular making it light weight and compact. The mixed exhaust gasses are hot and at high pressure. This high temperature necessitates the use of either nickel based heat resisting alloys or ceramics. The sheer volume of air to be transferred and the distance between the offtake and the remote fan means that a metallic system will have considerable weight. Ceramic matrix composites offer a potentially viable system at an acceptable weight but substantial material development is required to make them affordable. Either option will require insulation to keep heat rejection to the fuselage down to an acceptable level.

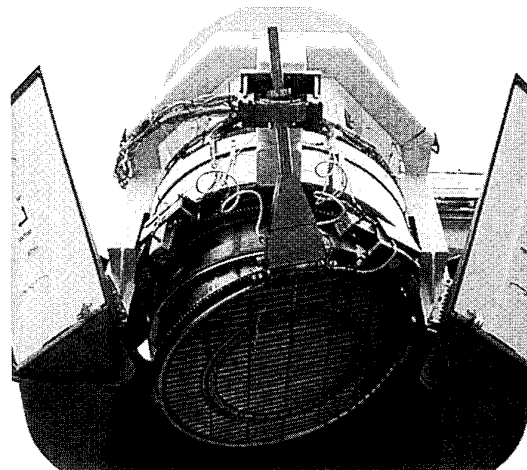
Once the gasses have been transferred to the lift fan the problem of achieving an acceptable manifold and distribution system is significant. In order to keep the outer diameter of the remote fan to a minimum the outer manifold is forced to be of a long toroidal cross section. This deviation from the optimum pressure vessel shape of a circular cross section means considerable strengthening must be added which contributes significant additional weight. From the outer manifold the hot gases must be ducted across the fan exhaust airstream. This causes significant thermal expansion mismatches in the vane which may necessitate the use of a dual skin vane construction.

The volume occupied by this gas transfer system is a major constraint on the airframe design, particularly for a common CTOL/STOVL aircraft.

Rolls-Royce has been involved in designing and manufacturing some of these components for the MDA/GE gas driven fan large scale powered model as shown in Figure 7.



Hot Gas Manifold



3 Bearing Nozzle

Fig.7 Gas Driven Fan LSPM Components

Also shown in Figure 7 is a 3 bearing type nozzle used to vector the thrust from the remote fan aftwards thus providing forward thrust during transition. This is a common requirement for all ASTOVL concepts with a remote front thrust post. The situation is made more complicated for the gas driven fan as the fan and turbine exhaust streams must be kept separate through the nozzle due to their different pressures.

Numerous designs of nozzle to provide front thrust post vectoring have been proposed e.g.

- o 3 Bearing (contra rotating duct) nozzle
- o Cascade nozzles
- o Post exit deflectors
- o Hooded nozzles

All these types of nozzle are feasible and their effectiveness has been evaluated by model and full size testing. The solution employed is very dependent on the particular airframe configuration, especially the amount of vertical height available for the stowed nozzle and the degree of vectoring required.

5.4 Lift Plus Lift/Cruise

Apart from the Harrier, the only other operational fixed wing STOVL combat aircraft is the YAK 38 Forger which uses the lift plus lift cruise propulsion concept. This system, as shown in Figure 8, uses one or more engines mounted vertically and used only during jet borne flight and transition to provide lift. Numerous other lift plus lift/cruise demonstrator aircraft have been built and flight tested successfully, notably;

YAK 141
VFW-Fokker VAK191B
Dassault Mirage 111-V
Short SC1
Dorier DO31

With the exception of the Russian aircraft, all the above used multiple Rolls-Royce lift jets, either the 2 300 lbf thrust RB108 or the 6000 lbf thrust class RB162. A third generation lift jet the XJ99 was also developed jointly by Rolls-Royce and Allison for a US/German project which was unfortunately cancelled before first flight.

The problems generated by mounting an engine vertically in an aircraft, shutting it down just after take off and then restarting it prior to landing are numerous. However, the experience generated on the programmes listed above is invaluable in understanding the issues and identifying likely solutions.

The major design criteria for lift engines are that they should be;

- reliable
- occupy a small space envelope (diameter and length)
- lightweight
- low cost
- posses a low exhaust temperature.

The fuel consumption of the engine is relatively unimportant as it will only be operated for a few minutes per flight. High engine cycle efficiencies such as can be obtained by high bypass ratios, overall pressure ratios and cycle temperatures are not warranted as they add to weight, length, cost and complexity. Indeed it can be readily shown that the highest specific thrust cycle (thrust per unit airflow) for an engine is obtained at a relatively low overall pressure ratio of between 10 and 15 dependent upon turbine entry temperature. (See Figure 9). Specific thrust does increase monotonically with increasing turbine entry temperature. However, this parameter must be limited to ensure an acceptably cool exhaust for avoidance of ground erosion and hot gas ingestion problems. It should be noted that the length constraints imposed upon the lift engine installation will probably preclude efficient mixing of the fan and core exhaust streams. It is therefore the core stream exhaust temperature which is the critical parameter for ground erosion which again effects the choice of engine cycle.

Severe length constraints are placed upon the lift engine to limit the required depth of the aircraft fuselage. This is particularly true for an airframe intended for both CTOL and STOVL variants and necessitates some unconventional design features such as;

- o Minimal length fan spinner
- o Low length/depth ratio combustors
- o High aspect ratio turbine blading
- o Deletion of exhaust vanes and case



Lift+ Lift/Cruise engines

SPV 12599

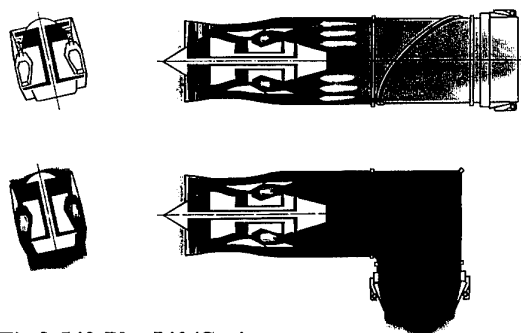


Fig.8 Lift Plus Lift/Cruise

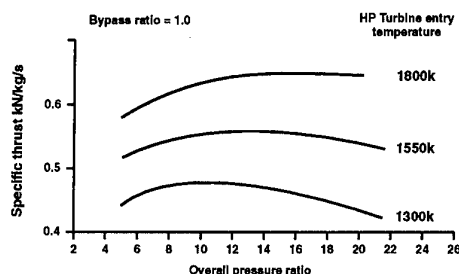


Fig.9 Turbofan Specific Thrust vs. Overall Pressure Ratio

Such features require great attention to detail during the engine design. Performance degradations relative to the state of art may have to be anticipated to ensure the engine functions effectively from a mechanical point of view.

Perhaps the major challenge associated with the lift plus lift cruise concept is the integration of the powerplants with the airframe.

Of concern must be the interaction of the control systems for the two engines particularly if, as is likely, the lift engine depends upon the lift/cruise engine for services such as starting and fuel supply.

The installation aerodynamics for the vertically mounted lift engine require considerable attention. The achievement of acceptable intake distortion levels, so as to avoid engine surge, with the aircraft operating at significant forward speeds during transition is a particular concern. The generation of adequate airflow through the engine to windmill start must also be addressed. Thankfully, a large amount of research into these issues was carried out in the 1960s and 70s which provides an invaluable basis for defining solutions to these integration problems. A sample of this work is given in Reference 2.

6. GENERIC ASTOVL POWERPLANT CHALLENGES

There are a number of challenges associated with future ASTOVL powerplants which have to be addressed irrespective of which concept is chosen. Some of these issues are discussed below.

6.1 Vectoring Main Engine Exhaust Nozzles

All four concepts require a significant contribution to vertical thrust from the main engine exhaust. There are basically two options for achieving the required exhaust deflection;

- Block off the engine jet pipe and direct the engine exhaust flow through Pegasus type swivel nozzles.
- Articulate the main engine cruise nozzle such that it can vector vertically.

Neither approach is easy, especially at the high exhaust gas temperatures of modern military aircraft engines. Several different types of "block and turn" valves have been investigated by Rolls-Royce to suit the first option described above. These are principally based on thrust reverser technology of either the "clamshell" or target type. Issues such as sealing and mechanical integrity, particularly of the actuation system are, however, much more critical for the ASTOVL lift system. Leaks in the blocker system lead to significant lift thrust losses and possible overheating of the blocked off jet pipe and cruise nozzle. Failure of the blocker system during hover would almost certainly lead to loss of the aircraft due to uncontrolled vertical thrust loss and pitching moment.

The design of the block and turn system is further complicated by the need to maintain separate bypass and core airstreams across the valve during operation in the flight mode, in order to provide cooling for the jet pipe and cruise nozzle. Significant aerodynamic losses through the system are inevitable and require early design consideration to maintain a viable vertical thrust level. The most critical parameter affecting thrust loss is the total flow turning angle. This is inherently higher in a block and turn system than with an articulated cruise nozzle. Figure 10 shows the effect of turning on flow efficiency (Reference 4). For the Harrier Pegasus installation the total turning angle in each nozzle is 180° . This can be reduced by incorporating droop and trail as shown in Figure 11 but this feature requires careful integration with the airframe.

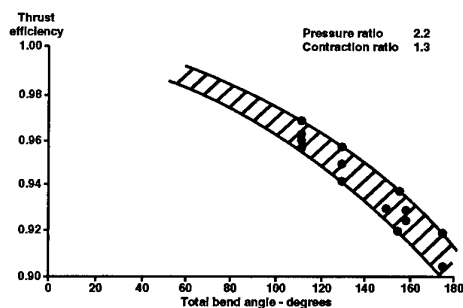


Fig.10 Effect of Turning on Thrust Efficiency

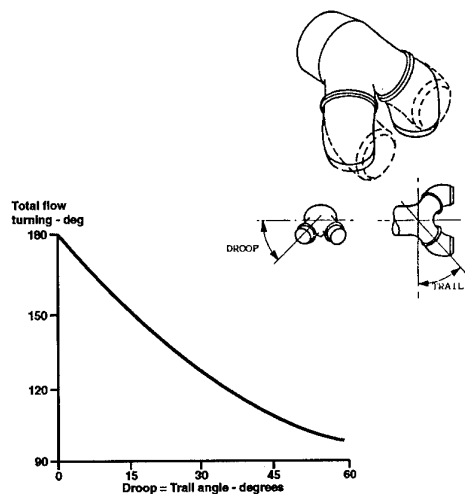


Fig.11 Effect of "Droop and Trail" on Total Flow Turning

Articulation of the cruise nozzle has been shown to be practical on the YAK 141 and other non-flying engine demonstrators. This is achieved by incorporating 2 angled bearings into the jet pipe together with a third bearing perpendicular to the engine axis. By differential rotation of these bearings, the jet pipe can be made to vector continuously from horizontal to vertical. Such systems are commonly termed "3 bearing nozzles".

Figure 12 shows such a system developed by MTU of Germany for the RB153 lift/cruise engine during the 1960s. As previously stated, the losses due to flow turning in an articulated cruise nozzle system are inherently lower than with block-and-turn systems. Additionally, the transition from lift to flight mode with such a system is simplified as no shut-off valve is required and, therefore, the exhaust system throat is maintained at the nozzle exit throughout. The engine cruise nozzle is variable area to allow for dry and reheat operations and therefore no additional actuation is required for those concepts which require a variable area rear lift nozzle. However, the resultant rear thrust post position is further aft than can be achieved with block-and-turn, which can lead to aircraft balance problems. Ground clearance is also a concern especially if a convergent-divergent cruise nozzle is required for high speed flight performance. Actuation of a 3 bearing nozzle is not easy as the drive has to be taken across the bearings but solutions have been found, albeit with some weight penalty.

An alternative means of providing a fully vectoring cruise nozzle is to employ a 2-D nozzle with a large vectoring flap range. Many conceptual designs have been proposed for such a nozzle as at first sight they appear to be simpler to engineer than a 3 bearing axisymmetric system. However, the challenge of designing a 2-D nozzle with acceptable weight and cost for a STOVL aircraft is significant. Figure 13 shows such a nozzle designed and built by Rolls-Royce for the Lockheed shaft driven fan large scale powered model demonstrator. This nozzle has demonstrated the aerodynamic feasibility of the concept. The design is however, very much a "boiler plate" construction and a significant challenge exists to turn such a system into a light-weight design.

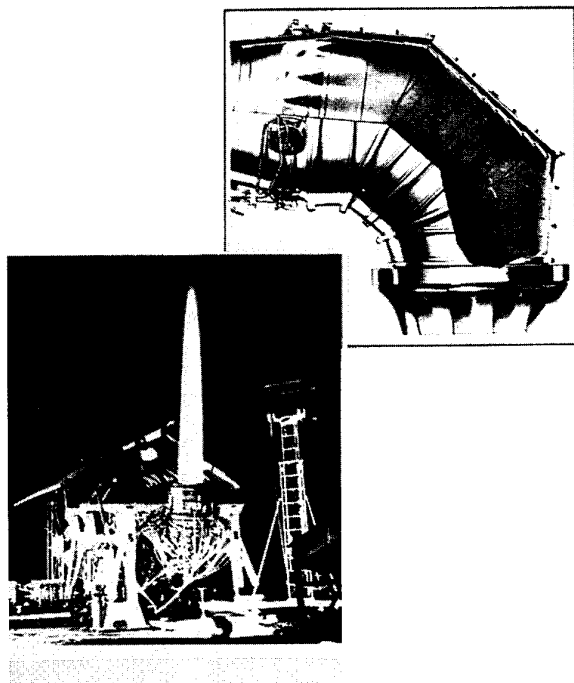


Fig.12 RB153 Deflected Reheat

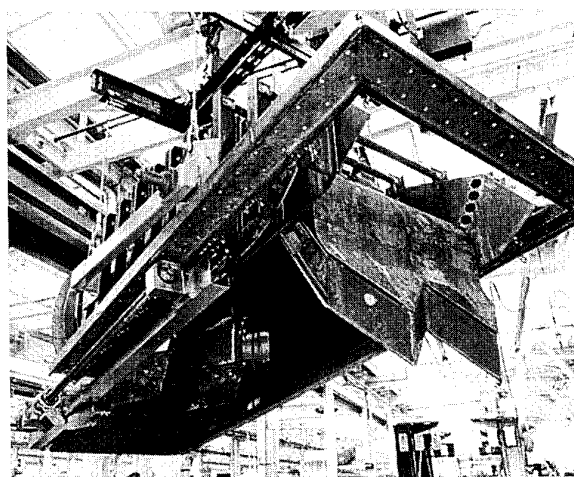


Fig.13 LSPM Fully Vectoring 2D Nozzle

6.2. High Temperature Capability Exhaust Nozzles.

The design of Pegasus style elbow nozzle for modern ASTOVL powerplants is complicated by the higher temperature of the hot jet efflux of such engines. Problems such as ground erosion, hot gas ingestion and fuselage heating are all exacerbated by increased jet efflux temperature. Therefore, the propulsion system designer must strive to minimise this parameter. However, it is fundamental that powerplant Thrust/weight ratio increases with higher engine exhaust temperature leading to a significant conflict, particularly if the same basic powerplant is to be used for both STOVL and CTOL variants.

The environmental issues mentioned above have been the subject of many papers in the past, notably References 4 and 5 and it is not, therefore, intended to discuss these issues further in this paper.

Pegasus nozzle are fabricated from Nickel based alloy sheet which can tolerate jet temperature up to around 800°C. It is anticipated, however, that rear jet temperatures of the production JAST powerplants could be over 100°C hotter than Pegasus. The nozzle designer is therefore faced with three options;

- Use a material capable of withstanding the the higher temperature.
- Cool the nozzle using fan bypass air.
- Insulate the nozzle from the high temperatures.

All three of these approaches are currently being investigated by Rolls-Royce for either large scale powered models or proposed production JAST/ASTOVL powerplants.

Option (a) is somewhat restricted as few materials have greater temperature capability than nickel base alloys. The options are basically limited to either turbine blade casting alloys or ceramics. At first sight, the option of casting such a large component in a nickel or cobalt based alloy appears daunting. The potential benefits of reduced cost and timescales, particularly if stereo lithography modelling techniques are employed, are however worthwhile. A small but significant improvement (~50°C) over a fabricated nozzle is achieved with such a route. The final component can be heavy, but Rolls-Royce have recently demonstrated that the casting process is feasible.

The ultimate materials for both high temperature capability and low weight are ceramic matrix composites. Temperatures of 1000°C can be readily tolerated. Problems of durability and manufacturability of large ceramic composite components are being addressed. However, further advances are required before they could be successfully employed in the high load and vibration environment of an ASTOVL swivel nozzle.

Option (b) cooling requires the nozzle to be double skinned, similar to a conventional military engine jet pipe construction. The outer load carrying skin is separated from a hot inner liner by a flow of relatively cool air extracted from the fan bypass stream. The inner liner would be nickel alloy, or possibly Titanium Aluminide, and could be run to high temperatures as it is not required to transmit the main nozzle pressure and thrust loads. As fan bypass temperature does not exceed 270°C for the envisaged powerplants, it is possible to conceive of an outer nozzle skin in lighter lower temperature materials such as Titanium or even Organic Matrix Composite depending on the amount of cooling air available. Difficulties have been identified with this approach with regard to attachment of the liner to cater for differential expansion, together with localised pressure loads on the liner caused by the acceleration of the flow into and along the nozzle. An attraction of this type of nozzle design is that the outer skin is relatively cool and therefore does not transmit significant heat into the aircraft structure.

Option (c) (insulation) has been used successfully by Rolls-Royce to construct nozzles for one of the JAST/ASTOVL large scale powered models currently being tested. A nickel Alloy nozzle is lined both inside and outside with an insulation blanket. Again attachment is a problem, especially as the insulation material can be easily dislodged by the nozzle internal airstream. The outside insulation is used to minimise differential expansion and to reduce the outside skin temperature.

6.3. Attitude Control

Control power to maintain aircraft attitude in jet - borne flight must be provided from the Powerplant. Four different options have been investigated for this purpose.

- HP Compressor delivery bleed air
- Engine exhaust bleed air
- Differential vectoring of thrust posts
- Re-distribution of thrust between thrust posts.

Option (a) (HP bleed) is the system used successfully in the Harrier. Air is bled from a manifold around the combustion chamber of the Pegasus engine. This has two major effects on the engine:

- o Turbine entry temperature has to be increasing to maintain thrust requiring additional cooling to maintain life.
- o The HP compressor working line falls, increasing surge margin but reducing choke flutter margin.

The above effects mean that the amount of HP bleed air from an engine is limited, generally to around 10% of the engine core mass flow. The amount of attitude control power required for the ASTOVL aircraft currently being studied is yet to be fully defined but studies based around simulation work such as Reference 6 indicate HP bleed flows in excess of the projected powerplant capabilities if all axes are controlled by this method.

The temperature of HP delivery bleed air (around 700°C) for the majority of projected ASTOVL powerplants requires the reaction control system air ducts to be constructed from temperature resistant material and valves such as nickel alloy (heavy) or ceramics (high cost/risk). Note: air cannot be bled from part way up the HP compressor without seriously compromising engine operation. The ducts and valves are, however, relatively compact due to the high air pressure and can therefore be relatively easily incorporated into the aircraft.

This is a well proven system but does require the engine to be configured to provide the bleed flow which compromises CTOL/STOVL commonality of the main powerplant core.

Option (b) (Engine exhaust bleed) generally does not suffer from the capacity restrictions of HP bleed. In such a system air is limited to a pressure at or close to fan delivery (i.e. approximately 5 times lower pressure than HPC delivery). This means that any ducting must be of a significantly larger cross-sectional area. It is possible to conceive of systems using fan bypass flow, core exit flow or a mixture of the two. However, the high temperature of the core exit gases (900°C or more) mean that, as with HP bleed, ducts and valves would need to be constructed in either nickel alloys or ceramics. Such considerations mean the ducting of hot exhaust air over significant distances is not practical. Fan bypass air attitude control

systems can, however, use light weight Titanium alloy or organic matrix composite ducts and valves making them a relatively attractive option, provided that the engine bypass ratio is sufficiently high to deliver the ACS flow together with any cooling requirements for the rest of the powerplant.

Option (c) (Re-distribution of thrust) is theoretically an elegant solution to the problem of providing attitude control. In practice, however, it poses significant difficulties. The remote fan systems, including lift plus lift/cruise, offer scope for pitch control due to the large axial spacing of the front and rear thrust posts. However, current studies indicate that high rates of change of pitching moment are required to stabilise the aircraft implying rapid thrust transients from the forward and rear posts. This implies a rapid increase of power to the remote fan (whether gas driven, shaft driven or lift engine), which is difficult to achieve due to lags caused by control system computing time, control system response time and combustion lags (or hydraulic lags in a gas driven system)

One method of improving the response of an engine is to utilise variable geometry in the fan system i.e. variable pitch blades or inlet guide vanes. Variable pitch blades are very difficult to engineer on any fan, especially the high speed high pressure ratio designs employed on ASTOVL powerplants in order to reduce size and weight. The variable inlet guide vane is simpler to engineer but does add significant length, cost and weight to the engine. The inclusion of variable geometry allows the flow through the fan to be rapidly changed (limited only by actuator response) making use of the stored energy in the engine LP spool to increase thrust very rapidly. If, however, no action is taken to increase the energy input into the systems, the fan will decelerate and the thrust boost will be lost.

Figure 14 illustrates this effect for a projected lift engine with variable inlet guide vanes. This data taken from a transient performance model of the engine shows separately the thrust change due to IGV change and fuel flow increase followed by the combined response.

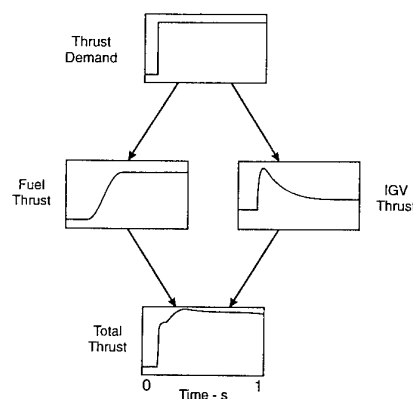


Fig.14 Lift Engine Thrust Response - Effect of VIGV and Fuel Modulation

Another method of thrust redistribution is to employ variable area lift nozzles on the powerplant. This technique can for instance be used on a pair of Pegasus type lift nozzle to provide roll control by simultaneously reducing the area of one nozzle while increasing the other. The large force changes achievable by this method offset the small moment arm to give acceptable control power. The thrust change occurs instantaneously with the nozzle area variation and is therefore limited only by the response rate of the actuation system. The basic difficulties with this type of system is its application on nozzles carrying hot exhaust gases and the complexity of carrying the area variation actuation across the vectoring nozzle bearing plane. These problems are not insurmountable and indeed the nozzle shown in Figure 15, designed and built by Rolls-Royce for one of the CALF/JAST large scale powered models, incorporates a clamshell door to provide area variation. The challenge is, however, to engineer such a system at an acceptable weight and reliability. It is essential with such systems to ensure that the total engine exhaust nozzle area is held constant at all times to maintain the fan working line in its correct position.

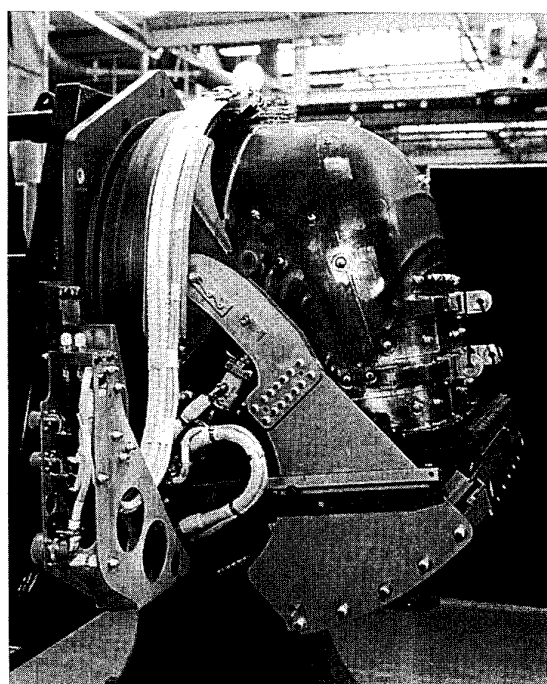


Fig.15 LSPM Pegasus Type Nozzle with Variable Exit Area

Option (d) (differential vectoring) has been investigated mainly for attitude control in the yaw axis. Numerous options are possible depending on the particular powerplant layout utilising either

- differential vectoring of a pair of Pegasus type lift nozzles (one vectored forward the other vectored aft).
- Post exit vanes, again usually on Pegasus type nozzles.

- A nozzle with side to side vectoring (\pm approx 15°) on the front thrust post.

Rolls-Royce studies indicate that this latter option is the most feasible due to the lower exhaust temperature allowing a relatively light weight vectoring nozzle coupled with the larger effective movement arm of a side force applied at the front nozzle position. In all cases the effect of such systems on the ground cushion (fountain) and hot gas ingestion characteristics needs to be carefully considered.

For all concepts the attitude control requirements have a significant effect upon the size and complexity of the ASTOVL powerplant. Piloted simulator studies, similar to those reported in Reference 6 are essential using the proposed aircraft and powerplant characteristics in order to define more accurately the level of control power required and also the transient response demanded of the system. These studies should be carried out as early as possible in the weapon system design process.

6.4 Complexity and Reliability

A fundamental feature of ASTOVL powerplants is their complexity compared to conventional engines, and indeed the Pegasus/Harrier.

This is indicated in Figure 16 which lists the number of control actuations required for the different concepts together with those for the Harrier. In all cases a failure in any of these systems could lead to the loss of the aircraft if failure occurs in jet-borne flight.

	Harrier	DL	SDF	GDF	L+L/C
Remote fan post exit door/front nozzle vectoring		✓		✓	✓
Remote fan clutch			✓		
Remote fan variable pitch			✓		
Lift engine fuel valve					✓
Rear vectoring nozzle angles	✓	✓	✓	✓	✓
Rear lift nozzle variable area			✓	✓	
Rear nozzle sleeve valve (forward) &/or bypass blocker	✓	✓	✓	✓	✓
Hot gas to remote fan offtake sleeve valve			✓	✓	
Jet pipe block and turn device		✓	✓	✓	✓
Bypass offtake valve		✓	✓		
Fan inlet guide vanes		✓	✓	✓	✓
HP compressor VIGV's and blow-off valves	✓	✓	✓	✓	✓
RCS bleed valve	✓	✓	✓	✓	✓
Core engine fuel flow	✓	✓	✓	✓	✓
Afterburner fuel flow		✓	✓	✓	✓
Flight propulsion nozzle variable area		✓	✓	✓	✓
Yaw control	✓	✓	✓	✓	✓
Pitch control	✓	✓	✓	✓	✓
Roll control	✓	✓	✓	✓	✓

Fig.16 Control Actuations Required For Various ASTOVL Concepts

Although differences in the detailed implementation of the powerplant concepts may marginally alter the number of actuation systems required, it is clear that the number of safety critical control functions for the ASTOVL concepts is approximately twice that of the Harrier. Therefore, unless action is taken to improve the reliability of these systems, the rate of aircraft loss due to propulsion system failure will be significantly worse than the Harrier.

Figure 17 shows a fault tree for failures leading to the loss of an aircraft. Aircraft loss may be due to either operational reasons (pilot error, bird strike etc.) or technical failures. Technical failures can be due to either the airframe or the propulsion system. Propulsion system failures may be due to either the basic engine or its control features. The typical percentage of aircraft losses attribute to each of these factors is also shown on Figure 17 for a conventional aircraft.

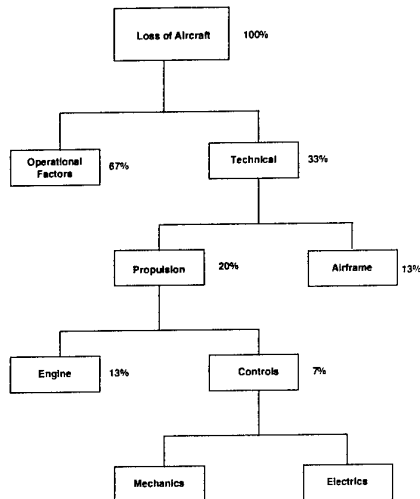


Fig.17 Fault Tree For Single Engine CTOL Aircraft

For an ASTOVL aircraft the fault tree is expanded as shown in Figure 18. In addition to propulsion system failures due to the basic engine and basic control, the contribution of the "STOVL elements" must be added. These STOVL elements can

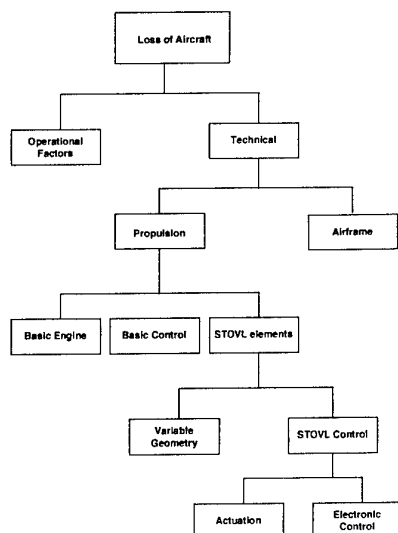


Fig.18 Fault Tree For ASTOVL Aircraft

themselves be split into hardware (ducts, nozzles etc.) and control features (actuation and electronics). This type of analysis can be used to set the reliability requirements for the STOVL elements. It is clear, however, that these complex system will make a significant contribution to the failure rate of the weapon system. If the overall aircraft loss rate is to remain at the same level as a conventional aircraft, improvements to the reliability of the basic engine and its control, and indeed the airframe reliability must be achieved to allow for the STOVL elements. This represents a challenge to both airframer and engine maker alike. Even so, the task of achieving an acceptably reliable control system for the STOVL features will be extremely demanding. In particular, the actuation of large mechanical structures such as blocker valves and nozzles is a major concern. The reliability issues of such actuation systems are discussed in Reference 7.

6.5. Affordability

The foregoing discussion describes some of the major technical issues associated with ASTOVL powerplants. There is, however, little doubt that all the concepts described could be made to work given an unlimited amount of resources. The major challenge is therefore to design and develop such systems at an affordable cost.

The current JAST initiative to develop a common CTOL and STOVL airframe is potentially a significant step towards providing an affordable ASTOVL aircraft for those operators who need such a capability. Even so, stringent attention must be paid to the means by which we design, develop and manufacture future powerplants. This includes;

- o True Concurrent Engineering, i.e. designing for minimum development, acquisition and support cost from day one.
- o Utilising existing hardware where possible - if not complete engines then make use of existing cores.
- o Utilisation of "lean manufacturing" techniques and development of reduced cost processes.

7. CONCLUSIONS

All the STOVL powerplant concepts currently being studied for the competing JAST airframes present major challenges for the engine company. Some of these challenges are specific to a particular concept, many others have to be addressed for any ASTOVL system.

The JAST program philosophy of utilising a common airframe for both CTOL and STOVL introduced additional constraints and challenges for the propulsion systems.

Any successful JAST propulsion concept must offer an affordable solution to these challenges. It is likely that the optimum concept may not be the same as that for a purely STOVL aircraft.

8. REFERENCES

1. Mitchell, N.A., "ASTOVL Propulsion Systems, configuration and Concept Choice" in Proceedings of the international Powered Lift Conference, 29-31 August 1990", The Royal Aeronautical Society.
2. Coplin, J.F., "Lift Jet Installational Experience", Aircraft Design and Technology Meeting, Los Angeles, November 14-18, 1965
3. Lewis, W.J., "V/STOL Propulsion System Aerodynamics", Paper No.6, AGARD report No.710 in "Special Course on V/STOL Aerodynamics, May/June 1984
4. Penrose, C.J., "Influence of Headwind on Hot Gas Reingestion and Consideration of Pressure Ratio Scaling", Paper 17 of AGARD Symposium on Computational and experimental Assessments of Jets in Cross Flow, Winchester, UK, April 1993.
5. Moss, G.M. and Penrose, C.J., "Development of Modified Lift Improvement Devices for the AV-8B Harrier", paper AIAA 95-0532, 23rd Aerospace Sciences Meeting and Exhibit, January 9-12, 1995, Reno, USA.
6. Franklin, J., "Criteria for Design of Integrated Flight/Propulsion Control System for STOVL fighter aircraft", NASA Technical Paper 3356,
7. Northcott, A.J., "Actuation System Requirements for ASTOVL Powerplants", paper presented at I Mech E Seminar on the future of Engine Accessory Drives, Birmingham, UK, October 19

9) ACKNOWLEDGEMENTS

The author wishes to acknowledge the assistance of his colleagues at Rolls-Royce, and the directors of Rolls-Royce plc, for their permission to publish this paper. The preparation and presentation of this paper has been assisted by the Engineering and Physical Science Research Council through the Warwick University Engineering Doctorate programme. The views expressed in this paper are those of the author, and do not represent any commitment by or policy of Rolls-Royce plc.

Figure 7 is reproduced courtesy of General Electric Aircraft Engines.

Paper 8: Discussion

Question from F Scorer, Defence Research Agency, UK

You said that to provide attitude control via fore/aft thrust modulation with a lift plus lift/cruise system, inlet guide vanes or variable area nozzles would be needed on the lift engines. The Russian Yak 38 uses fuel control to achieve this. Did the Rolls-Royce analysis examine different kinds of lift engine which were not as responsive as those used in the Yak 38?

Author's reply

Yes, the Yak 38 does use thrust modulation for pitch altitude control in the hover. However it is not known what rate of pitch response is provided by their system. Currently the JAST study teams are seeking very fast response to take account of all possible pitch disturbances. There is some Harrier evidence to suggest that the rates demanded are excessive and, that should these be relaxed, it may be possible to stabilise the aircraft with thrust response through fuel modulation alone. Two aspects of the lift engines used in the Yak 38 help in this respect. Firstly, they are turbojets rather than turbofans and therefore the spool inertias are relatively small. Secondly they use a hydromechanical fuel system which, if properly designed, could give a better response rate than the digital systems envisaged for the JAST aircraft. This is because the finite computing time delay is avoided. On the other hand, Rolls-Royce studies have shown that turbofans offer significant advantages over a turbojet for the proposed systems - notably, reduced engine plus fuel weight (even with variable geometry) and reduced exhaust gas temperature. Also digital fuel control will be essential in the JAST concepts, due to the highly integrated nature of the aircraft systems.

Developing Affordable Gas Turbine Engines

Charles A. Skira
 WL/POTA Building 18
 1950 Fifth Street
 WPAFB, OH 45433-7251
 USA

Summary

The cost of advanced, high performance gas turbine engines for future military fighter aircraft application are explored. The impact of increasing engine performance on the cost of the aircraft was examined and was found to have a favorable impact on the cost of the weapon system. From an engine viewpoint, advanced component performance and improved, cost effective manufacturing methods combine to significantly lower the cost of gas turbine engines on a per pound of thrust basis. Engine component costs were compared and analyzed for a modern fielded engine and an advanced technology, high performance engine. Manufacturing costs and the implication to overall engine cost reduction for advanced technology engines was explored.

List of Symbols

BAI	Battlefield Air Interdiction
CMC	Ceramic Matrix Composites
DoD	Department of Defense
IHPTET	Integrated High Performance Turbine Engine Technology
LPT	Low Pressure Turbine
MMC	Metal Matrix Composite
NASA	National Aeronautics and Space Administration
OMC	Organic Matrix Composite
O&S	Operating and Support
T/W	Thrust-to-Weight Ratio
TOGW	Take-off Gross Weight
\$/lb Fn	Dollars per Pound of Thrust

This paper is declared a work of the U.S. Government and is not subject to copyright protection in the United States.

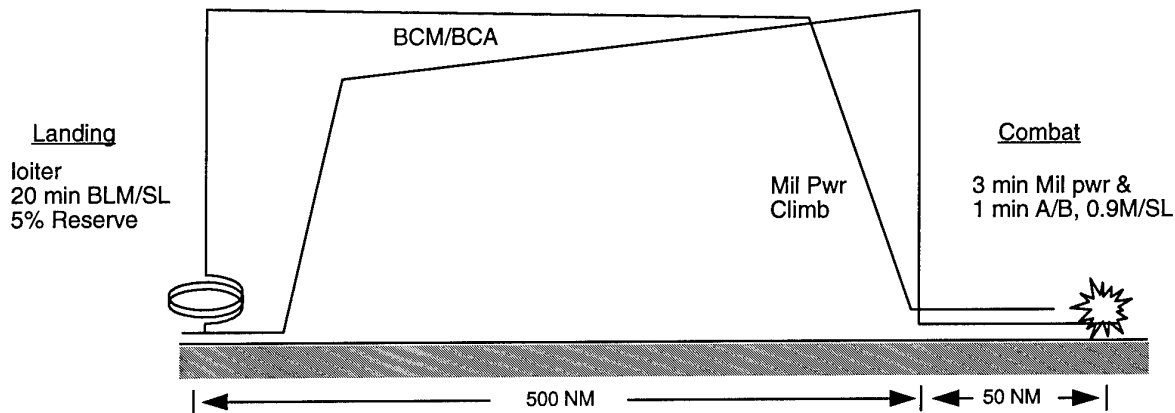
Introduction

Due to the historic and dramatic changes in recent global events, the United States military services have been undergoing a drawdown in size. Since 1989, our military forces have been reduced by 30%. While the reduction in troop strength is the most visible sign of this drawdown, all elements of the military have been involved, including research and development for future systems.

By the year 2010, more than half of the Air Force fighter fleet will consist of existing F-15's, F-16's and F-117A's -- well beyond their expected service life. Nonetheless, the need exists to replace our most aged fleets of aircraft despite the uncertainty of future defense budgets. The environment within today's defense establishment is unprecedented in recent history. Costs, more than any other factor, will determine military force structure.

Recognizing the importance of this challenge, the Aero Propulsion and Power Directorate of Wright Laboratory began to investigate the issues of affordability and cost of future aircraft turbine engine propulsion systems being developed under the DoD/NASA/Industry Integrated, High Performance Turbine Engine Technology (IHPTET) Initiative. The goal of the IHPTET program is to demonstrate technology by the turn of the century that will double the propulsion capability for a wide range of aircraft and missile applications. The IHPTET program has added cost reduction to its list of program goals. The two (2) principal aspects of engine life cycle cost that are being addressed within IHPTET are engine acquisition cost (unit sell price) and operating and support (O&S) costs. This paper

Battlefield Air Interdiction



GENERAL NOTES

MISSION

Warm up: 5 min T/W=.2
 Short Take-off: 1/2 min Max A/B
 Short Landing: 1/2 Min Mil Pwr
 5% Reserve Fuel at Landing
 5% Fuel flow conservatism
 No Range/Fuel Credit for Descent
 External Fuel: 3500lbs
 Payload: 2xTDM
 2xASRAAM
 500 Rds 20mm Ammo

ECONOMIC

FY 1990 \$'s
 Fuel Cost: \$0.551/Gal
 750 Aircraft over 10 Years
 Single Engine Aircraft
 750 Engines + 25% Spares
 20 Year Life Cycle
 Engine is Two Level Maintenance
 Costs quoted for 250th Unit

Figure 1 : BAI Mission Schematic

will describe the efforts that have been made to identify the cost of future, advanced turbine engine powerplants, identify the cost reduction potential for these engines, and define the technology developments required to lower the cost of future engines.

Weapon System Affordability

A unique aspect of the aircraft powerplant is its positive influence on the size and weight of the aircraft. The application of high performance propulsion systems results in a smaller, lighter and lower cost aircraft. Traditional thinking dictates that high performance also implies high cost. This cost versus performance issue does not necessarily have to be a trade-off or compromise. Both high performance and low cost can be achieved at the same time.

One of the first issues to be addressed was to determine the influence of propulsion system performance and cost on the overall cost of an aircraft. In an earlier in-house Air Force study conducted by WL/PO, the impact of engine performance, defined as thrust-to-weight ratio (T/W), on aircraft take-off-gross-weight (TOGW) was investigated. A battlefield air interdiction (BAI) mission was selected as the mission that would size the aircraft and engine. Figure 1. shows a schematic of the BAI mission and also lists the groundrules and assumptions that were used for the mission and for the cost analysis.

The initial study task focused on identifying the aircraft TOGW and engine weight required to satisfy the mission. Figure 2. shows a plot of aircraft weight and engine weight as a function of engine T/W. As

shown in the figure, the size and weight of the aircraft shrinks as the engine T/W increases. The base engine identified in figure 2. is similar in performance to the Pratt & Whitney F119. This engine results in an aircraft that weighs a little over 41,000 pounds. Conversely, the aircraft powered by an engine whose performance is characterized by levels that will be demonstrated in Phase III of the IHPTET program weighs a little over 29,000 pounds. In the aircraft weight analysis, all mechanical components were considered. To arrive at aircraft TOGW, most components of the aircraft were scaled by weight. Some components, such as the cockpit and weapons are not scaleable and therefore their weights remained constant. The final aircraft weight was the sum of the scaled and unscaled component weights.

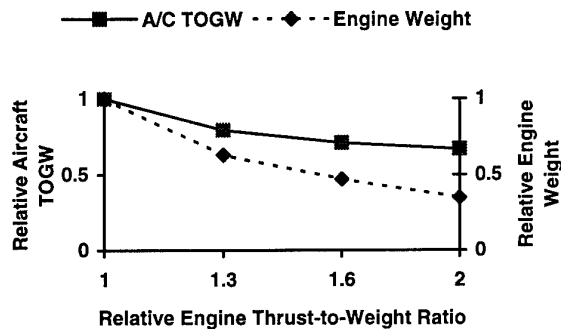


Figure 2.

Two interesting phenomena occur. As the aircraft gets smaller, the engine thrust required to accomplish the same mission also gets smaller. This is coupled with the fact that the IHPTET initiative will result in a smaller engine for a given thrust size. The dashed line in figure 2. shows how the engine weight is impacted by these two phenomena.

Acquisition costs were determined for the aircraft and engine combinations. For the aircraft, a simple

conversion of \$775 per pound of weight is used to arrive at the aircraft cost. The primary purpose of the study was to determine the engine impact on aircraft structural weight. In the analysis, avionics weight and costs were not considered. From a weight viewpoint, the avionics is not a significant factor. However, from a cost perspective, avionics is one of the most significant contributors to the cost of a modern fighter aircraft.

An estimate of engine cost was determined by examining the historical costs of modern fighter engines. The subset of modern aircraft investigated included the Air Force F-15 and F-16 and the Navy F-18. Figure 3 shows a normalized plot of engine cost expressed in terms of dollars per pound of thrust (\$/lb Fn) versus relative engine thrust-to-weight ratio.

In addition to the fielded engines described above, the data base also includes cost estimates for the IHPTET Generation 4 and Generation 5 engines. The cost data for the fielded engines represented the unit sell price negotiated as of the last engine buy. All costs were then converted to constant FY90 dollars. Figure 3 indicates that the cost (\$/lb Fn) of modern fighter engines is relatively constant. Using this relationship, the engine costs were derived for our study configuration. Table 1 shows the results of the cost analysis for both the airframe and the engine. The only factor influencing engine cost is the

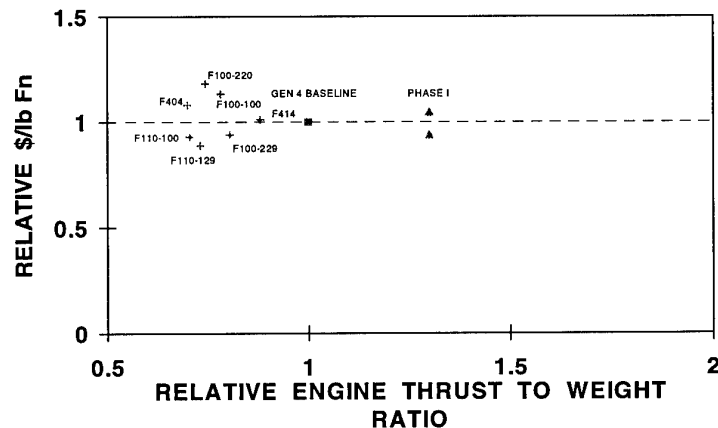





Figure 3. Historical Trend of Engine Acquisition Cost

engine size, which is a function of technology level. The engine and aircraft cost payoff due solely to advanced technology, high performance propulsion systems is quite significant -- illustrating the importance of advanced technology from a system point of view.

ENGINE GOALS/PAYOFF	PHASE I	PHASE II	PHASE III
			
• THRUST/WEIGHT	+30%	+60%	+100%
• FUEL BURN ⁽¹⁾	-20%	-30%	-40%
	PAYOFF ⁽¹⁾		
• AIRCRAFT ACQ COST (FY90)	-19%	-25%	-30%
• ENGINE ACQ COST (FY90)			
- AT CONSTANT \$/lb F _n	-15%	-25%	-30%

(1) Based on typical mission/system

Table 1. Cost Analysis Results:
Historical \$/lb F_n

Cost Reduction

Having investigated the affordability aspect of advanced propulsion systems, the next issue to address was to identify what could be done to lower the manufacturing cost of advanced technology engines.

The engines of the future will achieve their incredible performance primarily through improvements in aerodynamics and materials technology. The materials used in these engine cycles will have higher temperature capability, improved strength and will be lighter in weight than the materials used in today's aircraft engines. Advanced technology engines of the future will be characterized by the application of high temperature organic matrix composites (OMC) for the fan, front frame, ducts and cases. Advanced titanium metal matrix composites (MMC) will be used in the compressor rotor. Compressor blades and vanes will be made of advanced intermetallic titanium offering high strength and temperature capability. Advanced intermetallics will also be used extensively in the diffuser, combustor and in the exhaust nozzle.

Advanced ceramic matrix composites (CMC) will be required for the combustor, low pressure turbine (LPT), turbine rear frame and in the exhaust nozzle. High pressure turbine blades will be designed to require less cooling air through the application of advanced integral convective cooling methods. Multi-alloy turbine discs will provide localized creep and fatigue resistance at the rim and hub, respectively.

Compared to the mostly monolithic materials of present day engines, the high temperature, high strength composite materials for future engines present significant processing and manufacturing challenges. Developing cost effective methods to fabricate and manufacture engine components with these advanced materials is the key to future engine cost reduction. In the IHPTET program, cost reduction goals have been established. The goals were defined based on an evaluation of cost reduction potential, and an assessment of the development programs required. The assessment of programs included an evaluation of technical and schedule risk. Accomplishing these goals requires an integrated emphasis on innovative design and improved material processes and manufacturing science.

Figure 4 illustrates the impact of the IHPTET cost reduction goals relative to the historical trend shown previously in figure 3. As indicated in the figure, a significant shift in the state-of-the-art is required to attain these goals. Table 1 described the cost payoff associated with higher engine performance. Recall that these payoffs were due solely to the reduction in engine size needed to accomplish the mission. Cost was assumed to follow the historical trend. Table 2 shows the total cost benefit (in terms of the unit price of the engine) when cost reduction technologies are applied.

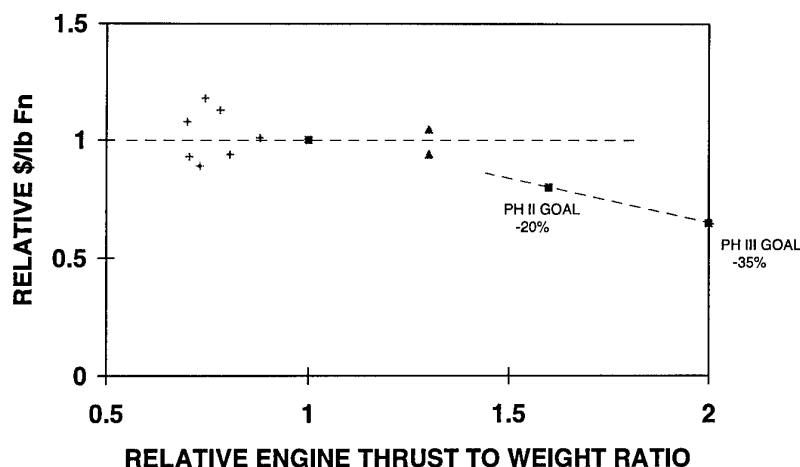


Figure 4. IHPTET Engine Acquisition Cost Goal

ENGINE GOALS/PAYOFF	PHASE I	PHASE II	PHASE III
• THRUST/WEIGHT	+ 30%	+ 60%	+ 100%
• FUEL BURN ⁽¹⁾	- 20%	- 30%	- 40%
		PAYOFF ⁽¹⁾	
• AIRCRAFT ACQ COST (FY90)	- 19%	- 25%	- 30%
• ENGINE ACQ COST (FY90)			
- AT CONSTANT \$/lb Fn	- 15%	- 25%	- 30%
- AT "GOAL" \$/lb Fn ⁽²⁾	----	- 40%	- 55%

(1) Based on typical mission/system

(2) Integrated IHPTET innovative design and adv manufacturing technology

Table 2. Cost Analysis Results: Goal \$/lb Fn

Engine Manufacturing Cost

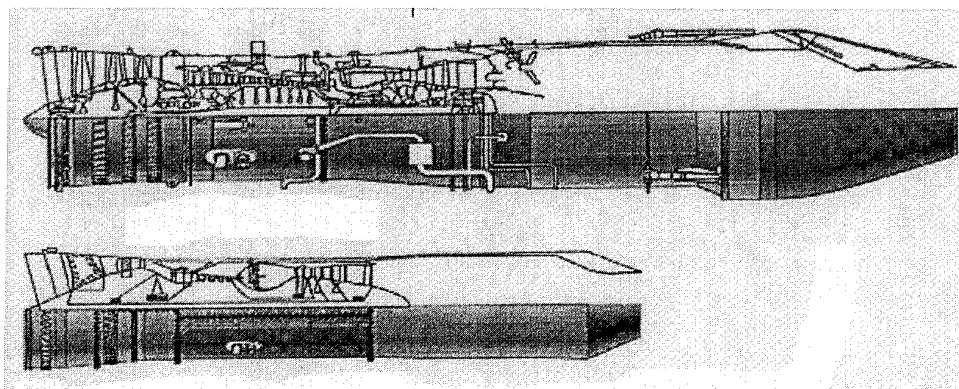
Once the impact of cost reduction and advanced performance had been determined, the next step in the analysis involved an investigation of the impact of cost reduction on the manufacturing cost of an engine. In the previous analysis, propulsion technology to perform a given mission was examined. Required thrust levels changed as technology improvements were made. These changes in required thrust, in turn, had an impact on both the aircraft and the engine size, and subsequently, cost.

In order to focus only on manufacturing costs, a cost comparison was made for two engines whose thrust levels were held constant. In this way, mission requirements would not be an influence on engine size and cost. The level of technology for the two engines, however, did change. The engines chosen for comparison were the F100-229 and an advanced IHPTET Phase II engine scaled to produce the same

level of thrust. The F100-229 was chosen because it is a relatively new engine in the inventory and it represents an engine whose manufacturing methods are mature, well established and in place.

Figure 5. shows a cost comparison between these two (2) engines. The engine schematics illustrate the impact of advanced technology on size and cost. The Phase II advanced technology engine requires less airflow to produce the same thrust as the F100-229, so it is smaller in diameter. In addition, improvements in aerodynamic and aeromechanical technology dramatically reduce the number of fan and compressor stages in the Phase II engine. The principal factors contributing to lower manufacturing cost for the advanced technology engine are its smaller size (as a result of advanced turbine engine cycle design), reduced parts count and the development of cost effective manufacturing methods. Figure 5 also shows the cost breakout for the two (2) engines by major sub-module. The numbers in parenthesis represent the percentage contribution of each sub-module to the total engine cost.

It is interesting to note the change in the cost distribution between the cold section and the hot section for the two engines. The most dramatic parts count reduction is in the fan and compressor, hence, the highest cost reduction potential lies in that area. In the hot section area, the cost is expected to rise slightly despite the fact that the



COST	COLD SECTION	HOT SECTION	AUG/NOZZLE	EXTERNALS	TOTAL
F100-229	\$1,257,000 (36%)	\$887,000 (25%)	\$444,000 (13%)	\$924,000 (26%)	\$3,500,000
IHPTET PHASE II	\$821,000 (29%)	\$936,000 (34%)	\$282,000 (10%)	\$755,000 (27%)	\$2,794,000

Figure 5. Cost Comparison between F100-229 and Equivalent Thrust IHPTET Engine

engine is smaller. This is due to the application of advanced materials and cooling schemes necessitated by higher turbine inlet temperatures. Parts count reduction is also a small, but not significant factor in the hot section.

The augmentor/nozzle and externals areas are also expected to show a reduction in cost. The cost reductions for these two areas are driven by design innovation, such as fixed A8/A9 exhaust nozzles and integral fuel/hydraulic pumps, as well as the smaller engine size.

Implications of Cost Reduction on Manufacturing Cost

The previous example comparing the F100-229 to an equivalent thrust IHPTET Phase II engine offers some interesting insights into the manufacturing cost area. A closer examination of the cold section was made by breaking down the cost for the high pressure compressor into the costs for the rotating and non-rotating components. The high pressure compressor blades and disks for the F100-229 are made of conventional monolithic titanium material. For the IHPTET Phase II engine, the blades will be made of gamma titanium and the disks will be made of a monolithic titanium incorporating titanium metal matrix composite ring inserts. The

manufacture of MMC reinforced compressor disks involves more processing steps than for a monolithic disk. Consequently, the manufacturing cost for a MMC disk would be expected to be higher.

This brings up an interesting issue. How can this higher expected manufacturing cost be conducive to cost reduction -- especially in the cold section? The answer to this question is presented in table 3. Table 3 shows a comparison of cold section costs for the F100-229 and the IHPTET Phase II engine. When analyzing the cost of the fan and compressor rotor stages, the cost per stage for the IHPTET engine can be up to forty percent (40%) greater than for a conventional forged monolithic rotor and still meet the targeted cost reduction goal.

F100-229	IHPTET PHASE II ENGINE
ROTOR COST: \$ 520,000	ROTOR COST: \$ 342,000
AVE. COST/STAGE: \$ 40,000	AVE. COST/STAGE: \$ 57,000
STATIC STRUCTURE \$ 737,000 COST:	STATIC STRUCTURE \$ 479,000 COST:
AVE. COST/LB (APPROX): \$ 1100	AVE. COST/LB (APPROX): \$ 2050

Table 3. Manufacturing Cost Comparison: Cold Section

Similarly, for static components in the cold section the cost per pound for the IHPTET engine can be up to eighty-five percent (85%) higher than for the conventional engine and still achieve the cost reduction goal. In some respects, the old adage that higher technology costs more holds true. However, the allowable growth of the manufacturing cost must be controlled through the development of improved manufacturing methods.

Summary

Analysis has shown that advanced technology turbopropulsion systems being developed under the DoD/NASA IHPTET program will offer a significant payoff with respect to the size, weight and cost of future aircraft. Cost reduction goals have been incorporated into the IHPTET program. The goals address engine unit acquisition cost and maintenance costs. The cost reduction goals are compatible with IHPTET performance goals and both are designed to be met concurrently.

Satisfying the engine cost reduction goals requires the development of innovative designs and improved, cost effective manufacturing methodologies for advanced material systems. In some cases, the advanced engine material systems are incompatible with conventional manufacturing methods. A good example of this incompatibility is investment casting of high temperature materials such as gamma TiAl. Conventional core and shell materials adversely react with the gamma TiAl causing poor quality castings and low yields. In this case, a new core or shell material must be developed.

An analysis of advanced technology turbopropulsion systems has shown a promising consensus between the benefits of higher performance and the reduced cost goals of the IHPTET program. This analysis indicates that manufacturing cost targets are compatible with the advanced material systems and lower engine cost.

Acknowledgements

The Author wishes to gratefully acknowledge the outstanding contribution made in support of this paper to Mr Richard E. Quigley III and to Mr Thomas W. Shaffer for their technical assistance, and to Mr Zane D. Gastineau for his help in preparing the manuscript.

References

1. Nelson, J.R. and Timson, F.S., Relating Technology to Cost: Aircraft Turbine Engines, Rand Report WN-7882-PR, July 1972.
2. Shishko, R., Technological Change Through Product Improvement in Aircraft Turbine Engines, Rand Report R-1061-PR, May 1973.
3. McConnell, V.P., Aerospace Applications: Affordability First, High Performance Composites, March/April 1995.
4. Dix, D.M. and Riddell, F.R., Projecting Cost-Performance Trade-offs for Military Vehicles, Aeronautics & Astronautics, September 1976.
5. Curry, C.E., Earle, R.V. and Pedersen, G.H., Turbine Engine Cost Reduction Using Life Cycle Cost Techniques, SAE 781031, November 1978.
6. May, T.T., Maj, Operating and Support Cost -- A Primer, ASD/ACCL, WPAFB, Ohio, May 1982.

Paper 10: Discussion

Question from A T Webb, Edwards AFB, USA

The engines used for illustrations in this paper are basically derivatives of engines designed in the late 1960s and early 1970s. Given the emphasis on affordability and costs, could you comment on the desirability and feasibility of using derivatives of today's advanced engines, say the F119 in the F22, to meet at least partially the IHPTET goals?

Author's reply

Yes, IHPTET goals could possibly be partially reached using derivatives of the F119, but this would not take sufficient advantage of the latest technology advances. For instance, reduction in the number of fan and compressor stages, which the new technology could provide, could not be realised without designing a totally new engine.

Advanced Small Turbopropulsion Engines

C. Rodgers
3010 N. Arroyo Dr.
San Diego, CA 92103
USA

ABSTRACT

Candidate advanced turbopropulsion engines to fulfill the requirements of the next generation military small aircraft, drones, & missiles are, turbojets, turboprops, turbofans, air turboramjets pulsejets, & combinations thereof.

Prime requirements are to provide significant range increases with higher flight Mach numbers, & in some applications extended endurance above the tropopause, both of which are primarily dependent upon the propulsion system specific fuel consumption trends.

Other combinations of turbojets, rockets, & ramjets are being studied for operation at even higher Mach numbers, but generally involve variable geometry inlets & exhausts difficult to incorporate on small propulsion vehicles.

Preliminary design studies of a variety of advanced small turbopropulsion concepts was conducted recently by the author, & associates, including ;

. Advanced small Turbojets with near stoichiometric combustion.

. Small Stoichiometric Airturboramjets.

. High pressure ratio Intercooled Turboprop.

. Semi-Constant Volume (SCV) turbojet.

. Regenerative Feedback Turbine Engine.

This paper compiles the results of these studies & highlights the design features necessary to attain advanced levels of performance.

NOMENCLATURE.

A	Area Frontal
APU	Auxiliary Power Unit
ATR	Airturboramjet
BTU	British Thermal Unit
Cp	Specific Heat at constant pressure
Condi	Convergent Divergent
GG	Gas Generator
F	Thrust, or deg F
CG	Gas Generator
HRR	Heat Release Rate
ICR	Intercooled Recuperative
JPT	Jet Pipe Temperature
LHV	Lower Heating Value
N	Rotational Speed
OD	Outer Diameter
RFTE	Regenerative Feedback Turbine Engine
SCV	Semi-Constant Volume
SFC	Specific Fuel Consumption
SL	Sea Level
T	Temperature
TJ	Turbojet
T.I.T	Turbine Inlet Temperature
Rc	Pressure ratio
W	Massflow
	Subscript
c	Compressor
t	Turbine

1. INTRODUCTION.

Advanced turbopropulsion engines to fulfill the requirements of the next generation military small aircraft, drones, & missiles are, turbojets, turboprops, turbofans, air turboramjets pulsejets, & combinations thereof. Prime requirements are to provide significant range increases with higher flight Mach numbers, & in some applications extended endurance above the tropopause, both of which are primarily dependent upon the propulsion system specific fuel consumption trends depicted on Fig 1. For flight numbers in the range of 0.8 to 2.0 the simple (or leaky) turbojet is seen to provide the lowest specific fuel consumption (SFC).

Other combinations of turbojets, rockets, & ramjets are being studied for operation at even higher Mach numbers, but generally involve variable geometry inlets & exhausts, difficult to incorporate on small propulsion vehicles, with attendant cost implications. Preliminary design studies of a variety of advanced small turbopropulsion concepts was conducted commencing in the early 1990's by the author including;

- . Advanced small Turbojets with near stoichiometric combustion.

- . Small Stoichiometric Airturboramjets

- . High pressure ratio Intercooled Turboprop

- . Semi-Constant Volume (SCV) turbojet.

The studies focused towards improving both SFC & specific thrust (F/W) through higher "uncooled" (non - internally cooled) turbine inlet temperatures, higher compressor pressure ratios, while still attempting to minimize complexity & maximize durability.

Major constraints for the design of these small turbopropulsion engines for high speed flight were;

- . Minimum number of components, to minimize cost
- . Low frontal area to reduce drag
- . Low mission total weight
- . High start reliability

2. ADVANCED SMALL TURBOJETS

The attributes of several turbomachinery design configurations suitable for small high power density turbojets & low manufacturing cost are discussed in Ref 1. Most typical small expendable turbojet flowpaths tend to embody single stage compressors & turbines, with the exception of multistage axial compressors cast as a single monolithic rotor assembly.

The simplicity & reduced cost features of the single stage centrifugal compressor are ideal assets for

small expendable turbojets especially when mounted back-to-back with a radial inflow turbine, & cantilever supported from a forward, cool location bearing capsule, as typified by the TJ90 turbojet cross section (Ref 1) shown on Fig2.

The thermodynamic performances of small turbojets is dominated by the choice of compressor pressure ratio & turbine inlet temperature, the former basically effecting SFC(pph/lbf), & the latter specific thrust (lbf/ airflow). The two parameters have a profound effect on engine & vehicle sizing.

.Under supersonic flight conditions the influence of inlet pressure recovery & exit nozzle performance become equally important. The combined effect of the three parameters are illustrated by the cycle performance shown on Fig 3 representative of small advanced turbojets with "uncooled" hot end carbon/carbon components, where it is seen that although higher turbine inlet temperatures (TIT) increase F/W, SFC eventually starts to increase.

An indication of the relative range is provided by the parameter :

$$\text{Relative Range} = f \sqrt{F/W / (\text{SFC})}$$

Translating the results from Fig 3 into terms of relative range on Fig 4, it is observed that the relative range plateaus at TIT's approach stoichiometric limits. Engine frontal area & volume constraints imposed by the installation plus the demands of higher TIT's precipitate increasing the combustor heat release rate, as defined by:

$$\text{HRR} = \text{Fuel flow} \times \text{LHV} / (\text{Volume} \times \text{Pressure Ratio})$$

The estimated effect of combustor HRR & compressor pressure ratio on small turbojet engine volume (Ref 1), & is shown on Fig 5 to illustrate their importance in attaining compact propulsion packages. HRR's of the order 30×10^6 BTU / atm cuft with pressure ratios of at least 4.0 are preferred.

The results of thermodynamic studies for small advanced turbojets are summarized as follows:

- .Higher TIT's provide increased specific thrust F/W at all Mach numbers.

- .High TIT's may provide unboosted supersonic acceleration.

- .Optimum cycle pressure ratio decreases with increasing Mach number.

- .Increased TIT's are very desirable for maximum thrust but must be traded against higher SFC for range.

- . SFC & F/W trends at the higher Mach numbers are highly dependent upon the inlet & exhaust nozzle performances.

3 . SMALL AIRTURBORAMJETS

The airturboramjet(ATR) is being reconsidered as an alternate to the rocket & turbojet (TJ) as a propulsion system for short range tactical missiles. Potential advantages of the ATR are both high thrust per frontal area, & high specific airflow lbf /airflow, permitting smaller cross section , thus potentially supersonic missiles ,as compared to the TJ. The major disadvantage of the ATR is high specific fuel consumption, or in rocket terminology- low specific impulse.

The ATR cycle is shown schematically on Fig 6, with the gas generator gases first driving the turbine ,& subsequently mixing with the compressor airflow, ignition & stoichiometric "afterburning"to provide propulsive thrust. The ATR is in effect a hybrid turbojet & rocket, embodying both the advantages & disadvantages of both propulsion systems.

The potential use of the ATR in small propulsion systems,& especially the necessary utilization of advanced small turbojet technology ,motivated an interim evaluation of the ATR in comparison to the TJ.

Starting with Ref 1, TJ90 turbojet technology, the ATR cycle listed in Table 1 was optimized to match the compressor flow ,pressure ratio, & speed, at SL 59F static conditions. Neat Hydrazine was selected as the fuel ,due to uncertainty regarding the combustion efficiency of advanced solid fuels.

After several iterations a turbine inlet pressure & temperature of 580 psia ,& 2000 F respectively, were considered the best compromise between turbine efficiency. SFC, & inlet manifold thermal/structural design constraints.

Table 1 ATR Design Point

SL 59 F Mach = 0

GG gas properties $k=1.21$ $C_p=0.71$ LHV 4000

Compressor Pressure Ratio	4.75
Airflow Wc pps	1.52
Compressor efficiency %	69.6
Turbine efficiency %	59.0
Net Cycle Pressure Loss %	15.0
GG Flow Wt pps	0.50
GG Pressure psia	580
T.I.T deg F	2000
JPT deg F	3496
Net Thrust lb	281
SFC pph/lbf	6.4
Specific Impulse sec	566

The ATR design point SFC over four times that of the TJ90 turbojet, but with double the specific thrust.

Mixed gas temperature in the afterburner is 3496 F ,probably requiring high temperature composite materials technology for both the liner & nozzle.The computed turbine nozzle area was 0.125 sq in with an expansion ratio of 8.31, requiring a small supersonic probably partial admission turbine. Note that candidate solid fuels have nearly the same gas properties as Table 1, but potentially higher LHV's. Several versions of the baseline TJ90 design were examined as candidates for an ATR technology demonstrator initially including both aft mounted concentric GG/ afterburner, & forward mounted GG.The aft mounted GG posed many problems including throttle pintle provision, the high temperature GG environment, cramped afterburner volume, & extended length.

Although the forward mounted GG is preferred, the high pressure 1700 F gases need to be manifolded through the compressor flowpath to the turbine nozzle, complicating the mechanical design & compromising the compressor diffuser performance.

A forward mounted solid fuel GG,ATR configuration is shown on Fig 7, with an OD of 6.2 inches. The airflow enters from a retractable side inlet & is sucked in by the impeller ,discharged into the diffuser & subsequently flows around & into the afterburner for mixing with the turbine exhaust GG gases. The design of the missile air inlet , its sensitivity to incidence, flow distortion. & high Mach number is critical to the performance of the ATR.

The GG gases are throttled by a twin port rotary sliding hot gas valve, & pass through the hot gas transfer tubes ,which penetrate the compressor diffuser & feeds into the turbine nozzle manifold. The flow blockage in the diffuser is assumed to penalize compressor efficiency by 2% points.The GG gases then accelerate supersonically through the 0.07 sq in turbine nozzle,& drive the small radial inflow rotor with cantilevered impulse blades.

The highly swirling turbine exhaust flow then mixes with the airflow for near stoichiometric afterburning, & expulsion through the aft supersonic propulsion nozzle. If feasible the afterburner volume could be preloaded with the booster grain ,& an ejectable boost nozzle contained within the propulsion nozzle. The afterburner volume depicted is representative of an HRR of 30×10^6 which may be difficult to achieve with current low LHV candidate solid fuel GG's. Alternate boron based solid fuels are being researched.

The concerns relating to solid fuel GG turndown limitations , throttle type, actuator regulation &

sizing, plus GG gas particulate accumulation led to consideration of the selected hydrazine fueled ATR depicted schematically on Fig 8. Apart from environmental implications, this approach offers many system advantages:

- . Throttle control on liquid side via current TJ90 shaft mounted high speed pump, thus no hot gas valve.
- . Small externally mounted catalytic bed.
- . No high energy ignition system required.
- . Clean burning exhaust.
- . No carbon or metallic deposition.

. Proven demonstration of a workhorse ATR Ref (2). Unfortunately Hydrazine gas properties produce low specific work, low heating value, & comparative SFC increases some 40%, compared to proposed solid GG fuels.

This study indicated that the ATR could double the specific thrust (lbf/pps), but with over four times the specific fuel consumption of the turbojet.

Application to small ground launched missiles may therefore be limited due to excessive fuel weight (& volume) for typical tactical mission profiles.

Small ATR propelled air launched supersonic missile applications were considered as a more optimal operating scenario.

4.0 HIGH PRESSURE RATIO INTERCOOLED TURBOPROP

High altitude long endurance unmanned aircraft impose unique constraints on candidate engine propulsion systems & types. Piston, rotary, & gas turbines have been proposed & developed for such special applications. Of prime importance is the requirement for maximum thermal efficiency (minimum SFC) with minimum waste heat rejection.

Engine weight although secondary to fuel economy must be evaluated when comparing the various engine candidates. Weight can be minimized by either high degrees of turbocharging with the piston or rotary engines, or high the power density capabilities of the gas turbine.

The design features of a conceptual high pressure ratio intercooled small turboprop are discussed in Ref 3, for application to a long endurance aircraft flying above 60,000 ft altitude, with a thermal efficiency exceeding 40% & an overall pressure ratio of 66.0. Aircraft gas turbine thermal efficiencies greater than 40% (SFC 0.33 lb/hp.hr) can be obtained with compressor intercooling &/or exhaust heat recuperation. Fig 9 shows the results of design point cycle computations for recuperative, intercooled/recuperative(ICR), & intercooled operation above the tropopause, from which the following is concluded:

- . All three cycles can provide SFC's in the 0.3 lb/hp/hr realm.
 - . Higher pressure ratios improve the straight intercooled cycle performance.
 - . Lower pressure ratios improve the recuperative & ICR cycle.
 - . TIT has least influence on the intercooled cycle.
- The advantages & disadvantages of all three cycle options are listed on Table 2. Although the ICR embodies the best of both other cycles, it results in the most complex flowpath, & also incorporates the thermally difficult heat exchanger component.

Table 2 Comparison of Turboprop Engine Designs		
Type	Advantages	Disadvantages
Intercooled	.No high temperature heat transfer surfaces .Reduced leakage potential .Small responsive HP spool	.Requires very high pressures .High number of stages .Intercooler heat rejection
Heat Exchanged	.Low pressure ratio reduced stage number	.Low specific power .Requires high effectiveness with large regenerator. .Poor transient response .Variable geometry for optimum part load fuel economy. .Surface fouling.
ICR	.Lower number of stages	.Complicated flowpath, & higher pressure drops. .All heat exchanger concerns

Overall pressure ratios of 64.0 were demonstrated in the 1980's with a three stage intercooled small turbocharger (Ref4). The attainment of such high pressure ratios in combination with increased TIT's offers the feasibility of improved Brayton cycle thermal efficiencies competitive with those of the Diesel cycle. A conceptual high pressure ratio intercooled turboprop engine is shown on Fig10, & comprises triple spool arrangement with a separate free power turbine. Intercoolers are positioned after the first low pressure (LP) compressor, & after the second intermediate pressure (IP) compressor. Reheat may be used between the LP turbine & power turbine for power boosting. The small high pressure spool is offset aft behind the intercoolers, & provides an acceptable frontal area presentation for aircraft applications.

The estimated performance of this conceptual high pressure ratio turboprop is listed on Table 3 at sea level standard, & 60000 ft altitude, for a constant 400 hp output rating, where the engine is "throttled back" for SL operation. Optimum intercooler effectiveness for maximum endurance was determined to be in the range of 65 to 75 %.

Table 3. High Altitude Intercooled Turboprop.

Ambient		60kft	SL
Compressor Stage Ratios		4.8, 3.94, 3.78	2.5, 2.4, 2.3
Compressor Stage Efficiency	%	79	78
Intercooler Effectiveness	%	75	75
Intercooler pressure drop(s)	%	4	4
Overall pressure ratio		66	12.3
Combustor pressure drop(s)	%	6	6
Combustor efficiency(s)	%	98	98
TIT	F	2000	1400
Turbine stage efficiency	%	86	86
Mechanical efficiency	%	95	95
Leakage	%	1.0	1.0
Airflow	pps	1.65	4.9
Gross output	hp	432	437
Cooler power	hp	32	37
Net output	hp	400	400
SFC	lb/hp/hr	0.30	0.53
LP krpm		26.1	18.9
LP Compressor tip diam	inch	13.3	-
MP krpm		40.7	29.4
MP Compressor tip diam	inch	8.6	-
HP krpm		56.6	41.0
HP Compressor tip diam	inch	6.2	-
Power turbine pressure ratio		11.2	2.4
Estimated dry weight	lb	805	-

The specific application & its unique requirements result in a specialized propulsion system with somewhat limited commercial viability coupled with extensive design & development costs, as compared to the highly turbocharged piston or rotary engine with possibly some degree of commonality to existing product lines & hardware. The offset core concept resolves the mechanical difficulties associated with multiple concentric shafts at the ultra pressure ratios envisioned.

5. SEMI -CONSTANT VOLUME TURBOJET.

The author has been associated over the past several years with the study of small semi-constant volume gas turbine (Atkinson Cycle) as a means of potentially providing improved SFC & F/W, plus the feasibility for self-starting. In the SCV cycle additional significant compression occurs in the combustor as a consequence of sequential closing of the combustor inlet in phase with fuel injection & ignition. The first successful commercial gas turbine worked on this principle, being built by Holzwarth in the early 1920's. The combustion process is described as semi-constant volume (SCV), since the combustor exit is not entirely closed, being throttled by the ratio of the combustor volume to the turbine nozzle area, or segments thereof. Experimental demonstration of the pressure rise during SCV combustion is described in Ref 5. Single pulse detonation testing with propane fuel indicated a pulse pressure rise within a simulated SCV combustor of 4.0 atmospheres. The pulse pressure rise increasing with the ratio of combustor volume to exit area.

The ideal thermal efficiencies of the Atkinson & Brayton cycles are plotted against mechanical compression ratio on Fig 11. It is easy to see why the Holzwarth gas turbine was so successful in an era during which mechanical compressor performance was so poor as to make the Brayton cycle impracticable. With zero or very small mechanical precompression it was possible to obtain by constant volume combustion, overall cycle pressure ratios of 15 or more. At this level of overall pressure ratio, ideal thermal efficiencies of 40% or more

are indicated. Holzwarth readily obtained a working efficiency of 13%.

The efficiency advantage of the Atkinson cycle, as compared to the Brayton cycle applies over the full range of mechanical pressure ratios from unity upwards, independently of engine size. Practical limits are set only by the maximum allowable peak temperature & pressure, i.e., only by stoichiometric combustion & mechanical stress limitations. Successful application of the cycle to a gas turbine does, however, depend on the effectiveness of the combustion process in producing the desired combustion chamber pressure rise & on the efficiency of the expansion process. Past experience using a combustion chamber exhaust valve has shown this to be mechanically undesirable & a source of turbine inefficiency. If this valve is replaced by a choked first stage turbine nozzle, then the turbine efficiency will be improved by providing a continuous throughflow with a nozzle efflux velocity variation no greater than the square root of the chamber pressure variation. Thermodynamic modeling of the SCV combustion can be computed using modified constant volume combustion algorithms in which flow escapes proportional to the nozzle area & square root of the internal pressure.

Such algorithms were used to compute the potential performance gains that may be attainable with the conceptual small SCV turbojet depicted on Fig 12. The concept features a small single stage centrifugal compressor delivering a pressure ratio of 4.0 to a single can SCV combustor with self modulating flapper valves, closed by pressure rise accompanying fuel injection & ignition, & opened in the air charge mode by the compressor pressure differential. Alternatively self-positioning compressor diffuser vanes might provide the valving process as described in Ref 5.

A virtue of applying SCV to the turbojet is that most of the "free" compression is expanded across the jetpipe nozzle, which in this particular adaptation is depicted as a bifurcated type.

Projected gains in thrust & fuel economy for this SCV turbojet concept are shown on Fig 12, as a function of average pulse pressure rise, which if the SCV process can be successfully developed should reach 1.4.

It may be argued that the potential improvements with SCV are small, & may be diluted by further technology advancement of the Brayton cycle gas turbine. The impending approachment of stoichiometric combustion & plateauing aerodynamic expertise, however, gives all the more credence to re-investigate alternate gas turbine engine cycles discarded in the past due to lack of design technology,

6.0 REGENERATIVE FEEDBACK TURBINE ENGINE (RFTE).

A research program is currently being sponsored by NASA in order to demonstrate proof of concept for a novel gas turbine based on the Coleman cycle, identified in Ref 6. The justification for this program lies in the unique characteristics & advantages of the RFTE cycle which can double the specific power of current state-of-the-art gas turbine engines with nearly constant SFC over 80% of the power range, & reduced emissions. The thermodynamics of the Coleman cycle have been independently validated by the author as well as a number of government & commercial agencies. Since the cycle is in the patent application process, details of the process cannot be described at this time. It is anticipated that the patent will issued by the time of this conference.

7.0 CONCLUSIONS.

A technology review of advanced small turbopropulsion concepts recently investigated by the author has been presented covering the high temperature turbojet, airturboramjet, high pressure ratio turboprop, & the semi-constant volume gas turbine. These investigations were focused towards both improving thermal efficiency & specific thrust which in some aircraft applications may seem to be in conflict, but when examined in relation to specific aircraft mission profiles it is found that both influence range, since thermal efficiency influences fuel weight, & specific thrust can influence aircraft drag. The motivations to increase thermal efficiency will continue to increase pressure ratios, whether this is accomplished in the traditional manner of increased stage number & stage loadings, or amplified by pulse combustion (either SCV or wave rotors) depends on developmental efforts devoted towards these intriguing methods of compression. The introduction of heat exchanged engines for propulsion is another latent alternate to plateauing cycle pressure ratios & cycle temperature ratios, a precipitous future

increase in oil prices could trigger its introduction to main propulsion engines. As discussed in the preceding text, the intercooler could be a key element in the quest for very high thermal efficiency since it facilitates recuperation in both very high pressure ratio systems, & the RFTE cycle.

8.0 REFERENCES.

1. Rodgers .C., " Smaller Expendable Turbojets" . AGARD-CP-526. 1992.
2. Lilley.J.S., Hecht.S.E., "Experimental Evaluation of an Airturboramjet". AIAA -94-2710. 1994.
3. Rodgers.C ., " High Pressure Ratio Intercooled Turboprop Study". ASME 92-GT-405. 1992
4. Rodgers.C., "Unusual Centrifugal Compressors & Applications". AIAA-95 -2346.1995.
5. Blackburn. R.B., Moulton.J.L., "Semi-Constant Volume Pulse Combustion for Gas Turbine Starting". AIAA-89-2449. 1989.
6. Acurio. J., "Small Gas Turbines in the 21st Century". Aerospace Engineering. Aug 1993.

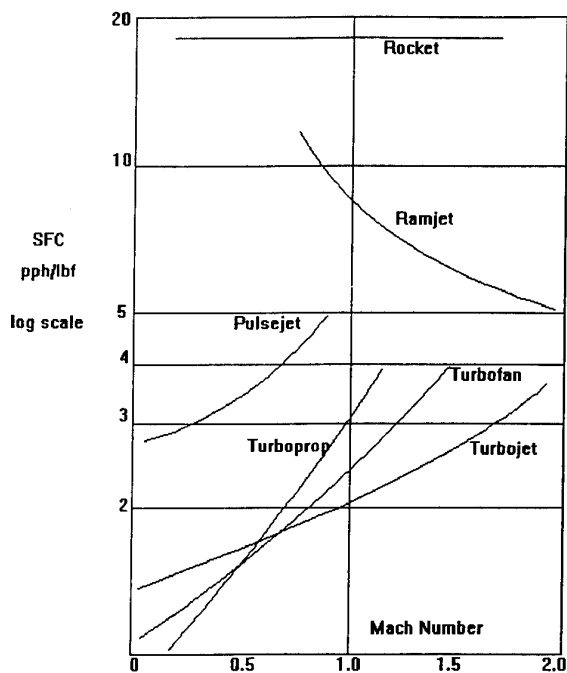


Fig 1. SFC's OF SMALL PROPULSERS

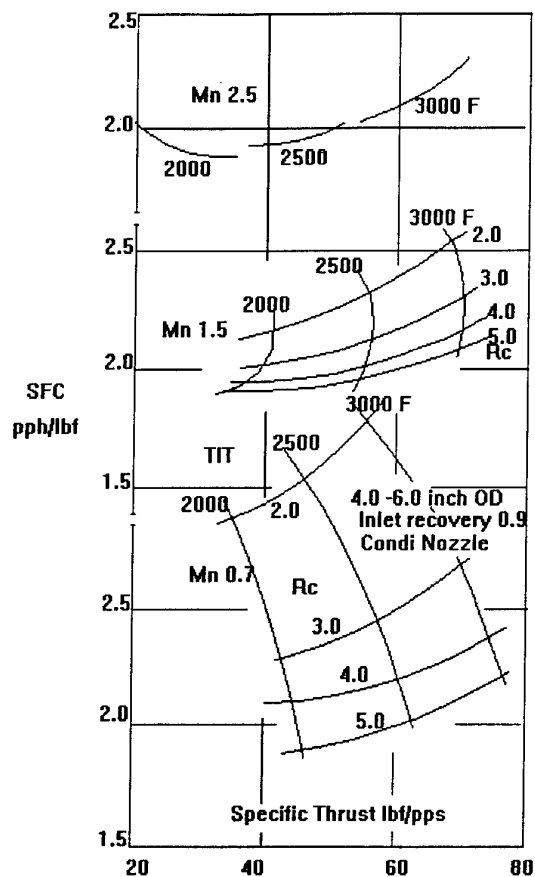


Fig 3. SMALL TURBOJET CYCLE PERFORMANCE

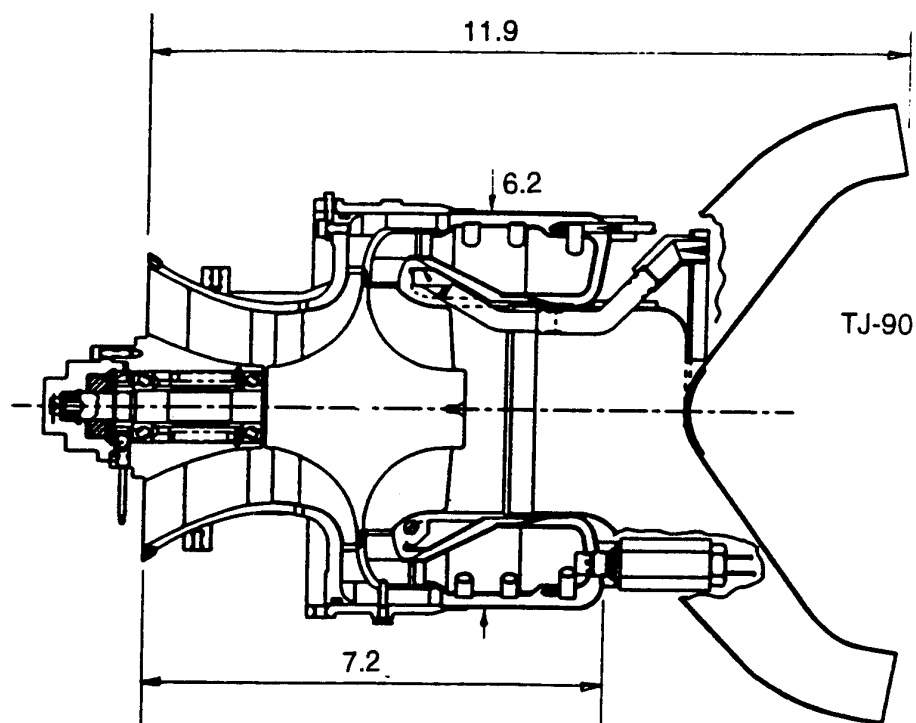


Fig 2 TJ90 Turbojet Cross Section

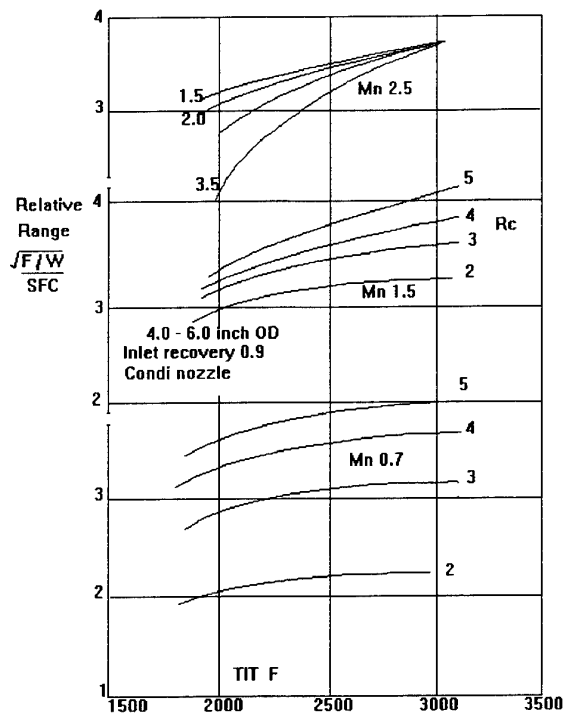


Fig 4. RELATIVE RANGE PARAMETER SMALL TURBOJETS.

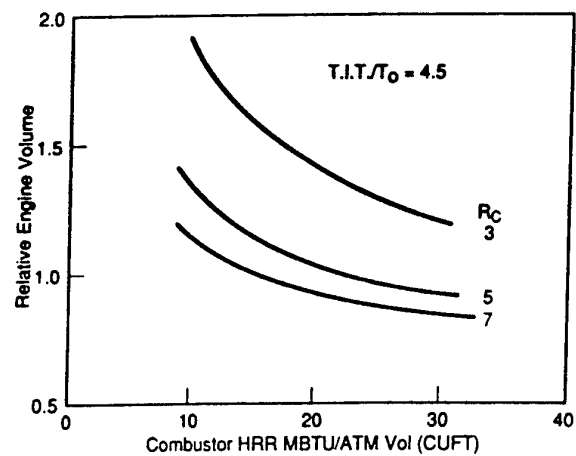


Fig 5. Effect of Combustor HRR on Turbojet Volume

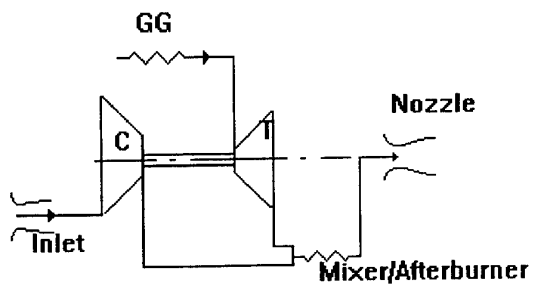


FIG 6 ATR CYCLE SCHEMATIC.

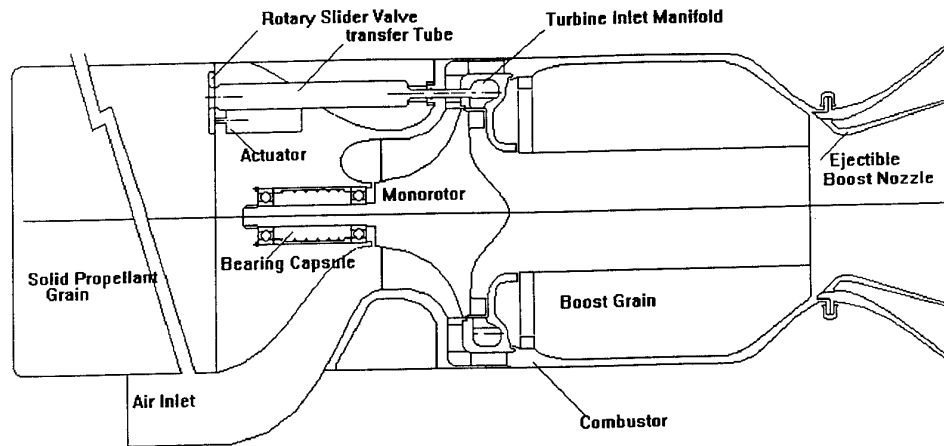


FIG 7. SOLID FUEL GG TJATR

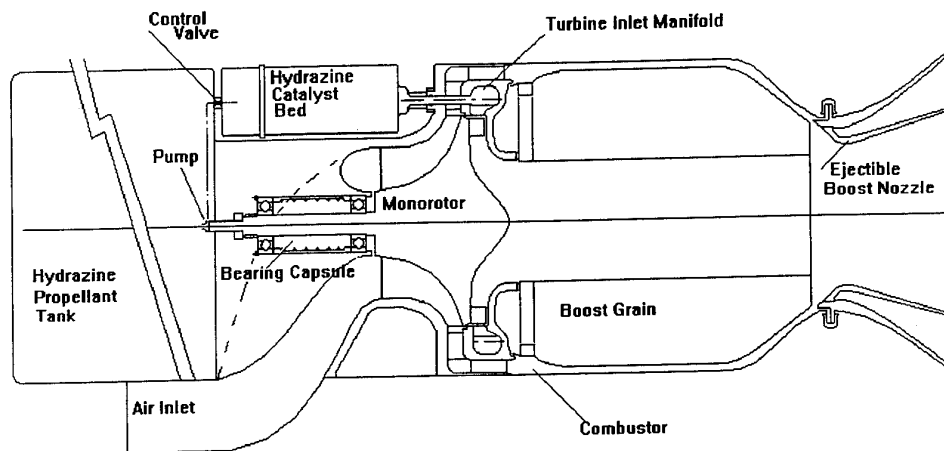


FIG 8. HYDRAZINE FUELED ATR

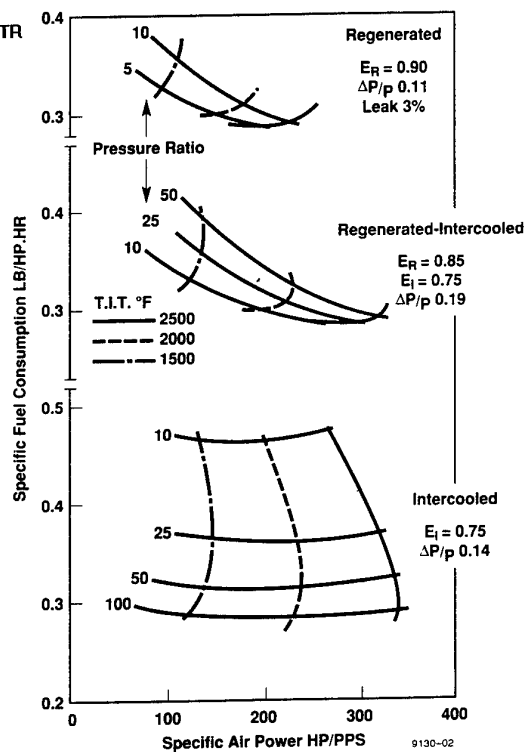


Figure 8. Gas Turbine Cycle Performances (Ambient Temp. - 70°F)

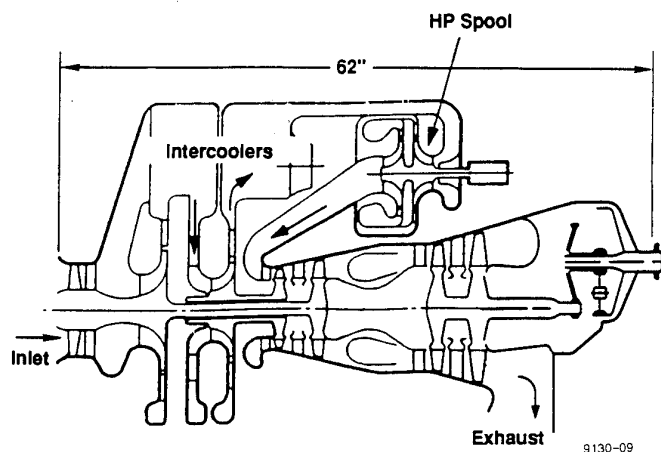


Figure 10. Conceptual Pusher Turboprop Installation (400 HP 60 KFT)

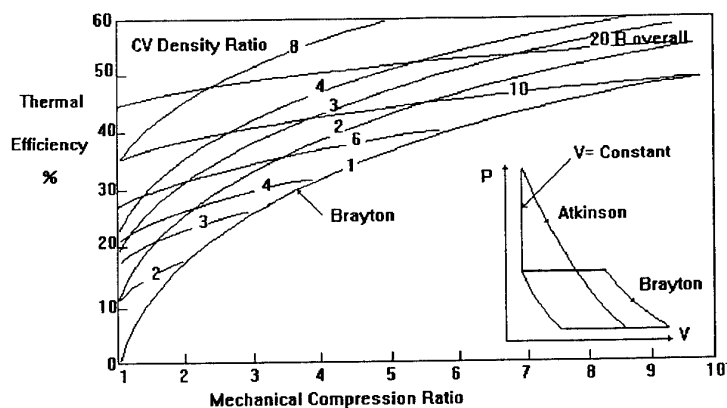


Fig 11. IDEAL THERMAL EFFICIENCIES OF ATKINSON & BRAYTON CYCLES.

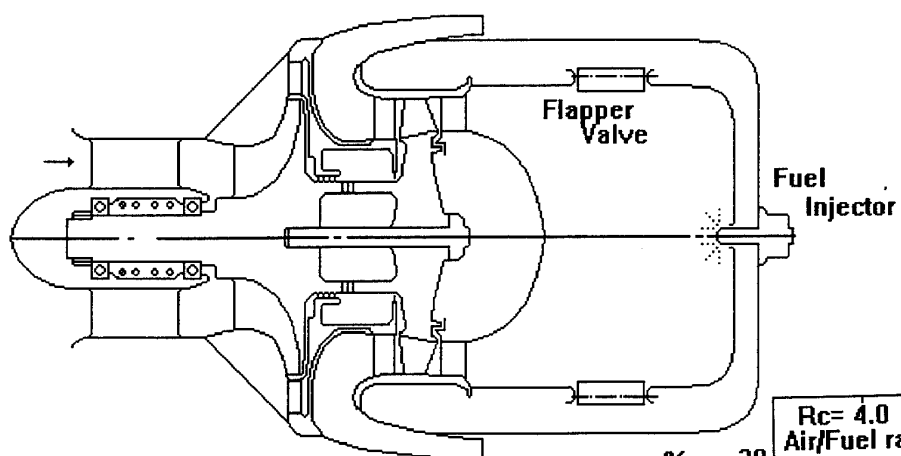


Fig 12 CONCEPTUAL SCV TURBOJET

%
SFC & F
Increase

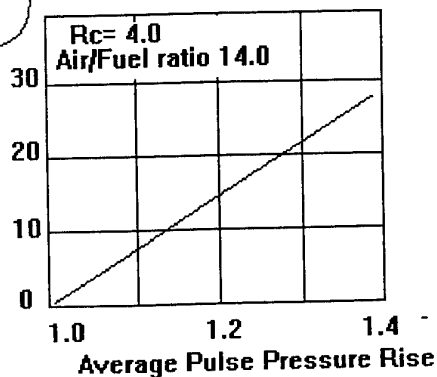


Fig 13 Projected SCV Turbojet Gains

Paper 11: Discussion

Question from A T Webb, Edwards AFB, USA

In the semi-constant volume cycle, what is the effect of the pulses on the structure of the rotating machinery?

Author's reply

Clearly this would be an important design consideration, but a full understanding of the problem could only be gained by building and testing such an engine.

Question from Prof Ir W B de Wolf, NAL, Netherlands

Could you comment on the fact that you chose for the high altitude turboprop the same reference output of 400 hp at both altitude and sea level. Optimising the aircraft mission with respect to maximum endurance at altitude would require a fast climb at higher power than 400 hp, also improving sfc. Could you comment also on engine weight aspects?

What is the reason for the low compressor and turbine efficiency values used in your ATR study?

Author's reply

A 'flat' rating of 400 hp was selected for the preliminary design study even though it was realised that higher power would be available to permit a faster initial rate of climb. The design trade-offs between take-off and cruise power ratings are discussed thoroughly in NASA CR195469, together with the effects on total aircraft weight.

In the ATR study, conservative compressor and turbine efficiencies were selected as being typical of small high speed turbomachinery.

PRELIMINARY DESIGN AND PERFORMANCE ANALYSIS OF A VARIABLE GEOMETRY RECUPERATIVE TURBOSHAFT

S.Colantuoni, A.Colella, G.Mainiero, G. Santoriello, L.Cirillo, C.Iossa

ALFA ROMEO AVIO - Societa' Aeromotoristica per Azioni
R&D - Design Technologies - Propulsion & Aerothermodynamics
80038 Pomigliano d'Arco (NAPOLI) - ITALY

ABSTRACT

The paper describes a performance study developed on a compact turboshaft engine based on two concepts that can contribute to the performance gains of advanced future propulsion systems : the recuperative cycle and the variable geometry.

Cycle optimization is done for a medium helicopter application, trying to minimize the fuel consumption and taking into account moderate levels of peak gas temperature, to guarantee adequate life of the most critical engine hot components.

The engine architecture (1000 kW class turboshaft with free turbine) is based on minimum number of turbomachinery components, in order to reduce the weight of the propulsion system and its global cost (initial and operative).

The three gas-generator components are: 1) a transonic, high-performance, 8 to 1 pressure ratio single stage centrifugal compressor; 2) a very compact, reverse-flow annular flame-tube, having 1600 K combustor exit temperature; 3) a high-loaded cooled axial flow turbine stage.

The variable geometry free-power turbine is counter rotating respect to the gas-generator rotor and the power output is available at the rear-end on the engine. Heat-Exchanger recuperator, placed behind the power turbine, contributes to the significant reduction of the engine specific fuel consumption.

The components of the engine gas-generator section are based on the results of company research projects in the field of the application of the most advanced CFD techniques to the aerothermal-design of turbomachinery and combustors.

LIST OF SYMBOLS

CET	Combustor Exit Temperature
CFD	Computational Fluid Dynamics
C	Heat Capacity rate ($W \cdot Cp$)
EGT	Engine Exhaust Gas Temperature
ER	Expansion Ratio
h	Heat Transfer Coefficient
HE	Heat Exchanger
NUT	Number of Transfer Units

OEI	One Engine Inoperative
EMP	Emergency Power
ETA	Efficiency
MCSP	Maximum Continuous Power
MCYP	Maximum Contingency Power
PR	Pressure Ratio
PT	Power Turbine
OTDF	Overall Temperature Distribution Factor
RTDF	Radial Temperature Distribution Factor
SFC	Specific Fuel Consumption
TET	Turbine Entry Temperature
TOP	Take Off Power
W	Mass Flow Rate
ϵ	Heat Exchanger effectiveness

Subscript

a	Air
g	Gas
ratio	Quantities Ratio
tt	Total-to-Total
0	Engine Inlet
1	Compressor Inlet
2	Compressor Exit
21	Cold Side Heat Exchanger Exit
3	Combustor Exit
4	HP Turbine Exit
5	Power Turbine Inlet
6	Power Turbine Exit
61	Hot Side Heat Exchanger Inlet

INTRODUCTION

Over the years there have been steady improvements in helicopter engine performance: higher specific powers, lower SFC and improved power/weight ratios. The gains have been the result of improving materials, cooling technologies and better aerodynamic design methods. These advances have allowed higher compressor pressure ratio, combustor temperatures and component efficiencies, with direct benefit to both specific power and SFC. The higher turbomachinery stage loading has been mainly exploited to improve reliability, maintainability and to reduce acquisition costs of the engine.

For a simple cycle engine, low SFC demands high temperatures, high pressure ratios and high component efficiencies, all of which become more difficult to achieve as

the engine becomes smaller.

One possible way to overcome this problem is to use the recuperative cycle [1,2]. Recuperative cycle engines for aircraft applications have not been considered sufficiently attractive in the past: these were bulky, heavy, and with poor reliability. Although preliminary studies pointed out their feasibility [3].

Nowadays heat exchanger is widely used in the gas turbine for industrial and vehicular applications although used in the different manner with several HE options. These used in more complex cycles, allow efficiency levels considerably above that simple cycles.

The remaining bastion of gas turbine technology to take advantage of HE is the propulsion field, because fuel price is still low and overhaul costs for the HE engine higher. Therefore more demanding mission requirements and new recuperator technology [4] would make such cycles interesting.

Here we are going to present the off-design performance of a turboshaft, with the layout based on a recuperative cycle. The aim was to minimize rotating components respect to a simple cycle engine with the same performance level.

RECUPERATIVE CYCLE FOR 1000 kW CLASS TURBOSHAFT ENGINE

The application is for a turboshaft with free power turbine having a max power level of 1000 kW for the propulsion of 4-5 ton class helicopter, which is typically required for many military or medium lift applications.

Fig 1 shows the comparison between simple Brayton cycle and the recuperative cycle with 0.7 HE effectiveness. With the same TET the recuperative cycle allows a significant reduction of SFC. Moreover, this can be obtained at the lower cycle pressure ratio with evident advantages of fewer turbomachinery stages and a lightening of engine casings.

The parametric study, based on max cycle temperature of 1600K and current technology of the compressor, turbine and combustor, has dictated a range from 8 to 10 of the overall pressure ratio as the optimum for engine thermodynamic efficiency.

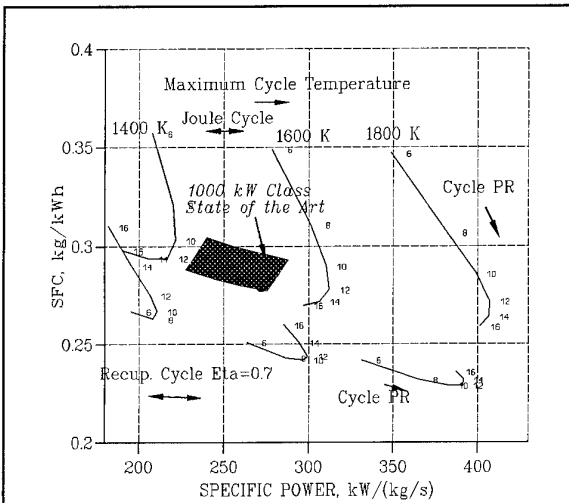


Fig 1 - SFC vs Specific Shaft Power

ENGINE RATINGS

The performance study has been done with the aim to define a performance level of 1000 kW class turboshaft. This application is typically required for many military or medium lift helicopters, powered with twin engines.

The power ratings taken as reference to assess the performance of the engine are outlined in Table I.

The Emergency and Max Contingency ratings are referred to an engine failure. The former has been chosen as reference condition for preliminary thermal analysis of the engine hot section components, since it is the most severe rating with a maximum TET of 1800 K.

Table I - Power Ratings

Rating	kW
EMP (Emergency, ISA +15°, 30sec)	995
MCYP (Max Contingency)	945
TOP (Take Off)	851
MCSP (Max Continuous)	783
50% TOP	425

ENGINE LAYOUT

The engine layout of fig 2 is referred to a rear drive turboshaft.

Core engine section consists of a single spool gas generator with a single-stage centrifugal compressor, a reverse flow annular combustor and a single-stage axial flow HP turbine. The output shaft is driven by a free axial flow turbine, counter rotating respect to that of the gas generator.

The core engine components are derived from units developed and tested in the company research programs [5,6,7], while a preliminary design has been done for the power turbine and the recuperator.

COMPRESSOR

The centrifugal compressor is a single stage with 8/1 as pressure ratio, developed for a turboprop application, here equipped with an enhanced diffuser system in order to improve the surge margin and efficiency at high operating speed.

The impeller has 13 full and 13 splitter blades, designed to work efficiently with an inducer tip relative Mach number of 1.2 at the rotational speed of 40000 rpm.

The diffuser was designed with an average absolute Mach number entering the semi-vaneless of 1.2, while at the exit the requirement was for near axial discharge with 0.15 as Mach number. The diffuser flow path was optimized to enhance the aerodynamic behaviour of semi-vaneless space and to maximize pressure recovery of the channel portion. The design feature was a 3-D diffuser geometry having 25 mixed-flow vanes (radial inlet - axial outlet) and 25 axial blades placed among the vanes at the diffuser exit.

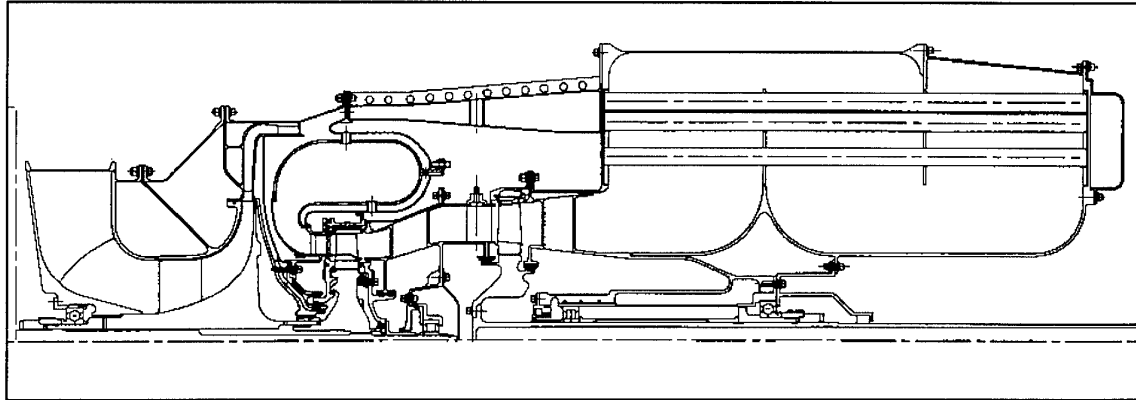


Fig 2 - Engine Layout

COMBUSTOR

The combustor has a double wall to take the advantage with air flow (8.6 % W2), to cool the combustor dome, directly from the compressor instead of that hotter at HE exit. The fuel injection system consists of 12 air blast atomizers of spray angle 90° . The liners are cooled by angled cooling holes, for which the manufacturing technology by laser drilling has been provided in house.

The combustor performance has been assessed by a 3-D reactive flow analysis using a mesh size of $137 \times 31 \times 51$ built on a combustor angular sector of 30° .

The 3-D mesh is shown in fig 3, while the figs 4,5 are concerning the vector plot and gas temperature at the fuel injector plane.

Overall performances at the combustor exit are presented in fig 6. Here is the average temperature profile and that of the maximum peak temperature.

The air inlet temperature is 1000 K, the mean outlet is 1800 K , so that the computed OTDF is 15.7%, while the RTDF is 8.4%.

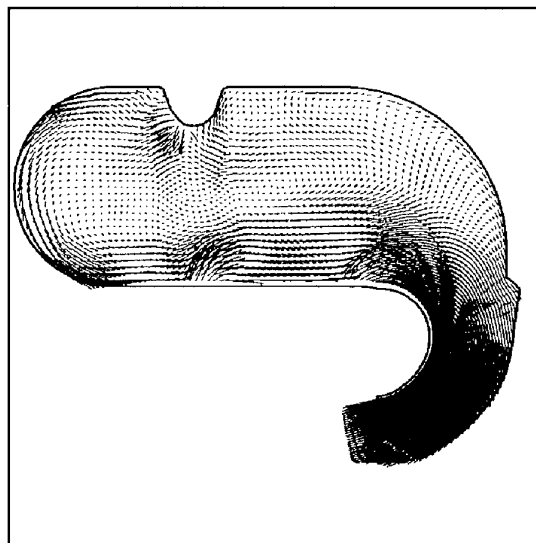


Fig 4 - Velocity Vector Plot at Fuel Injector Plane

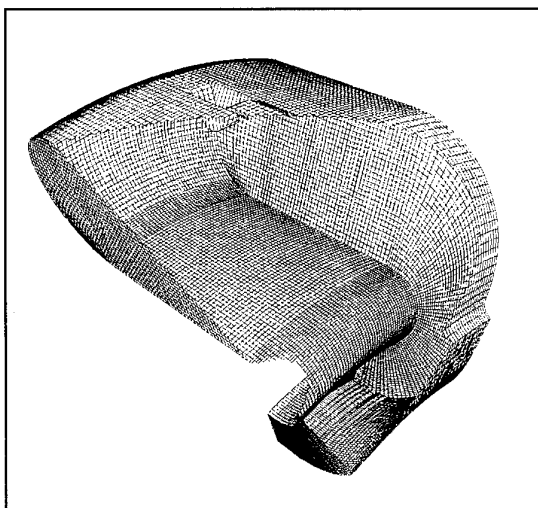


Fig 3 - CFD 3-D Mesh

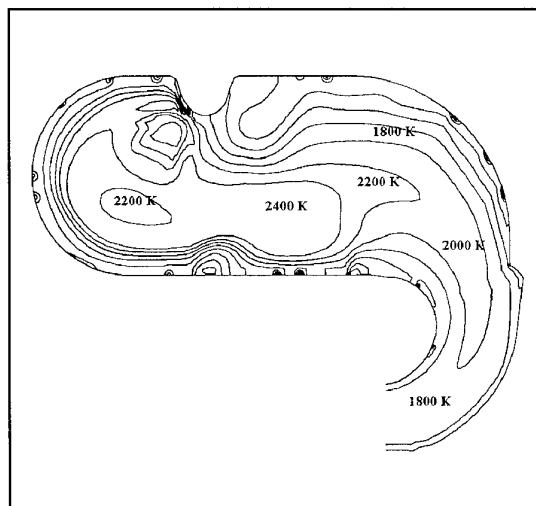


Fig 5 - Gas Temperature at Fuel Injector Plane

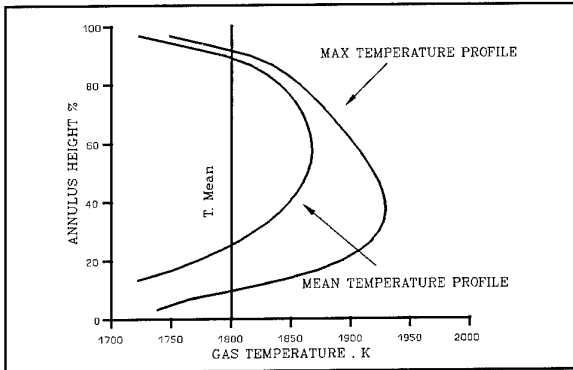


Fig 6 - Combustor Exit Temperature Profile

Gas temperatures evaluated above have been used to verify the thermal behaviour of the combustor liner. The FEM analysis has been performed with ANSYS and results are in fig 7.

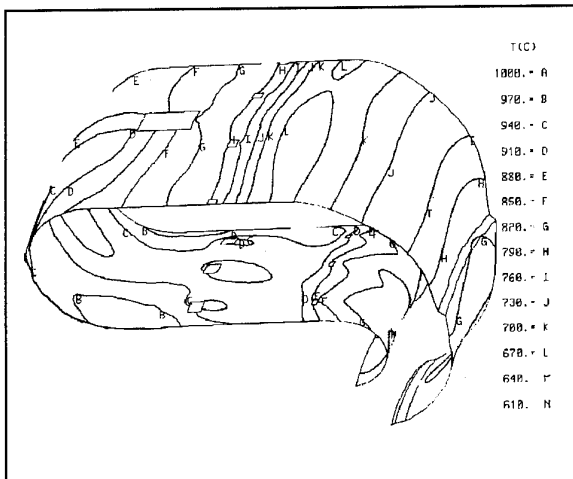


Fig 7 - Combustor Liner Metal Temperature

The highest temperature is 984 °C located upstream dilution holes of inner liner. Moreover to keep the wall temperature far enough from that allowable a ceramic coating (thermal barrier coating TBC) on the internal surface of liner can be applied. This can drop metal temperature by ~60° C.

HP TURBINE

As said before the HP turbine was designed for a core engine demonstrator to withstand to maximum TET of 1600 K. Here, as engine ratings ask for highest TET, to assure adequate operating life of NGV and ROTOR some modifications are needed.

The NGV cooling has been increased from 8% to 12% W2 with some modifications applied to internal cooling passages. Forced convection plus impingement is used to cool the forward internal surface. After impingement cooling the air is injected in the main stream at leading edge, pressure and suction side by six hole rows. The rearward portion of the blade is cooled internally by an enhanced convection cooling and film cooling at the trailing edge pressure side. The platforms are cooled by film cooling holes.

Fig 8 shows the metal temperature distribution at the blade pressure side obtained by means of FEM thermal analysis performed at EMP, using the span-wise distribution of gas temperature relatively to the maximum profile "hot spot" of fig 6.

The maximum metal temperature (1042 °C) is at the trailing edge near the blade mid span.

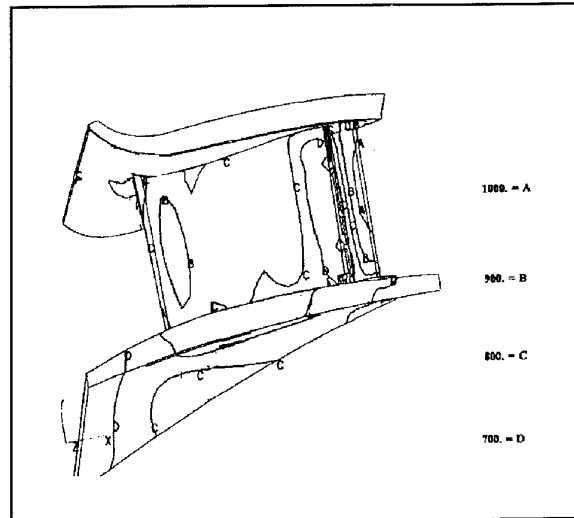


Fig 8 - Metal Temperature Distribution of HP Turbine NGV

Regarding the rotor blade it has been considered a thermal barrier of 0.5 mm applied both on blade and platform and 5% W2 as cooling flow. The cooling system provides air flow to cool the internal blade surface by means of multi-pass forced convection and impingement. Air flow is then discharged in the main flow through the blade tip and through film cooling holes, placed at the leading edge and in the rear part of the blade pressure side.

The FEM analysis is done on whole rotor assembly (rotor disk and blade). Fig 9 shows metal temperature distribution on the blade pressure side, where maximum peak temperature (922°C) is at the tip in the region of trailing edge.

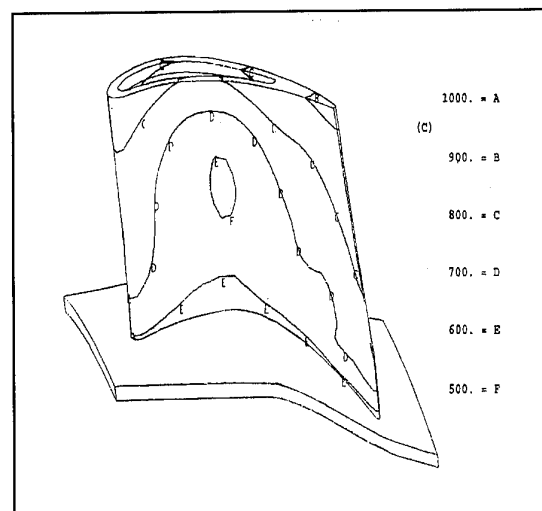


Fig 9 - Metal Temperature Distribution of HP Turbine Rotor

Since the thermal coating produces some substantial variations of the rotor blade profile, and the increasing cooling flow modifies the thermodynamics, an assessment of overall turbine performance has been done.

The fig 10 reports the computed performance map obtained taking as reference point the following conditions:

Inlet Temperature, T_{ET}	1720. K
Rotational Speed, N	38562 rpm
Expansion Ratio, ER_{tt}	2.4
NGV Cooling Flow, % W3	15.0 %
Rotor Cooling Flow, % W3	6.2 %

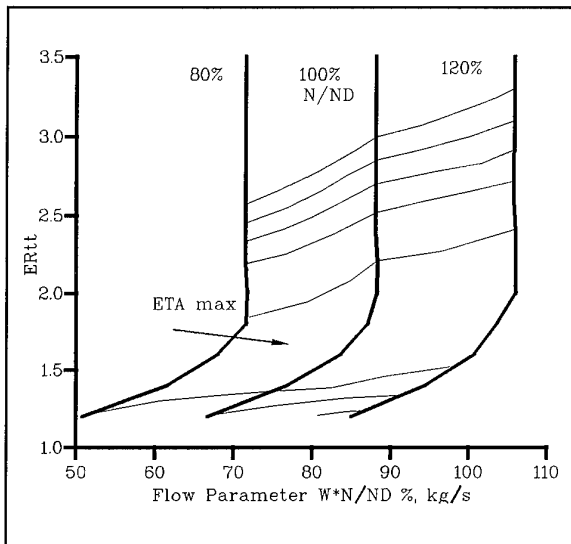


Fig 10 - HP Turbine Performance Map

POWER TURBINE

The power turbine is a single stage design with following reference performance:

Inlet Temperature, T_s	1284 K
Expansion Ratio, $ER_{tt,56}$	2.7
Rotor Disk Cooling, W_{c56}	1%W5
Rotational Speed, N	33000 rpm

Until now only the preliminary design of this engine component has been done.

The conceptual design of the turbine is based on two choices featuring the turbine : 1) variable geometry for the NGV; 2) counter rotating PT shaft respect to HP one.

The latter have the advantage to reduce the amount of turning in the PT nozzle and the gyroscopic effects.

The variable geometry allows to optimize the performance of the engine in terms of surge margin, HE running temperature and part load SFC.

The performance map of the PT relatively to nominal position of the NGV, is presented in fig 11.

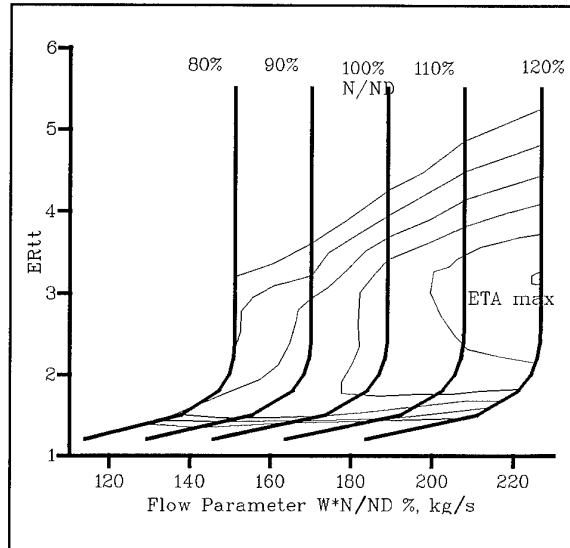


Fig 11 - Power Turbine Performance Map at Nominal NGV position

The change of NGV geometry makes the turbine flow function variably in the range of $\pm 15\%$.

Fig 12 reports the design speed efficiency relatively to four NGV stagger positions. The turbine was designed to have a flat efficiency over a range of $ER_{tt} 2 \div 3$.

When flow capacity reduces, the efficiency progressively drops, this because of the mismatch between NGV and the rotor blade. In turn an increase is observed when higher mass flow is through the turbine, even if optimum ER_{tt} is reduced, because of earlier rotor choking.

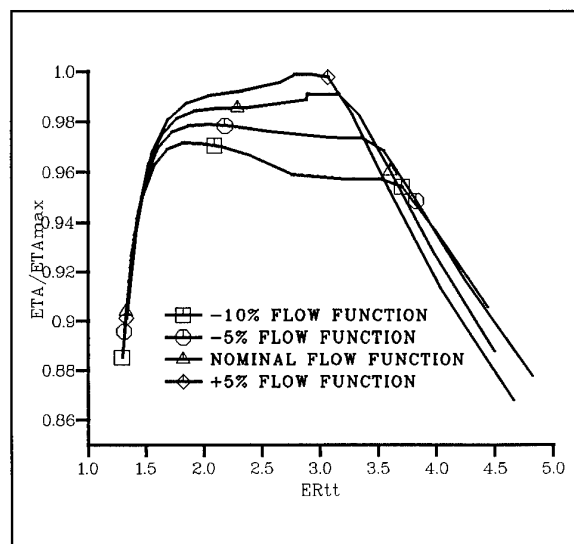


Fig 12 - Power Turbine 100% N/ND - Flow Function Variation Effect on Efficiency

HEAT EXCHANGER

The gas heat energy at the PT exit is extracted by the HE to heat air coming from the compressor. So that the air flow at combustor is available at higher temperature. The basic idea was to design something compact, easy to manufacture and adaptable with the exhaust turbine duct, even if with medium effectiveness. The selected geometry is cross-flow type, with mixed hot stream crossing three times a tube matrix while cold air makes a double pass through the tubes.

Here, to define the engine layout, the HE has been considered with six tube-bundle modules. Ceramic material, having high thermal shock and temperature resistance, and low thermal expansion coefficient, can be used. In fact recently technology developments show that the ceramic HE (Silicon-Nitride) can be manufactured and successfully tested up to $T_g=700^\circ\text{C}$ [8].

In the preliminary phase of the design, six staggered tube rows with total of 576 tubes have been selected. For each row the tubes are equally spaced along the circumference.

The tube cross section has elliptic shape in order to maximize the number of tubes per row and to reduce the hot side pressure loss [9]. Furthermore each tube has a straight fin, to enhance heat transfer performance.

Fig 13 shows the cross section of the HE, while main design characteristics at the MCSP rating are the following:

Effectiveness	67.9 %
Cold Side Pressure Loss	4.8 %
Hot Side Pressure Loss	5.2 %
T_a	557 K
T_g	1010 K
\dot{W}_g	2.95 kg/s
\dot{W}_a/\dot{W}_g	0.72

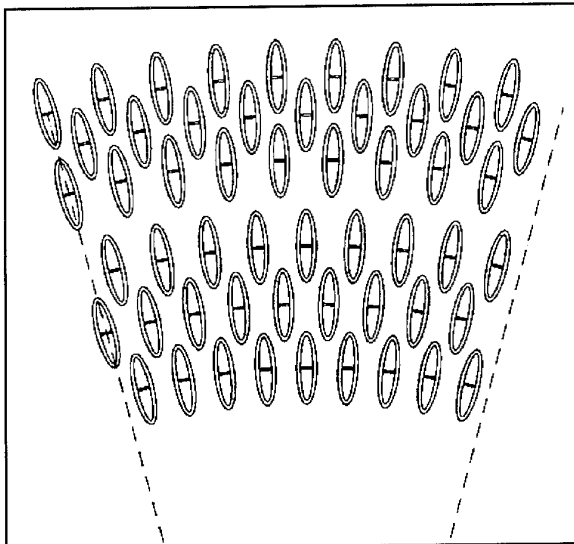


Fig 13 - Heat Exchanger Tube Matrix Layout

Fig 14 presents off-design performance of the HE in terms of effectiveness vs non-dimensional parameters NUT and C_{ratio} , defined as follows :

$$NUT = \frac{1}{\frac{1}{h_g A_g} + \frac{1}{h_a A_a}} \frac{1}{C_{min}}$$

$$C_{min} = \min(C_{P_a} \dot{W}_a, C_{P_g} \dot{W}_g)$$

$$C_{ratio} = \frac{C_{min}}{C_{max}}$$

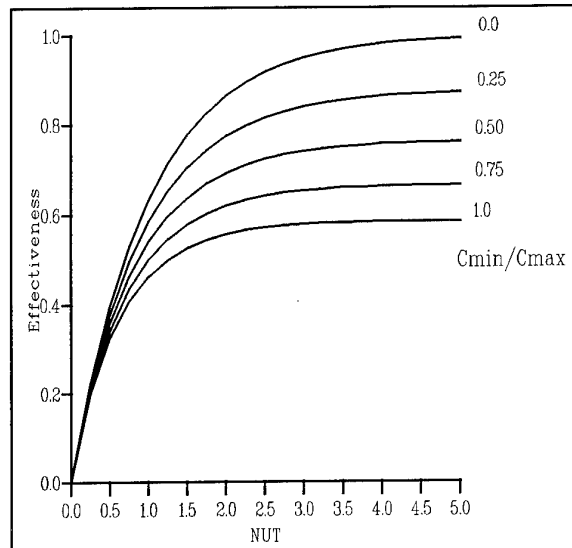


Fig 14 - Heat Exchanger Off-Design Performance

OFF-DESIGN PERFORMANCE

Off-Design engine performance is evaluated by means of an iterating procedure based on energy balance and mass continuity through the turbo-machineries and HE.

The code uses components performance maps described above, while the power turbine has been simulated by means of several maps, each of them with a fixed NGV position, in such a way to cover the range of $\pm 15\%$ of its nominal flow function. For off-design behaviour of the HE the effectiveness of fig 14 has been used.

The use of correlations allows to evaluate the h_g and h_a needed to define NUT. The non-dimensional group " C_{ratio} " is computed by thermodynamic characteristics of hot gas at the PT exit and those of cold air at compressor discharge. The cold and hot side losses are assumed proportionally to the flows through the HE.

Moreover, since a percentage of compressor discharge air flow bypasses the HE entering directly in the combustor the off-design study accounts for the different temperature of two streams.

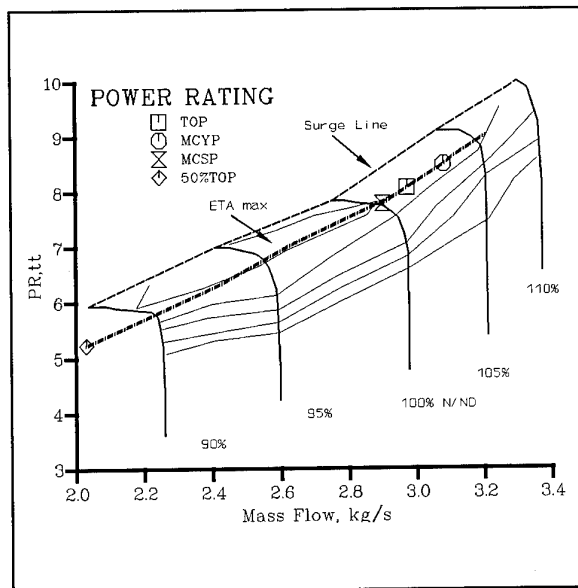


Fig 15 - Engine Operating on the Compressor Map

As observed in fig 15, the engine operating line on the compressor map lies near the peak efficiency line with enough surge margin for the transient engine behaviour. Table II is outlining the engine performance at the power requirements.

Table II - Engine Performance at Power Ratings

Rating	Power kW	TET K	SFC g/kWh
EMP	995	1800	240
MCYP	945	1702	243
TOP	851	1648	248
MCSP	783	1605	252
50% TOP	425	1480	280

Fig 16 shows SFC vs shaft power with and without variable geometry of the PT. It can be seen that a significant gain in SFC is attainable at the part load while no improvement exists at the high power rate. The gains of the recuperative cycle are still more evident, when compared to two engines representative of current simple cycle technology in the 1000 kW class.

Lower SFC of the HE cycle engine reduces the take off gross weight, or allows an improvement of mission endurance. Moreover, low EGT for warfare operations makes this engine less vulnerable to infrared tracking missiles.

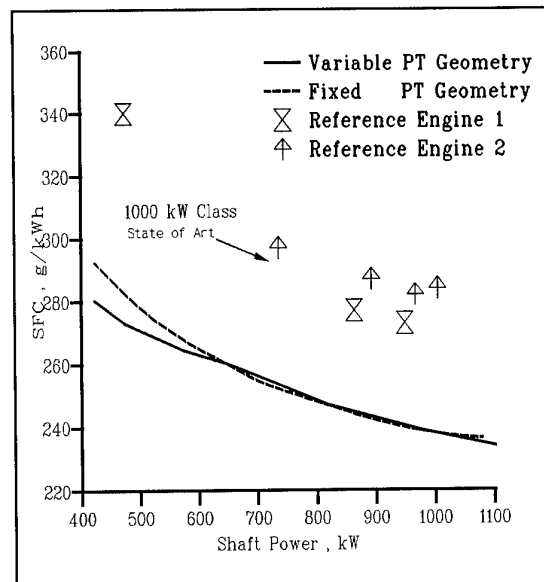


Fig 16 - SFC vs Shaft Power

A further significant advantage of the variable geometry coupled with a recuperative cycle engine is observed looking at fig 17, where the HE inlet temperature vs power is presented. Variable geometry allows the HE working with near constant inlet temperature ($\Delta T \sim 80$), when the engine running condition moves from max power towards part load conditions, while fixed geometry shows a wider range of $\Delta T \sim 200$ K. This reduces HE thermal stresses induced during transients and HE performance lack due to thermal inertia.

Furthermore a substantial benefit on the life of the hot-section engine components, combustor, NGV and rotor blade can be obtained.

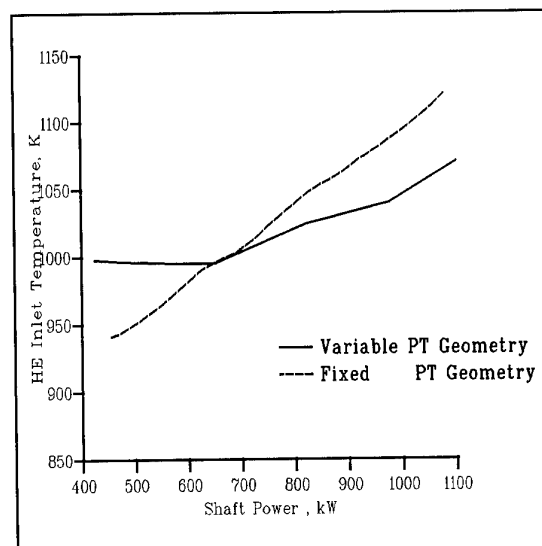


Fig 17 - HE Inlet Temperature vs Shaft Power

CONCLUSIONS

The use of a recuperative cycle applied to 1000 kW class turboshaft, results very attractive for its low SFC and simple engine layout.

In fact to reach the same power levels, a simple cycle engine should have an overall pressure ratio in the range of 13-14, which would lead to more compressor and turbine stages. Increased complexity due to HE is almost compensated by a fewer rotating components, with a direct impact on engine first cost as well as that for ownership.

Here it has been described a possible layout of a recuperative engine, which is built taking advantage of existing components for the core engine, while for the power turbine and heat exchanger geometry a preliminary design has been used.

The engine duty cycle is based on maximum TET of 1600 K for which 8/1 as overall pressure ratio allows SFC near optimum for recuperative cycles with 0.7 HE effectiveness.

In comparison with the simple cycle, the reduction of the SFC of recuperative cycle impacts on the helicopter take off gross weight or allows an improvement of mission endurance. This and lower EGT are two important factors, especially for military applications, where wider operative range and reduced infrared signature make this engine type more attractive.

Very important would be making use of the recuperative cycle with high technology level of combustor and turbo-machineries in civil applications, where significant reduction of pollution would result from the less fuel consumption.

REFERENCES

- [1] A.D. Beweley
"Cycle Analysis for Helicopter Gas Turbine Engines", ASME Paper 89-GT-328
- [2] Colin F. McDonald
"The Increasing Role of Heat Exchanger in Gas Turbine Plants", ASME Paper 89-GT-103.
- [3] H. Grieb, W. Klusmann
"Regenerative Helicopter Engines - Advances In Performance And Expected Development Problems", AGARD CP302,1981
- [4] Robert A. Wilson, Daniel B.Kupratis and Satyanarayana Kodali
"Future Vehicular Recuperator Technology Projections", ASME Paper 94-GT-395
- [5] S.Colantuoni, A.Colella, L.DiNola, D.Carbone, D. Marotta
"Aero-Thermal Design of a Cooled Transonic NGV and Comparison with Experimental Results", AGARD CP 527, 1992
- [6] S.Colantuoni, A.Colella, G.Santoriello, L.Cirillo, C. Iossa
"Aerothermal Design of 1600 K TET Core Engine Hot-Section Components for High-Technology Compact Propulsion Systems", AGARD CP 537,1993
- [7] S.Colantuoni, A.Colella
"Aerodesign and Performance Analysis of a Radial Transonic Impeller for a 9:1 Pressure Ratio Compressor", Trans. ASME, Jrl of Turb. July 1993, Vol 115/573
- [8] Y.Yoshimura, K.Itoh, K.Ohori, M.Hori, M.Hattori, T.Yoshida, K.Watanabe
"Development of Shell-And-Tube Type Ceramic Heat Exchanger for CGT301", ASME Paper 95-GT-208
- [9] G.Pellischek, B.Kumpf
"Compact Heat Exchanger Technology for Aero Engines", ISABE 91-7019

Paper 12: Discussion

Question from Dr M G Philpot, Defence Research Agency, UK

What is the impact of the additional weight and volume of the recuperative engine on the performance of the helicopter, compared with a single cycle engine?

What is the impact of the life and reliability aspects of the heat exchanger on life cycle cost, compared with a simple cycle engine?

Author's reply

Using a medium effectiveness heat exchanger with a rear drive turboshaft we have only a small volume increase, resulting from the greater axial dimension. The additional weight of the heat exchanger is balanced by fewer turbomachinery stages. Also the helicopter has a lower gross take-off weight, due to the lower sfc. The life cycle cost for the heat exchange engine becomes competitive when the annual flying hours are high.

Question from G Bobula, NASA Lewis, USA

Can you explain why your cycle used a power turbine rotational speed of 33000 rev/min? By choosing this rather than a speed closer to 20000 rev/min, the propulsion system including the drive train, must involve at least one extra gear stage, ie one more set of reduction gears. Could an engine with a lower power turbine speed produce a lighter system weight?

Author's reply

We chose 33000 rev/min in order to have the loading factor near optimum efficiency, accepting the increased complexity in the reduction gearbox.

Question from B Leroudier, Dassault Aviation, France

Why did you not mention reduced infra-red signature reduction as an advantage for a military helicopter?

Author's reply

There is no significant reduction at partial power.

Question from Dr P Pilidis, Cranfield University, UK

How does the transient response time of the engine compare to that of a state-of-the-art simple cycle helicopter gas turbine?

Author's reply

At this time no evaluation of the transient response has been done. However several authors state that a fast acceleration rate is a further advantage of an engine with a variable geometry power turbine.

Question from C Rodgers, USA

The recuperator effectiveness was relatively low and the pressure drops relatively high. Was this the result of seeking to minimise recuperator volume and weight?

Author's reply

One of the design requirements was to keep the outer diameter of the recuperator within the engine/accessories envelope. To improve the effectiveness with this constraint, we had to use a finned tube (low hydraulic diameter)/multipass configuration for the hot stream.

Variable Cycle Engine Concepts

J.E. Johnson

Manager - Advanced Systems
GE Aircraft Engines
1 Neumann Way MD-G326
Cincinnati, Ohio 45215-1988
USA

SUMMARY

General Electric Aircraft Engines has been involved in both the study and development of variable cycle engine concepts for over 30 years. During this time GEAE, working closely with the advanced technology centers in government, has been seeking an engine concept that could combine the attributes of a high temperature turbojet - high dry specific thrust and low max power SFC, with those of a turbofan - low part power SFC and low exhaust gas temperature. Also sought were engine concepts that could reduce inlet spillage drag and nozzle closure drag during part power dry operation.

This paper describes several of the concepts evaluated during the last three decades, starting with the Air Force defined VAPCOM (an acronym for Variable Pumping Compressor) and concluding with a general description of the YF120 VCE that flew in the YF22 and YF23 ATF prototype aircraft.

LIST OF SYMBOLS

VCE	variable cycle engine
SFC	specific fuel consumption
VAPCOM	variable pumping compressor
A8	exhaust nozzle throat area
A9	exhaust nozzle expansion area
HP	high pressure (spool or turbine)
LP	low pressure (spool or turbine)
T3	compressor discharge temperature
T41	HP turbine rotor inlet temperature
TACE	turbo augmented cycle engine
AIV	annular inverter valve
MOBY	modulating bypass engine
VABI	variable area bypass injector
SST	supersonic transport
ATEGG	advanced turbine engine gas generator
JTDE	joint technology demonstrator engine
ATF	advanced tactical fighter
IHPTET	integrated high performance turbine engine technology

1.0 INTRODUCTION

General Electric Aircraft Engines has been involved in both the study and development of variable cycle engine, (VCE) concepts for over 30 years. During this time GEAE, working closely with the advanced technology centers in government, has been seeking an affordable engine concept that could combine the attributes of a high turbine temperature turbojet, i.e., high dry specific thrust and low max power specific fuel consumption, (SFC), with those of a turbofan, i.e., low part power SFC with low exhaust gas temperature. Also sought

were engine concepts that could further improve part power SFC levels by reducing inlet spillage and nozzle closure drag by retaining high operating airflows at reduced power settings.

Section 1.1 of this paper contains descriptions of several of the novel engine concepts that have been evaluated during the last three decades, starting with the Air Force defined VAPCOM (an acronym for Variable Pumping Compressor) and concluding with a general description of the YF120 type VCE that ran in the YF22 and YF23 ATF prototype aircraft. Section 1.2 contains descriptions of the family of YJ101 derived VCE concept demonstrators that were jointly funded by the Air Force, Navy, and NASA during the 1975-1981 time period. Section 1.3 describes the final evolution of the F120 type VCE and Section 1.4 briefly addresses the current status of VCE development.

1.1 Concept Descriptions

The following paragraphs describe, in chronological order, the major types of VCE's evaluated by GEAE during the past 30⁺ years.

1.1.1 VAPCOM - The Original Variable Cycle Concept

A major change in fighter and fighter/bomber propulsion began in the 1960 time period when augmented turbofans began to replace augmented turbojets as the preferred propulsion concept due to their improved subsonic cruise SFC potentials. These initial turbofan systems were not without their own problems however. The lower part power SFC's were accompanied with very high max afterburning SFC's, relatively more complex augmentors and huge exhaust nozzle sizes that required very large nozzle throat area (A8) variations between max dry and max A/B power settings.

The VAPCOM engine concept was conceived by a group of engineers at Wright Patterson in this 1960 time period as a possible alternative to the augmented turbofan. They envisioned an engine that could combine the improved lower power SFC's of a turbofan with the max power SFC's of a very high temperature turbojet that required little or no augmentation to produce equivalent max power relative to these first generation augmented fans. This was to be accomplished by using variable stator fan, compressor, and turbine systems in a unique manner that actually changed the engine operating mode from that of a pure turbojet, essentially a near zero bypass ratio dual rotor turbojet, to a bypass 1.0 class dual rotor separated flow turbofan.

Figure 1 contains an engine schematic of the original VAPCOM engine. As shown, the concept had a dual spool arrangement with a bypass duct that was only used during the turbofan mode of operation. The exhaust system had two variable nozzle throat areas, and for this schematic illustration, a common expansion area, A9. A two stage fan with all variable stators was driven by a single stage fan turbine that incorporated a variable area nozzle diaphragm. The core was comprised of an all variable stator six stage compressor, a high delta T combustor and a two stage HP turbine that had a variable area stage one vane system. Turbine temperatures in excess of 3000° were envisioned for this extremely advanced engine. Afterburning was also considered but this was not the preferred approach to making high thrust levels. The turbojet mode, with high turbine inlet temperature, was the high specific thrust mode of choice since this would produce max combat SFC levels lower than J79 type augmented turbojets and nearly 50% lower than the TF30 class of augmented turbofan. Also, exhaust nozzle areas would be minimized since thrust was being created with both increased nozzle pressure and temperature and not by just temperature alone as is the case of augmented engines.

For this high specific thrust mode the core stator systems were full open to allow all of the fan discharge flow to be accepted by the core engine. Fan speed and fan stator schedules coupled with turbine temperature usage and turbine vane control were optimized to maximize engine thrust at all flight conditions. For these high power modes only the core stream A8 system was utilized as depicted in the top view of Figure 1. For part power operation the core stators were systematically closed and fan stators and fan operating line were adjusted to build up the operating bypass ratio from the 0⁺ level at max power to the 1.0 class at part power. The variable area turbine vane systems were now being utilized to allow both core speed, core operating line, and turbine temperature to be optimized to achieve minimum possible fuel flow at each part power setting. Both A8 systems were utilized for part power performance optimization.

Another aspect of performance improvement potential was made possible with the unique spool speed/flow control offered by the VAPCOM. Throttle dependent spillage drag losses and exhaust system boattail drags (nozzle closure) can be minimized if fan airflow can be maintained as thrust is reduced. In both turbojets and conventional turbofans only limited capabilities are available for part power airflow tailoring before large penalties are incurred in basic uninstalled performance. The variable stator VAPCOM components and the twin A8 exhaust system allowed high levels of fan flow to be maintained to relatively low power settings.

As studies progressed several basic problems became apparent with the VAPCOM approach to providing both a turbojet and turbofan operating mode. First, the all variable fan and compressor components did not achieve their target efficiency goals. Also the variable area turbine systems needed in both the HP and LP turbines proved to be complex and relatively high loss devices. Most importantly, however, was the fundamental problem associated with achieving the turbofan

operating mode. In order to obtain a 0-1 bypass swing the core stator system had to be low flowed which results in an accompanying loss of core compressor pressure potential (similar to reducing speed to reduce flow). Also, a reduction in fan operating line was also required to achieve the final increment of bypass increase. This further reduced overall cycle pressure ratio so that when the full conversion from 0-1 bypass was achieved over 25% of the 0 bypass mode cycle pressure potential had been lost, negating a major position of the cycle mode change advantage. This loss, in conjunction with the lower efficiency levels and relative complexity of all variable stator fan, compressor, and turbine systems, lead to an abandonment of this concept in the 1965 time period.

Even though an engine didn't result from the VAPCOM program the basic research conducted on the variable stator fan, compressor and turbine systems provided valuable knowledge about how to design and utilize these innovative engine features. Also, high temperature rise combustor technology and advancements in basic heat transfer and turbine cooling were integral parts of the overall technology programs that addressed the needs of the VAPCOM concept. This early research in very high temperature cooled turbine technology helped form the tech base for General Electric's very successful high temperature turbine systems.

The author of this article is greatly indebted to the VAPCOM program. His initial assignment at GE involved hand matching of all of the VAPCOM variable geometry components and manually calculating the performance potentials of this machine. Having been introduced to this industry with a turbomachinery concept of nearly infinite flexibility has made the study and definition of ensuing variable cycle concepts relatively easy.

1.1.2 Composite Cycle - Turbojet & Turbofan Modes

Another attempt at combining both a turbojet and turbofan mode in one turbomachinery design was the Composite Cycle concept defined by a General Electric engineer in the early 1960's. His original concept was examined during the initial supersonic transport program while the version depicted in Figure 2 was evaluated in several high speed advanced bomber and fighter studies in the 1965-1970 time period.

As shown in Figure 2, this concept had a two spool design that incorporated a conventional fan and core system and an unconventional bypass duct and low pressure confluent flow turbine system. The bypass duct contained a second main burner type combustor that fed into a variable area turbine vane system and the tip section of this confluent flow turbine rotor. The hub and tip portion of this turbine plus, for the version shown, three additional conventional fan turbine stages supply the power needed to drive the fan. In the max power, or turbojet mode, both the core burner and the bypass burner are on producing a concentric turbojet operating mode. The flow streams entering the tip and hub of the confluent flow turbine are constrained to have equal static pressure levels and a reasonably homogenized flow exits from the confluent flow turbine for flight speeds from SLS to Mach 2⁺. For max thrust operation beyond Mach 2 the core system can be phased out and the power required to operate the fan can be fully derived

from the tip section of the confluent flow turbine. This ability to phase out the core allowed very high overall cycle pressure ratios to be examined for an engine that could also operate in the Mach 3⁺ flight regime since core engine speed and temperatures (compressor discharge, T3, and high pressure turbine inlet temperature, T41) could be minimized with little loss in thrust potential. For part power operation the outer burner was shut off and the engine cycle converted into a mixed flow type turbofan. Special demands were placed on the confluent flow turbine tip section during this outer burner off mode. Very large changes occurred in corrected turbine speed, turbine flow function, and turbine energy function that caused untenable swings in turbine exit swirl and high system losses. These losses (verified in a turbine rig) offset the potential turbofan mode advantages and the concept was abandoned. There were some later studies that examined variable pitch confluent flow turbine rotor designs to help handle the swirl problem but those designs proved to be too heavy and complex to pursue beyond the concept study phase.

Interest in VCE's lay dormant at General Electric from 1970 to 1973 when a series of both in-house and government funded studies were begun to see if a variable cycle engine could be defined that offered distinct advantages over a conventional turbofan while also being both practical and affordable.

1.1.3 Combined Turbofan and Turbojet Revisited

Another attempt at defining an engine with two basic operating modes was made in early 1973. Figure 3 illustrates the basic architecture of this engine concept called a Turbo Augmented Cycle Engine or TACE for short. This engine was basically two separate engines connected by a unique set of crossover ducting. The front engine shown is a conventional dual rotor turbofan. The aft engine is a single rotor turbojet that acts as a bypass stream augmentor for the turbofan during high thrust production.

Two operating modes are shown in Figure 3. In the top view the aft turbojet is shut off and the core and duct streams of the turbofan are mixed in the common duct surrounding the aft turbojet and are exhausted through the outer nozzle. In the bottom view the aft turbojet is on and is supercharged by the bypass stream from the turbofan. In this mode the turbojet adds efficient augmentation to the bypass stream. The hot turbofan core discharge is bypassed around the aft turbojet and exhausted through the outer nozzle.

This concept offered very good part power performance with the aft jet shut off and exceptional max power SFC with the aft jet on due to the efficient augmentation that the supercharged turbojet supplied. However, some very obvious drawbacks are readily apparent. Two full engines are really required to make this concept. Length, weight, complexity, and cost overwhelmed the cycle advantages and the concept was dropped.

1.1.4 Series/Parallel Mode VCE Concepts

In the early 1970's The Boeing Company designed, built, and successfully tested a unique flow augmentation series/parallel mode VCE concept demonstrator by adding an annular inverter valve, AIV, to a JT3D commercial engine. General Electric

evaluated the merits of this concept in the 1973-1974 time period and also looked at several variations on the basic scheme to try to overcome some of the deficiencies found.

1.1.4.1 Full Span Annular Inverter Valve VCE Concept

Figure 4 illustrates the conceptual layout of an annular inverter valve added to the fan of a YJ101 engine. This valve permits two distinct modes of engine operation. In the series mode all of the front fan stage discharge flow is fed into the rear fan section and passed on to the core engine and bypass duct, just as in a conventional engine. In the parallel mode all of the front fan discharge flow is diverted around the rear fan section and is then exhausted through a separate outer nozzle system. When the AIV diverts stage one flow around the rest of the engine it also opens up an ambient air delivery duct for the rear section of the fan. This auxiliary inlet flow is compressed by the aft fan stages and then divided in a conventional manner between the core and inner bypass duct. For the YJ101 fan used in this study, total inlet mass flow is increased about 60 percent and the operating bypass ratio increased from a bypass 0.2 class to a bypass 2 class. Due to the loss of stage one fan supercharge overall cycle pressure ratio in the parallel mode is about 40% lower than in the series mode.

This loss of core supercharge results in diminished core energy, and, for a given parallel mode thrust class requirement, results in a core size penalty that amplifies the weight problems associated with this concept. Also, the loss of overall pressure ratio that results during parallel mode operation reduces the potential cycle benefit derived from the increased operating bypass ratio. A special oversized inlet system would also be needed to accommodate the increased fan total flow levels that result during the parallel mode of operation.

1.1.4.2 Part Span AIV - Constant Core Supercharge

Figures 5 and 6 illustrate a modified inverter valve design that retains core supercharging during the series - parallel mode change for a separated flow duct burning turbofan and a mixed flow afterburning turbofan. The splittered fan designs retain full core supercharge while the hinged valve opens and closes the inlet to the rear fan tip section. With this approach core size is minimized for a given thrust size engine; however, the amount of fan flow enhancement is greatly reduced since only the tip portion of the fan rear section is opened to ambient air during the parallel high flow mode.

These concepts obviously add weight, length and cost to a basic turbofan engine and were found to have little improvement to offer in fighter, fighter/bomber, and supersonic transport aircraft systems during evaluations conducted in the 1973-1975 time. The series/parallel mode concept reappears occasionally, most recently in the Tandem Fan STOVL Concept. Core size penalties and system weight increases again proved to be unacceptable.

1.1.5 Three Spool Modulating Bypass Ratio VCE-MOBY

In the 1973 time period attention was starting to be focused on throttle dependent inlet and afterbody drag levels for the turbofan powered fighter and bomber systems coming on line. Also, NASA had restarted research on efficient low noise

capable propulsion concepts for a Mach 2.2-2.7 supersonic transport.

In order to address these needs General Electric defined a very versatile (and very complex) three spool duct burning engine that allowed nearly independent rotor speed and operating line control for use in optimizing installed part power performance. The Modulating Bypass Engine, or MOBY, shown in Figure 7 had three spools, three variable area turbines, three variable nozzle throats, two variable stator fan systems and two bypass ducts, one of which contained a high temperature rise duct burner. The core compressor was conventional, having only a variable inlet guide vane. For max thrust production all of the front fan flow was passed through the second fan to maximize fan pressure ratio. As in the VAPCOM system there was essentially no flow in the outer bypass duct during this max dry and max augmented operating mode. The discharge flow from the second fan was divided between the core and the inner bypass duct that contained the duct burner. Full temperature rise in this augmentor produced the max thrust rating for the engine. The bottom view of Figure 7 illustrates this mode of operation.

The unique part power operating mode of this cycle concept is shown in the top view of Figure 7. Front fan flow could be maintained to very low thrust levels by systematically phasing out the core system and intermediate spool pressure rise as core fuel flow was reduced. (The duct burner was not on during part power operation at subsonic flight speeds.) Use was made of the intermediate and low pressure turbine variable stators to optimize core speed and intermediate spool speed during part power operation. The high pressure turbine variable vane system was used to control core operating line. Front fan and second fan operating lines were controlled by utilizing the independent A8's associated with each bypass duct. Finally, the second fan IGV could be scheduled, in conjunction with second spool speed, to regulate the build-up of flow in the outer bypass duct to further improve part power performance by optimizing operating bypass ratio.

This VCE did do something useful relative to a conventional turbofan. All of the variable geometry allowed both optimum uninstalled and, more importantly, optimum installed performance to be achieved, especially at low power settings. Also, the ability to hold full fan flow at reduced thrust provided an ability to reduce exhaust gas velocity, the prime ingredient in jet noise production, and therefore tailor noise at reduced power settings such as community cut back and approach. As with the other VCE's discussed so far, the concept was too complex to be pursued in the form shown in Figure 7, but many valuable lessons were learned about the attributes that a VCE should have to offer a significant advantage over a conventional propulsion system.

1.1.6 Initial Dual Cycle Single Bypass VCE

The studies conducted on the MOBY concept provided insight into what each variable geometry feature contributed to overall engine operational flexibility and performance improvement potential. Figure 8 illustrates how one of the MOBY engine operating modes could be added to a conventional dual rotor mixed flow turbofan engine. The bottom view shows the basic

engine mode of operation when the bypass flow and low pressure turbine flows are joined and exit together through a single exhaust system. A constraint in this operating mode is the requirement for a balanced static pressure to be maintained at the point where the two streams first come together. This constraint which affects rotor speed/T41 relationships can be removed by introducing a diverter valve system that transfers the bypass flow around the basic exhaust stream as a secondary exhaust stream is opened. The mixed flow engine concept has now been converted into a separated flow turbofan concept with two independently variable nozzle area systems which allow spool speed/T41 flexibilities for fine tuning max dry thrust and part power fan airflow scheduling.

This form of single bypass VCE retained the advantage of a mixed flow afterburning turbofan relative to the separated flow duct burning MOBY concept, i.e., all of the fan flow is augmented to provide maximum thrust, while also having the rotor speed flexibility offered by a separated flow turbofan with two variable area nozzles. However, it did not have as much fan pressure ratio control and bypass ratio adjustment as the three spool double bypass arrangement MOBY concept.

1.1.7 Initial Double Bypass VCE Configurations with 3 Stream Exhaust

1.1.7.1 1*2 Fan Stage Split

Figure 9 shows the first attempt at combining some of the additional flexibilities of the MOBY concept to the mixed flow afterburning VCE shown in Figure 8.

Two spools were retained, but, as shown in Figure 9, the three stage fan was divided into two sections, a single stage front block and a two stage rear block. Variable stators were added to the rear fan block as were a second bypass duct and third A8 system. Also included was a variable area vane set for the low pressure turbine. As shown in the bottom view of Figure 9, the engine retained a basic mixed flow afterburning mode where all of the stage one fan flow was accepted by the two stage rear block. (The outer bypass duct has essentially no flow during max power production just as in the VAPCOM and MOBY cycle concepts.) The fan flow is then divided between the core inlet and inner bypass duct. Basic mixed flow engine operation produces a static pressure balance between the core and inner bypass duct discharge flows that now mix and burn in the afterburner and then are exhausted through a single A8 nozzle.

For max dry power the engine can be operated in a mixed flow mode or, with the diverter valve and second A8 system, in the separated flow mode previously discussed for the preceding VCE concept. The unique split fan architecture and bypass duct/nozzle arrangement for the VCE concept shown in Figure 9 allows a part dry power mode of operation that comes close to having the fan pressure ratio/fan flow/bypass ratio control offered by the more complex three spool MOBY concept. The variable fan stators of the rear fan block (an original VAPCOM feature) allow nearly the same flexibility as a third spool, especially when variable turbine vanes are also used in the low pressure turbine.

1.1.7.2 2*1 Fan Stage Split

Figure 10 illustrates another version of this VCE concept. Instead of dividing the fan into a 1*2 stage arrangement the fan was split into a 2*1 configuration. Max power single bypass mode performance (no flow in the outer bypass duct) was identical between the two but part power performance, outer duct sizing, and total A8 demands were impacted.

The simplicity of two spools plus the mixed flow afterburning max power mode made either of these initial double bypass VCE concepts more attractive than the MOBY concept; however, the three stream nozzle still added an unacceptable level of complexity and cost.

1.1.8 Single and Double Bypass VCE Simplification

1.1.8.1 Rear VABI

As previously discussed, mixed flow turbofans have a cycle balancing constraint of requiring equal static pressure levels in the core and bypass duct exit streams where the streams first come together. The diverter valve used in the preceding single and double bypass VCE's effectively eliminated this cycle operational constraint but did introduce the complexity of an additional rear duct and exhaust system. In the 1976 time period an approach to simplifying this was defined. This new concept called a VABI, an acronym for variable area bypass injector, is shown in Figure 11. Instead of closing off the duct entry into the primary exhaust stream as was done by the diverter valve, this concept varied the areas at the static pressure balance plane which allows bypass duct and core discharge total pressure levels to be optimized for both max and part power operation. While not supplying the same level of fan pressure ratio, speed, and turbine temperature control as a fully separated flow mode, most of the cycle advantages were retained and the exhaust system was greatly simplified with this single bypass VCE only requiring one variable A8. The variable area low pressure turbine system added additional spool speed optimization.

1.1.8.2 Front and Rear VABI

Shortly after defining the cycle tailoring potentials of the rear VABI it became apparent that this same principle could be applied to the inner and outer bypass flows of the double bypass VCE, resulting in a much simplified version of this cycle concept. Figure 12 illustrates a potential double bypass VCE that has both a rear VABI and a first generation front VABI. Note that there is now only one common bypass duct and one conventional exhaust nozzle. This improved mixed flow afterburning double bypass VCE had a major augmented thrust advantage over the separated flow duct burning MOBY VCE while retaining most of the part power performance optimization potential with one less spool and two fewer exhaust nozzle systems.

The variable area low pressure turbine vane system shown in Figures 11 and 12 were found to add an improved level of rotor speed control for optimizing low power performance for this double bypass VCE concept.

1.1.9 Core Fan Architecture for Additional Simplicity

As mentioned previously variable cycle engines were also being investigated under a NASA sponsored supersonic transport propulsion study. Several of the VCE concepts described in this paper were analyzed. The flow holding and part power cycle tailoring of the MOBY concept appeared to have potential during these 1973-1974 studies. Therefore, as the basic double bypass VCE concept was evolved in the 1974-1976 time period, it too was evaluated and found to have merit from both a noise and performance standpoint. A specialized version of the double bypass VCE emerged from these studies. Figure 13 illustrates the features of this VCE and also includes an acoustic nozzle concept that provided Stage II noise goal levels. The basic engine is quite similar to the military version shown previously in Figure 12. Closer inspection shows that the third fan stage is really attached to the high pressure spool rather than being on the low pressure spool as was the case in Figure 12. This unique core engine architecture is called a core fan since the extended tip section of stage one of the core functions as an additional fan stage relative to providing higher bypass duct pressure levels when the engine operates in its single bypass mode.

With the help of the front and rear VABI's, this core fan version operates in a similar manner to the initial double bypass concept discussed previously. A distinct configurational advantage results from the core fan architecture in that a favorable work split occurs between the high pressure, HPT, and low pressure, LPT, turbines. Since more of the compression work load is given to the HPT a reduced inlet temperature results for the LPT. This saves a large amount of cooling air and simplifies the LPT design. Also, the LPT loading is minimized since part of the overall fan work is now supplied by the HPT.

1.2 VCE Concept Demonstrators Based on YJ101

Hardware

The rapid definition of attractive VCE concepts in this 1974-1975 time period attracted the interest of both General Electric management and the advanced technology centers in government. This mutual interest coupled with an unsolicited VCE planning brief started the most successful, cost effective concept demonstration program in jet engine history.

Fortunately for this program several YJ101 engines, initially produced for the YF17 light weight fighter, were available for use in a series of proof-of-concept VCE demonstrators that were sponsored by the Air Force, Navy, and NASA during the 1975-1981 time period.

1.2.1 Air Force Sponsored 1x2 Split Fan VCE

The first double bypass VCE demonstrator was sponsored by the Air Force and is shown in Figure 14. As can be seen, it has the basic architecture of the original double bypass VCE shown in Figure 9. The three stage YJ101 fan was divided in a 1*2 fan stage arrangement and an outer bypass duct and rear diverter valve were added. A three stream, three variable A8 nozzle system completed this initial VCE that was tested in the 1975-1976 time period. Figure 15 illustrates the four unique engine concepts that were tested with this one basic configuration, these being:

- A) Baseline mixed flow turbofan
- B) Separated flow mode-single bypass VCE with two variable A8's
- C) Mixed flow mode - double bypass VCE with two variable A8's
- D) Separated flow mode - double bypass VCE with three variable A8's

Each version ran as predicted with each increased level of engine complexity offering both better uninstalled part power SFC plus improved airflow holding that would provide additional performance improvement potentials from reduced inlet spillage drag.

1.2.2 Navy Sponsored 2*1 Split Fan + Rear VABI

A second build of this double bypass VCE was sponsored by the Navy and is shown in Figure 16. A 2*1 fan stage split was selected for this build and the first rear VABI system was added. Also, a fully variable low pressure turbine nozzle system was designed, built, and tested on this two stream nozzle concept demonstrator. The following tests were conducted in the 1976-1977 time period.

- 1) First 2*1 fan split test
- 2) First drop chute rear VABI test
- 3) First augmented VCE testing
- 4) First variable LPT test
- 5) Fixed Cycle, Single Bypass, Double Bypass mode testing

1.2.3 NASA Sponsored Front VABI & Acoustic Nozzle Test

NASA took the basic Navy VCE vehicle and added the worlds first front VABI system. The resultant concept demo now required only one variable area exhaust nozzle. Figure 17 contains both single and double bypass mode geometry settings for this engine. The engine ran extremely well and everything performed as predicted.

As was mentioned previously, the double bypass VCE concept was being evaluated in the ongoing NASA sponsored SST studies. A very simple Stage II noise capable acoustic nozzle concept had been evolved for this type engine and a YJ101 sized version was built and added to the NASA sponsored front VABI VCE concept demo. Figure 18 shows the complete engine test configuration that produced very successful acoustic test results.

1.2.4 NASA Sponsored Core Fan Concept Demo

One last YJ101 VCE Concept demo configuration was defined, built, and tested in the 1979-1981 time period and is shown in Figure 19. Stage 3 of the YJ101 fan was removed and a core fan stage was added to the seven stage YJ101 compressor. This unique compression system architecture was successfully demonstrated and closed out the highly successful YJ101 based VCE concept demonstration testing. (Several additional VCE tests were conducted in the 1982-1984 time period as part of the Air Force and Navy sponsored GE23 ATEGG/JTDE program that was based on an upgraded F110 class core and a new advanced technology counter rotation low pressure spool.)

1.3 ATFE Configuration Definition

Lessons learned from these demonstrations were built into the VCE cycle and configuration studies that were evolving during the pre-ATF aircraft and mission studies conducted in the 1978-1982 time period. Figure 20 contains a typical cross section of one of these double bypass VCE study engines that was latter evolved into the F120 type VCE.

The final architecture selected for the XF, YF, and F120 engines is illustrated in the configuration schematic shown in Figure 21. Both the XF120 and YF120 and the proposed F120 had two stage front fan systems and five stage core compressors. Both compression components were driven by single stage turbines. Stage one of the core compressor had an extended tip (core fan stage) that served as a third stage for the fan system. Counterrotating spools plus the optimum turbine energy split made possible by the core fan architecture greatly simplified the design of the low pressure turbine system. As shown in Figure 21, the ATFE concepts retained the single and double bypass modes that were initially tested on the YJ101 VCE concept demonstrators. The successful test stand results from the XF120 lead the way to an even more successful series of proof-of-concept flight testing of the YF120 in both the YF22 and YF23 ATF prototype aircraft. The worlds first flight VCE's performed as predicted and powered both aircraft to their maximum attained supercruise flight speeds.

1.4 Continuing VCE Developments

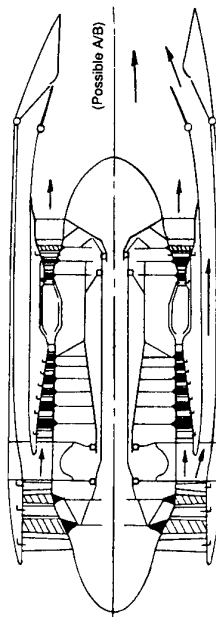
Fundamental VCE development work continues to be an integral part of General Electric's ATEGG and JTDE programs. More advanced versions of the basic YF120 VCE were defined and tested during the XTC/E45 ATEGG and JTDE program that ran during the 1984-1991 time period. A new type of VCE was defined in the 1991-1992 time period and is now being jointly pursued with Allison Advanced Development Company under the joint XTC/E76 ATEGG and JTDE programs. The performance and architectural simplicity of this new engine will allow the full Phase II IHPTET goals to be achieved by 1998.

FIGURE 1

Variable Pumping Compressor (VAPCOM) Engine Schematic

- All Variable Stator Fan & Compressor System
- Variable HP & LP Turbine Vane Systems
- Twin Variable A8 Nozzle System with Common A9

Top View - Min Bypass/Max T41/Max Power Mode: (BPR ~ 0, $PR_{OA} = \text{Max}$)



Bottom View - Max Bypass/Part Power Mode: (BPR ~ 1.0, $PR_{OA} \sim .75 \text{ Max}$)

1960 - 1965 Time Period

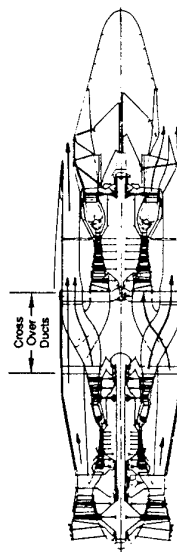
1-AUG-62

FIGURE 3

Turbo Augmented Cycle Engine (TACE) Configuration

- Combined Turbofan & Turbojet Architecture
- Twin Variable A8 Plug Nozzle System

Top View - Turbofan Mode Only, Aft TJ Off for Low Power



Bottom View - Combined Mode, Aft TJ On for Max Power

1973 - 1974 Time Period

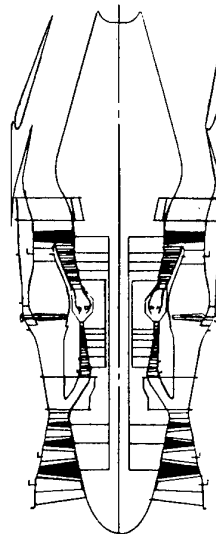
8-AUG-64

FIGURE 2

Composite Cycle Engine Schematic

- ② Spool Design for Mach 3+/Mixed Mission Applications
- Unique LP Spool Turbine System Architecture
 - Key Component = Aft "Confluent Flow" Turbine

Top View - Turbofan Mode for Part Power - Outer Burner Off



Bottom View - Concentric Turbojet Max Power Mode - Outer Burner On

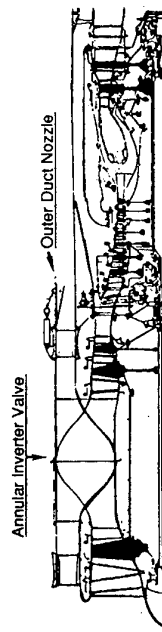
1965 - 1970 Time Period

1-AUG-63

FIGURE 4

Annular Inverter Valve VCE - Series/Parallel Modes

- Modified J101 Hardware Shown
- Full Span AIV
- Desupercharged Core in Parallel Mode



- Base BPR = 0.2 in Series Mode, $W/\sqrt{\theta}/\delta = 127$
- BPR = 2 Class in Parallel Mode, $W/\sqrt{\theta}/\delta_{\text{Total}} = 203$

- Flowpath Study Only - No Hardware Built

1973 - 1974 Time Period

1-AUG-67

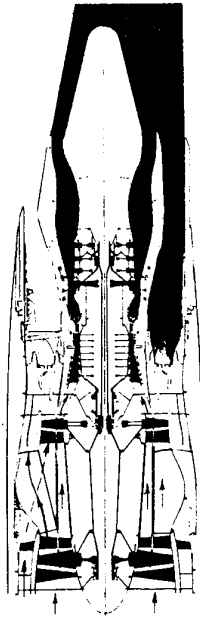
GE Aircraft Engines

FIGURE 5

Series/Parallel Variable Cycle Concept - Separated Flow Version

- Separated Flow ② Spool Duct Burning Turbopan
- Constant Core Supercharge Design

Top View - Parallel Mode: Max Bypass Ratio for Part Power



Bottom View - Series Mode: Max Fan PR/Min Bypass Mode for Max Power

1973 - 1975 Time Period

13-8

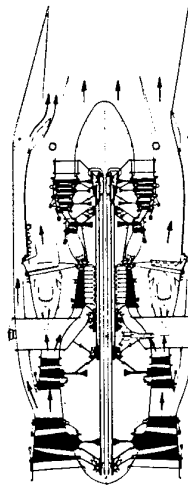
GE Aircraft Engines

FIGURE 7

Modulating Bypass Ratio (MOBY) Engine Configuration

- Separated Flow ③ Spool Duct Burning Turbopan
- ③ Variable Turbine Vane Systems
- ② Bypass Ducts, ③ Variable A8's

Top View - Part Power Double Bypass Mode, Duct Burner Off



Bottom View - Max Power Mode, Duct Burner On

1973 - 1974 Time Period

13-8

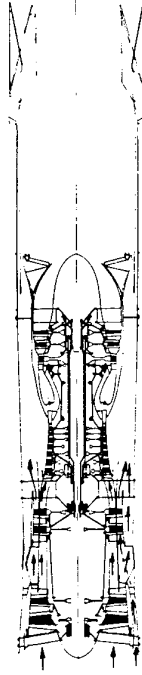
GE Aircraft Engines

FIGURE 6

Series/Parallel Variable Cycle Concept - Mixed Flow Version

- Mixed Flow ② Spool Afterburning Turbopan
- Constant Core Supercharge Design

Top View - Series Mode: Max Fan PR/Min Bypass Ratio for Max Power



Bottom View - Parallel Mode: Max Bypass Ratio for Part Power

1973 - 1975 Time Period

13-8

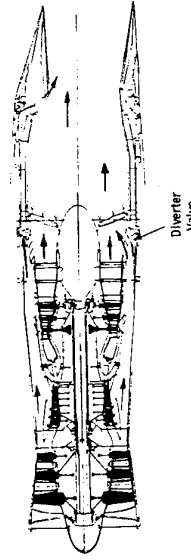
GE Aircraft Engines

FIGURE 8

Initial Dual Cycle Single Bypass VCE Configuration Example

- ② Spool Mixed Flow Turbopan for Max A/B Thrust
- Separated Flow Mode Option for Dry Power
- Twin Variable A8 Nozzle System with Common A9

Top View - Separated Flow Mode for Special Dry Operation



Bottom View - Mixed Flow Mode

1974 - 1976 Time Period

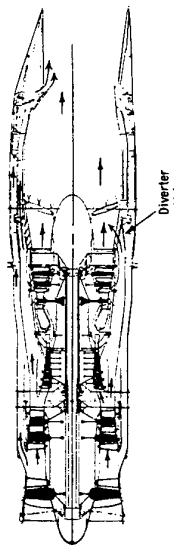
13-8

FIGURE 9

Initial Double Bypass VCE Configuration - ③ Stream Exhaust

- 1+2 Fan Stage Split
- ② Spool Mixed Flow Turbofan
 - Separated Flow Double Bypass Mode for Part Power
- ③ Variable A8 Nozzles with Common A9

Top View - Double Bypass Separated Flow Mode for Part Power



Bottom View - Single Bypass Mixed Flow Mode for Max Power

1974 - 1976 Time Period

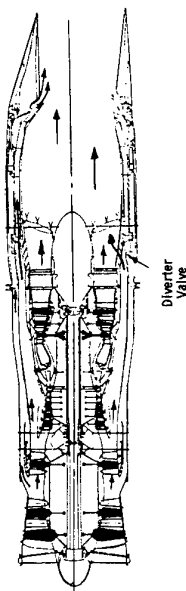
8. J. AUGUST 18

FIGURE 10

Initial 2+1 Fan Stage Split Configuration - ③ Stream Exhaust

- ② Spool Mixed Flow Turbofan
 - Separated Flow Double Bypass Mode for Part Power
- ③ Variable A8 Nozzles with Common A9

Top View - Double Bypass Separated Flow Mode for Part Power



Bottom View - Single Bypass Mixed Flow Mode for Max Power

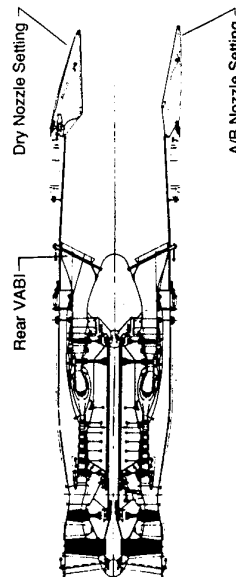
1974 - 1976 Time Period

8. J. AUGUST 18

FIGURE 11

Improved Dual Cycle Single Bypass VCE Configuration

- Mixed Flow Mode Only
- ① Variable A8 Nozzle System
 - Rear VABI Replace Diverter & 2nd A8 System
- Variable Area LP Turbine Vane Payoffs Investigated



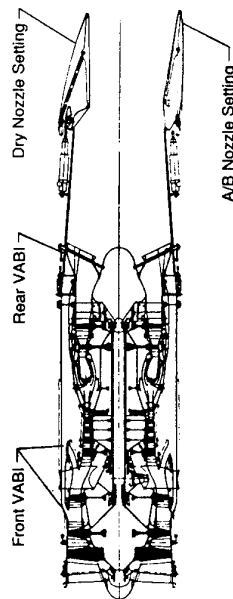
1976 - 1978 Time Period

8. J. AUGUST 17

FIGURE 12

Improved Double Bypass VCE Configuration

- Mixed Flow Mode Only
- ① Exhaust Nozzle
 - Front & Rear VABI's Replace Diverter & ② Var. A8 Systems
- Variable Area LP Turbine Vane Payoffs Investigated



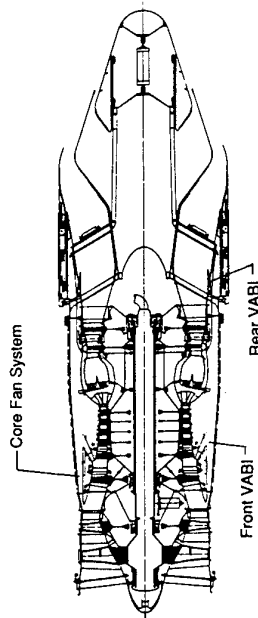
1976 - 1978 Time Period

8. J. AUGUST 18

FIGURE 13

Double Bypass VCE with Core Fan Architecture

- From NASA Sponsored SST Studies
- Stage ① of Core has an Extended Tip
- Acts as Stage ③ of the Fan
- Co-Annular Acoustic Nozzle Shown



1975 - 1981 Time Period

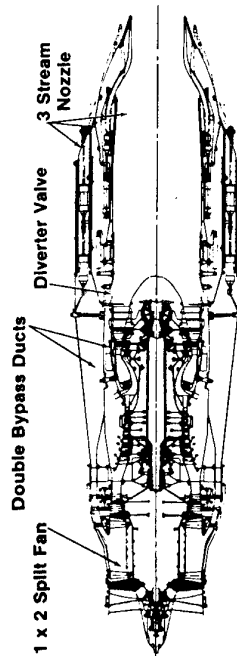
13 AUGUST 18

FIGURE 14

Air Force Sponsored 1 + 2 Fan Split Double Bypass VCE

(Modified YJ101 Hardware)

- 1+2 Fan Split
- Diverter Valve VABI
- 3 Stream Nozzle
- Augmentor Removed
- Fixed Cycle, Dual Cycle, Double Bypass Modes Tested



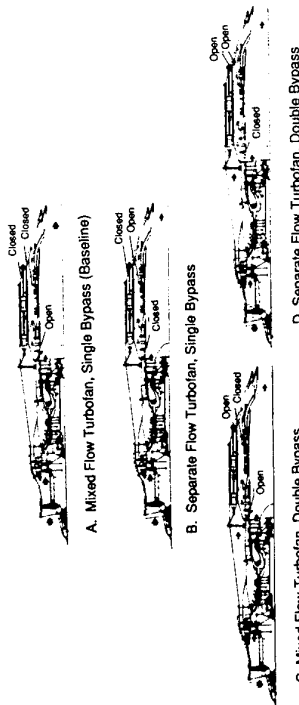
1975 - 1976 Time Period

13 AUGUST 18

FIGURE 15

Test Mode Flexibility of 1+2 Fan Split VCE Concept Demo

- Initial Air Force Sponsored VCE Derived from YJ101 Hardware



1975 - 1976 Time Period

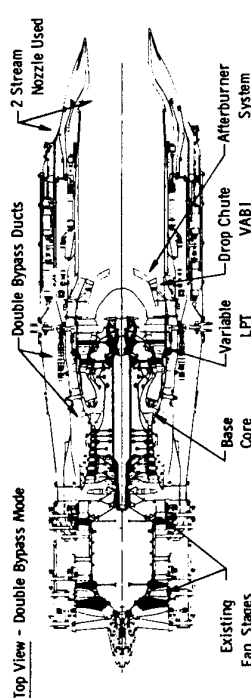
13 AUGUST 18

FIGURE 16

2+1 Fan Split Double Bypass VCE

(Modified YJ101 Hardware)

- First 2+1 Fan Split Test
- First Drop Chute VABI Test
- First Augmented VCE Testing
- First Variable LPT Test in VCE Configuration
- Fixed Cycle, Single Bypass, Double Bypass Modes Tested



Bottom View - Single Bypass Mode

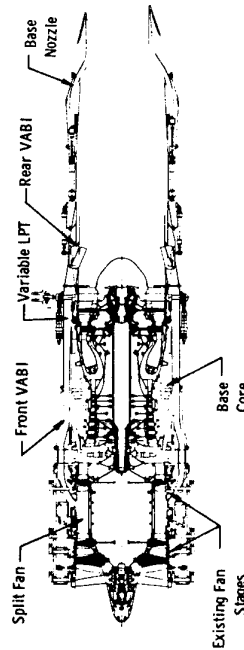
1976 - 1977 Time Period

FIGURE 17

NASA Front VABI Test Demo - Single Stream Exhaust

- Derived from Navy 2-1 J101 Based VCE Concept Demo

Top View - Double Bypass Mode for Part Power



Bottom View - Single Bypass Mode for Max Power

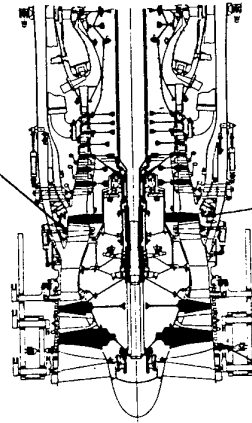
1977 - 1978 Time Period

13-11-19

FIGURE 19

NASA Core Driven Fan Stage VCE (Modified YJ101 Hardware + New Core Fan)

Top View - Double Bypass Mode



YJ101 Fan Stages

New Stg 3 Fan Attached to HP Compressor Shaft

Bottom View - Single Bypass Mode

1979 - 1981 Time Period

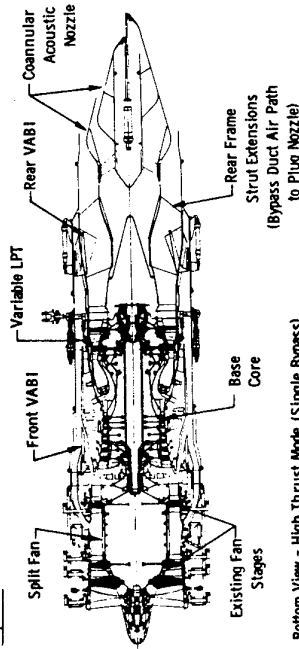
13-11-20

FIGURE 18

NASA Acoustic Test VCE (Navy 2-1 Fan with Acoustic Nozzle)

INITIAL DOUBLE BYPASS VCE NOISE TEST CONFIGURATION

Top View - Low Noise Test Mode (Double Bypass)



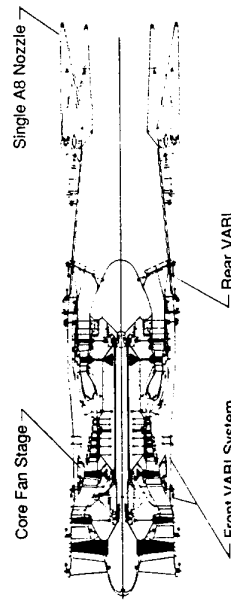
Bottom View - High Thrust Mode (Single Bypass)

1977 - 1978 Time Period

FIGURE 20

Double Bypass VCE with Core Fan Architecture

- Evolved from NASA AST/SST Studies/Demonstrators
- Very High Fan PR Potential
- Better Balanced Turbine Work Split



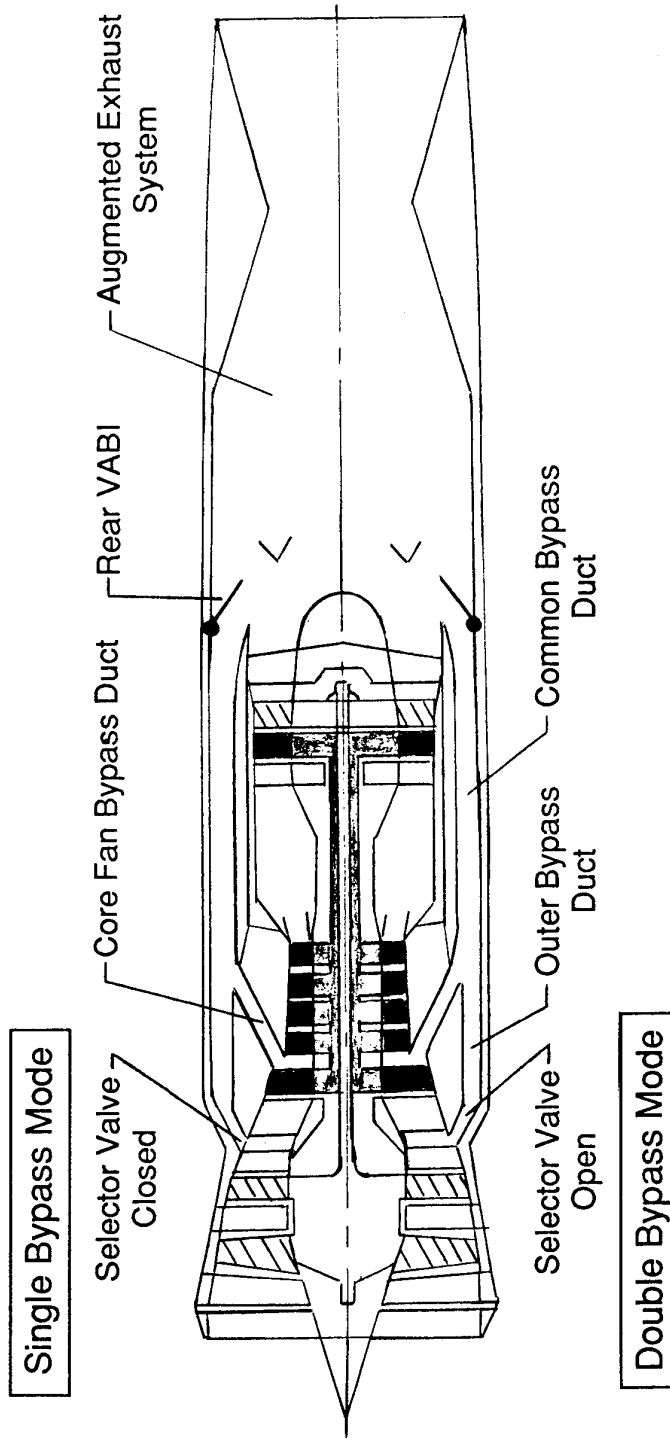
1978 - 1982 Time Period



FIGURE 21

XF, YF, & F120 Variable Cycle Configuration Schematic

- ② Spool Counterrotation Design
 - 2 Stage Fan
 - 5 Stage Core with Core Fan
 - 1*1 Turbine System



1983 - 1990 Time Period

STUDIES ON NO_x-EMISSIONS OF SST ENGINE CONCEPTS

F. Deidewig; A. Döpelheuer
 Institut für Antriebstechnik
 Deutsche Forschungsanstalt für Luft- und Raumfahrt
 Postfach 90 60 58
 51147 Köln/Cologne, Germany

SUMMARY

To predict the engine performance at subsonic and supersonic design and off-design flight conditions a thermodynamical calculation procedure has been developed, which describes the engine performance with the help of generalized turbine and nozzle characteristics. To demonstrate the advantages of new engine concepts - including variable cycle and/or intercooler - on an aircraft with the payload of about 10000kg a realistic flight trajectory has been chosen, which involves every phase along the whole flight path: take off, climb, supersonic acceleration, cruise and descent. The results for chosen flight routes including fuel flow rates and NO_x-emissions are compared to a zero bypass engine, the Olympus593 Mk610, producing comparable thrust.

LIST OF MAIN SYMBOLS

b	= booster
c_{pA}, c_{pG}	= specific heat air and gas
c_d, c_l	= drag and lift coefficient
$by, core$	= bypass and core
D	= design-values
EI	= emission index
hpc, hpt	= high pressure compressor, turbine
$IC - TF$	= Intercooled Turbofan
\dot{m}_{red}	= corrected mass flow ($\dot{m}\sqrt{T_t}/p_t$)
Ma	= Mach number
MTF, TF	= Mid Tandem Fan, Tandem Fan
lpc, lpt	= low pressure compressor, turbine
LPP	= lean premixed prevaporised combustor
RQL	= rich quick quench lean combustor
$SBVCE$	= Selective Bleed Variable Cycle Engine
SFC	= specific fuel consumption
η_p, η_{in}	= polytropic and intake efficiency
κ	= ratio of specific heat values
μ	= bypass ratio
Π	= pressure ratio

1. INTRODUCTION

Looking at the second generation engines for supersonic-transport it should be possible to achieve an improved performance against Concorde powered by Olympus-engines. Especially the specific fuel consumption and the noise levels during start and the subsonic phase of the flight have to be decreased significantly. This would be possible by introducing a bypass ratio, whereas at supersonic cruise conditions there is a benefit using an engine mode with a near zero bypass ratio. The variable cycle engine is a possible concept to take advantage of the benefits of these two modes. The Mid Tandem Fan could be a design concept to tackle a variable bypass concept with minimum outer diameter.

In detail it has to be investigated whether the engine compressor - and fan characteristic - match the operating line due to a great mass flow variation during the whole flight trajectory.

To investigate the advantages and disadvantages of the new engine concepts a realistic flight trajectory has been chosen, which involves every phase during the whole flight path: take off, subsonic and supersonic acceleration, cruise and descent. The Concorde is being taken as a reference supersonic aircraft with take off weight of 180t and a payload of 10t. A flight mechanics procedure must be available to estimate the thrust settings of the engines with respect to the actual flight conditions. Critical flight phases, e.g. take off and drag rise during transonic acceleration, can be analyzed. Benefits of these engine concepts, depending on the flight route and therefore the duration of subsonic and supersonic flight can be underlined.

In addition a semiempirical correlation for the NO_x-production during the whole flight is applied, which describes the emission index (in g NO_x per kg fuel burnt) as a function of the combustor inlet conditions. This correlation is based on characteristic time values during the combustion process.

2. SST ENGINE CONCEPTS

In Figure 1 the so called Mid Tandem Fan is shown. For decreasing the drag according to the inlet area the fan is integrated within the tail of the engine behind the booster. For the core part of the engine the fan will be characterized to produce a pressure loss (2%). After the exit of the lpt the hot and cold engine streams are mixed to expand in one convergent-divergent nozzle. This concept is a symbiosis of the Snecma MCV99 engine concept and of Rolls Royce Tandem Fan RB 576-05. The laval-nozzle is fully adjustable which means area 8 and 9 can be adapted to the actual nozzle pressure ratio (ideal expansion). In case of higher supersonic cruise Mach numbers area 8 decreases in a way that area 9 remains constant, without exceeding the maximum engine diameter.

The Tandem Fan, Figure 2, works in a 'bypass' mode during subsonic flight. The blow indoors are open to deliver booster inlet air. Through the blow outdoors the fan exit air expands in a separate nozzle. At high Mach numbers both doors are closed, the engine works in 'series' mode similar to a mere turbojet, the bypass nozzle is no longer active. A main advantage of this concept is lowering the total combustor inlet pressure during take off and climb to prevent autoignition in case of using LPP-combustors ($p_3 \leq 20\text{bar}$, strongly depending on T_3). Furthermore better thermal efficiencies are reached by compressing 'cold' intake air by the booster [1].

The third concept discussed here is the so called Selective Bleed Variable Cycle Engine or Double Bypass Engine which combines the advantage of higher bypass ratios within the subsonic flight regimes by lowering the bypass ratio down to near zero for supersonic cruise, Figure 3 (Nascimento et al.[11]). Therefore two valves controlling the bypass ratio are designed after the fan respectively booster. Problems may occur in case of varying the bypass ratio which causes a change of the compressor steady state operating lines. The compressors must tackle these wide variety with the help of adjustable stator vanes.

Lowering the burner inlet temperature causes a significant reduction of thermal NO_x production. Trying to achieve this goal without changing the power output the following intercooled concept was generated, Figure 4 (IC-TF). The bypass duct cools down the core engine airflow and generates additional thrust by increasing the total temperature of the bypass flow. A low pressure ratio for the outer fan ($\Pi \approx 1.1$) enables the outer bypass duct to produce thrust even at sea level static conditions and Mach numbers equal to zero.

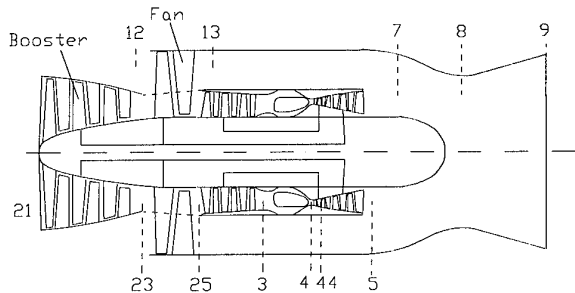


Figure 1: Mid Tandem Fan (MTF), concept 'A'

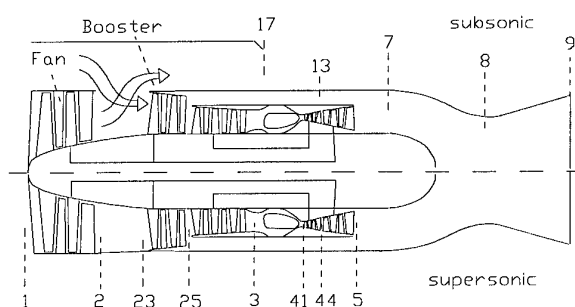


Figure 2: Tandem Fan (TF), concept 'B'

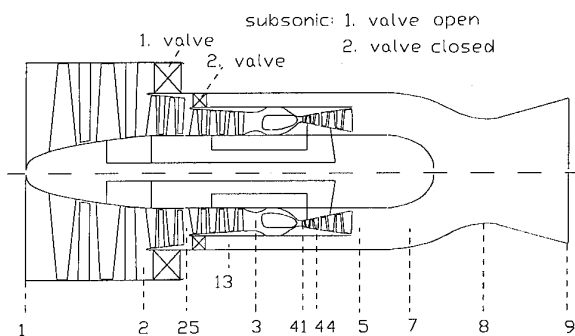


Figure 3: Selective Bleed Variable Cycle Engine or Double Bypass Engine (SBVCE, DBE), 'C'

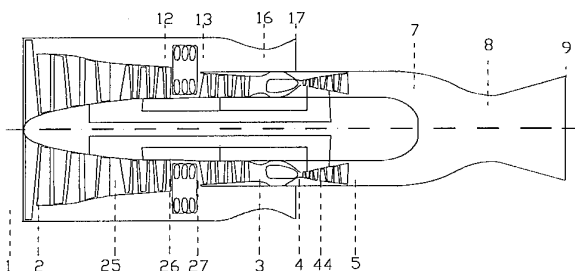


Figure 4: Intercooled Turbofan (IC-TF), concept 'D'

3. THERMODYNAMICAL CALCULATION PROCEDURE

To describe the behaviour of the discussed engine concepts a simple design and off-design procedure is developed. The basic principles of these methods are listed in Wittenberg [16] and Saravanamouttoo [13]. In a first step to get an overlook about fundamental engine behaviour it is useful to design an engine which is based only on a few main parameters:

1. flight Mach number and altitude
2. compressor ratios
3. turbine inlet temperature
4. bypass ratio
5. absolute amount of airflow through the engine

The calculation of the design point is based on the power balance of the low-pressure and high-pressure spool, the continuity equation, the pressure balance through the engine and the connection of the turbines with the hot core nozzle. The rotational speed does not attack the flow function for the hpt and lpt in the off-design mode. One generalized massflow-pressure ratio function for each turbine is taken into account depending only on the critical pressure ratio and therefore only depending on the number of stages. Realistic pressure losses and efficiencies for intake, compressors, turbines, hp- and lp-shaft, combustor and nozzles are assumed. The amount of cooling air is due to the maximum allowed material temperature of the hpt stator. Formulating the mixing condition after lpt and fan is to reach static pressure identity. Polytropic efficiencies for compression and expansion allows to simplify the off-design calculation relationships. Keeping the polytropic efficiencies constant for the whole flight trajectory in a first run should be improved in a practical manner for detailed analysis. For this case some empirical suggestions are made. Regarding these preliminary design studies no compressor maps are involved in the procedure, only the compressors of the SBVCE has been looked at in more detail because of a wide variety of the operating lines. The transonic fan of the MTF concept is also a critical point due to the small operating range having good efficiencies and adjustable fan stator vanes.

The intake pressure loss or intake recovery $\Pi_{in} = p_{t1}/p_{t0}$ depending on the flight Mach number is due to the following equations:

low subsonic $Ma_0 \leq 0.4$ ($\eta_{in}=0.92$), v.d.Velden [15]:

$$\Pi_{in} = 0.98 - 2.5 \cdot (0.4 - Ma_0) \cdot (1 - \eta_{in}) \quad (1a)$$

subsonic $0.4 < Ma_0 \leq 1$:

$$\Pi_{in} = \text{const.} = 0.98 \quad (1b)$$

supersonic $Ma_0 > 1$ ($\eta_{in} = 0.976$):

$$\Pi_{in} = \left(1 + (1 - \eta_{in}) \cdot \frac{(\kappa - 1)}{2} \cdot Ma_0^2 \right)^{\frac{\kappa}{1-\kappa}} \quad (1c)$$

Looking at the off-design performance calculation it is essential that the gas generator (hp-spool) is independent from the lp-spool for those points, where the lpt does not change its corrected mass flow. In this case the operating point of the hpt is fixed: no change in pressure ratio, mass flow and efficiency will occur. This assumption is commonly used in analytical engine calculation programs but only true for high power settings of the engine (see [1]). If no mixing after lpt with the bypass has been considered and the hot core nozzle is choked this assumption is also correct, because constant corrected mass flow in the core nozzle causes a fixed operating point in the lpt and therefore a fixed operating point in the hp-turbine. During take off, climb and cruise modes turbojet engines always run with choked core nozzles so that this simplifying assumption can be made.

For the off-design the hp-compressor ratio can easily be evaluated by assuming a new hpt inlet temperature $T_{t\epsilon}$:

$$\Pi_{hpc} = \left[1 + \frac{T_{t\epsilon}/T_{t25}}{(T_{t\epsilon}/T_{t25})_D} \cdot \left(\Pi_{hpcD}^{\frac{m}{\eta_{pD}}} - 1 \right) \right]^{\frac{\eta_p}{m}} \quad (2)$$

with $m = (\kappa - 1)/\kappa$.

In this equation the hpc inlet temperature at off-design conditions T_{t25} is unknown for the first iteration step. The calculation is described later. Using eqn.(2) the corrected mass for the hpc is found to be:

$$\dot{m}_{red,hpc} = (\dot{m}_{red,hpc})_D \cdot \sqrt{\frac{(T_{t\epsilon}/T_{t25})_D}{T_{t\epsilon}/T_{t25}}} \cdot \frac{\Pi_{hpc}}{\Pi_{hpcD}} \quad (3)$$

Having a simple turbofan consisting only of lpc and hpc the low pressure ratio of the compressor can be expressed in a similar way like (2) with the help of the power balance of the lp-spool:

$$\Pi_{lpc}^{\frac{m}{\eta}} = 1 + q \cdot \left(\Pi_{lpcD}^{\frac{m}{\eta}} - 1 \right) \cdot \frac{1 + \mu_D}{1 + \mu} \cdot \frac{1 - \Pi_{lpt}^{\frac{m}{\eta}}}{1 - \Pi_{lptD}^{\frac{m}{\eta}}} \quad (4)$$

where q in this case is depending on the engine inlet and low pressure turbine inlet temperature respectively: $q = \frac{T_{t44}/T_{t1}}{(T_{t44}/T_{t1})_D}$.

Some simplifications in (4) can be made if the engine is a mere turbojet. Then of course the bypass ratio at design and off-design is equal to zero and the pressure ratio of the lpt does not change for the off-design mode.

The mixing of hot core mass flow at the lpt-exit with the cold bypass massflow is based on static pressure identity in the mixing chamber. Reaching this constraint over the whole flight envelope even at the design point the values of T_{t5} , μ , Π_{Fan} , Π_b , Π_{hpc} had to be chosen in a way, that the two total pressure values at the intake of the mixing chamber are close to each other (e.g. $(p_{t5})_D = 1.86 \text{ bar}$, $(p_{t13})_D = 2.05 \text{ bar}$ in the case of MTF-concept). Having a constant mixing area leads to:

$$A_5 + A_{13} = A_7 = A_{mix} = \text{const.} \quad (5)$$

The total temperature after mixing can easily be calculated by using the energy equation. The pressure loss according to the different velocities entering the mixing chamber are found by using the momentum equation. In spite of keeping the inlet areas constant each Mach number at the inlet mixing chamber can be evaluated by achieving a static pressure balance. A very useful procedure to find the unknown outlet Mach number and outlet total pressure at the mixing chamber is to rewrite the momentum equation in the so called 'FM-method': $\dot{m} \cdot v + p \cdot A = \dot{m} \cdot \sqrt{R \cdot T_t} \cdot FM$, where FM is only a function of Mach number and ratio of the specific heats [4]. Using the method for engine section 7 will give:

$$FM_7 = \frac{1}{\dot{m}_7 \sqrt{R \cdot T_{t7}}} \cdot (\dot{m}_{By} \cdot v_{13} + p_{13} \cdot A_{13} + \dot{m}_{core} \cdot v_5 + p_5 \cdot A_5) \quad (6)$$

With the help of the known FM-value the outlet Mach number can directly be calculated without any iteration procedure solving the biquadratic equation:

$$Ma_7^2 + \frac{2 - FM_7^2}{\kappa - \frac{\kappa-1}{2} \cdot FM_7^2} \cdot Ma_7^2 +$$

$$\frac{1}{\kappa \cdot \left(\kappa - \frac{\kappa-1}{2} \cdot FM_7^2 \right)} = 0 \quad (7)$$

Then the nozzle total pressure can be calculated by means of the continuity equation or the gasdynamic relationship combining static and total pressure. Finally the transformation of the corrected mass flow from the exit lpt to core nozzle once for design and once for off-design involving pressure loss of the mixing chamber and the bypass ratio is due to (8). In this case Π_{lpt} is a value greater one and the corrected mass flow of the lpt is kept constant ($\dot{m}_{red,lpt} = \text{const}$; $\Pi_{lpt} = p_{t5}/p_{t5} > 1$):

$$\frac{\dot{m}_{red,core}}{(\dot{m}_{red,core})_D} = \frac{\Pi_{lpt}^{1 - \frac{\eta_p \cdot m}{2}}}{\Pi_{lptD}^{1 - \frac{\eta_p \cdot m}{2}}} \cdot \sqrt{\frac{T_{t7}/T_{t5}}{(T_{t7}/T_{t5})_D}} \cdot \frac{1 + \mu}{1 + \mu_D} \cdot \frac{(p_{t5}/p_{t7})}{(p_{t5}/p_{t7})_D} \cdot \frac{A_{8D}}{A_8} \quad (8)$$

The necessary amount of cooling flow is connected to the cooling efficiency $\epsilon_{cool} = \frac{T_{gas} - T_{metal}}{T_{gas} - T_{cool}} = 50 \dots 60\%$. Corresponding to [10] a linear assumption of the cooling air \dot{m}_{cool} due to the material temperature of 1200K, the cooling temperature of hpc exit and turbine inlet temperature is made. The absolute amount can be derived from (9). In the program half of the cooling air is injected between stator and rotor to lower the rotor inlet temperature of the hpt and half of the cooling air is mixed behind the hpt.

$$\frac{\dot{m}_{cool}}{\dot{m}_{25}} = 0.106 \cdot \frac{T_{t5} - T_{metal}}{T_{metal} - T_{t3}} \quad (9)$$

The engine concepts A,B,C consist of fan and booster compressors both driven by the lpt with the same rotational speed. Taking into account that the working balance between both - fan and booster - does not change from design to off-design operating conditions, e.g. $(\Delta H_{Fan}/\Delta H_b)_D = \Delta H_{Fan}/\Delta H_b$ a useful connection between both pressure ratios can be given:

$$\Pi_b = \left[1 + (\Pi_{Fan}^m - 1) \cdot \frac{(\Pi_{bD}^m - 1)}{(\Pi_{FanD}^m - 1)} \cdot \left(\frac{\Pi_{FanD}}{\Pi_{Fan}} \right)^m \right]^{\frac{1}{m}} \quad (10)$$

The intercooler in concept 'D' causes a pressure loss in the bypass and core ducts. The efficiency of the intercooler allows to calculate the lower inlet temperature of the second part of the hpc (11).

$$\eta_{IC} = \frac{T_{25} - T_{26}}{T_{25} - T_{12}} \quad (11)$$

The position of the intercooler is at $\sqrt{\Pi_{hpc}}$ (regarding a single intercooled process, the maximum specific work output of the gas is due to the location of the intercooler at $\sqrt{\Pi}$). All engines have convergent-divergent nozzles. As mentioned in the description of the future SST engines the laval nozzles are treated as fully adjustable. According to the nozzle pressure ratio the outlet area at engine stage 9 is varied to improve optimal thrust. To avoid outlet areas greater than the maximum engine diameter the nozzle area at engine point 8 must be decrease in case of high nozzle pressure ratios.

4.COMPRESSOR PERFORMANCE MAPS

Evaluating the steady state operating lines with the help of the thermodynamic program it is essential for an engine whether the compressor can match the required operating lines or not. Furthermore the distance between surge margin to any engine operating point should be somewhat greater than 20%. Nevertheless good efficiencies even at off-design running points should be reached to prevent increasing SFC-values. Having adjustable core nozzle areas (section 8) like in this case causing a wide variety in low pressure compressors working lines the whole overall performance of the compressors must be looked at. The most critical compressors of the four engine concept are the fan and booster of the concept 'C' because of significant change of the bypass ratio during the flight phase due to the two valves.

To generate compressor performance maps a one dimensional calculation procedure was developed [2]. Based on fundamental turbomachinery relationships including an empirical relationship for total pressure losses related to the incidence and Mach number effects good agreement between practical and calculated performance could be achieved. For positive incidence a reduction of the flow turning angle in spite of deviation effects is also taken into account.

Figures 5 and 6 show the pressure ratio of the fan for the MTF-concept (A). Closing the inlet guide vanes about 30° led to an increasing operating range with less maximum pressure ratio.

Figures 7 and 8 show in which way the fan and booster had to be adjusted to match the different operating lines for the low pressure and high pressure mode (fan -30°, Booster -40°). The lp-mode is running during subsonic flight with the first valve open. Closing the first and opening the second valve characterises the hp-mode.

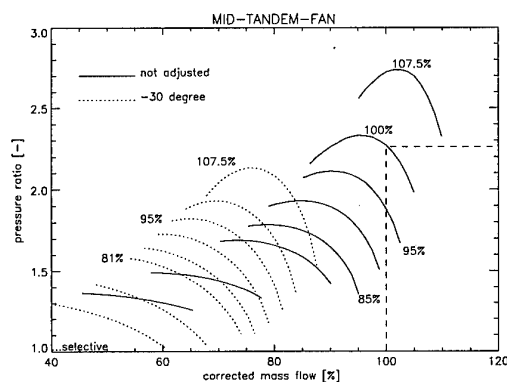


Figure 5: Fan for the MTF-concept, 'A'

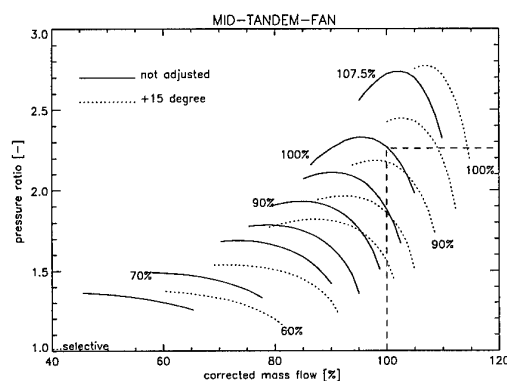


Figure 6: Fan for the MTF-concept, 'A'

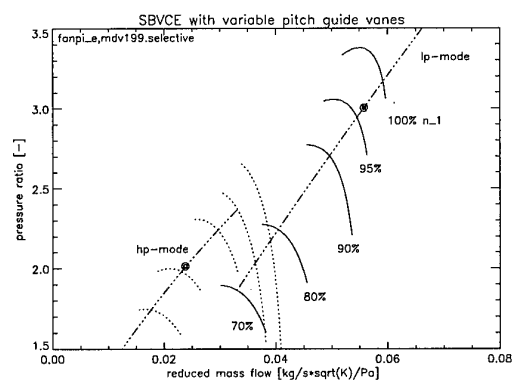


Figure 7: Fan for the SBVCE-concept, 'C'

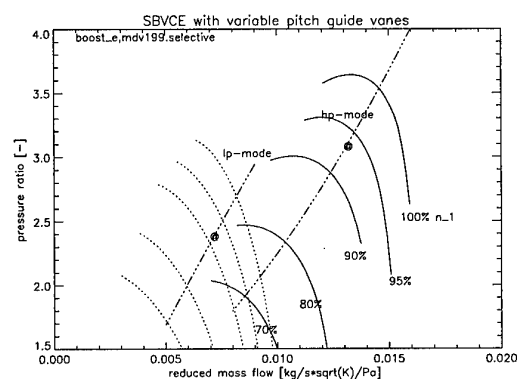


Figure 8: Booster for the SBVCE-concept, 'C'

5. CALCULATION OF NO_x

Due to environmental aspects it is essential to improve the engine characteristics for the next generation of supersonic aircrafts. In this paper no new combustor technology is being looked at to reach the SST goal of 5g NO_x per 1kg burned fuel. For all discussed new engine concepts in this paper a conventional combustor is assumed. Unfortunately increasing maximum turbine entry temperature having a better thermal efficiency causes an increased level of produced thermal NO_x ($= NO + NO_2$).

Concerning the certification of a turbofan or turbojet engine the manufactures are obliged to measure the emissions of the engines under sea level static conditions. This measurements for different power settings of the engines built up the ICAO database (ICAO Exhaust Emission Data Bank [6]). Till now, measured values under flight conditions are not published except inflight measurement due to actual research investigations (Schulte et al.[14]). Taken this into account, values for nitric oxides during realistic flight phase have to be assessed using calculated engine parameters and semiempirical NO_x correlations.

Looking at several existing NO_x correlation methods they can be classified in three main categories: The first category are procedures which use the measured EI-values at sea level (from ICAO) as a reference and try to find the actual flight emission index with the help of formulas based on kinetic relationships or on 'best fit' curves related to typical combustor inlet values. The second category can be named 'absolute'. In this $EINO_x$ -correlations the amount of NO_x can be derived without having typical reference values at sea level using only combustor inlet parameters. The third category can be summarized as the so called 'fuel flow methods'. In this case only available engine monitored fuel flow and ambient flight conditions resp. measured EI-values at sea level are necessary (anyway, informations from the ICAO-datasheet are involved in this method).

For certified engines reference values from ICAO at sea level (EI_{SL}) the following equation is used:

$$EI_F = EI_{SL} \cdot \frac{e^{\left(\frac{67500}{T_{\lambda=1}}\right)_{SL}}}{e^{\left(\frac{67500}{T_{\lambda=1}}\right)_F}} \cdot \frac{(p_3)_F}{(p_3)_{SL}} \cdot \frac{(\dot{m}_L)_{SL}}{(\dot{m}_L)_F} \cdot \frac{(T_3)_{SL}}{(T_3)_F} \quad (13)$$

These example of a 'relative' correlation needs engine data at sea level (SL) and the measured EI-values. In principle there are two different ways to handle equations like (13). First of all, the $EINO_{x,SL}$ -value can be treated as a fixed reference (for instance at 100% thrust). Then of course all combustor inlet

parameters at sea level must be referred to this single point. The second possibility is the use of the reference EI-value at sea level as a gliding reference point. Then all sea level values ($(T_{\lambda=1})_{SL}$, $(\dot{m}_L)_{SL}$, $(p_3)_{SL}$) are functions of the combustor inlet temperatures at sea level conditions.

If no reference values are available for the discussed concepts the following 'absolute' correlation is used to calculate the $EINO_x$ -value (Odgers et al. [12]):

$$EI_F = 27.03 \cdot \exp\left(-\frac{21670}{T_{\lambda=1}}\right) \cdot p_{BK_E}^{0.66} \cdot \left(1 - \exp\left[-0.7325 \cdot \left(\frac{V_{PZ} \cdot p_{BK_E}^{0.6}}{\dot{m}_L \cdot T_m^{0.5}}\right)^{0.4047}\right]\right) \cdot \Phi_{PZ}^{0.269} \quad (12)$$

With the stoichiometric flame temperature $T_{\lambda=1}$, the equivalence ratio in the primary zone Φ_{PZ} , $T_m = 0.5 \cdot (T_3 + T_{\lambda=1})$, and the combustor inlet pressure p_3 in Pa.

Problems can occur if the volume of the primary zone is unknown (V_{PZ}). For high thrust civil engines (e.g. CF6-80C2) the value of V_{PZ} is in the range of $V_{PZ} \approx 0.07m^3$. Assuming nearly constant combustor reference velocities, V_{PZ} can be derived from the volume flow through the combustor.

Essential for thermal NO_x formation is the influence of combustor inlet temperature as shown in Figure 9. Constant residence time in the combustion chamber during design and off-design operating mode is caused by nearly constant volume flow through the engine.

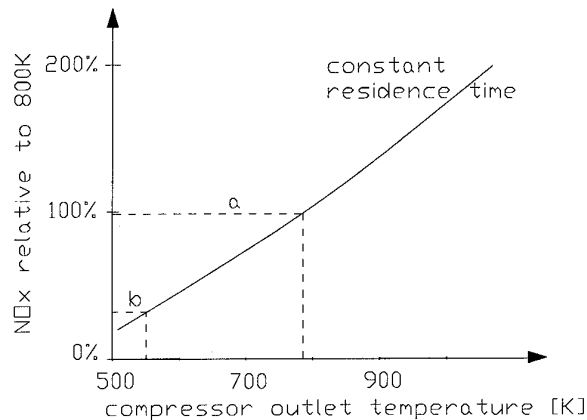


Figure 9: Influence of compressor outlet temperature on the NO_x formation having constant residence time in the primary zone (according to Kerrebrock [8]). The marked lines (a) and (b) denote the difference between potential of NO_x for the IC-TL-concept compared to the Olympus593, see Table 1.

6. FLIGHTMECHANICS

Describing the aerodynamical behaviour of the Concorde the following flight-polars are used, Figure 10. These polars are calculated by Döpelheuer [3], on the base of measured values [5]. The compressibility effect (Mach number influence) plays an important role for supersonic aircraft lift-over drag-polars. In this simplified method the parabolic polar is described neglecting different flap settings and rudder effects.

To calculate the drag coefficient c_w only one single equation (14) is necessary. The lift coefficient c_l is directly convertible from known parameters like flight-velocity, ambient air-density, wing area and gross weight.

The other variables can be expressed as:

$c_{w(\frac{L}{D})opt}$: drag coefficient at the best gliding point
(due to the incompressible polar)

$c_{l(\frac{L}{D})opt}$: lift coefficient at the best gliding point
(due to the incompressible polar)

c_{w_0} : minimum drag coefficient

c_{l_0} : lift coefficient at minimum drag coefficient

K_1, K_2 : both semiempirical factors depending on the flight Mach number and aspect ratio of the airfoil

$$c_w = K_1(Ma) \cdot c_{w_0} + K_2(Ma) \cdot [c_{w(\frac{L}{D})max} - c_{w_0}] \cdot \left(\frac{c_l - c_{l_0}}{c_{l(\frac{L}{D})max} - c_{l_0}} \right) \quad (14)$$

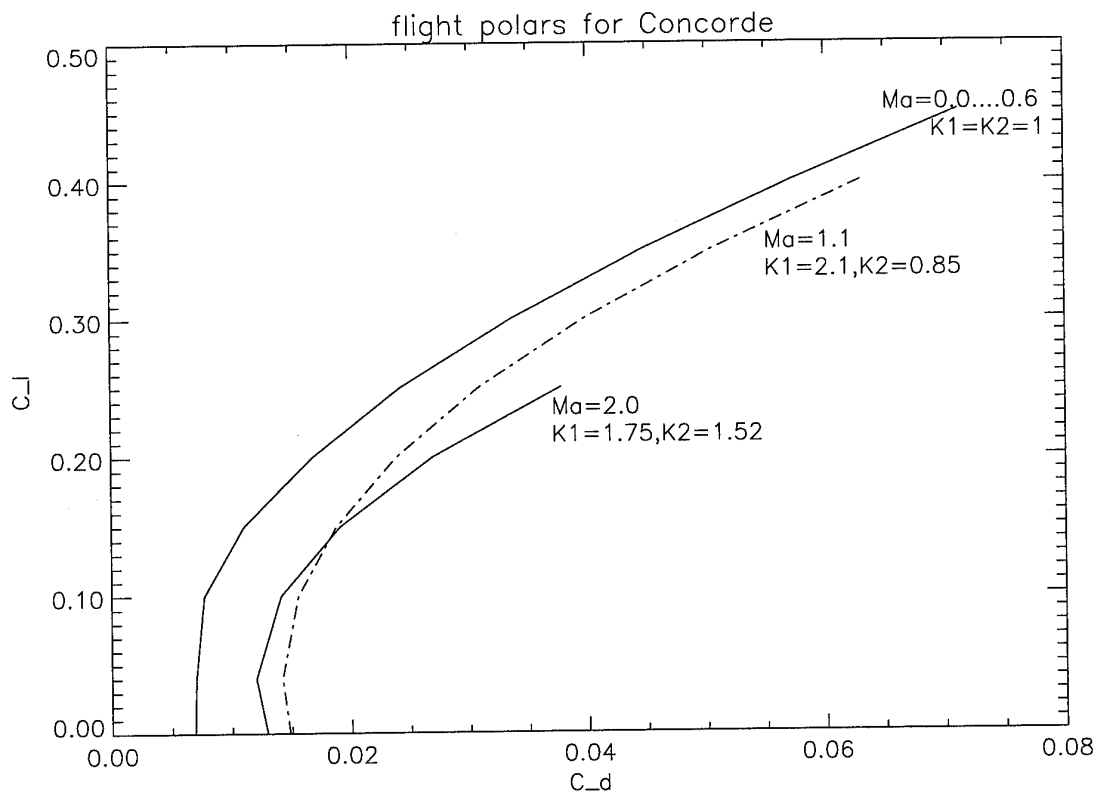


Figure 10: Influence of the Mach number for the used flight-polars due to the Concorde ([3])

7. RESULTS OBTAINED

For three main flight operating points - take off, transonic acceleration and cruise - the most important values are listed in Table 1 showing the advantages of the new engine concepts with respect to the reference engine Olympus 593 Mk610. In this Table following abbreviations are used: OPR=Overall pressure ratio, AB=Afterburning, TET=Turbine entry temperature. Marked values with * are calculated with eqn.(12). The EI_{NO_x} -value for the Olympus without afterburning is connected to the fuel flow in the main combustor. The $EI_{NO_x,AB}$ -value is due to the additional amount of fuel burned in the afterburner. The reduction of NO_x for the IC-TF-engine compared to the Olympus can be obtained from Figure 9 marked lines (a) and (b). At take off conditions the core velocity could be decreased drastically using MTF and TF engines. The noise level is connected to this velocity, so it should be possible to achieve future noise requirements using these power units, Figure 11. The MTF and TF tables are not complete because of restrictions from Rolls Royce and Snecma.

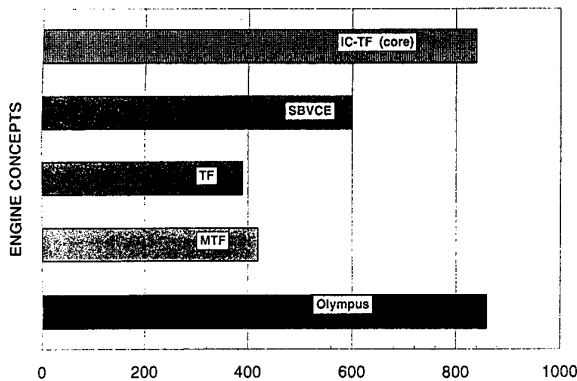


Figure 11: Exit velocities (core) at take off in (m/s).

Because of different bypass ratios even at supersonic cruise conditions and of course due to different TET- and OPR-values the following Table 1 showing the specific thrust, gives an idea of the required engine size. These investigations are neglecting any installation effects and additional drag according to greater engine sizes.

Benefits in decreasing fuel consumption could be noticed for the MTF and the TF concepts. For the chosen supersonic cruising point a 16% fuel reduction using MTF-engines and a 10% reduction using the TF-engines can be achieved. Unfortunately the emission index increases drastically with higher combustor inlet temperatures and pressures. The calculated EI_{NO_x} -values of the most efficient engines are in the range of 35...40g NO_x /kg fuel, far away from the SST-target of 5g/kg.

Basis of these calculations are current technology combustors. Future concepts like double annular combustor or RQL- respectively LPP-concept, have not been taken into account.

The Selective Bleed Variable Cycle Engine uses a higher bypass ratio during take off conditions ($\mu = 2$) to reduce the noise levels and decreases its bypass ratio at higher flight regimes to reach high specific thrust levels, Table 1. Improvements in fuel reductions compared to the Olympus engine are reached during take off and low subsonic flight. During the low pressure mode at subsonic flight with an open first valve the fan operates at high corrected mass flows, Figure 7. While throttling the engine - closing the first valve - the fan operating line sweeps to lower mass flow parameters requiring adjustable fan stator guide vanes. The opposite happens to the booster stages. In spite of opening the second valve at higher flight Mach numbers the stators of the booster have to be opened Figure 8.

Looking at the last discussed engine concept, with an Intercooled-Turbofan, the emission index for NO_x fulfils the environmental constraint for the second generation of supersonic aircraft. The intercooler must be designed to achieve high heat exchanges. The efficiency is assumed to $\eta_{IC}=80\%$ and the pressure losses on both ducts - bypass and core - to be $\Pi_{IC}=5\%$.

For a chosen flight distance of 6000km and a maximum take off weight of MTOW=180000kg and for fixed aerodynamic behaviour (Concorde) the following total fuel burnt has been calculated, Figure 12.

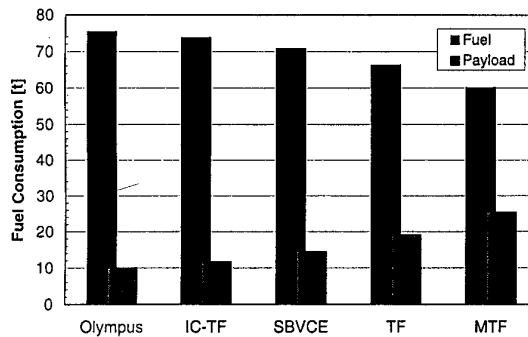


Figure 12: 'Concorde-like SST' with different engine types. Calculated amount of burnt fuel for a range of 6000km.

According to highest benefits in SFC for the MTF during cruise the total amount of fuel can be reduced from approx 75.4t down to approx. 61.5t.

	Take off Ma=0, H=0	Transonic Ma=1.36, H=10700m	Cruise Ma=2.0, H=16100m
Olympus 593Mk610	$F = 169kN$ $F_{dry} = 144.7kN$ $SFC = 1.38kg/daN/h$ $SFC_{dry} = 0.90kg/daN/h$ $F_{spec} = 738m/s$ $TET = 1350K$ $\Pi_{NDV} = 3.14$ $\Pi_{HDV} = 4.79$ $T_3 = 673K$ $A_8 = 0.486m^2$ $A_9/A_8 = 1.11$ $EINOx = 12.9g/kg$ $EINOx,AB = 6.2g/kg$ $v_9 = 862m/s$	$F = 101.9kN$ $SFC = 1.20kg/daN/h$ $F_{spec} = 659m/s$ $TET = 1520K$ $\Pi_{NDV} = 3.47$ $\Pi_{HDV} = 5.23$ $T_3 = 725K$ $A_8 = 0.486m^2$ $A_9/A_8 = 2.14$ $EINOx = 17.0g/kg$ $v_9 = 1058m/s$	$F = 44.1kN$ $SFC = 1.28kg/daN/h$ $F_{spec} = 472m/s$ $TET = 1390K$ $\Pi_{NDV} = 2.52$ $\Pi_{HDV} = 3.88$ $T_3 = 779K$ $A_8 = 0.486m^2$ $A_9/A_8 = 2.58$ $EINOx = 16.2g/kg$ $v_9 = 1058m/s$
MTF	$F = 187.4kN$ $SFC = 0.53kg/daN/h$ $F_{spec} = 420m/s$ $\Pi_{Fan} = 2.16$ $OPR = 31.6$ $EINOx = 34g/kg \star$ $v_9 = 419m/s$	$F = 98.1kN$ $SFC = 0.972kg/daN/h$ $F_{spec} = 341m/s$ $\Pi_{Fan} = 2.12$ $OPR = 36.4$ $EINOx = 39g/kg$ $v_9 = 739m/s$	$F = 44.5kN$ $SFC = 1.06kg/daN/h$ $F_{spec} = 235m/s$ $\Pi_{Fan} = 1.78$ $OPR = 19.6$ $EINOx = 40.2g/kg$ $v_9 = 821m/s$
TF	$F = 179.3kN$ $SFC = 0.533kg/daN/h$ $F_{spec} = 383m/s$ $\Pi_{Fan} = 2.21$ $OPR = 22.5$ $EINOx = 24.4g/kg \star$ $v_9 = 388m/s$	$F = 97.4kN$ $SFC = 0.995kg/daN/h$ $F_{spec} = 417m/s$ $\Pi_{Fan} = 1.88$ $OPR = 31.0$ $EINOx = 35.9g/kg$ $v_9 = 815m/s$	$F = 44.2kN$ $SFC = 1.158kg/daN/h$ $F_{spec} = 312.5m/s$ $\Pi_{Fan} = 1.47$ $OPR = 16.3$ $EINOx = 35.3g/kg$ $v_9 = 899m/s$
SBVCE	$F = 176.2kN$ $SFC = 0.565kg/daN/h$ $F_{spec} = 462m/s$ $TET = 1540K$ $\Pi_{Fan} = 3.00$ $\Pi_{NDV} = 2.40$ $\Pi_{HDV} = 3.6$ $T_3 = 808K$ $\mu_1 = 2, \mu_2 = 0$ $A_8 = 0.583$ $A_9/A_8 = 1$ $EINOx = 30g/kg \star$ $v_9 = 597m/s$	$F = 101kN$ $SFC = 1.134kg/daN/h$ $F_{spec} = 595m/s$ $TET = 1750K$ $\Pi_{Fan} = 2.17$ $\Pi_{NDV} = 3.51$ $\Pi_{HDV} = 4.38$ $T_3 = 889K$ $\mu_1 = 0, \mu_2 = 0.4$ $A_8 = 0.453$ $A_9/A_8 = 2.19$ $EINOx = 27.1g/kg$ $v_9 = 993m/s$	$F = 44.4kN$ $SFC = 1.26kg/daN/h$ $F_{spec} = 442m/s$ $TET = 1660K$ $\Pi_{Fan} = 1.84$ $\Pi_{NDV} = 2.72$ $\Pi_{HDV} = 3.57$ $T_3 = 950K$ $\mu_1 = 0, \mu_2 = 0.4$ $A_8 = 0.453$ $A_9/A_8 = 2.51$ $EINOx = 25.7g/kg$ $v_9 = 1028m/s$
IC-TF	$F = 168.8kN$ $SFC = 0.92kg/daN/h$ $F_{spec} = 485m/s$ $TET = 1390K$ $OPR = 20.0$ $T_3 = 461K$ $A_8 = 0.352$ $A_9/A_8 = 1.25$ $EINOx = 4.6g/kg$ $v_9 = 841m/s$	$F = 101.5kN$ $SFC = 1.20kg/daN/h$ $F_{spec} = 420.5m/s$ $TET = 1420K$ $OPR = 20.2$ $T_3 = 470K$ $A_8 = 0.352$ $A_9/A_8 = 2.28$ $EINOx = 4.9g/kg$ $v_9 = 1059m/s$	$F = 44.5kN$ $SFC = 1.27kg/daN/h$ $F_{spec} = 322m/s$ $TET = 1322K$ $OPR = 10.3$ $T_3 = 551K$ $A_8 = 0.352$ $A_9/A_8 = 2.69$ $EINOx = 5g/kg$ $v_9 = 1054m/s$

Table 1: Comparison of mean engine parameters for the discussed new engine concepts with respect to the reference engine Olympus 593 Mk610. For all three flight points - take off, transonic and cruise - the absolute produced thrust is nearly equal for every engine concept.

That means, the payload can be increased with the new engine concept or of course the maximum range could be improved up to 9000km. All other concepts are between this gap of Olympus and MTF-concept, where the potential of fuel savings for the IC-TF is nearly negligible.

Totally different are the results for the calculated NO_x -emissions as seen in Figure 13. The reference level $\sum NO_x = 1197\text{kg}$ of all Olympus-engines for these range is more than doubled by MTF and TF concepts. Drastical NO_x reduction is found using IC-TF engines.

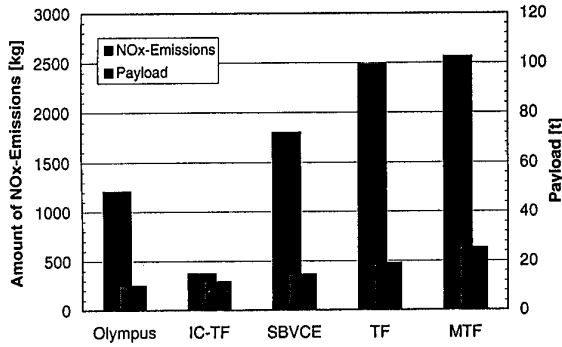


Figure 13: Concorde with different engine types. Calculated amount of emitted NO_x for a range of 6000 km.

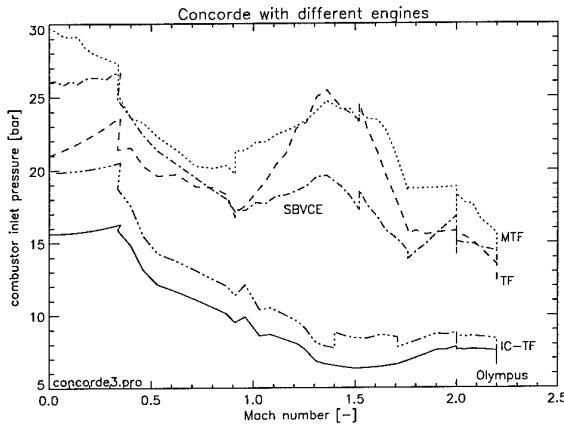


Figure 14: Concorde with different engine types. Variation of combustor inlet pressure versus flight Mach number.

The combustor inlet pressure and temperature versus flight Mach number during take off, climb and cruising phase are shown in Figure 14 and 15. Due to operating in a 'bypass' modus at take off the TF-concept could avoid maximum pressures of 30bar in contrast to MTF. The TF-concept reduces this pressure level below 25bar at take off and if at the beginning of the climb phase a lower power setting of the engines is used, the LPP-constraint of $p_{3,max} \approx$

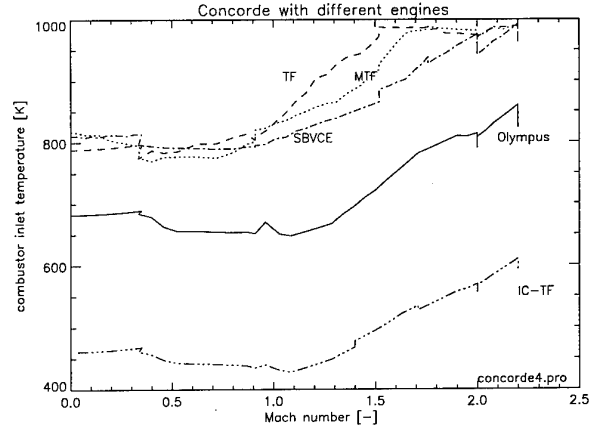


Figure 15: Concorde with different engine types. Variation of combustor inlet temperature versus flight Mach number.

20...22bar (depending on T_3 and therefore due to the compressor efficiencies) is reachable. Combining high overall pressure ratios of these three engine concepts with high flight velocities led to compressor delivery temperatures of $T_3 > 950\text{K}$ at the end of supersonic acceleration. Again, the IC-TF-engine shows untypical low values, the maximum of T_3 is in the order of 600K.

To calculate the climb trajectory the aerodynamic constrain of dynamic head value below $q_{max} = 30\text{kPa}$ has to be fulfilled. Depending on the actual engine concepts the following engine constraints have to be taken into account: $(\dot{m}_{red})_{max}$, $(\dot{n}_{red})_{max}$, $(TET)_{max}$, $(T_3)_{max}$, $(\Pi_{Fan})_{max}$ and $(\Pi_b)_{max}$. If one of these constraints are in danger to be exceeded due to the previous climb trajectory the actual climb path has to be modified. In the case of MTF- and TF-concepts it was necessary to reduce the cruise altitude of the first step cruise down to 15100m in contrast to Olympus (Alt=16100) to avoid compressor delivery temperatures greater $T_3 = 1000\text{K}$ at top of climb. The second cruise level for those engines, according to lighter gross weight was reduced from 18000m (Concorde with Olympus) to 16600m, too. Even the T_3 -values shown in Figure 15 are still on a high level which requires a certain amount of cooling mass flow if standard materials are used.

In general the transonic acceleration should be at lowest altitudes as possible. Reaching 'top of climb' optimal trajectories are supersonic acceleration at low altitude with respect to the maximum dynamic head value and low climb rates combined with high climb rates at near cruise Mach numbers.

In the case of Concorde powered with common Olympus593 Mk610 engines the following calculated engine or aircraft restrictions appears during climb

and lead to modify climb trajectories and engine power settings:

- During take off and transonic climb the most important engine parameters to take care about is never exceeding the corrected mass flow of the low pressure compressor over $\dot{m}_{lpt,max}=138\%$ respectively stay beyond the corrected rotational speed of $n_{1,cor}=126\%$ for the low pressure spool [7] (100% \approx cruise-phase).
- During the first part at supersonic climb the dynamic head is the stringest constraint.
- Finally, to stay lower than $T_{3,max}=850K$ (assumed value) at higher flight Mach numbers till cruising speed, these engine parameter should be critical looked at.

For the maximum take off weight of MTOW=180t the Concorde with four Olympus engines uses the afterburning modus only for take off and transonic acceleration (Mach number between 1 and 1.7). When reducing MTOW by 20t, no afterburning is necessary either for take off nor for transonic flight.

When looking at the fuel saving potential of all discussed variable cycle engine concepts in this paper it seems astonishing that only a relative low fuel benefit compared to Olympus can be achieved. To investigate the SFC-reduction for supersonic engines some general design calculations for a mixed turbojet are presented in Figures 16-19. All studies are for design cruising speed of $Ma=2.0$ at an altitude of 16100m. The Figure 16 shows SFC plotted versus bypass ratio for a compressor delivery temperature of 800K, the last three pictures, Figures 17-19, for a delivery temperature of 900K.

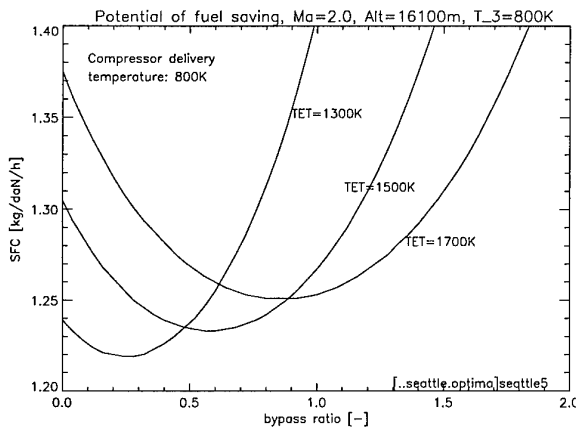


Figure 16: SFC versus bypass ratio at supersonic flight conditions. $T_3=800K=const.$ Influence of different TET.

Increasing the bypass value from $\mu=0$ up to higher values the SFC decreases - depending on the turbine

inlet temperature - down to an optimal bypass value. Keeping the material temperature of the turbines constant, leads to a higher cooling mass flow with

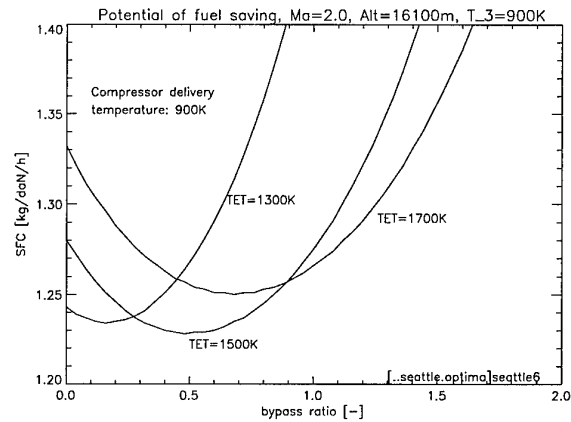


Figure 17: SFC versus bypass ratio at supersonic flight conditions. $T_3=900K=const.$ Influence of TET.

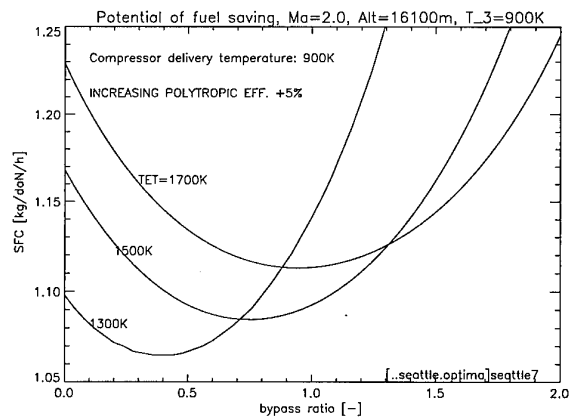


Figure 18: SFC versus bypass ratio at supersonic flight conditions. Same as Figure 17, all turbocomponent efficiencies plus 5%.

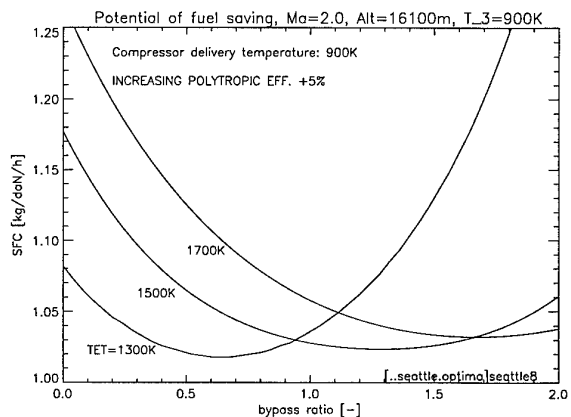


Figure 19: SFC versus bypass ratio at supersonic flight conditions. Same as Figure 18, all turbocomponent efficiencies plus 5% with improved turbine materials ($\Delta T_{material}=200K$).

higher TET according to equation (9) and therefore to worse overall efficiencies, that means, higher TET causes higher SFC values. Introducing a bypass ratio - however - is connected with a strong decrease of specific thrust.

If the compressor delivery temperature is set to 900K (Figure 17-19), a benefit in SFC can be obtained, see Figure 17.

The Figure 18 and 19 are showing the advantages by increasing all turbocomponent efficiencies plus 5%. Only if the cooling rate could be decreased by improved turbine materials ($\Delta T_{\text{material}}=200\text{K}$) introducing higher TET-values are useful regarding engine size and fuel burnt, Figure 19.

LITERATUR

- [1] Deidewig, F.; Döpelheuer, A.; Lecht, M.
Leistungs- und Emissionsverhalten zukünftiger Überschalltriebwerke
DGLR-paper: 94-F4-103, (1994)
- [2] Deidewig, F.
Ein Beitrag zur Berechnung von TL- und ZTL-Triebwerken
DLR, Interner Bericht, IB-325-12-91, (1991)
- [3] Döpelheuer, A.
Brennstoffverbrauch und NO_x -Emissionen von Überschall-Verkehrsflugzeugen
Diplomarbeit RWTH Aachen/DLR Köln, (1994)
- [4] Frenk, A.
Triebwerksmodellierung für ein Staustrahltriebwerk mit Überschallverbrennung im Machzahlbereich 5 bis 15
Diplomarbeit RWTH Aachen/DLR Köln, (1991)
- [5] Humpert, K.
Untersuchungen über den Einfluß aerodynamischer Parameter auf den Entwurf eines Überschallverkehrsflugzeuges
Konstruktiver Entwurf SA 472, TU Braunschweig, (1992)
- [6] ICAO ENGINE EXHAUST EMISSION DATA-BANK
ICAO committee on aviation environmental protection working group 3 meeting 10-13 October 1989, Mariehamn, Aland
- [7] Journal of the Royal Aeronautical Society, Vol.70, 7/66, (1966)
- [8] Kerrebrock, J.L.
Aircraft Engines and Gas Turbines
Massachusetts Institute of Technology, (1992)
- [9] Mellor, A. M.
Semi-empirical correlation for gasturbine emissions, ignition and flame stabilization
AGARD-CP-275, 180, paper no. 24
- [10] Münzberg, H.G.; Kurzke, J.
Gasturbinen - Betriebsverhalten und Optimierung
Springer-Verlag, Berlin/Heidelberg/New York, (1977)
- [11] Nascimento, M.A.R.; Pilidis, P.
The selective bleed variable cycle engine
ASME paper: 91-GT-388, (1991)
- [12] Odgers, J.; Kretschmer, D.; Pearce, G.F.; Wang, G.
The Prediction of thermal NO_x in Gas Turbine Exhausts
ISABE paper: 93-7022, (1993)
- [13] Saravanamouttoo, H.I.H.
Overview on basis and use of performance predictions methods
AGARD lecture series 183: Steady and transient performance prediction of gas turbine engines, (1992)
- [14] Schulte, P., Schlager, H.
Inferred NO_x emission indices of jet engines at cruise altitude from in situ NO and CO_2 measurements within aircraft plumes
Impact of Emissions from Aircraft and Spacecraft Upon the Atmosphere, DLR, Mitteilung 94-06, (1994)
- [15] V.d.Velden, A.J.M.
Aerodynamic Design and Synthesis of the Oblique Flying Wing Supersonic Transport
Stanford University, SUDAAR 621, (1992)
- [16] Wittenberg, H.
Prediction of Off-Design Performances of Turbojet and Turbofan Engines Based on Gasdynamik Relationships
Delft University of Technology, Department of Aerospace Engineering, (1976)

Paper 14: Discussion

Question from A T Webb, Edwards AFB, USA

In your paper and in others, most attention seems to have been given to reductions in Nox. Do you think that combustor design has reached the point where we no longer need to worry about emissions of unburnt hydrocarbons?

Author's reply

It depends on the type of combustor selected. For some types combustion efficiency can be as high as 99.5%, and unburnt hydrocarbons would not be a problem. For lower efficiency combustors, unburned hydrocarbons become an important consideration.

Analyse des performances d'un superstatoréacteur en fonction des paramètres de combustion **Scramjet Performance Analysis in function of Combustion Process Parameters**

Ir. P. HENDRICK
 Ecole Royale Militaire
 Chaire de Mécanique Appliquée
 Avenue de la Renaissance 30
 1040 Brussels - BELGIUM

RÉSUMÉ

Avec un monoétagé (S.S.T.O.) utilisant la propulsion aérobique, un gain significatif en fraction de charge utile ne peut être obtenu que si on atteint au moins Mach 14-15 en mode aérobique. Pour atteindre ce niveau de performances, l'emploi d'un superstatoréacteur au carburant hydrogène est obligatoire.

Ce travail donne les résultats d'une analyse de sensibilité des performances d'un moteur scramjet appelé Hyperjet Mk.3 (avant-corps, rampe externe à trois segments, diffuseur supersonique, isolateur, chambre de combustion et tuyères d'éjection interne et externe) utilisant de l'hydrogène slush comme carburant stocké et le refroidissement actif des parois de la cellule et du moteur pour réchauffer le carburant avant l'injection. L'étude est réalisée à Mach 15, pour une pression dynamique de 60 kPa et un angle d'incidence total constant égal à 11°. Le code utilisé est un code d'aérodynamique 1.5-D avec effets visqueux où l'air est considéré comme un mélange (à 9 éléments) de gaz parfaits réagissant chimiquement entre eux.

L'influence des paramètres les plus importants du processus de combustion est étudiée : le rendement de combustion (rendement de mélange inclus), l'angle injection, l'angle de propagation de flamme, les pertes par mélange fuel-air, les pertes de traînée dans la chambre de combustion, la pression et la température d'alimentation en hydrogène et, enfin, la pression d'injection de l'hydrogène. A chaque fois, les résultats sont comparés avec les valeurs présentées dans la littérature théorique et expérimentale, ce qui permet de fixer les valeurs d'avant-projet de tous ces paramètres en vue d'études futures.

Tout au long de cette étude paramétrique, l'importance de la gestion de l'énergie (donc de la récupération thermique) apparaît clairement : l'impulsion spécifique du carburant doit être utilisée aussi efficacement que possible et toutes les pertes présentes dans le processus de combustion et dans sa préparation doivent être limitées au strict minimum.

LISTE DES SYMBOLES

Symboles

A	(m ²)	section
C _f	(-)	coefficient de frottement de surface
C _D	(-)	coefficient de traînée
D	(N)	traînée
d	(-)	dosage (m _f /m)
δ	(°)	déflexion ou angle
dj2	(°)	angle d'injection du carburant
dz	(°)	angle de propagation de flamme
EFc	(-)	rendement de combustion
ER	(-)	rapport d'équivalence (d _r /d _{sto})
F	(N/m)	poussée (par mètre de largeur)
H	(m)	hauteur
i ₀	(°)	angle d'incidence
ISP	(s)	impulsion spécifique (F/m _f)
ISP _e	(s)	ISP effective ((F-D)/m _f)
km	(-)	coefficient de perte par mélange
Kcf	(-)	rapport de coefficient de frottement dans la chambre
L	(m)	longueur
M	(-)	nombre de Mach
m	(kg/s)	débit d'air
m _f	(kg/s)	débit de carburant
P	(kPa)	pression statique
Q	(kW)	pression dynamique
q	(kW)	transfert thermique
T	(K)	température statique
V	(m/s)	vitesse

Indices

o	conditions non perturbées
1	entrée du diffuseur
2	sortie du diffuseur
3	entrée chambre de combustion
4	sortie chambre de combustion
5	sortie de la tuyère interne
6	sortie de la tuyère externe
c ou k	chambre de combustion
jo	entrée injecteur
j2	sortie injecteur
r	réel
t	total (condition d'arrêt)

1. INTRODUCTION

Une alternative pour le véhicule monoétage transatmosphérique lanceur de satellites (Single-Stage-To-Orbit ou S.S.T.O.) est l'avion à décollage et atterrissage horizontal propulsé par un moteur à cycles combinés. Ce concept possède en effet de nombreuses qualités intrinsèques vis-à-vis des lanceurs classiques à décollage vertical comme Ariane, de part son caractère complètement réutilisable, ses possibilités de retour en cas d'incident ('abort capability'), sa grande flexibilité (longues fenêtres de lancement) due à la possibilité de vol de croisière et sa mise en oeuvre plus rapide.

La propulsion de cet avion doit être assurée par un moteur dérivé de la technologie fusée (Rocket Based Combined Cycle ou RBCC) dont le dernier mode en propulsion aérobie doit fonctionner jusque Mach 14 ou 15 minimum pour obtenir une fraction de charge utile (véhicule inhabité) de l'ordre de 3 à 4 % (Réf. 1).

Le superstatoréacteur (scramjet) à hydrogène est un mode de propulsion aérobie permettant, théoriquement, d'atteindre des vitesses de vol de l'ordre de Mach 15 à 20. Il est depuis 35 ans l'objet d'intenses travaux de recherche théorique et expérimentale aux U.S.A., en Russie, au Japon et en Europe dans le cadre de l'avion hypersonique transatmosphérique à propulsion aérobie, dont le défunt X-30 (ou NASP) fut le porte-drapeau au niveau des recherches et des essais (Réf. 2). Mach 15 était aussi le nombre de Mach choisi pour le programme d'essais HySTP de l'USAF, fin 1994.

2. LE SUPERSTATORÉACTEUR

Au-delà de Mach 6 - 6.5, les chocs nécessaires à l'obtention d'un flux subsonique à l'entrée d'une chambre de combustion classique (ramjet) conduisent à des pertes en pression totale très importantes, ainsi qu'à des pressions et températures très élevées à l'entrée de cette chambre. Ceci implique des structures lourdes et une augmentation de la production de l'entropie irréversible. La compression dynamique est plus grande que la compression optimale et la diffusion subsonique est défavorable (Réf. 3) : la diffusion doit rester limitée et l'écoulement à l'entrée de la chambre de combustion doit rester supersonique, d'où le nom de Supersonic Combustion Ramjet ou Scramjet ou superstatoréacteur.

Avant l'entrée de cette chambre, on trouve par conséquent un convergent supersonique appelé diffuseur supersonique donnant à l'entrée de la chambre un nombre de Mach M_3 compris entre 0.25 et 0.4 M_0 .

La chambre de combustion doit aussi être précédée d'un isolateur qui stabilise le train d'ondes de choc présent en avant de la chambre suite à l'injection et à la combustion du carburant. Cet isolateur évite les interactions de ces chocs avec l'entrée d'air (voir réf. 4). Il doit être suffisamment long pour contenir le 'precombustion shock train'. En fait, il est dimensionné à relativement bas M_0 (en mode ramjet dual) : dans le moteur considéré ici, sa longueur est d'environ 50 cm (plus de deux fois la hauteur H_3).

La chambre doit être légèrement divergente (ici, le rapport de divergence est de 2.2) afin d'assurer un écoulement supersonique à sa sortie jusqu'en-dessous de Mach 7.

3. LE MOTEUR HYPERJET MK.3

Le moteur utilisé pour la propulsion de ce S.S.T.O. est un moteur à cycles combinés RBCC appelé Hyperjet Mk.3. Il fonctionne suivant les modes suivants depuis Mach 0 jusqu'à la transition à Mach 15 : éjecteur à air, ramjet, scramjet et, finalement, fusée. Ces modes exigent quelques reconfigurations de géométrie en fonction du nombre de Mach, comme représenté schématiquement à la fig. 1. On notera toutefois la complexité des sous-ensembles à géométrie variable qui est un sérieux obstacle à la construction et à l'utilisation d'un tel moteur dont les différents modes sont optimisés.

Le carburant est obligatoirement de l'hydrogène car le carburant stocké doit permettre de refroidir les parois fortement échauffées du véhicule et les parois du moteur, et le LH_2 est le seul carburant possédant les capacités de refroidissement adéquates. On choisit en fait de l'hydrogène slush (50% liquide - 50% solide) stocké dans les réservoirs à 13.8 K, pour sa densité qui est 16 % plus élevée que celle de l'hydrogène liquide.

Le moteur Hyperjet Mk.3 est léger et compact si on le compare aux moteurs utilisant des turboréacteurs comme mode de propulsion à basse vitesse. Son rapport poussée/poids par mètre d'envergure est de l'ordre de 16 kg/kg. Sa longueur totale (de 1 à 5 sur la fig. 1) est de 3.87 m.

A Mach 15, le rapport de contraction de l'entrée d'air est égal à 22.7, valeur comparable à celle de la référence 4. La hauteur de la section d'entrée de la chambre de combustion H_3 est égale à 24 cm et la pression statique dans cette section est d'environ 100 kPa (110 kPa dans la réf. 4).

4. ETUDE DE L'INFLUENCE DES PARAMÈTRES LIÉS À LA COMBUSTION SUR LES PERFORMANCES DU MOTEUR

a. Avant-propos

L'étude de l'influence de quelques paramètres importants liés à la combustion dans un superstatoréacteur est étudiée à l'aide du code Hyperjet dans les conditions suivantes : $M_0 = 15$, $Q_0 = 60$ kPa et $i_0 = 5^\circ$ ($\delta_0 = 6^\circ$). L'angle d'incidence total, défini comme étant $\delta_0 + i_0$, est donc égal à 11° .

Le code Hyperjet est un code 1.5-D d'aérothermodynamique avec dissociations (à 9 éléments) où l'air est considéré comme un mélange de gaz parfaits réagissant chimiquement entre eux. Il prend en compte les chocs, le frottement de surface et les transferts thermiques par convection et radiation.

Dans un superstatoréacteur à Mach 15 (et déjà dès Mach 11-12), les notions classiques vues dans l'étude des turboréacteurs et des ramjets deviennent caduques. Cela est principalement dû à la richesse excessive en hydrogène du mélange dans la chambre de combustion : on y rencontre des rapports d'équivalence ER bien supérieurs à 1, de l'ordre de 3 et même parfois plus. Ainsi la contribution du carburant à la poussée ($m_f V_6$) est bien plus importante que la contribution du débit d'air ($m(V_6 - V_0)$).

De même, si on travaille avec de tels ER et une injection d'hydrogène relativement parallèle à l'écoulement (angle d'injection entre 5 et 20°), la température totale diminue entre l'entrée et la sortie de la chambre de combustion. Cette diminution est compensée par un gain énorme en quantité de mouvement (énergie cinétique) apportée par l'hydrogène injecté quasi parallèlement.

Dans le moteur Hyperjet Mk.3, avec un angle d'injection de 15° , on a :

M_0	15
M_3	4.19
T_{t3}	11048 K
ER	2.09
M_4	2.99
T_{t4}	7957 K

Vu la température d'entrée de chambre très élevée, aucun problème d'autoallumage de l'hydrogène ne devrait se produire ; celui-ci devrait même être très rapide (quelques cm).

On retrouve cette même évolution dans la référence 5, où, à Mach 15, on a, à l'entrée de la chambre de combustion :

M_3	5.19
T_{t3}	12182 K

et les valeurs suivantes de T_{t4} en fonction du dosage :

ER	M_4	T_{t4} (K)
2.0	3.39	9593
3.0	3.17	8151
4.0	3.02	7125

On remarque donc bien la diminution de plus en plus forte de la température totale si le dosage augmente.

b. Injecteurs de carburant

Dans un véhicule à Mach 15, les injecteurs doivent donner un bon mélange air-hydrogène sur une distance courte malgré la faible différence de vitesse et de direction existant entre les deux flux. Cela ne peut être réalisé que grâce à une recirculation, à des tourbillons (vortex) tridimensionnels importants et à une diffusion turbulente comme cela se produit derrière des injecteurs-trous (*flush-wall orifice*) ou derrière des injecteurs-rampe avec flèche et détente et plusieurs fentes d'injection verticales (*swept-expansion ramp injector with discrete vertical slots*, voir réf. 6).

Ces deux concepts semblent être ceux qui réalisent le meilleur mélange, l'avantage de l'injecteur-rampe étant de mieux accrocher la flamme tandis que le flush-wall provoque moins de pertes en pression totale.

c. Influence du rendement de combustion

Le rendement de combustion (global) EFC est, dans cette analyse, le produit du rendement de mélange et du taux de réaction de l'hydrogène mélangé.

Dans le code utilisé, EFC joue un rôle dans la sous-routine thermochimique qui calcule la composition chimique des gaz avant et après la chambre de combustion. Si EFC diminue, le nombre de moles d' H_2 brûlées diminue également. Ci-dessous, on trouve un tableau donnant les valeurs de différentes grandeurs pour trois valeurs de EFC.

Grandeur	EFC = 0.95	EFC = 0.90	EFC = 0.85
T_4 (K)	2845	2814	2781
P_4 (kPa)	96.51	95.41	94.24
V_6 (m/s)	4809	4801	4791
q_k (kW)	143.3	142.9	142.3
F (kN/m)	104.0	101.9	99.7
ISP (s)	1191	1172	1151

La vitesse d'éjection des gaz diminue, facteur qui réduit la poussée et l'impulsion spécifique (dans ce cas-ci où m et ER sont quasi constants).

On remarque que les diminutions en poussée (-4%) et en ISP (-3%) sont d'une part linéaires (voir fig. 2) et d'autre part bien inférieures à celle en EFC (-10%). Ceci est dû à la grande impulsion spécifique du carburant qui, même sans brûler, apporte déjà une contribution appréciable à la poussée (et donc à ISP). On remarque aussi la diminution du transfert de chaleur dans la chambre avec la diminution de EFC, ce qui est logique. Mais cette diminution est relativement faible (-1%).

La référence 7 donne des résultats expérimentaux et analytiques très intéressants de JHU/APL : on peut y voir qu'à $M_0 = 12$, la variation de ISP avec EFC est linéaire et qu'une diminution de EFC de 0.9 à 0.8 donne une diminution de ISP de 3.3 %, ce qui correspond parfaitement aux résultats obtenus dans cette étude.

Une question assez débattue est de savoir si une température d'alimentation en hydrogène élevée (700 K et plus, comme dans ce moteur) défavorise le rendement de mélange, étant donné qu'une température élevée (voir point j) donne une vitesse d'éjection du fuel proche de celle du flux d'air, ce qui réduit le taux de mélange. Une étude approfondie (Réf. 8) a montré que, dans le cas d'une injection parallèle, des valeurs de l'ordre de 80 % n'étaient pas exagérées pour le rendement de combustion global à condition de disposer d'une chambre de combustion pas trop courte, c'est-à-dire de 80 à 85 cm. Dans ce moteur, la longueur de la chambre est de 70 cm, ce qui constitue un bon compromis entre rendement de combustion élevé et traînée de frottement dans la chambre pas trop importante (dans un véhicule de grande finesse, cette traînée peut devenir une contribution importante de la traînée totale).

d. Influence de l'angle d'injection de l'hydrogène

L'angle d'injection de l'hydrogène gazeux d_{j2} peut varier entre 90° (injection normale) et 0° (injection parallèle). Bien que les interactions entre l'angle d'injection et d'autres paramètres, comme le rendement de combustion, soient évidentes, seule l'influence de d_{j2} est étudiée dans un premier temps.

La variation de F et de ISP en fonction de d_{j2} est donnée au tableau ci-dessous et à la fig. 3.

d_{j2}	90°	20°	0°
T_4 (K)	2987	2822	2811
V_4 (m/s)	3608	3864	3882
V_6 (m/s)	4697	4797	4803
q_k (kW)	143.0	142.9	142.9
ER (-)	2.096	2.094	2.086
F (kN/m)	91.8	101.6	102.1
ISP (s)	1047	1165	1174

Avec une injection parallèle, la poussée F croît de 11.2 % par rapport à un cas avec injection normale, ce qui pourrait permettre de diminuer le poids du moteur ou d'améliorer le rapport F/D. De son côté, l'ISP augmente d'un pourcentage un peu plus élevé (12.1%).

La forte augmentation de F est due à une grande augmentation de V_4 et donc de V_6 vu la contribution de la vitesse d'injection du carburant proportionnelle à $\cos d_{j2}$. Si cette contribution cinétique diminue (cas où d_{j2} croît), la contribution thermique du carburant va croître et donc aussi T_4 , le transfert de chaleur et donc ER, ce qui explique pourquoi ISP diminue plus que F lorsque d_{j2} croît.

On peut dire qu'au-delà de Mach 10, la quantité de mouvement apportée par le carburant devient un élément de plus en plus important de la poussée du moteur et que, par conséquent, il faut obligatoirement choisir un *angle d'injection faible*, tout en assurant toujours un bon mélange.

Dans le domaine des valeurs de d_{j2} intéressantes à Mach 15 (entre 0° et 20°), la variation de ISP est environ égale à 0.5 s° .

e. Influence de l'angle de propagation de flamme

L'angle de propagation de la flamme dz est un paramètre dimensionnant de la chambre du moteur Hyperjet Mk.3 : au plus petit dz , au plus longue la chambre. Dans le code de calcul utilisé, un facteur limitant dz est d_{j2} : dz ne peut être supérieur à d_{j2} , ce qui n'est peut-être pas vrai en réalité mais va dans le sens de la sécurité.

Les figures 4 et 5 donnent l'influence de cet angle sur F, ISP, ER et la longueur de la chambre de combustion L_c . La forte augmentation de l'ISP avec l'angle dz peut être expliquée par le raccourcissement de la chambre et donc l'importante diminution de ER qui entraîne aussi une chute de V_6 . L'évolution asymptotique de ISP est en relation directe avec l'évolution de $L_c = H_3/(2 \tan dz)$.

f. Influence des pertes par mélange

L'énergie nécessaire au mélange de l'air et du carburant n'est pas négligeable comme l'ont montré les travaux du Prof. J. Swithenbank. Si cette énergie doit venir de l'écoulement, une perte importante en vitesse est à prévoir. L'énergie perdue lors de ce mélange est généralement exprimée proportionnellement à un coefficient km , appelé 'fuel air mixing losses coefficient' et exprimé en %. Il a une influence directe sur V_4 et donc sur T_4 .

L'évolution de F et de l'ISP en fonction de km est donnée à la fig. 6. La chute de ISP et de F est constante et continue : ceci est dû à la diminution

de V_4 qui entraîne une diminution de V_6 et aussi une augmentation de T_4 donc du transfert thermique et de ER, ce qui explique la chute plus importante de ISP. Un effet favorable doit cependant être noté : le frottement dans la chambre (C_{fc}) diminue vu la diminution de la vitesse et la température plus élevée.

g. Influence de la traînée due à l'injection

Dans la chambre de combustion, il existe aussi une perte d'énergie (et de vitesse) due à la traînée créée par les injecteurs et l'injection dans un flux supersonique (voir, par exemple, l'étude détaillée en réf. 9).

L'énergie perdue est proportionnelle au facteur $C_D S_3 / A_3$ où S_3 est l'augmentation de la surface interne due au système d'injection et C_D un coefficient de traînée de frottement et de pression. On peut introduire un coefficient K_{cf} , appelé 'friction coefficient ratio in combustor', qui multiplie le coefficient de perte par frottement C_{fc} ($K_{cf} \geq 1$). Dans la chambre de combustion, C_{fc} , le nombre de Stanton et le flux de chaleur lui sont donc proportionnels. Le coefficient K_{cf} va donc avoir un effet non négligeable sur ER, F et ISP.

Le tableau suivant donne quelques caractéristiques de l'écoulement et les performances en fonction de K_{cf} (avec km égal à 0.05).

Grandeur	$K_{cf} = 1.0$	$K_{cf} = 1.5$	$K_{cf} = 2.0$
V_4 (m/s)	3908	3878	3849
P_4 (kPa)	89.72	95.41	100.77
V_6 (m/s)	4795	4801	4803
C_{fc} (-)	0.00323	0.00482	0.00641
q_k (kW)	94.6	142.9	191.2
ER (-)	1.7750	2.0859	2.3906
F (kN/m)	96.1	101.4	106.2
ISP (s)	1297	1167	1068
ISP _e (s)	778	700	641

(Pour ISP_e, T/D = 2.5 a été considéré)

Si K_{cf} double, C_{fc} double aussi, ce qui fait croître ER de 35%. Cette augmentation de ER entraîne une augmentation de F (+10.5%) due aussi à une plus grande V_6 . Vu que ER croît beaucoup plus que F, l'ISP et l'ISP_e diminuent fortement.

h. Influence combinée de km et K_{cf}

En réalité, les effets de km et de K_{cf} sont couplés, ce qui amène certains auteurs à introduire un seul et unique coefficient k_E . On peut donc comparer l'influence du couple ($km + K_{cf}$) à l'influence de k_E . On a donc déterminé l'influence de ce couple en comparant les performances moteur obtenues avec le couple ($km = 5\%$, $K_{cf} = 1.5$) (cas 1) à

celles obtenues dans le cas idéal ($km = 0$, $K_{cf} = 1.0$) (cas 2).

Grandeur	cas (1)	cas (2)
ER (-)	2.0859	1.7750
F (kN/m)	98.4	100.6
ISP (s)	1167	1360
ISP _e (s)	700	816

(ISP_e avec un rapport T/D égal à 2.5)

On voit que l'influence sur la poussée est faible (car ER augmente fort) mais que l'ISP_e du couple (1) est 14.2% inférieure à celle du couple idéal (2), ce qui correspond très bien aux résultats donnés dans la référence 3. Ces mêmes conclusions peuvent être tirées de la figure 7 (conditions différentes du tableau) qui représente l'évolution de l'ISP en fonction de km et de K_{cf} combinés.

i. Influence de la pression d'alimentation des injecteurs

L'hydrogène est détendu d'une pression d'alimentation P_{j0} à une pression d'injection P_{j2} dans des petits injecteurs-tuyères supersoniques.

Si on modifie la pression P_{j0} sans modifier P_{j2} , la section col doit être adaptée ; tandis que pour un P_{j0} constant (donc une section col de l'injecteur constante également), on fait varier P_{j2} , T_{j2} et V_{j2} en faisant varier le taux de divergence de la tuyère (voir point k).

Si, par exemple, P_{j0} croît (la section col diminue) et que P_{j2} reste constante, T_{j2} diminue et V_{j2} augmente ce qui donne une poussée un rien plus grande mais une ISP quasi constante vu l'augmentation de ER qui compense celle de F. Cette augmentation de ER est due à un plus grand transfert thermique dans la chambre consécutif à une augmentation de C_{fc} et donc du nombre de Stanton dans la chambre de combustion.

Le tableau suivant donne l'influence de P_{j0} (kPa) sur les performances du scramjet ($P_{j2} = 110$ kPa) :

Grandeur	$P_{j0} = 880$	$P_{j0} = 1760$	$P_{j0} = 2640$
T_{j2}	564	465	417
V_{j2}	3613	3996	4181
ER	2.320	2.330	2.331
F	95.7	96.1	96.2
ISP	1137	1137	1138

j. Influence de la température d'alimentation

Le carburant est d'abord utilisé comme fluide de refroidissement. C'est seulement après son passage dans des échangeurs de chaleur servant à refroidir la structure externe de l'avion et la structure interne du moteur (active cooling) qu'il est amené

à l'entrée des petits injecteurs-tuyères à une température d'alimentation T_{j0} relativement élevée (dans tout ce qui précède $T_{j0} = 1000$ K).

Une température T_{j0} élevée apporte de gros avantages au niveau des ISP's comme on peut le voir à la fig. 8 (cf. aussi Réf. 4 & 10). On peut ainsi remarquer, à cette figure, qu'à haut M_0 , il est presque indispensable d'avoir une T_{j0} élevée pour que l'ISP_e soit supérieure à celle d'une bonne fusée. La chute de F liée à l'augmentation de T_{j0} est en grande partie due à la diminution de ER qui, en pourcentage, chute plus que F.

k. Influence de la pression d'injection

Les sensibilités sont identiques à celles du point i. Au plus petite P_{j2} , au plus grands V_{j2} et le poids de l'injecteur et au plus petit T_{j2} . Une haute pression à l'injection sera donc désavantageuse pour la poussée et pour l'ISP mais l'effet est très limité : F passe de 96.1 kN/m pour $P_{j2} = 110$ kPa à 95.7 kN/m pour $P_{j2} = 200$ kPa tandis que l'ISP passe de 1137 s à 1127 s.

l. Influence combinée de plusieurs paramètres

Il faut aussi étudier l'influence combinée d'au moins deux paramètres sur les performances comme cela a été fait pour le couple (km, Kcf). On doit, par exemple, étudier l'influence combinée de l'angle d'injection d_{j2} et de Kcf car l'intensité des chocs créés par l'injection de carburant va dépendre de d_{j2} et cet angle va donc avoir un impact direct sur Kcf (et sur km et sur Efc).

Les figures 9.a et 9.b donnent l'évolution de ISP en fonction des couples (d_{j2} , Kcf) et (d_{j2} , km). On y voit qu'une augmentation de d_{j2} peut mener à une diminution de l'ISP bien plus importante que la valeur de 0.5 s par degré de d_{j2} obtenue au point d ci-dessus, puisqu'on peut ici atteindre (cas (d_{j2} , Kcf)) jusqu'à 1.2 s°, soit plus du double.

5. VALEURS D'AVANT-PROJET DES PARAMÈTRES

On choisit les valeurs suivantes vu la concordance qu'elles apportent avec la littérature expérimentale et théorique :

- ♦ Efc = 80% (voir réf. 6, 8 & 9)
- ♦ $d_{j2} = 10^\circ$ (cette valeur donne une poussée et une ISP élevées sans introduire trop de chocs dans la chambre, elle permet aussi un meilleur mélange que l'injection parallèle)
- ♦ $dz = 10^\circ$, valeur qui implique un bon mélange
- ♦ km = 5% et Kcf = 1.5
- ♦ On pourrait choisir une valeur de P_{j2} élevée malgré les inconvénients cités au point k car cela peut nous procurer un gain important en poids mais on choisit plutôt un rapport P_{j2}/P_2 petit (égal

à 1.1) pour une toute autre raison : l'hydrogène injecté doit être sous-détendu vis-à-vis du flux d'air pour favoriser le mélange mais pas trop pour ne pas provoquer un choc à l'injection trop grand (Réf. 11). Aussi P_{j2} sera-t-il choisi égal à 110 kPa. On pourrait aussi surdétendre le fuel (90 kPa, par exemple) et ainsi aussi favoriser le mélange (Réf. 8) mais cela aurait relativement peu d'influence sur les performances.

♦ $P_{j0} = 1760$ kPa (cette valeur est dictée par le choix de P_{j2} et une détente P_{j0}/P_{j2} relativement faible vu le faible gain apporté par une détente importante qui, en plus, impose une pompe à hydrogène plus grosse)

♦ $T_{j0} = 1000$ K (cette valeur est peut-être un peu pessimiste en regard des matériaux futurs mais dépasse quand même les possibilités des alliages actuels).

Avec ce jeu de valeurs, les performances (F et ISP) obtenues à Mach 15 sont en bonne concordance avec les résultats de nombreuses autres études (Rudakov, Maurice, Miki, Baranovsky, etc.).

6. CONCLUSION

L'importance du management énergétique, et en particulier de la récupération thermique apparaît clairement tout au long de cette analyse : un carburant réchauffé vous permet de disposer d'une impulsion spécifique du carburant élevée et/ou d'une grande énergie cinétique du carburant à l'injection. Cette énergie apportée par le carburant doit être utilisée le plus efficacement possible : l'angle d'injection doit être petit et toutes les pertes dans le processus de combustion et sa préparation doivent être strictement limitées. C'est pourquoi les valeurs d'avant-projet de tous ces paramètres ont été déduites de cette étude afin de disposer d'un moteur où les pertes sont réduites.

Cette étude contourne toutefois le problème fondamental qui est d'arriver à Mach 15 avec le même scramjet fonctionnant depuis Mach 6-6.5. La solution évidente serait de réduire fortement le nombre de Mach de transition aérobie→fusée de Mach 15 à Mach 8-9, limitant ainsi le domaine de fonctionnement nécessaire du scramjet. Ceci n'est envisageable qu'avec un seul concept : la collecte d'oxygène (avec séparation O_2-N_2) pendant la phase de vol avec propulsion aérobie en vue de l'emploi ultérieur de cet oxygène stocké lors du mode fusée (Réf. 12). Ce concept pourrait même mener à une transition autour de Mach 6 avec un véhicule légèrement plus lourd qu'à Mach 7, mais en évitant l'emploi (et le développement risqué et coûteux) d'un scramjet (Réf. 13).

REMERCIEMENTS

Je tiens à remercier Jean Vandekerckhove pour m'avoir fait partager sa passion de l'hypersonique, ainsi que Luc Smeets pour le traitement de nombreux résultats de calcul.

RÉFÉRENCES

1. VANDENKERCKHOVE J. A., "A Peep beyond S.S.T.O. Mass Marginality", IAF-92-0656, Sep 1992.
2. VOLAND R. & ROCK K., "NASP Concept Demonstration Engine and Subscale Parametric Engine tests", AIAA-95-6055, Chattanooga, 3-7 Apr 95.
3. CSYSZ P. A., "Hypersonic Convergence", Course for St Louis University, Parks College, Aerospace Engineering Dept., Apr 1988.
4. BILLIG F. S., "Research on Supersonic Combustion", AIAA Journal of Propulsion and Power, Vol. 9, n° 4, Jul-Aug 1993.
5. BILLIG F. S., "Thermochemistry issues in the design of high-speed propulsion systems", von Karman Institute, Lecture Series 1995-04, 24-28 Apr 1995.
6. SEKAR B., "Conceptual studies of high speed combustors for mixing enhancement mechanisms", AIAA-95-6095, Chattanooga, 3-7 Apr 95.
7. THOMPSON M. W. & FRIEDMAN M. A., "Issues associated with long-duration high-enthalpy scramjet combustor testing", AIAA Journal of Propulsion and Power, Vol. 9, n° 3, May & June 1993.
8. WENDT M. & STALKER R. & JACOBS P., "Effect of fuel temperature on supersonic combustion", AIAA-95-6029, Chattanooga, 3-7 Apr 95.
9. RIGGINS D. & McCLINTON C. & BITTNER R., "Investigation of scramjet injection strategies for high Mach number flows", AIAA Journal of Propulsion and Power, Vol. 11, n° 3, May & June 1995.
10. VANDENKERCKHOVE J. A. & BARRERE M., "Energy Management for S.S.T.O.'s", ISABE-93-7019, XI ISABE Symposium, Tokyo, Sep 1993.
11. ABBITT J. & McDANIEL J., "Experimental supersonic hydrogen combustion employing staged injection behind a rearward-facing step", AIAA Journal of Propulsion and Power, Vol. 9, n° 3, May-Jun 1993.
12. BILLIG F. S., "Propulsion systems from takeoff to high-speed flight", chapter 1 of book "High-speed flight propulsion systems", AIAA series Progress in Astronautics & Aeronautics, Vol. 137, 1991.
13. VANDENKERCKHOVE J. & BALEPIN V. & CZYSZ P. & MAITA M., "Assessment of SSTD performance with in-flight LOX collection", AIAA-95-6047, Chattanooga, 3-7 Apr 95.

Figures

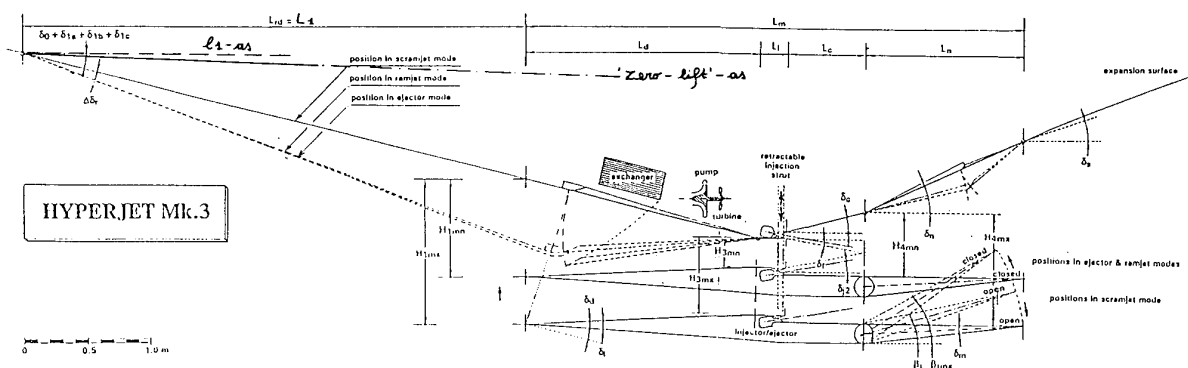


Figure 1

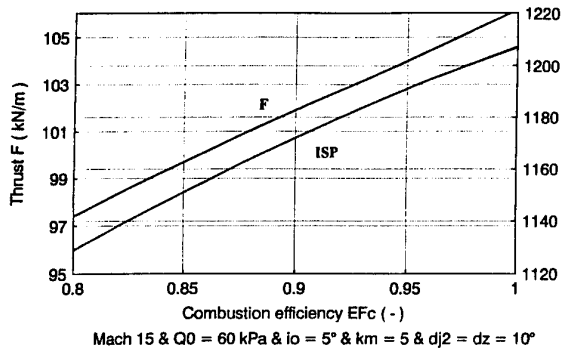
Influence of the combustion efficiency EF_c 

Figure 2

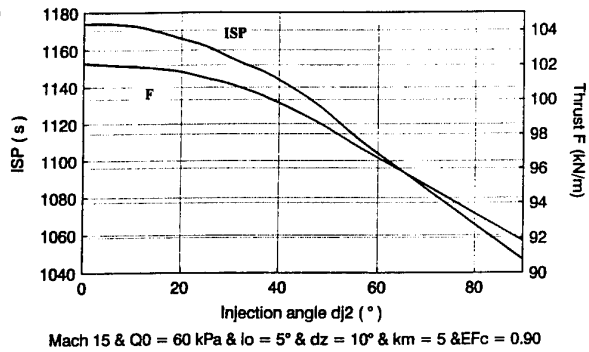
Influence of the injection angle dj_2 

Figure 3

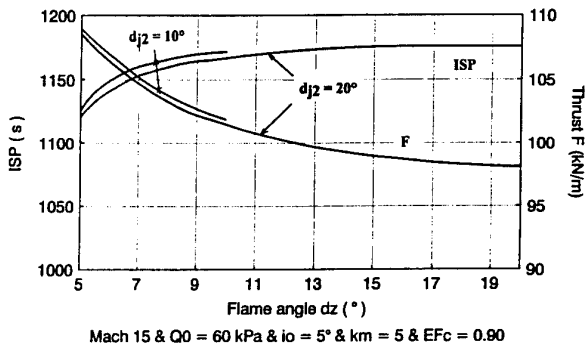
Influence of the flame propagation angle dz 

Figure 4

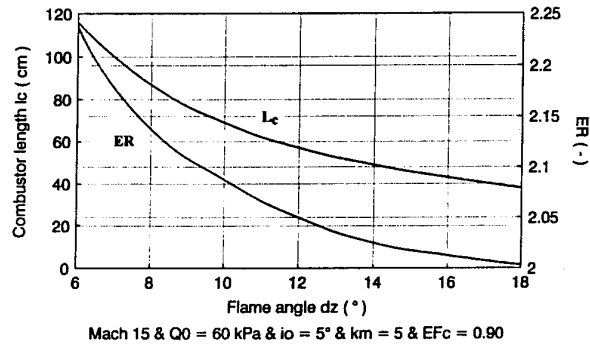
Influence of the flame propagation angle dz 

Figure 5

Influence of fuel-air mixing losses

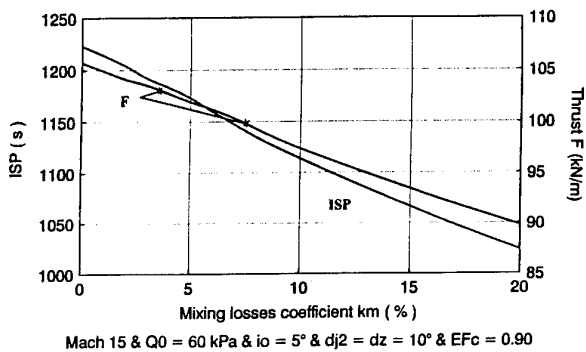


Figure 6

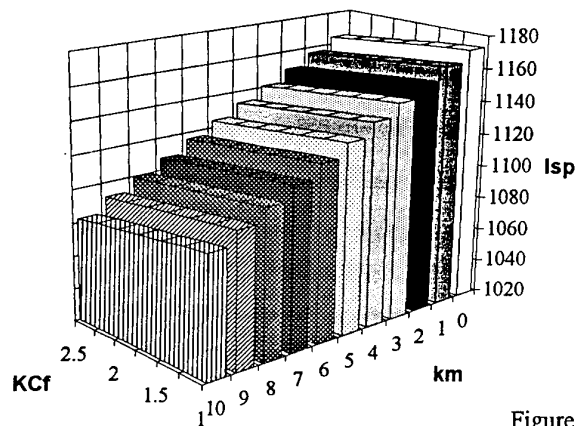
 $I_{sp} = f(KC_f, km)$ 

Figure 7

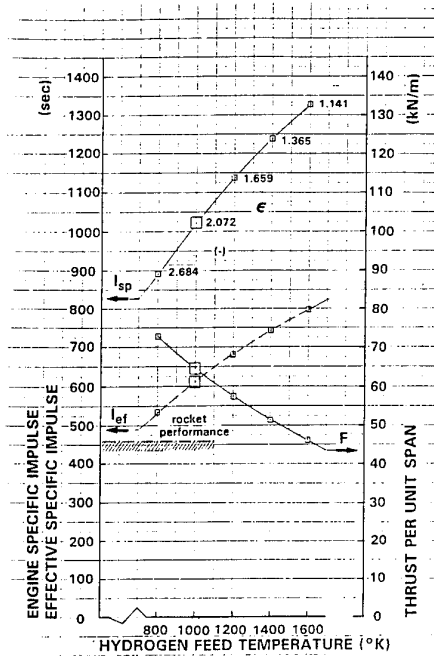


Figure 8

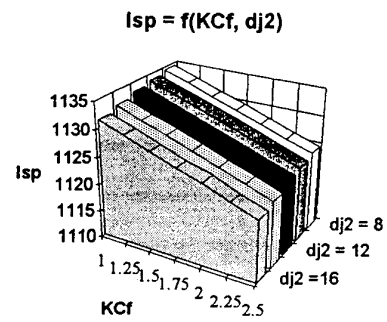


Figure 9.a

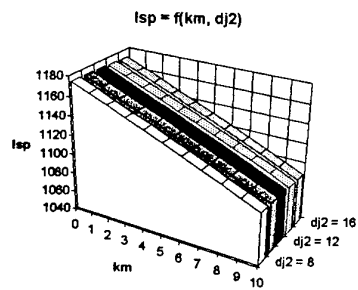


Figure 9.b

Paper 15: Discussion

Question from Prof L de Luca, Milan Politechnic, Italy

In general, combustion losses depend on the interplay of many factors. Did you check whether 80% efficiency is compatible with your specific configuration?

Author's reply

A combustion efficiency of 80% is rather optimistic, but corresponds to results given in other studies with similar combustion chambers and combustion conditions, eg Reference 8 cited in my paper, or the paper by G B Northam of NASA Langley at the 1995 ISABE Conference in Melbourne. Perhaps I would need to extend the length of my combustion chamber (say 100 cm instead of 70 to 75 cm) to ensure that 80% efficiency can be attained at these rather high equivalence ratios. We did not carry out any tests to measure this efficiency. However the effect on performance will be limited.

COMBINED-CYCLE ENGINES FOR HYPERSONIC APPLICATIONS

F.J. Heitmeir
MTU Motoren- und Turbinen-Union München GmbH
Postfach 50 06 40
80976 Munich, Germany

Summary

Since the early days of manned flight the aim has always been to increase speed and range. Propellers were able to cover speed ranges well below sonic speed, jet engines pushed the boarder to the supersonic regime. For hypersonic applications combined engines are mandatory if the vehicle has to operate at different speed levels throughout the whole flight regime. This makes the design of such engines very complex. Control, thermal management and secondary power generation became decisive factors influencing the engine design.

on a reference concept which operates in the speed range between Mach 0 and Mach 7.

This paper highlights the technological challenges associated with combined-cycle engines for hypersonic flight. At first, different possible engine concepts are discussed. The number of possible combined-cycle engine concepts is very high. Operating requirements and other boundary conditions are selection criteria to narrow the number of concepts down. Furthermore, the technological challenges associated with combined-cycle engines are presented with respect to the selected baseline engine.

1. Introduction

It has always been the aim of mankind to push existing frontiers into unknown areas. This also holds true for the speed of manned and unmanned aircraft. Continuous development starting with propeller engines of the first days of flight and speeds well below the sonic range finally led to the jet engines which have the potential to accelerate the vehicle to supersonic speed. This is state of the art nowadays. In the universities and engineering departments in various countries propulsion systems for hypersonic flight are being investigated. But beside missile application which operate in only one design point no operative vehicle emerged up to now since the technology needed to cover the whole speed range is not jet available.

During the last few years an application in space transportation surfaced: since expandable rockets are very cost intensive and have inherent safety disadvantages, airbreathing propulsion systems for winged space transportation systems were investigated in various countries.

To lay the technological foundations in Germany, the Federal Ministry of Research and Technology initiated a hypersonic technology readiness programme /1/. The engine investigations were based

2. Engine Classification

Different propulsion systems are available for the various speed ranges. They are classified by their working principles or by regimes of increasing flight speed:

For subsonic cruising speeds up to Mach 0.6 the TURBOPROP is the best choice, owing to its excellent propulsive efficiency (bypass ratio BPR > 40).

Higher subsonic flight speeds up to Mach 0.9 are covered by TURBOFANS with bypass ratios up to 8.

The lower supersonic flight regimes are typical applications for TURBOFANS with smaller bypass ratios (BPR < 1) and medium pressure ratios. Their specific fuel consumption (sfc) is better than that of a turbojet owing to the bypass mass flow. Alternatively, a TURBOJET with lower pressure ratio could be installed which offers some advantages in the upper Mach number regime with respect to its thermodynamic cycle.

Pure TURBOJETS with low compression ratios are dominant in the upper supersonic regime (Mach < 3).

Lower hypersonic speeds (Mach > 3) may be covered by a low-compression TURBOJET with very high turbine entry temperatures and with reheat; greater advantages are offered by a combination engine with a small low compression gas turbine (TURBOJET OR TURBOFAN) combined with a

subsonic RAMJET COMBUSTOR. Increased ram entry temperatures ask for extremely high combustion temperatures, otherwise the thrust per air mass flow would be too low.

The upper hypersonic regime ($Mach > 6$) could be covered by SCRAMJETs, a ram duct with supersonic combustion. In this case turbo components would become unnecessary since at this Mach numbers the multi-shock pre-compression intake already provides for sufficiently high pressures.

Even higher Mach numbers can be achieved with rocket engines. A rocket engine operates on the jet propulsion principle, and carries its fuel and an oxidizer to burn the fuel either in the rocket itself, or aboard the vehicle that the rocket propels. Unlike ramjets, pulsejets and gas turbine engines, a rocket engine is not an airbreathing engine; therefore, it is completely independent of the outside atmosphere and can even be operated in the airlessness of outer space.

Based on the different jet engines types described above, a lot of different propulsion system concepts are possible. There is a strong dependence on the required Mach number range and flight trajectory.

Fig. 1 summarizes the above classification. The Mach number regime versus the specific impulse is shown for different aero engines such as turbo engines, ramjets and scramjets as well as for the rocket engine. This plot indicates that for a vehicle

which has to cover a wide Mach number range different propulsion principles must be combined unless a rocket-type engine is selected. However, owing to the fact that the oxidizer must be on board rocket engines have a poor specific impulse.

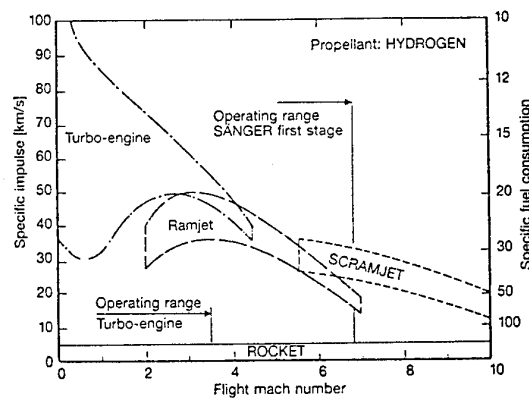


Fig. 1: Operating regimes of airbreathing engines

The different engine principles can be combined in various manners. The number of possible combinations is nearly unlimited, Fig. 2. Application of further components such as air liquefaction devices, ejector systems, pre-coolers or other heat exchangers, increases again the number and complexity.

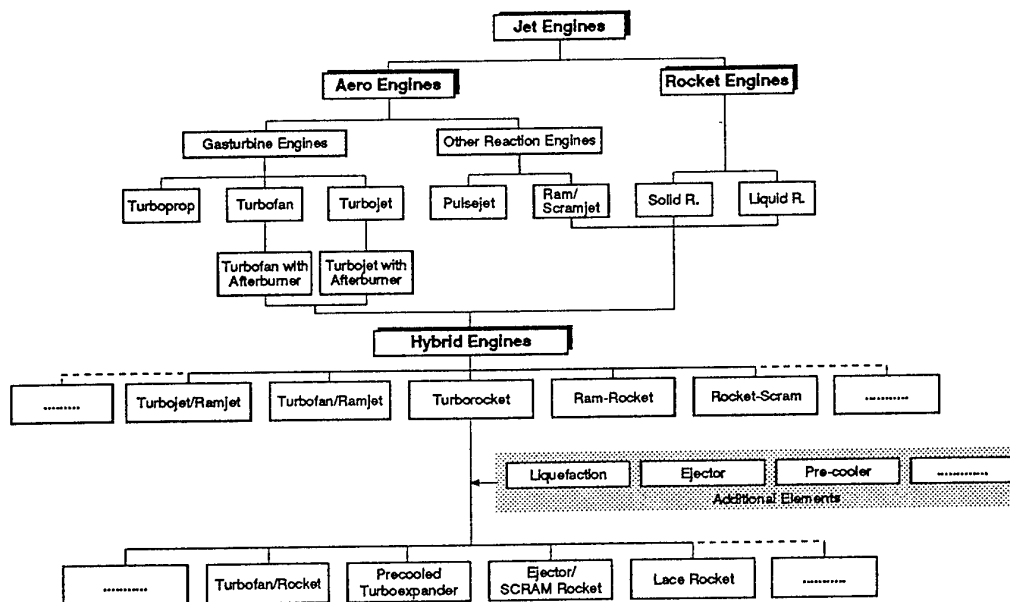


Fig. 2: Propulsion system classification

But most of the combinations are of academic interest only. Achieving the specified thrust over the entire flight path is the ultimate goal. This means that major selection criteria are a low overall engine weight, high engine efficiency together with a good acceleration capability leading to a low overall fuel consumption. The engine installation must be optimized with regard to low installed drag. Further, and very strong selection criteria are the requirements for high reliability, good maintenance and no sophisticated infrastructure to operate the vehicle. From an environmental point of view the engine must have low noise and low emissions. Last but not least engine development and operation must be at low cost and at an acceptable risk.

The answer to the constraints described above and with it the selected engine concept depends very strongly on the flight mission the vehicle has to perform. In the German Hypersonic Technology Programme a two-stage to orbit space transportation reference concept was the baseline. The engine selection process [2, 3] lead to a coaxial turbo ram engine. This is taken as a baseline in the further discussion of the technological challenges associated with combined-cycle engines for hypersonic flight.

3. Engine Reference Concept

The selected propulsion system, outlined in Fig. 3, consists of a rectangular inlet, a boundary layer diverter, a turbine engine featuring a front and a rear closure mechanism to protect the rotating machinery during ramjet operation at extreme temperatures, an afterburner/ram combustor representing the only source of propulsion beyond approx. Mach 3.5 and a rectangular nozzle. The vehicle afterbody is designed for use as a single expansion ramp nozzle. The entire assembly is characterized by a high degree of airframe/powerplant integration. The propulsion system operates in the Mach number range from Mach 0 up to Mach 7. Fig. 4 shows the total intake temperature for different Mach numbers. It is one measure for the technological gap which must be bridged to operate a Mach 7 propulsion system. Detailed descriptions are given in [4, 5].

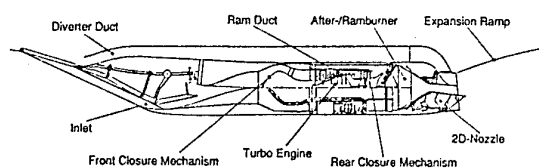


Fig. 3: Sanger propulsion system reference concept

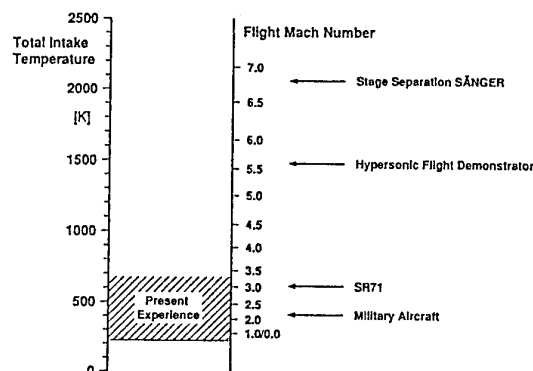


Fig. 4: Total ram temperature for different Mach numbers

4. Challenges associated with the Combined-Cycle Engine Design

In the design and development process of a combined-cycle engine for hypersonic applications features became very important which are of minor importance in engine design for subsonic applications. The additional aspects which must be given special attention are:

- component design at different operation points,
- variable geometry,
- transition in operating mode,
- engine airframe integration,
- thermal management,
- control,
- secondary power systems,

These items will be discussed briefly in the following on the basis of the above reference engine.

Component design points

One key area for the successful development of a hypersonic vehicle is the design of the engine components. They cannot be designed individually without considering their interaction. For example, the size of the intake is determined by the thrust required at maximum flight speed. This, however, has a severe impact on the turbine engine sizing. The turbine engine is designed for the transonic regime at approximately Mach 1.2. In this flight regime the intake usually delivers a mass flow in excess of engine demands. The excess mass must be spilled around the intake cowl thus producing an additional spillage drag. The higher the thrust requirements at Mach 6.8 the greater the intake capture area and, in consequence, the greater the size of the turbine engine necessary to overcome the additional drag. But owing to the larger engine bay the thrust demand at Mach

6.8 rises again and the loop must be entered again. The design points for the different engine components are depicted in Fig. 5. A detailed discussion of the interaction of component size and thrust, fuel consumption and engine weight is given in /6/.

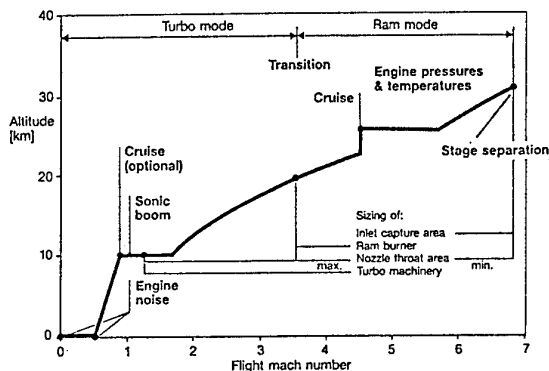


Fig. 5: Engine critical flight conditions

Mode Transition

Combined-cycle engines require transitions from one operating mode to another. Transition will take place in the powered and nearly unpowered descent flight regime. During the powered flight, especially at high Mach numbers, no significant thrust decrease is allowed. This makes sophisticated control procedures necessary.

The following example gives an impression of the transition from turbo to ram mode for the reference concept shown in Fig. 3.

The transition process is subdivided into four phases, Fig. 6. At first the fuel flow to the turbo engine is reduced and the nozzle throat area will open to allow a constant intake mass flow. This avoids additional intake control. The front closure mechanism starts to move when pressure equilibrium at the rear mixing plane is achieved. In the second phase the flow passes simultaneously through the turbine engine and the ram duct. The turbine engine will run down completely and afterwards the turbine engine compartment will be closed and vented. From this point on the mass flow is not restricted by the turbo engine any more so that the intake can be further opened to swallow the maximum possible mass flow. Finally, the boundary layer diverter duct will be closed and all the mass flow is fed through the ram combustor.

During descent the transition process is reversed with the additional complication that the turbine engine must be started in flight.

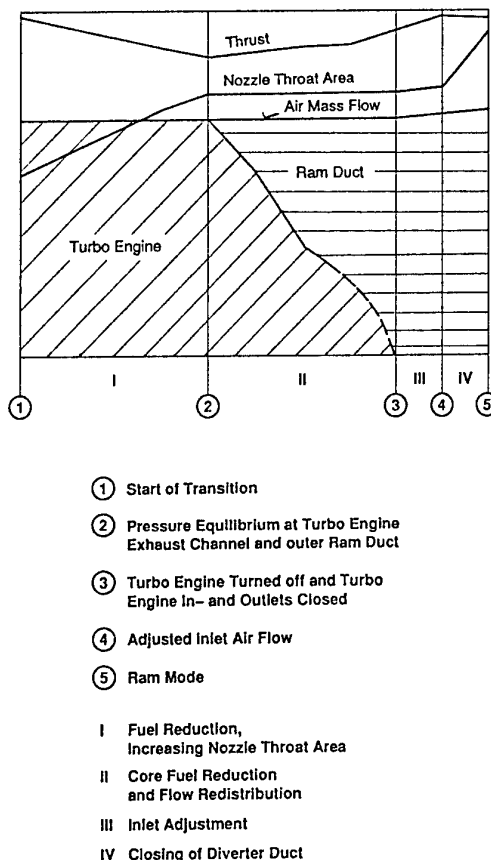


Fig. 6: Transition from turbo to ram operation

Variable Geometry

The intake is one of the most critical parts of an airbreathing propulsion system. Its design must be such that it delivers air to the engine at the desired mass flow rate and flow conditions for all flight Mach numbers. This makes variable ramps mandatory to adjust the intake at each flight point.

The air delivery must be accompanied by as little losses, drag, weight and complexity as possible. This task is often very difficult because the intake is at the interface between the vehicle and the engine /7,8/. Thus, many factors such as vehicle configuration and its overall performance affecting the design of an intake are outside the responsibility of the intake engineer. Therefore, the engineers responsible for external aerodynamics, intake design, vehicle stability and vehicle performance must find a compromise for the final forebody/intake configuration.

An other point of interest is the nozzle design. Nozzle systems for combined-cycle hypersonic engines must be operated from the low-speed range (take-off and landing) up to the maximum flight

Mach number required. The scope of nozzle pressure ratios (i.e. internal total to static ambient pressure) ranges from about 2 to 500 or even 1000 depending on the inlet recovery achieved and the flight trajectory. Therefore, a high variability in nozzle throat area and/or nozzle exit area is required to obtain adequate internal performance. The problem arising is the absolute size of the nozzle exit area for high flight Mach numbers required to avoid detrimental overexpansion losses, which lead to undesired internal and/or external losses. Optimum nozzle design at high Mach numbers leads to unfavourable afterbody angles and flow detachment at base areas in the transonic and low supersonic flight regime, where the nozzle operates in extreme off-design modes. For axisymmetric and symmetric two-dimensional convergent/divergent nozzles these demands result in severe technical problems and unacceptably high weights. Nozzles with single expansion ramp are attractive solutions for the challenging variation requirements outlined above due to their better off-design adaptability. Throat area variation can be achieved with comparably small flaps, which is important with respect to weight, especially in the high-pressure convergent part of the nozzle. The maximum usable nozzle end area is shaped to a large extent by the aircraft fuselage itself.

Engine/airframe integration

The successful approach to hypersonic flight is engine/airframe integration. Fig. 7 indicates that a very close collaboration between the different parties involved is essential for the development of an optimized airframe/propulsion system. The integration requirements depend on the selected engine configuration and on the Mach numbers in which the different engine cycles operate. Detailed information is given in /4, 5, 9/.

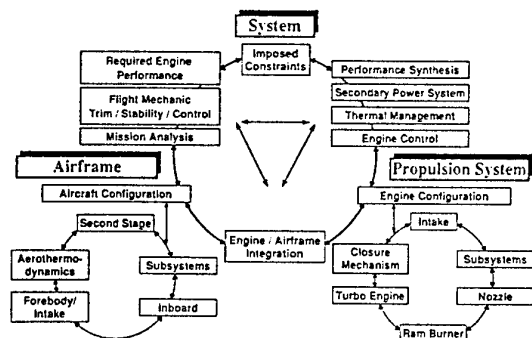


Fig. 7: Integrated team work

5. System Aspects

Secondary Power System

For safe operation of the propulsion system and the vehicle itself secondary power is needed for the engines and the airframe throughout the entire flight.

In conventional turbine-engine powered aircraft all the fuel pumps, hydraulic pumps and electric generators are driven mechanically by the turbine engines. For combined-cycle engines this is usually not possible since different engine cycles operate in different flight phases with and without delivering mechanical energy. An independent secondary power system (SPS) is therefore required, designed as a light-weight system with low fuel consumption, operable in the whole flight regime. Furthermore, the SPS shall ensure the starting of the engines on the ground, provide sufficient energy in the event that no engine is running (emergency power unit), and supply the cooling fluids for the thermal management system.

The thermal management involves the cooling of the propulsion system, air inlet, cockpit and avionics (see below). Owing to the high flight Mach numbers, the cooling systems for hypersonic propulsion systems are of a size and a complexity, unknown for conventional aircraft. Usually hydrogen fuel is used as a heat sink for the whole vehicle while compressed and cooled air is used for sealing and secondary cooling purposes. The SPS is therefore highly integrated not only with the engine but also with the cooling system and, of course, with the overall engine control system.

Again, the SPS system for the Sänger reference concept will be presented as an example /10/. The evaluation of all constraints resulted in a secondary power system comprising five units, which operate in different flight segments, Fig. 8 and 9. It drives three LH_2 pumps for the varying hydrogen fuel demands (a large one for reheated turbo-engine and ramjet operation during ascent; a medium-size pump for turbine engine operation; a small pump for the SPS combustion gas turbine fuel supply, for turbo-engine starting and idling and for ram combustion and cooling during descent), a cooling air compressor for the cooling air after it leaves the LH_2 heat exchanger, a hydraulic pump, a generator and an oil pump for the SPS lubrication system. To reduce the fuel consumption of the SPS the energy for these components is generated by several sources. Two bleed-air turbines (one for SPS ground start and to drive the hydraulic pump, generator, small LH_2 pump and lubrication oil pumps during turbo-engine

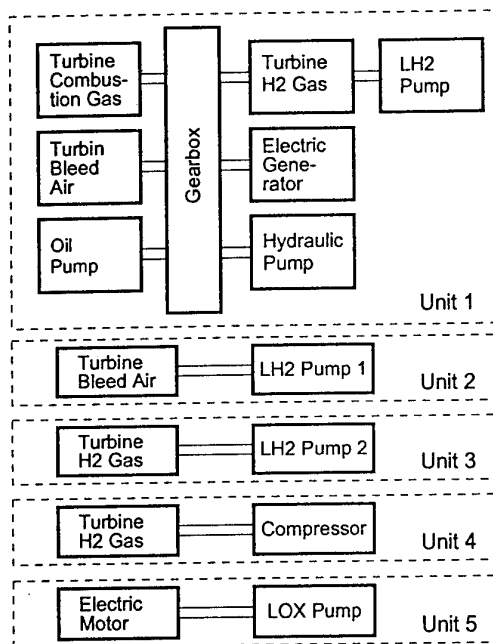


Fig. 8: Sänger secondary power system concept

operation, the other for the turbo-engine fuel pump), three expansion turbines (one for hydraulic pump, generator or small LH_2 pump and oil pumps, one for the ram/afterburner fuel pump, one for the cooling air compressor), using heated H_2 from the cooling system and one combustion gas turbine driven by H_2 and H_2O from the gas generator (for hydraulic pump, generator, small LH_2 pump and oil pumps, for use during low Mach number descent and as an emergency power unit).

To increase the redundancy of secondary energy supply and to simplify the pipe connections each of the five main engines has a separate SPS.

Thermal Management System

High intake air temperatures owing to the high Mach numbers and high internal combustion temperatures demand for active cooling of most parts of the propulsion system. The standard metallic materials presently in use are limited to temperatures in the range of 1200 K to 1300 K. Materials such as ceramics and ceramic composites, which are still under development, are capable of withstanding temperatures of about 2000 K. But even if these materials are available, a sophisticated design and an efficient cooling system are necessary in any case.

The design of the cooling system to ensure maximum cooling effectiveness combined with minimum pressure losses is a cumbersome task. Hydrogen is used as a direct coolant as well as a heat sink. Thermal management is also closely linked to the operating mode of the engine, and influences the secondary power system to a large extent. Fig 10 shows, as an example, the thermal management system for the combined turbo ram propulsion system of Sänger /11, 12/.

The design of effective cooling systems requires detailed knowledge of the heat transfer from the hot gas to the structure and from the structure to the coolant flow /13 - 15/. Phenomena similar to those encountered in aerothermodynamics such as separation, transition and shock wave/boundary layer

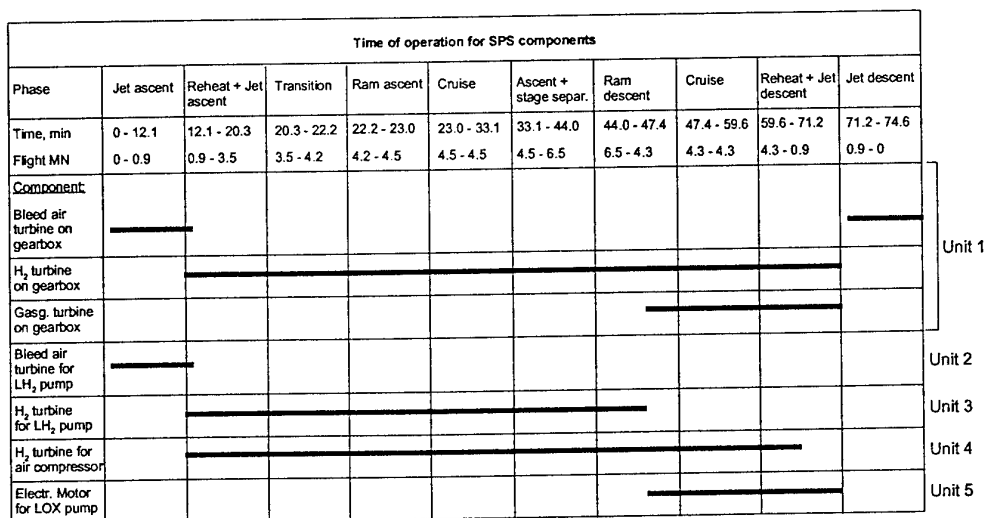


Fig. 9: Operation phases of individual components

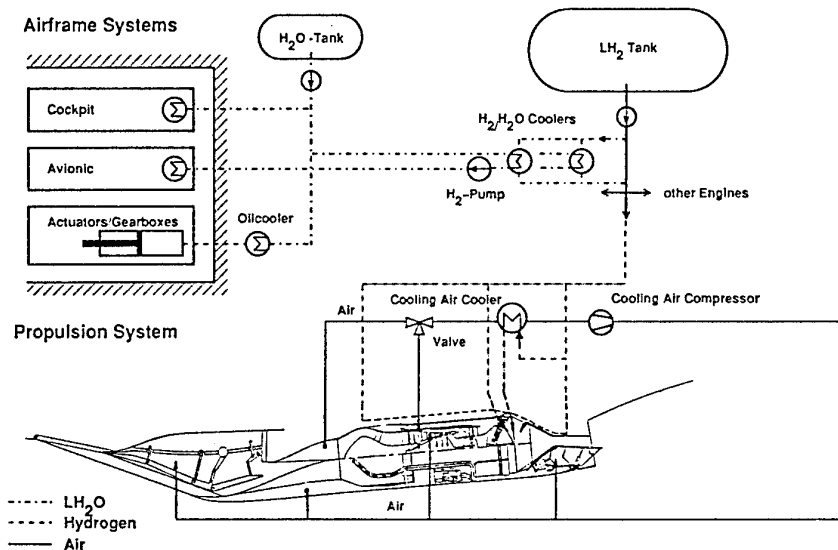


Fig. 10: Thermal management system

interaction must be taken into account. The boundary layer may separate and reattach at some location downstream. At the reattachment point the boundary layer will be thin and as a consequence the heat transfer will be high. If the boundary layer is laminar before separation, there will often be a transition to turbulence depending on the pressure gradients. As a result, the heat transfer rate will increase with downstream distance. A careful balancing of the cooling passages and local heat transfer rates of the coolant is therefore necessary.

The hydrogen flow necessary for cooling purposes should not exceed the flow required for combustion to avoid penalties with respect to hydrogen tank size, since the structural weight of the vehicle largely depends on the tank volume. Excess hydrogen adversely affects the payload of Hypersonic vehicles.

In the ascent phase the Sänger system does not need any additional hydrogen for cooling purposes, see Fig. 11. But as expected, in the first phase of the nearly unpowered descent the hydrogen consumption for cooling purposes exceeds the hydrogen demand of the engines. The optimization of this flight sector is very important and can be achieved either by introducing new materials and structures which can withstand higher temperatures and/or by changing the mission profile and operating modes so that the hydrogen consumption of the propulsion system equals the amount of hydrogen needed for cooling purposes.

Control System

Variable-cycle engines cover a wide Mach number range in which the engine has to deliver thrust. This has a severe impact on the engine control system. Different components and subsystems must be controlled. For the Sänger these are mainly the intake, the turbine engine and the closure mechanism, the ram combustor and the nozzle but also the secondary power system which has to deliver the necessary energy for all pumps, compressors, actuators etc. and the thermal management system.

The engine control is shown in greater detail in Fig. 12. The control functions are subdivided into groups in accordance with the main propulsion components. The measured engine variables are also listed. These are data from the aircraft including the pilots demand data and a variety of data from the

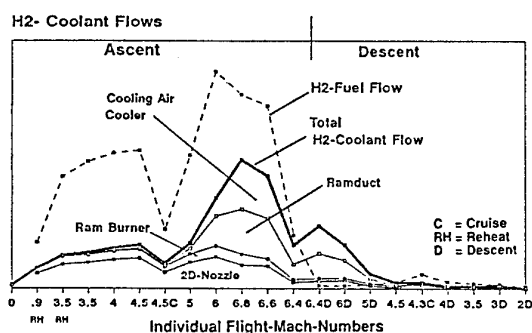


Fig. 11: Hydrogen cooling requirements

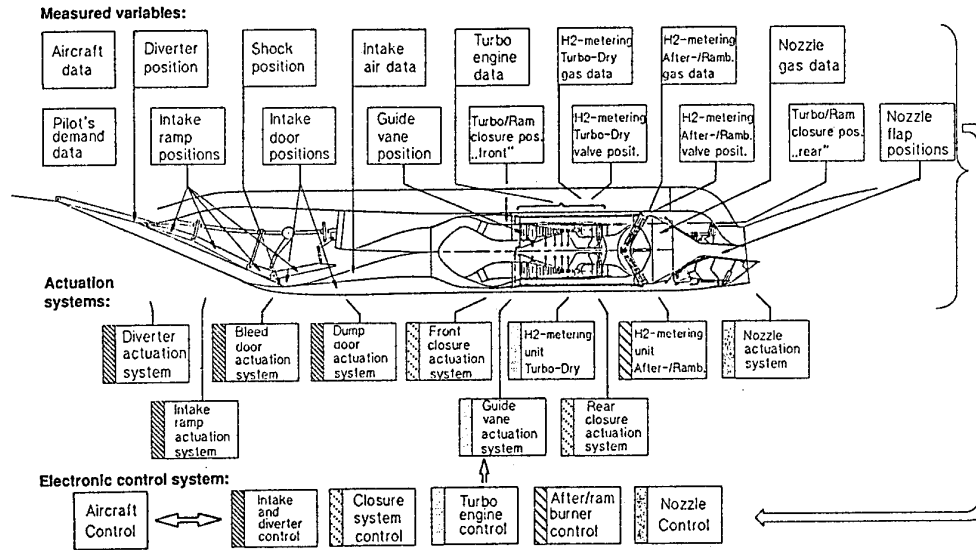


Fig. 12: Control layout of the propulsion system

different engine components. They are all used as input parameters to the electronic control system of the powerplant indicated in Fig. 13. The control unit comprises two major parts: one for the engine itself and the other for the secondary power and cooling systems. Both are closely linked together. Actual values and target values are compared and a signal is given to the various actuation systems for adjusting the desired position.

All major components including the secondary power system and the thermal management system have to be constantly monitored and/or controlled by using open-loop or closed-loop algorithms. A large number of actuation systems then allow the correct matching of actual to rated values throughout the various flight phases of the mission.

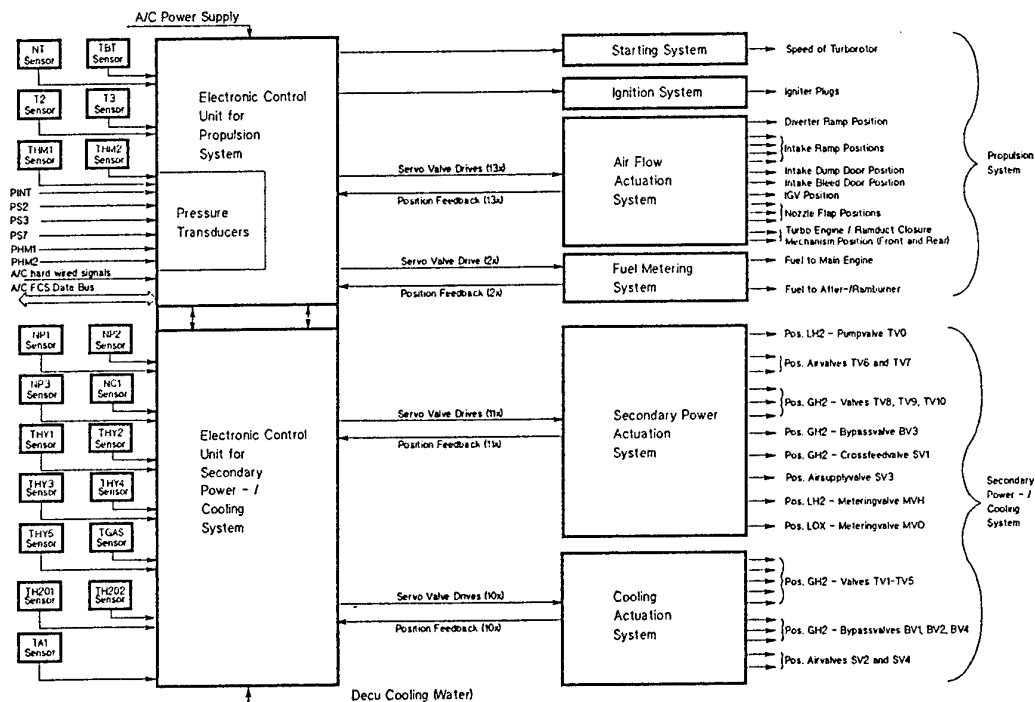


Fig. 13: Control concept for propulsion system and secondary power- / cooling system

7. Conclusions

Airbreathing engines for hypersonic applications are in any case combined-cycle engines. This adds another order of complexity to the propulsion system. There is a great variety of possible engine concepts. But if the goal is to have reliable engines flying the number of promising concepts is declining very rapidly, because apart from the engine weight, development time and risk, reliable operation and maintenance are important selection criteria.

Nevertheless, airbreathing propulsion systems are promising powerplants for reusable space transport systems. They offer significant economic and operational advantages over rocket-based systems. However, a great number of the key technologies needed are still not available today. Furthermore, owing to the highly integrated design and the close interaction of all components, the development of such an airbreathing system requires highly skilled engineers who must also be efficient team workers.

In the design of each engine component as well as the sub-systems design engineers have to face a lot of technological challenges. For flight Mach numbers above 4 nearly all metal structures require cooling. It would be preferable to use advanced materials like ceramic composites, or carbon-carbon composites to keep the total weight of the propulsion system at a minimum. For this purpose advanced materials with high specific strength at high temperatures must be developed.

A step by step approach is necessary. At first basic component technologies have to be developed using sophisticated subscale models, numerical calculations and advanced measurement techniques. In the next step integrated tests have to be carried out, and the results have to be fed back into the component design as well as into the overall system concept. The next goal is ground testing of a complete subscale propulsion system. Since ground testing offers only limited possibilities of simulating actual flight conditions the development process must also be supported by flight testing. Of course CFD calculation must be applied during the whole design process.

Acknowledgements

The authors wish to acknowledge the assistance and contributions of colleagues from MTU DASA and Volvo. This work was funded by the German Ministry for Education, Science, Research and Technology (BMBF).

References:

- /1/ Federal Ministry for Research and Technology, *Hypersonic Readiness Programme* Bonn, BMFT, 1988
- /2/ Voss N., Albers M., *Sänger Propulsion System Options* 2nd EAC Conference, Bonn, 22.-24 May 1988
- /3/ Albers M., Proske S., Kramer P., Voss N., Krebs H., *Evolution of Airbreathing Propulsion Concepts Related to the SÄNGER-Space Plane*, IAF-Paper IAF-88-247
- /4/ Heitmeir F., Schmitt-Thomas K., Dietl U., *Hypersonic Propulsion, Challenges in Design and Materials*, Proceedings of the 2nd Space Course, TU-München, Vol. 2, 1993, pp. 22.1 - 22.28
- /5/ Heitmeir F., Lederer R., Voss N., Bissinger N., Herrmann, *Turboramjets and Installation* AIAA Proceedings of High-Speed Flight Propulsion Systems, edited by Muthy S.N.B., to be published, Oct, 1995
- /6/ Schaber R., Heitmeir F., *Einfluß der Komponentendimensionierung auf die Leistung eines Hyperschallantriebs* DGLR-Jahrestagung, Göttingen Sept. 1993
- /7/ Wilson G., Davis W., *Hypersonic Forebody Performance Sensitivities Based on 3-D Equilibrium Navier Stokes Calculations* AIAA Paper 88-0370, 1988
- /8/ Monnoyer F., *Hypersonic Configuration Optimization with Euler/Boundary Layer Coupling Technique*, AIAA Paper 93-3116, 1993
- /9/ Heitmeir F., Lederer R., Herrmann O., *German Hypersonic Technology Programme, Airbreathing Propulsion Activities* AIAA Paper 92-5057, 1992
- /10/ Trolheden S., Streifinger H., *Secondary Power System Study for the Sänger First Stage Vehicle* AIAA Paper 93-5033, 1993
- /11/ Rüd K., Ebenhoch G., Mark H., *Thermal Management of Propulsion Systems in Hypersonic Vehicles* AIAA Paper 92-0516, 1992
- /12/ Rüd K., Mark H., Götz G., *Heat Management Concepts for Hypersonic Propulsion Systems* AIAA/ASME/SAE/ASEE Joint Propulsion Conference Paper No. 91-2492, 1991
- /13/ Patankar S., *Recent Development in Computational Heat Transfer* ASME Journal of Heat Transfer, Vol. 110, 1988, pp. 1037-1045
- /14/ Launder B. E., *On The Computation of Convective Heat Transfer in Complex Turbulent Flows* ASME Journal of Heat Transfer, Vol 110, 1988, pp. 1112-1128
- /15/ Pletcher R., *Progress in Turbulent Forced Convection* ASME Journal of Heat Transfer, Vol 110, 1988, pp. 1129-1144

Paper 16: Discussion

Question from G Bobula, NASA Lewis, USA

Please could you outline what programmes might be in progress to address the material barriers to the hypersonics programme you presented.

Author's reply

Materials and structures are very important issues in hypersonics. Within the propulsion part of the German hypersonic technology programme a lot of research has been done on these aspects. For example, in the case of the engine nozzle this work resulted in a sophisticated cooling structure for the nozzle itself, which is actively cooled with liquid hydrogen, and in an uncooled carbon/carbon expansion ramp. After two test series, with gas temperatures up to 2800K and ramp wall temperatures up to 1800K, the nozzle was still in a very good condition. The airframe part of the programme also included one work package focused on materials and structures.

DESIGN AND OFF-DESIGN SIMULATION OF HIGHLY INTEGRATED HYPERSONIC PROPULSION SYSTEMS

Th. Esch, S. Hollmeier, H. Rick

Lehrstuhl für Flugantriebe
Technische Universität München
Arcisstr. 21
D-80290 München, FRG

ABSTRACT

The propulsion system for the lower stage of a two-stage-to-orbit transport system (TSTO) is presented with its main components: mixed compression air inlet, combustion chamber and single expansion ramp nozzle (SERN).

Using an implicit finite-volume Navier-Stokes code the flow fields in these components are studied. Comparisons between experimental data and CFD calculations are presented for a two-dimensional high speed inlet, a high temperature reacting three-dimensional combustion chamber flow and a two-dimensional nozzle/afterbody flow field.

For the determination of the forces and moments acting on the propulsion system, comprehensive studies have been performed from transonic to hypersonic flight Mach numbers. The results of the studies form the basis for an accurate description of performance and operating behaviour of the propulsion system by performance analysis.

At hypersonic speeds the effects of the propulsion system on flight-mechanical behaviour is substantial, especially in the event of engine failures. Two failure scenarios have been considered: flame out and inlet choking. For both cases the forces acting on the propulsion system are shown.

c_{fg}	[-]	gross thrust efficiency
h	[J/kg]	enthalpy
p	[Pa]	pressure
q	[Pa]	dynamic pressure
x, y, z	[m]	Cartesian coordinates (aircraft/model fixed)
σ	[°]	thrust vector angle
Π	[-]	pressure ratio
α	[°]	angle of attack
η_b	[-]	combustion efficiency
η_{ke}	[-]	kinetic energy efficiency
κ	[-]	ratio of specific heats
μ	[-]	mass flow ratio

Subscripts

e	exit
g	gross
i	inlet
id	ideal
n	nozzle
w	wall
x, y, z	direction of Cartesian coordinates
t	total
∞	free stream
$*$	nozzle throat
0	inlet entry plane
2	exit plane of inlet
3	inlet plane of combustion chamber
4	outlet plane of combustion chamber
9	exit plane of nozzle

LIST OF SYMBOLS

A	[m ²]	area
F	[N]	thrust vector
Ma	[-]	Mach number
T	[K]	temperature
V	[m/s]	velocity
c_p	[-]	pressure coefficient

1 INTRODUCTION

Horizontal take-off and landing spacecraft meet the main requirements for reusing virtually all space transport system components and considerably simplify the ground operations and flight preparations [1]. Due to lower thrust requirements compared to conventional

rockets or single-stage-to-orbit (SSTO) systems, the two-stage-to-orbit (TSTO) concept allows the use of a combined variable cycle air-breathing turbo-ramjet engine with subsonic combustion. Using parts of the airframe as parts of the propulsion system (e.g. pre-compression along the forebody of the aircraft, "Single Expansion Ramp Nozzle", SERN) can considerably reduce the propulsion system's size and weight. This leads to a strong coupling between the airframe and the engine, making it impossible to consider these two components separately [2].

Within the Special Research Programme (SFB) 255 this subject is studied by the Technische Universität in Munich in co-operation with Daimler Benz Aerospace (DASA).

2 REFERENCE TSTO CONCEPT

Figure 1 shows the reference TSTO concept and its main characteristic data. This concept has been developed by the industry in co-operation with universities in Germany.

The propulsion system of the considered generic TSTO concept is composed of a two-dimensional inlet with mixed external/internal compression, a diffuser with a cross-section changing from rectangular to circular, a two-spool low-bypass turbofan engine, a closure mechanism to seal off the turbo engine section during ramjet operation mode, a reheat/ram combustor and a (quasi-) two-dimensional single expansion ramp nozzle.

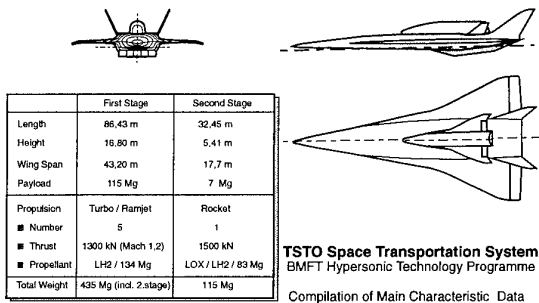


Figure 1: Reference TSTO Concept

The nominal ascent trajectory up to stage separation is shown in Figure 2. After take-off the aircraft climbs to an altitude of approximately 10,000 m where a flight Mach number of 1 is reached. The afterburner is turned on and the aircraft accelerates further. At a flight Mach number near 3.5 the turbofan engine is shut off, the turbo-engine is bypassed and the afterburner is used as ramjet combustion chamber. Stage separation occurs at an altitude of 35,000 m at a Mach number of 6.7.

For the feasibility of a transport system it is not sufficient to consider regular flight operation alone. The behaviour of the system in the event of certain failures has to be investigated as well. For the propulsion system two failure scenarios have been simulated: (1) an

all-engine flame out and (2) an inlet choking, both at a flight Mach number of 6.

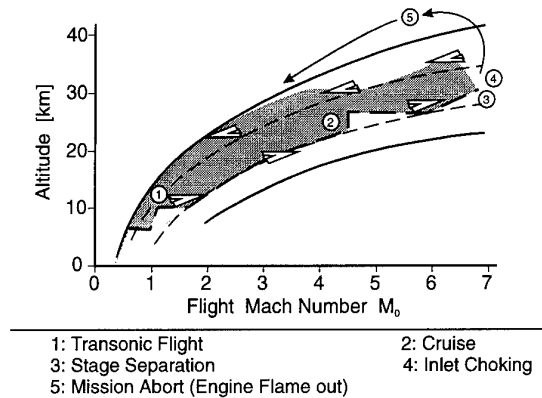


Figure 2: Nominal ascent trajectory with two selected propulsion system failures and a mission abort scenario

3 PROPULSION SYSTEM SIMULATION

To create a compatible formulation of all forces acting on airframe and propulsion system, an overall bookkeeping system has to be defined. In the bookkeeping system used for this study, all forces that are influenced by the engines are summarised in the propulsion data set (with resulting net thrust vector and moment), while all forces that are mainly influenced by the flight vehicle aerodynamics are contained in the aerodynamic data set.

To permit the numeric representation of steady and dynamic engine behavior ('performance analysis') the engine is subdivided into separate modules such as: inlets, compressors, combustion chambers, turbines, nozzles etc. Within each module the basic physical behavior of a component is described by an appropriate set of equations and/or characteristic maps. The engine components are coupled not only via the laws of mass, momentum and energy conservation but also via the engine control system. Therefore the recombination of the different components ("synthesis"), forming the propulsion system results in a large, nonlinear, coupled set of equations that has to be solved by means of an iterative numeric procedure.

The quality of the performance analysis strongly depends on the accuracy with which the basic physical processes within a single engine component are modeled. For example the inlet and the nozzle of airbreathing hypersonic aircraft propulsion systems are characterized by the high degree of integration of engine and airframe, by the extremely high geometric flexibility and thrust performance requirements, by the complex flowfield phenomena within the components and the wide area of largely different operating conditions. An extensive modelling of these components within the performance analysis is usually far too complex. The performance and operating behaviour is therefore

commonly described by characteristic maps, which are based on data provided by experiments and/or theoretical methods such as CFD-analysis. Creating accurate component maps is a key issue in simulating hypersonic air breathing engines, as will be shown in the next paragraph.

SENSITIVITY OF THE PROPULSION SYSTEM Especially at the maximum flight Mach number, the ratio between net thrust and gross thrust of the propulsion system is small. A sensitivity study was therefore carried out, showing the influences of various parameters on the net thrust vector [2]. The results of this study are summarized in Figure 3.

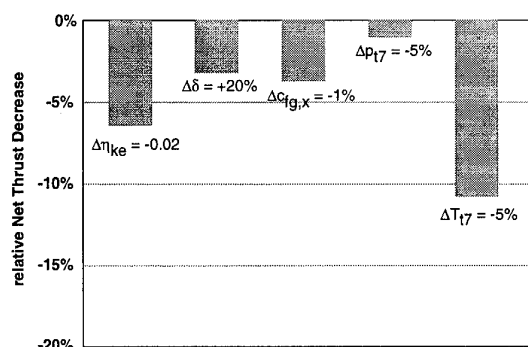


Figure 3: Sensitivity of net thrust vector [2]

A reduction in the kinetic inlet efficiency η_{ke} of 0.02 leads to a decrease in net thrust of about 6.4%. During ramjet operation this is mainly due to the total pressure loss, which amounts up to 30% at a Mach number of 6.8 or approximately 9% at $Ma_0 = 3.0$.

The thrust loss due to a 20% increase in the forebody boundary layer thickness has the same order as the thrust loss due to a 1% decrease in the axial thrust coefficient $c_{f,g,x}$.

A 5% loss in total pressure caused by the combustion process in the ram-combustor reduces the net thrust by roughly 1%, while a reduction of the combustor total temperature of the same order results in a net thrust loss of 8 to 10%.

The numbers shown in Figure 3 confirm that the propulsion systems for hypersonic aircraft are highly sensitive to even moderate changes in component efficiencies or the aircraft attitude.

4 NUMERICAL SIMULATION

For the complete simulation of hypersonic flow fields, not only geometric but also dynamic (Ma , Re) and thermal similarity (κ , T_w , ...) have to be fulfilled. The existing ground based test facilities usually do not allow a full simulation of hypersonic flow, making it difficult to transfer the experimentally obtained data to the full-scale configuration.

Theoretically there are none of those restrictions for the numerical simulation (CFD). Major restrictions (apart from limitations in computing time and storage) are imposed by the implemented physical models, as some physical processes, e.g., turbulence and combustion, are still not easily accessible to a full theoretical description. Furthermore, in order to simplify the computation, assumptions are made that are only approximations of the flow physics (e.g. gas behaviour at high temperature). Deficiencies in the physical models and the implementation of the numerics, e.g. the modelling of convective fluxes and the discretization of the computational domain ('grid density') also have effects on the numerical solution. In addition to grid dependence and other sensitivity studies it is therefore absolutely necessary to validate the numerical methods on the basis of experimental data.

4.1 CFD Method

The Navier-Stokes equations, describing the three-dimensional, steady and compressible flows in conservation form, are solved by means of a finite volume approach using a fully implicit time-stepping method with multigrid acceleration (TASCflow/ASC) [3].

The discretization of the convective terms is based on a skew upwind evaluation of the cell face fluxes together with a physically based correction term (Physical Advection Correction) which makes the method second-order accurate. All time-dependent terms are approximated by first-order backward differences.

To facilitate the computation and to guarantee that the solution method is strongly conservative a single-cell co-located grid with Cartesian velocity components is used.

To account for inter-variable coupling (e.g. pressure/velocity, pressure/density) a fully coupled solution algorithm is used for mass and momentum equations. The coupled algebraic linear system of equations is solved by a multigrid method running a W-cycle.

Two turbulence models are available in the code. The first model is the standard two-equation $k-\epsilon$ turbulence model with log-law wall functions. The second model is a two-layer turbulence model which combines the high Reynolds $k-\epsilon$ model in the fully turbulent outer region with a low Reynolds one-equation model in the viscous region near the wall.

Variable properties are modelled using temperature dependency (thermally perfect gas, $c_p = f(T)$) or temperature-pressure dependency (mixture of reacting gases in chemical equilibrium, $c_p = f(p, T)$).

4.2 VALIDATION OF NUMERICAL RESULTS

SCRAMJET INLET The hypersonic inlet calculated as first test case was originally tested at the NASA Ames 3.5 Foot Hypersonic Wind Tunnel at a nominal test Mach number of 7.4 and a free stream total temperature of 811 K. A schematic drawing of the considered configuration, known as 'P8' inlet, is

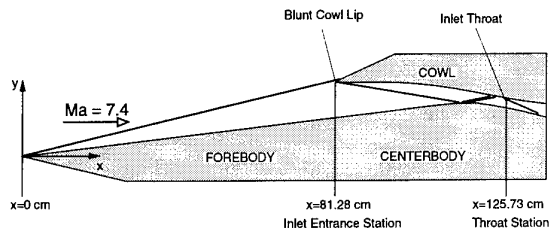


Figure 4: Scheme of hypersonic inlet (P8) and flow field structures

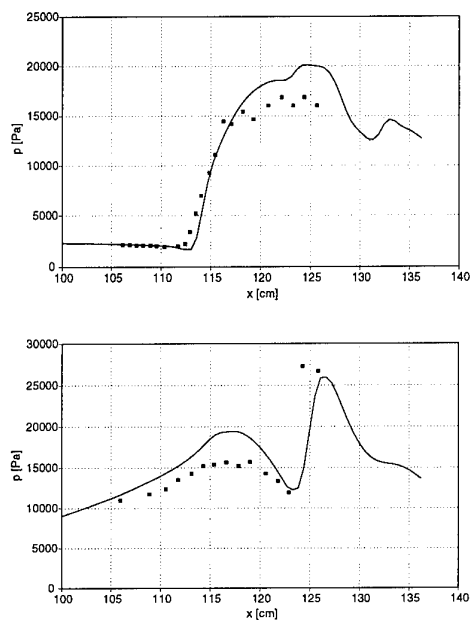


Figure 5: Hypersonic inlet, pressure distribution along centerbody and cowl

shown in Figure 4. The intake is a rectangular mixed-compression inlet with supersonic flow in the outlet region. On design the wedge produces an oblique shock that passes just outside the cowl lip and delivers a Mach 6 flow at the entrance to the internal inlet passage. A second shock is produced by the cowl lip. This shock traverses the internal flow passage and is reflected from the centerbody surface back onto the cowl (Figure 4).

Static pressure was measured along the ramp and the cowl surface. For further comparison pitot pressure and total-temperature profiles are available throughout the internal inlet passage.

The numerical simulations were performed on a grid with $250 \times 60 \times 3$ grid points. Turbulence was modelled using the $k-\epsilon$ turbulence model with wall functions. The gas was considered to be calorically perfect (i.e., constant specific heats) [4].

The static pressure distribution along the ramp/-centerbody and the cowl is shown in Figure 5. Experimental data is shown by the filled symbols, the two-dimensional calculations are marked by solid lines.

Moving downstream along the centerbody surface, the wall pressure stays nearly constant up to approximately $x=112.5\text{cm}$ (Figure 5, top). There the shock generated by the cowl strikes and is reflected from the centerbody surface. This leads to a strong pressure increase that is followed by a further, much slower, increase due to the contouring of the centerbody. The numerical code correctly predicts the shock location and pressure rise, but overpredicts the centerbody pressure further downstream.

Considering the pressure distribution along the cowl (Figure 5, bottom) the pressure increases slowly due to the cowl contour. Then the pressure decreases because of the expansion from the ramp shoulder. At $x=123\text{cm}$ the pressure sharply increases as the reflected cowl shock hits the surface. Considering the CFD results the location of the reflected cowl shock is predicted correctly. The shock strength is slightly underpredicted and the shock is smeared, probably due to a too low grid resolution in this area. The pressure along the front part of the cowl is overpredicted compared to the experimental data. The reason for this might be the overprediction of the displacement thickness of the cowl boundary layer.

Figure 6 (top) shows the comparison between the experimental and theoretical pitot pressure distribution at $x=104\text{cm}$. As before, the experimental data is given by filled symbols and the numerical calculations by solid lines. Considering the experimental data the thick boundary layer which has grown on the ramp surface can be seen in the lower part of the figure. The sharp increase indicates the cowl shock. The gradual pressure rise is caused by the compression on the inside of the cowl. At the top, the thin laminar boundary layer on the cowl is indicated by a sharp decrease in pitot pressure. As noted above, the shock location is predicted very well by the code. The boundary layer thickness for centerbody and cowl are equally well predicted. The pitot pressure in the core flow is overpredicted by the code.

Figure 6 (bottom) shows the comparison between the experimental and numerical pitot pressure distribution at $x=117\text{cm}$, just downstream of the reflection of the cowl shock from the centerbody. The boundary layer along the centerbody has been compressed by the shock. The reflected cowl shock can be seen just above the boundary layer. Due to the contouring of the cowl the pressure increases up to the edge of the cowl boundary layer. Again, the shock location is predicted very well by the code as is the boundary layer thickness at the centerbody. The pitot pressure in the core flow is once more overpredicted by the code, whereas the boundary layer thickness along the cowl is underpredicted.

The agreement between experimental data and numerical results, as shown in Figures 5 – 6, is quite good. Shock location and shock strength are well predicted. Boundary layer development and shock-boundary layer interaction are, at least qualitatively, well reproduced. As stated in [5] the reasons for the discrepancies in the pitot pressure distribution are assumed to be in consequence of differences between the actual test condi-

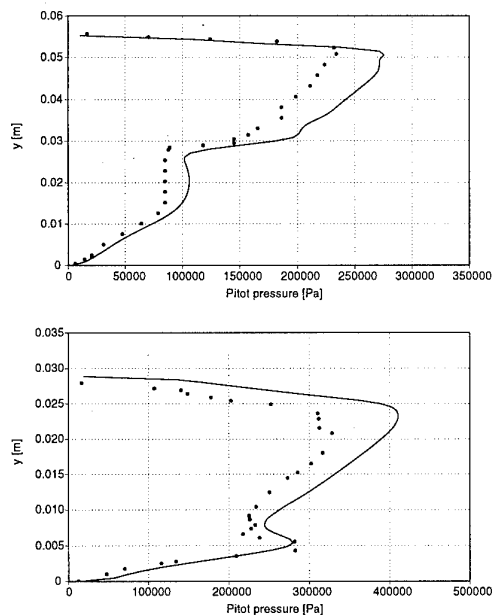


Figure 6: Hypersonic inlet, comparison between experimental and theoretical pitot pressure distribution at $x=104\text{cm}$ and $x=117\text{cm}$

tions and the inlet conditions used for the numerical investigation.

RAMJET INLET Figure 7 shows the experimental setup of the second test case. The ramjet inlet, designated S01A, was tested in the Trisonic Windtunnel at the DLR Cologne [6]. The inlet is again a rectangular mixed compression inlet with subsonic flow behind the inlet throat. At design Mach number ($Ma = 4.5$), the two oblique shocks produced by the inlet ramps are focused on the cowl lip. The shock emanating from the cowl lip is cancelled at the centerbody.

The first ramp of the model has a fixed angle of 10° , the second ramp is movable, to adapt the inlet to different free-stream Mach numbers. The wind tunnel model was equipped with static pressure taps along the ramp and the inside of the cowl. A movable throttle was attached to the divergent part of the inlet to adjust the inlet operating point and to determine the massflow ratio and the total pressure ratio. The model was mounted on a support that could be traversed into the wind tunnel boundary layer to simulate the effects of forebody boundary layer ingestion. The boundary layer that developed along the inlet ramps and the cowl could be removed by boundary layer control.

The calculations were done on a grid with $116 \times 82 \times 3$ grid points. As before the standard $k-\epsilon$ turbulence model was used. Calculations were performed over a Mach number region from 2.5 to 4.5. The free-stream total temperature was 293K, free-stream total pressure was adjusted such that a dynamic pressure $q (= \rho/2V^2)$ of 10^5Pa in the test section was achieved. Figure 8 shows the calculated Mach number distribu-

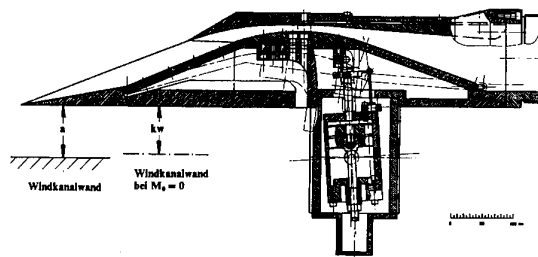


Figure 7: Wind tunnel model of ramjet inlet (S01A)

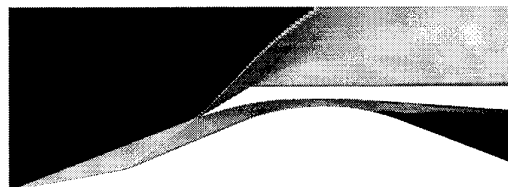


Figure 8: Mach number distribution in ramjet inlet at $Ma_0 = 4.5$

tion in the ramjet inlet. Clearly visible are the two oblique shocks in front of the intake and the final shock in the divergent part of the inlet

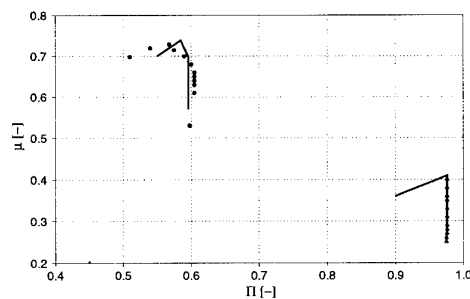


Figure 9: Ramjet inlet, comparison between experimentally and theoretically determined total pressure recovery as function of mass flow ratio

Figure 9 shows measured and calculated total pressure recovery as a function of the mass flow ratio for a free-stream Mach number of 2.5 and 4.5. The filled dots show the data for the inlet at $Ma = 2.5$, the filled triangles show the data for the inlet at $Ma = 4.5$. The bleed system of the inlet was not in use. The measured maximum pressure recovery Π_i for the isolated inlet was 0.729/0.4 at a mass flow ratio μ of 0.568/0.98. The agreement between experimental and numerical data (filled lines) is good, the maximum deviation is less than 2% for the massflow ratio μ_i and less than 2% for the total pressure ratio Π_i . All results are within

the experimental accuracy. Maximum differences occur at the free stream Mach number of 2.5.

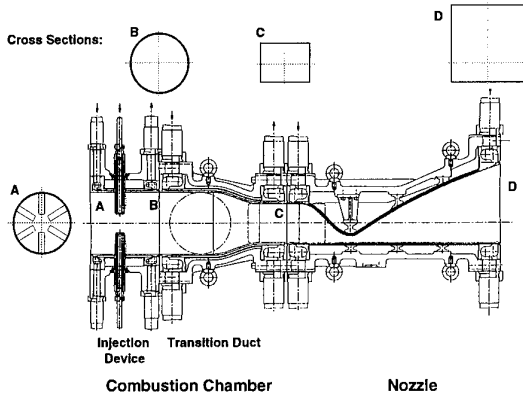


Figure 10: Experimental setup of combustion chamber and transition duct

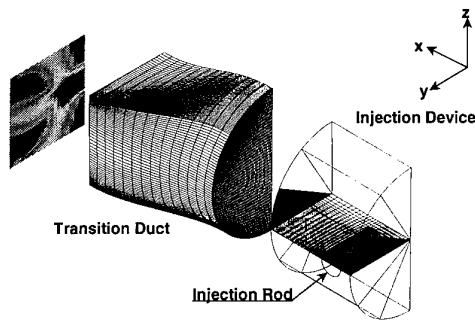


Figure 11: Numerical grids of combustion chamber and transition duct

3D-COMBUSTION CHAMBER To analyze the flow in a hydrogen combustion chamber for a hypersonic ramjet engine the flow code used for the inlet configurations was applied in three dimensions together with an Eddy-Break-Up (EBU) combustion-model for the chemical reactions [3].

The cylindrical combustion chamber has an injection device with 6 arms equally spaced on the circumference. Each of these arms injects hydrogen through a number of small holes in the axial direction of the combustion chamber. Further downstream the cross-section changes from circular to rectangular and the combustion chamber is followed by an asymmetric nozzle, Figure 10.

This configuration meets the basic features of a proposed hypersonic propulsion system and was extensively tested, with different laser methods, at the DLR ramjet test facility in Cologne [7].

First calculations of flows with chemical reactions showed that the flow fields were highly sensitive to the grid resolution. Since the EBU model assumes that the

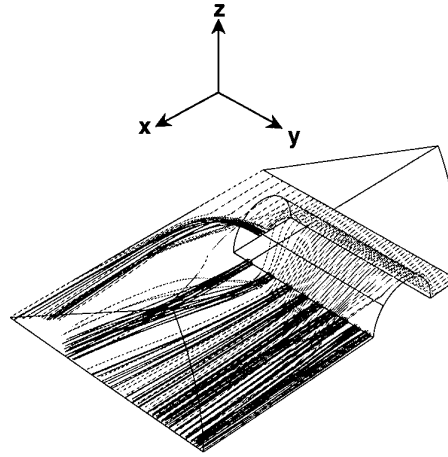


Figure 12: Streaklines in the combustion chamber; dark gray: H_2 , light gray: Air

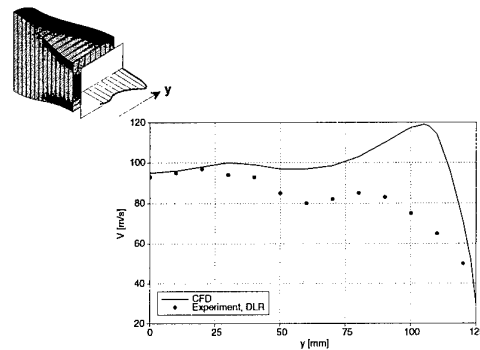


Figure 13: Comparison between experimental and theoretical velocity profiles at the combustion chamber exit plane

combustion process is mainly controlled by the turbulent mixing of fuel and oxidant, the thin shear layers between the fuel and the oxidant component had to be resolved. Modeling the complete combustion chamber at a resolution fine enough would have resulted in a computer model far too large for the computers available. The combustion chamber was split into two models: one for the injection zone and one for the transition duct.

To exploit the high degree of symmetry of the injection device, a 30 degree sector-model around one half of one of the injection rods was generated, containing about 60000 computational cells, Figure 11. The model for the transition duct assumes a symmetry plane in the middle of the duct and therefore only half of the cross-section is discretized with about 80000 cells.

The results from the injection zone are mapped to the inlet of the transition duct and the results at the end of the duct are compared with the measurements.

Because of the alignment of the injection holes with

the main flow direction, the combustion process takes place in stratified zones which extend down to the rectangular exit plane of the transition duct, see Figure 12. Figure 13 shows the calculated and measured (L2F) velocity profiles at the exit plane. The absolute speed corresponds within about 10% and the form of the profiles also agrees fairly well. Larger deviations can be seen near the duct wall ($y=125\text{mm}$), where the combustion model overpredicts the static temperature, leading to an overprediction of the speed near the walls. Nevertheless, since the flow field strongly depends on the chemical reactions in the combustion chamber the agreement found is encouraging.

2D-NOZZLE/AFTERBODY MODEL The performance of the exhaust system of a hypersonic aircraft is not only described by the thrust nozzle performance but it is also strongly influenced by the integration of the nozzle into the airframe [8, 12].

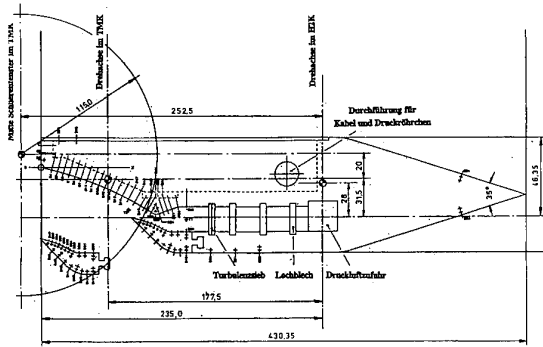


Figure 14: Wind tunnel model

To study the interference between the main nozzle flow and the ambient flow a generic windtunnel model (Figure 14) was built and tested in the Trisonic Windtunnel (TMK) and the Hypersonic Windtunnel (H2K) at the DLR in Cologne [13].

To provide an external flow with known flow conditions, the nose of the wind tunnel model is sharp and wedge-shaped. The model is further characterized by the blunt afterbody with a large lower nozzle flap compared to the combustor exit height. Air for the main nozzle flow is supplied through the model support strut. The model was equipped with sidewalls to ensure two-dimensionality of the flow in the test region. The locations of the static-pressure orifices along the expansion ramp and the lower nozzle flap are shown in Figure 14. Shadowgraph photographs were obtained in the afterbody region. The experimental tests were performed over a wide region of different free-stream Mach numbers and nozzle pressure ratios.

Figure 15 shows comparisons between calculated and measured wall pressure distributions along the upper nozzle wall plus expansion ramp and along the lower flap for two different flight Mach numbers, angles of attack and nozzle pressure ratios [8]. Experimental data are represented by filled symbols, solid lines show the results of the two-dimensional Navier-Stokes cal-

culations. Moving downstream along the upper nozzle wall the wall pressure remains constant up to the nozzle throat ($x = 0.97\text{m}$), where the flow is strongly accelerated and the static pressure drops sharply. The pressure decreases further along the external expansion ramp. The agreement with the experimental data is very good for both operating points shown. The code accurately predicts the pressure drop along the nozzle throat and is in very close agreement with the experimental data along the external ramp.

Discrepancies between the experimental and theoretical wall pressure distributions can be seen along the lower nozzle flap. The extension of the flow separation along the flap seems to be underpredicted by CFD regardless of the free-stream Mach number. Unfortunately, the exact position of the oblique shock preceding the separated flow cannot be determined by the experimental results. During the calculations it transpired that shock location and flow separation were highly sensitive to grid resolution and the turbulence model used [8]. The discrepancies along the lower side of the windtunnel model ($x > 0.12\text{m}$) for the simulation Mach number of 1.75 are probably due to disturbances of the flow field by the nose shock of the model, which is reflected at the windtunnel walls and the model itself. To avoid those undesired influences on the measurement in the transonic flight range, further experiments will be carried out at larger test facilities (TWG, DLR Göttingen).

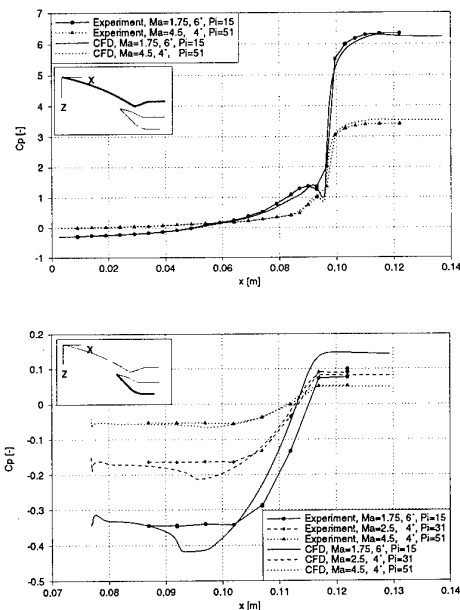


Figure 15: Afterbody model, wall pressure distribution

4.3 1-DIMENSIONAL METHODS

The use of costly 2D or 3D Euler/Navier-Stokes methods is not always possible, especially when the number

of different operating points that have to be considered is very large. In these circumstances it is necessary to use simpler methods that allow for a much faster and easier estimation of the performance of the propulsion system. Using 1D or quasi-1D methods it is possible to carry out parametric studies, identifying the main influences of changes in, for instance, geometry, operating conditions or component efficiencies on the performance- and operating behaviour of the engine.

In the next paragraphs 1D-models for the three major components of the considered propulsion system will be presented.

INLET The inlet is divided into an external and an internal flow field. The flow properties in the external flow field are described by oblique shock relations, the flow in the internal part of the inlet is influenced by a combination of oblique shocks, isentropic compression up to the inlet throat and a final normal shock. The position of the throat shock in the inlet duct is determined by the Mach number in front of the normal shock. For the calculations presented in this paper this Mach number was defined as $Ma_{throat} + 0.2$. The flow field behind the normal shock is fully subsonic.

The pressure ratio Π_i of the inlet is calculated from the pressure ratio across the shock system (oblique shocks and normal shock; $= \Pi_{inviscid}$) corrected by $(\Pi_{\eta_{ke}=0.92}/\Pi_{opt})$, i.e. the pressure ratio of an inlet with a kinetic inlet efficiency of $\eta_{ke} (= c_2^2/c_0^2) = 0.92$ divided by the maximum possible pressure ratio Π_{opt} for this specific inlet geometry, as determined after Oswatitsch [9]. Experience has shown that with this formulation it is possible to account for the total pressure losses due to viscosity, shock-boundary-layer interaction etc.

COMBUSTION CHAMBER The flow in the ramjet combustor is considered to be governed by the equations for one-dimensional flow with heat addition. The gas is regarded as thermally perfect, i.e. $c_p = f(T)$. With the prescribed conditions in the inlet plane of the combustor and along with the appropriate equation of state and the specified amount of heat added, these equations can be solved for the conditions in the exit plane of the combustor. To account for an incomplete combustion process, combustion efficiency η_b is used. Because no closed-form analytical expression can be obtained, a numerical solution is required.

SINGLE EXPANSION RAMP NOZZLE

Due to the asymmetric shape of the single expansion ramp nozzle (SERN), the thrust vector shows large variations (magnitude and direction) throughout a flight mission [10]. This is especially true for the region of transonic flight Mach numbers.

A one-dimensional description of the SERN is usually not possible, because of the flow leaving the nozzle at some arbitrary angle and the flow field values continuously changing along the nozzle exit plane.

In case of a fully two-dimensional problem definition the nozzle can be divided into a symmetric part up to the lower nozzle flap and a region in which the nozzle

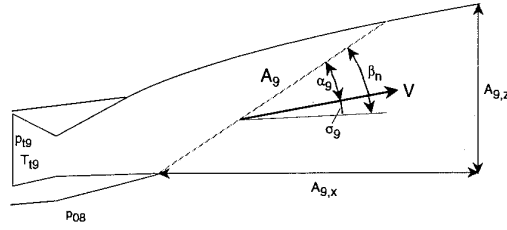


Figure 16: Single expansion ramp nozzle, geometry and definitions

flow expands around the trailing edge of the nozzle flap (Prandtl-Meyer expansion). Along the Mach lines the Mach number is constant, as are the static flow field values and the flow angle. This makes it possible to develop a one-dimensional method for the evaluation of the performance of a SERN nozzle.

In the case of an adapted flow, the nozzle flow expands to ambient conditions. The Mach number in the nozzle exit plane can then be determined by:

$$Ma_0 = \sqrt{\frac{2}{\kappa_0 - 1} \left[\left(\frac{p_{t9}}{p_{08}} \right)^{\frac{(\kappa_0 - 1)}{\kappa_0}} - 1 \right]}$$

The area necessary for the expansion to the ambient pressure is derived from the continuity equation:

$$A_0 = \frac{\dot{m}_0 RT_0}{p_0 \sqrt{\kappa_0 RT_0}}$$

This holds true as long as A_0 is smaller than $A_{0,max}$, with $A_{0,max} = \sqrt{A_{0,x}^2 + A_{0,z}^2}$. The angle between the nozzle flow in the exit plane and a reference line (e.g. fuselage datum line) is given by (see Figure 16):

$$\sigma_0 = \beta_n - \arcsin \frac{1}{Ma_0}$$

Assuming, that p_{ref} equals p_0 the gross thrust may be calculated by integrating the momentum of the nozzle flow in the exit plane A_0 .

For A_0 larger than $A_{0,max}$ the static pressure in the nozzle exit plane is higher than the ambient pressure (underexpanded nozzle flow). In this case, the exit area (i.e. $A_{0,max}$), the total pressure and the total temperature are known, but not the static flow field values in the exit plane. These values may be determined from the following relation:

$$Ma_0 = \sqrt{\frac{2}{\kappa_0 - 1} \left[\left(\frac{\dot{m}_0}{p_{t9} A_0^*} \sqrt{\frac{R}{\kappa_0} T_{t,9}} \right)^{\frac{2(1-\kappa_0)}{(\kappa_0+1)}} - 1 \right]}$$

This relation can be derived from the continuity equation $\dot{m} = \rho V A$ with the help of the ideal gas-law and the definitions of Mach number, total pressure and total

temperature. A_9^* is the area necessary for full expansion of the considered nozzle flow to ambient conditions and is therefore equal to A_9 shown above.

With the known values of p_9 and Ma_9 the gross thrust F_n and the gross thrust vector angle σ_n of the asymmetric nozzle can be calculated.

4.4 COMPARISON OF NUMERICAL RESULTS

$Ma_0 = 2.5$			
	Theory		Experiment [6]
	1D Inviscid	2D Viscous	
μ_i [-]	0.583	0.576	0.568
Π_i [-]	0.742	0.739	0.729
Max. Π_i for given throat area (0.00321 m ²)			
$Ma_0 = 4.5$ (Design Point)			
	Theory		Experiment [6]
	1D Inviscid	2D Viscous	
μ_i [-]	1.00	0.976	0.979
Π_i [-]	0.416	0.409	0.400
Max. Π_i ratio for given throat area (0.00102 m ²)			

Table 1: Ramjet integral performance parameters at $Ma_0 = 2.5$ and $Ma_0 = 4.5$, optimum ramp position, no bleed

INLET FLOW Table 1 compares integral performance parameters calculated by the 1D-method with results of 2D Navier-Stokes calculations and experimental data for the ramjet inlet as described in the paragraph above. The inlet was fully started and the boundary layer control system was not in use. The experimental values for μ_i and Π_i shown are the maximum values that could be achieved for a fixed inlet throat height. The pressure and massflow ratio calculated by the 2D Navier-Stokes code were obtained exactly as in the experiment by increasing the inlet back-pressure until the internal shock system was expelled (inlet unstart). The results of the 1D-calculation are based on the above-mentioned assumptions.

At the design point of $Ma_0 = 4.5$ both theoretical methods accurately describe the inlet performance. The maximum deviation in the massflow ratio is 2.1% for the 1D-method and 0.3% for the 2D Navier-Stokes code. The massflow through the inlet is overpredicted by the 1D-method because the boundary layer developing along the inlet ramps is neglected. The total-pressure ratio Π_i seems to be overpredicted by the theoretical methods, though both results are well within the accuracy of the experiment (+/- 3%).

At a Mach number of 2.5 the agreement between theory and experiment is not as good as before. The massflow ratio μ_i is again overpredicted by the theoretical methods (1D: 2.6%, 2D Navier-Stokes: 1.4%). Both numerical methods also overpredict the pressure ratio

of the inlet. Compared with the experiment, the values for Π_i are 2% too high for the 1D-method and 1.3% too high for the 2D Navier-Stokes calculation.

For an accurate prediction of the propulsion system performance throughout a flight mission, it is also necessary to consider situations, where the system has to be operated well outside the design specifications. For an inlet, this might occur when the internal shock system is expelled and a quasi-normal shock is in front of the inlet (inlet unstart). This case is shown in table 2. For the free stream Mach number of 3.0 the back-pressure was adjusted to a value given by the experiment, where it was known that the internal shock system is expelled. The final normal shock is now in front of the inlet cowl and subsonic fore-spillage exists. Compared to the case of nominal inlet operation at $Ma=3.0$ the massflow ratio μ_i is reduced by approximately 6.5%, whereas the pressure ratio Π_i is increased by nearly 17%.

For the one-dimensional calculation it was assumed, that the normal shock is just in front of the cowl lips. The flow in the internal inlet duct is fully subsonic and isentropic. The maximum possible massflow is now determined by the throat area. Due to the large total pressure loss across the normal shock in front of the inlet, this massflow is smaller than in the case of nominal operation. The performance values obtained by these assumptions are in good agreement with the experimental data ($\Delta\mu_i = -2\%$, $\Delta\Pi_i = 1\%$). The results of the 2D Navier-Stokes code show values that differ only slightly more from the experimental values ($\Delta\mu_i = 1.3\%$, $\Delta\Pi_i = 1.7\%$).

The comparison between the experimental data and the calculation has shown that for the considered ramjet inlet one- or two-dimensional calculations were sufficient to describe the inlet performance accurately. Usually it is necessary to perform 3D-calculations in order to capture all important inlet flow field structures (e.g. side-spillage, corner-flows).

$Ma_0 = 3.0$			
	Theory		Experiment [6]
	1D Inviscid	2D Viscous	
μ_i [-]	0.615	0.634	0.626
Π_i [-]	0.624	0.629	0.618
Max. Π_i for given throat area (0.00232 m ²)			

Table 2: Inlet Unstart, comparison of ramjet integral performance parameters at $Ma_0 = 3.0$

COMBUSTION CHAMBER FLOW In table 3 the arithmetic mean values in the model combustor exit-plane as calculated by the 1D-method, the 3D Navier-Stokes code with combustion model and the experiment [7] are shown.

At first sight the very low combustion efficiency of $\eta_b = 0.84$ in the experiment and the large discrepancies between the 3D results and the experiment are surprising. However, from a closer look at the experimental

		Theory		Experiment
		1D	3D	[7]
Π_b	[-]	0.995	0.995	n.a.
\bar{T}	[K]	1975	1385	1866 (- 2132)
\overline{Ma}	[-]	0.096	0.079	0.083
μ_b	[-]	0.84*	0.50†	0.84†
*: as given from the experiment				
†: calculated from unburnt H_2 in combustor exit plane				
$\dot{m}_{Air} = 400 \text{ g/s}$, $\dot{m}_{H_2} = 10 \text{ g/s}$, $\phi = 0.86$				

Table 3: Averaged flow field values in the model combustor exit-plane

setup (Figures 10, 12) it is obvious that the injection of H_2 parallel to the main flow direction leads to a very low mixing of fuel and air, resulting in a rather inefficient combustion process. While in the theoretical investigation a pronounced flow field structure in the combustor exit plane is the result of this axial injection, this structure is not as marked in the experiment. There are many possible problems for a theoretical description of this process, of which only some will be mentioned:

1. The calculation of the combustion chamber flow turned out to be a highly three-dimensional and unsteady problem, that cannot be accurately solved by the assumption of flow field symmetry and time- and space-invariant boundary conditions [11].
2. The numerical results turned out to be very sensitive to grid resolution. The number of grid-points used for the calculation (140.000) is probably still too low. The shear layers between the injected fuel and the oxidant (air) are not resolved sufficiently, so the combustion process cannot be modeled accurately.
3. A further source of uncertainty is the combustion model that was used for the calculations. This model ('Eddy-Break-Up' model) assumes, that the chemical reaction rates are directly related to the time required to mix the components. In turbulent flow the mixing time is dominated by characteristic turbulence time scales. In addition, the implemented model only allows one single-step reaction, i.e. one fuel component, one oxidant and a single product.

The average results of the 1D combustor code are in better agreement with the experimental data, though the prediction of flow field values in the combustor exit plane is sensitive to the combustion efficiency, that is not always known in advance.

SINGLE EXPANSION RAMP NOZZLE

In table 4 the integral performance parameters of a SERN calculated by the proposed 1D-method and results of 2D Euler/Navier-Stokes calculations are compared. For the Mach number of 1.5, 3.5 and 6.1 the results of the 1D-method and the 2D Euler solution agree very well, with deviation in $c_{fg,x}$ being below

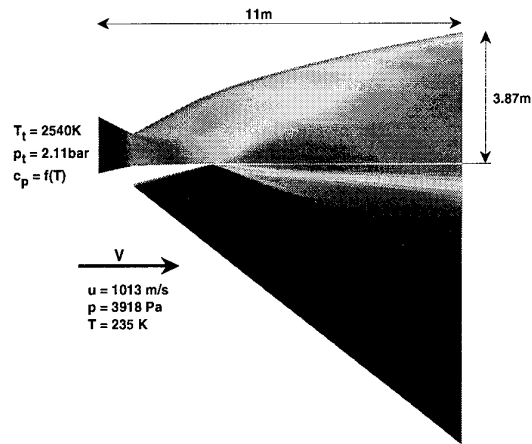


Figure 17: SERN, operating conditions and main geometric data, $Ma_{08}=3.5$

1.6%. The maximum difference in the thrust vector angle σ_n is also smaller than 0.4° .

A comparison between the 2D Euler (inviscid) and the 2D Navier-Stokes (turbulent, viscous) results shows, that the axial thrust coefficient $c_{fg,x}$ is reduced by 0.3% for the Mach number of 1.5 and by 0.7% for the Mach number of 3.5. There are no significant differences for the Mach number of 6.1.

Compared to the 2D Navier-Stokes calculation, the 1D method overestimates the nozzle performance at $Ma = 6.1$ by 0.6%. Referring to Figure 3, this results in a net thrust overprediction of approximately 3%.

5 SIMULATION OF COMBINED PROPULSION SYSTEM

Based on performance maps created by the previously described one- and two-dimensional methods, the reference propulsion system was simulated.

Figure 18 shows the engine force vectors and the resulting net thrust vector for a single two-dimensional engine at a flight Mach number of 6 and an angle of attack of 6 degrees for nominal operation and various engine failures.

At flame-out of the ram combustor the intake would still work normally, but the nozzle would produce less thrust due to the lower gas temperature. The resulting net force would have a small drag and lift component. Possibly due to a failure in the control system the intake could unstart, i.e. the internal shock system is expelled and subsonic fore-spillage exists. 10% flow reduction and 80% flow reduction through the intake were studied in a two dimensional analysis. Dependent on the degree of choking this could result in excessively large intake forces that might damage the air-

$Ma_0 = 1.5$				
		Inviscid		Viscous
		1D	2D	2D
σ_n	[°]	-13.2	-13.78	-13.47
μ	[-]	1.0	1.0	0.999
$c_{fg,x}$	[-]	0.975	0.966	0.972
$c_{fg,z}$	[-]	0.236	0.237	0.234
$F_{id} = 697 \text{ kN}$, $\dot{m}_{id} = 360.8 \text{ kg/s}$, $\Pi = 19$				
$Ma_0 = 3.5$				
		Inviscid		Viscous
		1D	2D	2D
σ_n	[°]	-5.95	-6.23	-6.37
μ	[-]	1.0	0.991	0.988
$c_{fg,x}$	[-]	0.981	0.972	0.965
$c_{fg,z}$	[-]	0.102	0.105	0.108
$F_{id} = 661.7 \text{ kN}$, $\dot{m}_{id} = 297.3 \text{ kg/s}$, $\Pi = 53.9$				
$Ma_0 = 6.1$				
		Inviscid		Viscous
		1D	2D	2D
σ_n	[°]	4.5	5.87	5.86
μ	[-]	1.0	1.0	1.0
$c_{fg,x}$	[-]	0.960	0.954	0.954
$c_{fg,z}$	[-]	0.042	0.098	0.098
$F_{id} = 915 \text{ kN}$, $\dot{m}_{id} = 337.2 \text{ kg/s}$, $\Pi = 583.9$				

Table 4: Single expansion ramp nozzle, integral performance parameters, no base drag due to lower nozzle flap

frame structure.

The disturbed flowfield in front of an unstarted intake might also lead to a sympathetic unstart in the adjacent intakes. Although the three dimensional forces acting on an engine are possibly smaller than those shown in this two-dimensional analysis, an unstarted intake should be avoided under all circumstances.

6 CONCLUSIONS

Within this study different numerical methods have been successfully used to calculate the integral performance parameters for (1) a ramjet inlet, (2) a combustion chamber and (3) a single expansion ramp nozzle of an integrated hypersonic aircraft engine.

Validation of the numerical methods and the physical models was performed by recalculating a set of well-defined experiments and comparing local and global experimental and numerical results. The agreement

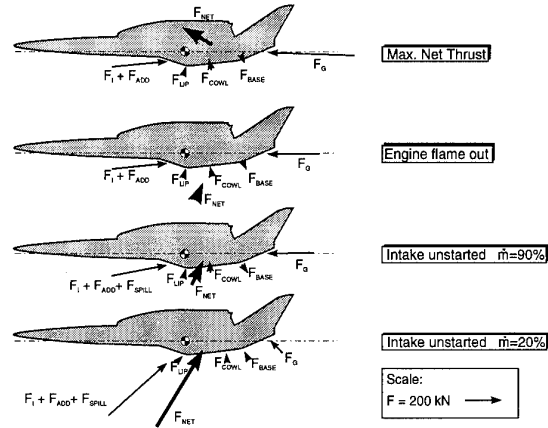


Figure 18: Propulsion system forces and net thrust at Mach 6 for nominal operation, engine flame-out and two different degrees of engine choking

between measurement and calculation was quite good in nearly all the test cases. The high-temperature, reacting flow field in a model combustor presented difficulties to the numerical codes. The combustor performance, as predicted by 3D Navier-Stokes calculations is still subject to large errors.

One-dimensional methods for the estimation of the performance of ramjet-inlets, combustion chambers and asymmetric SERNs were presented together with comparisons between results of 1D-/2D-calculations and experimental data. It could be shown, that the one-dimensional methods can describe the propulsion system over a wide range of operating conditions. This makes it possible to use costly CFD methods only for recalculating operating points of special interest.

A study was carried out to show the sensitivity of the net thrust on changes in component efficiencies or operating conditions. It was found that the propulsion system of hypersonic aircraft is highly sensitive to changes in component efficiencies or the aircraft attitude.

The forces acting on the combined propulsion system were simulated not only for nominal operation but also for two engine-failure situations.

7 ACKNOWLEDGEMENTS

This study was carried out within the framework of the German Hypersonic Technology Programme funded by the BMFT and within the Special Research Programme 255 (SFB 255, Project B1, Prof. Dr.-Ing. H. Rick) funded by the DFG. The authors are grateful for the support given by the MTU München, the DLR Cologne and the Technische Universität München, Lehrstuhl für Flugantriebe. Special thanks to Marcus Giehl, MTU München, for supplying the results of the combustion chamber flows.

References

- [1] Weingartner, S., "Sänger - The Reference Con-

- cept of the German Hypersonics Technology Programme", AIAA-93-5161, Munich, 1993
- [2] Bauer, A., "Betriebsverhalten luftatmender Kombinationsantriebe für den Hyperschallflug unter besonderer Berücksichtigung der Triebwerksintegration", Dissertation, TU Munich, 1994
 - [3] Advanced Scientific Computing Ltd. "Theory Documentation", Waterloo, Ontario, Canada, 1992
 - [4] Bader, R., Esch, Th., "Numerische Berechnung von Hyperschall-Einlaufströmungen", Interner Institutsbericht LFA-Ba/Es-3/95, LFA, TU Munich, 1993
 - [5] AGARD ADVISORY REPORT 270, "Air Intakes for High Speed Vehicles", AGARD-AR-270, September 1991
 - [6] Krohn, E.-O., Triesch, K., "Parametrische Untersuchung am ebenen Einlauf S01A im TMK", Technical Report IB-39113-90C17, DLR-WT-WK, Cologne, 1993
 - [7] Zielinski, M., "Ergebnisse der Meßkampagne mit verschiedenen Lasermessverfahren am Austritt der H₂-Brennkammer", MTUM-B94 EEN-0003, 1994
 - [8] Esch, Th., "Navier-Stokes-Rechnungen zur Triebwerksstrahl Interferenz beim MTU-Heckmodell, Vergleich Experiment - Rechnung", Interner Institutsbericht LFA-Es-2/93, LFA, TU Munich, 1993
 - [9] Oswatitsch, K., "Grundlagen der Gasdynamik", Springer Verlag, 1976
 - [10] Esch, Th., Giehrl, M., "Numerical Analysis of Nozzle and Afterbody Flow of Hypersonic Transport Systems", ASME, 94-GT-391, Den Haag, Netherlands, 1994
 - [11] Mühleck, P., "Numerische Untersuchungen turbulenter, reagierender Strömungen in Brennkammern und Schubdüsen von Hyperschall-Staustrahltriebwerken", Dissertation, Ruhr-University Bochum, 1995
 - [12] Herrmann, O., Rick, H., "Propulsion Aspects of Hypersonic Turbo-Ramjet-Engines with Special Emphasis on Nozzle/Aftbody Integration", ASME, 91-GT-395, Orlando, Fl., 1991
 - [13] Niezgodka, J., "Druckverteilungsmessungen zur Simulation der Interferenz des Triebwerksstrahles auf das Heck der Sänger-Unterstufe (MTU-Heckmodell)", Technical Report IB-39113-93C15, DLR-WT-WK, Cologne, 1993

Performance Optimization of a Turboramjet Engine for Hypersonic Flight

B. Bareis, W. Braig
 Institut für Luftfahrtantriebe, Universität Stuttgart
 Pfaffenwaldring 6, 70569 Stuttgart
 Germany

SUMMARY

For an acceleration flight mission of the lower stage of a two-stage space transportation system a turboramjet engine is investigated. This propulsion system uses a burner behind the turbo engine which acts as an afterburner in turbo mode and as a ramburner in ram mode. Engine performance calculations are applied to evaluate the effect of design features and to optimize the engine operation. Special emphasis is taken on the influence of the power limiting controls and variable geometries. In a multistep calculation procedure the interference between the vehicle aerodynamics and engine performance is considered. The engine control parameters are varied systematically to evaluate the effects on the engine performance and on the mission fuel consumption. The engine control parameters are optimized for a fuel efficient mission using an energy-state approach. Furthermore the changes in operation mode are investigated such as the transition from turbo to ram operation. Exemplary, variable geometries are utilized to minimize the time for the shut-down of the turbo engine.

1 INTRODUCTION

The feasibility of a two-stage space transportation system with airbreathing propulsion systems has been investigated extensively in the recent past, [1]. These studies have shown a strong dependency of the overall system efficiency on the technological standards assumed. The accurate prediction of the propulsion system performance has been identified as a key element for a successful development of space transportation systems.

Engine performance calculation programs have been developed for the investigation of several engine concepts, considering the special installation requirements of the engine in a hypersonic vehicle ([2], [3], [4], and [5]). The results show a strong, highly nonlinear sensitivity of thrust and fuel flow to the flight conditions and engine control parameter settings. Because of the interference between engine performance and flight conditions a valuation of the mission fuel consumption was only possible in connection with mission performance calculations, as presented in [6].

The recent studies have been focused on the equivalence ratio as the most promising control parameter for the performance of a turboramjet engine using a burner behind the turbo engine which acts as

an afterburner in turbo mode and as a ramburner in ram mode. For this type of engine the utilization of other control parameters, especially variable geometries, hasn't been investigated in a similar extent before. Also the potential in fuel flow reduction of the control parameters should be considered in more detail. During the transition from turbo to ram operation variable geometries have to be used to change the flow path in the engine. An important question is the way of performing the transition to keep on high engine thrust and save operating conditions.

The method described in this paper allows an optimization of the engine control parameters in parallel to the engine performance calculation. For a turboramjet engine the results of the optimization for an ascent flight mission as well as for the transition from turbo to ram operation are presented.

2 PROBLEM DESCRIPTION AND APPROACH

The mission optimization of new space transportation vehicles implies vehicle and propulsion system design and vehicle and engine control parameter optimization along the entire mission ([7]). An accurate determination of vehicle aerodynamic properties and engine performance requires high computational expenses and is not practical within the mission optimization. Therefore approximate techniques must be employed whereby the vehicle and the engine properties, each determined in separate analyses, are represented by performance maps. For the mission optimization it is almost sufficient only to consider the most decisive parameters in the engine performance model as long as the influence of the less decisive parameters can be neglected compared to the influence of variations in flight path or vehicle design.

In this study a turboramjet engine is investigated for a fixed vehicle design. Applying an engine performance calculation program, the thrust and fuel flow are calculated for given flight conditions and engine control parameter settings, which determine the fuel supply and the variable geometries in the engine. In conjunction with the performance calculation the engine control parameters are optimized using an energy state approach to minimize the ascent flight mission fuel consumption. Furthermore, the engine control parameters are optimized to minimize the time for the transition from turbo to ram operation at a given flight Mach number.

The vehicle data of the two-stage space transportation system of the Sänger concept investigated in the German Hypersonic Technology Programme serve as a baseline for the investigations described in this paper. All vehicle data relevant for the engine design and the aerodynamic model used refer to an early design of the Sänger space transportation vehicle with a total launch mass of $m_{V0} = 340$ Mg, [8].

The ascent flight mission corresponds to the mission of the Sänger system without any cruise flight and with a staging flight Mach number $M \approx 6.8$. The trajectory is formed by the horizontal take-off, an initial accelerated climb to an altitude of $H = 11$ km, followed by a subsequent acceleration at constant altitude, until the dynamic pressure limitation of $q_{\max} = 50$ kPa requires a further climb to an altitude of $H = 28$ km reached at $M \approx 6.8$. The pull-up maneuver to staging conditions and the flyback mission segment are not considered in this study. The ambient temperature and pressure are used according to the standard atmosphere.

The turboramjet engine is similar to that of Sänger, using a combustion chamber behind the jet engine as an afterburner in turbo mode. During ramjet operation the air is guided around the jet engine through a bypass duct to the combustion chamber. Fig. 1 illustrates the engine concept with the two positions of the closure mechanism in front and behind the turbo engine for turbo and ram operation conditions. Hydrogen is used as fuel in both combustion chambers, regarding the cooling requirements and the high mass specific energy.

3 ENGINE PERFORMANCE CALCULATION AND OPTIMIZATION

3.1 Engine thrust calculation

The computer program used for engine performance calculations is described in [9]. Fig. 1 shows the definition of the control area used for the calculation of the thrust and drag forces in forward x and upward z direction on the engine inlet, the bypass door and the nozzle as proposed in [10].

The inlet calculation considers the ramdrag due to the air entering the inlet and the spilling drag due to the air diverted around the inlet lip, both dependent on the Mach number M_{01} upstream the inlet. As for all flight conditions a diverter separates the forebody boundary layer, the effect of this boundary layer on the flow entering the inlet can be ignored in the engine performance calculation. The resulting diverter drag must be included in the aerodynamic data of the vehicle. At the end of the subsonic diffuser a bypass door is used to pass excessive air under $\vartheta_{91} = 45^\circ$ overboard. Thus the bypass door acts as a convergent nozzle providing thrust in forward and upward direction. The effect of the bypass air on the external flow field has been ignored. The nozzle performance including the basedrag is calculated using the thrust coefficient $c_F = F/F_{id}$ and the thrust vector angle σ_9 dependent on the pressure ratio p_{t8}/p_{09} and on the nozzle throat area ratio $A_8/A_{s,min}$ describing a one di-

mensional variability of the lower ramp configuration, ([11]). For a calculation (see [10]) of the engine thrust and drag consistent with the aerodynamic forces on the vehicle, which are based on the ambient pressure p_0 , the difference between the ambient pressure and the local pressure (see Fig. 1) is considered in terms of an additional pressure force, specified in Table 1.

3.2 Performance optimization along a trajectory

The optimization of the engine thrust and fuel flow values requires a careful consideration of the interaction between flight conditions and engine performance. Therefore the engine performance program is coupled with a vehicle performance program within the engine performance calculation as depicted in Fig. 2.

In a first step the thrust and fuel flow values are calculated with the engine performance program for given flight conditions and engine control parameters, both depending on the flight Mach number. With the aerodynamic data of the vehicle the equations of motion are evaluated in a second step for a flight in a vertical plane over a spherical earth in flight

$$m_V \dot{c} = F \cos(\alpha + \sigma) - D - m_V g \sin \gamma \quad (1)$$

and lift direction

$$m_V c \dot{\gamma} = F \sin(\alpha + \sigma) + L - m_V g \cos \gamma \left(1 - \frac{c^2}{(r + H)g} \right). \quad (2)$$

Incorporating the flight-path angle $\sin \gamma = dH/cdt$ and approximating $\dot{\gamma} = 0$, the acceleration \dot{c} and the angle of attack α can be determined. Since the angle of attack α calculated in step 2 differs from the estimated input value α_e used for the engine performance calculation in step 1, an iteration is carried out as shown in Fig. 2. Because the angle of attack is mainly dominated by the aerodynamic forces on the vehicle and by the vehicle mass, only few iterations are necessary.

For optimizing the engine performance for an ascent flight segment characterized by its initial and final point along the trajectory, it is assumed that the effect of vehicle mass changes on engine performance can be neglected, thus the engine control parameters are the independent parameters only. In the ascent flight mission from beginning of ground acceleration to staging, the engine converts chemical energy of the fuel into energy of the vehicle E as depicted in Fig. 3. To minimize the fuel consumption at a point along the trajectory, according to a proposal in [12] the increase of energy dE related to the fuel energy dQ consumed is used to optimize the engine control parameter settings. With the time derivative for vehicle mass $\dot{m}_V = -\dot{m}_F$, for vehicle energy

$$\frac{dE}{dt} = m_V c(\dot{c} + g \sin \gamma) + \left(\frac{1}{2} c^2 + gH \right) (-\dot{m}_F) \quad (3)$$

and for fuel heat release $dQ/dt = \dot{Q} = \dot{m}_F h_c$, the

efficiency of the energy conversion

$$\eta = \frac{dE}{dQ} = \frac{c(F \cos(\alpha + \sigma) - D) - \dot{m}_F(\frac{1}{2}c^2 + gH)}{\dot{m}_F h_c} \quad (4)$$

can be calculated. For the transportation systems considered, the specific energy $\frac{1}{2}c^2 + gH$ divided by the specific heat of combustion h_c is less than 0.02. Explaining the dominating effects this portion can be neglected in eq. 4. With $F_x = F \cos(\alpha + \sigma)$ the efficiency

$$\eta = c \left(1 - \frac{D}{F_x} \right) \frac{F_x}{\dot{m}_F h_c} \quad (5)$$

can be expressed in the relevant flight parameters, i. e. flight velocity, excessive thrust and fuel specific thrust, which means thrust related to the heat of combustion $\dot{m}_F h_c$.

Optimizing the engine operation for a fuel efficient ascent flight segment, the vehicle performance program is applied in two different ways, see Fig. 2. For the vehicle mass given as an estimate the engine control parameter settings are varied systematically to evaluate and optimize the efficiency η . In a subsequent run of the engine and vehicle performance program vehicle mass is calculated by numerical integration of the vehicle equations of motion and mass flux $m_V = m_{V0} - \int \dot{m}_F dt$ starting from the initial conditions m_{V0}, t_0 . These two steps - optimization and integration - should be repeated until a satisfactory convergence of vehicle mass has been obtained. Calculating the vehicle mass at the end of the ascent flight mission the increased payload capability due to optimized engine control parameter settings can be predicted.

3.3 Optimization of the turbo ram transition

During the transition from turbo to ramjet operation the flow path in the engine is changed using variable geometries. The transient process is assumed to be fast compared to the change of the flight conditions. Therefore the conditions at the engine inlet are taken as constant.

The only instationary effect considered in this study is the moment of inertia of the rotor, other effects like combustion efficiency changes, heat soakage, and tip clearance changes have been neglected. The change of shaft speed

$$\frac{dn}{dt} = -\frac{1}{4\pi^2 \Theta_R} \frac{\Delta P}{n} \quad (6)$$

depends on the moment of inertia of the rotor Θ_R , the deceleration power ΔP , and the shaft speed n itself. At a time with the shaft speed given, the deceleration power only is a function of engine control parameters (fuel flow, variable geometries), determining the performance of the engine components. To achieve minimum deceleration time, deceleration power has to be maximized.

For the optimization, a control parameter setting without any time delay has been assumed, what

means that e. g. the moment of inertia of variable geometries compared to that of the rotor is small and the speed of the control gears is high. Using the engine performance program in a first step, the shaft speed and the engine control parameters are varied systematically to maximize the deceleration power and to minimize the time respectively. In a second step the instationary shut-down process is calculated with optimized engine control parameters $EC^{opt} = f(n)$.

4 RESULTS

4.1 Engine design and reference operating conditions

The components of the engine configuration are designed for their critical flight conditions as described in [13]. Table 2 gives the design values of representative engine components. Special emphasis has been focused on the turbo engine design. For an adequate acceleration potential in the transonic flight regime, regarding the cross section available, the turbo components have been sized at $M = 1.2$ for maximum mass flow capability to provide maximum thrust. A low compressor design pressure ratio of $(p_{t3}/p_{t2})_D = 8$ has been selected, reducing the thermal loading which occurs at high flight Mach numbers, thus enabling an acceptable performance in the turbo mode at flight Mach numbers above 3. The performance of the components is described in maps, enabling an accurate and time efficient calculation of the component characteristics.

The engine off-design performance depends on the flight conditions, on the fuel supply to the main burner and to the afterburner and on the variable geometries. For the investigation of different engine control parameters

- the turbine inlet temperature T_{t4} ,
- the overall equivalence ratio Φ and
- the turbine guide vane angle α_G

are considered. Changing the fuel flow in the burner the temperature T_{t4} can be adjusted to values between the compressor exit temperature T_{t3} and a maximum value of $T_{t4} = 2000$ K according to the maximum thermal loads admitted. The overall equivalence ratio $\Phi = \left(\frac{\dot{m}_F}{\dot{m}_A} \right)_g / \left(\frac{\dot{m}_F}{\dot{m}_A} \right)_{st}$, is defined with the overall fuel flow in the engine related to the amount necessary for stoichiometric combustion of the air ducted through the engine. Starting from a minimum value of the equivalence ratio Φ_{min} determined by the fuel flow in the main burner the equivalence ratio can be varied over a wide range $\Phi \geq \Phi_{min}$. For a good performance in the low speed range, a high compressor pressure ratio is desirable. But for a fixed turbine geometry, this results in excessive compressor outlet temperatures at Mach numbers above $M \approx 3$, requiring an early power reduction of the turbo engine and a transition to ram operation at an unfavourable low Mach number. The turbine capacity is the parameter mainly determining the pressure ratio and variable turbine guide vanes would allow an adjustment to the varying requirements according to the different Mach

numbers. To evaluate the potential of this technology, variable turbine guide vanes have been assumed, although the realisation is difficult. The dependency of the turbine characteristics on the turbine guide vane angle α_G is taken into account considering α_G as a third independent parameter of the turbine characteristics. According to previous studies [11], the variable nozzle throat area A_8 hasn't to be investigated as an additional engine control parameter since it is used to achieve maximum mass flow through the engine regarding the limited working range of the inlet and turbo components.

For the investigation of the engine performance on the ascent flight segment, at subsonic flight the operation with maximum temperature $T_{t4} = 2000$ K and without afterburning serves as a reference, whereas at supersonic flight maximum temperature T_{t4} and stoichiometric afterburning are used for reference. The turbine guide vanes were fixed in the nominal position $\alpha_G = 0^\circ$ for all reference calculations. Fig. 4 shows the temperatures and rotor speeds for the flight segment considered in this study. At subsonic and transonic flight, the mass flow is limited by the maximum reduced speed $\frac{n}{\sqrt{RT_t}}$ of the compressor. According to the increasing stagnation temperature T_{t0} , at constant $\frac{n}{\sqrt{RT_t}}$ the rotational speed n increases, until at $M \approx 2$ the limiting value of n is reached. For a further increase in flight Mach number, the speed parameter $\frac{n}{\sqrt{RT_t}}$ has to be reduced to prevent exceeding of maximum n . At a flight Mach number $M \approx 2.5$, the turbo engine ingests all the air delivered by the intake. Thus for higher Mach numbers the engine rotational speed has to be reduced slightly according to the intake maximum mass flow. The small change in n indicates the proper matching of inlet and turbo engine off-design performance in this flight segment. Finally, at flight Mach numbers $M > 3.5$ the increasing stagnation temperature $T_{t2} = T_{t0}$ and hence compressor exit temperature T_{t3} requires a considerable reduction of the compressor pressure ratio and hence mass flow, keeping the compressor exhaust temperature at its limit of $T_{t3} = 1000$ K. Above $M \approx 3.8$ for effective operation transition is required into ramjet mode.

Fig. 5 illustrates the performance characteristics of the turboramjet engine running under these reference operating conditions. By operating the engine at maximum temperature T_{t4} in the dry mode a high fuel specific thrust $\frac{F_x}{\dot{m}_F h_c}$ is achieved at subsonic flight. In the transonic flight regime high installation losses in combination with afterburning result in a considerable loss of fuel specific thrust. In the low supersonic flight regime, with increasing Mach number spillage and ram drag related to gross thrust decrease causing a more favourable fuel specific thrust again. The interaction of vehicle aerodynamics and engine performance determines the relative excessive thrust $1 - \frac{D}{F_x}$. The minimum value of excessive thrust occurring in the transonic flight regime is caused by the vehicle aerodynamics giving a minimum lift to drag ratio at $M \approx 1.2$. Increasing lift to drag ratio with rising Mach number causes high values of relative excessive thrust over a wide flight range beginning from $M \geq 1.5$. The efficiency is the result of superimpos-

ing the fuel specific thrust and the relative excessive thrust as described by eq. (5).

4.2 Performance optimization along a trajectory

4.2.1 Turbo mode, supersonic flight

The thrust and fuel flow values largely depend on the overall equivalence ratio Φ . A higher equivalence ratio causes increasing fuel flow and thrust, resulting in a reduced mission time and therefore positively affecting fuel consumption. The contradictory effect of fuel flow at a time and time span with respect to the mission fuel consumption can be valued using the change of relative efficiency $\frac{\Delta \eta}{\eta_{ref}} = 1 - \frac{\eta}{\eta_{ref}}$ compared to reference operating conditions at each point along the trajectory.

For the supersonic flight in turbo mode with maximum turbine inlet temperature $T_{t4} = 2000$ K and turbine guide vane position fixed at $\alpha_G = 0^\circ$, the influence of the equivalence ratio on the relevant flight parameters is shown in Fig. 6 - 8. With increasing equivalence ratio and hence fuel supply to the engine, the excessive thrust $1 - \frac{D}{F_x}$ is increasing as indicated in Fig. 6. In the transonic flight regime, where poor engine performance occurs, afterburning is mandatory to get an excessive thrust at all. The fuel specific thrust $\frac{F_x}{\dot{m}_F h_c}$, shown in Fig. 7, is determined by the efficiency of the thermodynamic process and the propulsive efficiency. Over a wide range of flight Mach number, with increasing equivalence ratio and afterburning rate both the thermodynamic and the propulsive efficiencies deteriorate, resulting in a drop of $\frac{F_x}{\dot{m}_F h_c}$. This influence is opposite to the one shown in Fig. 6, where due to the prevailing effect of thrust generation on $1 - \frac{D}{F_x}$ over the whole Mach number range a high equivalence ratio is advantageous. In Fig. 7 at transonic flight Mach numbers only, afterburning increases the fuel specific thrust. There for low equivalence ratio high installation losses and hence low propulsive efficiency mainly determined by the nozzle base drag occur, but with higher equivalence ratio an increasing nozzle throat area reduces nozzle base drag and leads to a better propulsive efficiency. Combining excessive thrust and fuel specific thrust, Fig. 8 shows the influence of equivalence ratio on the efficiency, compared to the efficiency at reference operating conditions. In case of low excessive thrust, the change of efficiency mainly depends on the change of excessive thrust, determining the acceleration capability. The results in Fig. 8 indicate almost slight improvements applying overstoichiometric combustion with $\Phi \approx 1.2$ up to $M \approx 1.2$. In case of high excessive thrust $(1 - \frac{D}{F_x}) \rightarrow 1$ the influence of equivalence ratio on fuel specific thrust prevails that on excessive thrust. Therefore lower than stoichiometric equivalence ratios providing an increased fuel specific thrust are advantageous to improve the efficiency, according to eq. (5). This effect becomes important at Mach numbers $M \approx 2.5$, where understoichiometric combustion results in an improvement up to 2.5% in efficiency. But equivalence ratios as low as $\Phi = \Phi_{min}$ lead to a prevailing effect of ex-

cessive thrust and therefore are disadvantageous. In cases with the temperature T_{t3} limiting the performance and decreasing the thrust, as both the excessive and the fuel specific thrust become lower again, stoichiometric combustion is required. In Fig. 8 the uppermost line shows the benefit of optimizing the equivalence ratio Φ_{opt} for efficiency compared with the reference operating conditions.

As long as the turbine guide vanes are fixed, for the nozzle throat control used in this study the turbine inlet temperature T_{t4} is the control parameter, which mainly determines the working conditions of the compressor. Reduced temperatures lead to a decrease in pressure ratio and, except the cases with mass flow limitation by the inlet, to an increase in engine mass flow. To run the turbo engine at the maximum mass flow, given by the intake or by the turbo engine itself, reduced T_{t4} requires an increased nozzle throat area. The restricted variability of the nozzle enables only a small band-width between maximum temperature $T_{t4,max} = 2000$ K and $T_{t4,min}$ corresponding to a fully opened throat area $A_{s,max} = 1.6$ m². As long as the increase in mass flow prevails the reduction in nozzle pressure ratio, a reduced temperature T_{t4} is advantageous.

In Fig. 9 the gain in efficiency and the engine control parameters are given for a simultaneous optimization of the equivalence ratio and the turbine inlet temperature at supersonic flight conditions. Compared with the results described above (see Fig. 8), the additional optimization of the temperature results in a small benefit in the transonic flight regime. This is due to the fact, that the lines of reduced speed in the compressor map are very steep, so a lower temperature T_{t4} causes mainly a decreasing pressure ratio with no or only small increase in mass flow. But in the flight regime, where the engine is running at maximum compressor exit temperature T_{t3} and close to the compressor choking line, the compressor pressure ratio according to $(p_{t3}/p_{t2}) = (T_{t3}/T_{t2})^{\frac{\gamma}{\gamma-1}}$ stays approximately constant too, as there is a small change in compressor efficiency only, unless choking conditions at the compressor exit are reached. Hence for approximately constant values of turbine capacity and compressor exit pressure, a reduction of temperature T_{t4} enables an increased engine mass flow at almost constant pressure ratio and therefore a higher thrust compared to reference operating conditions.

In future variable turbine guide vanes may be used as an additional control parameter. Opening the guide vanes ($\alpha_G < 0$) leads to a higher mass flow capacity of the turbine. This enables a higher engine mass flow at maximum T_{t4} and rotor speed, occurring from $M \approx 1.0$ to $M \approx 2.5$, and at maximum T_{t4} and T_{t3} , occurring above $M \approx 3.6$. Closing the turbine guide vanes enables higher pressure ratios and in case of the mass flow limited by the inlet without any effect on the mass flow.

As indicated in Fig. 9, optimizing the guide vane position additionally to equivalence ratio and turbine inlet temperature gives a small improvement in efficiency over the whole flight range only. The gain is even decreasing with increasing flight Mach number, as the

share of the turbo engine pressure ratio $\frac{p_{t3}}{p_{t2}}$ on the overall pressure ratio $\frac{p_{t3}}{p_{01}} = \frac{p_{t3}}{p_{t2}} \frac{p_{t2}}{p_{01}}$ compared to inlet diffuser pressure ratio $\frac{p_{t2}}{p_{01}}$ falls with rising flight Mach number. Altogether at supersonic flight, the benefit utilizing variable turbine guide vanes is small.

4.2.2 Turbo mode, subsonic flight

Regarding the nozzle control, in the case of engine operation without afterburning the turbine inlet temperature is the only control parameter determining the fuel supply in the engine, as long as the turbine guide vanes are fixed. As the variable nozzle is accommodated to keep the compressor running at maximum reduced speed at subsonic flight, the parameters relevant for the thermodynamic process $\frac{p_{t3}}{p_{t2}}, \frac{T_{t4}}{T_{t2}}$ can be affected considerably at almost constant engine mass flow. Because of the low design pressure ratio and the high turbine inlet temperatures the fuel specific thrust increases with falling turbine inlet temperature due to an improved propulsive efficiency.

Fig. 10 shows the gain in efficiency for optimized turbine inlet temperature and - in case of afterburning - for optimized equivalence ratio. Because of the high relative excessive thrust for flight Mach numbers $M < 0.7$, as depicted in Fig. 5 for reference operating conditions, reduced turbine inlet temperatures are required to improve the efficiency. This is due to the effect that the increasing specific thrust prevails the loss of excessive thrust in case of $(1 - \frac{p}{F_x}) \rightarrow 1$. With rising flight Mach number $M \geq 0.7$ due to falling excessive thrust maximum turbine inlet temperature and afterburning are advantageous. The optimization results in an operation without afterburning at low Mach numbers, what is advantageous regarding the noise emission additionally.

Fig. 10 shows the gain in efficiency for the variable turbine guide vanes additionally used to improve the engine performance. At low flight Mach numbers $M < 0.7$, the operation with more closed turbine guide vanes yields to an improved efficiency of almost $\frac{\Delta \eta}{\eta_{ref}} = 15\%$ in this flight segment. This is due to the beneficial effect of a higher engine pressure ratio associated with lower turbine inlet temperature. At higher flight Mach numbers, where the optimization leads to afterburning operation, as high pressure ratio is no more beneficial opening the turbine guide vane gives a small improvement in the efficiency only.

4.2.3 Fuel consumption on ascent flight mission

After optimizing the engine control parameter settings at different points along the ascent flight segment using the efficiency, the overall fuel consumption is calculated by integrating the vehicle equations of motion. This shows the result of the optimization in terms of fuel mass required for a flight segment and the overall ascent mission.

Table 3 gives the overall fuel consumption for a different level of performance optimization with

- reference operating conditions,
- optimized fuel flow (T_{t4} and Φ),
- optimized fuel flow and turbine guide vane angle (T_{t4} , Φ and α_G)

for the ascent flight mission divided into three flight segments. In the ramjet mode the equivalence ratio is the only engine control parameter to be considered. As the influence of equivalence ratio on ramjet performance is already well understood for this type of engine (see [6]) the optimization of the ramjet operation is not described in this paper.

Running the turboramjet engine under reference operating conditions requires a total fuel mass of $m_F = 40\,630$ kg for the engine design considered. The simultaneous optimization of equivalence ratio and turbine inlet temperature enables a considerable reduction in fuel consumption $m_{F,ref} - m_F = 690$ kg compared to the reference engine control parameter setting. Table 3 shows that in turbo mode in both the subsonic and the supersonic flight segment the fuel consumption is reduced by the optimization, but in the ramjet mode a slightly higher fuel mass is required. This is according to the effect, that with a take-off mass fixed fuel savings at low flight Mach numbers result in higher vehicle mass associated with higher vehicle drag forces at the end of the mission, corresponding to the higher payload achieved by the fuel savings. The optimization of the variable turbine guide vane angles additional to that of the fuel supply in the engine enables improvements in fuel consumption of $m_{F,ref} - m_F = 1140$ kg compared to reference operating conditions. Related to the efforts required for the realisation variable turbine guide vanes the gain in fuel consumption is small.

4.3 Optimization of the turbo ram mode transition

For the transition from turbo mode to ram mode the closure mechanism up- and downstream the turbo engine are used as additional variable geometries necessary to change the flow path in the engine as illustrated in Fig. 11. The closure mechanisms considered for this engine are

- two plane doors separating the flow into three rectangular cross-sections, followed by a duct guiding the flow into the two circular cross-sections of bypass-duct and compressor inlet,
- variable flaps at the end of the turbine.

In the turbo mode the front doors are open for the flow entering the compressor, additionally preventing the hot pressurized gas from recirculating from the turbine exit to the compressor inlet. The variable flaps are in a position where they are outside of the hot gas flow leaving the turbine in order to lower the thermal loads. As with rising flight Mach number the pressure ratio provided by the turbo engine becomes less than $p_{t5}/p_{t2} = 1$, the front doors can be opened to an intermediate position enabling an additional mass flow passing the bypass duct. As long as the turbo engine is running at high rotational speed and mass

flow, therefore being sensitive to inlet disturbances, the front door position must leave a sufficiently large passage to the compressor. Hence the flaps at the turbine exit can be used as an additional control parameter only. They act as a throttle at the expansion side of the turbo engine, having a strong influence on the pressure ratios and mass flows in the turbo engine and giving a potential to optimize the transition, i. e. to minimize the shut-down time of the turbo engine. By closing the variable flaps, shaft speed and mass flow are reduced so far, that the front doors can be closed without any harmful effect on the compressor. Then ramjet operation conditions are reached with the front doors and flaps are in closed position for the turbo engine.

The investigation of the turbo engine shut-down at a flight Mach number of $M = 3.8$ concentrates on the transition beginning from parallel mode with open front doors and the main burner still fired. Fig. 12 shows the compressor map for the shut-down process with a flap controller to realize different stall margins during deceleration alternatively. Beginning at a stationary point with $T_{t4} = 1540$ K, the fuel flow to the burner is stopped, causing an sudden drop of pressure ratio and, according to the shape of the compressor characteristics, a rise in mass flow. Due to the reduced turbine power, the rotor would decelerate to stationary windmilling conditions, providing the variable flaps would stay in the open position. To shut down the turbo engine, the flaps have to be closed, resulting in a rise of compressor p_{t3}/p_{t2} and turbine p_{t5}/p_{t4} pressure ratio with increasing specific work of the compressor a_C and decreasing specific work provided by the turbine a_T . When the flaps are closed fast, the engine mass flow \dot{m}_2 falls according to the shape of the compressor shaft speed line. Because for closing the flaps the deceleration power $\Delta P = \dot{m}_2(a_C - a_T)$ depends on the contradictory effects of rising specific work and falling mass flow, an optimization problem occurs for the change of speed described by eq. (6).

Fig. 13 shows the compressor mass flow and shaft speed in case of utilizing the variable flaps according to the different stall margins in the compressor map depicted in Fig. 12. Between shut-down of the fuel flow and closing the flaps a certain space of time is assumed. In Fig. 13 a flap operation resulting in a minimum stall margin and a flap operation optimized for minimum deceleration time is depicted. For reference, also the data for open flaps, finally resulting in stationary windmilling conditions with a shaft speed of $n/n_D = 0.37$, are given. It has been assumed, that at a shaft speed of $n/n_D = 0.1$ the flaps and the front doors can be closed completely without any harm for the turbo engine, regarding the aerodynamic forces and the rotor kinetic energy, which mainly is converted to heat of the turbo engine structure. The optimization of the flap control enables a 30% reduction of the time required from $n/n_D = 0.46$ compared to an operation with minimum stall margin.

5 CONCLUSION

The results of the engine performance calculations presented have shown a potential of fuel savings by optimizing the engine control parameters. Engine operation with reduced combustion temperatures in the turbo mode enables a considerable reduction in mission fuel consumption for the ascent flight segment. The optimization results in an operation without afterburning in the flight segment after take off, being advantageous relative to noise emission additionally. Although variable turbine guide vanes allow a further reduction of fuel consumption especially in the subsonic flight regime, the benefit in mission fuel consumption is not clear enough to justify the development of the difficult technology required. For transition from turbo to ramjet operation, the closure mechanism upstream and downstream the turbo engine must be operated to change the flow path in the engine. Optimizing the control of the rear closure mechanism, acting as a throttle behind the turbine, the time for decelerating of the rotor can be reduced considerably.

ACKNOWLEDGEMENTS

These investigations have been sponsored by DFG (Deutsche Forschungsgemeinschaft) as a part of the work done in the collaborative research center (SFB 259) "High Temperature Problems of Reusable Space Transportation Systems" at Stuttgart University.

References

- [1] Proceedings. AIAA/DGLR 5th International Aerospace Planes and Hypersonics Technologies Conference, Munich, Germany, Nov./Dec. 1993
- [2] Bauer, A.; Ludäscher, M. and Rick, H.: Leistungsrechnung und Simulation des Betriebsverhaltens von Antriebssystemen für Hyperschallflugzeuge. Jahrbuch 1993 I der DGLR, Göttingen, Sept. 93
- [3] Steinebach D.; Kühl W. and Gallus H. E.: Design Aspects of the Propulsion System for Aerospace Planes. AIAA/DGLR 5th International Aerospace Planes and Hypersonics Technologies Conference, Munich, Germany, Nov./Dec. 1993
- [4] Schaber, R. and Heitmeir, F.: Einfluß der Komponentendimensionierung auf die Leistung eines Hyperschallantriebs. Jahrbuch 1993 I der DGLR, Göttingen, Sept. 1993
- [5] Zellner B.; Sterr W. and Herrmann O.: Integration of Turbo-Expander and Turbo-Ramjet-Engines in Hypersonic Vehicles. International Gas Turbine and Aeroengine Congress and Exposition, ASME 92-GT-204, June 1992
- [6] Sachs, G.; Bayer, R.; Lederer, R. and Schaber, R.: Improvement of Aerospace Plane Performance by Overfueled Ramjet Combustion. Z. Flugwiss. Weltraumforsch. 17 (1993) 25-32
- [7] Rahn, M. and Schöttle, U.M.: Decomposition algorithm for Flight Performance and System Optimization of an Airbreathing Launch Vehicle. IAF-94-A.2.018, 45th IAF Congress, Jerusalem, Israel, Oct. 1994
- [8] Kuczera, H.; Hauck, H. and Sacher, P.: The German Hypersonics Technology Programme Status 1993 and Perspectives. AIAA-93-5159, 5th International Aerospace Planes and Hypersonics Technologies Conference, Munich, Germany, Nov./ Dec. 1993
- [9] Therkorn, D.: Fortschrittliches Leistungs-Berechnungsverfahren für luftatmende Turbotriebwerke. Dissertation, Universität Stuttgart, Institut für Luftfahrtantriebe, Jan, 1992
- [10] Lehrach, R. P. C.: Trust/Drag Accounting for Aerospace Plane Vehicles. AIAA 23rd Joint Propulsion Conference, AIAA-87-1966, June 1987
- [11] Bareis, B.: Einfluß der Auslegungs- und Betriebsparameter auf das Leistungsverhalten eines Kombinationstriebwerks. Interner Bericht ILA - 93 B 04, Institut für Luftfahrtantriebe, Universität Stuttgart, 1993
- [12] Bryson, A. E. and Desai, M. N.: Energy-State Approximation in Performance Optimization of Supersonic Aircraft. Journal of Aircraft 6 (1969), no. 6, 481-488
- [13] Schwab, R.R.: Airbreathing Propulsion Integration. SPACE COURSE Aachen 1991, pp. 1-33, RWTH Aachen

Table 1: Thrust and drag calculation for inlet I, bypass door B, and nozzle N

F_{Ix}	$=$	$- \left[2 \left(\frac{A_{01}}{A_{01x}} \right) + \left(\frac{F_{spill,x}}{q_{01} A_{01x}} \right) \right] q_{01} A_{01x}$	$-$	$A_{01x}(p_{01} - p_0)$
F_{Iz}	$=$	$\left(\frac{F_{spill,z}}{q_{01} A_{01z}} \right) q_{01} A_{01z}$	$+$	$A_{01z}(p_{01} - p_0)$
F_{Bx}	$=$	$\dot{m}_{g1} c_{g1} \cos \vartheta_{g1}$		
F_{Bz}	$=$	$\dot{m}_{g1} c_{g1} \sin \vartheta_{g1}$	$+$	$A_{g1z}(p_{0g1} - p_0)$
F_{Nx}	$=$	$F_{id} c_F \cos \sigma_9$	$+$	$A_{9x}(p_{09} - p_0)$
F_{Nz}	$=$	$F_{id} c_F \sin \sigma_9$	$+$	$A_{9z}(p_{09} - p_0)$

Table 2: Design values of representative engine components

geometry of engine components		design criterion
$w = 2.36\text{m}$	max. installation width	vehicle design, 5 engines
$A_{01} = 3.14\text{m}^2$	inlet capture area	thrust requirement at staging
$A_2 = 1.77\text{m}^2$	compressor	max. diameter
$A_3 = 0.88\text{m}^2$	main burner	max. diameter
$A_5 = 1.68\text{m}^2$	turbine exit	max. diameter
$A_{12} = 0.80\text{m}^2$	bypass duct	mass flow capacity at transition
$A_6 = 3.33\text{m}^2$	ram burner	mass flow capacity at transition
$A_{8,\text{max}} = 1.60\text{m}^2$	nozzle throat	mass flow capacity at transition
$A_{8,\text{min}} = 0.60\text{m}^2$	nozzle throat	performance at staging

Table 3: Optimized fuel consumption m_F and $\frac{\Delta m_F}{m_{F,\text{ref}}} = \left(1 - \frac{m_F}{m_{F,\text{ref}}}\right) 100\%$ for segments of the acceleration flight mission

operating conditions	turbo mode		ram mode		overall mission	
	$0.2 \leq M \leq 1.0$		$1.0 \leq M \leq 3.8$		$3.8 \leq M \leq 6.8$	
	m_F	$\frac{\Delta m_F}{m_{F,\text{ref}}}$	m_F	$\frac{\Delta m_F}{m_{F,\text{ref}}}$	m_F	$\frac{\Delta m_F}{m_{F,\text{ref}}}$
reference	6 770 kg		18 490 kg		15 370 kg	
opt. T_{t4}, Φ	6 650 kg	1.7 %	17 870 kg	3.3 %	15 420 kg	-0.3 %
opt. T_{t4}, Φ, α_G	6 480 kg	4.5 %	17 570 kg	5.0 %	15 440 kg	-0.5 %
					39 490 kg	2.8 %

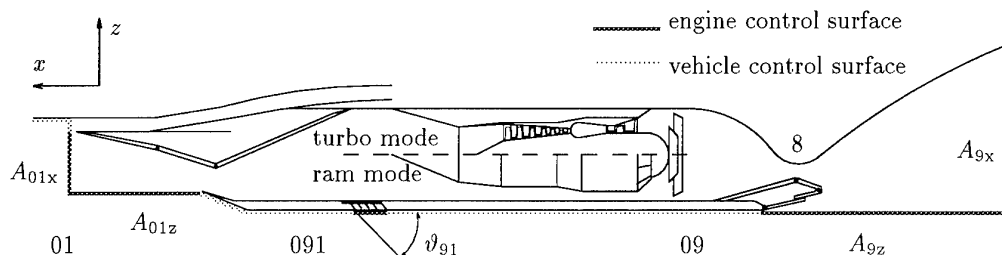


Figure 1: Turboramjet engine concept with propulsion and vehicle surface definition for thrust and drag accounting

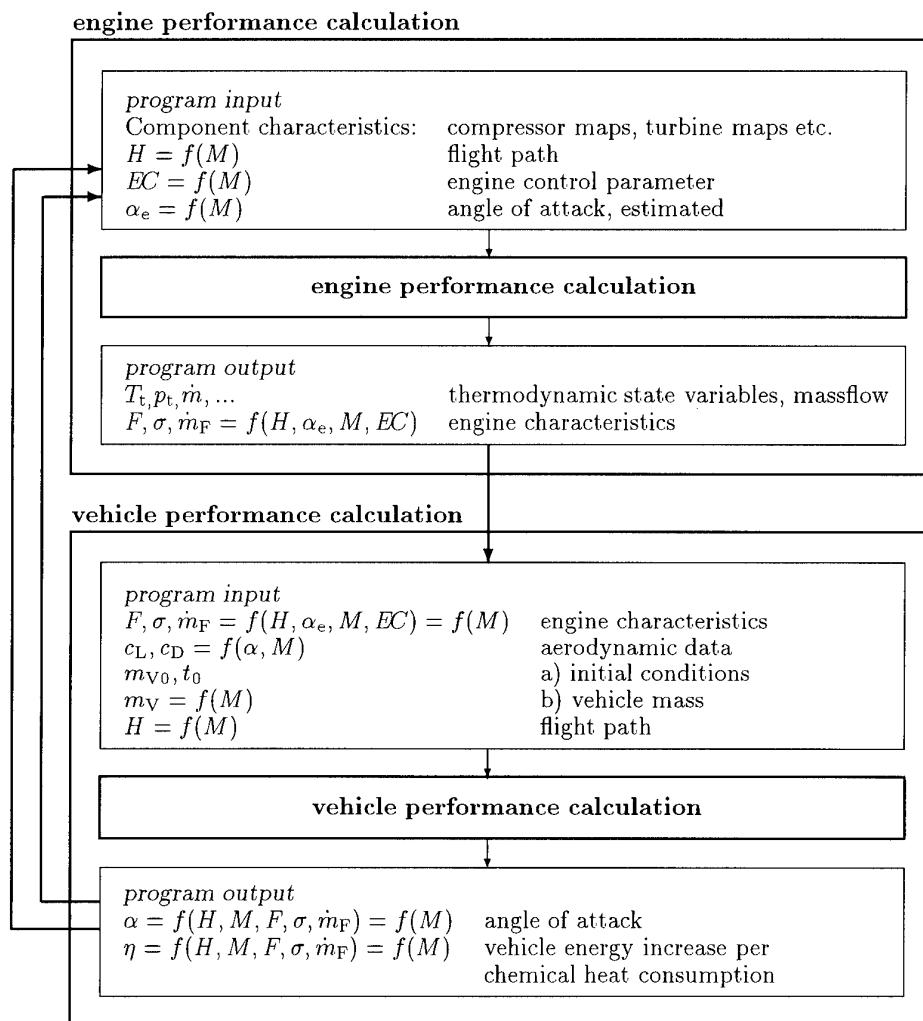


Figure 2: Iterative multistep procedure coupling the engine and the vehicle performance calculation programs
a) numerical integration of the vehicle mass b) calculating the efficiency η for the vehicle mass given

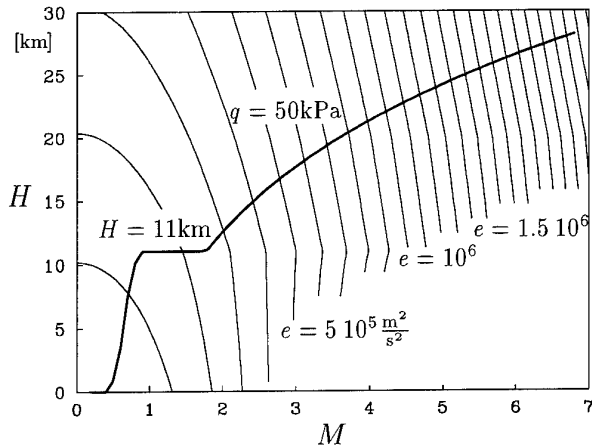


Figure 3: Trajectory for the ascent flight mission with lines of constant specific energy $e = \frac{1}{2}c^2 + gH$

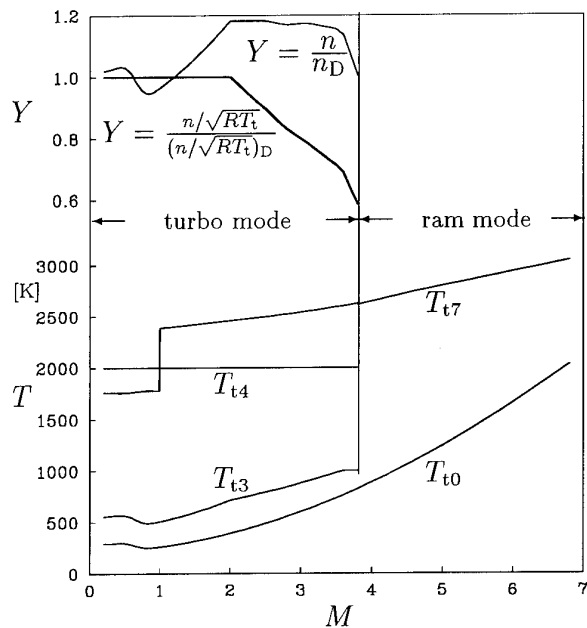


Figure 4: Rotational speed and temperatures in the turbo-ramjet engine running under reference operating conditions

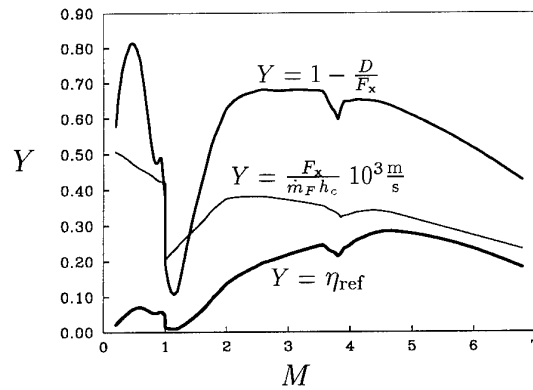


Figure 5: Performance characteristics of the turbo-ramjet engine, running under reference operating conditions

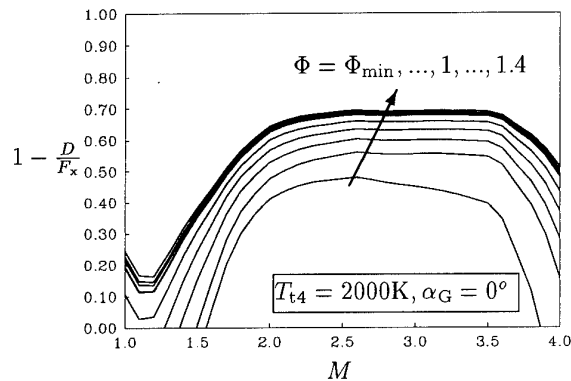


Figure 6: Excessive thrust $1 - \frac{D}{F_x}$ as a function of flight Mach number and overall equivalence ratio

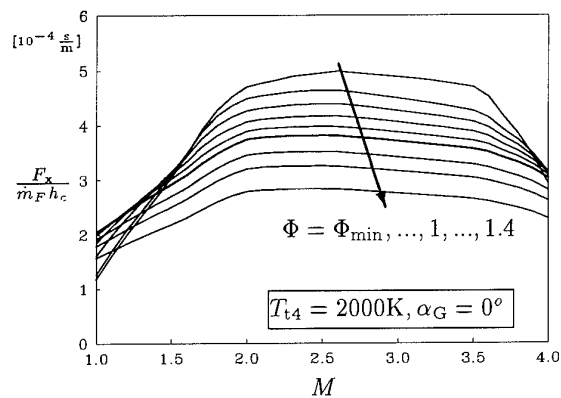


Figure 7: Fuel specific thrust $\frac{F_x}{m_F h_c}$ as a function of flight Mach number and overall equivalence ratio

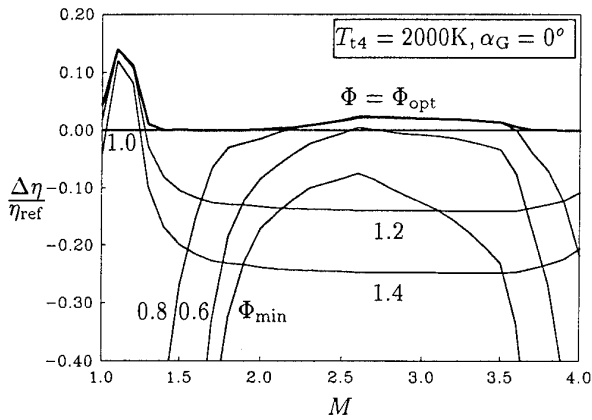


Figure 8: Influence of the overall equivalence ratio Φ on the relative efficiency $\frac{\Delta\eta}{\eta_{ref}}$ in turbo mode at supersonic flight

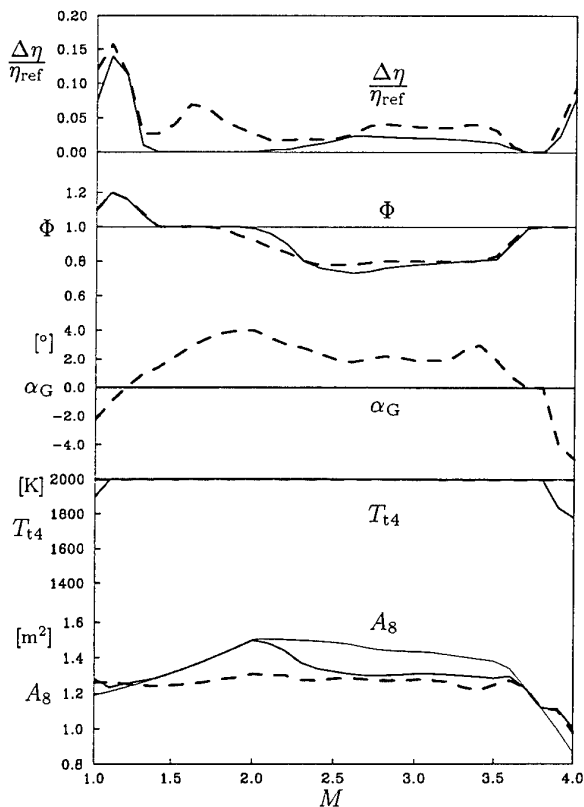


Figure 9: Gain in efficiency $\frac{\Delta\eta}{\eta_{ref}}$ compared to reference operating conditions for optimized control parameters at supersonic flight
— optimized Φ, T_{t4}
- - optimized Φ, T_{t4}, α_G

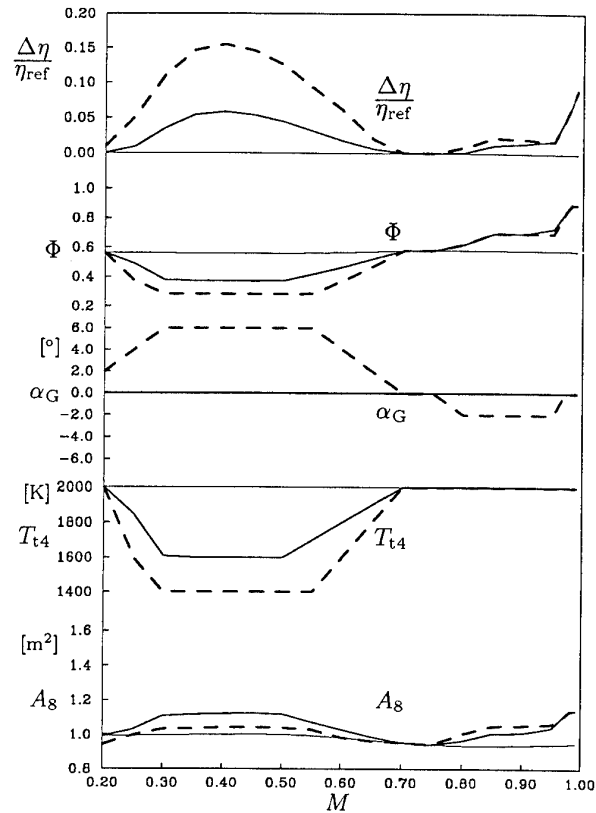


Figure 10: Gain in efficiency $\frac{\Delta\eta}{\eta_{ref}}$ compared to reference operating conditions for optimized control parameters at subsonic flight
— optimized Φ, T_{t4}
- - optimized Φ, T_{t4}, α_G

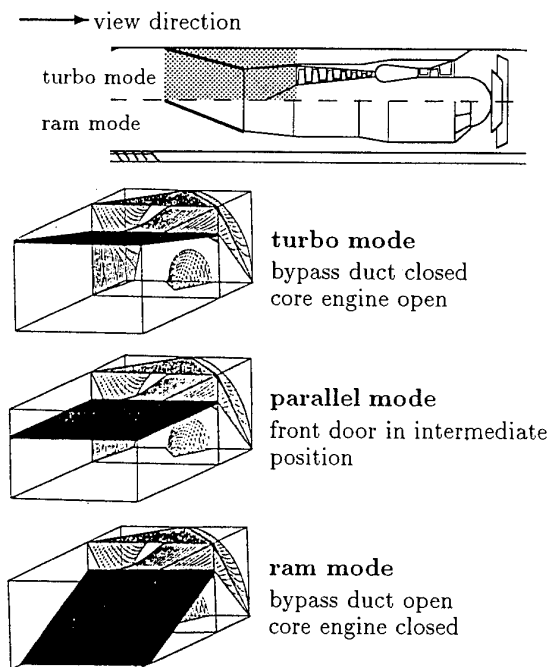


Figure 11: Turbo engine with closure mechanism, position of the upper front door corresponding to different engine operation modes

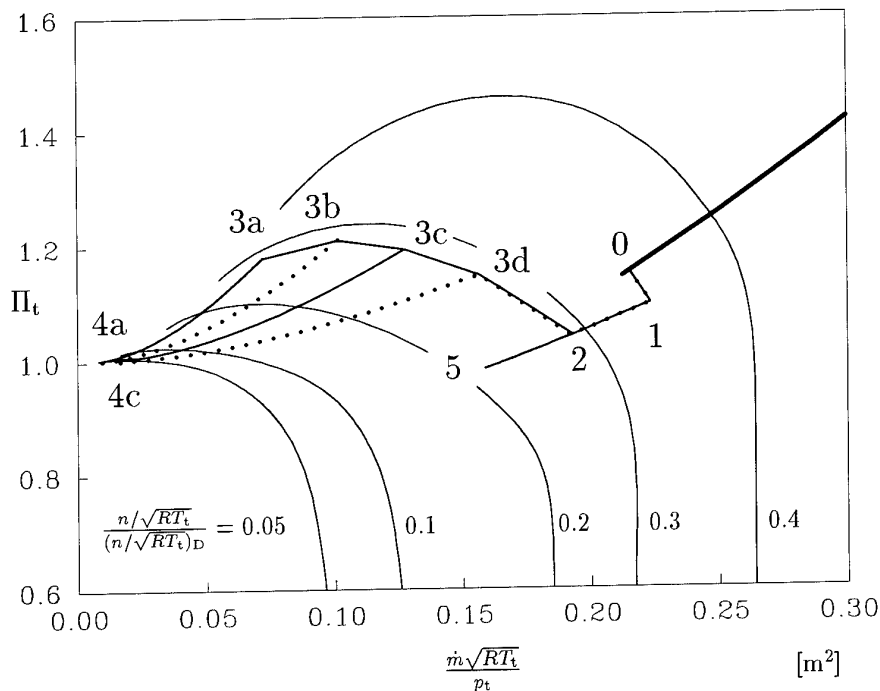


Figure 12: Compressor map for a controlled shutdown of the turbo engine at $M = 3.8$, beginning from parallel mode with front doors already in intermediate position

- turbo-ramjet mode for $3.5 \leq M \leq 3.8$ before shutdown
- 0 operation at $M = 3.8$ with $T_{t4} = 1540\text{K}$
- 0 to 1 shutdown of the fuel flow in the main burner
- 2 to 3 fast closing of the variable flaps according to a given stall margin a, b, c, d
- 3 to 4 variable flaps are continuously closed according to the stall margin
- 4 rotational speed remains under maximum tolerable value
- 5 stationary windmilling conditions

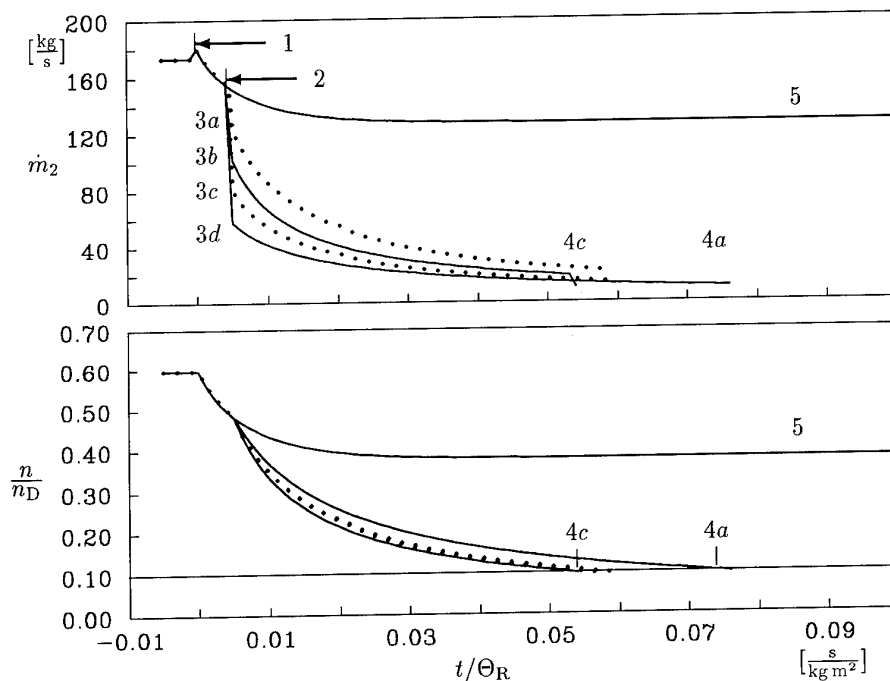


Figure 13: Compressor mass flow and speed during the controlled shut down of the turbo engine at $M = 3.8$, considering different stall margins (see Fig. 12)

Application of a System for the Monitoring of Aerodynamic Load and Stall in Multi-Stage Axial Compressors

H. Hönen

H.E. Gallus

Institut für Strahlantriebe und Turbomaschinen
RWTH Aachen
Templergraben 55
52062 Aachen
Germany

1. SUMMARY

As a part of a complete health monitoring system the observation of aerodynamic compressor load and the detection of stall in multi stage axial compressors is explained in detail.

At first the definition of monitoring parameters and the choice of the suitable measuring technique is demonstrated. Based on the design of the system structure the hard and software solution is shown. Checking modules and a failure detection for all components take a great part of the software. With help of suitable input and output interfaces the system can be adjusted to different applications and the monitoring results can be made visible.

Furthermore, the experiences with this system applied to three multi-stage compressors are reported. The behavior of the monitoring parameters shows a good agreement with the different operating conditions of the compressor as well as for design conditions and for operation near the stability limit.

2. INTRODUCTION

The requirement of reduced weight and high thrust in modern jet engines leads to higher power densities and increasing efficiencies in the components. For the compressor part this is directly connected with operating points close to the stability limit. Therefore, a permanent and real time observation of the operating conditions is necessary. Whereas in the past only the inlet and outlet conditions of a turbo component were used for a calculation of the operating point now so called artificial intelligence is applied to these monitoring tasks in order to provide a high number of information for a detailed view inside the machine.

Rule-based and model-based expert systems and gas path analysis find more and more entrance to diagnosis processes in turbo machines. The enormous progress in the field of computer technology allowed an increasing engagement in the on-line analysis. In addition to measuring data at the inlet and outlet information about the flow conditions inside the machines is required in order to provide exact statement about the momentary operating conditions.

The combination of suitable measuring techniques with a corresponding data enhancement and analysis allows the definition of several monitoring tasks. The detection of the stability limit of a turbo compressor is one main field of the research work. It is the basis for further activities in the field of stable compressor operation, e.g. the operating line management.

3. MEASURING TECHNIQUE AND MONITORING PARAMETERS

The choice of a suitable measuring technique and the definition of monitoring parameters are two tasks which influence each other. The calculation of instructive results depends on the correct measuring position in the compressor.

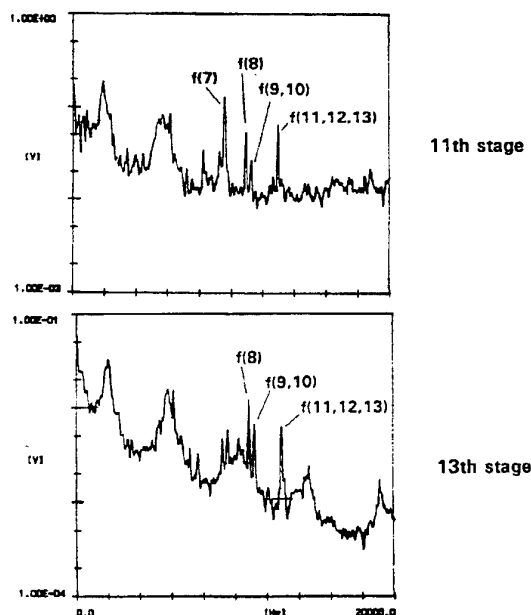


Fig. 1: Frequency Spectra in the Stages 11 and 13 for normal Operating Conditions

Long term investigations in the 14-stage high pressure compressor (HPC) of a LM5000 gas turbine provided detailed results concerning the influence of the aerodynamic load onto the pressure fluctuations in a compressor stage /1/. With increasing compressor load in the

end stages a stall region near the casing occurs. Pressure sensors at the casing behind the rotor showed a sharp reduction of the periodic information for that case.

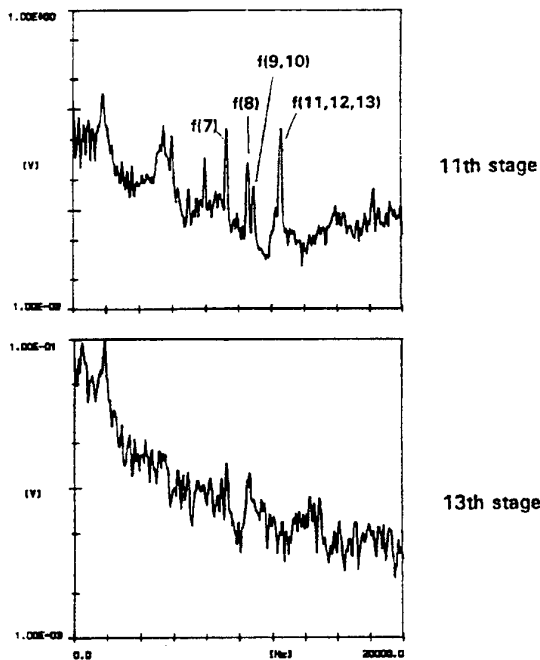


Fig. 2: Frequency Spectra in the Stages 11 and 13 for Operation near the Stability Limit

The figures 1 and 2 demonstrate the behavior of the frequency spectra of sensors in the 11th and 13th compressor stages. For normal operating conditions (fig. 1) the characteristic frequencies of the measured and the neighbouring stages can be detected. The stages 9 and 10 and 11 to 14 have the same blade numbers. At operation near the stability limit of the compressor all periodic information in the 13th stage disappeared (fig. 2). Due to the higher blade load in the 11th stage the characteristic peak was elevated.

Investigations in a single stage research compressor at high aerodynamic load produced similar results [2]. Measurements with hot wire probes in the stator channel and with hot film glue-on probes on the blade surfaces found strongly damped periodic fluctuations inside the separation regions.

This effect has been used for the design of a monitoring system for compressor load. By means of dynamic pressure sensors the periodic fluctuations at the casing between rotor and stator are observed and analyzed. The behavior of these data provides an information about the operating conditions of the compressor.

Since at design speed the highest aerodynamic load occurs in the end stages pressure measurements in the stages 11, 12, and 13 with piezo-electric sensors were required. Due to the high pressure ratio of 27 in the 13th stage a temperature of about 500° C had to be

considered. The maximum allowable temperature of quartz sensors is 200° C to 250° C. Therefore, special cooling adapters had to be developed which reduce the temperature down to 200° C at the sensor position (fig. 3).

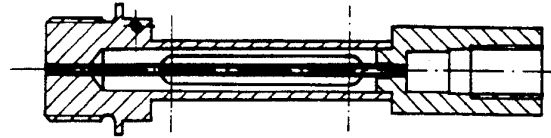


Fig. 3: Cooling Adapter for Pressure Measurement at the Compressor Casing

For the design of these adapters the sonic behavior of a thin tube had to be taken into account. There should be no resonance frequencies of the tube in the observed frequency range. Furthermore, the damping should be as little as possible.

During experiments in a special calibration facility the length/diameter ratio of the tubes could be optimized. A comparison between a reference transducer mounted directly to the pressure generator and the sensor in the adapter a calibration correlation could be defined. Calculations with an acoustic method described by Tijdeman and Bergh [3, 4] demonstrated a good agreement between theory and experiment. Now it is possible to calibrate the transmission behavior of such a cooling adapter so that from the output signal of the sensor the real pressure fluctuations at the bottom of the tube can be calculated.

Since there is a great number of data coming from the pressure sensors in the three compressor stages a data reduction is necessary. The real time signals are analyzed by a FFT. Then only the characteristic frequency peak of the observed stage is used for the further calculations.

The results shown in figs. 1 and 2 demonstrated that the extend of this frequency peak is a measure for the aerodynamic load of the stage. Therefore, a parameter p_{val} was defined to

$$p_{val} = \frac{p_{fre} - \overline{p_{fre}}}{p_{fre}}$$

In this equation the value p_{fre} is the amplitude of the characteristic frequency peak and $\overline{p_{fre}}$ is the mean value of the complete frequency spectrum (fig. 4).

While this parameter is a value for the aerodynamic load of one stage an additional information has to be provided as a measure for the load of the whole com-

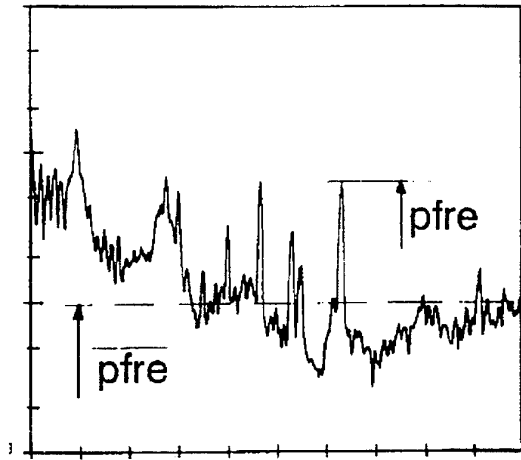


Fig. 4: Definition of p_{fre} and p_{fre} in the Frequency Spectrum

pressor and the detection of the stability limit. With increasing compressor load the casing stall region observed in the last stage also occurs in the upstream stage and so forth. The parameter p_{val} shows the same behavior in all observed stages. Thus, a new load parameter SL can be defined as an addition of the calculated p_{val} values.

$$SL = a_{13} \cdot p_{val13} + a_{12} \cdot p_{val12} + a_{11} \cdot p_{val11}$$

Figure 5 demonstrates the behavior of this compressor load parameter for increasing pressure ratio. In order to provide a constant growth of SL the calculation has to be switched after the casing stall in the 13th stage has been detected. The maximum value of p_{val} (13th stage) is kept constant and inserted into the above equation.

One main problem in the detection of the stability limit is the exact prediction of the limit value for the monitoring parameters. In this case the system itself defines this limit. From the long term measurements it was known that the compressor showed a stable operation although casing stall in the 13th stage occurred. When the control system of the machine released a shut down no casing stall was detected in the 11th stage.

Thus, the stability limit has been defined as that point when casing stall occurs in the 12th stage. Since the stages 11 to 13 have the same geometry it can be estimated that the unsteady behavior in these stages look similar. Therefore, the definition of the limit value of SL can be provided by the software itself. When the parameter p_{val} (stage 13) exceeds its maximum the first time the same value can be inserted into the above equation as the maximum for the 12th stage. The SL

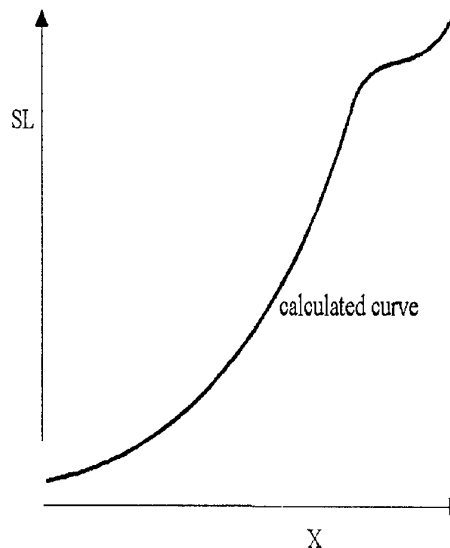
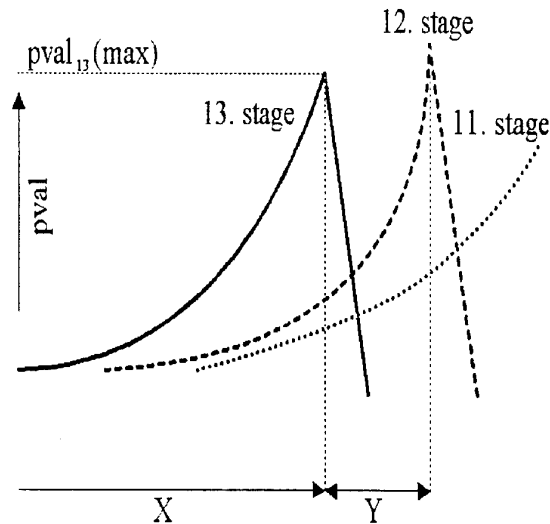


Fig. 5: Behavior of the SL Parameter for Increasing Compressor Pressure Ratio

which is calculated now is the limit value for operation close to the stability limit of the compressor.

By this procedure the observation of stable compressor operation is independent from the compressor itself. The system defines its parameters and the limitations by learning during operation.

4. SYSTEM STRUCTURE

The hardware structure of the monitoring system is demonstrated in figure 6. The surface mounted pressure sensors at the casing in the stages 11 to 13 are connected to the analog-to-digital converters controlled by the three signal processors in the monitoring computer. This computer system for the measurement and the data enhancement is based on an industrial computer which contains a 386 CPU. It is connected to a host computer

for the visualization of the results and trend analysis. Each signal processor controls four analog-to-digital converters.

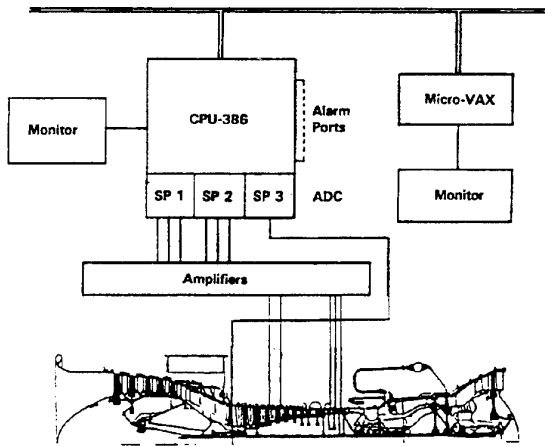


Fig. 6: Hardware Structure of the Monitoring System

In the 386 CPU only the control of the signal processors, the comparison of the FFT-results, and the communication with the network is established. All the other tasks are running on the signal processors. The optimal usage of the capacities of all processors is the requirement for the least possible monitoring time. A detailed investigation provided information about the number of the necessary computing cycles for each task. Only in case all processors are permanently in action the shortest time for a measuring and analyzing cycle could be reached.

Therefore, the monitoring software was divided in a number of modules which are capable to run either on the CPU or on each of the signal processors. By a comparison of the necessary computing cycles and times the tasks could be equally divided. In order to keep the program clearly arranged each module was kept as one unit. Thus, it was not possible to run the several tasks absolutely parallel (all processors permanently in action).

One major aim in the design of the software was the compatibility to different monitoring tasks. Therefore, the main calculation and observation parameters have to be changeable. Furthermore, the monitoring results should be stored for later analyses and visualization. Figure 7 demonstrates the software structure of the system.

By a three-parted structure of the software it is possible to define interfaces in front of and behind the closed monitoring part in order to exchange the data with other systems or users.

The input interface at first allows the changing of all parameters for data acquisition, e.g. ADC-channel,

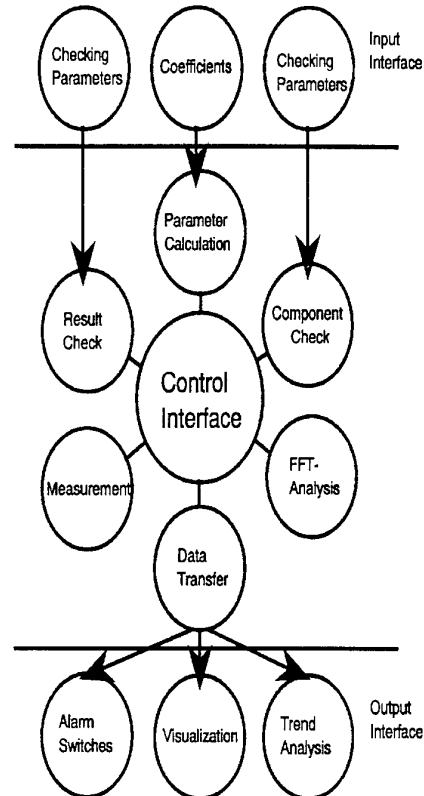


Fig. 7: Software Structure of the Monitoring System

time base, gain, etc.. Thus, it is possible to fit the program to different measuring equipment or measuring tasks.

Since checking procedures for the pressure sensors and transmission lines are integrated in the software different measuring equipments have to be considered by changing the checking parameters. Furthermore, the coefficients for the calculating algorithms and the limit values for the result check are variable so that the system may be fitted to different stage groups or machine types.

The output interface provides the user with three main data and signal groups. At first there are the alarm switches, which switch information to digital output channels depending on the monitoring result in each cycle. In the second group the data are transferred to a host computer for visualization, storage and further analyses.

5. FAILURE CHECK

For a failure free operation of a monitoring system the correct operation of the soft- and hardware components has to be checked. Thus, the observation of the system components is the basis for a high diagnosis safety.

Therefore, a large part of the monitoring system presented here deals with the detection and the interception of malfunctions. Different modules are integrated in the

program for the verification of the correct function of the soft- and hardware. At each time step a malfunction warning and analysis is possible. Furthermore, the design of the system allows a continuation of the monitoring tasks under negligence of the defect components. This tolerant behavior is archived by a suitable change of the monitoring algorithms or selection of different monitoring parameters.

For the monitoring of compressor load and stability several sensors are installed in the machine. In case of malfunction of one sensor or the related transmission line to the computer the corresponding signal is blanked out in the calculation of the monitoring parameters.

Component	Parameter
pressure sensors/ transmission lines	RMS values of the signals
signal processors	calculation of a test FFT
rotor speed sensors	$n \text{ (HPC)} / n \text{ (LPC)}$ ratio
connection to the host computer	error level in the net
function of the moni- toring computer	transfer of a calculated test value to the host

Table 1: Control parameters for the monitoring system

Table 1 shows the control parameters for the soft- and hardware components. From the analyses of the long term experiments at the compressor the influence of different operating points onto the sensor behavior was derived. Damaged sensors or amplifiers provide a measuring signal with a very low noise so that the RMS values will drop under a defined limit. In case of disturbances due to problems with the cabling a very high noise is produced which can be detected in a growth of the RMS values. By defining suitable filter algorithms the information about the sensors can be calculated from the real time signals.

After the detection of a malfunction the related software routines are switched to other calculating algorithms for the monitoring parameters. Thus, the recording of monitoring data is continued with reduced safety of the diagnosis until the failure is removed.

Similar to the monitoring parameters for the compressor operation suitable and characteristic values have to be defined for the judgement of the system function.

The permanent connection between monitoring and host computer allows a reciprocal check of both computers.

The pressure sensors and the transmission lines are checked by the PC itself. In the case of malfunction or damage to one of these components the RMS values of the signals drop under a defined limit or disturbing signals are superposed. By comparison with a limit value the failure can be detected.

6. OPERATING EXPERIENCES

The monitoring system has been installed in three LM5000 gas turbines. Several tests should show the behavior of the Stall Level in dependance from the compressor load. The figures 8 and 9 demonstrate the effectiveness of this parameter. The diagrams show a comparison between the Stall Level, the compressor inlet temperature, and the VSV positions in the HPC. The pressure ratio (fig. 10) and the rotor speed (fig. 11) kept nearly constant during the entire test range of about one hour.

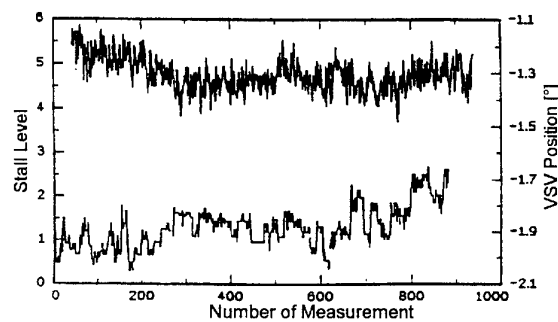


Fig. 8: Comparison between Stall Level and Compressor VSV Position

A strong influence of the VSV angle onto the Stall Level can be observed. With decreasing angle position (higher compressor load) the Stall Level increases an vice versa. This effect occurs without any time lack so that the compressor load can be made visible from the Stall Level directly.

The operation of the monitoring system connected to the three gas turbines during the first three years allowed several changes and completion of the software to improve the safety of the diagnosis results.

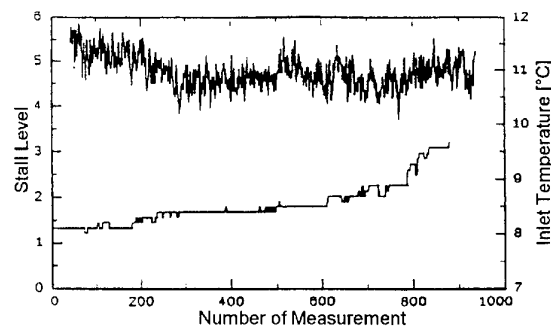


Fig. 9: Comparison between Stall Level and Compressor Inlet Temperature

The system was designed for operation at design load of the gas turbines. In this case the HP rotor runs with full speed of about 10,300 RPM and the highest aerodynamic load occurs in the end stages of the HPC. In order to detect the convergence to the stability limit at design load the measuring equipment was mounted in these stages.

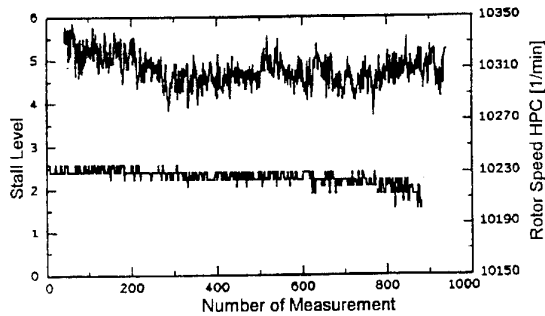


Fig.10: Comparison between Stall Level and Rotor Speed of the HPC

Nevertheless, measurements at lower speeds showed a good reliability of the monitoring parameters even at part load. During an acceleration from part load to full load of the gas turbine the increasing aerodynamic load was observed by the Stall Level.

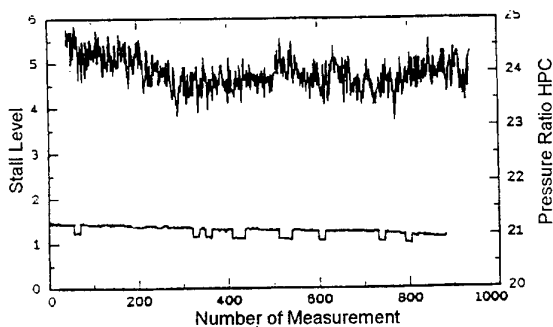


Fig.11: Comparison between Stall Level and Pressure Ratio

Since the pressure sensors and their connections to the amplifiers were very often destroyed during inspections of the compressor bladings a new sensor type was developed by the manufacturer. The transducer itself and also the new designed cooling adapter had quite a different signal characteristic compared to the old ones.

Nevertheless, the monitoring parameters showed the same behavior and the calculated values had the same level as before the transducer change. After about half a year experience with the new measuring equipment the system has shown that no change of the algorithms as of the coefficients is necessary.

This demonstrates the independence of the monitoring parameters and algorithms from the measuring equip-

ment. Thus, the system can be transferred to different applications without changing the fundamental parameters.

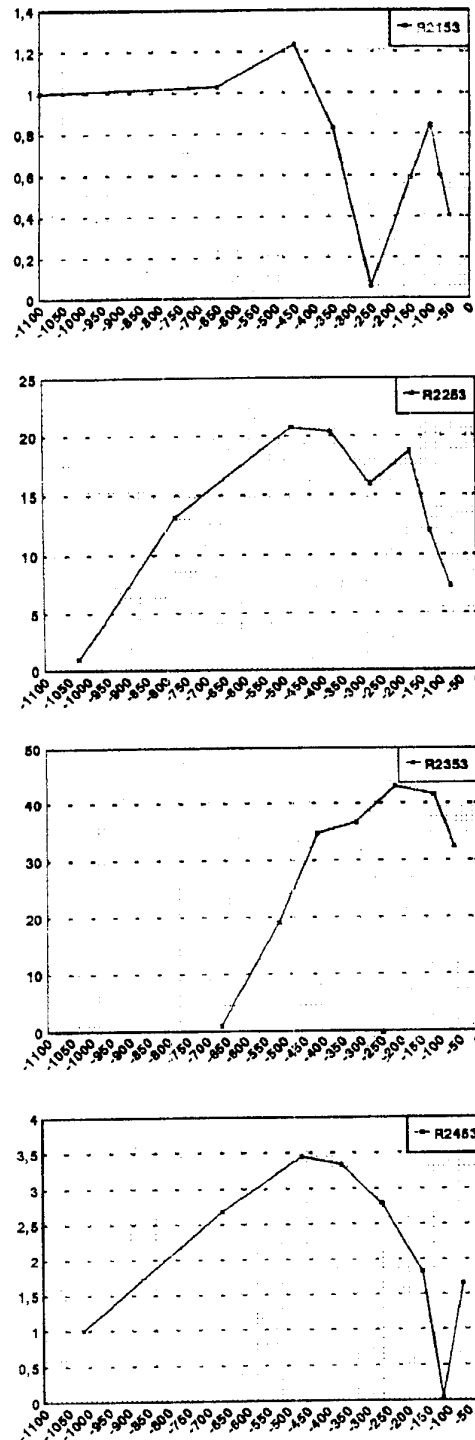


Fig.11a: Distribution of P_{val} (second stage) for increasing Compressor Load



Fig. 12b: Distribution of p_{val} (first stage) for increasing Compressor Load

The principles of this monitoring theory also were applied to a 17-stage axial compressor. In different experiments at part load the operating points of the compressor were shifted to the stability limit and into the unstable region of the performance map. The compressor was equipped with surface mounted dynamic pressure transducers at the casing in the first and second stage.

In order to improve the exactness of the parameter definition p_{val} was calculated from the measuring signals. The figures 12a and 12b show the distribution of this parameter calculated from the measuring data of the transducers in both stages. The four diagrams show the condition for different compressor operations at the four test runs.

This first evaluation of measuring data demonstrate quite a similar behavior of this monitoring parameter in the observed stages. The parameters on the x-axis shows the remaining distance to the stability limit. The right border of each diagram is equal to the compressor surge. After a slight increase of the curves up to a maximum a sharp decrease follows and provides a precursor for the beginning instabilities of the compressor.

The measuring position in the compressor and the operating conditions are different in comparison to the conditions in the compressor of the LM5000 gas turbines. Nevertheless, the monitoring result demonstrates the good compatibility of the principles and algorithms to other compressor types and other operating conditions.

In order to check the possibilities to decrease the cycle times for one measuring and analyzing cycle the software was installed on PCs with a 486/50 and a Pentium/90 processor. The 486 CPU allowed a cycle time of about 0.9 s and could be reduced with the Pentium to 0.1 s.

On the signal processor boards three measuring tasks are running together on one processor. In an additional test for each task an own processor was installed. For this case the cycle time dropped to about 0.01 s. This demonstrates the capability to run the system in real time applications with very short reaction times.

7. CONCLUSIONS

The version of this monitoring system described here was designed for a stationary gas turbine based on the CF6-50 jet engine. The results provide a fundamental base for further activities on operation line management. The short times for one complete measuring and analyzing cycle show that an application in a real jet engine is possible.

The main advantages of the system are

- good compatibility to different compressor types,

stages, and measuring equipment

- low effort for the measuring equipment
- stable operation of the system and high safety of the monitoring results
- failure tolerant operation of the system

The experiences with the system under operating conditions show a very good agreement with the operating parameters of the compressors. The diagnosis safety has been approved on a high level so that functional errors are nearly impossible.

Further activities will include test runs of the monitoring system on the test field in order to check the behavior for part load. The main goal however is to estimate the remaining reaction time after detection of the stability limit and to redefine the alarming parameters.

8. REFERENCES

1. Hönen, H., Gallus, H.E.: "Monitoring of Aerodynamic Load and Detection of Stall in Multi Stage Axial Compressors", ASME Paper No. 93-GT-20, 1993 International Gas Turbine Conference, Cincinnati, USA
2. Hönen, H., Gallus, H.E.: "Experimental Investigations of Airfoil- and Endwall Boundary Layers in a Subsonic Compressor Stage", ASME Paper No. 86-GT-143, 1986 International Gas Turbine Conference, Düsseldorf, Germany
3. Tijdeman, H., Bergh, H.: "Theoretical and Experimental Results for the Dynamic Response of Pressure Measuring Systems", National Aero- and Astronautical Institute, Amsterdam, 1965
4. Tijdeman, H.: "On the Propagation of Sound Waves in Cylindrical Tubes", National Aero- and Astronautical Institute, Amsterdam, 1975

Paper 19: Discussion

Question from K Garwood, Rolls-Royce, UK

You suggest a model of surge that has quiescent air at the casing, unable to transmit the pressure signals from neighbouring stages. This appears to be a variance with experience with stall anticipation devices that operate by detecting stall cells. Please would you comment on this.

Author's reply

There have been several investigations of methods relating to the detection of stall cells, ie so-called "stall precursors". Such models are quite different from mine, because my method indicates the approach to the stability limit much earlier. I believe stall cell detection methods only work well at part speed. When a rotating stall is detected at full speed there is no chance of escaping from this unstable situation because there is a hysteresis between entry to and exit from stall operation. My model can prevent such unstable operation arising in the first place.

Application of Thrust Vectoring to Future Aircraft Design

Hannes Ross, Peter Huber
Dasa, Military Aircraft LME01
Postfach 801160
81663 Munich, Germany

Abstract

Configurations with thrust vectoring of about 20° of their aft fuselage mounted engines have been studied for more than 25 years. In the last decade significant advantages in thrust vectoring systems and their integration in the digital aircraft control system have been made. Thrust vectoring has become a viable control effector.

This paper reports about studies and flight test results demonstrating the effective utilization of thrust vectoring within the conventional and expanded (into the Post-stall regime) flight envelope.

It addresses also new design options provided by the use of thrust vectoring, in particular the option to reduce the vertical tail surface.

1. INTRODUCTION

Thrust vectoring is not exactly a brandnew feature in airvehicle design. In the second world war it was used for missile control and in the fifties and sixties it was essential for the design of a new class of vehicles: aircraft which can take off and/or land vertically.

However, for these configurations thrust vectoring was only used for the take-off and landing phases with deflection angles of at least 90 degrees and max engine power. Another important characteristic of VSTOL configurations is the fact, that the thrust vector of the propulsion system must go through the centre of gravity to avoid unwanted thrust moments. Desired control moments were generated by nozzle rotation (Harrier), Thrust modulation (VJ-101) and external flap deflection (XV-5A).

The VTOL aircraft had, -for the reasons mentioned above-, one performance penalty: the propulsion system arrangement usually resulted in a cross section distribution which precluded supersonic flight.

The fighter generations developed since the late sixties resulted in configurations which had thrust to weight ratios close to and in excess of one. They all have good supersonic capability and the high thrust to weight ratio

would theoretically allow vertical take-off and landing but rear fuselage mounted engines would require a 90 degree attitude for the aircraft. This option, -though also already test flown (Ryan X-13)-, has so far not caught on.

A new idea of thrust vectoring utilization was developed in the mid seventies by the late Dr. Wolfgang Herbst at MBB in Munich, Germany. He had the idea to use thrust vector control in the pitch and yaw axis to achieve a new level of maneuverability in the stall and post-stall arena and thereby improve the close-in combat capability of an aircraft. This could be done for the "conventional" aft fuselage engine installation and would require only deflection angles in the order of 10 to 20 degrees.

Another option investigated already at that time was the utilization of this thrust vectoring concept for take-off and landing.

With the successful flight testing of this kind of thrust vectoring on the X-31 aircraft and its impressive demonstration at the 1995 Paris Air Show and the development of engine integrated pitch/yaw vectoring nozzles, a new era of thrust vectoring has started.

This paper addresses some of the results achieved in the X-31 program, the potential pay-offs of thrust vectoring and some of the challenges, which still wait for solutions.

2. X-31 FLIGHT TEST OBJECTIVES AND RESULTS

The primary flight test objectives were the demonstration of the

- technical feasibility of Post-stall (PST) maneuvering
- tactical utility of post-stall capability

At post-stall flight conditions control power provided by conventional aerodynamic control surfaces is insufficient. Therefore, thrust vectoring is required to provide the control power necessary for pitch and yaw moments around the body axes.

2.1 The X-31 Thrust Vectoring System

Why did we need a thrust vectoring system for the X-31? While pitch control and trim could be provided throughout the entire angle of attack (AoA) range by using the trailing edge flaps and the canard, body axis yaw control power is greatly reduced above 25° AoA. The rudder has no efficiency at all above 45° AoA (Fig. 2.1-1) and the directional stability turns negative at high AoA. However, the thrust vectoring system had no problem to provide the stability and control functions at the power settings required for PST maneuvering.

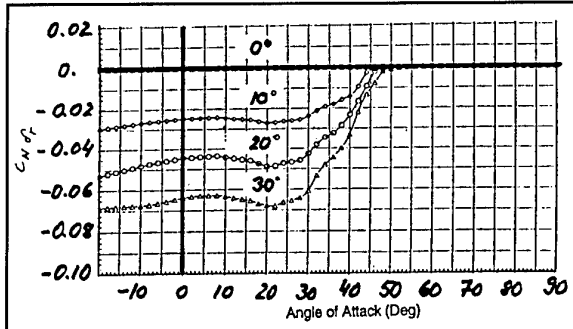


Fig. 2.1-1 X-31 Rudder Power vs. Angle of Attack

Fig. 2.1-2 shows some of the initial specification values for a thrust vectoring system as developed by MBB in 1978.

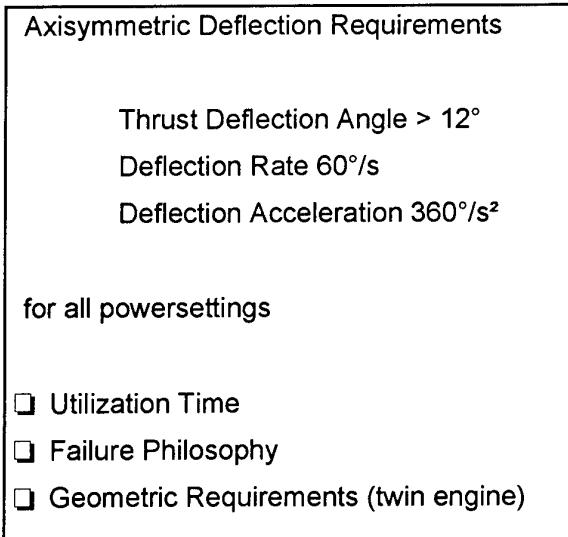


Fig. 2.1-2 Thrust Vector Nozzle Specification

At the time the X-31 program was started in 1985, the development of an engine integrated vector nozzle was not a realistic option. Therefore the "poor man's" solution, -using three vanes mounted at the aft fuselage to vector the engine jet-, was developed.

This solution was highly successful, very efficient and proved to be the right concept for a low cost demonstrator.

Fig. 2.1-3 shows the principle characteristics of this system.

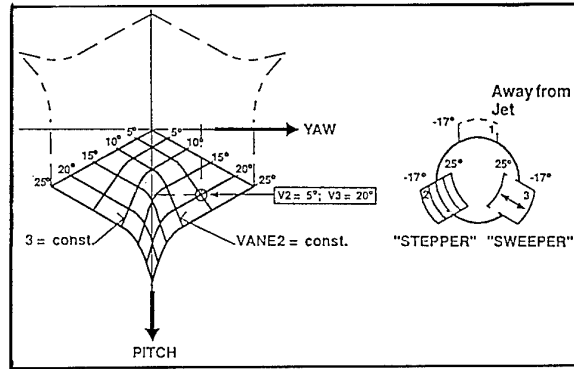


Fig. 2.1-3 T.V. System Characteristics

Maximum vane deflection capability was 35 degree and limited by structural interference of two vanes. This results in about 16 degree deflection of the actual jet over a wide range of nozzle areas. Deflection rate of the single system hydraulic actuators was 60 degrees/sec for the vanes at no load condition and approximately 45°/sec effective jet deflection rate. Bandwidth of the system is about 10 Hz.

Fig. 2.1-4 shows the thrust vectoring characteristic of a single vane vs the deflection angle. The X-31 flight control system contained a whole table of T.V. information regarding powersetting, flight altitude and Mach number including information about the jet plume boundary to avoid any dead zones during a deflection command.

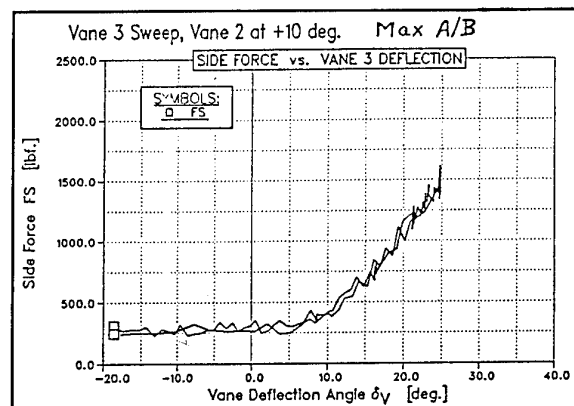


Fig. 2.1-4 Sideforce vs. Deflection Angle

Some of the operational data observed in flight tests are given in Fig. 2.1-5. Temperature and vibration levels were relatively low and did not cause any problem. Also the simple bushing attachment of the vane to the metal back-up structure was not a problem.

Some metallic parts of the rear attachment were exchanged about every 12 to 15 hours to maintain freeplay requirements.

Utilization	
Conventional Envelope	80% Mil - Max AB
Poststall Envelope	Mil - Max AB
Total Time in Operation	190 flight hours
Vibration Level	up to 20 g
Max Temperature	
Carbon Vane Back Side	600 Deg C
Metal Structure	200 Deg C
No material nor functional problems	

Fig. 2.1-5 T.V. System, Operational Data

The design of the X-31 did consider the installation of a thrust vectoring system from the very beginning, i.e. the impact of the additional mass at the end of the fuselage and its impact on wing location, centre of gravity etc. was taken into account. However, for cost reasons the thrust vectoring system was not designed as a primary control surface: It was only to be utilized during PST flight and during transition into and out of this regime. Therefore, there was the requirement that the aircraft must be recoverable from high AoA even in the event of a T.V. system or engine failure.

2.2 X-31 Flight Test Results, Post stall Capability

The feasibility of post-stall maneuvering was demonstrated by four major milestones

- transition into and out of the PST regime up to 70 degree trimmed angle of attack
- 360 degree (or more) velocity vector rolls at up to 70° AoA
- high "g" entry into PST, up to 6g and $M = 0,7$
- a "clinical" 180° heading reversal maneuver which involves all of the above elements, called "Herbst maneuver"

The flight envelope in which the X-31 was cleared to perform PST maneuvers is shown in fig 2.2-1.

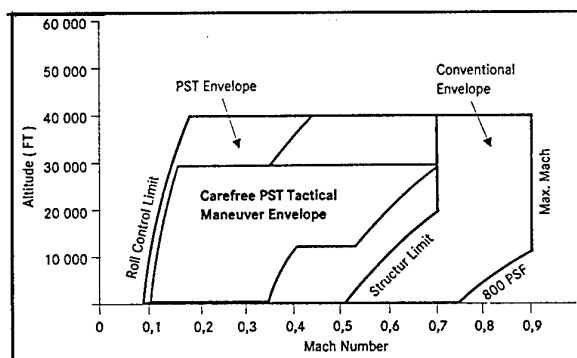


Fig. 2.2-1 X-31 Flight Envelopes

After the technical clearance of the system, close in combat engagements were flown and evaluated against

F-14, F-15, F-16 and primarily against the F-18 aircraft. The results are indeed impressive (fig.2.2-2), in particular, when it is considered that the X-31, -when limited to 30° AoA-, is markedly inferior to the F-18.

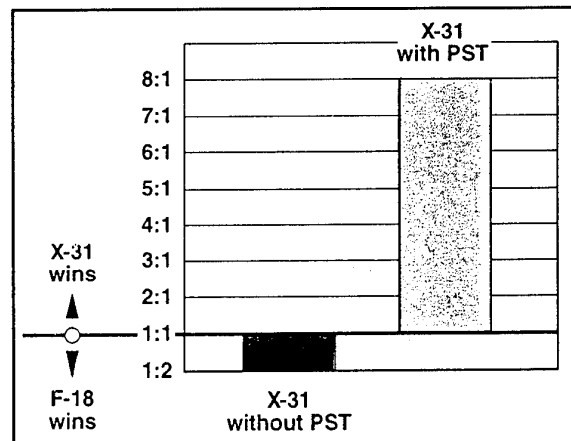


Fig. 2.2-2 X-31 Close in Combat Exchange Ratio

3. POTENTIAL UTILIZATION OF THRUST VECTORING

Basically, a thrust vectoring device can be treated and used like any other control effector. However, there are some fundamental differences when compared to an aerodynamic control surface:

- For a given flight condition the amount of deflected thrust is in addition to the deflection angle also dependent on the power setting. That means, that if for any reason the power is reduced (intentionally by the pilot or unintentionally by a propulsion system failure), the vectored thrust component is reduced accordingly. This can be compensated by a higher deflection angle up to the maximum allowable value and/or by increasing the aircraft drag and (e.g. partial speedbrakes) and thereby maintaining a higher thrust level.
- The second fundamental difference is that the effectiveness of an aerodynamic control effector is directly proportional to dynamic pressure or M^2 (assuming a constant coefficient) while the thrust is basically proportional to $(1+M^2)$ assuming a constant power setting (fig.3-1). Therefore, the ratio of sideforce generated by thrust vectoring divided by the aerodynamic force generated by a control surface tends to get smaller with increasing dynamic pressure.

This really means that there are two critical areas:

- flight conditions where the control power of the thrust vectoring system is too low because of the low thrust level

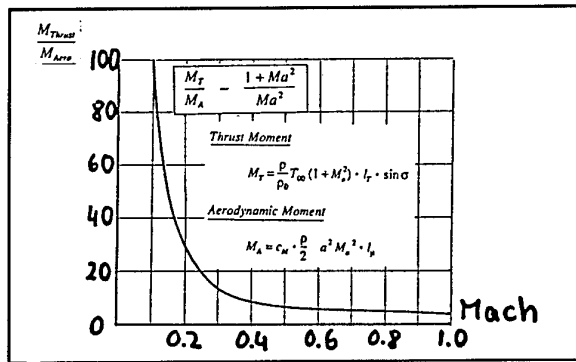


Fig. 3-1 Thrust Moment vs. Aerodynamic Moment

- flight conditions where the aerodynamic forces or disturbances are very high so that even with full power the thrust vectoring system may be insufficient to provide enough control power

The location of an aircraft engine is dictated by many design considerations, which normally do not include the moment arm of a thrust vectoring device. For fighter aircraft the engines are usually installed in the aft fuselage with no (single engine) or little lateral separation from the aircraft centreline. Therefore, thrust vectoring utilization to generate a rolling moment around the body axis is null or limited. Primary utilization of thrust vectoring is therefore expected to be for the generation of pitch and yawing moments.

Two different applications will be discussed:

- T.V. for flight performance improvement
- T.V. for stability and control purposes. Both functions can and should be combined for optimum utilization of a T.V. system.

3.1 Performance Improvements

Field Performance

Take-off performance can be favourably effected by thrust vectoring if

- the lift-off speed can be reduced by an earlier rotation (this could be the case for heavy, forward c.g. A/G loadings)
- the lift off speed can be reduced by a better trim concept (resulting in a higher lift coefficient for a given ground clearance AoA). In this case the pitch down moment of a larger trailing edge flap deflection will be compensated by a pitch up moment generated by thrust vectoring.

Thrust vectoring during take off is not a problem since the power setting is high.

Landing performance can similarly be improved. This requires, however, that the power setting for approach and that required to generate the control forces and moments can be matched.

Fig.3.1-1 shows calculated field performance improvements for a typical modern fighter configuration, to which a thrust vectoring nozzle has been added.

Another option for thrust vectoring utilization as related to field performance is a steep approach at post-stall angles of attack and landing in post-stall mode/attitude. While steep approach is not a problem and has been demonstrated numerous times during X-31 flight test, a post-stall landing is certainly a challenge for the flight control system and the landing gear.

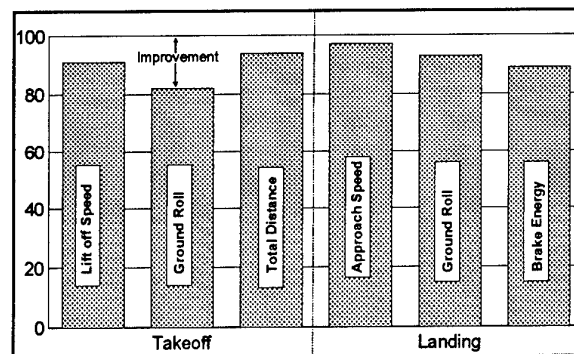


Fig. 3.1-1 Field Performance Improvements

Two options can be considered:

- approach and landing in a "steep approach/conventional attitude" where the aircraft has a very high sinkrate which exceeds the current capability of even carrier landing gears (Fig.3.1-2). The reduction of the sinkrate can be achieved by either increased attitude or increased forward velocity.

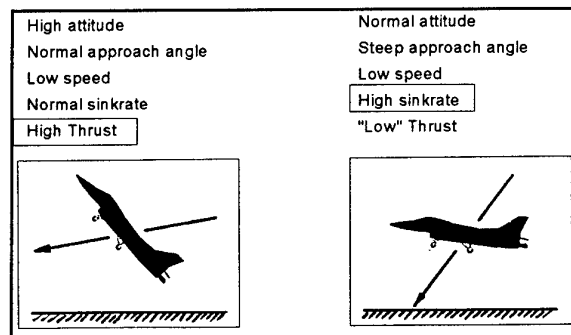


Fig. 3.1-2 Post-stall Landing Options

- landing at PST angles of attack but with a normal glide slope. This would require a special (grashopper) landing gear which provides the necessary ground clearance and results in a lengthy derotation sequence which tends to eat up the benefit of a low approach speed. Fig.3.1-3 shows a configuration concept studied by MBB in the mid seventies. It included a "Grashopper" landing gear and assumed a derotation sequence which would maintain the c.g. position vertically above the wheel axis.

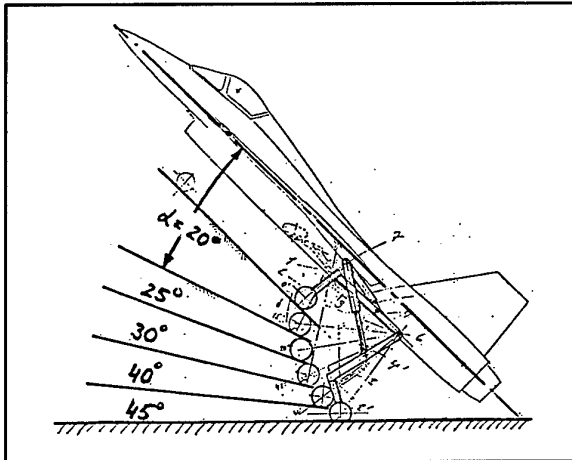


Fig. 3.1-3 Post-stall Landing Gear, Grashopper

Pilot vision was to be provided from lower fuselage sensors with the image put on a cockpit display.

Landing performance improvement using PST capability on a normal horizontal runway is still a challenge and remains to be proven. An alternate landing concept at a vertical wall (as considered by Grumman with their "Nutcracker" 20 years ago) seems to be much more feasible now with the availability of the vectoring nozzle.

Cruise and Maneuver Performance

The potential reduction in trim drag is the benefit to look for. It should be noted that the potential pay-off is decreasing, if the basic aerodynamic concept is already optimized.

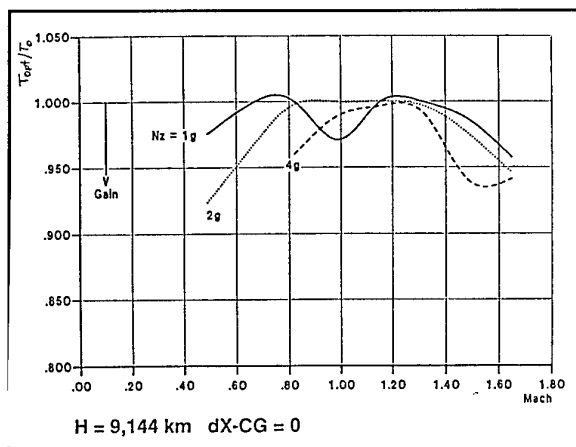


Fig. 3.1-4 Maneuver Performance Improvements

Calculated improvements are shown in Fig. 3.1-4 for the X-31 for various g-levels and in Fig. 3.1-5 at various altitudes for a 1g condition. Improvements are in the order of a few percent which -if considered at constant performance level- could also be converted in an improved range/radius. Flight tests to measure the trim drag improvements for the X-31 were scheduled, but could not be performed due to time constraints.

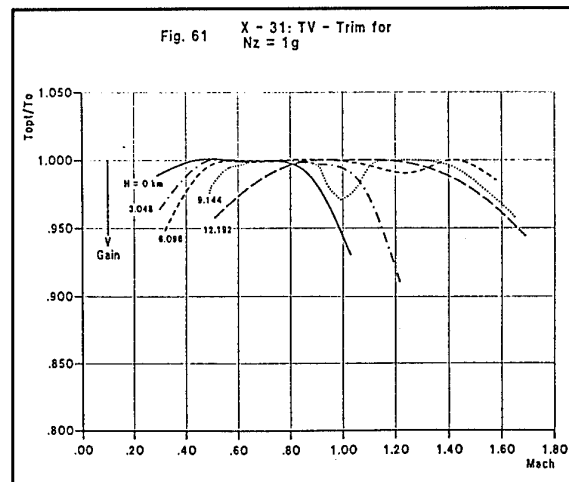


Fig. 3.1-5 Cruise Performance Improvements

3.2 Stability and Control

When the very successful X-31 demonstrations of the PST capability with the enabling thrust vectoring system became apparent, the utilization of the T.V. system in other parts of the flight envelope and for other purposes became a goal for subsequent flight tests.

The maximum benefit of the incorporation of a thrust vectoring device can be achieved, if it is designed like a primary control effector with the intent to minimize or eliminate other aerodynamic control surfaces.

To prove the feasibility of this concept Rockwell suggested to demonstrate the utilization of the thrust vectoring system to stabilize the aircraft around the yaw axis. This idea led to the conception of the "quasi tailless" experiment with the X-31. Quasi tailless is an in flight simulation of the directional stability characteristics of the aircraft, as if the vertical tail is reduced in size or totally removed. Rudder and ailerons are being used to destabilize the aircraft and the thrust vectoring system for directional control and to re-establish the desired lateral/directional flying qualities of the configuration. This concept allows to simulate an aircraft with a reduced vertical tail/lateral stability without actually removing it.

The initial flight test was performed at 37500 ft at Mach 1.2. The tests consisted of doublets, bank to bank rolls and 2g turns. The aircraft showed good handling qualities and met level 1 Dutch-Roll flying qualities requirements up to 100% tail reduction. This was possible, because the power setting and, hence, the control power was high enough at this flight condition.

Further tests were conducted later on as part of a flight test contract by the JAST program office. Subsonic cruise conditions, formation flights, and air to ground weapon delivery runs were tested in addition to the a.m. carrier approaches [Ref.1]. Fig. 3.2-1 shows the test conditions within the X-31 flight envelope.

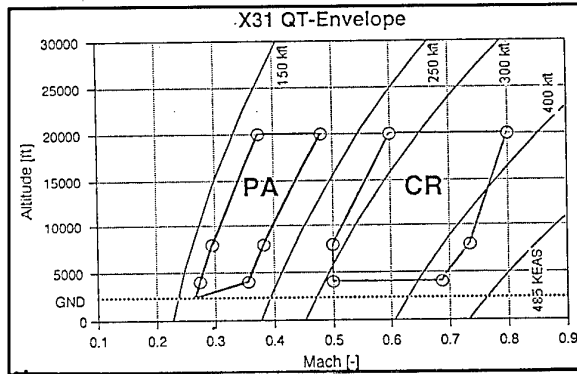


Fig. 3.2-1 Quasi Tailless Flight Test Regime

The modifications of the flight control laws are listed in Fig.3.2-2.

- ☐ Provides possibility to perform QT-tests at various subsonic flight conditions with improved robustness against T.V. control saturation
- ☐ Main features are:
 - 12 destabilization gain sets selectable by the pilot
 - Maximum roll rate and roll acceleration command as a function of estimated thrust
 - Maximum sideslip and sideslip command rate as a function of estimated thrust
 - Safety disengagement if specified envelope parameters are exceeded

Fig. 3.2-2 Flight Control Law Modifications

Three ground attack profiles with simulated tail reductions up to 50% were flown, a 45° Dive Attack started at 18000 ft AGL/250KCAS, a 15° Dive Attack started at 4000 ft AGL/350 KCAS and a Pop-up Attack was flown from 1000 ft AGL/400 KCAS. Level 1 flying qualities were achieved for fine tracking tasks for all profiles, gross acquisition was rated at level 2.

A comparison of the directional stability derivative cn_{β} tail on and tail off for various modern fighter aircraft at low subsonic Mach numbers reveals (see Fig. 3.2-3) that the X-31 has the highest tail-off instability. Therefore, it was a very good testbed to cover critical configurations and flight conditions.

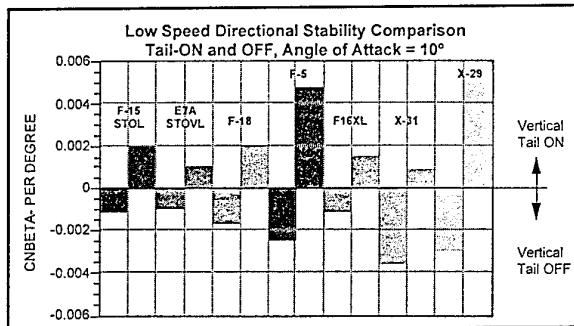


Fig. 3.2-3 CNBETA. Tail on and Tail off

Fig.3.2-4 shows the variation of cn_{β} versus Mach number for two different configurations with and without vertical tail. This indicates that even with a tail on, conventional fighter configurations can get close to neutral or beyond lateral stability at high speed.

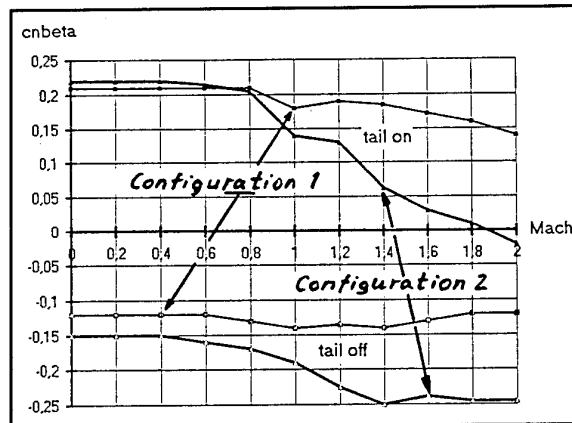


Fig. 3.2-4 CNBETA Variation with Mach Number

Approach and landing, considering cross wind requirements, are most demanding for a thrust vectoring system because of the relatively low power setting required.

For the precision approach task, a field carrier approach was chosen, because it represents a challenging high gain pilot task. The approaches were flown with speed brakes extended and up to 50% tail reduction. The aircraft exhibited good flying qualities in the lateral/directional axes.

4. DESIGN CONSIDERATIONS

4.1. Early MBB Studies

Design studies for configurations using thrust vector control from engine integrated axisymmetric nozzles were already performed in the late sixties at MBB [Ref.2]. Fig.4.1-1 shows the twin engine baseline configuration (an early Tornado version with a variable sweep wing) and the configuration using thrust vectoring for the pitch and yaw axis.

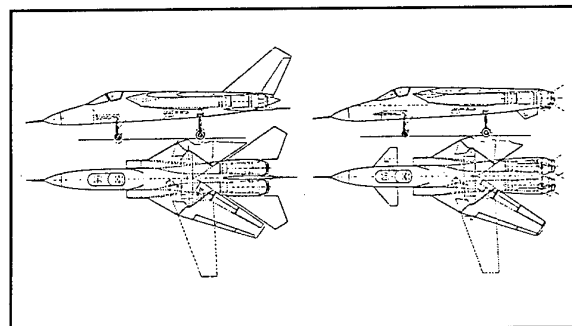


Fig. 4.1-1 Configuration with T.V. Control

The conclusion at that time was that

- a small canard was required to provide adequate pitch trim capability throughout the whole Mach/altitude envelope at all maneuver conditions. This was based on a nozzle design with 30° thrust vectoring and a subsonically unstable configuration.

- two ventral fins were required at the lower side of the fuselage to generate a neutrally stable configuration.

If the deflection capability assumed at that time is reduced to about 20 degrees, it can be concluded that the size of the trim surfaces for that configuration need to be increased.

Another study was performed 1975 for a single engine configuration (Fig.4.1-2) and a strake type wing [Ref.3] with an axisymmetric nozzle with 30° vectoring capability.

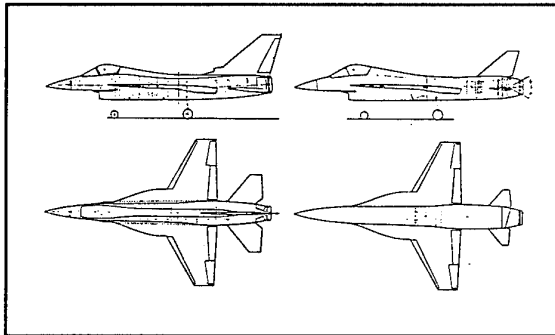


Fig. 4.1-2 Single Engine Configuration with T.V.

The conclusions at that time were similar:

- a small horizontal control surface was required to provide adequate pitch trim capability throughout the flight envelope
- a small all-moving vertical tail was necessary to satisfy the cross wind landing requirement

4.2 The "Tailless" Configuration!?

For the X-31 the mass of the thrust vectoring system and its c.g. effects were taken into account in the configuration development.

However, for a retrofit of a configuration with an axisymmetric thrust vectoring system the idea of saving the mass of the vertical tail is very attractive, because the additional weight of the T.V. nozzle is about at the same aft fuselage location and, therefore, the mass and the c.g. balance might be maintained.

Mass Properties (kg)		
Vanes (3)		47
Carbon/Carbon	17	
Metal Back-up	30	
FCS Components		36
T.V. Support Structure		14
Aft Fuselage Frames		13
Total Mass		110
System mass related to engine mass		11,3%
System mass related to TOGW		1,5%

Fig. 4.2-1 X-31 T.V. System, Mass Properties

Fig.4.2-1 shows the mass properties for the X-31 nozzle system.

Mass Properties (kg)		
Vanes (3)		47
Carbon/Carbon	17	
Metal Back-up	30	
FCS Components		36
T.V. Support Structure		14
Aft Fuselage Frames		13
Total Mass		110
System mass related to engine mass		11,3%
System mass related to TOGW		1,5%

Fig. 4.2-1 X-31 T.V. System, Mass Properties

The mass for an axisymmetric nozzle system is in the order of 8-10% of the engine mass and located at the very end of the fuselage. If no compensation, -e.g. by vertical tail reduction-, at the rear fuselage is feasible, additional mass has to be added in the front of the aircraft (e.g. ballast, lengthening of the forward fuselage etc).

Fig.4.2-2 presents mass properties of the vertical tail including its actuation system mass for operational fighter aircraft plus the X-31.

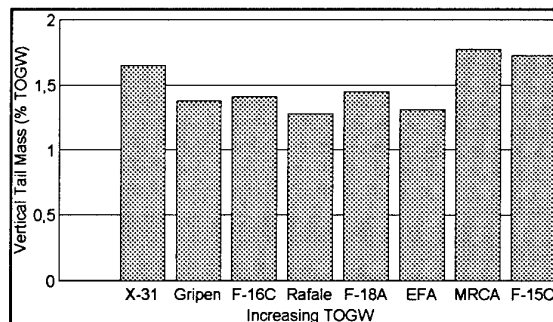


Fig. 4.2-2 Vert. Tail Mass Prop., incl. Actuation

Average mass is about 1.5% of the Take-off Gross Weight. This is the maximum weight saving potential for a vertical tailless configuration.

Similarly the smaller wetted area of a reduced or tailless configuration can be considered in the friction drag and can result in a fuel saving. Fig.4.2-3 reflects the percentage of vertical tail contribution to the wetted area for some modern fighter configuration. Between 5 and 10% of the friction drag could be saved.

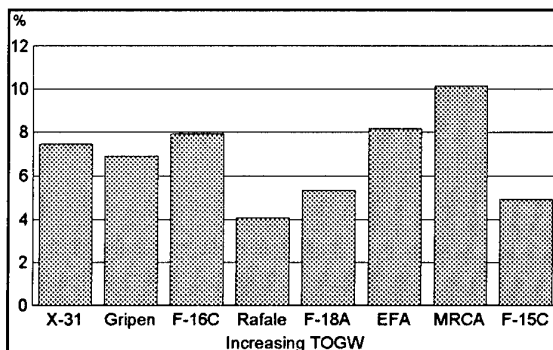


Fig. 4.2-3 Vert. Tail Contribution to Wetted Area

According to the study results described in 4.1 which are confirmed by the "Quasi Tailless" flight test results with the X-31, thrust vectoring can augment the reduced directional stability of a fighter aircraft if the configuration is about neutrally stable. The amount of possible tail size reduction and the associated weight drag saving needs to be determined for each aircraft considered.

If the whole vertical tail is to be removed and the aircraft becomes directionally unstable, additional aerodynamic devices are required to cover flight conditions with unsufficient thrust vectoring control power. Potential solutions are

- split flap ailerons (B-2) or
- differential trailing edge deflection (inboard/outboard)
- surfaces which are deflected in critical flight conditions

Another consideration in favour of a reduced vertical tail is the aircraft signature. Fig. 4.2-4 shows the radar signature distribution of a F-117 type aircraft in the horizontal plane as calculated with physical optics plus PDT + RT for a horizontal polarization.

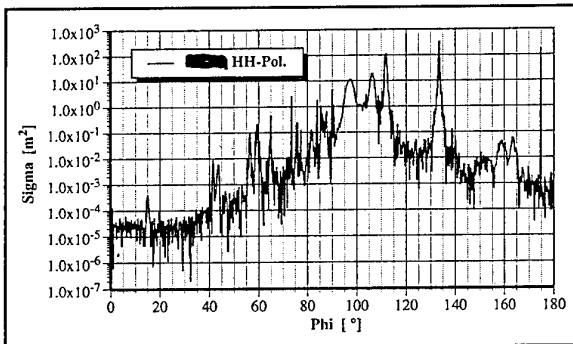


Fig. 4.2-4 Radar Signature Distribution, F-117 Type

The reduction of this signature by removal of the vertical tail is presented in Fig.4.2-5. The impact is primarily visible in the side aspect and can reach significant peak values.

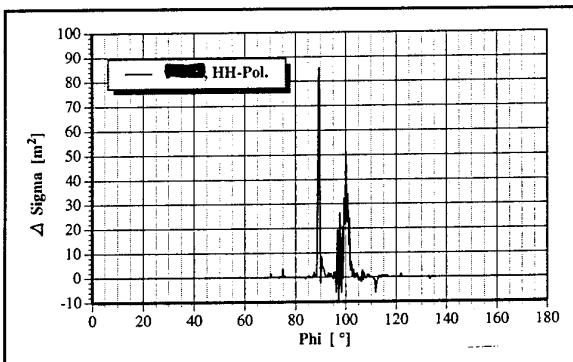


Fig. 4.2-5 Vertical Tail Signature Contribution

The smaller the signature of the vertical tail by initial design, the smaller is the signature reduction by its removal.

In conclusion: "Vertical Tailless" configurations are feasible, however, require special attention and aerodynamic devices.

4.3 Civil Aircraft Application

Application of thrust vectoring technology to civil aircraft is more difficult due to the following facts:

- civil aircraft have a significantly lower thrust to weight ratio and, hence, smaller control forces by thrust deflection
- only configurations with aft mounted engines provide a reasonable moment arm to generate pitch and yaw moments
- civil engines do not have a variable nozzle geometry which is suitable to modify for thrust vectoring. A different deflection or nozzle concept needs to be developed.

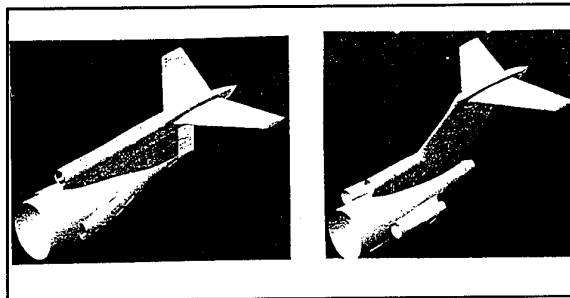


Fig. 4.3-1 Thrust Vectoring for Civil Aircraft

Fig.4.3-1 shows a Dasa study for thrust vectoring application for an aft fuselage mounted three engine civil aircraft. The same aircraft type has been used in model flight tests with thrust vectoring [Ref.3] by the Jet Laboratory of the Israel Institute of Technology with funding provided by the US DOT and FAA (Fig.4.3-2).

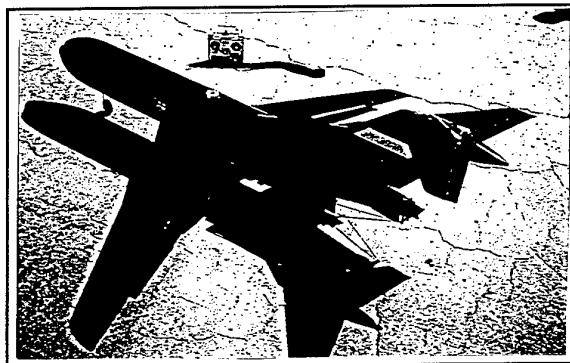


Fig. 4.3-2 Civil Aircraft Flight Test Model with T.V.

An application to supersonic transport vehicles with a higher thrust to weight ratio seems to be more promising, however, the (currently) preferred underwing engine installation reduces the required momentarm for pitch and yaw vectoring. The potential saving of a few percent fuel by the combination of reduced trim drag, friction drag and mass of a smaller vertical tail are certainly attractive goals for the civil aircraft designer.

4.4 Challenges

Though a lot of studies, demonstrations and flight tests have been performed in the last decade, there are a few challenges left.

If the nozzle is to be used as a primary control effector, its reliability, -in particular for single engine configurations-, should be no less than current aerodynamic control surfaces.

Utilization of the nozzle for continuous trim optimization will increase nozzle deflection time and may require special attention to avoid thermal or mechanical fatigue by long time asymmetric flow conditions.

Critical flight conditions in terms of low engine power setting (such as approach, crosswind landing, deceleration etc.) must be considered in the configuration design or modification. It may be necessary to integrate automatic thrust/drag management into the control laws as well as to schedule maneuvering performance of the aircraft, i.e. maximum roll rate and maximum sideslip, with engine thrust.

Utilization of available aerodynamic control surfaces to generate yawing moments may help to achieve real vertical tailless designs.

Integration of vector nozzles into existing configurations without exceeding the aft c.g. limit is another challenge.

5. SUMMARY

Thrust vectoring is not a "new" design option as studies from the late sixties and seventies confirm. But thrust vectoring has now become a realistic option.

The current development status of engine integrated multiaxis thrust vectoring devices will allow in the near future the

- integration of such systems into existing aircraft, e.g. as a weapon system upgrade (as shown in the F-16 MATV, F-15 ACTIVE, Su-35) or the
- incorporation of a T.V. system into new configurations such as JAST or other projects

The combined benefits of thrust vectoring as demonstrated in various flight test programs in the last decade (F-15 SMTD, X-31, F-18 HARV, YF-22, F-16 MATV), and theoretical estimates will assure, that this technology will find its way into current and future aircraft.

Application to civil aircraft still needs further exploration.

After one hundred years of aviation, thrust vectoring technology is just at the beginning of its application and holds a great potential for the future.

Abbreviations

A/G Air to Ground

AoA Angle of Attack

c_M Aerodynamic moment coefficient

L_T Moment arm of Thrust Vectoring System

l_μ Mean aerodynamic chord

Ma Mach number

PTD Physical Theory of Diffraction

RT Multiple reflection

T_{00} Sea level static thrust

ρ Air density

References

- [1] Huber, Peter: "Control Law Design for Tailless Configurations and in Flight Simulation using the X-31 Aircraft". AIAA Conference, August 1995, Baltimore
- [2] Mederer/Croy: "Untersuchungen über Entwurfsstudien für ein strahlgesteuertes Kampfflugzeug". MBB Bericht UFE 411-69
- [3] Ross, Hannes: "Reglergestützte Flugzeuge - Integration sämtlicher CCV- Möglichkeiten in einen AS/CAS Entwurf". MBB Bericht UFE 1141, Jan. 1975

Paper 21: Discussion

Question from D Kidman, Edwards AFB, USA

What is the next step for the X31 thrust vectoring programme?

Author's reply

Rockwell and DASA are trying to obtain funding for a new programme which would address the utilisation of thrust vectoring throughout the whole flight envelope. In particular, the areas of take-off and landing would be addressed and also the issue of reduced tail surface area.

The F-15 Active Aircraft "THE NEXT STEP"

Roger Bursey *
 Pratt & Whitney
 MS 715-85, P.O. Box 109600
 West Palm Beach
 Florida 33410-9600, USA

ABSTRACT

As the aerospace industry adjusts to post cold-war budgets, emphasis is shifting rapidly to demonstrating technologies of the future with current modern-day fighters before committing them to production. Pratt & Whitney, together with NASA Dryden, U.S. Air Force Wright Laboratories, and McDonnell Douglas, have developed such a system based on the F-15. This testbed aircraft has the capability of demonstrating a wide array of aerodynamic and propulsion integration technologies that will apply to future commercial and military aircraft design. This paper will present the "ways & means" of how Pratt & Whitney designed, manufactured, and flight tested affordable axisymmetric exhaust nozzles incorporating multidirectional thrust vectoring for the Advanced Control Technology for Integrated Vehicles (ACTIVE) Program.

INTRODUCTION

The F-15 ACTIVE Program is a prime example of using an existing fighter aircraft as a flying testbed for evaluating

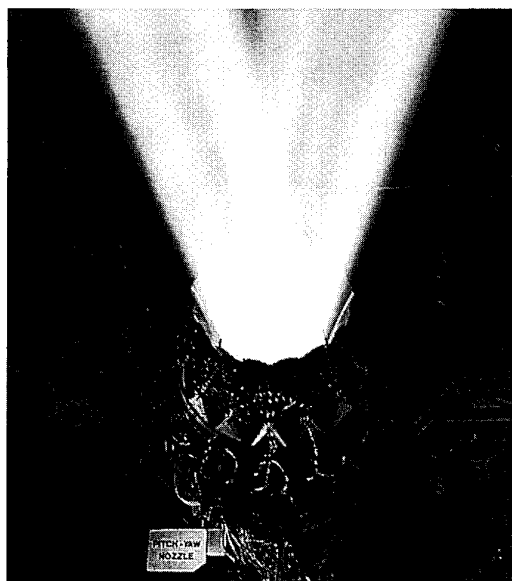


Figure 2. Axisymmetric Thrust Vectoring Nozzle

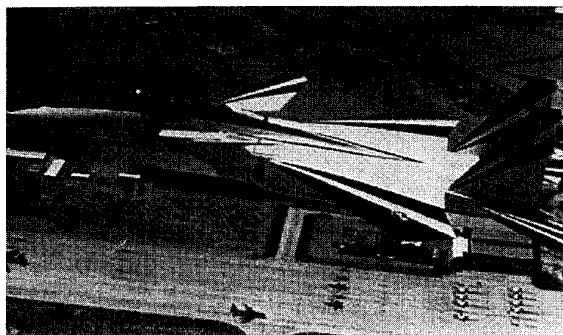


Figure 1. ACTIVE Aircraft

near-term, high-payoff technologies. A small, dedicated team comprised of Government and Industry personnel has, with a minimum of resources, brought this vehicle to flight readiness. In addition, numerous second-tier suppliers have contributed resources ensuring program success at minimum cost. Selection criteria for the technologies demonstrated in this program are that they offer a high degree of system performance improvement, yet are relatively low cost and minimum risk. Evolutionary, rather than revolutionary, approaches tend to best fill these needs.

THE ACTIVE PROGRAM

Having first flown in 1988, in the Short Takeoff and Maneuverability Demonstrator (SMTD) Program, the ACTIVE aircraft, shown in Figure 1, demonstrated highly integrated flight control with 2-dimensional convergent/

COPYRIGHT ©1995 BY PRATT & WHITNEY. PUBLISHED BY THE ADVISORY GROUP FOR AEROSPACE RESEARCH & DEVELOPMENT, WITH PERMISSION. RELEASED TO AGARD TO PUBLISH IN ALL FORMS.
 * PROGRAM MANAGER

ID	Task Name	1993	1994	1995	1996
1	Design & Fabrication	■	■		
2	Software Integration		■	■	
3	Instrumentation & Aircraft Mods			■	■
4	Flight Tests			■	■

Figure 3. ACTIVE Demonstrator Program Schedule

divergent pitch vectoring/thrust reversing nozzles, in-flight. The ACTIVE aircraft has evolved from the SMTD Program, which completed flight testing in Sept., 1991. The SMTD Program has contributed significantly to maturing thrust-vectoring technologies, which have been incorporated into the F-22 design. Significant accomplishments of this program were:

- Demonstrated a 40% reduction in takeoff distance with rotation achieved at speeds as low as 30kt
- In-flight deceleration time from Mach 1.6 to 0.8 reduced by 30%
- Improved pitch-down rates

Many of the SMTD program assets have been transferred to ACTIVE as a further means of reducing cost. The aircraft has been reconfigured to incorporate a more highly integrated aircraft/propulsion control system by

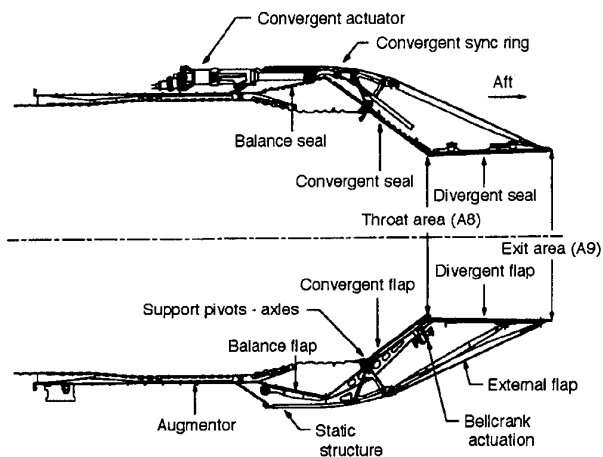


Figure 4. Balanced Beam Nozzle

incorporating two axisymmetric, multi-axis thrust vectoring nozzles provided by Pratt & Whitney. These nozzles, shown in Figure 2, provide thrust vectoring throughout the flight envelope with independent exit area control. The ACTIVE Program has four goals: (1) to demonstrate multi-axis

thrust vectoring through-out the flight envelope with attendant range improvements; (2) to investigate adaptive logic that can determine and adjust in real time the optimum settings of the engine for maximum performance; (3) to quantify the interaction between the vectoring nozzles and the airflow they induce over the airframe; and (4) to verify a method for reducing noise produced by the jet velocity of the vectoring nozzles. This last goal is important for the High Speed Civil Transport (HCST) Program, for which excessive noise could be an issue.

The ACTIVE Program was formally initiated in the last quarter of 1992 with a program schedule shown in Figure 3.

Incorporating multi-axis thrust vectoring into the ACTIVE Program offers a prime opportunity to evaluate the effectiveness of this technology in flight. Pratt & Whitney, in conjunction with Government agencies and the airframer contractor, has successfully evolved such a concept that provides a revolutionary step in tactical aircraft performance. This is the pitch/yaw balanced beam nozzle (P/Y BBN). As shown in Figure 4, this is the nozzle concept that has evolved from the basic F100 axisymmetric BBN.

This nozzle provides a full 360 degrees of axis thrust vectoring at angles up to 20 degrees, yet retains maximum commonality with the basic nozzle that has accumulated over 11.5 million hours of operation in the F100 series of engines.

Predicted payoffs for incorporating thrust vectoring on combat aircraft are numerous. Thrust vectoring has been shown to significantly increase aircraft agility with the additional benefit of improving survivability. Fighters can be made much more maneuverable, especially at very low speeds and high angles of attack, giving them a better chance of swinging the nose around to snap a shot at an adversary or dodge hostile missiles.

Operational deployment flexibility is increased, since the ability to thrust vector with thrust reversing decreases required landing and takeoff distances. This increases operational effectiveness by using bomb-cratered runways, while maintaining the ability to carry full weapons loads.

Also, vectoring can result in a more aerodynamically efficient overall aircraft configuration. Conventional tail surface sizes can be reduced or ultimately eliminated by replacing their trim drag function with thrust vectoring. The resultant drag count reduction can lead to significant range improvements and improves survivability by reducing the radar signature produced by large tail surfaces. These nozzles may provide the capability to reduce

signature by quickly shifting the nozzle position and hiding the engine components.

THE ACTIVE PROPULSION SYSTEM

The ACTIVE propulsion system consists of modified F100-PW-229 engines with strengthened fan and augmentor ducts, P/Y BBN, and attendant control revisions. The modified ducts are designed to be compatible with thrust growth up to 35,000 lb, although the ACTIVE engines are in the 29,000 lb thrust category. Pratt & Whitney's F100-PW-229 Improved Performance Engine (IPE) is the world's highest performance production fighter engine currently available with a thrust-to-weight in the 8-to-1 class. Since entering production in 1989, it has accumulated over 150,000 engine flight hours in the U.S. Air Force.

As previously noted, the P/YBBN has evolved from the BBN and maintains maximum commonality to the F100 configuration. The balanced beam feature has been retained, which results in a lightweight convergent/divergent exhaust system that provides optimum contour and performance. Minimum weight is attained through balanced air loads and by using high strength-to-weight ratio materials, such as in the divergent, convergent, and balance seals. Cooling air is used to reduce the operating temperature of various nozzle components, such as the convergent and balance flaps, convergent synchronous ring and static structure, thus allowing the use of lower density materials. The convergent actuation system provides throat area (A8) control and engine match to optimum engine pressure ratio (EPR) and thrust. This innovative design of the BBN concept, minimizes actuation system loads required to position A8. This is accomplished by using cooling air pressure to offset the actuation force required to drive the throat to the nozzle kinematic system optimum area.

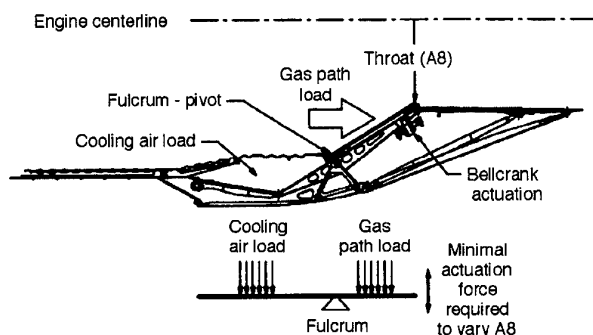


Figure 5. BBN Balanced Flap and Actuated Convergent Section

The individual components and their functions for the BBN and its vectoring derivative are the same, with the exception of the divergent section. Vectoring is accomplished by adding multi-axis control to the divergent flaps. This requires the addition of a synchronizing ring, a divergent flap actuation system, and an aft static structure. The divergent synchronous ring is supported by the aft static structure to permit three degrees of motion of the divergent flaps.

P/Y BBN DESIGN DESCRIPTION

To provide full thrust vectoring, only three new major components were added to the basic nozzle assembly. First, a synchronizing ring was added to ensure proper positioning of the divergent flaps at all vector and area ratio settings. Second, three dual redundant hydraulically powered actuators were added to provide multiplane

Table 1. P&W's Full Envelope Thrust Vectoring (FETV) System Has Completed Ground and Flight Clearance Tests

<i>Ground Demonstration Program 1990-1992</i>	
Total, hr	82
Total A/B, hr	8.5
Vectoring, cycles	>1300
Vectoring Angle/Sideforce, lb	$\pm 20^\circ/4000$
Slew Rate	45°/sec
<i>ACTIVE Flight Clearance Program 1992-1994</i>	
Total, hr	48
Total A/B, hr	12.0
Vectoring, cycles	50,250
Vectoring Angle/Sideforce, lb	$\pm 20^\circ/4000$
Slew Rate	120°/sec

control of divergent flap position. Third, an aft static structure was added to support the vectoring mechanism. This basic concept has evolved from initial kinematic development that began in 1986 and continued through flight acceptance testing, which was completed in December 1994 for the ACTIVE Program.

The P/Y BBN for the ACTIVE aircraft retains the BBN balanced flap feature, as shown in Figure 5, and a pneumatically actuated convergent section that is fail safe/operational.

This configuration completed a highly successful sea-level demonstration in 1992 and flight clearance testing for the ACTIVE Program in 1994. The results of these tests are summarized in Table 1.

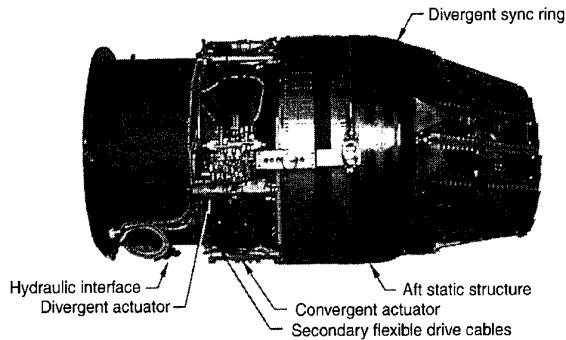


Figure 6. ACTIVE Flight Test Nozzle

In addition, a rigorous series of bench tests was successfully completed for the flight actuation system. The divergent actuators accumulated 572 bench hours and 280,000 cycles. In similar testing, the convergent actuators accumulated 168 hours and 1,030,000 revolutions at the actuator input drive shaft. These tests also included the following:

- Explosion Proof
- Lightning
- Vibration
- Impact
- Limit Load
- Burst Pressure
- High Pressure
- Room Temperature Endurance
- Low Temperature
- Fire Resistance

As shown in Figure 6, the system has evolved into pre-production flight nozzles and is currently in flight testing.

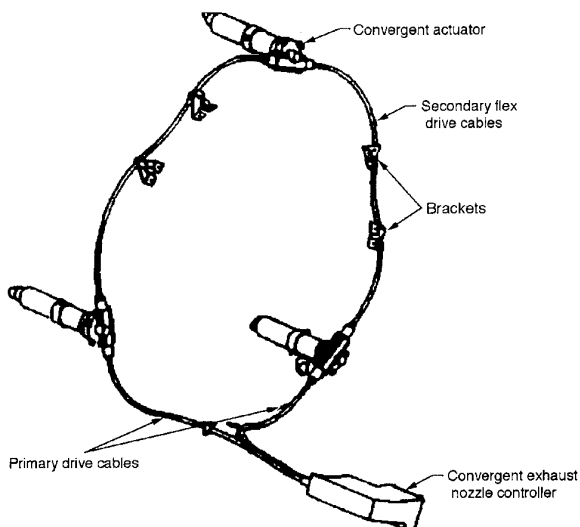


Figure 7. Convergent Control

CONVERGENT FLAP SYSTEM

The convergent flap system is functionally the same as the F100 system, except that the number of actuators has been reduced to accommodate envelope requirements for the divergent actuators unique to the vectoring system. In addition, a rotary variable displacement transducer (RVDT) has been added to provide throat area feedback. The convergent exhaust nozzle control (CENC) is identical to the F100 CENC. The convergent actuators, shown in Figure 7, are driven by redundant flexible drive cables from the CENC. The system is pneumatically driven by engine air.

DIVERGENT FLAP SYSTEM

Vectoring is accomplished by axisymmetric modulation of the independent divergent actuators powered by the hydraulic system. This results in an angular rotation of the sync ring. The ring, in turn, positions the divergent flap and seal assemblies, as shown in Figure 8.

Axisymmetric modulation is used to vary the nozzle area ratio to optimize performance at all flight conditions. The vectoring and area functions are blended by the nozzle

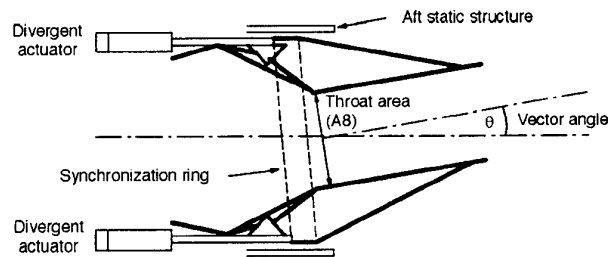


Figure 8. Divergent Flap System

control system to ensure smooth operation. In the case where actuator rate limits are reached, priority is given to satisfy flight control vector requests to prevent degradation of vehicle handling characteristics.

NOZZLE COOLING

The internal divergent flap and seal assemblies are constructed of high-temperature-capability alloys and are cooled by fan duct air. Although heat resistant coatings have been tested on the divergent seals, no coatings have been deemed necessary due to the highly efficient cooling system design.

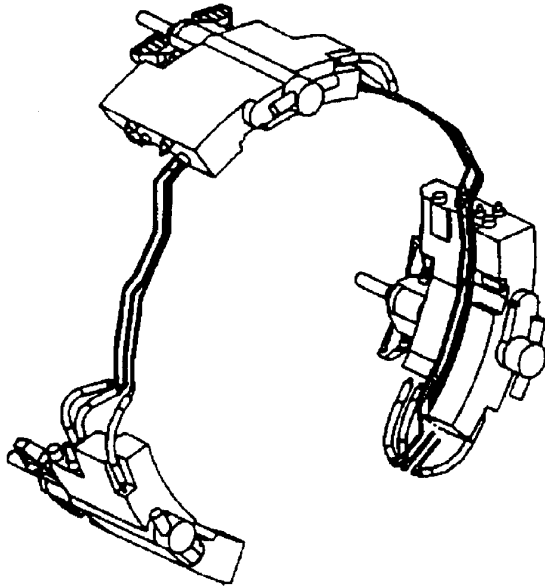


Figure 9. Divergent Flap Actuator and Servovalve Modules

CONTROL SYSTEM DESIGN AND FUNCTION

The nozzle control configuration consists of two independent systems: a pneumatically controlled convergent drive system using engine compression system bleed air, and a hydraulically powered divergent/vectoring system.

The divergent actuation system is designed with reliability as primary importance, and is configured with hydraulic and electrical redundancy specifically directed toward thrust vectoring as a critical flight control function. The divergent actuators are a dual-piston design, adaptable to either single- or dual-hydraulic sources. Reliability studies have shown that redundant hydraulic pumps are a necessity to achieve acceptable flight critical failure rates. These redundant hydraulic pumps, reservoirs, coolers, and related accessories already exist in most aircraft, and the P&W design is configured for ease of incorporation into current systems. The remainder of the divergent control system (servovalves, control valves, and fail-safe system) is arranged in modular fashion for ease of maintenance and adaptability to customer requirements (see Figure 9).

SYSTEM SAFETY

In the event where one or more of the divergent actuators can no longer respond to position commands, the system has been configured with a fail-safe feature that overrides other electric and hydromechanical control components and locks the vectoring system in an axial orientation, providing an expansion ratio schedule that affords nozzle

performance and thrust capability similar to the BOMB BN. A variant of this approach has also been successfully tested. This variant can independently lock a signal of the offending actuator and reconfigure the control software to allow limited thrust vectoring, while sacrificing optimum nozzle expansion ratio. Safety is also of utmost concern during nozzle operation. During vectoring, the nozzle structure, engine ducts, and mounting components operate at higher loads due to the forces generated normal to the engine centerline by the deflected exhaust efflux. Typical installations require strengthening in these areas to avoid component overstress. The generated normal forces are a function of engine gross thrust, vector angle, and induced aero effects and must be calculated in real time during flight to limit the maximum achieved vector angle. Although engine gross thrust is calculated in flight with reasonable accuracy, induced aero effects are not, since no direct measurements are readily available. Induced effects are caused by the internal and external flowfield interactions and *can be very powerful* in generation of additional normal force. An example of this was the S/MTD 2-D/C-D nozzle configuration where 53.4 kN (12,000 lb) of normal force could be generated at some flight conditions by deflecting the nozzles only one degree.

Although industry has had success predicting internal effects using advanced computational fluid dynamics tools, the external flowfield has shown to be much more difficult to characterize because of its aircraft configuration dependency. Experience has shown that these investigations are better left to model testing of the actual configuration in wind or flight test.

SUMMARY

The "Next Step" is underway with flight testing of a fully integrated multi-axis thrust vectoring nozzle system in the ACTIVE aircraft. This evolution extends the jet engine beyond being a mechanism for merely supplying propulsive force, by providing designers of future aircraft with alternative aerodynamic solutions. No longer will the designer have to rely solely on aerodynamic surfaces for pitch and yaw moments. Vectoring thrust is rapidly emerging as a technology to push aircraft capability well beyond the vision of aircraft designers of the 1950s and 1960s. The F-15 ACTIVE aircraft, fitted with Pratt & Whitney 29,000 lb thrust class engines, modified with full envelope thrust vectoring nozzles, will lead this technology into the next century.

The "Next Step", building on the success of past pioneer vectoring nozzle systems such as the F-18 HARV, X-31, F-15 SMTD the F-16 VISTA and F-22, will establish a new foundation for future fighter aircraft design.

Paper 24: Discussion

Question from Dr H Toenskoetter, IABG, Germany

What is the weight increase of the balance beam vectoring nozzle compared with the equivalent conventional nozzle? Is it intended to use composite materials and, if so, in which parts?

Author's reply

The target weight difference between the vectoring balanced beam nozzle and the basic nozzle is 245 lbs. The article that will be flight tested in the ACTIVE aircraft is heavier due to cost saving measures taken in the construction of these prototypes.

The conceptual evaluations completed to date indicate that Organic Matrix Composites could be effectively used on construction of the external flaps, some actuator kinematics components, and control housings.

Question from G T Shanks, Defence Research Agency, UK

What criteria were addressed during flight clearance testing of the nozzle?

Author's reply

First and foremost was safety of flight. The nozzle was designed with dual redundant electrical and hydraulic actuation system components. Extensive endurance bench tests were conducted on all subsystems to ensure that the durability and safety requirements were met. The dual redundancy features ensured the system could be used in single engine applications, such as the F16 VISTA.

Optimization of Actuation and Cooling Systems for Advanced Convergent-Divergent Nozzles of Combat Aircraft

C. Sánchez-Tarifa, M. Rodríguez-Fernández, R. Rebolo, G. Corchero

SENER INGENIERIA Y SISTEMAS, S.A.
Parque Tecnológico de Madrid
C/ Severo Ochoa nº 4, 28760 Tres Cantos - Madrid - Spain

and M. Rodríguez-Martín, I. Ulizar Álvarez

INDUSTRIA DE TURBO PROPULSOIRES, S.A. (ITP)
Carretera Torrejón-Ajalvir km.3.5, Torrejón de Ardoz 28850 .Madrid - Spain

1. SUMMARY

The system or components of a convergent-divergent (CON-DI) nozzle that offer better perspectives for improvement and optimization are the actuation and cooling systems.

Performance offers little margin for a direct improvement, and the utilization of advanced materials in many components of the nozzle presents no specific problems as compared with those of other parts of the engine, with the exception of the petals, in which the introduction of ceramic materials has a direct influence on cooling and performance, and it will be included in the cooling optimization.

The introduction of a thrust vectoring capability is a major improvement, though not the subject of this paper.

The problem of the optimization of the actuation system was preliminary discussed in ref. 1, mainly in connection with the utilization of one versus two parameters actuation system. Since that time, SENER and ITP have carried out many studies and tests on actuation systems and on cooling optimization. They have also accumulated experience by means of theoretical and experimental studies on the utilization of ceramic petals.

Some results and the main conclusions of these studies and tests are presented in the present work.

2. ACTUATION SYSTEM

Conceptual design of nozzles involves primarily a device optimization based on a set of missions for which the whole weapon system is to be designed. Optimization of the actuation mechanism is closely linked with the nozzle concept itself, and therefore is one of the main issues established during the conceptual design phase.

Basically the function of the nozzle as an engine component is the air flow and back pressure control. It can be covered in a military engine by means of a simple variable convergent nozzle. However this type of devices are far of being optimum regarding the produced thrust. The second function of the nozzle is to convert as much thermal energy as possible into thrust. As the supersonic flight capabilities of fighter

airplanes seem more and more important, thrust at high nozzle pressure ratio starts to be one of the limiting constraints for sizing the engines. That is the case of the following typical design cases:

- Supersonic cruise & escape dash.
($M = 1.5$, $h = 30\text{kft}$, $R = 130\text{ n.mi.}$, Max dry)
- Weight specific excess power at high Mach num.
($M = 2.0$, $h = 40\text{ kft}$, Max reheat)
- Accelerations to supersonic.
($0.8 \leq M \leq 1.6$, $h = 30\text{ Kft}$, $t < 50\text{s}$, Max reheat).

A convergent nozzle working in the first condition is producing 6% less thrust than the optimum convergent-divergent nozzle, or in other words, aircraft is requiring 0,5% WTO to perform the supercruise missions phase (5% of the typical payload of an air to air fighter-AAF). For the weight specific excess power at high Mach number the loss of thrust relative to the optimum convergent divergent is in the order of 7% which represents roughly the required excess power. For comparison purposes the optimum CON-DI nozzle will be used as a baseline. Optimum CON-DI nozzle means an axisymmetric convergent-divergent nozzle with a fixed aircraft interface producing the highest thrust for a giving total thermodynamic conditions of the exhaust gases. Convergent and divergent petals length are kept constant as well as the required cooling flow.

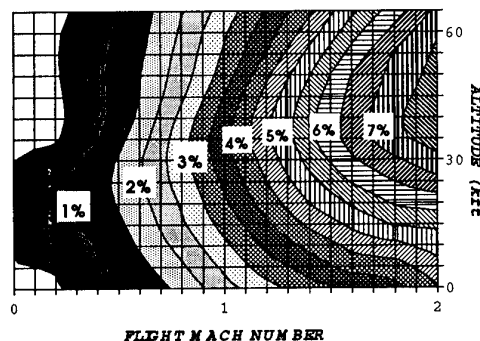


Fig.1.- Thrust losses of a convergent nozzle (dry)

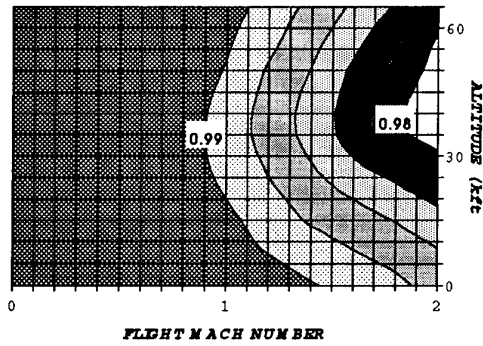


Fig.2.- Optimum thrust coefficient for a CON-DI nozzle (dry)

Figure 1 shows the thrust losses of a convergent nozzle relative to the optimum CON-DI operating in dry conditions, and the optimum thrust coefficient contours attainable with the described CON-DI nozzle are plotted in figure. 2. Nozzle optimization has been performed based on a typical engine for an AAF operating up to Mach number 2 an 65 kft altitude. Exit to throat area ratios (A_9/A_8) corresponding to optimum thrust coefficients are included in Figs.3. Optimum A_9/A_8 ratios vary from 1 to 1.9 for this kind of applications.

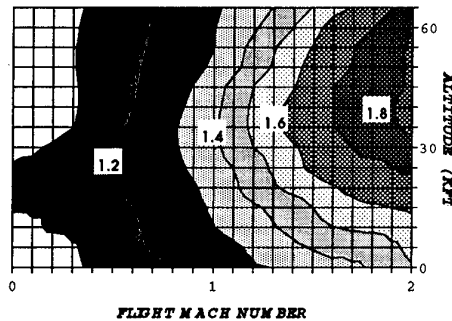


Fig.3.I.- Optimum exit to throat area ratio (dry)

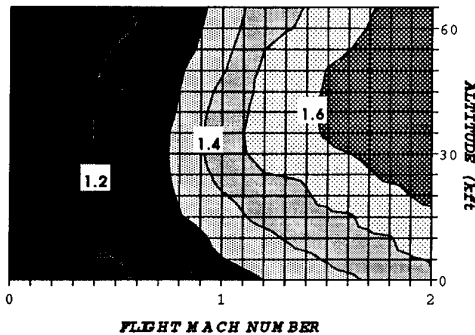


Fig.3.II.- Optimum exit to throat area ratio (reheat)

From figures 3.I. and 3.II. above, where the mentioned A_9/A_8 relationship for dry engine rating and reheated operation respectively are shown, the following conclusions can be derived:

- Best A_9/A_8 ratio for supercruise mission phase is ~ 1.6 . (Fig. 3.I).
- Optimum A_9/A_8 for weight specific excess power requirement at $M=2.0/40$ Kft is again around 1.6. (Fig.3.II).

It has been mentioned that supercruise or excess power at high Mach number are the limiting constraints at high speeds, but on the other hand there is another fundamental constraint at low speed: the take off requirements. Preferred solutions for A_9/A_8 ratio for take off conditions are around 1.1. That introduces one of the main problems of the nozzle actuation system. Nozzle performance demands a system capable of producing variations of A_9/A_8 ratio from 1.1 to 1.6, independently of the throat area value, this means, a two degrees of freedom mechanism or biparametric CON-DI nozzle. But all the other aspect to be taken into account in the design optimizations indicate the opposite. Weight, Maintainability and Reliability considerably worsen when a biparametric nozzle is studied.

Classical CON-DI nozzle designs are based on the articulated struts construction, where A_9/A_8 relationship is kinematically linked to actual throat area. Large A_8 produces high A_9/A_8 ratio, when reheated engine operations is required at supersonic Mach number. Lower A_8 implies low A_9/A_8 , suitable for continuous subsonic operations.

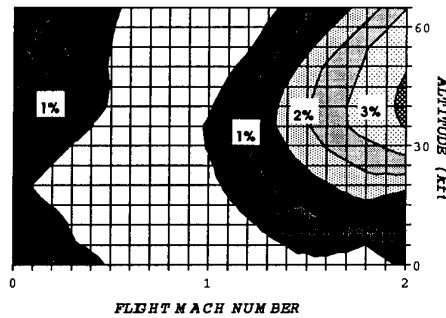


Fig.4.I.- Thrust losses for a monoparametric nozzle (dry)

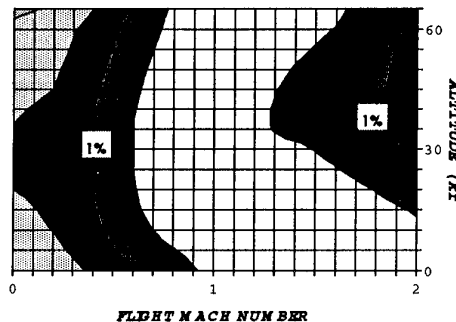


Fig.4.II.- Thrust losses for a monoparametric nozzle (reheat)

In figures.4.I and 4.II the thrust losses contours for a typical monoparametric nozzle are presented. For take off conditions 1.5% of the available thrust is lost. At supercruise flight

conditions the thrust losses are approximately 2%. For excess power requirement point the thrust losses are around 1%.

Figures 5, 6 and 7 present the thrust losses, at dry power, for a nozzle with fixed exit to throat area ratios of 1.2, 1.55 and 1.9 respectively, with the reheat losses being very similar to the dry ones.

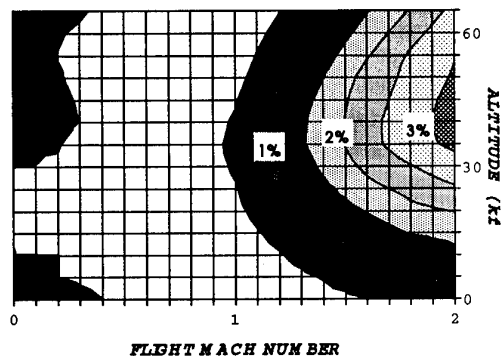


Fig. 5.- Thrust losses for a a CON-DI nozzle with $A_9/A_8=1.2$ (dry)

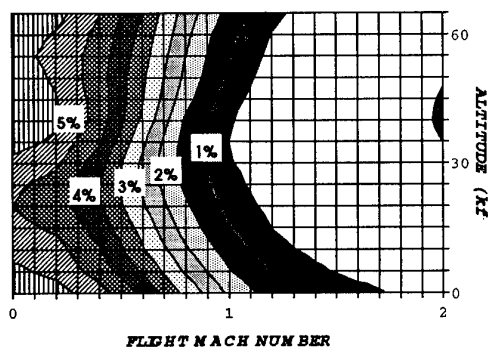


Fig. 6.- Thrust losses for a a CON-DI nozzle with $A_9/A_8=1.55$ (dry)

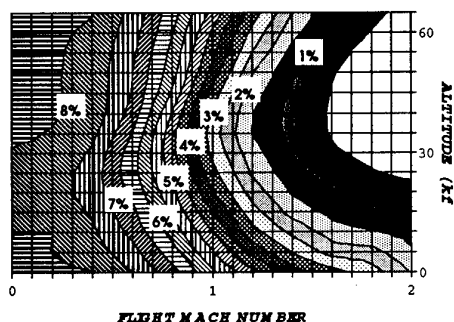


Fig. 7.- Thrust losses for a a CON-DI nozzle with $A_9/A_8=1.9$ (dry)

An important conclusion arises from the previous figures. The whole speed-altitude range, from Mach number 0 to 2, and from sea level to 65 kft, can be flown with thrust losses below 0.5% using a nozzle with two fixed A_9/A_8

relationships, 1.2 for subsonic flight and 1.55 for supersonic flight, either in maximum dry rating or maximum reheat operation. This kind of bistate CON-DI nozzle is being currently investigated for future applications. Bistate nozzle can be nearly as efficient as the biparametric ones, but lighter and more reliable provided that the change between the two expansions ratios could be done using the appropriate system, such as electrical micro actuators.

Up to this point missions phases involving maximum thrust requirements have been discussed. To finalize with the optimization of the actuation mechanism some attention must be paid to the cruise conditions. A substantial part of the fuel required for a mission is spent in cruise conditions. Typical subsonic cruise phases are:

- Subsonic cruise climb ~ 40 Kft/ $M=0.9$, 150 n.mi.
- Loiter 10 Kft/ $M=0.65$.

Engine pressure ratios for these flight cases are well below 3. The most critical case is the loiter mission phase. Performance of a perfectly sealed CON-DI nozzle as described in previous paragraphs is very poor. The reason of such a bad behavior is due to the large A_9/A_8 employed for the actual cruise nozzle pressure ratio. Discharge static pressure P_{s9} is lower than the ambient pressure, and this nozzle over-expansion causes a rapid descent of thrust coefficient. A method to alleviate the mentioned effect is to leave the divergent part of the nozzle floating. As static pressure inside the nozzle is lower than the ambient pressure there is a moment relative to the hinge at the throat plane which tends to close the divergent part of the nozzle. Hence over-expansion can be drastically reduced leaving the divergent petals floating up to a position where the moment of external pressure forces is in equilibrium with the one generated by the internal ones. That device has been called floating nozzle. Figure 8 (solid line) shows the increase in thrust, when the floating system is employed, relative to a nozzle with a fixed A_9/A_8 ratio of 1.2.

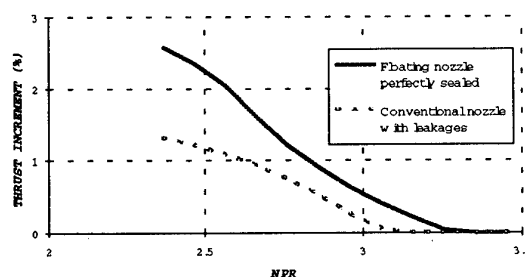


Fig. 8.- Thrust increment for a CON-DI nozzle with floating and leakage

However floating mechanisms present some problems difficult to overcome. Pressure oscillations in the divergent part of the nozzle induce vibrations at low A_9/A_8 , when the floating nozzle could give the biggest benefits. Moreover, load maneuvers in flight would induce nozzle ovalization. Pressure fluctuations in the external cavity, between nozzle and the flaps, in a twin engine aircraft installation, would produce in flight vibrations.

Fortunately real nozzles are not perfectly sealed, specially at low NPRs where pressures inside the nozzle are below the ambient pressure. In that situation slave divergent petals tend to be separated from the master ones. External air is really being ingested through the existing gaps between master and slave divergent petals. This incoming flow reduces the effective exit to throat area ratio, hence diminishes over-expansion producing an increment in thrust coefficient. Fig. 8 (dashed line) gives the thrust increment due to the described effect. At least half of the benefit theoretically recoverable by means of a floating nozzle can be obtained from the real geometry of a conventional CON-DI. For that reason, nozzles with floating mechanism have been discarded, because the potential benefits can not compensate the problems that it introduces.

3. COOLING

The simplest way to cool a CON-DI nozzle is to take the air needed for the cooling at the end of the reheat liner. This air flows downstream as a film protecting the walls from the high temperature of the main flow. The cooling effectiveness decreases with the distance from the injection due to the mixing of the (cold) film cooling layer with the (hot) main stream.

There are alternative ways to cool a CON-DI nozzle but with a high mechanical complication in the design of the nozzle petals and/or mass penalty not compensated with the possible increment on thrust due to the hypothetical reduction on cooling.

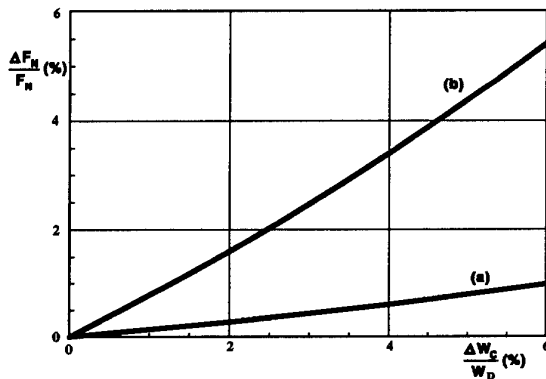


Fig. 9.- Delta thrust vs. delta cooling reduction. (a) with decoupled R/H system; (b) with coupled R/H system.

The appropriate nozzle cooling has to be obtained as a compromise with the jet pipe cooling. For example, a reduction on nozzle cooling flow does not implies an equivalent increment on engine thrust if there is not an appropriate coupled design of the complete reheat system as can be seen in Fig. 9. The reason to have the difference between curves a and b of Fig. 9 is because, for a given reheat configuration, the reduction on nozzle cooling implies a redistribution of the cooling flow across the reheat system and only a small part of the reduced cooling is utilized (burnt in the reheat system) to increase the thrust. Nevertheless, if the reduction is complemented with a coupled design of the reheat system the increment on thrust can be as high as given in curve b of Fig. 9.

3.1. THROAT COOLING

Independent of the thermal design is the passive cooling that can be obtained in some flight conditions, i.e. for some nozzle pressure ratios, throughout the gaps between petals left for mechanical reasons.

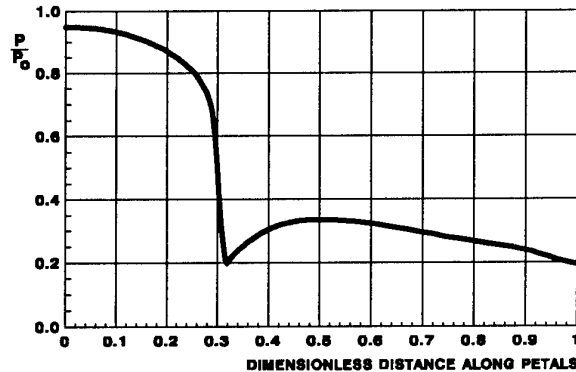


Fig. 10.- Typical pressure distribution along the petals of a CON-DI nozzle

A CON-DI nozzle with a sharp throat produces a local expansion downstream the throat, as sketched in Fig. 10, when the nozzle is choked. The pressure at the nozzle wall suddenly decreases down to approximately 50% of the one-dimensional value immediately downstream the throat, followed by a gradual increasing up to the one-dimensional value in a petal length of approximately 20% of the throat diameter as pointed out by experimental results.

The local expansion around the throat region could be utilized to introduce some amount of cold air from the surrounding nozzle cavity to the nozzle main flow. This cold air can be used as extra-cooling air for the divergent petals. To pump the cold air from the cavity, a slot in the throat is needed. The flow direction downstream the throat near the nozzle wall is complicated to analyze in a theoretical way because there is a supersonic flow at distances sufficiently apart from the nozzle wall, together with a shear layer starting at the throat slot in presence of the boundary layer originated upstream of the nozzle throat.

It is clear that to have positive flow from the cavity to the nozzle, the cavity pressure, p_c , must be larger than the local pressure inside the nozzle near the wall just downstream the throat slot, but this pressure depends on the local geometry of the nozzle around the throat and on the main flow characteristics.

The slot in the throat area of a CON-DI nozzle is inherent to its design unless special features are provided so as to seal that region. Nevertheless, the slot is of small dimensions compared with the throat diameter, so that the local flow can be considered two-dimensional.

Let us assume the simple two-dimensional configuration of Fig. 11 when the nozzle is choked. The flow at the throat is sonic and the sonic line starts perpendicular to the end of the convergent petal. The relative angle between the convergent

and the divergent petal is $\alpha + \beta$, being α and β the convergent and the divergent petal angles, respectively, with respect to the symmetry axis of the nozzle. In the case of an ideal flow, a tangential discontinuity separates the nozzle flow from the cavity air. For a value ψ of the angle of this tangential discontinuity with the divergent petal, the total turning of the flow is $\alpha + \beta + \psi$. As the pressure across the tangential discontinuity must be continuous, the total flow turning is function of the ratio p_c/P_0 , P_0 being the total pressure of the main flow. On the other hand, the velocity at both sides of the discontinuity can be different but its component normal to this surface must be zero, and therefore the mass flow is zero.

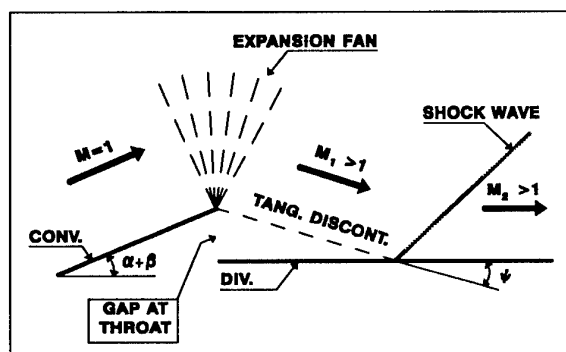


Fig. 11.- Sketch of the ideal flow in the region close to the throat slot and the nozzle petals.

In a real flow the tangential discontinuity does not exist, being instead a layer where the viscous effects take place and some amount of flow goes inside or outside the cavity as sketched in Fig. 12.

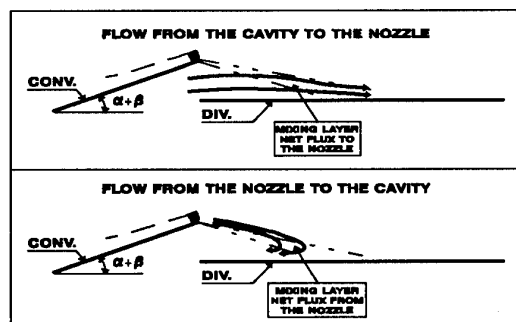


Fig. 12.- Sketch of the real flow in the region close to the throat slot and the nozzle petals

From the analysis of this layer, the additional condition comes that determines the cavity pressure as a function of the mass flow. The analysis of this layer is complicated, but if we are looking for small values of the mass flow (compared with the main flow) ejected from and to the nozzle, the mixing layer is narrow and can be taken as a discontinuity when we are calculating the expansion fan. Using the method described in Ref. 4, it is possible to obtain the angle ψ of the effective separation surface between the nozzle and cavity (see Fig. 13) as a function of the cavity pressure p_c .

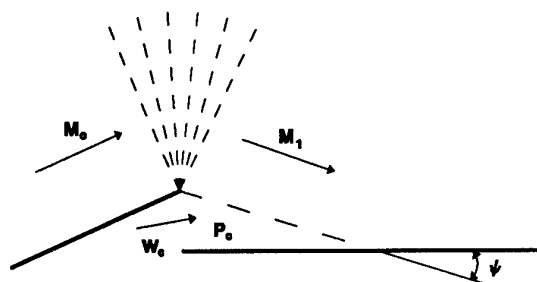


Fig. 13.- Sketch to obtain the mass flow ejected from or to the nozzle

Once the angle ψ is known as a function of P_c , the Mach number M_1 downstream the expansion fan is also known. As the angle ψ can also be written as (see Ref. 4),

$$\psi(M_1, C_w) = f_1(M_1) + C_w \cdot f_2(M_1)$$

where C_w is the dimensionless mass flow (positive or negative) and $f_1(M_1)$ and $f_2(M_1)$ are known functions of the Mach number M_1 , the dimensionless mass flow can be obtained from the above relation. The definition of C_w is given in terms of the mass flow ejected W_c , the density ρ_1 and the velocity v_1 (both known) and the boundary layer momentum thickness before the expansion fan (also known from the analysis of the flow field in the convergent nozzle). Therefore, the ejected mass flow can be obtained.

The mass flow W_c shall be positive (to the nozzle) or negative (from the nozzle). The important point is to know what is the nozzle pressure ratio, NPR_0 , for which W_c is zero. When $NPR < NPR_0$ we have a positive value of W_c , that means an extra-cooling for the divergent petals. On the other hand if $NPR > NPR_0$, W_c is negative and there is a loose of cooling for the divergent petals.

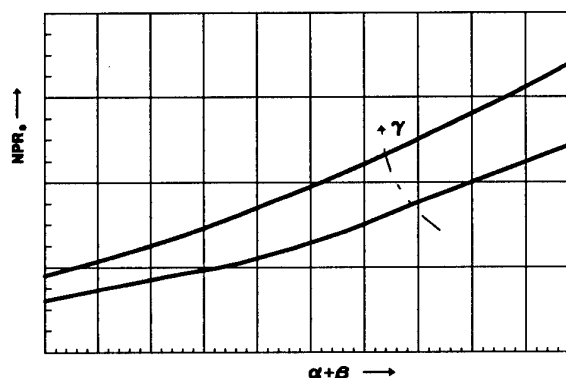


Fig. 14.- Nozzle pressure ratio for zero cooling flow throughout the nozzle slot.

Tests have been performed with a nozzle throat ejector in order to determine the ejection capability and the value of NPR_0 (see Refs. 6 and 7). The experimental data can be easily correlated using the method of Ref. 4 above described. The value of NPR_0 is a function of the total turning angle

$\alpha + \beta$ and the specific heat ratio γ , for fixed values of the total cavity pressure (assumed to be equal to ambient pressure) and slot geometry. The results are given in Fig. 14.

The operating NPR of a CON-DI nozzle can be, in some flight conditions, higher than NPR_0 and, as mentioned above, the nozzle will lose some amount of cooling flow throughout the gap. As it can be seen in the sketches of Fig. 12, for W_c to have negative values, a reversal flow pattern needs to be generated at the throat, this meaning that the value of the NPR to lose an appreciable amount of cooling mass flow is too high, outside of the operating values. This was confirmed with the ejector tests and also with engine tests measuring petal temperatures distribution for NPR's lower and higher than NPR_0 (see Fig. 15).

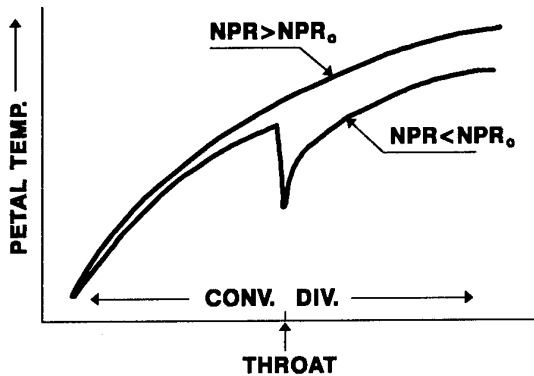


Fig. 15.- Effect of throat cooling on petal temperature.

3.2. CERAMIC PETALS, COOLING REDUCTION.

CON-DI nozzle will benefit from the general development of advanced materials, as in the field of advanced titanium alloys (actuation ring, struts); polyamides composites (external fairing flaps), and specially ceramic matrix composites for the petals.

The development of ceramic composite materials have progressed steadily, but rather at a slow pace. This development is being hampered by the size of the potential market, which is rather small. As a consequence the high cost of these materials will probably continue to be a problem.

AVERAGE SiC/SiC CHARACTERISTICS		
Density	T ~ 20 °C 2.3-2.5 gr/cm ³	T ~ 1400°C -----
Tensile strength	180-340 MPa	~150 MPa
Flexure strength	300-550 MPa	~280 MPa
Shear strength	35-45 MPa	
Thermal difussivity	~ 6 × 10 ⁻⁶ m ² /s	~ 2 × 10 ⁻⁶ m ² /s
Total emissivity	0.75 - 0.80	-----

Table 1.

The most advanced type is the ceramic composite silicon carbide matrix and silicon carbide fiber (SiC/SiC). Some of its more important characteristics (averages values from several manufacturers) are shown in Table 1.

The utilization of SiC/SiC petals up to temperatures of about 1200°C is feasible. Above this temperature a protective coating would be needed, or else the utilization of other carbon matrix materials, such as the C/SiC, not yet sufficiently developed. However, at such high temperature, radiation from the petals might originate serious problems in other nozzle components, specially in the actuation system and fairing flaps.

The value of the cooling flow is usually determined by the maximum admissible temperature in the divergent petals. Therefore the utilization of SiC/SiC in these petals would permit reduction of cooling flow up to the limitation in the temperature now imposed by the convergent petals. Reductions of the order of a 5% are possible (fig. 16) with a thrust increase of about 4% (fig. 9). In addition, SiC/SiC divergent petals could reduce the total mass of the nozzle by about a 5-6%. However, the introduction of this ceramic matrix continues being hampered not only by its high cost, but by a certain insufficient knowledge of some mechanical properties specially with relation to life.

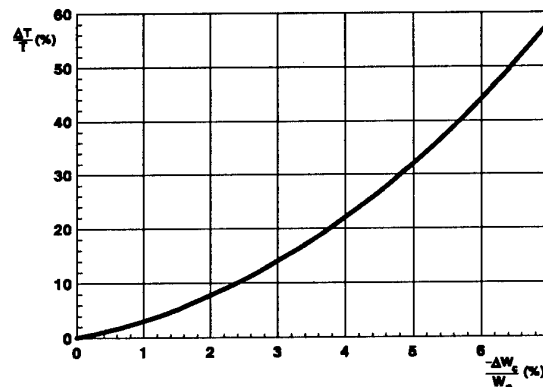


Fig. 16.- Petal temperature increment vs. nozzle cooling reduction

The utilization of SiC/SiC in the convergent petals would allow a further reduction of the cooling flow, with a total reduction of the order of a 6% and a thrust increase of about a 5% (fig. 16 and 9); assuming maximum temperature of 1400°K. However it would imply that the master convergent petals would require a new configuration, with a SiC/SiC surface plate in contact with the hot gases and the rest of the petal of a metallic material with a minimum contact with the SiC/SiC.

Finally, another factor to be considered is that a high temperature ceramic petals nozzle would have a much higher infrared emissivity than that of a metallic petals nozzle.

3.3. SYMBOLS.

NPR Nozzle pressure ratio (P_o/P_a)

A_g	Nozzle throat area.
A_9	Nozzle exit area.
C_w	Mass flow coefficient.
F_N	Net thrust.
M	Mach number.
P	Pressure.
P_o	Total pressure at nozzle entry.
P_a	Ambient pressure.
P_c	Cavity pressure.
W_p	Total engine mass flow.
W_c	Cooling mass flow.
α	Convergent petal angle.
β	Divergent petal angle.
ψ	Angle of effective separation (see Fig. 13).
γ	Specific heat ratio.

4.- REFERENCES

- [1] Sánchez-Tarifa, C. & Mera-Díaz, E. "A Study on the optimization of Jet Engine for Combat Aircraft". (8th International Symposium on Air Breathing Engines. Cincinnati, USA, 1987.
- [2] Huntley, S. C. & Yanowitz, H., "Pumping and Thrust Characteristics of Several Divergent Cooling-Air Ejectors and Comparison of Performance with Conical and Cylindrical Ejectors", NACA RM E53J13, 1954.
- [3] Carrière, P. & Sirieix, M., "Facteurs D'Influence du Recollement d'un Écoulement Supersonique", ONERA, Publication n° 102 (Nov. 1961).
- [4] Carrière, P., "Aérodynamique Interne. Tuyères et Jets", Ecole Nationale Supérieure de L'Aéronautique et de L'Espace", Toulouse, 1980.
- [5] Brooke, D.; Dusa, D. J.; Kuchar, M. P. & Romine, B. M., "Initial Performance Evaluation of 2DCD ejector Exhaust Systems", AIAA-86-1615, 1986.
- [6] Rodríguez, M., "Throat Ejector. Cold Flow Tests Results-Phase I", SENER, SN-RP7-004, 1988.
- [7] Rodríguez M., "Throat Ejector in a CON-DI Nozzle (Results of Phases I and II of Cold Flow Tests", SENER, SN-RP7-001, 1989.

Paper 26: Discussion

Question from K Bradbrook, BAe Defence Ltd, UK

You referred to thrust losses for convergent nozzles. Were these losses for installed or uninstalled nozzles?

Author's reply

The losses are for the uninstalled case. For a pure convergent nozzle the installed losses will be higher. However, in the case of an ejector nozzle they will be lower because it forms an aerodynamic convergent-divergent nozzle. In most cases such a nozzle will be larger than a conventional single parameter nozzle.

AN ADVANCED CONTROL SYSTEM FOR TURBOFAN ENGINE : MULTIVARIABLE CONTROL AND FUZZY LOGIC. (APPLICATION TO THE M88-2 ENGINE)

Alain GARASSINO, Patrick BOIS
Control and Accessories Division
SNECMA
MELUN-VILLAROCHE
77550 MOISSY-CRAMAYEL
FRANCE

ABSTRACT :

The search for better performance of present and future turbofan engine involves an increase on the number of variable geometries and thus of control loops.

As we can not or do not want to disregard the interaction between loops any more, the future control systems will therefore be multivariable. The aim of the architecture of multivariable control presented here is to optimize a performance index during transients.

This architecture consists of an inner loop which optimizes the performance index taking in account the limitations, an outer loop which brings the nominal steady-state offsets to zero and a trajectory which allows to take into account the topping schedule limitation.

This basic architecture can be improved by fuzzy supervisor.

Indeed, two control outputs are generated according to the description above :

- the first one optimizes the thrust and does not care very much about LP stall margin limitation,
- the second one optimizes again the thrust and strongly takes low pressure stall margin limitation into account.

The fuzzy logic then allows to do a compromise between these two control outputs according to the engine state.

Simulation results showing the efficiency of the method are given.

XN2R Corrected Fan Speed
X* the desired value of X

1 - INTRODUCTION :

1.1 - Control Architecture of the M88-2 engine :

In order to manage thrust, two engine parameters are controlled: the fan speed, XN2, which is an estimator of the fan airflow and the pressure ratio, $\Delta P/P = (PT23 - PS23)/PT23$, where PT23 is the total pressure and PS23 the static pressure between the LP and HP compressors, $\Delta P/P$ is an estimator of the mach between the two compressors. The LP stall margin, SM, can be computed versus $\Delta P/P$ by :

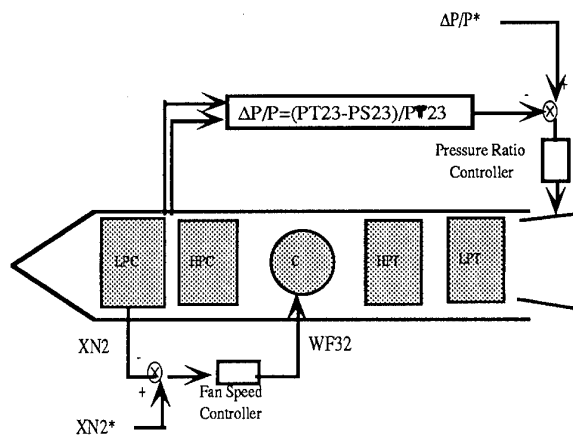
$$SM = f(\Delta P/P, XN2R)$$

where the corrected fan speed XN2R has a very low influence.

Usually, the fan speed XN2 is controlled by the main fuel flow, WF32, and the pressure ratio $\Delta P/P$ is controlled by the exhaust nozzle area, A8 :

Symbols and Notations :

A8	Exhaust Nozzle Area
C	Combustion Chamber
$\Delta P/P$	Pressure Ratio
F _n	Thrust
H/L P	High/Low Pressure
HPC	High Pressure Compressor
HPT	High Pressure Turbine
LPC	Low Pressure Compressor
LPT	Low Pressure Turbine
LQ	Linear Quadratic
SM	Low Pressure Stall Margin
WF32	Main Fuel Flow
XN2	Fan speed



There are also the control of the inlet guide valve and the variable stator valve. The engine does not directly appear in the feedback of these two loops. It is the reason why we do not consider these two loops in this study.

1.2 - Application of the Linear Quadratic Regulator :

In Linear Quadratic (L.Q.) multivariable control, the controller gains are computed in order to minimize a performance index. The choice of this performance index depends on the requirements for an operational mode.

In the thrust mode, the thrust F_n must be optimized and the performance index is :

$$J = \int F_n^2 dt$$

In order to have the same steady state values for any engine, we have the same number of integrators as the number of variable geometries. Therefore, the thrust value in steady state is worked out by control demands. So optimizing the above criteria J means optimizing the time response.

An engine having physic limitations, the actual optimization must take into account constraints. The low pressure (LP) stall margin is one of the main limitations for transients. Thus, the performance index becomes :

$$J = \int (F_n^2 + a SM^2) dt$$

where SM is the LP stall margin, a parameter used to manage the compromise between performance and the available LP stall margin.

Optimizing J means keeping low pressure stall margin nearly constant.

Thrust optimization and keeping LP stall margin nearly constant are contradictory: the best accelerations involve lower LP stall margins at the beginning of transient.

Therefore, it would be very interesting to adapt a versus time, in order to optimize the LP stall margin in the beginning and thrust at the end.

Unfortunately, the linear quadratic method does not allow that variable weighting.

2 - SUPERVISED ARCHITECTURE :

In order to perform this variable weighting, the gains of two multivariable controllers are computed by L.Q. method :

- K_{secu} which optimizes the LP stall margin rather than thrust (a big)
- K_{perf} which optimizes the thrust rather than LP stall margin (a small)

The actual control output is then computed by the weighted sum :

$$u = [(1-\lambda) K_{perf} + \lambda K_{secu}] X$$

where

u is the control output vector
 X is the states vector
 λ a weighting factor.

- when $\lambda \rightarrow 0$, performance is improved rather than LP stall margin.

- when $\lambda \rightarrow 1$, the LP stall margin is optimized rather than performance.

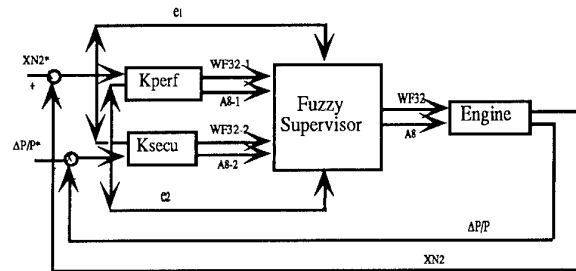
The management of λ becomes the critical point in this concept. Therefore we use fuzzy logic because :

- the λ computation can be evaluated by rules such as
 " If the difference between $\Delta P/P^*$ (desired) and $\Delta P/P$ is big then $\lambda \rightarrow 1$ "

where $\Delta P/P$ is an estimator of the LP stall margin.

- fuzzy logic allows smooth and continuous evolutions of λ .

So, the following control architecture is selected :



where

$XN2$ is the LP rotor speed,

$\Delta P/P$ the pressure ratio

$WF32$ the fuel flow

$A8$ the exhaust nozzle area

$e1 = XN2^* - XN2$ with $XN2^*$ the desired LP rotor speed,

$e2 = \Delta P/P^* - \Delta P/P$ with $\Delta P/P^*$ the desired pressure ratio.

3 - APPLICATIONS :

3.1 - L.Q. Gains computation :

The K_{perf} and K_{secu} gains are classically computed by LQ method optimizing the thrust and LP stall margin, respectively.

3.2 - λ computation :

3.2.1 - Approach :

By considering the two following errors :

$$e1 = XN2^* - XN2,$$

what we call the LP rotor speed error.

The faster this error reaches zero, the more performant the controller is.

Thus, $e1$ can be considered as a performance indicator.

$$e_2 = \Delta P/P^* - \Delta P/P,$$

what we call the Pressure Ratio error.

$\Delta P/P$ being a LP stall margin estimator, $\Delta P/P^*$ being worked out to keep LP stall margin nearly constant, e_2 is an indicator of the loss of LP stall margin.

λ can be computed with both differences:

$$\lambda = f(e_1, e_2)$$

Then it is necessary to :

- define a domain of variation (called universe of discourse) for each variable e_1 , e_2 and λ .
- divide each universe of discourse in sub-parts called fuzzy sets.
- define rules as :

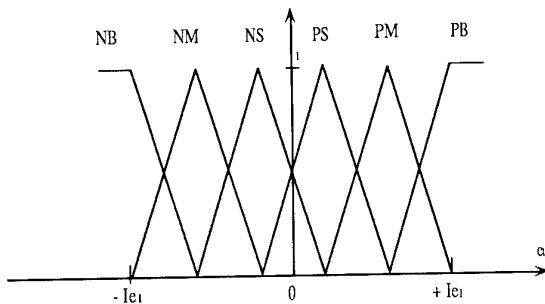
IF (e_1 is ...) and (e_2 is ...) THEN (λ is...)

3.2.2 - Universes of discourse :

. Universe of discourse of the Rotor speed error :

The universe of discourse of e_1 is divided in six fuzzy sets :

NB : Negative Big
 NM : Negative Medium
 NS : Negative Small
 PS : Positive Small
 PM : Positive Medium
 PB : Positive Big

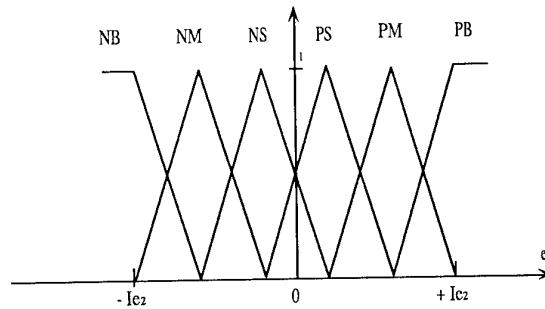


Ie_1 is a tuning parameter. An obvious value of Ie_1 is the transient amplitude :

$$Ie_1 = XN2^* - XN2 (T=0)$$

. Universe of discourse of the Pressure Ratio error :

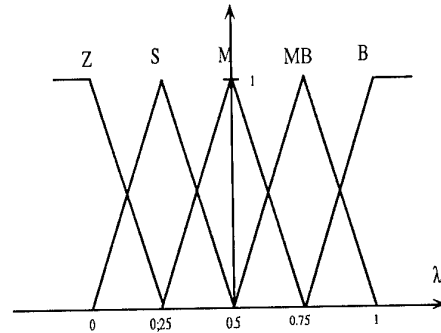
The universe of discourse of e_2 is also divided in six fuzzy sets :



In the same way, Ie_2 is a tuning parameter. Ie_2 can be chosen as the biggest value of the difference between $\Delta P/P^*$ and $\Delta P/P$ during the transient : flight idle --> full power.

. Universe of discourse of λ :

λ must be included in $[0 ; 1]$, its universe of discourse is divided into five fuzzy sets :



where: Z stands for Zero,
 S for small,
 M for medium,
 MB for medium big,
 B for big.

3.2.3 - The Rules :

Keeping in mind e_1 and e_2 expressions :

$$e_1 = XN2^* - XN2$$

$$e_2 = \Delta P/P^* - \Delta P/P$$

We know that during an acceleration :

- IF $e_1 > 0$ or $e_2 < 0$: quite normal behaviour,
 we can optimize the thrust : $\lambda \rightarrow 0$

- IF $e_2 > 0$, the LP stall margin becomes smaller,
 we have a loss of LP stall margin, so we must
 optimize LP stall margin : $\lambda \rightarrow 1$

- IF $e1 < 0$, there is an overspeed, the optimization depends on LP stall margin loss.

The following look-up table can be deduced :

	$e1$						
		NB	NM	NS	PS	PM	PB
Overspeed	$e2$	NB	Z	Z	Z	S	MB
	NB	Z	Z	S	S	MB	B
	NM	Z	Z	S	S	MB	B
Performance Seeking	NS	Z	Z	S	S	MB	B
	PS	Z	Z	S	S	MB	B
	PM	Z	Z	S	S	MB	B
	PB	Z	Z	Z	S	MB	B
		Performance Seeking			Stall Margin lost		

The middle square of this table stands for nearly steady-state behaviour.

The choice of λ value for the steady state (λ_{ss}) is also a tuning parameter.

A choice of $\lambda_{ss}=0.25$ implies a controller that performs a compromise between thrust and LP stall margin optimization at the end of transients.

Physically, this choice makes no sense and the choice of $\lambda_{ss} = 0$, which implies a controller which performs a complete thrust optimization at the end of transients, would lead to better performance. But a complete thrust optimization at the end of transients could involve an overspeed due to the integral control.

Therefore, simulation results of two controllers ($\lambda_{ss} = 0.5$ and $\lambda_{ss} = 0.25$) are shown and the consequences of the choiced λ_{ss} on performance is exhibited.

4 - Results :

The following results are obtained with linear models of the engine.

The method is tested at two points :

- M1: near flight idle with $\lambda_{ss} = 0.5$ and $\lambda_{ss} = 0.25$.
- M3: near full power with only $\lambda_{ss}=0.5$.

For each variable X, the response was simulated for an input step :

- with a classical multivariable controller which performs the best compromise between the thrust and LP stall margin optimizations, Xref.

- with a classical multivariable controller which performs only the LP stall margin optimization , Xsecu.

- with a classical multivariable controller which performs only the thrust optimization , Xperf.

- with a controller supervised by fuzzy logic, Xfuzzy.

The last controller leads to a minimum loss of LP stall margin: it is the same as those obtained with only LP stall margin optimization. On the other hand this controller also leads to a significant gain of thrust compared with the first one.

These results are mainly due to the desired response of the nozzle area, more efficient in the beginning of transients.

λ evolution shows of course a LP stall margin optimization at the beginning of the transient, $\lambda > \lambda_{ss}$, and a thrust optimization at the end $\lambda < \lambda_{ss}$.

We can also compare the different behaviour of the system for the two values of λ_{ss} . The smaller value of λ_{ss} involves the best performance. Indeed, that means a more complete thrust optimization at the end of transient, these complete thrust optimization being limited by overshoots which forbid $\lambda_{ss}=0$.

5 - Conclusion :

The results exhibit a significant gain in thrust response for an equivalent LP stall margin loss.

Of course, this method will have to be evaluated with non-linear models. But its application with non-linear models may not introduce particular problem because non-linearities are managed by LQ architecture itself.

On the other hand, stability must be proved at each time:

If $u1$ and $u2$ are stable control outputs, $(1-\lambda) u1 + \lambda u2$ is not automatically stable.

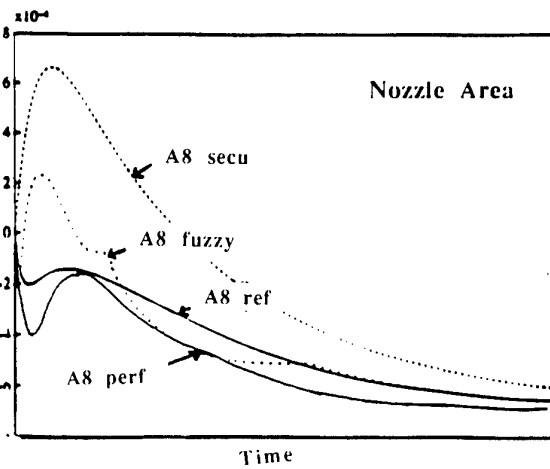
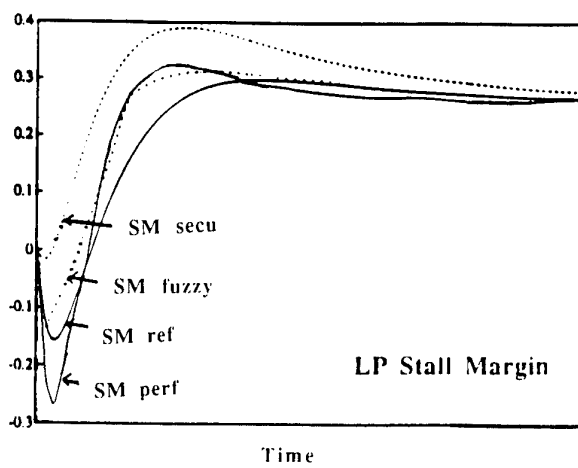
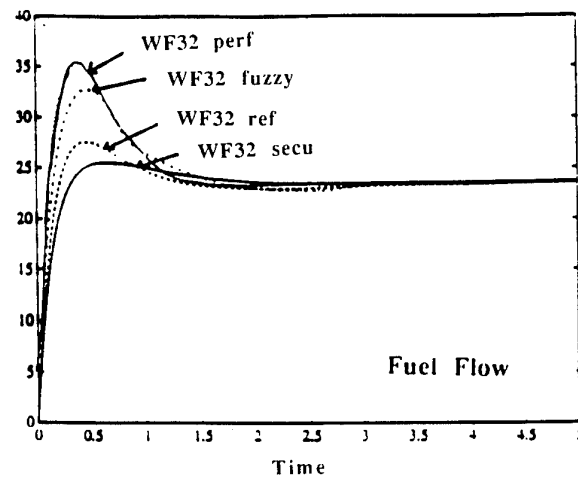
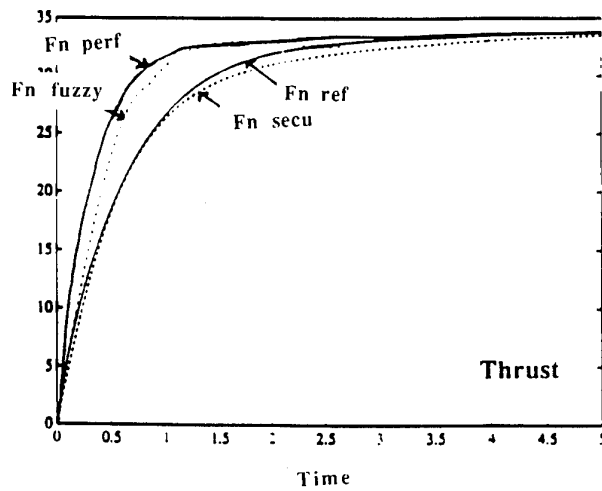
In consequence, when K_{perf} and K_{secu} are computed, it must be necessary to verify that $(1-\lambda) K_{perf} + \lambda K_{secu}$ is also stable for $\lambda \in [0 ; 1]$

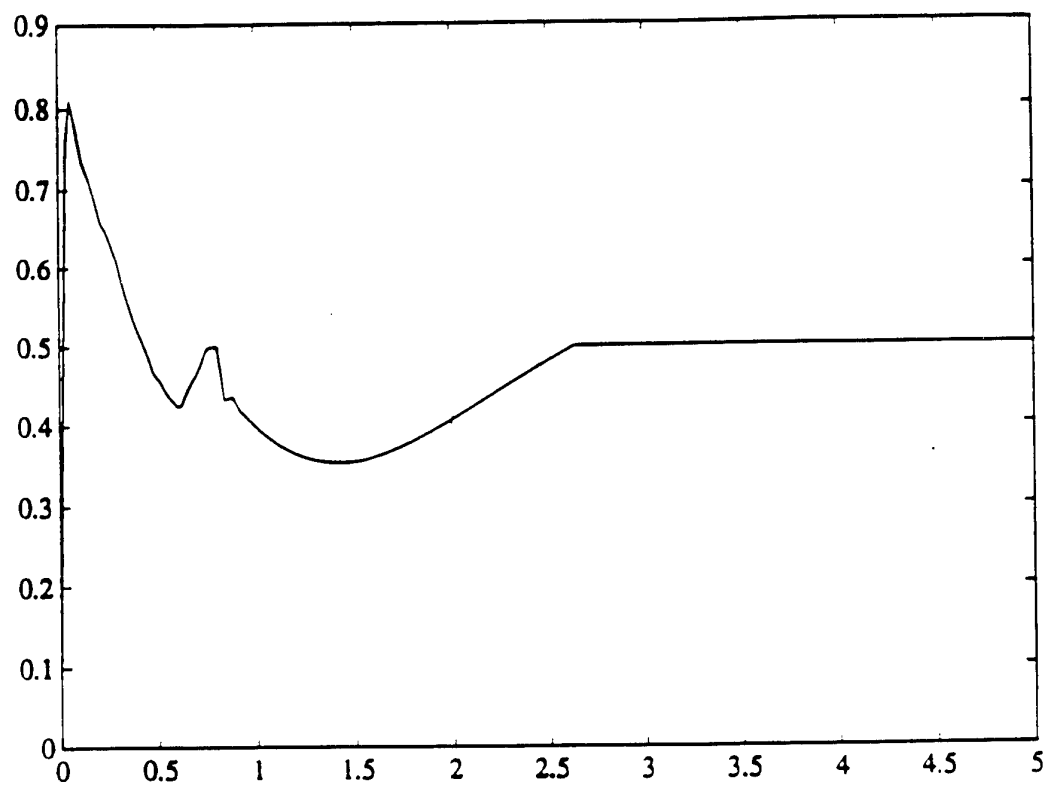
This architecture implement in a real ECU also involves the computation of control outputs twice plus the computation of λ using fuzzy logic.

References :

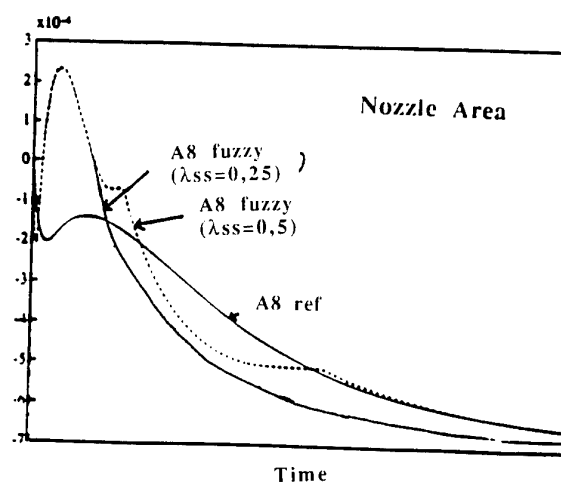
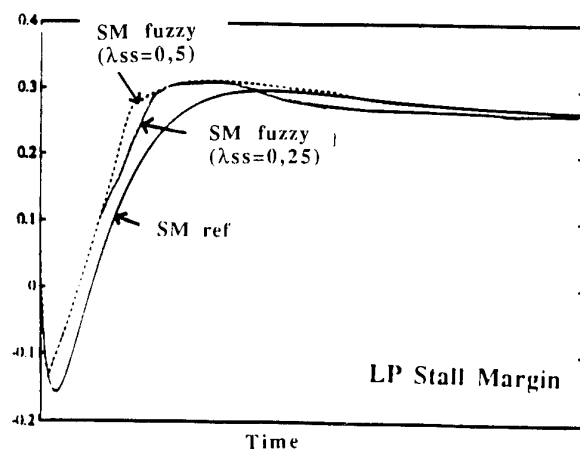
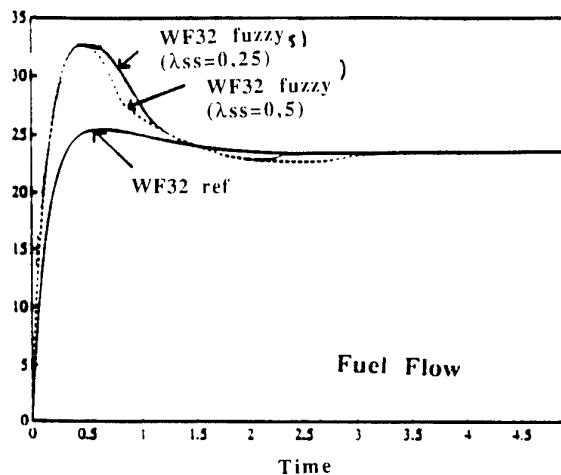
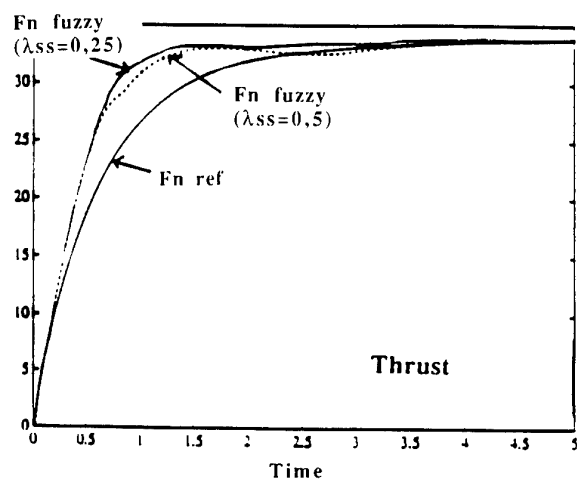
- FRITSCH M.C and WENDLINGE. "Les atouts de la logique floue". Technologies internationales, N°3, avril 1994, p27-33.
- DUBOIS D., PRADE H., "Fuzzy sets and systems". Mathematics in science and engineering, 1980, p297-316.
- KING P.J. and MANDANI E.M. "The applications of fuzzy control systems to industrial processes". Automatica, 1977, vol 13, p235-242.
- HUET T. "Application de la théorie des ensembles flous à la commande". C.N.A.M., 1994, chp2 and 3.

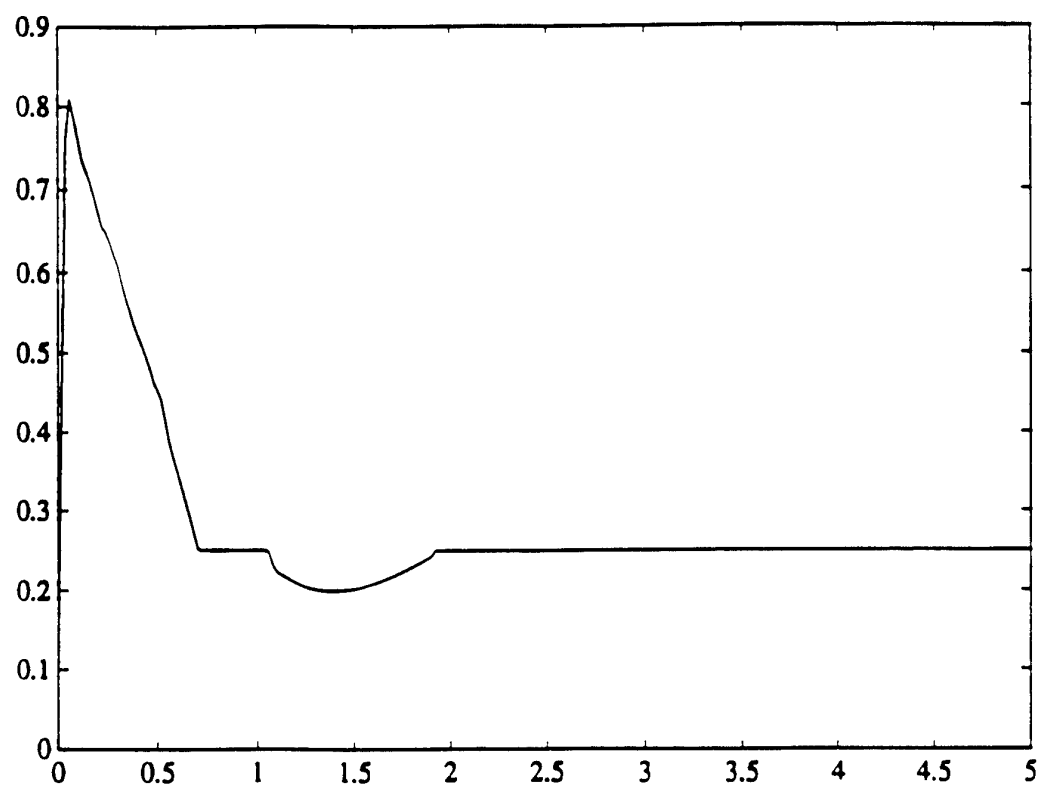
Point M1

 $XN2 = 7876 \text{ tr/min}$, $\lambda_{ss}=0,5$ 

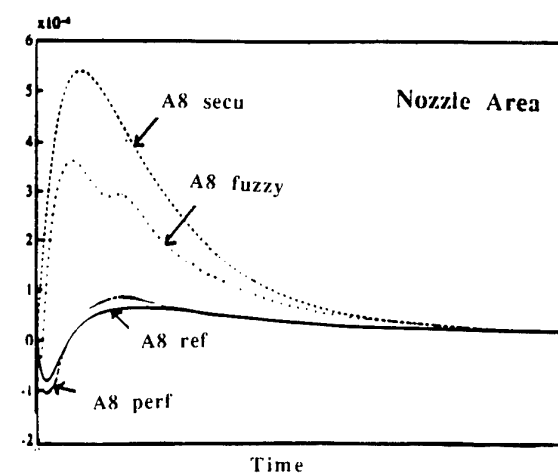
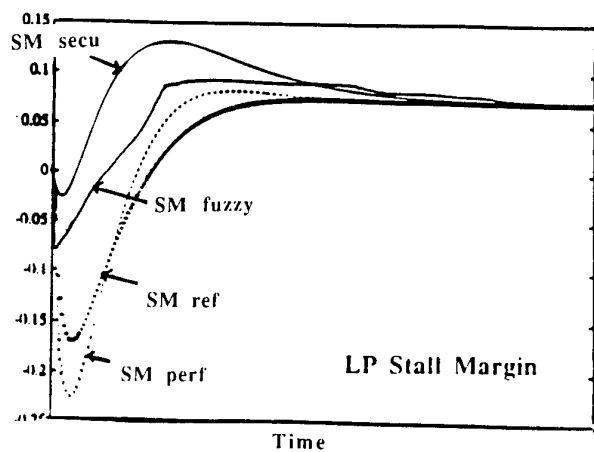
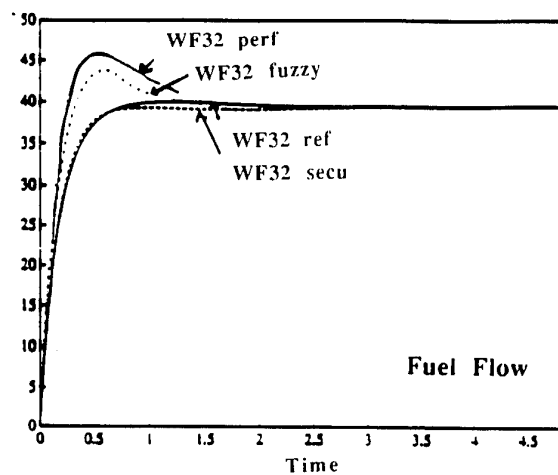
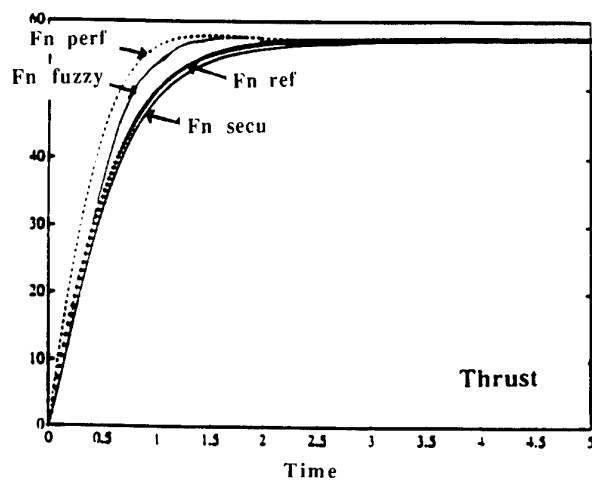
Point M1**XN2 = 7876 tr/min , $\lambda_{ss}=0,5$**  λ evolution

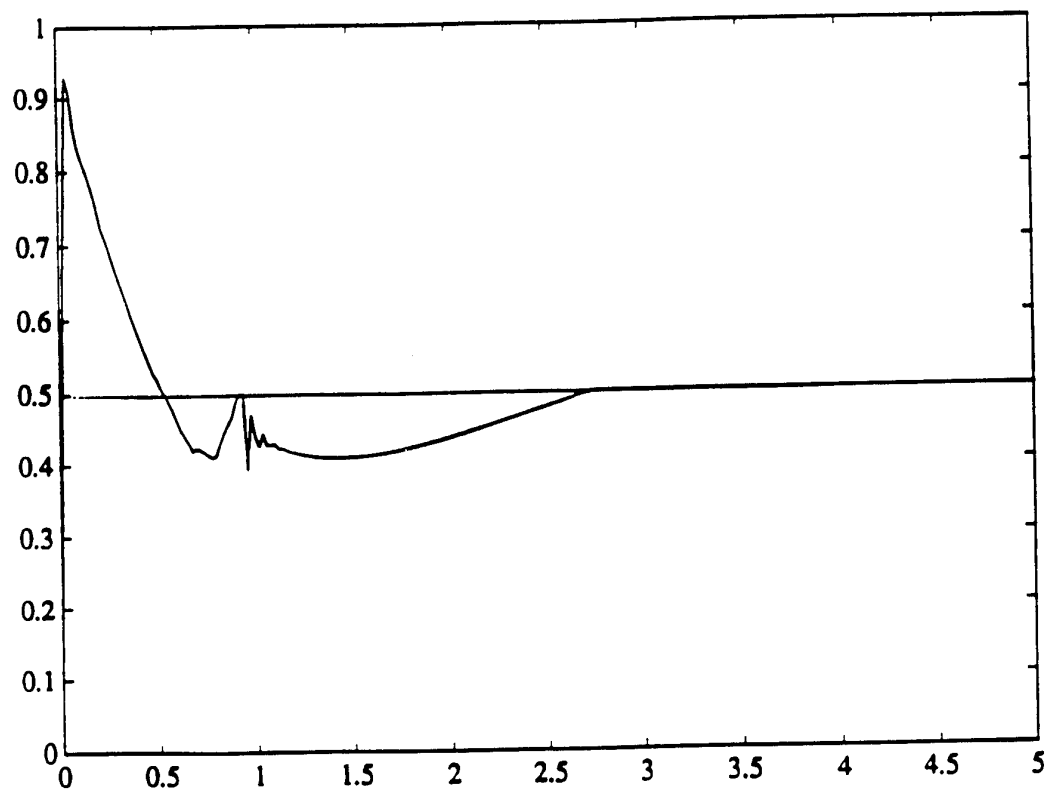
Point M1

 $\text{XN2} = 7876 \text{ tr/min}$, $\lambda_{ss}=0,25$


Point M1**XN2 = 7876 tr/min , $\lambda_{ss}=0,25$**  λ evolution

Point M3

 $XN2 = 10042 \text{ tr/min}$, $\lambda_{ss}=0,5$


Point M3**XN2 = 10042 tr/min , $\lambda_{ss}=0,5$**  λ evolution

Paper 27: DiscussionQuestion from L Larkin, Pratt and Whitney Aircraft, USA

Did you address the HP stall margin in the study as well as the LP margin?

Author's reply

HP stall margin is a function of fuel flow only and was therefore not included in our study.

Question from B Leroudier, Dassault Aviation, France

Can the fuzzy logic approach incorporate inputs from LP tip clearance sensors and flight altitude sensors.

Author's reply

Yes, but the system will be more complex.

MULTIVARIABLE CONTROL OF MILITARY ENGINES

G J Dadd, A E Sutton, A W M Greig
 Propulsion Technology Department
 Defence Research Agency
 Farnborough, GU14 0LS, UK

SUMMARY

Multivariable control (MVC) of aircraft powerplants has been viewed in the UK as a means of gaining more precise control of conventional engine operation. This offers the prospect of improved engine performance and throttle response, leading to gains in aircraft range and agility. More importantly MVC is also regarded as an essential enabling technology for future variable cycle engines (VCE), as well as for powerplants for ASTOVL applications which feature significantly increased numbers of input variables (actuators).

Research in this technology at the Defence Research Agency (DRA) Pyestock in association with Rolls-Royce and Lucas Aerospace, has been undertaken at both theoretical and practical levels in the context of conventional, VCE and ASTOVL engine cycles. Tools and Methods have now been established to support technical demonstration of flight capable multivariable controls. These have been validated by means of engine tests.

The paper reviews this research, illustrating that MVC offers potential for tighter and more responsive control of conventional engines. Component and engine designers may be able to exploit this control capability in performance terms. The controls capability to support VCE and ASTOVL engine technology has, in most respects, been established in the UK.

LIST OF SYMBOLS AND ABBREVIATIONS

ACU/DCU	acceleration/deceleration control schedules
ASTOVL	advanced short take off vertical landing
DECU	digital engine control unit
HP	high pressure component
IGV	compressor inlet guide vanes
LP	low pressure component
LPC	low pressure compressor
MN	bypass Mach number - actually $\Delta p/p = f(M)$
MOU	Memorandum of Understanding
NH	rotational speed of high pressure spool
NHDOT	high pressure spool acceleration rate
NL	rotational speed of low pressure spool
NOZ	nozzle area
P + I	proportional plus integral control
PLA	pilot's lever position
PR	pressure ratio
ps ₁	static pressure at engine inlet
ps ₃	static pressure at HP compressor outlet
RAE	Royal Aircraft Establishment (now DRA)
SISO	single input single output controller
TBT	pyrometer measured turbine blade temperature
T6	thermocouple measured LP turbine exit temperature
WFE	core engine fuel flow
θ	ratio of engine actual inlet temperature to standard day temperature

1. INTRODUCTION

The aero engine controls group at the Defence Research Agency (Pyestock) - formerly RAE - has been routinely involved with engine control laws research both military and civil over many years. Research programmes for controls hardware, actuators, sensors etc. have also been managed within the UK supply industry through DRA Pyestock over the same period.

A significant feature of the in-house control laws research since the mid 1980s has been multivariable engine control. This has been motivated by the realisation that future proposals for VCE and ASTOVL powerplants are likely to feature increased numbers of engine input variables. The present approach to control on conventional engines, ie closed loop control of fuel with other variables open loop scheduled, would almost certainly prevent precise control of these more complex engines because of the accumulation of tolerances on many more open loop scheduled actuators. Hence the endeavour has been to establish the technical capability to implement multivariable engine controls and to understand the benefits conferred and the restrictions that would need to be accepted by their use.

As a result of collaboration between NASA, DOD in the USA and the MOD-UK in 1987 under the ASTOVL MOU, RAE undertook studies to produce a model of an 'Advanced Vectored Thrust' (AVT) engine and to design an appropriate engine controller¹. The engine, a 'Pegasus' derivative, included a pair of forward thrust nozzles of variable area with plenum chambers for fuel burning (PCB) situated within them. Independent control of the thrust from these nozzles and the core nozzle indicated the need for MVC since cross coupling between thrust centre and thrust magnitude had to be minimised for effective aircraft pitch, height and roll control.

A three input three output MVC was proposed to control the engine during hover mode. This allowed independent control of the three downward facing nozzle thrusts. The design included multivariable structural limiters to control maximum engine spool speeds and temperatures. The study showed that fore and aft thrust centre management alone, involving main engine fuel and spool speed variation, was not fast enough for effective aircraft pitch control. In contrast the response to changes in roll demand were achieved rapidly by differential nozzle area variation and differential PCB fuel variation. Thus besides producing useful generic ASTOVL lessons for future studies this exercise also advanced MVC design experience.

The study confirmed the requirement to reinforce the UK programme on multivariable engine control to underpin the ability to address similar project studies in the future.

This multivariable controls research within DRA has had the additional benefit of stimulating the UK engine and controls supply industry to undertake complementary research in

multivariable control to establish the more detailed understanding necessary for project application. The results of this industry research which began in the early 1990s may now be considered to have provided the climate and state of readiness to evaluate MVC within Technology Demonstrator Programmes (TDPs).

This paper will review the research initiatives, within the DRA, Rolls-Royce and Lucas Aerospace which have culminated in the achievement of this position. Finally, a brief view of the likely way ahead and the outstanding areas which require further work will be considered.

2. OVERVIEW OF MVC PROGRAMMES

The programmes considered in this review have been conducted by Lucas Aerospace, Rolls-Royce (RR) and the Defence Research Agency. Universities of Salford, Leicester, Strathclyde and Southampton have been involved to varying degrees. Cambridge Control and Stirling Dynamics, specialist control houses, have also been subcontracted in these studies. Financial sponsors for this work include the Ministry of Defence (MOD-UK), the Department of Trade and Industry (DTI) and the Science and Engineering Research Council (SERC). In all instances where control laws have been brought to engine test this has taken place at DRA Pyestock in the Glen Test House (described in Section 4.2). Engines available for test have been conventional military turbofan engines (RB199 - the Tornado powerplant, and Spey Mk202). Where research has been directed at more complex cycles or full flight envelope investigation, work has been limited to the various simulation laboratories located at the research centres listed above.

A brief résumé of the research programmes concerned with MVC is given in table 1 (see end of paper). It will not be possible within the scope of this paper to review each item in complete detail. Instead, the intention is to provide background information while highlighting the particular contributions which each item has made to meeting the functional requirements of an MVC for aero engine application. Consideration is given in the next section as to what these functional requirements are.

3. FUNCTIONAL REQUIREMENTS

Detailed functional requirements for engine control necessarily depend on the precise nature of the engine to be controlled and its application. Therefore only generic functional requirements can be considered here. Many of these requirements are common to existing single loop (plus open loop schedule) controllers which represent the present standard of control in project use. However, the very nature of MVC - the fact that multiple closed loops have to co-exist - introduces some new requirements not previously encountered.

The following list serves to define some of the basic functionality which an MVC design will need to meet.

1. Accommodation of widely varying engine dynamics (due to both flight envelope and throttle setting)
2. Response and stability levels comparable to, or better than, those of existing controllers (ie single closed loop plus open loop scheduled actuators).
3. Acceptable de-coupling between the MVC multiple loops. This is a new requirement arising from the nature of MVC.

4. Disturbance rejection dynamics which are as rapid as the command response and de-coupling dynamics.
5. The integration of MVC structural limiters with bumpless selection dynamics (eg for turbine temperature, combustor pressure etc).
6. The integration of MVC acceleration and deceleration (rate) limiters (eg. NHDOT)
7. The integration of open loop scheduled limits for actuator positions to constrain the authority of the MVC during periods of engine malfunction (surge), system failure or component error.
8. The assurance of adequate levels of control robustness to ensure that changes in the engine and control system dynamics, through manufacturing variability and propulsion system degradation, do not precipitate inadequate dynamic stability.

In none of the research programmes identified in table 1 were all these requirements addressed simultaneously. However, across the totality of the programmes identified, they have all been considered. The obvious situation where these requirements, plus those specific to the engine configuration and application, would next be brought together is within a TDP or project application. (eg HIPECS - see paper 2, this conference)

Because no one programme addresses all requirements at once, there will be instances in the results presented where various aspects of performance are less than acceptable for flight application. Collectively, the results presented within this paper serve to show what minimum standards are achievable with MVC. Undoubtedly improvements can be made in most areas given well defined objectives and research and development resource. For the present however, the work already undertaken is considered to have established a robust capability within the UK for MVC of aero gas turbines.

4. RESEARCH FACILITIES

An important aspect of the research programme is to provide experimental verification of the MVC concepts; this is essential for reducing the technical risk associated with a TDP. Two principal types of facility were used for MVC research as follows:-

1. simulation and analysis laboratories for conducting preliminary investigations using thermodynamic engine simulations
2. a sea level test bed (The Glen) for engine validation of the control laws developed.

4.1 Simulation Laboratories

When the work first started, VAX 11-750 computers with attached processors were in use at DRA Pyestock to host both the thermodynamic engine simulations and the experimental control laws. Run times were typically five times slower than real time. Now this facility features three VAX 4000.90 stations and one DEC 3000 Alpha station. Typical engine simulations run slightly slower than real time on the former and roughly twice as fast as real time on the latter.

In terms of software support and analysis tools, when work began, software tools such as TSIM and NAG library routines only were available. Now MATLAB and SIMULINK are facilities upon which the staff rely heavily for synthesis, dynamic identification and of course data presentation.

These facilities are broadly typical of those at Rolls-Royce, Lucas and within the Universities.

4.2 The Glen sea level test bed

The Glen test bed is a conventional sea level facility which traditionally has been dedicated to digital controls research for application to reheated turbofan engines of up to 95kN reheated thrust.

The test engine may be controlled through conventional or experimental actuators which are commanded by a programmable microprocessor control system, linked in turn to the engine sensors and thrust command lever. When engine trials of MVC first began, this equipment used Intel 8086 with 8087 maths processors for control law implementation. However, various upgrades have been undertaken and the system is now configured around the Intel 486 microprocessor. This digital hardware hosts a software environment, OLMP (on-line monitor programme), which has been in use at DRA Pyestock over several years. This incorporates the control law as a subroutine which is called in response to a clock driven interrupt. Spare processor time and computer memory are employed by other lower priority keyboard selected routines within OLMP for controlling data capture, data storage, control variable modifications and display of engine data for purposes of managing engine trials.

The research control laws, which have all been written in FORTRAN, have been simplex (rather than dual or triple redundant), but independent overspeed governors and temperature trips have been installed in addition to manual emergency shut down features for purposes of safeguarding the engine and facility.

4.3 Test Engines

A variety of multivariable control laws have now been engine tested on either RB199 or Spey Mk202 engines as shown in Table 1. These have been distinguished largely by the combinations of feedback sensors used, there being little flexibility in terms of the actuators available. The feedback signals employed have included spool speeds, pressure ratios, bypass duct Mach number and turbine temperatures. These signal requirements have been met using specially designed probes where necessary in conjunction with both experimental and standard bought out sensors.

The first engine to which MVC was applied was the RB199. The simplicity of this engine in control terms, while providing a benign introduction to engine application of MVC, allowed only dual loop systems to be studied. As MVC capability was established by work with this engine, attention was transferred to the more challenging military Spey engine with a potential for three loop MVC systems. Although no longer in service, this engine shares its basic architecture, as far as controls is concerned, with modern engines such as EJ200, the powerplant for Eurofighter. To support the MVC testing, modifications were made to the IGV and handling bleed valve actuator systems of the Spey to enable independent control through the test facility control computer.

As yet, no suitable VCE test vehicle exists in the UK. All studies of MVC applied to VCEs have therefore been based on aerothermodynamic simulations.

5. MVC RESEARCH PROGRAMMES

In this section most of the items in table 1 will be considered in more detail and are indicated in the section sub-headings.

5.1 Early programmes

The first direct engine experience in MVC techniques was gained in 1986/7. RAE collaborated with the University of Salford to produce a MVC for the RB199 engine. This was to be based on the compensator design methods due to Porter and Bradshaw² and run on the Glen Test Bed.

For simplicity the controlling signals chosen were the error between the demanded and measured values of (1) HP spool speed, NH, and (2) bypass Mach number, MN, as these signals had previously been used successfully for a controller using two separately designed single input, single output loops. The demanded NH was set by the pilot's lever and the demanded MN was scheduled according to non-dimensional LP spool speed, NL. The control outputs determined the actuator demands for engine fuel flow and nozzle area.

The control was of straightforward P+I design, in which the open loop combination of plant and control approximated to a matrix containing simple integrators in the leading diagonal. The Salford method determined a control which diagonalised the plant and control combination at high and low frequencies and included a diagonal tuning matrix. For simple plants this is equivalent to designing a controller by inverting the plant matrix and adding integrators in series.

The system operated satisfactorily in most aspects although the performance of the disturbance rejection was less than would normally be desirable. However the experience gained through the design and by running this practical system proved extremely valuable for future work. It also showed that the RB199 engine did not present a particularly challenging control problem, although the integration of all the required limiters required significant effort. It was also found that schedules used for creating closed loop demands had to be 'identified' with the engine when establishing system dynamics for compensator design.

In 1990 during engine tests on the RB199 in the Glen Test House, time was allocated for a second phase of development and test of a MVC³ using the experience gained within DRA during the previous study with Salford University and on the ASTOVL simulation project. The two input two output designs were extensions of a very flexible single input single output controller designed in an MOD-UK TDP (AMECS), that had performed well in previous flight tests in Tornado.

The dry engine multivariable range control set fuel and nozzle area demands using a selected pair of engine parameters as control feedbacks. Three separate range controllers were designed and tested on the engine, the feedback pairings being:

1. NH and Bypass Mach Number
2. NL and Bypass Mach Number
3. NL and Fan Pressure Ratio Error.

In each case the Pilot's Lever Demand determined the rotational speed demand (NH or NL) and a schedule depending on a non-dimensional engine LP speed set the demand for the other engine variable. Each of the three control designs included acceleration and deceleration control, based on NHDOT, and structural limiters for turbine blade

temperature and for two maximum rotational speeds. A scheduled ACU/DCU fuel demand limit, based on HP compressor pressure, was included in the DECU programme downstream of all other controllers for surge and flame out protection. All control loops were gain scheduled and used multivariable P + I control.

Although there was no intention to fly the controls all were fully non-dimensional to allow operation over a wide flight envelope.

The block diagram (Figure 1) shows the third control identified above (NL and Fan Pressure Ratio Error control) including the limiters in a simplified form. These were integrated within the system by means of Hanus⁴ bumpless transfer and integrator anti-windup code.

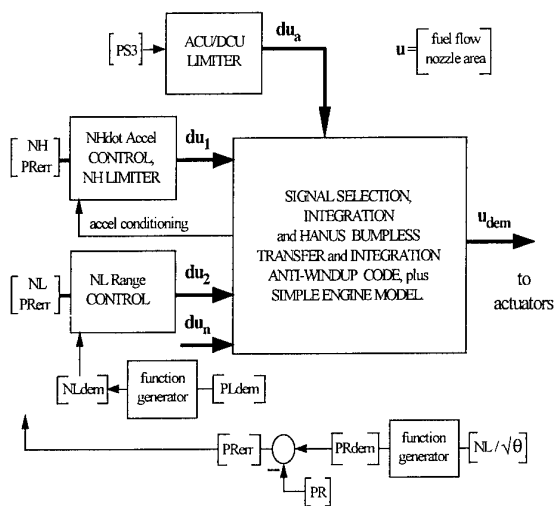


Figure 1 Early MVC controller

A block diagram of the 'Hanus' conditioning for a simple P+I multivariable control is shown below (Figure 2). Here u_{sel} is selected in some way (eg lowest fuel demand) as one of the vectors u_1 to u_4 . If u_1 is not the controlling vector, integrator conditioning takes place automatically. This method was used in several other projects mentioned in the text, including the ASTOVL study already referred to in the introduction.

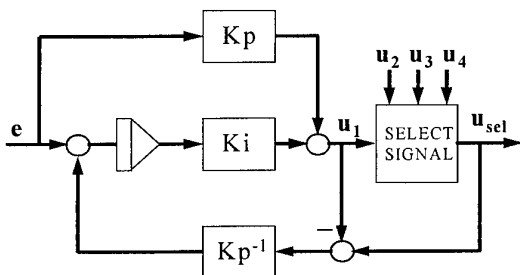


Figure 2 Arrangement for Hanus conditioning - P+I control

Figure 3 below shows the result of a step change in fan pressure ratio demand during tests on the third controller. The result is typical of all three controllers, there being an adequate response with little cross coupling (in this case on the NL signal).

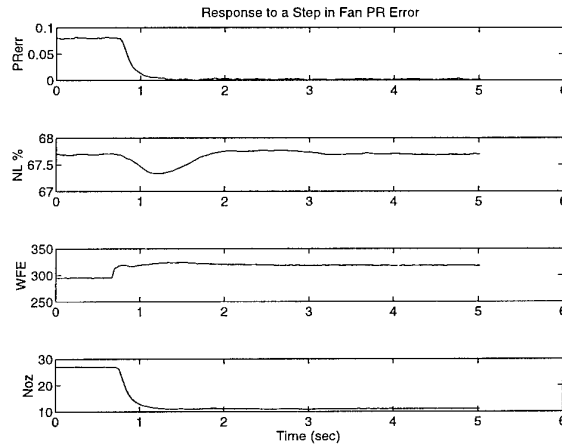


Figure 3 Controller performance

A full scale acceleration onto a reduced TBT limit set at 680°C is shown below (Figure 4), indicating smooth take over as 4 different loops operate at various times during the manoeuvre. Diagonal tuning matrices in each control or limit block allowed easy tuning of the complete system.

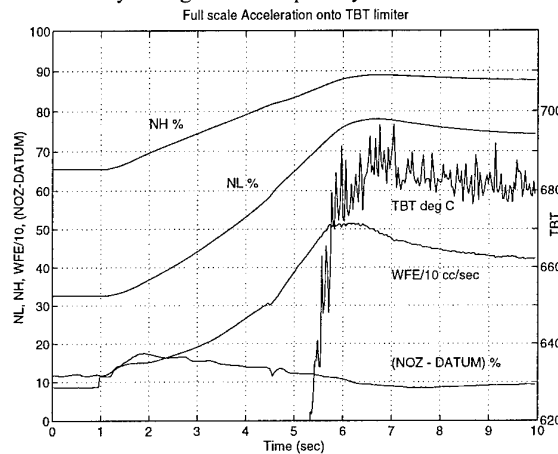


Figure 4 Loop changing

5.2 Recent programmes at DRA Pyestock

5.2.1 Fast response control law (item 5)

The case for establishing a MVC capability can be made most strongly to support VCE and ASTOVL engine applications. For conventional engines where adequate control methods already exist, the need for change is not overwhelming. However, from the studies shown in Table 1 a number of advantages have become apparent which could justify the additional complexity of MVC. Of these, the results of item 5, Table 1 are a good example. In this programme⁵, it was demonstrated that engine variables such as guide vanes and final nozzle area could be managed unconventionally by a MVC to provide fast large scale thrust response should this be desirable. This unconventional operation could possibly induce compressor blade flutter. This was not considered in detail, it being assumed that any intention to exploit this control mode in a project would include appropriate steps at the time of compressor design to avoid this potential problem.

The input-output groupings for the fast response MVC were dictated largely by the fast response requirement rather than consideration such as robustness etc. There was some latitude

for different choices to be made but essentially a thrust parameter, LP working line parameter and HP spool speed were central to the objective. The input output parameters chosen were:-

Inputs	Outputs
Main engine fuel	LP Spool Speed
Inlet guide vanes	HP Spool Speed
Final nozzle area	Bypass duct Mach number

The basic approach to obtaining improved thrust response was to hold the HP spool speed constant while varying the LP spool speed. Thus the HP spool did not need to be accelerated during a thrust transient, allowing the energy which would otherwise be required to change the rotor state to be applied wholly to changing engine thrust. Furthermore, the loss of surge margin anticipated for the LP compressor due to rapid handling could be compensated by opening the final nozzle. The working line control loop provides this latter function automatically.

By way of contrast, the conventional SISO controller for the Spey embodies just one closed loop for NH. The IGV and nozzle demands are subsequently generated by open loop schedules driven from other measured engine outputs.

For simplicity the MVC control again featured P+I compensation and employed the Salford design technique to decouple the engine transfer function at high and low frequencies. As long as the engine dynamics remained well behaved in the mid frequency ranges, adequate decoupling is then achieved throughout the frequency range.

For purposes of assessing the MVC, a SISO controller, broadly typical of a conventional engine control was used to generate comparative results for the Spey engine during large manoeuvres. The significant improvement obtained in thrust response using the MVC over the top 50% of the sea level static thrust range is demonstrated in Figure 5 below.

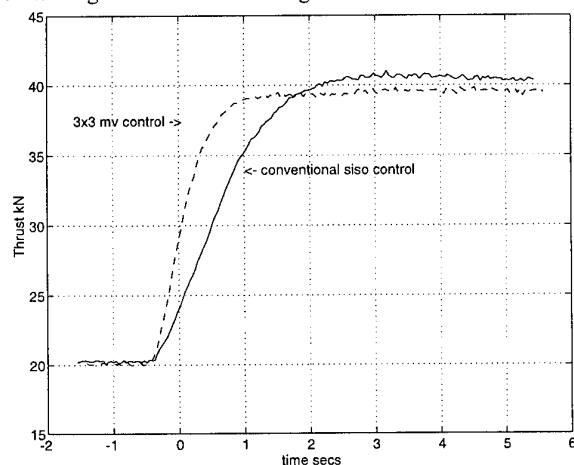


Figure 5 Comparison between MVC and SISO control

At low thrust in this high response mode, the guide vanes are closed but the HP spool speed is high. This off-design operation does not materially change the HP compressor working line, but during thrust transients the working point did not exhibit the usual strong movement to or from the surge line either. However, it remains to be established where the in-engine surge points are for these unconventional guide vane settings. It is thus possible that the transient handling surge

margin allowance could be reduced and cashed at the design stage as a performance or weight benefit.

At very low power settings the HP compressor inlet guide vanes are driven on to their closed position end stop as the controller attempts to maintain NH at a constant value. In this range of operation, the guide vanes can no longer exert any control authority making it necessary to reduce the MVC to a 2 x 2 controller (fuel and final nozzle controlling LP spool speed and bypass duct Mach number). In this thrust range NH is no longer controlled and the HP spool speed reduces as thrust is regulated to lower levels. Both the 2 x 2 controller and 3 x 3 controllers were run simultaneously with authority being switched between them as the guide vanes either approached or moved off the inner end stop.

Under sea level static test of this fast response control law it was found that the specific fuel consumption of the engine was not affected significantly, while the thermal cycling range of the turbines was reduced over the fast response thrust range. The operational 'costs' of using the fast response mode may thus be relatively minor assuming compressor integrity can be maintained.

5.2.2 Alternative Loop Selection Procedures (item 5)

Most of the MVC systems described in this paper employed the Hanus method (described in section 5.1) for the selection of competing MVC compensators (eg limiter loop structures and range governor). This implies that each compensator contains its own set of integrators upstream of the selection point, and these then have to be managed when the compensator in question is de-selected. For the fast response control law on the Spey (Table 1, item 5), an alternative approach, aimed at software simplification, was investigated. This used just one set of unity gain integrators. The P+I control compensators were modified to provide the time derivative of the actuator demands (\dot{u}) as shown in Figure 6.

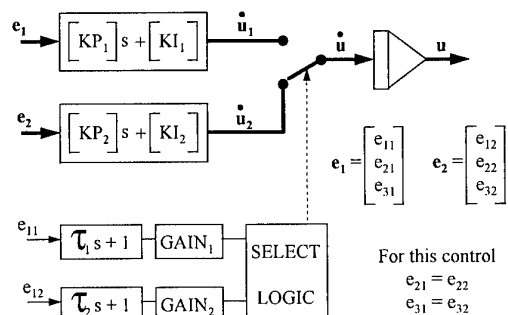


Figure 6 Alternative loop selection

The \dot{u} signals from these were then selected on the basis of the lowest of their respective phase advanced error signals (eg. $TBT_{LIMIT} - TBT$), but first being converted to a common set of units by appropriate gains. Subsequently a single bank of three integrators formed the u vector from the selected \dot{u} vector. Operation of this structure is shown in Figure 7 for the case of transfer from NL range governing onto a TBT temperature limit. Open loop override of the closed loops (eg for surge protection or recovery etc - see section 3 item 7) was implemented by overwriting the integrator outputs with the scheduled values.

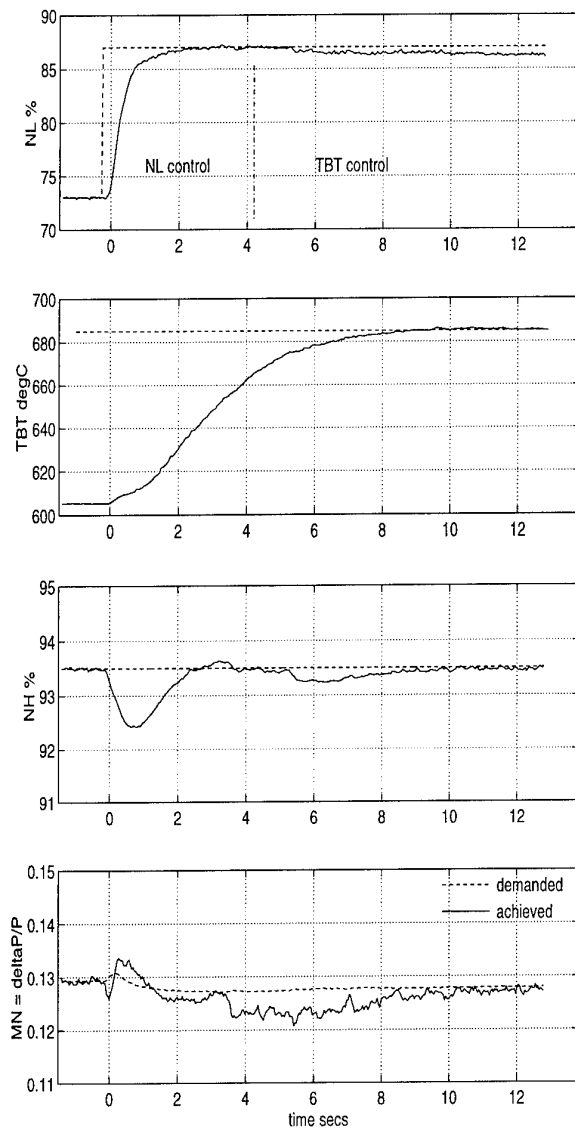


Figure 7 Limiter loop exchange

5.2.3 Disturbance Rejection Dynamics (item 6)

In Section 3, the basic functional requirements included the need to ensure disturbance rejection dynamics which are as rapid as the command and decoupling dynamics. Good disturbance rejection is most important for engine limiter loops and of these, the turbine blade temperature is probably the most critical. This is because modulation of unmeasured secondary aircraft demands such as power off-take and environmental conditioning air bleed can cause significant transient limit exceedance. The extent and duration of these exceedances will consume engine life and therefore reasonable steps need to be taken in the controller design to minimise these effects. An approach taken at DRA Pyestock within item 6 in Table 1 is described in the following.

Many of the MVC compensator designs, eg the Salford method, rely in effect on pole-zero cancellation (or plant inversion methods). It is known that these can give quite acceptable command and decoupling responses with simple P+I controllers for the general dynamics prevalent in aero engines. However, it is also known that uncertainties in the

position of plant poles can give rise to unwanted components in the command response when exact cancellation of these by control zeros is not achieved. More importantly for disturbances, when the engine dynamics contain slow modes these can appear in the disturbance response transfer function resulting in slow rejection of the disturbance. This is commonly the situation encountered with the turbine blade temperature limiters obtained with pole-zero cancellation compensator design methods because of the slow thermal dynamics of the engine.

The simple expedient investigated at DRA Pyestock, to overcome this problem was to hasten the "slow" closed loop poles of the pole-zero cancellation design which represented the source of the poor disturbance rejection, while permitting the "fast" closed loop poles to be slowed down. This shifting of poles was achieved by manipulating the integral gains alone through a function minimisation process. The function was defined in terms of the distances (in the direction of the real axis) of the closed loop poles from a central gathering point. This point was chosen to be consistent with the command response rise time implied by the choice of proportional gains. Constraints were imposed to prevent large imaginary components in the closed loop poles, thus suppressing very oscillatory responses. The effects of this re-tuning process are illustrated as follows.

The closed loop poles of the MVC turbine blade temperature limiter are shown in Figure 8. In this case the limiter is essentially a regulator in which fuel, IGV and nozzle area are used to control TBT, HP spool speed and bypass duct Mach number. The proportional gains of the compensator were selected to provide a closed loop rise time of 0.25 seconds for the notional TBT command response.

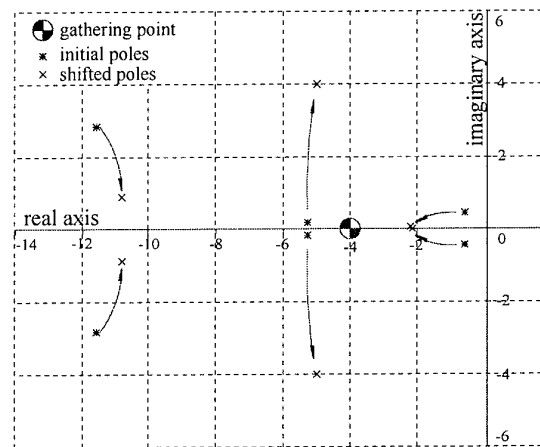


Figure 8 Closed loop poles of system

The ideal gathering point objective for the closed loop poles was therefore -4 rad/s (ie $-1/.25\text{sec}$). Manipulation of the integral gains was managed automatically by a function minimisation routine giving rise to the closed loop pole migration indicated in Figure 8. The main impact of this was that the slowest mode contributing to MVC responses (ie. the poles nearest the imaginary axis) was speeded up by a factor of approximately $3\frac{1}{2}$.

A comparison of the TBT command and NH , MN decoupling responses before and after pole gathering is made in Figure 9.

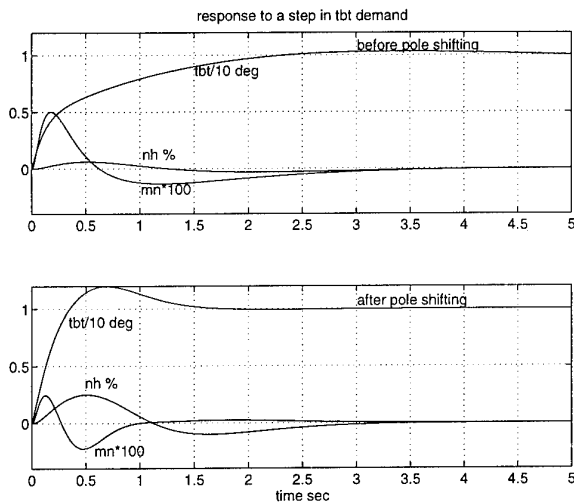


Figure 9 Effect of pole shifting technique

Here the deficiency of imperfect plant cancellation in the original design using P+I compensation, evident in the slow TBT command response, is remedied with the shifted pole integral gains. Despite the relatively major change to these integral gains, evident by comparing Tables 2a and 2b, the decoupling response for NH has only deteriorated slightly, to a degree which is still acceptable (ie a 0.2% NH transient perturbation for a 10°K change in temperature limit).

Table 2a

Integral gains before pole shifting		
10.7	5.29	1580
-0.730	14.1	-134
0.0319	-0.615	1260

Table 2b

Integral gains after pole shifting		
102	-163	15200
-3.52	25.8	-376
-0.290	4.75	3290

In exchange, a very significant speeding up of disturbance rejection (represented by a fuel step - this being a close analogue of the power off-take loading) has been secured as shown in Figure 10.

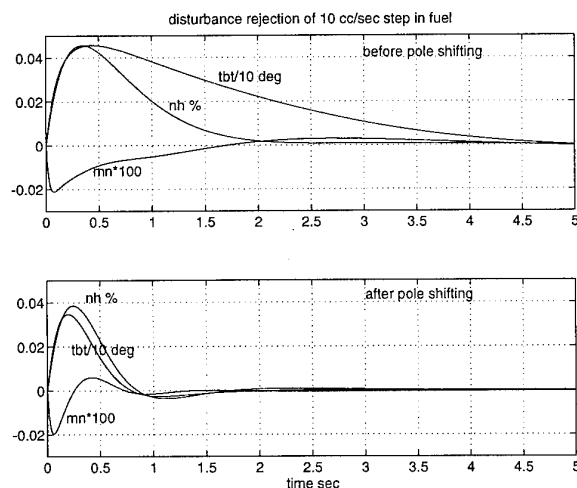


Figure 10 Disturbance rejection

The impact of pole shifting on system robustness should not be overlooked. In Figure 11, the original and pole shifted compensators are compared in terms of their worst case stability sensitivity to changes in system gains. These can manifest themselves at the input (eg actuator changes) and at the output (engine and sensor changes). These results show that in this case the pole shifting exercise has caused little loss in system robustness.

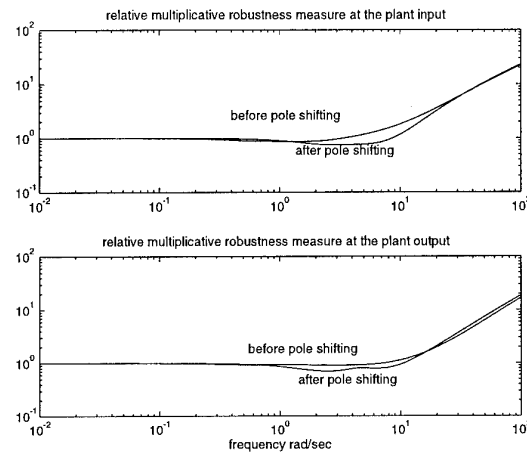
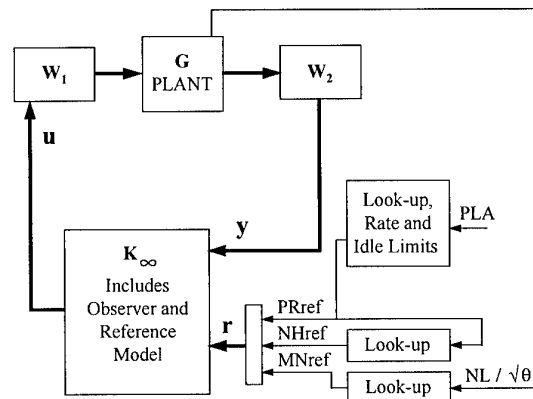


Figure 11 Robustness

5.3 Complimentary University research (item 7)

Between 1992 and 1995 Lucas, three Universities and DRA collaborated in an effort to produce novel MVCs for the Spey engine. The objective was to investigate fresh control concepts arising from centres of expertise with a wide ranging controls background (ie. not focused solely on the needs of gas turbines). As a result Leicester University⁶ designed a controller, the block diagram of which is shown below.

Figure 12 H[∞] Multivariable controller

As part of the project the 'best' engine control parameters had to be determined. Leicester, by using a methodology involving practical considerations, right half plane zeros, the relative gain array, the condition number and Hankel singular values, determined that (1) engine static pressure ratio $PR = p_{s3}/p_{s1}$, (2) HP spool speed NH , and, (3) bypass duct Mach number, MN , should be the engine variables chosen as control parameters for the range control in order to give the most robust control.

Engine accelerations and decelerations are controlled by rate limiting the demands of PR and NH derived from the pilot's lever and the demand of MN is determined as a function of non-dimensional NL. Referring to the block diagram W1 and W2 are the plant shaping matrices, with W1 involving dynamic terms. The K_∞ block is a linear H_∞ designed control for the shaped plant, and includes an observer and a simple reference model. No gain scheduling is used within the block.

A similar arrangement was used to design structural limiters for maximum fan spool speed NL and for maximum T6. The T6 maximum value replacing the demanded PR signal in the reference vector r , and the T6 engine signal replaced PR in the shaped plant vector y . Obviously no rate limiting is needed in these controllers, because the limiting is applied in the demand signals.

The minimum fuel flow was selected from the outputs of the various loops together with the other corresponding plant input demand signals. 'Hanus' conditioning was used to integrate the limiters with the main range control. This ensured bumpless transfer of control between the loops and prevented integrator windup.

The control was initially tested against an aerothermodynamic model of the Spey engine before being offered to the engine on the Glen test bed. Extensive use of engine non-dimensional groups fitted the control to operate across the complete flight envelope. Computer simulations of engine and control at various altitudes and Mach numbers confirm this.

The control was engine tested under sea level static conditions at Pyestock in 1994. Figure 13 below shows a full scale acceleration in response to a pilot's lever change.

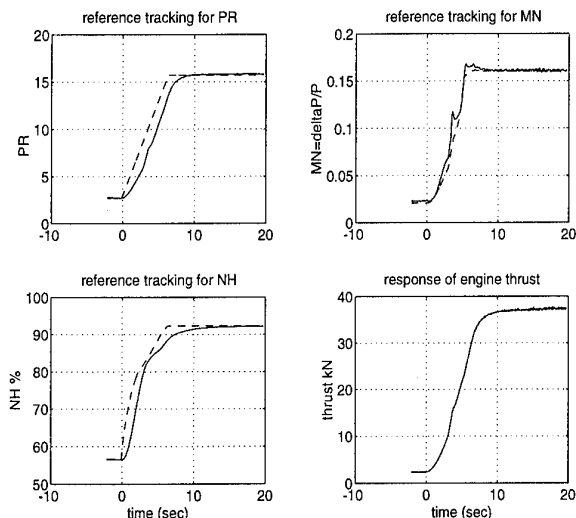


Figure 13 Large range acceleration

The figures show the engine signals (solid) tracking the reference demands (dashed) for the pressure ratio (PR=ps3/ps1), bypass Mach number MN, and HP spool speed NH for a change from idle to near maximum power. The engine thrust measurement during the transient is also shown.

Figure 14 below shows a manoeuvre from about 80% NH onto the jet pipe thermocouple temperature limit, so that loop switching occurs. In this case it can be seen that the

temperature signal vector takes over from the PR signal vector just before the end of the acceleration phase. MN and spool speed NH continue to track their reference values.

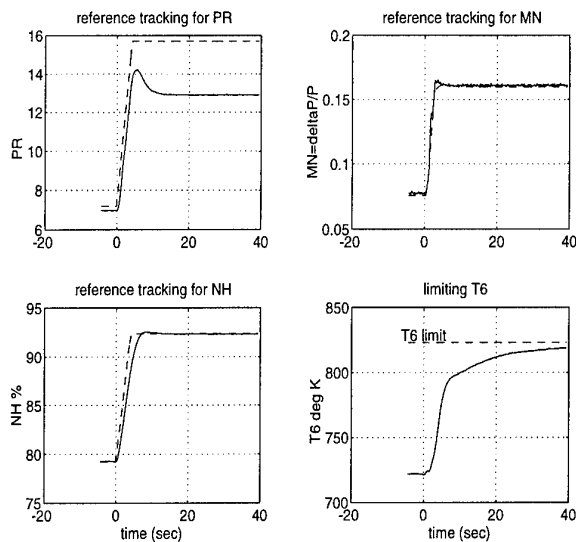


Figure 14 Small acceleration performance

The control reference tracking has been substantially improved since the engine tests by changing the anti wind-up code. Robustness measures for the system are good and it is claimed that this control is robust enough in terms of step response to require no gain scheduling (besides that endowed by the use of non-dimensional parameterisation) over the entire flight envelope.

5.4 Practical implementation issues of MVC (items 8 & 9)

The demands on projected flight propulsion systems for improved fuel economy and wide flight envelope and mission capability are likely to be met by engine designs which incorporate more active internal variable geometry devices. The VCE engine is entirely dependent on accurate control of the variable geometry to ensure that the compressors and turbines run at the design conditions of pressure ratio and airflow. Since the design conditions vary with the operational mode (loiter, combat, etc.), it is unlikely that the control concepts adopted for current engine types can be simply extended to the VCE. The reasons are simply;

1. there is a limit to the accuracy with which engine geometry can be positioned by open loop scheduling,
2. the relationships between pressure ratios, air flows and geometry settings vary both from engine to engine and with engine degradation.

For these reasons, it is clear that the VCE will require additional closed-loop controls to provide accurate control of the measurable engine outputs which may be used to define the key efficiency and safety parameters. This leads to a third relatively new control system design problem area,

3. options will arise as to which engine parameters should be included in closed-loop controls and which variables can be positioned by open-loop schedules in the conventional way.

The increased requirements for sensors and actuation components associated with the VCE must be offset by the benefits to be gleaned from greater control capability, lower cost of ownership, and improved thrust-to-weight ratios.

However, the points made above emphasise the need for a much greater comprehension of the interactions between the engine performance and the variable geometry components. Of particular concern must be the behaviour of such a complex system to various failure modes and the requirements for safe and controlled recovery from such events.

Building on the work already undertaken by DRA and faced with this set of new engine design challenges, Rolls-Royce embarked on a series of exercises aimed at a thorough investigation of the potential control law definition, design, and implementation problems which might arise in future VCE projects. Existing design methods and procedures were to be assessed in order to develop a complete multivariable engine control system design methodology, ensuring avoidance of 'blind alley' designs, in a project-type environment. It was also important to make an assessment of the impact that realisation of such a system would have on controller parameters such as software capacity and speed, system validation and verification and failure modes and effects specific to multiple closed-loop controllers.

The first Rolls-Royce MVC design activity (item 8 table 1) was directed at engine tests of the Spey Mk202 engine in the Glen at Pyestock. This served to validate the design methodology as it then existed in a fully practical way. The block structure employed for this 3input-3output control is shown in Figure 15. Acceleration and deceleration control was administered by rate limiting the NL demand signal. Recommendations for further work proposed independent NHDOT limiting.

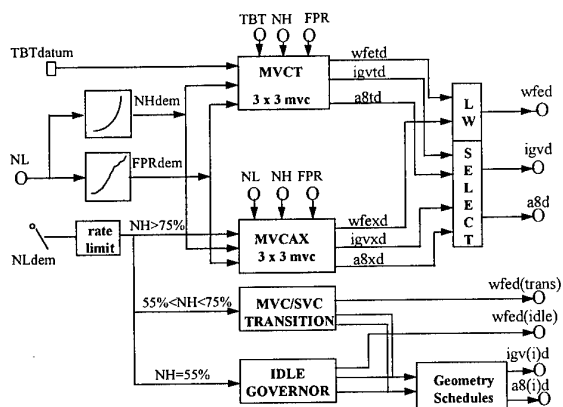


Figure 15 Rolls-Royce MVC structure

The first multivariable variable cycle engine (MVVCE) simulation exercise⁷ (described briefly as Item 9 in Table 1) comprised the design of a thrust, acceleration, turbine blade temperature, and fan working line control over a very wide flight envelope.

Positive conclusions included the proving of the value of control configuration design methods to avoid poor choice of parameters, successful integration of the several multi-loop controllers and experience of the rapidity with which loop designs of simple structure could be achieved using the Edmunds⁸ method, and the achievement of accurate fan working line control. It was possible to keep the full envelope controller structure simple by scheduling the proportional and integral gains (16 gains for each chosen flight condition) against corrected NH. At all design stages of the exercise

advanced methods were evaluated for inclusion in a Design Methodology.

The present Rolls-Royce MVC design methodology is shown in figure 16.

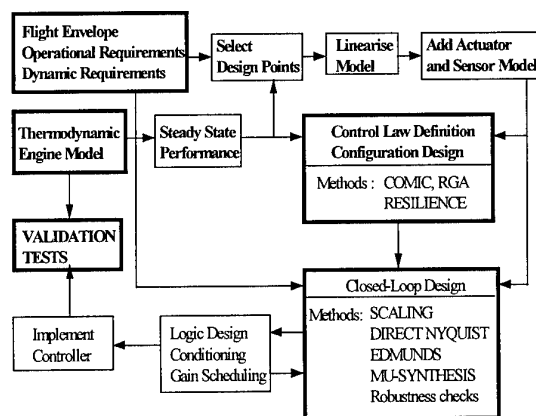


Figure 16 Overall design methodology

In the control law definition and configuration block, COMIC (Control Mode Investigation and Comparison) is a steady state sensitivity matrix method which relates all engine performance and safety parameters of interest to all engine input variables. It can be used to highlight engine control system sensitivities (ie. system errors) induced by sensor or actuation position errors for any chosen control configuration (choice of parameters and loop structure). The RGA (Relative Gain Array) technique can be used to explore subsequent decentralisation of a multiple loop control. RESILIENCE is a technique which allows selected closed-loop options to be compared in terms of achievable bandwidth and robustness criteria. The merits of these methods is that they highlight poor parameter combinations at an early stage and avoid nugatory design work.

The closed-loop design methods most suitable for systems such as the VCE controller, where gain scheduling is required to cover a wide flight envelope, are those in which the designer has control over the control structure. The Direct Nyquist technique provides a high level of visibility as the design proceeds (ie. de-coupling design followed by separate single loop designs in the frequency domain) but there is little control over the order of the control compensation algorithms. In contrast Edmunds is a numerical optimisation method of loop design in which the designer nominates a preference for a closed-loop frequency response (for each input and output) and also decides on a particular control structure. Controller gains are then evaluated by the optimiser to match the achieved and desired closed-loop transfer functions most closely. The method can be automated quite simply and therefore is suitable for mass calculation of controllers - which is a matter of some value for wide envelope control design tasks in which gain scheduling is contemplated. For both of these design methods, robustness checks are carried out on completion of the designs. This is not satisfactory from the point of view that complete designs may have to be repeated. More advanced ideas are available in the Mu-Synthesis technique in which known system uncertainties are included within the compensator design and robustness targets are set at that stage.

5.5 Way ahead (item 10)

The most recent area of study at DRA Pyestock associated with MVC is on-line engine performance optimisation. Similar in concept to the US PSC programme⁹, this aims to exploit the "indirect approach" where a model is configured which accurately tracks engine sensor outputs and acts as the subject of optimisation. Methods closely allied to MVC have been developed to provide the aerothermodynamic model tracking function and these yield estimates of engine degradation and temporal change as a by-product. These may be of significant value for health monitoring applications.

6. CONCLUDING REMARKS

The work reported here was undertaken at a number of UK work centres. Deliberate efforts were made to foster independent approaches - particularly with the University contributions through Lucas. The top level objectives were broadly the same in all cases of study with robustness being a characteristic of widespread interest. This being the case, it is noteworthy that there was little actual duplication of control input-output selections. It would seem that in practical terms therefore, there is a wide spectrum of possibilities for MVC of engines. This is of practical importance because many other factors which have not been raised in detail are also likely to influence feedback parameter choice. Sensor cost, weight and accuracy and the influence of engine heat soak on potential parameters are examples of such factors. In a project application of MVC the actual selection of controller structure will be the result of a wider based set of requirements than has been the case in these studies.

In the course of developing MVC the appreciation of engine dynamics and parameter interactions has been improved significantly. Engine dynamic identification methods - not given exposure in this paper - have been employed much more widely and effectively than previously. This has also helped in identifying the fidelity of aerothermodynamic models used in front-end studies.

Concerns regarding the effectiveness of single input-single output approaches for future ASTOVL and VCE engines have been one of the main influences in establishing a MVC capability in the UK. However, much of the generic experience gained through research programmes has derived from studies on conventional turbofan engines. From this it is evident that modest benefits to operators of conventional turbofan engines may be possible by adopting MVC approaches. Engine operation may be much more tightly prescribed by adding closed loop working line control for the LP spool and precisely specifying, for example, the relationship between the LP and HP spool speeds, instead of scheduling guide vane angle. It has been shown also that large scale thrust response may also be improved markedly while reducing handling surge margin consumption. This improved quality of control which can now, in principle, be offered may free the hand of the turbomachinery designer to seek performance gains through better optimised engine component matching. Undoubtedly the synthesis process to achieve the necessary control improvements is more complex than at present and the software needed will be more extensive both in execution time and memory requirement. But improvements occurring in parallel in electronics will accommodate these needs.

Ultimately it is expected that the factors determining whether an MVC approach is acceptable will be integrity and reliability considerations. The ease with which sensors and control lanes can be and are duplicated means the integrity required of sensors and electronics can be established with certainty - albeit at a possible cost in reliability. It is less easy to see how faults in the simplex regions of actuators will be managed. This represents perhaps the most important phase of work which yet requires detailed consideration because the assurance of system stability in the presence of such faults is harder to establish for MVC than for conventional systems. The next logical step toward project application of MVC is full demonstration within a controls TDP. An essential first phase of this will be to address the implications of simplex actuator failures on system stability.

ACKNOWLEDGEMENTS

The authors wish to thank Lucas Aerospace and Professor Ian Postlethwaite and Dr Raza Samar of the Department of Engineering Leicester University for the kind permission to use the figures and results shown in section 5.3 prior to their own full publication of this work.

Thanks are due also to Rolls-Royce and DFS(Air)4, MOD-UK for contributions made to section 5.4

REFERENCES

1. Sutton, 1989
'Design of a MVC for the advanced vectored thrust engine'
RAE Tech Memo, unpublished
2. Porter and Bradshaw, 1983
'Design of error-actuated controllers for multivariable plants with unknown dynamics and measurable outputs'
Int. Journal Control, vol. 37
3. Sutton, 1991
'Application of MVC to a turbofan engine'
IEE Control '91. Conference, vol 2 Edinburgh.
4. Hanus, Kinnaert, and Henrotte; 1987
'Condition technique, a General Anti-windup and Transfer Method'
Automatica, vol. 23
5. Greig, 1994
'Multivariable powerplant control - engine demonstration'
DRA customer report, unpublished
6. Postlethwaite, Samar, Choi and Gu, 1995
University of Leicester
'A digital multimode H_{∞} controller for the Spey engine'
The 3rd European Control Conference, Rome, Italy
7. Shutler and Betteridge, 1994
'Definition, design and implementation of control laws for variable cycle gas turbines'
RAeSoc conference, Bristol, UK
8. Matlab Multivariable Frequency Domain Toolbox
Users Guide Version 2.0 July 1990
GEC Eng. Research Centre, Cambridge Control Ltd
9. Glen B Gilyard and John S Orme
Performance - Seeking Control: Program Overview and Future Directions
NASA Dryden Flight Research Facility
A1AA - 93 - 3765 - CP

Table 1

Item	Period of Research	Participants	Control Law Details	Remarks
1	1985-89	DRA U Salford	Fuel and final nozzle controlling HP spool speed and LPC working line (through duct Mach no). Temperature limiters and open loop back up schedule included.	Based on RB199 engine simulation with test bed trials to conclude. Cross coupling of inputs and outputs not great.
2	1987-90	DRA	Control of thrust centre and magnitude on the Advanced Vectored Thrust ASTOVL concept (Plenum chamber burning Pegasus)	Simulation included an inertial hovering airframe. Engine throttle response poor for aircraft pitch control. Good roll control through lateral flow switching.
3	1989	DRA	Fan static pressure ratio and bypass duct Mach number. Thrust rating law with separate loops.	RB199 engine test to demonstrate flat thrust response and thrust estimating algorithm. No significant cross coupling encountered.
4	1989	DRA	1. NH and bypass duct Mach number 2. NL and bypass duct Mach number 3. NL and Fan pressure ratio	RB199 engine tested. Conclusion:- Hanus method validated performance consistent with conventional controls
5	1990-93	DRA	Three input/three output control:- fuel, IGV, nozzle (actuators); HP spool speed, LP spool speed and bypass duct Mach number (feedbacks). Limiters and open loop backups included. Fast thrust response mode.	Used Spey Mk202 engines with modified independent actuators for IGV and handling bleed. Large scale thrust response was improved over upper 1/2 of thrust range.
6	1993 1994	DRA	Same law as 5. Pole shifting by variation of integral gains used to improve disturbance rejection.	Spey Mk202 testing. Tests to map engine surge line for assessment of surge margin consumption in fast response mode, were frustrated by surge resistance of Spey.
7	1992-95	Lucas DRA U Strathclyde U Leicester U Southampton	Strathclyde - fan pressure ratio and HP speed to control fuel and nozzle IGVs scheduled Leicester - LPC pressure ratio, duct Mach number. HP spool speed to control fuel nozzle and IGV. Southampton - Neural nets and fuzzy logic.	Universities asked to assess engine model dynamics and input-output relationships to select "best" parameter pairing for robust control. Leicester H ∞ control engine tested Southampton have produced Reinforcement Control - an aid to tuning MVCs. Strathclyde - engine control trials imminent.
8	1992-94	Rolls-Royce	LP speed, HP speed and fan PR range governing with MVC TBT limiter (ie. TBT, HP spool speed, Fan PR). Actuators were fuel, IGV and nozzle area. Single loop idle schedule implemented, implying successful control structure change.	Engine tested using Spey Mk202 in Glen. Engine handling was by rate limited PLA but recommendation made to use dedicated NHDOT loops.
9	1992-94 (Phase I Phase II continues)	Rolls-Royce	Flight envelope capable MVC design of an ASTOVL powerplant in up-and-away mode. Continuous fan working line control (duct Mach number feedback) with one of the following: fan speed (range governing), TBT temperature limiting and NHDOT acceleration and deceleration limiting. Fuel and final nozzle actuators were closed loop, LP and HP guide vanes being open loop scheduled.	Definite evidence of performance and handling gains through active working line control. Assessment of processing requirements indicated manageable increase in overall control software load.
10	1994 to present	DRA	On line optimisation of multivariable controlled engines. MVC design methods exploited to achieve a real time thermodynamic simulation which tracks engine sensor outputs. This simulation represents the "vehicle" for optimisation trials.	Strategic research which anticipates much greater airborne computing power than currently available. Possible application to engine health monitoring, and alternative management of closed loop/open loop actuators in a MVC architecture.

Paper 28: Discussion

Question from A T Webb, Edwards AFB, USA

As is well known, compressor stall margin is lower in the upper left hand corner of the flight envelope. Has consideration been given to investigating this engine control system under these conditions, in an altitude test facility for example? Is this an issue for further testing?

Author's reply

Yes, this is an aspect that needs to be investigated and we are very interested in pursuing it. To date, all our testing has been at sea level static conditions. However, in one sense upper left hand corner operation helps, because flight idle occurs at higher core speeds in this region.

Question from Prof N Munro, UMIST UK

Comment: the historical perspective in the paper should perhaps be amended. The first multivariable engine control study was carried out by the University of Manchester Institute of Science and Technology (UMIST), with the then National Gas Turbine Establishment, in 1968.

Question: although the H-infinity approach produces good results, the resulting controllers are complex. There are newer, robust control techniques, eg QFT, developed by Houpis at Wright Laboratory, and Generalised Kharitonov, developed by Barmish at Wisconsin, which produce simpler controllers. Will these be included in future engine control studies?

Author's reply

In response to the comment, Prof Munro is correct. Reference to the earlier work he mentions was omitted from the paper inadvertently.

In response to the question, any new methods which offer robustness combined with simplicity should be evaluated. Both qualities are important for the successful clearance of multivariable control for aero-engines.

SYSTEME DE REGULATION AVANCE POUR TURBOMOTEUR

JL FREALLE

TURBOMECA

Division TURBOMECA MICROTURBO

Groupe LABINAL

64511 BORDES

FRANCE

Résumé

L'apparition de régulations de type FADEC sur les turbomoteurs d'hélicoptère ces dernières années a considérablement enrichi les fonctions de contrôle moteur. La mise en oeuvre de l'hélicoptère a été facilitée, la charge de travail du pilote réduite, le moteur et la chaîne de transmission de puissance étant automatiquement maintenus dans leurs limitations. La manoeuvrabilité de l'hélicoptère a été améliorée par les performances de régulation de vitesse rotor.

La possibilité de gestion rigoureuse de régimes d'urgence moteur, largement supérieurs au régime maximum continu, a permis d'améliorer de façon sensible les performances des hélicoptères bimoteurs en situation OEI (One Engine Inoperative). Des fonctions d'aide à l'entraînement du pilote à cette configuration de panne sont intégrées dans les fonctions de régulation.

L'application de la technologie FADEC à un moteur de petite puissance présente des spécificités, notamment par le gain de performances moteur et hélicoptère, par la pénalisation en terme de coût et de masse.

Les travaux de recherche en cours et à venir sont destinés à généraliser la technologie FADEC sur ce type de moteur, en réduisant coût et masse, tout en améliorant la tolérance aux pannes et les performances de régulation. Les thèmes suivants sont présentés : optimisation d'architecture régulation, mesure par capteurs optiques, application de la logique floue, utilisation d'un modèle interne.

1 - Introduction

L'application de la technologie FADEC aux turbomoteurs de nouvelle génération a permis d'offrir de nouvelles fonctions améliorant performances moteur et hélicoptère et diminuant la charge du pilote.

Une présentation détaillée des fonctions de régulation proposées sur un turbomoteur moderne est réalisée en première partie.

Par rapport aux réacteurs d'avions civils ou militaires, le turbomoteur d'hélicoptère présente des spécificités sur la fourniture de puissance nécessaire au vol, sur la structuration des régimes d'urgence, sur le couplage régulation et vol hélicoptère et sur la taille du moteur pour lequel les équipements de régulation entrent de façon non négligeable dans le bilan masse et coût.

Ces spécificités, favorisant ou pénalisant l'application de la technologie FADEC pour les turbomoteurs, sont présentées en deuxième partie.

L'orientation des travaux de recherche est axée sur la généralisation du FADEC pour les turbomoteurs de petite et moyenne puissance. Quelques thèmes, innovant par rapport à l'état de technologie des systèmes FADEC de dernière génération, sont présentés en troisième partie : optimisation d'architecture, capteurs optiques, logique floue et modèle interne.

2- Fonctions de régulation d'un turbomoteur moderne

Cette description présente les fonctions intégrées dans une régulation FADEC de turbomoteur pour hélicoptère bimoteur.

2-1 Fonctions de vol

-Démarrage

La séquence de démarrage du turbomoteur et d'atteinte du régime de ralenti sol est déroulée automatiquement (fig. 1). Les lois de démarrage sont adaptatives aux variations suivantes :

- altitude, température
- état thermique du moteur
- carburant (grade, température, viscosité)

Suite à un arrêt en vol la séquence de démarrage peut être relancée automatiquement ou sur simple ordre du pilote.

- Ralenti N1

En fin de démarrage, on peut éventuellement sélectionner un ralenti N1, utilisé dans deux cas de figure :

- quand l'hélicoptère possède un frein rotor et que celui-ci est engagé : la valeur du ralenti N1 est choisie pour respecter le couple limite du frein rotor, la sortie du ralenti N1 est impossible tant que le frein n'est pas relâché.
- quand le démarrage est effectué par temps très froid, pour permettre de mettre en température les circuits de lubrification.

Dans les autres cas, en fin de démarrage, on engage directement l'accélération du rotor.

- Accélération rotor

La mise en vitesse du rotor est automatiquement contrôlée (fig. 1). La mise en état prêt à décoller de l'hélicoptère est simple et rapide. Le contrôle automatique d'accélération du rotor augmente le confort des passagers en évitant les à-coups de couple et les mouvements de lacet de la cellule sur le train d'atterrissage.

- Maintien de la vitesse rotor

Il est assuré par la régulation de vitesse de turbine libre qui génère une consigne de vitesse de générateur de gaz (N1) (fig. 2).

La position du pas collectif du rotor est prise en compte afin d'anticiper les demandes de puissance. La consigne de vitesse rotor peut être si nécessaire ajustée par le pilote ou élaborée par le calculateur de bord hélicoptère en fonction de la vitesse, de l'altitude, de la phase de vol sur des critères de bruit, performance ou manoeuvrabilité.

- Equilibrage des deux moteurs

Les deux moteurs sont équilibrés en N1 ou en couple. Le paramètre d'équilibrage, N1 ou couple, est échangé sur un bus numérique entre les deux FADEC, le moteur le moins chargé corrigeant automatiquement sa demande de puissance pour atteindre l'équilibre.

-Respect des limites moteur

Le traitement de la demande de puissance calculée par la régulation de vitesse N2 transforme cette demande en débit carburant en assurant le respect des limites stabilisées (vitesse du générateur de gaz N1, température inter-turbine T4) et transitoires (pompage compresseur sur accélération, extinction chambre de combustion sur décélération).

-Respect des limites chaîne de puissance hélicoptère

La demande de puissance est corrigée pour ne pas dépasser les limites de couple de la boîte de transmission hélicoptère en condition AEO (All engines Operative), et OEI (One Engine Inoperative) en limitant le couple fourni par le moteur mesuré ou estimé à partir de N1, N2, PAMB et TAMB.

-Limitation de surcouple transitoire

Lors d'une demande de puissance importante, la vitesse rotor diminue transitoirement jusqu'à ce que la puissance du moteur, alors en accélération, équilibre la puissance absorbée par le rotor. Au delà, l'accélération du rotor pour rejoindre sa vitesse nominale est contrôlée pour éviter un surcouple pouvant endommager la boîte de transmission hélicoptère et une action du pilote de compensation sur le mouvement en lacet de l'appareil (fig. 3).

-Détection de panne moteur

La panne moteur est détectée par surveillance des paramètres moteur, et par comparaison avec le N1 ou le couple de l'autre moteur dans les phases où les deux moteurs sont normalement équilibrés (fig. 4). L'information panne moteur est envoyée au cockpit et au FADEC de l'autre moteur, les transmissions de données (N1, couple, détection panne moteur) sont réalisées via les bus numériques.

Dans certains cas, la détection de panne moteur est assurée par un dispositif hélicoptère travaillant sur une logique équivalente qui envoie un signal panne moteur au FADEC du moteur encore opérationnel.

- Gestion des limites moteur et hélicoptère en condition OEI.

En condition AEO (All Engine Operative), les limites moteur (N1, T4) et hélicoptère (couple) sont adaptées aux limites qualifiées en régime de décollage et en maximum continu.

En condition OEI (One Engine Inoperative), les limites moteur et hélicoptère sélectionnées sont des limites qua-

lifiées pour des régimes d'urgence, à temps limité d'utilisation (fig. 5).

Sur réception de l'information panne moteur émise par l'autre FADEC, les limitations appliquées commutent de AEO vers OEI. Le pilote, suivant la structuration des régimes qualifiée peut avoir le choix entre plusieurs régimes :

- "2 minutes 30" ou "OEI continu"
- "30 secondes" ou "2 minutes" ou "OEI continu"

Les temps d'utilisation de ces régimes sont gérés et comptabilisés avec génération d'informations pour le pilote (affichage cockpit) : zone de régime sélectionnée, zone de régime utilisée, temps d'utilisation dépassé.

En condition AEO ou OEI, le FADEC calcule une information de marge de puissance disponible synthétisée en écart N1 par rapport à la limite active, qui, transmise au cockpit, donne au pilote une image de son potentiel de puissance disponible.

- Entraînement à la panne moteur

Une logique d'entraînement à la panne moteur est intégrée au FADEC (fig. 6) dommage:

- la panne moteur est simulée par mise au ralenti d'un des moteurs
 - le moteur restant entraînant seul le rotor, l'hélicoptère se pilote comme en condition OEI réelle, mais avec des limites moteur détarées afin de ne pas comptabiliser de l'endommagement moteur.
- En situation d'entraînement, afin d'obtenir des trajectoires représentatives d'un hélicoptère en condition de pleine charge, la masse de hélicoptère est volontairement réduite à une valeur adaptée aux régimes détarés.
- en cas de perte d'un des deux moteurs, le mode entraînement est automatiquement désélectionné.

- Consigne de pilotage sur détection de panne régulation

Suite à une détection de panne en vol, le pilote est informé du niveau de dégradation des fonctions.

Trois niveaux d'information sont utilisés :

- défaut mineur : un élément redondant est détecté en panne, aucune fonction de régulation n'est altérée, l'information ne sera affichée au cockpit qu'au moment de la mise au ralenti ou à l'arrêt du moteur en fin de vol
- mode dégradé : la panne détectée conduit à la dégradation d'une ou plusieurs fonctions, les consignes de pilotages associées sont à appliquer
- panne totale : le débit carburant est figé.

1-2 Fonctions de Maintenance

Le FADEC utilise le bus numérique de dialogue avec le système hélicoptère pour fournir les renseignements de maintenance.

- Détection de panne

Suite à une détection de panne, un code est envoyé au système hélicoptère indiquant la fonction en panne et permettant de déduire le niveau de maintenance requis.

- Comptage de cycle

Pendant le vol, les cycles moteurs consommés sont automatiquement comptés. A l'issue du sol, la mémorisation des cumuls est remise à jour, les valeurs des compteurs sont émises sur le bus numérique de liaison avec le système hélicoptère.

- Contrôle santé moteur

Dans des phases de vol stabilisé, à la demande du pilote, le FADEC calcule pour le point de fonctionnement et les conditions d'utilisation courante, le couple minimum et le T4 maximum que doit fournir le moteur, ainsi que l'écart des paramètres réels du moteur par rapport à ces valeurs de référence. Le résultat est transmis sur le bus numérique de liaison avec le système hélicoptère.

- Comptabilisation des régimes OEI

Pour chaque régime d'urgence, le calculateur mémorise le nombre de fois où le régime est utilisé, le temps cumulé d'utilisation, le temps d'utilisation courante. Le contenu de ces compteurs est émis sur le bus numérique de liaison avec le système hélicoptère.

3 - Spécificités de l'application FADEC au turbomoteur

3-1 Aspect performances

3-1-1 Performances hélicoptère

Le vol, la trajectoire, la manoeuvrabilité d'un hélicoptère sont directement liés à la vitesse du rotor et au bon équilibre entre puissance absorbée et puissance motrice.

La régulation du moteur a un impact direct sur le pilotage de l'hélicoptère.

De part leur faibles capacités d'adaptation, les performances des régulations hydromécaniques sont un compromis comme, par exemple, pour assurer une régulation stable de vitesse turbine libre en condition rotor désaccouplé par la roue libre (autorotation, descente) et en condition rotor accouplé (fourniture de puissance), l'inertie pouvant varier d'un facteur 1 à 8.

Le FADEC permet de s'adapter aux différentes conditions de vol en maximisant la performance de régulation pour chacune d'elles.

Il permet également de mieux gérer les transitions entre ces différentes conditions de vol, limitant ainsi la charge du pilote (meilleur maintien de la vitesse rotor, respect des limites transitoires de couple...).

Les hélicoptères de nouvelle génération commencent à intégrer des concepts, désormais couramment utilisés sur les avions, destinés à faciliter la mise en oeuvre de l'appareil, diminuer la charge pilote, optimiser le vol, guider le pilote pour l'application des procédures de sécurité et optimiser la maintenance.

Cela se traduit, par exemple, par l'automatisation du démarrage jusqu'à l'état "prêt-à-décoller", par le respect automatique des limites du moteur et de la chaîne de transmission, par l'adaptation du régime rotor en fonction des phases de vol sur des critères de consommation, de vitesse, de manoeuvrabilité ou de bruit, par la simplification des informations transmises au pilote.

Cela se traduit également par une aide ou diagnostic et à la maintenance à partir d'informations générées par les calculateurs embarqués.

Sur les hélicoptères récents, la présence de calculateur de bord gérant les affichages cockpit, intégrant des capacités de mémorisation, de dialogue avec le FADEC et avec des équipements de maintenance au sol, ouvre de nouvelles possibilités d'intégration des fonctions hélicoptère / moteur.

3-1-2 Performances moteur

La réglementation d'accès aux plateformes de décollage dans un environnement non dégagé (ville, offshore ...) impose une certification en catégorie A : suite à une panne moteur au décollage, l'hélicoptère doit respecter un gabarit de trajectoire ainsi qu'un taux de montée. Les caractéristiques propres de l'hélicoptère induisent donc la demande d'un niveau de puissance en monomoteur.

Dans le cas d'une structuration de régime moteur proposant une puissance d'urgence "30 secondes", son niveau est en général plus élevé de 25 à 35 % par rapport au niveau de puissance "maximum continu".

La qualification de tels niveaux de régime se fait par la validation de niveaux élevés de température entrée turbine.

Ceci implique la nécessité de limiter les conditions d'accès à ces régimes, d'en contrôler leur temps d'utilisation, de faire respecter précisément par la régulation les limites qualifiées (par des limitations N1 ou T4).

De plus, des opérations de contrôle de performances moteur en vol doivent être réalisées périodiquement afin de garantir la disponibilité du niveau de puissance d'urgence au cours de la vie du moteur.

Ce contrôle santé moteur doit prendre en compte les conditions d'aviation du moteur influant sur les performances, par exemple la présence de filtres anti-sable.

Le FADEC permet de gérer directement l'utilisation des régimes d'urgence et le contrôle santé moteur.

3-2 Aspect masse

Sur un turbomoteur de petite puissance, la masse des équipements permettant d'assurer l'ensemble des fonctions de régulation représente de l'ordre de 15 % de la masse totale du moteur.

La masse des équipements de régulation est donc relativement sensible sur le bilan masse du moteur.

A niveau équivalent de complexité de fonctions, ce bilan masse est défavorable aux petits moteurs.

Par rapport à un système totalement hydromécanique relativement compact sur un turbomoteur, un système basé sur un FADEC altère le bilan masse (fig. 7):

- par l'ajout d'un calculateur
- par l'ajout de capteurs
- par l'ajout d'un faisceau électrique blindé et surblindé, de la connectique associée, permettant de tenir les niveaux d'agression électromagnétique et foudre spécifiés
- par la simplification de l'hydromécanique.

Du fait de la compacité d'un turbomoteur, des problè-

mes de ventilation de la zone moteur sous les capots, notamment moteur arrêté, le montage du FADEC sur moteur implique des spécifications d'environnement thermique qui conduiraient à un coût trop élevé.

Le FADEC est donc déporté en soute, ce qui allonge la longueur du faisceau électrique.

Le bilan est que, pour un petit turbomoteur, un système de régulation bâti autour d'un FADEC a une masse plus importante qu'un système purement hydromécanique.

Du fait de l'effet de taille, ce surplus de masse est sensible sur petit moteur.

3-3 Aspect coût

Sur un turbomoteur de petite puissance équipé de FADEC, le coût des équipements permettant d'assurer l'ensemble des fonctions de régulation représente de l'ordre de 20 % du coût total du moteur.

Le système de régulation est donc un poste très important sur les opérations de diminution de coût du moteur.

Au même titre que l'aspect masse, à niveau équivalent de complexité de fonctions, le ratio (coût système de régulation) / (coût moteur) est défavorable aux petits moteurs.

Par rapport à un système totalement hydromécanique, un système basé sur un FADEC altère le bilan coût par l'ajout d'un calculateur, des capteurs, d'un faisceau électrique, un système hydromécanique simplifié dont la réduction de coût ne compense pas l'augmentation sur les autres postes.

Il faut cependant prendre en compte que le service offert par une régulation FADEC au pilote et à l'opérateur est sensiblement plus important que celui offert par une régulation hydromécanique.

Deux exigences de conception et de qualification pèsent lourd sur le coût d'un système FADEC, du fait de l'introduction de l'électronique :

- garantir un bon fonctionnement pour des niveaux d'agression foudre et EMI demandés pour la qualification de l'hélicoptère : dispositif de protection du calculateur, faisceau électrique et connectique, capteurs
- garantir un taux de panne régulation conduisant à la perte du contrôle de la puissance du même niveau que celui d'un système totalement hydromécanique.

Les objectifs de maîtrise du coût d'acquisition et de réduction du coût d'utilisation sont très importants dans le cadre du redressement et du développement du marché de l'hélicoptère où le type d'utilisation et la structuration du marché en petits opérateurs ne facilite pas l'at-

teinte d'objectifs de rentabilité.

3-4 Bilan

L'amélioration des performances hélicoptère, l'optimisation des performances moteur, l'amélioration sensible des conditions d'utilisation de l'hélicoptère, l'aide à la maintenance favorisent la technologie FADEC.

Dans le cas des applications bimoteur, il permet d'intégrer la gestion des régimes d'urgence, et les contraintes associées, comptage, mémorisation, contrôle santé moteur. Les conséquences au niveau masse et coût du choix de la technologie FADEC pour la régulation d'un moteur ont plutôt eu un effet de frein sur son développement.

Par exemple, le nouvel hélicoptère léger d'EUROCOPTER, l'EC 120, optimisé sur des critères de coût, le moteur retenu, une variante de la famille ARRIUS de TURBOMECA, bien que technologie récente, est équipé d'une régulation hydromécanique.

Les travaux de recherche pour préparer la prochaine génération de système de régulation à FADEC ont pour but de repousser les limites actuelles pour conduire à la généralisation de cette technologie. En particulier, il faudra diminuer la masse et le coût à fonctions égales, améliorer la tolérance aux pannes, tout en assurant une immunité à des niveaux élevés d'agression EMI ou foudre.

Un autre axe de recherche est d'améliorer les performances de régulation par une meilleure adaptation aux différentes conditions de fonctionnement.

4- Axes de recherche pour les futurs systèmes de régulation

4-1 Optimisation de l'architecture

Sur les plus récentes motorisation à base de technologie FADEC, on trouve généralement deux catégories :

- FADEC simple canal associé à un dispositif de secours intégré au module hydromécanique, commandable depuis le cockpit par une liaison mécanique ou une télécommande électrique motorisée.
Le dispositif de secours doit permettre de commander la puissance du moteur en respectant les critères imposés par la FAR33 : pouvoir commander des transitoires de puissance en respectant les limites moteur (pompage et extinction), avec des conditions de temps maximum sur l'obtention de la puissance de décollage à partir d'un régime de ralenti vol.
- FADEC double canal avec ou sans dispositif de secours. Dans ce dernier cas le dispositif de secours est simplifié, il doit permettre la modulation de la puissance et l'arrêt du moteur, sans assurer de protection au pompage et à l'extinction.

Un système FADEC ne doit pas conduire à un taux de perte du contrôle de la puissance moteur supérieur à celui habituellement admis pour une régulation totalement hydromécanique, soit 10^{-5} / heure.

Or, avec calculateur FADEC simple canal, le taux de perte de la fonction de régulation est de l'ordre de 5.10^{-5} / heure, les éléments dimensionnant majoritairement ce taux étant l'alimentation et le processeur du calculateur ainsi que les éléments électriques de l'actionneur carburant.

Le choix d'une architecture double canal intégrant la redondance de ces éléments, permet d'atteindre un taux de perte de contrôle de la puissance meilleur que 10^{-5} / heure.

La solution mono canal conduit à calculateur FADEC plus simple, mais nécessite un dispositif de secours élaboré, plus ou moins complexe à réaliser suivant le domaine de vol à couvrir. Cela conduit à un module hydromécanique plus complexe ou à l'ajout d'un dispositif de télécommande ayant un taux de défaillance faible, impliquant une pénalisation en masse et en coût sur ces postes.

Une voie vers la diminution de masse et de coût peut être ouverte par la recherche d'une architecture conduisant à une meilleure optimisation sur la répartition des fonctions entre électronique, logiciel, électromécanique et hydromécanique.

Pour le FADEC, il s'agit de rechercher une architecture interne différente de celle d'un double canal classique conduisant à un taux de défaillance meilleur que

10^{-5} / heure, à un moindre coût et sans pénalisation de masse.

4-2 Capteurs optiques

La tenue des niveaux actuellement spécifiés d'agression EMI et foudre implique la protection des interfaces électriques du calculateur et le blindage et surblindage des faisceaux électriques.

Pour les capteurs, la substitution d'une technologie de mesure électrique par une technologie de mesure et de transmission optique de l'information conduirait à la simplification et à l'allègement des faisceaux électriques, à la suppression de dispositifs de protection des interfaces de mesure du calculateur. Nous avons commencé à dérouler un programme d'évaluation et de validation de dispositifs de mesure optique.

- Mesure de vitesse sur roue phonique ou sur pignon

Pour remplacer les capteurs électromagnétiques, nous évaluons des capteurs à effet FARADAY. Le principe est basé sur le changement de la polarisation de la lumière réfléchi sur un cristal, sensible aux variations de champ magnétique.

En interposant un polarisateur, on obtient une modulation de la lumière réfléchi sur la variation de l'entrefer capteur-roue. La lumière incidente, générée par une diode Led, et la lumière réfléchi sont véhiculées par la même fibre optique. Nous avons mis ce type de capteur en endurance sur une turbine industrielle, sa qualité de mesure est aussi bonne que celle d'un capteur électromagnétique classique et elle ne s'est pas dégradée au cours de l'essai.

Le type de cristaux utilisé limite la température d'environnement à 150 degrés centigrades.

Pour des températures supérieures, les recherches sont orientées vers l'utilisation de l'effet KERR, agissent sur la polarisation par sensibilité au champ électrique.

- Mesure de pression

Pour des environnements de -50 à +200 deg.C, différents principes de mesure sont proposés : variation de l'indice de réfraction avec la pression, variation de la différence de marche optique (interféromètre incluant un élément sensible à la pression).

Pour ces types de mesure, une seule fibre est utilisée pour véhiculer la lumière incidente et celle renvoyée par le capteur après transformation. L'élément de conversion de mesure peut être intégré au FADEC.

Des évaluations de ce type de chaîne de mesure sur moteur sont prévues dans le cadre de notre programme de recherche.

- Mesure de température

Pour des environnements de -50 deg.C à +200 deg.C, parmi les principes de mesures proposés, on peut citer la variation de caractéristique d'un matériau biréfringent ou variation de l'indice de réfraction en fonction de la température.

La chaîne de mesure est constituée du capteur, de la fibre et de l'élément sensible intégré au FADEC.

Pour des environnements au delà de 200 deg.C, on peut citer deux principes : la pyrométrie optique, la mesure de l'émission de micro corps noir inséré dans une gaine comme un thermocouple .

Pour ce type de mesures, un programme d'évaluation est également prévu.

A l'issue des différentes étapes de démonstration technologique, un bilan sera fait sur les avantages et les inconvénients liés à l'utilisation de la technologie optique.

S'il s'avère positif, la majorité des mesures sur turbomoteur pourraient être réalisées par des procédés optiques insensibles aux perturbations électromagnétiques, remplaçant une partie du faisceau électrique par des fibres optiques.

4-3 Logique floue

La particularité de la logique floue est de pouvoir encoder des raisonnements logiques exprimés en langage naturel en définissant des caractéristiques imprécises.

Par exemple : "si l'erreur est négative et que sa variation est importante, diminuer rapidement le débit carburant".

De l'évaluation des techniques de contrôle flou dans divers domaines, il ressort que :

- Ces techniques sont très intéressantes pour établir des lois de commande d'un système dont il est impossible d'obtenir facilement un modèle fiable mais dont le comportement peut bien être décrit en langage naturel par un expert.
- Ces techniques n'apportent en général rien par rapport aux techniques classiques pour établir des lois de commande sur un système dont le modèle est bien connu, et ne permettent pas la démonstration théorique du respect de marge de stabilité spécifiées.

Pour la régulation d'un turbomoteur, deux champs d'application peuvent être investigués.

Tout d'abord, le contrôle de démarrage, phase de fonctionnement du moteur dont il est très difficile d'extraire un modèle couvrant toutes les conditions.

Actuellement, les lois de démarrage sont adaptatives à la température ambiante, la pression ambiante, l'état

thermique du moteur. Pour couvrir tout le domaine du moteur, la logique d'adaptation peut être complexe et ne pas donner des qualités de démarrage uniformes.

Par contre, à partir de la connaissance de l'évolution des paramètres moteurs enregistrés lors d'essais au banc sol, au caisson climatique et en vol, on peut établir une logique exhaustive de pilotage de démarrage, décrite par des règles floues.

En ce qui concerne la régulation de vitesse rotor, en particulier le respect des marges de stabilité sur les modes propres en torsion de la chaîne cinématique de l'hélicoptère (arbres, rotors), un contrôleur conçu par application de la théorie des systèmes linéaires reste le plus efficace et permet la démonstration théorique des marges de stabilité.

Ce type de contrôleur classique est par contre pénalisant sur des transitions de régime stabilisé vers accélération ou décélération, en réponse à des variations de charge importantes.

La commande est calculée par la réponse naturelle des correcteurs jusqu'à des saturations variables par lesquelles sont limitées l'accélération et la décélération du générateur de gaz. La dynamique des correcteurs est limitée par les contraintes de marge de stabilité sur les modes du rotor, limitant ainsi les performances du contrôle de vitesse du rotor.

Il devient alors intéressant d'évaluer un contrôleur mixte flou-linéaire (*fig. 8*), ayant un comportement linéaire en régime stabilisé, évoluant vers un comportement non linéaire en réponse à un contrôleur flou en régime transitoire pour augmenter la dynamique de réponse.

La détection et le diagnostic de panne constituent un autre champ d'investigation des applications de la logique floue.

L'objectif est de diminuer les risques de fausse détection ou de non détection de panne en utilisant une logique plus robuste, pouvant encoder des tendances plutôt que des seuils de détection.

Des règles de décision, issues d'une spécification en langage formel pourront être codées et évaluées.

Un programme de maquettage et de démonstration de l'application des principes de la logique floue est réintégrée dans notre plan de recherche.

4-4 Modèle interne

La puissance des processeurs utilisés dans des applications embarquées augmentant rapidement, il sera dans l'avenir tout à fait possible de calculer simultanément en temps réel une commande de régulation et un modèle moteur.

Un moyen d'améliorer sensiblement les principes de

détection de panne de capteurs et d'actionneurs, est de pouvoir comparer des mesures de différentes grandeurs physiques, comparer commande et mesure.

Une logique de comparaison robuste dans tout le domaine de fonctionnement serait très difficile à réaliser et à tester.

Un modèle, même simplifié, couvrant tout le domaine de fonctionnement, permet de calculer la réponse à la commande appliquée au moteur réel sur les grandeurs physiques mesurées par le FADEC. L'étude des écarts calcul / mesure, de leur évolution, permet de mettre rapidement en évidence un défaut, une dérive importante d'une chaîne de mesure ou de commande.

Afin d'introduire plus de robustesse dans les règles de décision, celle-ci pourront être codées sur la base de règles floues (*fig. 9*).

On peut également envisager la mise à jour en temps réel d'un modèle de déviation de performances entre modèle moteur et moteur réel.

En cas de défaillance d'une chaîne de mesure, suivant sa criticité, sa valeur pourra être estimée à partir de la valeur donnée par le modèle moteur et corrigée par la déviation de performance mémorisée.

Une étude de faisabilité de principe détection de panne utilisant un modèle temps réel, intégrant une phase de démonstration sur moteur, est intégrée dans notre plan de recherche.

5 - Conclusion

L'application de la technologie FADEC aux turbomoteurs d'hélicoptères a permis des progrès importants sur la performance et l'utilisation de l'hélicoptère.

Pour généraliser cette technologie, des efforts restent à faire faisant appel à l'innovation sur les systèmes de régulation, visant particulièrement à améliorer le service offert en diminuant les coûts.

Ces actions de recherche contribuent à la démarche globale de réduction de coût d'acquisition et de coût d'utilisation de l'hélicoptère, nécessaire au redressement et au développement de son marché.

GLOSSAIRE

FADEC : Full authority Digital Engine Control

AEO: All engines Operative

OEI : One Engine Inoperative

N1 : Vitesse générateur de gaz

N2 : Vitesse turbine libre

T4 : Température interturbine

TAMB : Température ambiante

PAMB : Pression ambiante

EMI : Electro Magnetic Interference

"30 secondes" : Régime maximum d'urgence validé pour une utilisation pendant 30 secondes en OEI

"2 minutes" : Régime d'urgence validé pour une utilisation pendant 2 minutes en OEI

"OEI continu" : Régime validé pour une utilisation continue en OEI

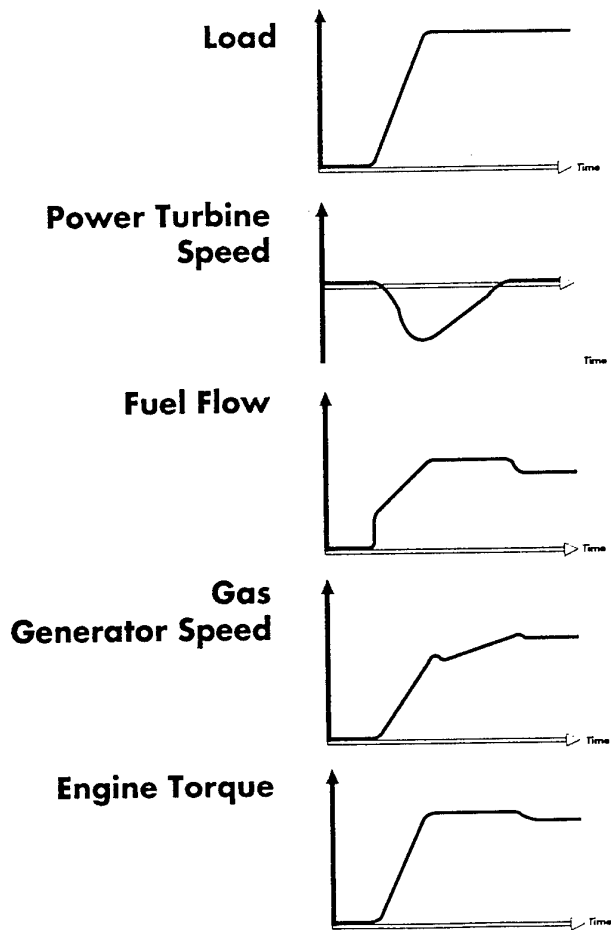


figure 3 : Mise de pas - limitation de surcouple transitoire

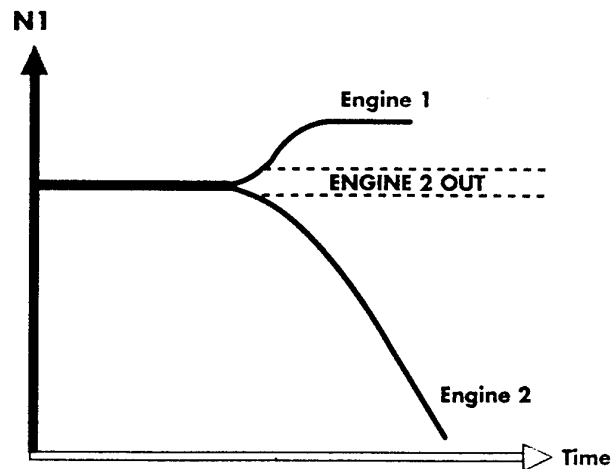


figure 4 : Détection de panne moteur

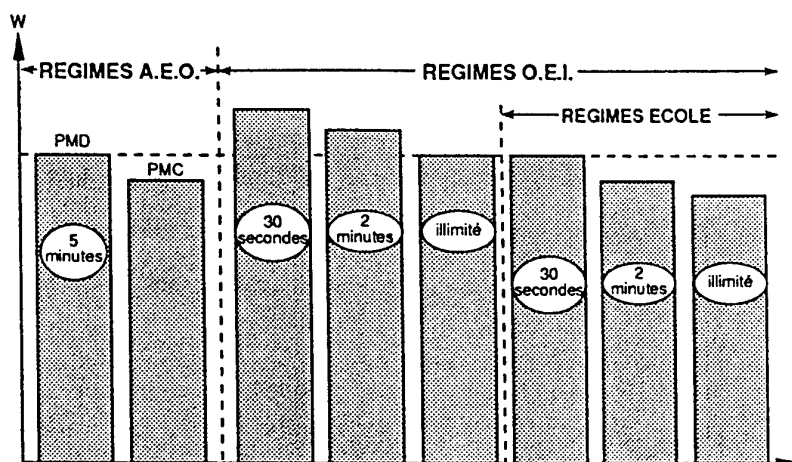


figure 5 : Structuration des limitations moteur

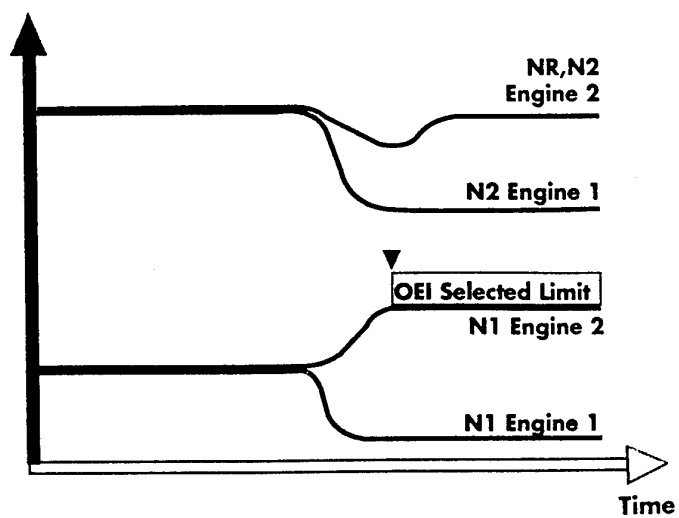


figure 6 : Entraînement à la panne moteur

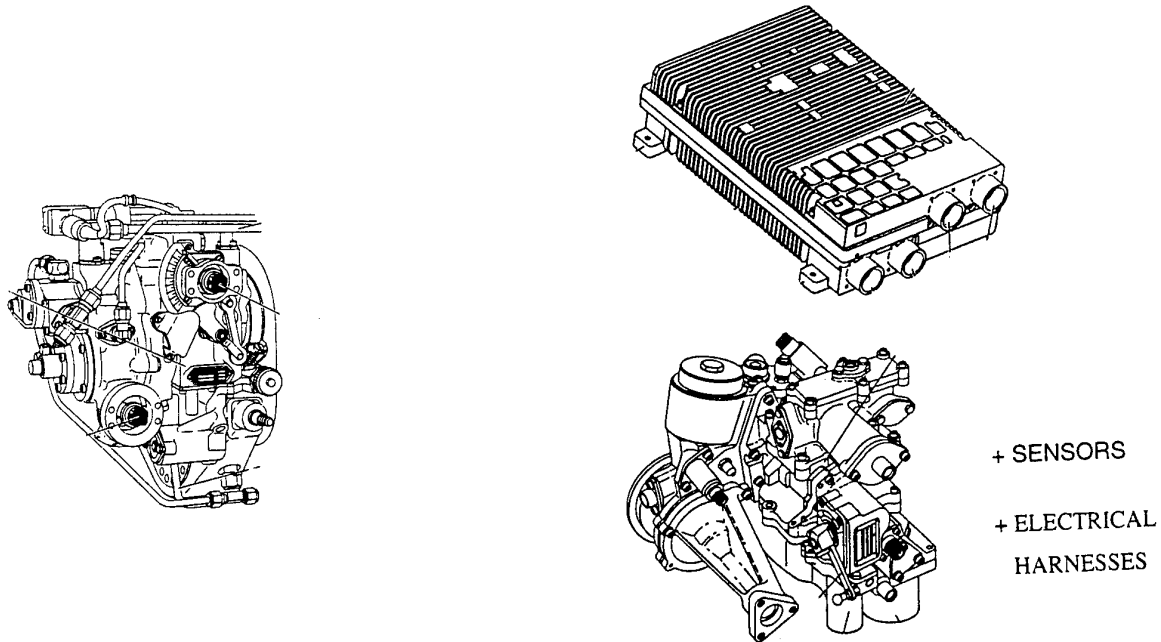


figure 7 : Système hydromécanique - Système FADEC

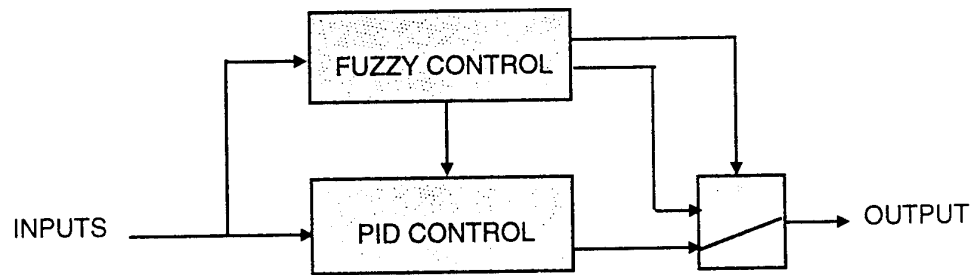


figure 8 : Structure de contrôleur mixte flou-linéaire

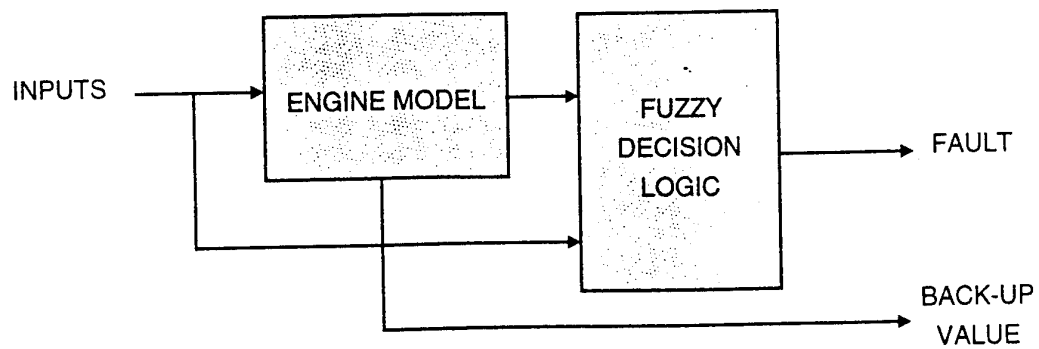


figure 9 : Modèle interne et détection de pannes

Paper 29: Discussion

Question from Dr W Merrill, NASA Lewis, USA

In the two engine/two FADEC architecture do the FADECs or the pilots have engine shut-down authority? What strategy is employed in the FADEC and what information is presented in the cockpit to prevent premature or incorrect engine shut-down?

Author's reply

The fuel shut-off valve is only actuated on a pilot cut-off demand, or as a result of power turbine overspeed detection (shaft failure case). The normal control system does not have authority over the fuel shut-off valve. Each FADEC is in charge of its own engine and has an engine-out discrete signal for the cockpit display (one display light per engine). The engine-out detection logic includes a discriminator between engine-out for its subject engine and high-side failure of the other engine.

Question from Ir P Hendrick, Royal Military Academy, Belgium

In the case of a failure of the shaft between the free power turbine and the main gearbox, how does the FADEC react? What happens to the gas generator spool speed after this reaction?

Author's reply

The overspeed detection system is an independent device from the normal control lane. When an overspeed is detected, the fuel shut-off valve is actuated in order to shut down the engine. For an engine qualified for blade off retention the overspeed detection device is optional. The choice of strategy, between engine shut-down and idle selection on overspeed, is dependent on the power turbine speed design choice and the amount of allowable overshoot.

CONTRIBUTION OF DYNAMIC ENGINE SIMULATION TO MILITARY TURBOFAN CONTROL SYSTEM DESIGN AND DEVELOPMENT

Laurent Pierre
Jean-Pierre Duponchel
Pierre Gérard

SNECMA Engineering Division
VILLAROCHE Site
77550 MOISSY CRAMAYEL FRANCE

SUMMARY

Transient performance and operational quality specifications applicable to modern military engines are getting increasingly important. In order to match such specifications, analysts in charge of transient behaviour extensively use dynamic models of the engine fitted with its control system.

This paper describes how dynamic simulations are analytically processed and highlights the role they play during performance of the main typical tasks based on concrete applications conducted during the development of the M88-2 engine and its control system.

This document is dedicated to the diverse tasks to be conducted as regards dynamic engine behaviour control and to be solved by using an analytical process that relies on dynamic simulations of the engine and its systems. The main features of the engine transient model, its real-time version and the identification tools that ensure evolution of the features are then presented.

Some applications of these contributing simulations cover for instance:

- the interpretation of tests: determination of in situ compressor surge line position, analysis of engine response during flight testing, etc.
- the design of control laws: effect of dynamics of a given element (T23) on the engine response, assessment of the response of the most critical engine.

Future prospects deal with improvements in engine handling and control monitoring likely to be brought about by incorporating a real-time engine model in the control software.

List of symbols

The symbols, notations and station identifications correspond to the SAE ARP 755A recommendations.

A8 Exhaust nozzle area
P2A Fan inlet total pressure

P23A	Fan discharge average total pressure
P23AQ2A	Fan total pressure ratio
P3Q25	HPC total pressure ratio
Ps 32	HPC discharge static pressure
P14	Fan discharge total pressure (by-pass flow)
P16	By-pass stream duct discharge total pressure
T2	Fan inlet total temperature
T23	Fan discharge total temperature (primary flow)
T31	HPC discharge total temperature
T14	Fan discharge total temperature (by-pass flow)
T41	HPT inlet total temperature
W2AR	Fan inlet total corrected flow
W23	Fan discharge flow (primary flow)
W25R	HPC inlet corrected flow
W13	Fan discharge flow (by-pass flow)
WF32	Fuel flow
XN2R	Fan corrected speed
XN25R	HPC corrected speed
Θ_{23}	$\frac{T_{23}}{288.15}$
WFQPR	$\frac{WF_{32}}{Ps_{32} \cdot \Theta_{23}^n}$ control parameter governing the acceleration rate of the engine
WFQP	$\frac{WF_{32}}{Ps_{32}}$
PRS	Fan or HPC surge margin, at constant corrected mass flow
TLA	Throttle lever angle
ECU	Engine Control Unit
HMU	Hydromechanical unit
IGV	Fan inlet guide vane
VSV	HPC variable stator vane

1. INTRODUCTION

The development of a propulsion system can be successful in terms of performance and operational qualities only if all the factors the system is due to be subjected to during operational use are identified early. Increasing requirements

as regards transient performance specifications and operational quality, call for the implementation of an elaborate engine/systems behaviour design and analysis process with the final goal of the specifications being complied with by the aero engine maker. The variety of aircraft missions and events to come, the integration of the propulsion system require that multiple simulation and analysis work dealing with engine transient behaviour be defined so as to ensure awareness at decision-making considering the various quality factors. Numerous cases of conflict in terms of engine characteristics emerge when designing and developing the engine. Each phase of development requires more and more detailed knowledge of engine operation as it gives ability to appreciate qualities and deficiencies of the engine and components and leads to pertinent modifications to reach the specified performance.

A detailed engine transient simulation, which approximates closely actual engine operation, is a must for successful logic development. The mathematical model that makes up the simulation code is recognized as the most valuable means of collecting information and an effective medium of communication, thus contributing highly to efficient development. Identification of in situ component performance, as well as overall engine performance and stability, can be derived from meticulous analysis of engine tests data. Development studies will be performed by model means, after updating each component submodel with the results of test analysis. These studies lead to clear evaluation of modifications under consideration to cure deficiencies. In many cases, simulation will give a good understanding of engine component interaction problems, particularly in flight. The aerothermodynamic calculation code is of a semi-analytic nature providing a flexible and dynamic tool, the contents of which reflect the best state of knowledge on engine components.

The simulation tool enables

- the designer, to define as accurately as possible in terms of costs the specifications applicable to engine and control components for given operational specifications
- the development analyst, to take advantage as much as possible of compressors margins (formulation of assumptions and checks thereof)

While the engine and its components are analysed and developed, progress is also going on for systems and particularly the control system. Choice of control parameters and definition of schedules have to be studied again, every time that a significant change has been recognized in the engine characteristics. Many control system functions are applicable to transient operations. So transient and dynamic simulation of the engine and its associated control system are of major interest. Flexibility of digital math models yields the opportunity to evaluate effects of possible components change on control schedule adaptability.

In that type of study, quality of control system modelling is of prime importance: careful integrated work with control designers is required to add the control system model to engine model programme. Control schedules have to be defined in order to optimize performance and particularly stability for the installed engine. Analysis of simulated

altitude and flight tests with the current control schedules permits to clearly establish the validity of the model before using it to optimize and re-define control schedules and system.

This paper describes a coherent engine and control system design/development process, incorporating up-to-date engine simulations, successfully used at Snecma for the M88-2 engine development.

2. ROLE AND INTEGRATION OF DYNAMIC MODELLING IN THE GLOBAL SIMULATION PROCESS

2.1 Computer-aided global simulation process

Engine properties in terms of steady state and transient performance and operational capabilities are the very expression of work made at the engineering functions of the aero engine manufacturer and, to a great extent, of the working methods used by teams in charge of developing the control system and evaluating engine aerothermodynamics. Efficiency of the control system design and development expressed in terms of costs, timescales and technical relevance implies controlling the diverse simulation and identification activities. This evolution has facilitated the development of computer-aided calculation codes. However these tools cannot be fully used unless specialists work in an integrated way so as to understand physical phenomena at the origin of a given engine behaviour as early as possible during the development programme (conventional process of understanding in order to act).

The objectives aimed at are mainly:

- to best pinpoint the need, in particular operational requirements. At the development stage of the individual specifications, the complete dynamic model of the specifications (engine components and control systems) must guarantee homogeneity of said specifications and highlight critical points very early.
- when the real characteristics of the components are identified and, as work progresses, the comparison specification model / identified model must allow to check that the operational requirements are still complied with. The simulation tool should contribute to define, if required, further flowpath development work that could prove necessary, and in particular in order to shorten testing time by reducing investigation time.

2.2 Simulation work

A consistent set of tools is then implemented in order to support the various steps of development of a propulsion system considered as a whole. Figure 1 presents the main lines of simulation and highlights the interaction between the individual tasks at the development steps of the programme. During the different steps of preliminary design, specifications, detail design, development and validation, simulation tools are used for organising tasks in order to meet specific needs of the development programme as a whole.

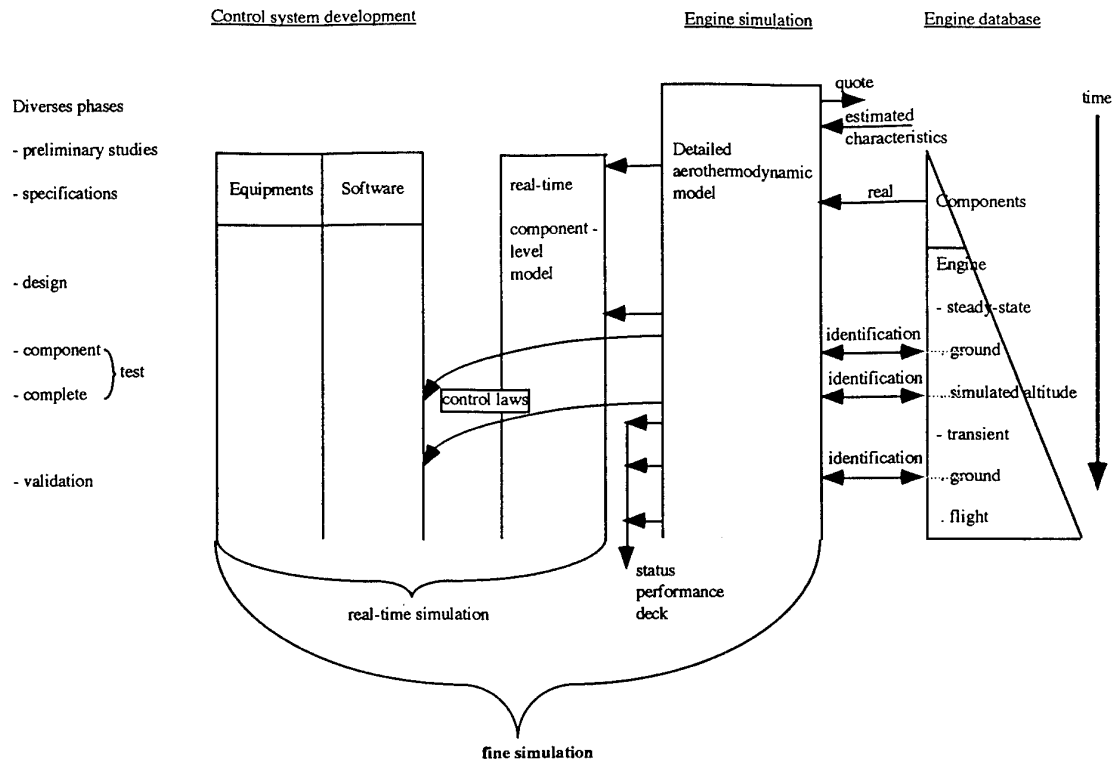


figure 1 - Global simulation process = engine and control system

As regards engine performance, the main steps are:

- definition of guaranteed performance level, referred to as Quote Deck.
- definition of detail specifications applicable to engine component characteristics (compressors, turbines, etc.).
- selection of expressions of engine command and control laws and taking into account of the operational requirements and programme constraints.
- definition of the real characteristics of engine components (location of deficiencies of certain components) based on steady state tests at ground and simulated flying test beds.
- working out of a component improvement approach and adjustment of engine control, best suited for complying with the Quote Deck.
- generation of the Status Engine Performance Deck indicating to the airframer the levels of performance as the programme proceeds.
- supply of diverse engine control laws at steady state and transient conditions, to be integrated in the airborne computer software (specification followed by enhanced versions).
- production of a real-time type engine model used for the definition and validation of equipment.
- connection of engine models with control models for achieving fine simulations of physical phenomena inherent to the processes, etc.

2.3 Simulation tools

Because of the scope of simulation, aspects of engine thermodynamic behaviour control are reviewed here in detail.

The global system is composed of

- specific modelling of the engine
- numerical solution methods
- databases entailing the measurements of testing and results of processing thereof.

2.3.1 Engine aerothermodynamic representation

As regards modelling the response of the basic engine, a detailed model of the non-linear aerothermodynamic representation of operation of the engine components is developed and used during every step of the development programme. It entails the compressors, combustion chamber and turbines characteristics maps as well as their respective secondary effects, i.e. IGV schedules (Fan) and stators (HPC), viscosity, bleeds, clearances, thermal growth, etc. and incorporates the diverse relationships enabling transient phases, i.e. rotors inertia moments, radial clearances, thermal fluxes, etc. to be processed.

This conventional method of modular representation of characteristics for various components calls for a great deal of data to be made available chiefly by aerodynamics functions (sometimes such data are not available at the

preliminary development step). Since knowledge related to assessed component real performance evolves during the development programme, the chief difficulty lies in managing all these data in such a way that, at every milestone, the status version of the engine model achieved is best describing the build-up of experience gained so far in terms of flow path quality characteristics.

Modular representation of the flow paths implies the coupling of the engine code with a numerical solution system of the equations system in order to accurately satisfy the diverse engine cycle compatibility equations (conservation equations) within the limits of convergence accuracy.

For the purpose of real-time engine simulation, another engine model with a simplified structure is implemented. This real-time non-linear model is based on simplified component representations, i.e. two bivariate representations are used for compressor, turbine and nozzle and a polynomial expression for the other modules. The aerothermodynamic relationships are based on constant gas properties and a correction is then made to the output values. Given the calculation time goal, this version entails no iterations for the mathematical solution (no influence coefficient matrix). The correction matrix of the NEWTON-RAPHSON method has been substituted by analytical expression in order to match mass-flow conservation (single pass per time step). This real-time engine model, based on simplified component representations, is designed in such a way that the code architecture permits dynamic/steady-state solution and easy adjustments/update (using the detailed aerodynamic model as a reference) as well.

Furthermore, any specific activity consists of developing fine modelling of the equipment which, once connected to the engine detailed code, yields a coupled model, i.e. the engine and its control. Such a fine model and the real-time version are used to evaluate FADEC hardware operability and performance requirements to allow early detection and correction of problems prior to actual engine test. Such studies simulate sensor and actuator transient responses and engine operability capabilities and provide evaluation of control schedules and logic. Engine Control System capability is analysed and demonstrated using the FADEC system including the HMU interfaced with the real time dynamic engine simulator.

2.3.2 Numerical methods and their applications

Figure 2 shows the numerical methods used for solving systems of equations developed and implemented at Snecma and likely to be connected to engine modelling as a function of the tasks. Some of these solving methods are detailed in reference [8].

It is to be noted that these solving methods are absolutely independent of the physical modelling available in the model; they are selected as a function of the problem to be solved, with their diversity enhancing the processing capabilities of the models.

For any calculation of engine cycle, the conservation equations must be accurately satisfied, hence the systematic use of method 1 (NEWTON-RAPHSON type method) for this sub-system of equations.

Resolution of a system of m equations and n unknowns

- | | |
|--------------------------|---------|
| (1) "square" system | $m = n$ |
| (2) "rectangular" system | $m > n$ |
| (3) Optimization method | $m < n$ |

optimization of a criterion to m-n degrees of freedom

(4) Simultaneous resolution of p systems, m equations and n global unknowns, nl local unknowns (multipoint method)

(5) Resolution of a system of differential equations (for transient calculation) calculation of local and global unknowns (integral criteria)

Figure 2 - Identification / optimization numerical methods

Further to aerodynamic and mechanical improvements in engine configuration, a significant share of work is devoted to determining components characteristics deviations by analysing steady-state tests on adjusted instrumentation engines (ground and simulated flight). Adjustments made to the model representation can be obtained by using a single-point (1) or (2) type method coupled with a regression method or a multipoint (4) type method applied to a set of p test points, each method having specific advantages.

However the multipoint (4) identification method allows faster solution of certain complex problems.

- Let us mention the engine thermodynamic design (at preliminary design step or at the stage of definition of specifications applicable to a new component) in order to match both
 - the Quote Deck for p flight conditions
 - a given know-how in the aerodynamic and mechanical fields.

The system of global unknowns is then constituted by the scalars that define the complete characteristics of compressor/turbine maps, the system of equations being made of inequalities that express all the requirements to be fulfilled.

- The adjustment of real-time model component characteristics to those of the detailed model is achieved by applying the multipoint method: the global unknowns are constituted by the scalars integrated in the real-time model component maps. The equations to satisfy concern the identity of the main engine state parameters as predicted by the two models for modes of operation covering the rotors unbalance range.

Working out certain laws used to control engine steady-state operation is facilitated by using the optimization method (3).

As regards the process of convergence, the guarantee of obtaining convergence and rapidity of the procedure is the main quality sought. To this purpose, the relevance of the initial values of the various guessed variables directly affects the efficiency with which the off-design cycle simulation computer programmes converge to a solution. To do so, the neuronal networks technique is successfully implemented for the preliminary estimation of the various guessed variables in the Snecma engine performance brochures.

2.4 Quality factors - Discussion

Suitability of these simulation methods (engine model and numerical tools) to the needs is a permanent concern. The main lessons learned allow several process quality factors to be expressed.

a) As regards the detailed engine model, desirably a unique structure must be sought,

- from Preliminary Design versions to final performance versions
- from Performance decks to the engine model used for engine tests analysis or for fine investigation into a given engine behaviour.

Only under such conditions, the different versions corresponding to the various levels of knowledge acquired on the components can be easily and readily introduced with minimum discontinuity in the Status Performance. As a result, capacities to improve the representation of physical phenomena are implemented at engine programme level thanks to the engine model ability to integrate new data supplied by aerothermodynamicists.

The main difficulty lies in defining the first version of the engine model at preliminary design step; at this level many data (for instance certain secondary effects of compressors/turbines) are missing. It is up to the engine maker to develop methods, even simplified ones, of representation of secondary effects that are general enough to be applied very early during the first modelling of the engine.

Another problem emerges as regards consistency of engine model versions concurrently used.

b) For the processing of component and core engine tests, some degree of consistency with the implemented methods should be sought, i.e. use of

- the same thermodynamic functions
- the same representation of the components at physical parameter level
- the same formulations and numerical methods (such as the multipoint method) for measurements processing.

c) In order to investigate into a given engine phenomenon more accurately a version particularly based on the knowledge of that behaviour can be worked out. In this case, the rectangular solution system 2 is the most suited one for determining the cycle for which the various experimental data best reconcile with the relationships drawn from former tests. It also allows to see where non-consistency of parameters occurs.

d) As regards build-up of experimentally acquired knowledge on the characteristics of a component, the use of statistical tools allows to quantify, at a given step during engine configuration, scalars dispersion on flow rate and efficiency. The standard deviation characterizing such a dispersion results from propagating uncertainties of the instrumentation implemented and from the quantity of test points and is necessary to assess the confidence level of parameters that quantify global engine performance.

e) The ability to rapidly deduce a real-time version from the detailed engine version then allows the Engine Control function to better define the various corrective networks as a function of the diverse engine characteristics (dispersion and component ageing, etc.).

f) The entire detailed model, i.e. engine and control system is a great help in the interpretation of flight tests since it allows to develop the engine transient handling laws (compared to the real-time model, the detailed model entails a finer representation of the various physical limitations, such as surge, blowout, etc.).

3. USE OF THE TRANSIENT MODEL IN THE M88-2 ENGINE DEVELOPMENT

3.1 Engine Operational Quality Qualification (French Bon de Vol)

Transient simulation methods are being extensively used as part of the preparation for Engine Operational Quality Qualification. Before presenting some applications, it is convenient to detail the main lines of this Qualification process.

As soon as the definition of the production engine standard is sealed, it must be sure that all the production engines will satisfy the operational quality requirements. The main risks covered by such engine quality requirements are:

HP/LP compressor surge

Unresponsive throttle/rollback

Combustion chamber blowout, fail start and relight,

Afterburner blowout, fail start

For any of these risks, faultless operation of all the production engines under the most critical individual conditions among the engine specifications is required. This result can only be achieved after a demonstration programme has been completed that includes engine bench testing and, in particular, flight testing on the combat aircraft the powerplant is destined for. In France, this programme is controlled by the Service Technique des Programmes Aéronautiques as a certifying organisation and conducted by the Centre d'Essais en Vol - CEV (Etablissement de la Direction des Constructions Aéronautiques DCAE). The efficiency in terms of costs and timescales of such a programme dedicated to preproduction verification is a constant preoccupation and is contingent upon highly integrated co-operation, at the preliminary steps, with the engine maker's engineering and flight test functions. Trials consist of completing a flight test campaign during which all the operational manoeuvres, in particular the most critical ones are completed versus a given hazard on engines deliberately selected in a setting condition so as to be representative of the most sensitive production engine. To do so, it is necessary

- to previously define dispersion of population by considering all the influencing parameters in terms of a given risk
- to previously classify a selection of engines by considering their respective limits; this step aims at sorting out the engine the most sensitive to a given hazard. The engine selected is then set so as to be representative of ultimate engine behaviour for a given hazard based on the dispersion characteristics detailed above.

Most of these risks emerge during engine transients. As an example, HP compressor stall is triggered during engine acceleration, LP compressor stall at afterburner ignition and combustor blowout during deceleration.

Transient simulation tools are used for each of the steps mentioned above. Dispersion of population versus a given hazard is obtained by calculating the contribution of each individual dispersion (turbines permeability, efficiency, acceleration schedules, fuel command quality, etc.) at transient, as global dispersion is obtained by square summation of each of the elementary dispersions. Such an approach has many advantages, in particular representativeness of simulation with regard to operational manoeuvres. It also makes it possible to directly assess the impact of parameters used in several engine control schedules. This applies to measuring T23 temperature whose dispersion affects both stators actuation and acceleration schedule control. However, after developing dynamic simulation tools, it was first used for restoring HP and LP compressors surge limits with a view to classifying the sample of engines retained for qualification.

3.2 Restoring non-measurable parameters: determination of engine surge line

3.2.1 General discussion

The development of an efficient and stable propulsion system relies on early recognition of all destabilizing influences to which the complete system will be subjected in real operation. Our experience shows that compressor component testing is only an initial step in development for surge evaluation and is incomplete to properly evaluate the adequacy of the compression system. Snecma corporate culture lays great emphasis on engine surge line determination in order to incorporate the important transient behaviour of the compression system in a realistic manner. Such an approach is possible provided the accuracy of obtained parameters and the limitations are acceptable at implementation. Such a technique implies the use of highly responsive instrumentation and the development of processing methods applicable to compressor operating point excursions during engine transients. The main representations of these transients are:

- representation directly using the measured parameters
- representation in the intrinsic coordinates system of compressor global characteristics

Compressor map	Measurable parameters	Intrinsic parameters
LP	A8 XN2R	P23A/P2A W2AR
HP	WFQPR XN25R	P3Q25 W25R

For the M88-2 engine, classification from parameters intrinsic to the compressors (pressure ratio, corrected flow rates) has been opted for. The thermodynamic calculation code (whose entries are the measured parameters including compensation for the bias inherent to the response of the whole measurement line) then allows to access to the

indirect parameters of the engine condition (here compressors corrected flow).

Thus, as an example, classification in terms of WFQPR depends on the dynamic response of the T23 temperature probe that acts in the reduction of this parameter and introduces a bias without any relation with the objective of classification of surge limits.

The first application of these tools is devoted to the restoration of these limits by calculating the operating points in the compressors maps from the measurements made on the engine.

3.2.2 Experimental procedure: testing and instrumentation

Testing proposed to provoke HP and LP compressor stall is representative of the operational manoeuvres likely to lead to such malfunctions. Hence, HP compressor stall occurs during acceleration, the test relies on a fuel step, with the nozzle remaining unchanged (Figure 3).

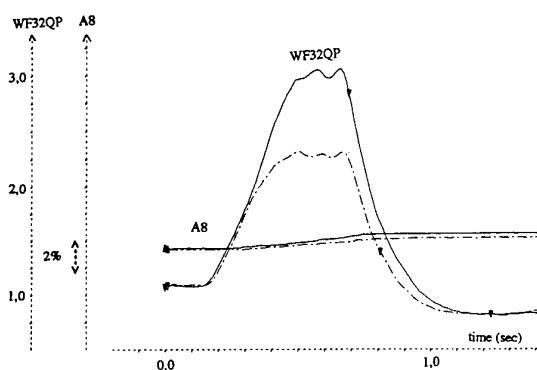


fig 3 H.P. transient : fuel step

Generally LP compressor stall is caused by thermal obstruction resulting from afterburner ignition; during the test, surge is provoked by obstruction, i.e. by closing the nozzle (extension tabs are used to further decrease the minimum exhaust area) and maintaining the acceleration schedule WFQPR (Figure 4). Keeping the acceleration schedule steady enables the LP compressor surge line to be determined in the high ratings zone while generating turbine temperatures acceptable for the engine.

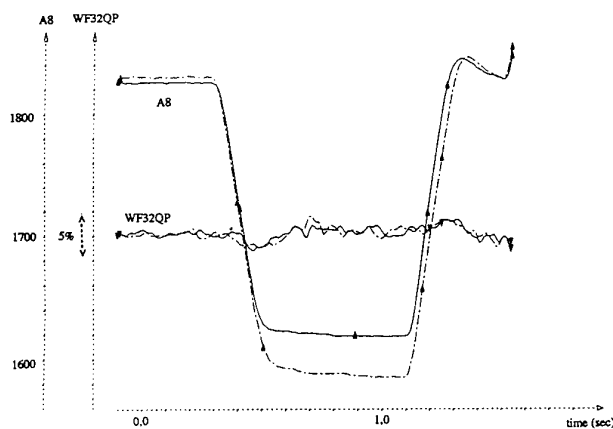


fig 4 L.P. transient : Exit nozzle closing

Instrumentation required for calculating the operating points in the compressors maps is identical to that used to identify steady-state performance data. On transient data processing and storage capacities grounds, only the individual measurements the most representative of averages per performance station are acquired. Furthermore, these individual measurements are used by the transient model and reset to the average values per performance station at static running conditions from steady state test results over a large engine operating envelope.

For these data, acquisition frequency is dictated by two constraints:

- Manoeuvre brevity (less than 1 sec.)
- Compensation for probe delay in time constants close to 0.5 sec.

All these constraints led us to use a 100Hz frequency.

3.2.3 Surge detection and limit plotting

From the measurement of the parameters defined above, the following parameters are calculated:

- primary air flow rate by solving continuity in the choked HP turbine nozzle (flow function assumed):
 $W23 = f(P31, T31, WF32)$
- by-pass air flow rate based on calibration of the secondary flow duct characteristic:
 $W13 = f(P16, P14, T14)$

Inlet air flow rate of the LP compressor is obtained by summing the two calculated air flow rates.

The correction parameters ($P2A$, $P23A$ pressure data, $T2A$, $T23$ temperature data) and pressure ratios ($P3/P25$, $P23A/P2A$) are directly calculated. For each transient manoeuvre, the following can be determined at any moment:

for the HP compressor: $W25R$ (time)
 $P3Q25$ (time)

for the LP compressor: $W2AR$ (time)
 $P23AQ2A$ (time)

The trajectories obtained during manoeuvres are:
 for the LP compressor (Figure 5)

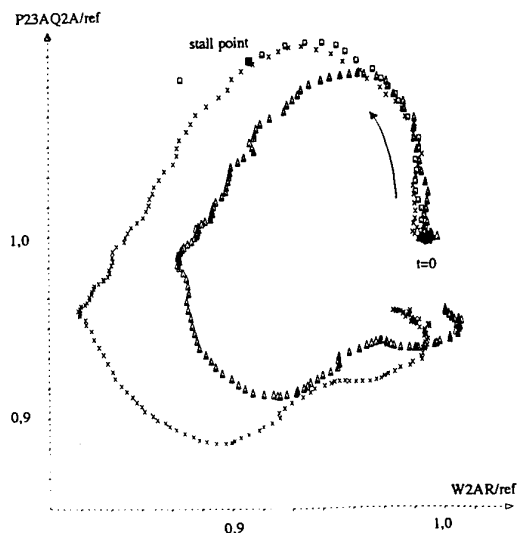


fig 5 L.P. transient : compressor map trajectories

for the HP compressor (Figure 6)

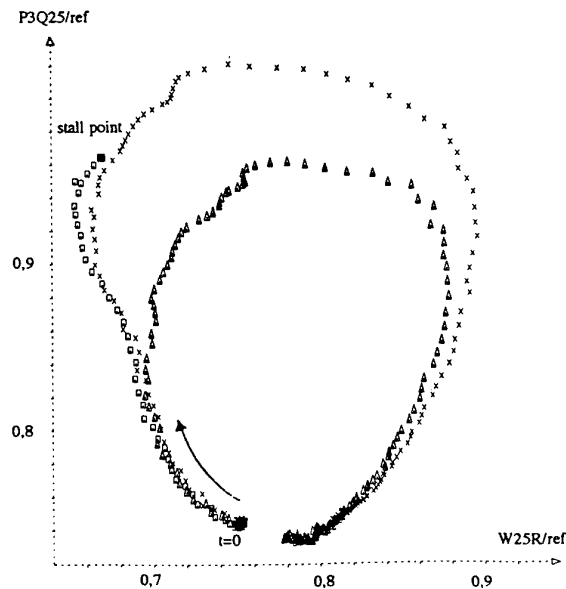


fig 6 H.P. transient : compressor map trajectories

When surge is provoked by a manoeuvre, detection is completed from a criterion on the evolution of the norm of the relative displacement vector.

The maximum value of the chosen parameter is determined during stall free tests and is the criterion beyond which the point dated at $t + dt$ (C) is deemed as being in the surge zone whereas the point dated at t (A) still is in the sound zone. The location of surge point (B) is then obtained from the last sound point (A) by interpolating the trajectory until $t + \frac{dt}{2}$ (Figure 7).

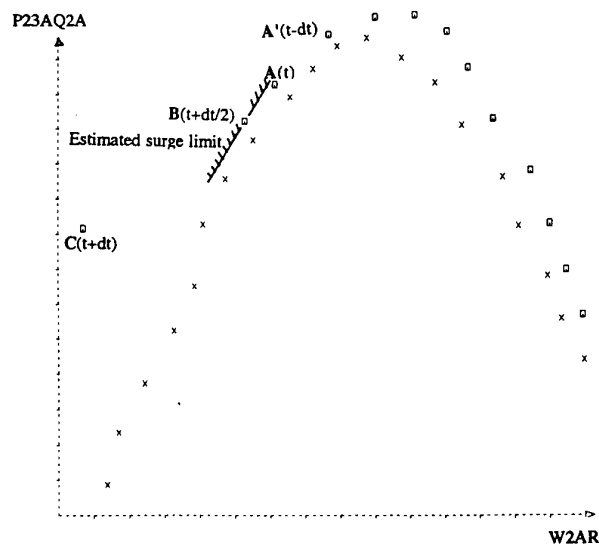


fig 7 Location of stall point

3.2.4 Application

Determination of the HP compressor surge line for two engines of dissimilar quality (engines pertinently choosed among a limited sample, in such a way that their compressor characteristics differ significantly) and comparison with the results from flight tests by classification performed by means of measurable parameters (Figure 8).

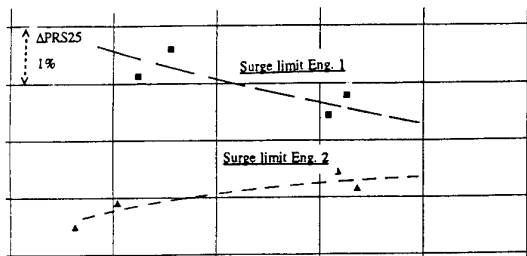


fig 8 Comparison of surge line between 2 engines

Parameter PRS25 describes the stall margin versus a reference line corresponding to the one deduced from component test rig.

$$PRS25 = 1 - (P3/P25_{current}) / (P3/P25_{ref})$$

The result shows the deviation of margin for the two engines is about 2% and it is detrimental to engine N°2. This result should be compared to observations made from flight testing of the same two engines that show a controllable acceleration schedule deviation of 8% which is equivalent to a difference of 2.3% of margin of the HP compressor considering influence factors. This verifies the level reported at ground.

Other elements strengthen the credibility of the result set up using the transient method.

The application of a correction allowing for variable stators offset during the transient manoeuvre brings back the stall limit noted on the engine near the stall limit recorded at the component test rig.

The first use of these transient tools thus enabled the selected engines to be classified versus the HP and LP stall risks.

3.3 Identification at transient

3.3.1 Calculation method

Now the model is used in order to determine some component characteristics best suited to engine transient measurements. In the proposed example, the guessed parameter is the afterburner efficiency and the identified measurement is engine thrust. In addition to the measurements mentioned above, the model also integrates afterburner flow rate, nozzle and thrust measurements.

3.3.2 Modelling and results

This study reveals that, upon ignition, the establishment of afterburner efficiency resembles a transfer function of the first order function applied to a step whose initial value is nil and whose final value is the steady-state point value (Fig. 9).

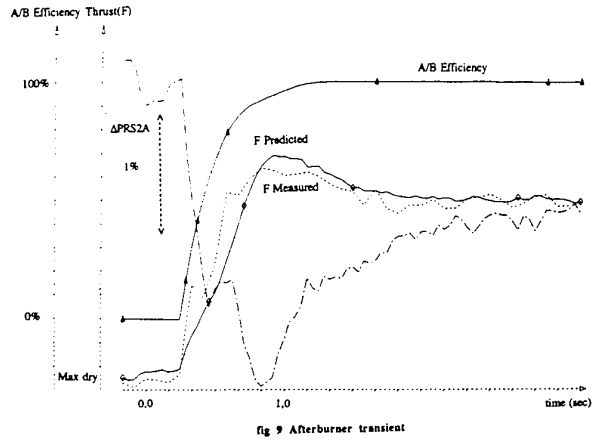


fig 9 Afterburner transient

This modelling enables in particular LP compressor surge margin upon afterburner ignition to evolve and it is used to calculate the influence of an engine parameter on the stall margin consumption.

3.4 Analysis using simulation

The examples given so far illustrate the contribution of the dynamic simulation model to the analysis and identification of characteristics of components involved in engine transient operation. As a result the establishment of afterburner efficiency is a transient phenomenon the knowledge of which allows the afterburner ignition control laws to be best defined. Functional interpretation of transient testing is another particularly prolific field of investigation which can be accessed by using a dynamic simulation model. The required model should be as exhaustive as possible and include, in addition to the thermodynamic model, a software (generator of schedules, correction networks, etc.) and control hardware (sensors, hydromechanical units, etc.) model as well as simulate the thermal phenomena inherent to the engine (heat fluxes, clearances, etc.).

The example presented herein deals with the interpretation of HP compressor operation from a snap acceleration to a bode transient. Such an analysis reveals a deviation of the surge margin between the two manoeuvres due thermal status differential and calls for the working out of an engine control strategy that differentiates the two manoeuvres.

3.4.1 Flight test analysis

The tests show that the maximum acceleration schedule that can be controlled during a bode transient can be significantly lower than that obtained upon a snap acceleration completed in the same flight conditions.

Acceleration schedule control entails a measurement of the HP compressor inlet temperature (T23) which lags behind the thermodynamic reality. The transfer function of the delay can be expressed as a first order. The delay results in:

- Overestimation of fuel flow rate needed during a bode transient, compared to a snap acceleration, resulting from the acceleration schedule expression:

$$WF32 = PS32x(WFQPR_{corrected})x(T23/288)^{EXPT41}$$

- Underestimation of the HP corrected RPM during a bode transient:

$$XN25R = XN25/(T23/288)^{0.5}$$

Overestimation of fuel flow rate is detrimental whereas underestimation of the corrected speed and resulting relative positioning of the stators are rather favourable.

Such deviations in operation have been corrected by introducing an analytical T23 that improves evaluation of the HP compressor inlet temperature. This analytical T23 is established from the LP compressor map parameters as P23AQ2A and XN2R, then reset to the control probe measurement.

3.4.2 Simulation and interpretation

Simulation completed from snap acceleration and bode transient tests with and without analytical T23 shows that T23 delay-induced effects are actually attenuated. On the other hand, the tests show that the extent of stall margin loss for bode transient is slightly the same. The acceleration schedule control has thus been devised to be able to differentiate bode transient from snap acceleration.

3.5 Control laws definition

Upstream of the test analysis step, such a dynamic tool can be used for defining engine transient operation control laws. In the example proposed below, the contribution of the dynamic model to the definition of the various acceleration schedule elements is detailed.

3.5.1 Definition of reference acceleration schedule

The expression retained for the generator acceleration schedule was elaborated in such a way that it should provide a bi-univocal correspondence, at a given XN25R corrected speed, between a level of the acceleration schedule and an operating point in the compressor characteristics map (for a given VSV schedule), whatever the value of temperature T23 at the compressor inlet. For this purpose, it was necessary to introduce a variable exponent that is a function of the estimated temperature T41, at the inlet of the HP turbine rotor, to take into account the dissociation effects occurring at high temperature levels.

$$\begin{aligned} P3Q25 &\Leftrightarrow WF32/PS32 \cdot (T23/288)^{\text{expt}41} \\ W25R &XN25R \end{aligned}$$

Furthermore, in order to optimize the schedule characteristics and the engine acceleration time as a result, correction terms that allow for the flight conditions are applied to a basic schedule.

These correction terms allow the acceleration schedule to be modulated as a function of viscosity (as measured at the HP compressor inlet), bleedings, distortion and heat conditions (Figure 10).

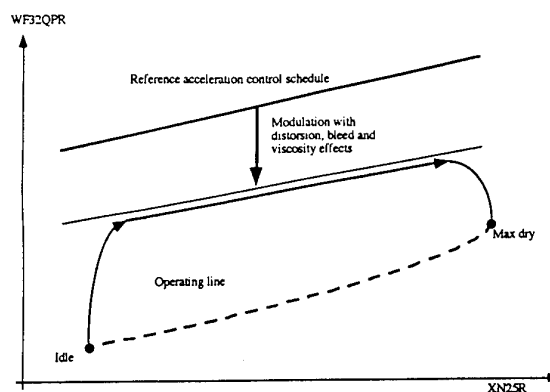


fig n° 10 Adaptive acceleration control schedule

The reference acceleration schedule is designed so as to protect the HP compressor against stall whenever the correction parameters are ineffective.

The surge tests carried out at the ground test bed are herein of particular interest as they match these conditions. The definition of the reference acceleration schedule is thus completed from surge tests effected at ground (Figure 11).

In this respect surge tests completed at the ground test bed are particularly interesting since they match these requirements. The design of the basic schedule is thus carried out from these tests.

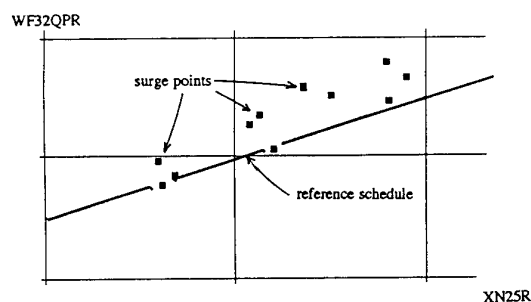


fig 11 Definition of reference acceleration schedule

3.5.2 Logic of protection against heat effects

The tests show that bode transients must be subject to special processing in the adaptive acceleration schedule. The logic implemented consists of temporarily reducing the acceleration schedule when a deceleration rate sufficient to modify the engine heat conditions is detected by engine control.

The transient simulation model is used herein to adjust the reduction value in the acceleration schedule which is required to protect the engine during mode transients (Figure 12).

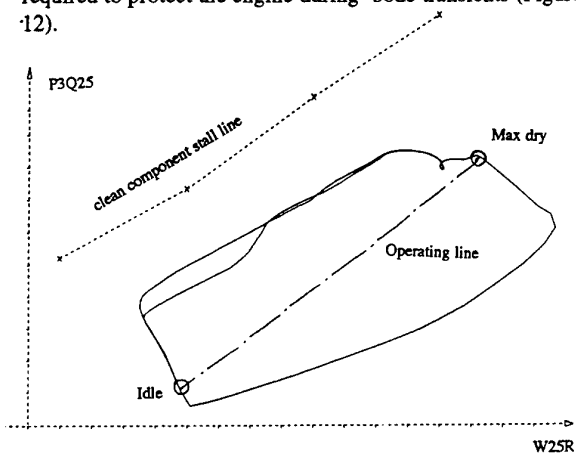


fig 12 Snap acceleration/mode transient : HPC paths

3.5.3 Adjustment of control laws

Adjusting the acceleration schedule that produces the best trade-off between stall margin and engine acceleration capabilities requires multiple iterations. During the iterations exchanges between tests results and model, simulations represent the convergent loop that allows such control laws to be defined under the best possible conditions. The example provided herein is the re-adjustment of the basic schedule for high RPM range that are too much sensitive to compressor stall. Two solutions are contemplated to improve this situation (Figure 13).

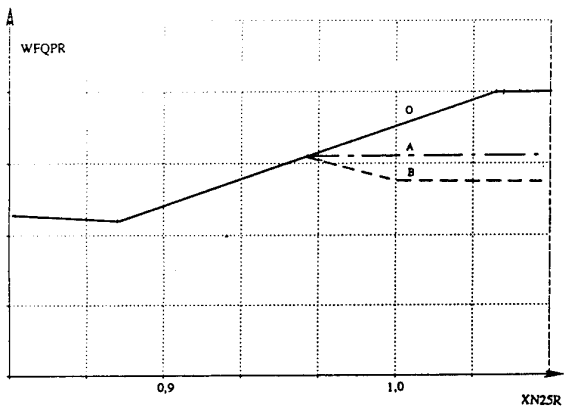


fig 13 Reference acceleration schedules

The results obtained by a model that simulates either of these solutions show that, for a given point in the flight envelope, solution A allows to control an acceleration schedule which shows an HP compressor margin (PRS25) which is by 1 % more protective compared to the referenced schedule (0) and that solution B extends this margin by an additional 2 %. (Figure 14).

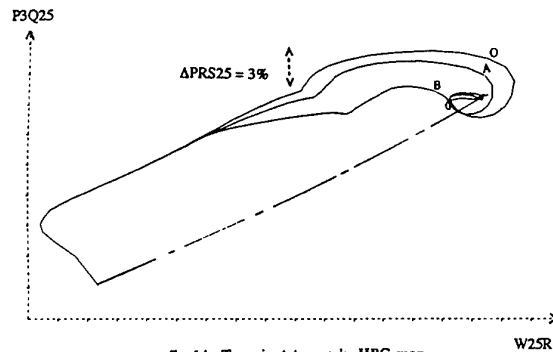


fig 14 Transient traces in HPC map

On the other hand, at ground static, acceleration time defined at 95% of the final thrust is slightly increased (Figure 15).

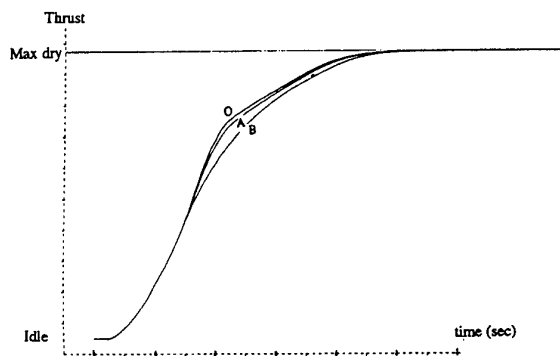


fig 15 Snap acceleration for 3 different accel. schedules - Thrust response

4. CONCLUSION

The design and development process of a propulsion system is strongly influenced by the quality of modelling and interpretation of the existing complex phenomena involved as regards engine components and control systems.

The analytical simulation tools described in this paper proved to be a valuable help in the M88-2 engine development. Most significant conclusions are:

- Comprehensive dynamic simulation tools enable the designer to define engine components and control systems specifications (in terms of costs and risks) best matching the operational specifications.
- Flexibility of the analytical process proves to be an essential feature in the main phases of production of simulation models applied to development aspects; by facilitating analysis, this integral approach (aerothermodynamicist, control designer, performance and system analyst) improves decision-making.
- Determination of in situ LP/HP compressor surge line position has been successfully implemented in the actual engine, using specific acquisition and processing systems associated with the dynamic engine model.
- Using control commands as input data of dynamic engine model permits to identify and analyse some specific engine response.
- Engine control schedules can be analytically reviewed in order to highlight the propagation of each individual feature as regards the engine response and to draw undesirable interactions. Such a simulation process is the mental support required for working out a set of control laws directed to engine transient handling intensification (concurrent fuel, nozzle and stators transient commands; AB light-on aided by controlled gas generator transient, etc.).

The integration of non linear component level engine model in the in-board engine control software will enable further strides in the field of relevance of commands, failure and abnormal events detection, engine condition monitoring, etc. Other effects from progress made in the engine modelling process can be expected on engine control quality versus components dispersion, engine behaviour either at steady-state (thrust control) or transient conditions (aircraft/engine transfer function improvement by close coordination with aircraft system).

REFERENCES

- [1] I.P.A. Monlibert "Les essais en vol d'avions de combat - Méthodes de validation employées par le CEV"
AGARD CP 293 October 1980
- [2] K. Kovach and P.R.Griffiths
"Engine compression system surge line evaluation techniques"
Third International Symposium on Airbreathing Engines Munich March 1976
- [3] S.J. Khalid
"Role of dynamic simulation in fighter engine design and development"
Journal of Propulsion and Power Vol. 8 - Num. 1.
January 1992.
- [4] G.T. Patterson
"Techniques for determining engine stall recovery characteristics" AGARD N° 324 Engine handling
October 1982
- [5] Aviation Week & Space Technology - 12 June 1995 -
Series of articles devoted to aircraft test programmes
- [6] "Guide to the measurement of transient performance of aircraft engines and components" AGARD WG 23
- [7] W. Merrill, B. Lehtinen and J. Zeller "The role of modern control theory in the design of controls for aircraft turbine engine" Journal of guidance, control and dynamics - December 1984.
- [8] J. P. Duponchel, J. Loisy, R. Carrillo
"Steady and transient performance calculation method for prediction, analysis and identification"
AGARD LS 183 May 1992

NEURAL ADAPTIVE CONTROL OF AN ENGINE EXHAUST NOZZLE

Alain GARASSINO
Control and Accessories Division
SNECMA
MELUN-VILLAROCHE
77550 MOISSY-CRAMAYEL
FRANCE

ABSTRACT :

This work deals with the application of neural techniques to control a turbofan engine exhaust nozzle area. The process exhibits strong non-linearities and thus it is difficult to control with classical methods. Neural Networks are used with an approach inspired by indirect adaptive control. The neural controller consists of two neural networks which communicate with each other. One achieves the identification task while the other controls the nozzle area. The simulation results of the process with neural controller are given and compared with the current results. The neural controller is better than the classical one and leads to a significant improvement of engine performance. Furthermore the method can be used easily to control any non-linear dynamic system. This work is a collaboration between Snecma/CEA/IUT Evry supported by the French Research Department.

1 - INTRODUCTION :

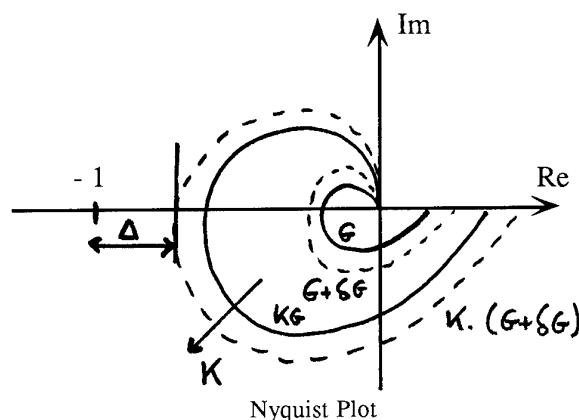
The theory of control provides tools perfectly suited for analysing and synthesizing linear systems. However the treatment of non linear processes still involves theoretical and practical difficulties. It has been shown by Hornik, Stinchcombe and White that a multilayered neural network with one hidden layer can approximate any continuous function. So, neural networks are candidates for identification and control for non linear systems. A particular interesting structure for a neural controller is based on the principle of indirect adaptive control. Therefore the main interests and theoretical point of view are discussed in part 2, then the control of a turbofan nozzle engine using neural networks is described in part 3. The results are shown and discussed in part 4.

2 - NEURAL ARCHITECTURE FOR CONTROL :

2.1 - Adaptive Control :

Compromise Performance/Stability :

It is well known that the greater the open loop gain of a system is, the better the closed loop performances are. Yet the greater the open loop gain is, the less the gain margin of the system is :

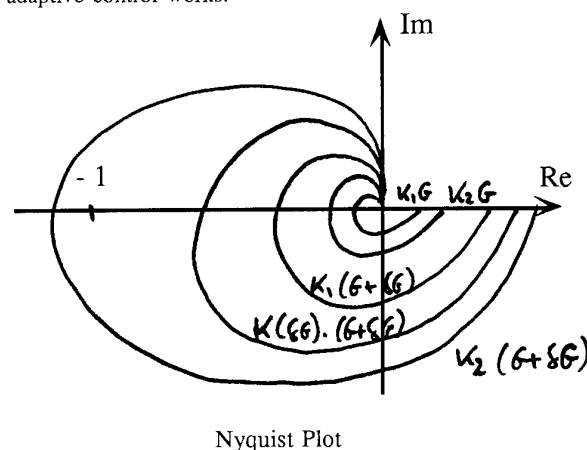


where K is the controller gain,
 G is the transfert function of the plant

Therefore, the choice of the open loop gain is the result of a dilemma :
- either K is small and the gain margin is good but the performance poor,
- or the performance is improved by the choice of a greater gain but the gain margin is small. Then the system may become unstable with disturbances.

Principle of the Adaptive Control :

In order to escape from this dilemma, it is possible to adapt the gain K according to the system evolutions : it is as the adaptive control works.



- the gain K_1 does not lead to good performance but the system remains stable when it changes
- the gain K_2 leads to good performance but the system can become instable,
- the gain K , by following the evolution of the system, allows stability with the best performances.

Indirect Adaptive Control Architecture :

To adapt the gain according to the evolution of the system means :

- to identify the system
- to have an algorithm to calculate the parameters of the controller leading to the best performance.

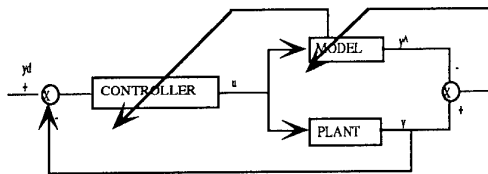
Identification Strategy :

- choice of a system model a priori
- adaptation of the parameters of this model in order to reproduce the plant output in the best way .

Control strategy :

- choice of a controller structure also a priori
- adaptation of the parameters of this controller in order that the system output is nearest to the desired output .

Thus, a possible architecture is what we call indirect adaptive control architecture :



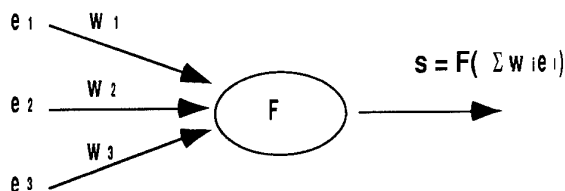
Most of the time, the model and controller structures are linear.

But physical is often non-linear. Therefore, it is interesting to use non-linear structures for both model and controller.

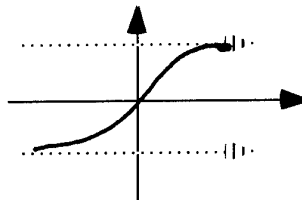
2.2 - Neurons and Neural Networks :

The Neuron :

The neuron is a cell in which the output is the evaluation of a transfert function for a sum of weighted inputs.

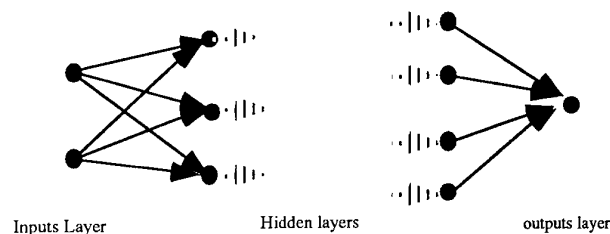


where e_i is the i th input, W_i the weighting factor of this input, called the synaptic weight, and F a transfert function which may be non-linear as a sigmoid :



The Neural network :

It is the connexion of several neurons :

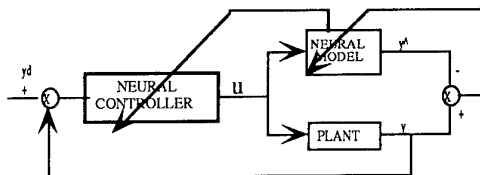


Some remarks :

- Any function can be represented by a neural network with one hidden layer.
- There is no method which allows us to design this network or to know its structure.

2.3 - Neural Control Architecture :

The architecture used is an Indirect Adaptive Control Architecture in which the model and the controller are neural networks.



For the identification task, the parameters of the model (the synaptic weights of the model network) are adapted by the backpropagation algorithm.

A feature of the backpropagation algorithm is that the control output error can be deduced. That is, the difference between the real and the optimal control outputs can be deduced from the backpropagation algorithm

Then, the parameters of the controller (synaptic weights of the controller network) are modified by the backpropagation algorithm in the way to obtain this optimal control output

2.4 - Backpropagation Algorithm Application :

This algorithm is based on the gradient method, the synaptic weights are calculated as the following way :

$$\Delta W(T) = -\eta \frac{\partial C}{\partial W} + \beta \Delta W(T-1)$$

where C is a cost function to minimize.

The term in $\Delta W(T-1)$ is introduced in order to improve the algorithm convergence.

Therefore, two parameters allow to manage the adaptation of a neural network, what it is called the learning:

η , the learning rate

β , the momentum

The synaptic weights computation is done from back to front, which is why the algorithm is called "backpropagation".

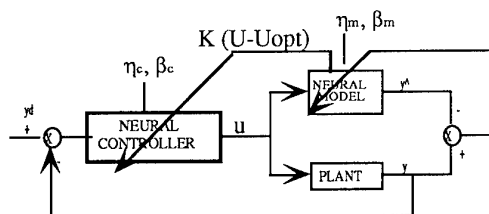
For the model, the synaptic weights are calculated in order to minimize the difference between the plant output and the model output for the same inputs.

The backpropagation on the neural model of the difference between the desired output and the plant output allows the deduction of the difference between the optimal control output and the real one.

Then the synaptic weights of the controller are calculated in order to minimize that difference between the real and optimal control outputs, this difference is multiplied by a gain factor.

In conclusion, five control parameters are used to optimize the system :

- the learning rate and the momentum for the neural model,
- the learning rate and the momentum for the neural controller,
- the gain factor

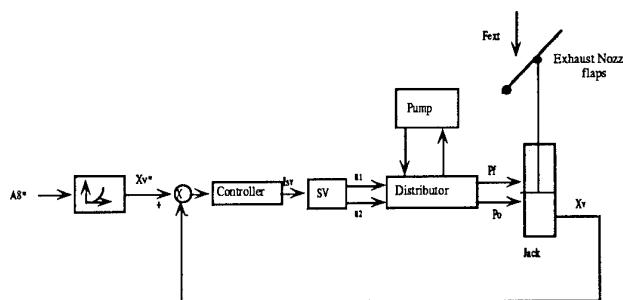


3 - TURBOFAN NOZZLE CONTROL APPLICATION :

The turbofan nozzle was chosen because it is a non-linear plant with strong disturbances, difficult to control.

3.1 - The plant :

It is the hydromechanical unit of the M88-2 engine exhaust nozzle :



- with
- $A8^*$ the desired exhaust nozzle area
 - Xv^* the desired jack position
 - I_{sv} the control output which is the servo-valve current
 - SV servo-valve
 - $u1, u2$ control pressures
 - F_{ext} external aerodynamic forces

The jack is actuated by two pressures P_f and P_o . These pressures are issued from a distributor, actuated by two modulated pressures $u1$ and $u2$. The pressure $u1$ and $u2$ are function of the current of the servo-valve, I_{sv} . The controller works I_{sv} out in order to minimize the error between Xv^* , the demanded jack position, and Xv , the sensed jack position.

The nozzle area can be deduced from the jack position by a cinematic law.

This system is of course non-linear, because :

- the external aerodynamic forces depends on flight envelop,
- the relation between the servo-valve current I_{sv} and the modulated pressures $u1$ and $u2$ changes according to the engine HP rotor speed.
- there are frictions, hysteresis,...

3.2 - The Neural Model :

The selected structure for the neural model is the following :

- an input layer with 7 neurons : the last four actuators positions and the last three control outputs.
- a hidden layer with 7 neurons,
- an output layer with one neuron which is the estimated nozzle actuator position.

Several structures were tested. The method to select the best one consists in simulating several transients and choosing the structure which minimizes the cumulative error between the plant output and the model output.

It must be noted that a big model, that means with a lot of neurons and layers, does not automatically imply good results.

The performance of the neural network depends of course on its size. There is an optimal size, which is unknown, and adding neurons or layers at these structure reduce performance.

3.3 - The Neural Controller :

The selected structure for the neural controller is the following :

- an input layer with 9 neurons : the four last actuator positions, the four last position errors and the last control output.
- two hidden layers with 7 and 4 neurons,

- an output layer with one neuron which is the control output.
The structure of the neural controller can be deduced, more or less, from the structure of the neural model.

4 - RESULTS :

The figures 1a and 1b show the actuator position compared with the desired one during a transient from the flight idle to the full power. Results using both the neural controller and the classical one are given.

The figure 2a and 2b show, in the same way, the results obtained during transient from full power to flight idle and figure 3a and 3b during random transient.

It appears that the neural controller has better performance than the classical one.

In addition, different value for the external aerodynamic forces were tested and the neural controller was found to be more robust than the classical one.

5 - CONCLUSION :

. About the neural model :

The neural model has very good performance: the difference between the output model and the output plant becomes quickly very small.

These results are obtained without any difficulty in finding the good values of the tuning parameters.

. About the neural controller :

The tuning parameters of the neural controller are more difficult to adapt. This difficulty is due to the fact that it is hard to understand the physical meaning of these parameters.

. About a real implementation :

The neural networks need a great amount of computation, which can lead to some difficulties for a real time application.

However, the neural controller has better performance and is more robust than a classical one. The studied architecture may fit any dynamic and non-linear system.

Due to the very good neural model performances and its simple structure, the use of neural networks would also involve significant improvements for failure detection methods.

REFERENCES :

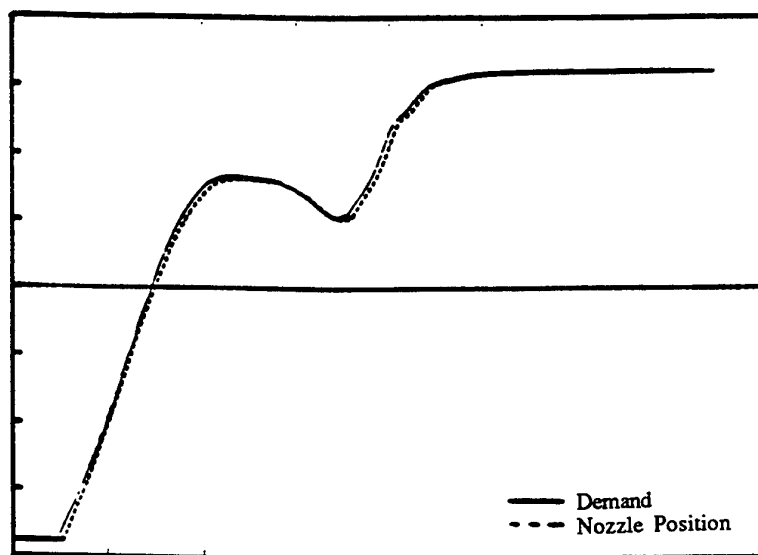
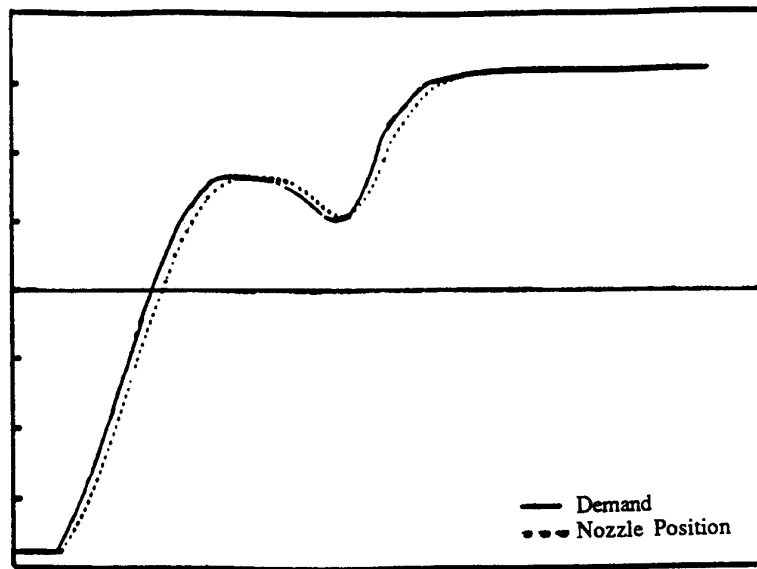
K.M. Hornik, M. Stinchcombe, H. White, "Multi-Layer Feedforward Networks are Universal Approximators", UCSD Department of Economics Discussion Paper, June 1988.

K.S. Narendra, K. Parthasarathy, "Identification and Control of Dynamical Systems Using Neural Network", IEEE Trans. On Neural Networks, Vol. 1, No. 1, March 1990.

D.E. Rumelhart, G.E. Hinton, R.J. Williams, Neurocomputing, Foundations of Research, Edited by J.A. Anderson and E. Rosenfeld, The MIT Press, Cambridge, Massachusetts, London, England.

Y. Lecun, "A Theoretical Framework For Back-Propagation", Connectionist Models, Summer School, Morgan Kaufmann Publishers.

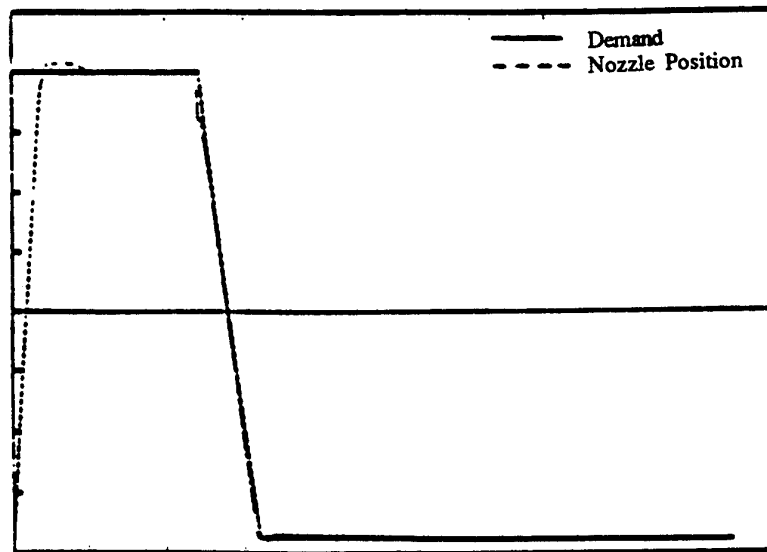
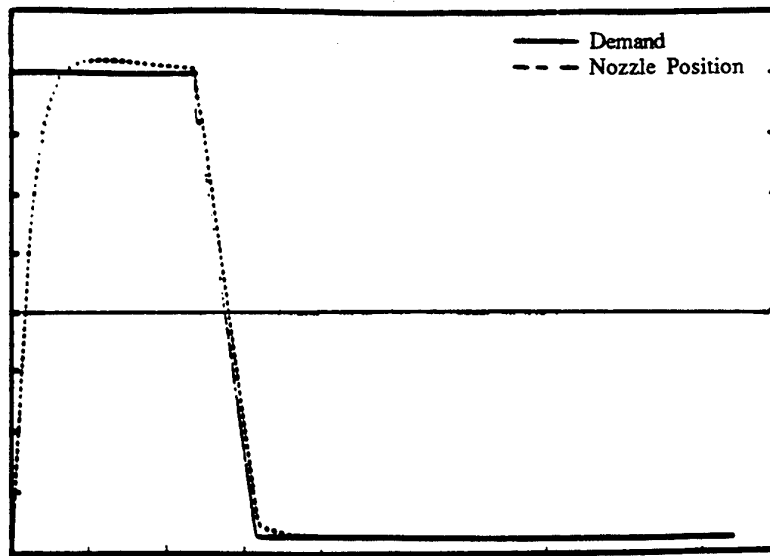
V.C. Chen, Y. Pao, "Learning Control With Neural Networks", International Conference On Robotics And Automation, 1989 IEEE.



Flight Idle --> Full Power

fig 1a : Actuator Position with PID controller

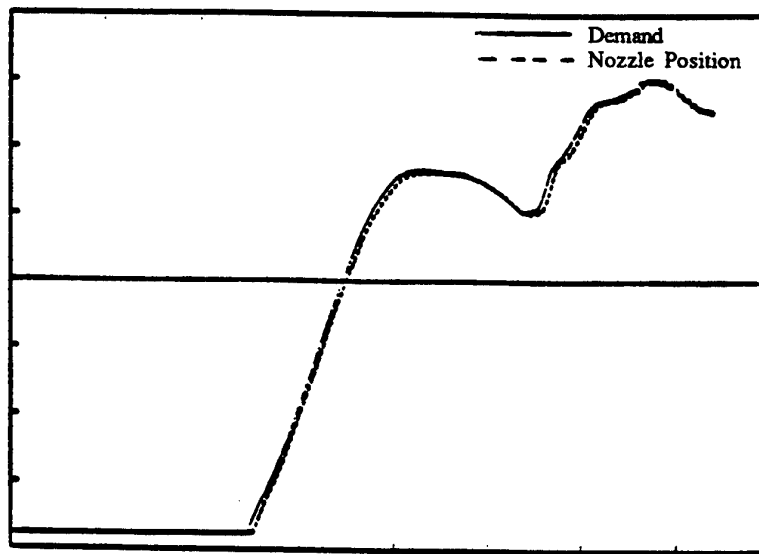
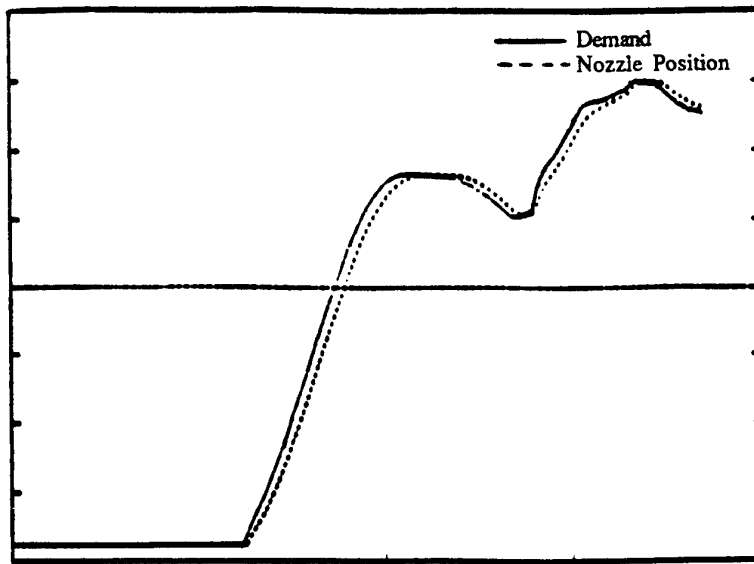
fig 1b : Actuator Position with Neural controller



Full Power --> Flight Idle

fig 2a : Actuator Position with PID controller

fig 2b : Actuator Position with Neural controller



Random Transcient

fig 3a : Actuator Position with PID controller

fig 3b : Actuator Position with Neural controller

Paper 33: Discussion

Question from Prof N Munro, UMIST, UK

You clearly obtained good results from your neural network approach at a particular operating condition. What happens when the system moves to a new operating condition? Also, what is the magnitude of re-learning time, with respect to real-time operation of the system?

Author's reply

The learning process of the model and controller is on-line, so that the model can readily be adapted to a new operating condition. This is possible in real time because the adaptation required by both model and controller is small. Indeed, neural networks have the capability of "generalisation". In the contrary case we would always take into account the operating condition in providing the inputs of the neural networks - for the model in particular.

Question from I Khalid, Pratt and Whitney Aircraft, USA

In your further studies do you plan to investigate hardware requirements for the neural network, in order to implement the approach in a real system? Do you know of any successful real hardware demonstration of a neural network engine model or controller, or is the necessary technology not sufficiently mature?

Author's reply

Experiments by SNECMA and others have shown that the software approach is difficult to implement because of long computation times. To overcome this difficulty, two solutions are possible: either reduce the computation times by a "smart" system architecture and/or do not perform on-line learning; or, use a hardware approach. The hardware approach is very attractive, but we must consider carefully the trade-off between the increased cost and the improved neural network performance. The system costs will include not only production cost, but also qualification and certification aspects. While we and others have achieved successful software demonstration, no such demonstration has yet been achieved in aeronautics with a hardware approach.

Adaptive Optimization of Aircraft Engine Performance Using Neural Networks

Donald L. Simon
Vehicle Propulsion Directorate
U.S. Army Research Laboratory
NASA Lewis Research Center
Cleveland, Ohio 44135

Theresa W. Long
NeuroDyne, Inc.
123 Hunting Cove
Williamsburg, VA 23185

ABSTRACT

Preliminary results are presented on the development of an adaptive neural network based control algorithm to enhance aircraft engine performance. This work builds upon a previous National Aeronautics and Space Administration (NASA) effort known as Performance Seeking Control (PSC). PSC is an adaptive control algorithm which contains a model of the aircraft's propulsion system which is updated on-line to match the operation of the aircraft's actual propulsion system. Information from the on-line model is used to adapt the control system during flight to allow optimal operation of the aircraft's propulsion system (inlet, engine, and nozzle) to improve aircraft engine performance without compromising reliability or operability. Performance Seeking Control has been shown to yield reductions in fuel flow, increases in thrust, and reductions in engine fan turbine inlet temperature. The neural network based adaptive control, like PSC, will contain a model of the propulsion system which will be used to calculate optimal control commands on-line. Hopes are that it will be able to provide some additional benefits above and beyond those of PSC. The PSC algorithm is computationally intensive, it is valid only at near steady-state flight conditions, and it has no way to adapt or learn on-line. These issues are being addressed in the development of the optimal neural controller. Specialized neural network processing hardware is being developed to run the software, the algorithm will be valid at steady-state and transient conditions, and will take advantage of the on-line learning capability of neural networks. Future plans include testing the neural network software and hardware prototype against an aircraft engine simulation. In this paper the proposed neural network software and hardware is described and preliminary neural network training results are presented.

INTRODUCTION

Performance Seeking Control (PSC) is an adaptive

model-based control algorithm which optimizes aircraft propulsion system performance in flight. The adaptive nature of the control system enables it to account for engine to engine manufacturing variations, off nominal engine component performance, or deterioration which may occur to the engine over time. This technology was a joint NASA, McDonnell Douglas, and Pratt & Whitney effort. The PSC algorithm has been flight tested on a NASA research aircraft at the NASA Ames/Dryden Flight Research Facility [1, 2, 3].

A NASA Small Business and Innovative Research (SBIR) contract which builds upon the previous NASA PSC effort has been established with NeuroDyne Inc. The objective of this effort is to investigate the use of neural networks for the implementation of a model-based adaptive control algorithm. Preliminary progress under this effort is presented.

Neural networks are computational representations of biological neurons in the human brain. Consisting of several layers of nodes connected by weighted synaptical connections, neural networks can be trained to recognize a pattern of inputs and provide desired outputs. They lend themselves very well to pattern recognition problems, or for this application, estimation of system parameters.

Neural networks have the promise of being faster and requiring less memory than traditional computer algorithms when implemented in specialized hardware. The original performance seeking control algorithm is only valid at near-steady-state conditions due to the computational burden of modeling transient maneuvers. A neural network implementation may be able to overcome this limitation. Neural networks also have the added benefit of being able to learn on line. Thus they may be able to adapt to new or unexpected conditions that the traditional PSC implementation could not account for.

PERFORMANCE SEEKING CONTROL

The objective of Performance Seeking Control is to adaptively optimize the near steady-state performance of an aircraft propulsion system in real-time by calculating engine control trims which are applied to the nominal engine schedules. Performance Seeking Control can select one of three modes for optimization. The modes are minimizing fuel consumption while maintaining nominal thrust, minimizing fan turbine inlet temperature (FTIT) while maintaining nominal thrust, or maximizing thrust while maintaining engine nominal FTIT. A block diagram of the PSC architecture is shown in Figure 1. It includes an estimator, a model of the propulsion system, and an optimizer. The estimator consists of a Kalman Filter using flight measurements to estimate five component deviation parameters. These component deviation parameters are those of the low pressure turbine efficiency (DELPT), the high pressure turbine efficiency (DEHPT), the fan airflow (DWFAN), the high pressure compressor airflow (DWHPC), and the high pressure turbine area (AAHT). The propulsion system model consists of linear and nonlinear models used to estimate unmeasured engine parameter based on flight measurements and the five component deviation parameters estimated by the Kalman filter. The model is continuously updated to adaptively model the dynamics of the actual propulsion system. The optimizer uses linear programming techniques to optimize control trim settings based upon the present operating condition of the

propulsion system and the optimization mode selected. The performance seeking control algorithm has been flight tested at the NASA Ames/Dryden Flight Research Facility on a NASA F-15 research vehicle. This aircraft is equipped with two Pratt & Whitney 1128 afterburning turbofan engines. The results from this testing has shown that Performance Seeking Control does indeed yield significant improvements over traditional control techniques. Thrust increases up to 15% at military power, turbine temperature decreases up to 120°F at military power, and Specific Fuel Consumption (SFC) improvements up to 2.0% at cruise have been achieved (ref. 4).

A limitation with the PSC algorithm is the speed at which it can be executed. The algorithm is rather computationally complex and is not able to achieve real-time performance when implemented in conventional computer processors where the calculations take place in a serial fashion. Therefore it is valid only at near steady state conditions. Also the accuracy of the algorithm is dependent on the accuracy of the adaptive model. Neural networks, because of their parallel nature and ability to learn on-line may help to overcome such limitations.

OPTIMAL NEURAL CONTROLLER

The proposed optimal neural controller is being developed to control a Pratt & Whitney 1128 engine simulation. The proposed architecture is shown in Figure

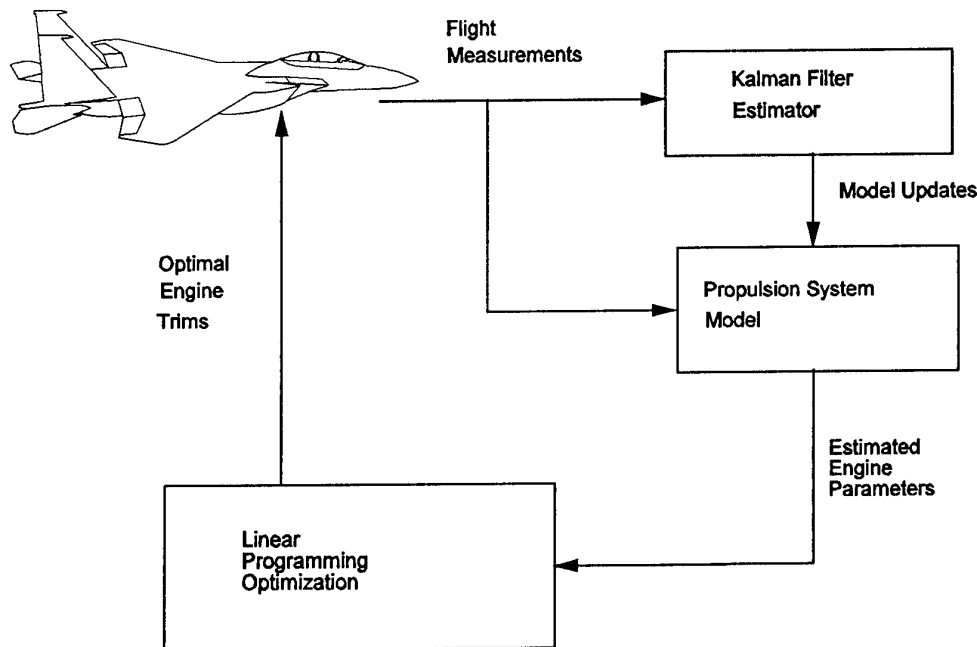


Figure 1. Performance Seeking Control Architecture

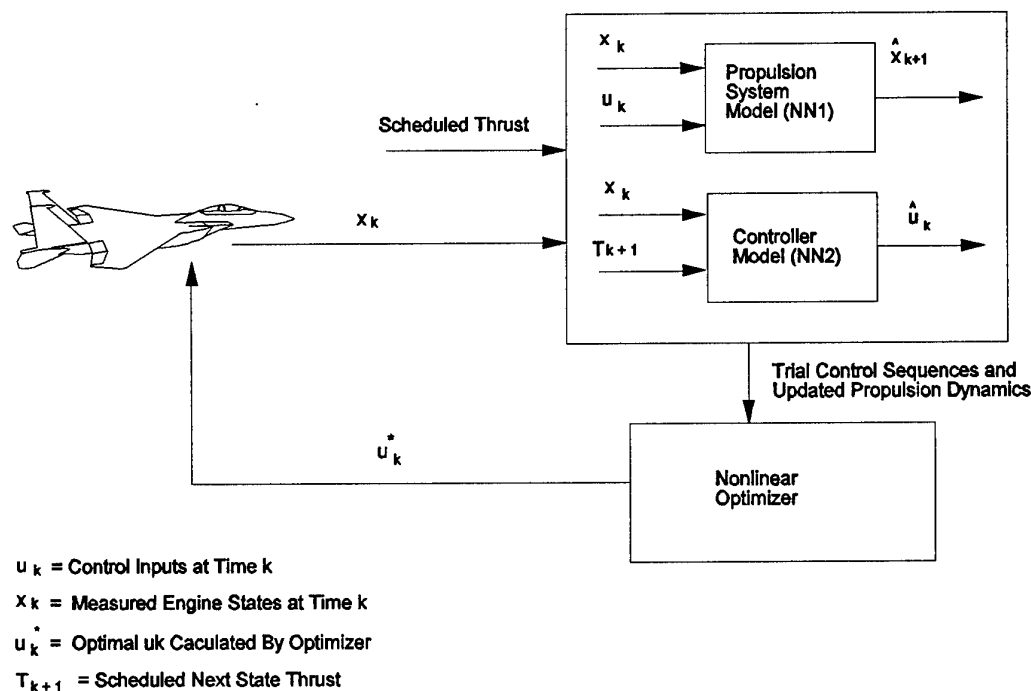


Figure 2. Optimal Neural Controller

2. It consists of a propulsion system model, a controller model, and a nonlinear optimizer. Plans call for implementing each of these components as neural networks. The propulsion system and controller models are used to generate trial control sequences n time steps into the future spanning the range of admissible control based on the present operating conditions and the scheduled thrust. These trial control sequences along with the dynamics of the propulsion system model are used by the optimization algorithm to perform an iterative optimal gradient search. After convergence, the optimizer produces the optimal control according the desired cost function. Logic is included to insure that the control and dynamic constraints are not exceeded. Prior to on-line operation the propulsion system model and the controller model neural networks are trained using simulation data. The controller model is further refined off-line by training on the optimizer outputs. On-line, the error between the propulsion system model predicted outputs and the measured outputs of the actual engine are monitored. If the error exceeds a certain threshold, the propulsion system model will be updated to maintain an accurate representation of the engine dynamics. A change in the propulsion system model will of course impact the response of the controller model as it's outputs adjust to allow the propulsion system to continue to provide the scheduled thrust. The optimizer then calculates a new optimal control for this condition using knowledge

of the updated propulsion system dynamics and the new trial control sequences. The new optimal control is fed back to the inner loop control to update control trims. It is also used to update the controller model neural net on-line.

Preliminary neural network versions of the propulsion system model and the controller model have been developed. The optimization routine is currently being coded in a higher level language, however future plans call for implementing this routine in a neural network also. Special purpose neural processing hardware is being developed for future implementation of the entire algorithm. By doing so we hope to demonstrate real-time operation. The development of the elements of the optimal neural controller are further discussed in the following sections.

The Propulsion System and the Controller Models

Pratt & Whitney has provided NeuroDyne data from an 1128 engine simulation for development of the propulsion system and controller neural network models. The data sets provided were collected from the engine simulation by perturbing the inputs around steady state operating points throughout the state space. This data consists of 8 measurable engine states and 6 control inputs. The engine state vector, x , is defined as

$$x = [PS20 \ T20 \ PB \ T45 \ P60 \ N1 \ N2 \ PAM]^T$$

PS20 : Engine Inlet Pressure
T20 : Engine Inlet Temperature
PB : Burner Pressure
T45 : Low Pressure Turbine Inlet Temperature
P60 : Nozzle Inlet Pressure
N1 : Low Rotor Speed
N2 : High Rotor Speed
PAM : Ambient Pressure

The control vector, u , consists of 6 elements

$$u = [WF \ AJ \ FVV \ CVV \ HPX \ BLD]^T$$

WF : Main Burner Fuel Flow
AJ : Exhaust Nozzle Area
FVV : Fan Variable Vanes
CVV : Compressor Variable Vanes
HPX : Horsepower Extraction
BLD : Bleed Flow

The Propulsion System Model

The propulsion system model (NN1) estimates the state at time $k+1$ from the states and control inputs at time k . There are 14 inputs to NN1 (8 states, 6 controls), and 8 outputs from NN1 (8 states). An initial propulsion system model has been developed by training a 1-hidden layer feedforward neural net consisting of 50 hidden nodes. The performance of this neural network in matching the response of the Pratt & Whitney engine simulation is very good. The average generalization error is 1.00% where the average generalization error is defined as:

$$e = \sqrt{\frac{\sum_{i=1}^n [x_i^* - x_i]^T [x_i^* - x_i]}{\sum_{i=1}^n [x_i^*]^T [x_i^*]}}$$

where

x_i^* is the target output for the i th data point of the training or testing set.

x_i is the neural net estimate of the i th data point of the training or testing set.

n is the total number of points in the training or testing set

Table 1 shows the generalization error for each output of NN1 as a percentage of the outputs operating range. Also shown in the table is the approximate accuracy of each

sensor as provided by Pratt & Whitney. On-line, the propulsion system model accuracy will be limited by the accuracy of the sensor measurements which are provided as inputs.

**Table 1 Propulsion System Model (NN1)
Estimation Error**

state	Estimation error (%)	Sensor error (%)
PS20	±0.34	±0.86
T20	±0.21	±0.41
PB	±0.61	±0.56
T45	±1.5	±1.59
P60	±0.55	±0.45
N1	±0.13	±0.13
N2	±0.10	±0.10
PAM	±0.20	±2.00

Figure 3 shows the P&W simulator output of T_{45} and NN1 estimated T_{45} for a steady state flight at mil power, 1.05 operating line, 60,000 ft altitude and Mach 2.0. As expected the neural net closely tracked the response of the simulator. Although the neural net was trained on steady state data it was desirable to check the networks ability to handle transient conditions. Figure 4 shows the simulator and NN1 estimated T_{45} for a transient condition of acceleration at 30,000 ft altitude and Mach 0.9. Once again the neural network was able to closely match the outputs of the simulation.

The Controller Model

The controller model (NN2) estimates the required control (u_k) based on the present state (x_k) and scheduled thrust (T). NN2 has 9 inputs (8 states, and 1 thrust), and 6 outputs (6 controls). Once again a 1-hidden layer neural net having 50 hidden nodes was selected for initial development. The controller model (NN2) will eventually be trained on the optimal control commands generated by the optimizer, but for an initial starting guess of the model weights the network was trained on the Pratt & Whitney engine simulation data. The average generalization error for this network is 7.54%. It should be noted that the accuracy requirement for the initial controller model is not as stringent as the propulsion system model NN1 because the controller model weights will be further refined by the optimizer. Table 2 shows the generalization error for each output of NN2 as a percentage of the outputs operating range. Measurement accuracy information is unavailable.

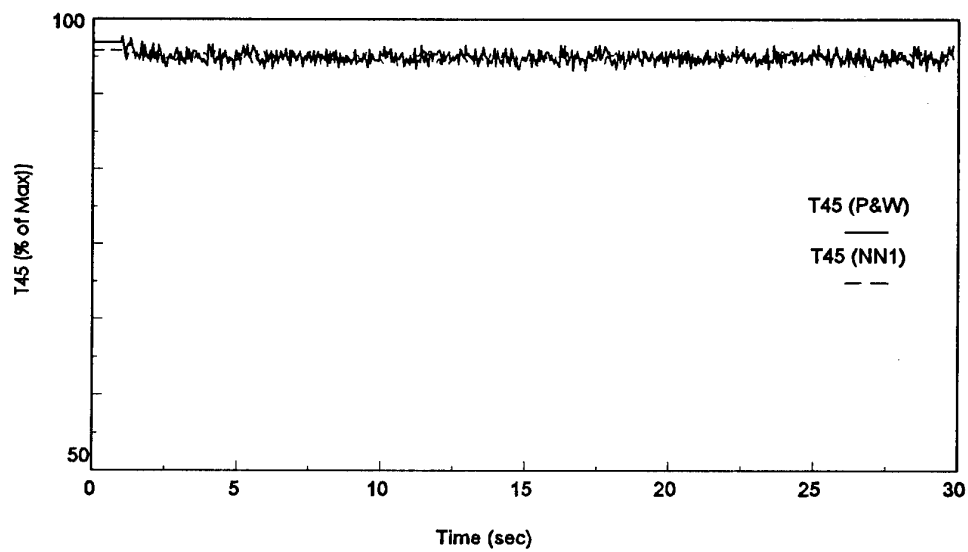


Figure 3. Simulator vs. NN1 Estimated T45
at Steady State Condition

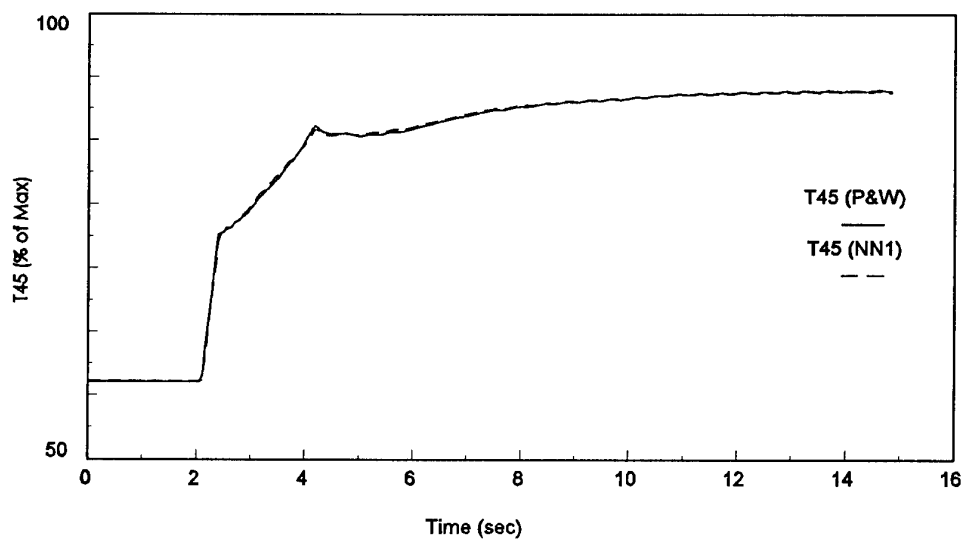


Figure 4. Simulator vs. NN1 Estimated T45
at Transient Condition

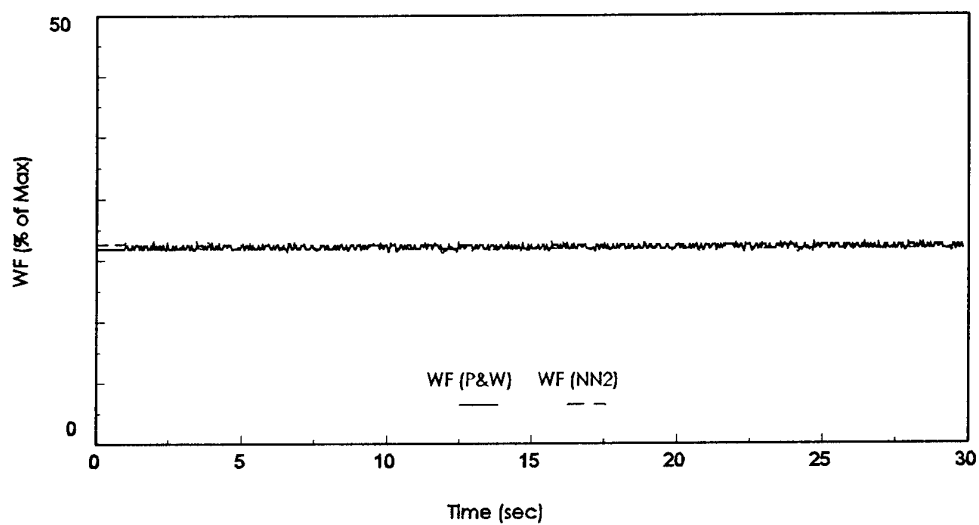


Figure 5. Simulator vs. NN2 Estimated
WF at Steady State Condition

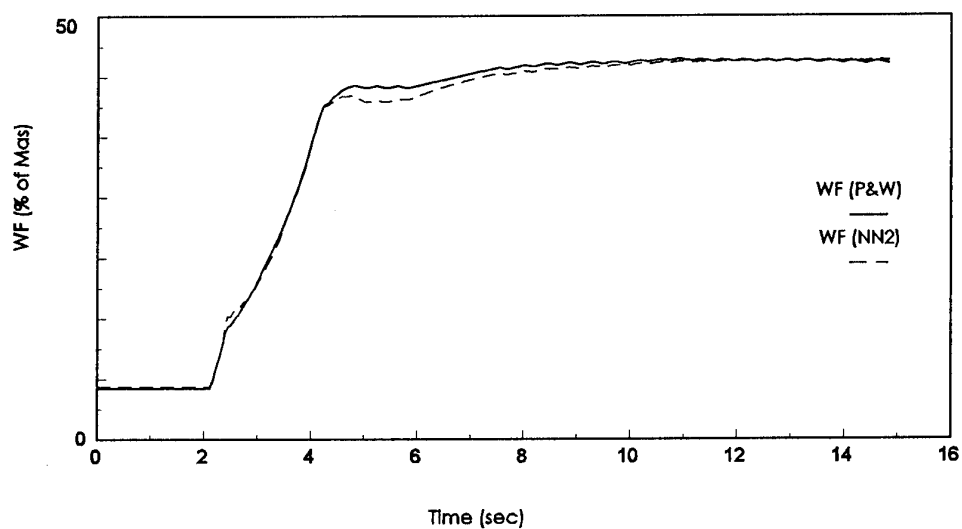


Figure 6. Simulator vs. NN2 Estimated
WF at Transient Condition

Table 2 Controller Model (NN2) Estimation Error

Control Input	Estimation error (%)
WF	1.14
AJ	1.22
FVV	6.19
CVV	3.51
HPX	4.86
BLD	8.00

Figure 5 shows the P&W simulator output of WF (fuel flow rate) and NN2 estimated WF for a steady state flight at mil power, 1.05 operating line, 60,000 ft altitude and Mach 2.0. Figure 6 shows the simulator and NN2 estimated WF for the transient acceleration condition at 30,000 ft altitude and Mach 0.9. Both figures show that NN2 did a fair job of tracking the simulator output.

On-Line Learning

Figure 7 illustrates the on-line learning of these two neural networks. The propulsion system model will be updated based on the error between its output and the actual measured propulsion system output. This will allow it to adapt to account for any off nominal engine behavior or any deterioration which may occur over time. The controller model will be updated based on the error between its output and that of nonlinear optimizer allowing it to update to account for any changes in the optimal control. The one hidden layer feed forward neural network used to obtain the initial results is probably not the best neural net architecture for on-line learning. Later in the paper alternative neural network architectures which are undergoing evaluation will be discussed.

Generating Trial Control and State Sequences

The nonlinear optimization routine requires an initial starting guess for the sequence of states and control inputs to meet the required constraints. This can be accomplished by cascading together the propulsion system model (NN1) and the controller model (NN2) as shown in Figure 8. For illustration purposes a constant net thrust constraint is used. The constraint can be altered to be an acceleration or deceleration schedule for thrust. Figure 8 shows that at time stage k given a next stage scheduled thrust, T_{k+1} , and the current measured state, x_k , the necessary control, u_k , can be computed from the controller model. Therefore, having selected a constant thrust value T , and an acceptable variation for the thrust (ΔT), m increments of thrust between $T - \Delta T$ and $T + \Delta T$ can be created.

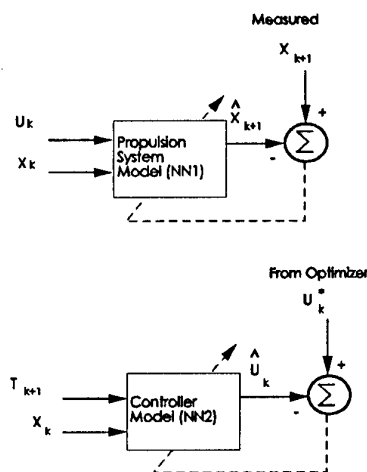


Figure 7. Neural Networks On-Line Update

With each of the m thrusts, a starting value of u_k can be computed using NN2. All the u_k 's are checked against constraints such as bounds and rate limit, and corrections are made to stay within the constraints. We will follow through the calculations for one of the m u 's. The rest would be similar. At time stage k , given the starting value of u_k (generated by NN2), the estimated next state \hat{x}_{k+1} can be predicted using the propulsion system model (NN1). Moving onto time stage $k+1$ using the NN1 estimated \hat{x}_{k+1} and the next stage scheduled thrust (T_{k+2}) as the inputs, the next stage estimate control input \hat{u}_{k+1} can be computed from NN2. This continues until the end of the horizon is reached, thus obtaining a sequence of states and control inputs as a starting guess.

Nonlinear Optimizer

The nonlinear optimization routine is currently being developed in the "C" language on a workstation computer. The calculations involved are highly parallel in nature and are dependent on the architecture of the propulsion system model (NN1) and the outputs of both the propulsion system model (NN1) and the controller model (NN1). NeuroDyne plans to investigate the implementation of the optimization routine in a neural network in the future.

The optimization routine uses a receding horizon cost function which is a function of engine states, x , and control inputs, u , over a finite number of time stages, n , into the future. The cost function has the following form at the present time stage k

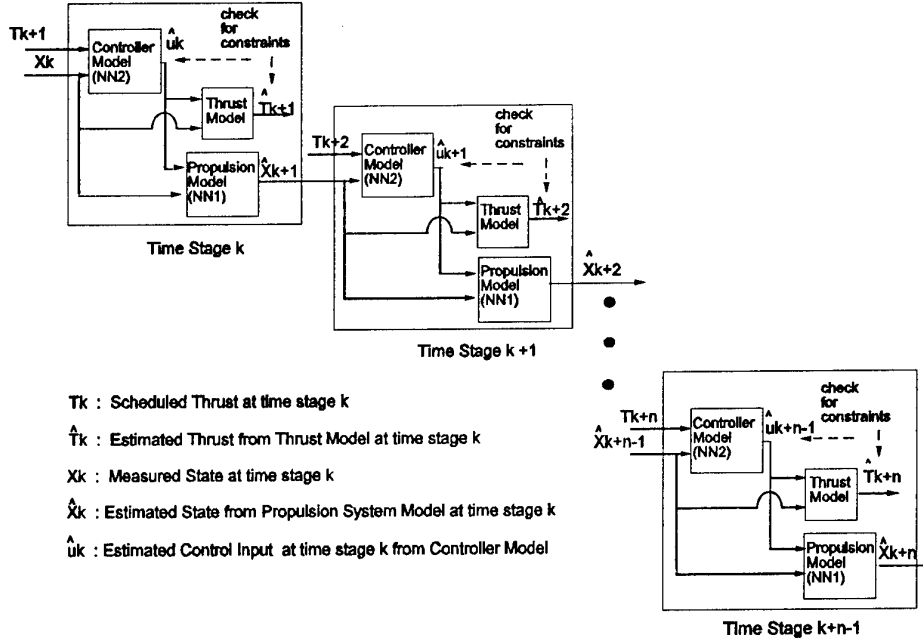


Figure 8. Generating Trial Control Sequences

$$J_k = \sum_{i=k}^{n+k-1} f(x_i, u_i) \quad (1)$$

where

x_i is the state at time i
 u_i is the control input at time i
 n is the size of the look ahead horizon.

One of the design issues of this optimization approach is selection of the horizon size used in the objective function. Theoretically, only an infinite horizon produces a global optimum. For a nonlinear system, it is necessary to use a receding (or limited) horizon. The size of the horizon depends heavily on the accuracy of the model. Therefore it is essential that the neural nets used for implementation provide good accuracy.

After NN1 and NN2 have been used to obtain an estimate of the propulsion system dynamics and an initial estimated sequence of state and control over the horizon of n , the sequence of estimated control inputs is corrected iteratively according to

$$U_{NEW} = U - \alpha \frac{\partial J}{\partial U} \quad (2)$$

where

U is a sequence of $[u_k, u_{k+1}, \dots, u_{k+n-1}]$

$\partial J / \partial U$ is dependent on the propulsion system model neural network architecture.

α is a step scaling factor between 0 and 1

Each time U_{NEW} is computed it is applied to NN1 to generate a new estimated sequence of states. These estimated states and U_{NEW} are then used as inputs to the thrust model. If the resulting net thrust at each time stage is still within $T \pm \Delta T$, U_{NEW} is saved as U , and the algorithm proceeds to the next iteration. Otherwise, the offending individual u_i is corrected, or the step size α in equation (2) is reduced and U_{NEW} is recomputed.

After convergence, the final J is computed and saved for this sequence of U . We then proceed to the next initial U . At each time stage k , there will exist m sequences of U and m J 's. The optimal control sequence will be the sequence which minimizes the cost function J . The optimal control, u_k^* , at the current time stage is the first control vector of that optimal control sequence. This is analogous to playing chess. At each point of the game, the player has an optimal sequence computed but only plays the first move of that sequence.

An example is provided below to illustrate operation of the optimization routine.

Optimizer Example

The optimization algorithm is set up so that various forms of the cost function can be used. For their preliminary work NeuroDyne has been working with a cost function suggested by Pratt & Whitney which penalizes high fuel usage and high low pressure turbine temperatures.

Equation (3) shows the instantaneous (1 stage) cost function J_{instant} . The receding horizon cost function of horizon n would be a sum of n of such functions.

$$J_{\text{instant}} = C_1 WF + \frac{C_2}{e^{[-C_3(T45 - T_{\text{ref}})]} - 1} \quad (3)$$

where

C_1 , C_2 , and C_3 are constants suggested by Pratt

WF: fuel flow

T45: LPT inlet temperature

T_{ref} = Reference temperature provided by Pratt

By dividing by C_1 the coefficient of WF becomes one. Then by defining $a = C_2/C_1$, $b = C_3$, and $c = C_3 \cdot T_{\text{ref}}$ you obtain:

$$J_{\text{instant}} = WF + \frac{a}{e^{[-b \cdot T45 + c]} - 1} \quad (3a)$$

Let us assume for multiple look ahead, a horizon size of 3 is used so all the terms can be shown in expanded form.

define

$$g_k = \frac{1}{e^{[-b \cdot T45_k + c]} - 1} \quad (4)$$

where the index k indicates time stage k .

The cost function at time stage k is:

$$J_k = WF_k + WF_{k+1} + WF_{k+2} + a(g_{k+1} + g_{k+2} + g_{k+3}) \quad (5)$$

Since T45 is the fourth element of x , and WF is the first element of U we obtain the following:

$$\frac{\partial g_k}{\partial x_k} = [0 \ 0 \ 0 \ \frac{b \cdot e^{[-bT45_k + c]}}{(e^{[-bT45_k + c]} - 1)^2} \ 0 \ 0 \ 0 \ 0]^T \quad (6)$$

$$\begin{aligned} \frac{\partial J_k}{\partial u_k} = & [1 \ 0 \ 0 \ 0 \ 0 \ 0]^T + a \left[\left(\frac{\partial g_{k+1}}{\partial x_{k+1}} \right)^T \left(\frac{\partial x_{k+1}}{\partial u_k} \right)^T + \right. \\ & \left. \left(\frac{\partial g_{k+2}}{\partial x_{k+2}} \right)^T \left(\frac{\partial x_{k+2}}{\partial x_{k+1}} \right)^T \left(\frac{\partial x_{k+1}}{\partial u_k} \right)^T + \right. \\ & \left. \left(\frac{\partial g_{k+3}}{\partial x_{k+3}} \right)^T \left(\frac{\partial x_{k+3}}{\partial x_{k+2}} \right)^T \left(\frac{\partial x_{k+2}}{\partial x_{k+1}} \right)^T \left(\frac{\partial x_{k+1}}{\partial u_k} \right)^T \right]^T \end{aligned}$$

$$\begin{aligned} \frac{\partial J_k}{\partial u_{k+1}} = & [1 \ 0 \ 0 \ 0 \ 0 \ 0]^T + a \left[\left(\frac{\partial g_{k+2}}{\partial x_{k+2}} \right)^T \left(\frac{\partial x_{k+2}}{\partial u_{k+1}} \right)^T + \right. \\ & \left. \left(\frac{\partial g_{k+3}}{\partial x_{k+3}} \right)^T \left(\frac{\partial x_{k+3}}{\partial x_{k+2}} \right)^T \left(\frac{\partial x_{k+2}}{\partial u_{k+1}} \right)^T \right]^T \end{aligned}$$

$$\frac{\partial J_k}{\partial u_{k+2}} = [1 \ 0 \ 0 \ 0 \ 0 \ 0]^T + a \left[\left(\frac{\partial g_{k+3}}{\partial x_{k+3}} \right)^T \left(\frac{\partial x_{k+3}}{\partial u_{k+2}} \right)^T \right]^T \quad (7)$$

For a horizon of n , the number of multiplications for equation set (7) would be $O(n^3) \times$ (matrix multiplication for 1 time stage). The matrix multiplication for 1 time stage is a function of the size of the neural net, the state vector, and the control vector. But a simple approximation for 1 time stage cost for a 1 hidden layer net would be $O(L^3)$, where $L = \max(N_u, R, P)$, with
 N_u : size of the control vector u
 R : size of the state vector x
 P : # of hidden nodes for a 1 hidden layer net.

Recursive calculation methods are being investigated to help reduce the computing cost of the gradients in equation set (7).

The architecture of the propulsion system model (NN1) determines the calculation of the Jacobians used in $\partial J / \partial U$. Assuming a 1 hidden layer net as shown in Figure 9 the Jacobians used in equation set (7) can be calculated as shown in equations (8) and (9).

$$\frac{\partial x_{i+1}}{\partial x_i} = W^{(1)} \frac{\partial x_i^{(1)}}{\partial s_i^{(1)}} W^x \quad (8)$$

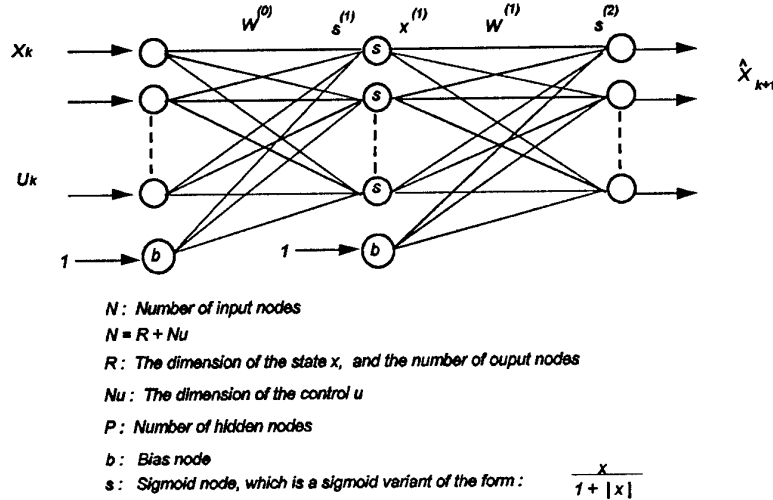


Figure 9. One Hidden Layer Net

$$\frac{\partial x_{i+1}}{\partial u_i} = W^{(1)} \frac{\partial x_i^{(1)}}{\partial s_i^{(1)}} W_u^{(0)} \quad (9)$$

$$\left[\frac{\partial x_i^{(1)}}{\partial s_i^{(1)}} \right]_j \quad \text{for the } j\text{th hidden node is : } (1 + |x_i^{(1)}(\text{jth node})|)^{-2}. \text{ They form the diagonal of a } P \times P \text{ matrix.}$$

NEURAL NETWORK ARCHITECTURES

where

$x_i^{(1)}$: hidden layer output at time stage i

$s_i^{(1)}$: input to the hidden layer at time stage i

$W^{(1)}$: weight matrix coming out of the hidden layer nodes to the output layer nodes, but the weights from the bias node is not included. dim. $R \times P$

$W_x^{(0)}$: weight matrix coming out of the state input (x_k) nodes to the hidden layer nodes, note that the weights from the bias node are not included. dim. $P \times R$
note also that $R + N_u = N$ at the input

$W_u^{(0)}$: weight matrix coming out of the control input (u_k) nodes to the hidden layer nodes, note that the weights from the bias node are not included. dim. $P \times N_u$ with N_u the dimension of the control u vector.

The sigmoid nodes of the neural net used in this project will use an Elliott nodal function of the form $x/(1 + |x|)$. This implementation computes faster than the frequently used hyperbolic tangent, and achieves similar accuracy. Therefore,

Three important considerations for the selection of the neural network architectures used for the implementation of the optimal neural controller are :

1. Accuracy , specifically the generalization ability of the neural networks.
2. Speed of Computation : This often means the size of the network should be as small as possible.
3. Redundancy : The redundancy helps to increase the stability or memory retention of the neural network.

The accuracy of the propulsion system model affects the accuracy of the control command, as well as the size of the look ahead horizon. As an example, if the network has a 98% accuracy in predicting the outcome at time stage $k+1$, based on information gathered up to time stage k (the current stage), then to predict the outcome at time stage $k+10$, we can repeat the same process 10 times, each time using the predicted outcome as the input for further forward prediction. The accuracy of the prediction at time stage $k+10$ would be proportional to 0.98^{10} , which is about 80% accuracy. On the other hand, if the one stage prediction accuracy is about 90% accurate then the 10th stage prediction is only about 35% accurate. So the accuracy of the neural network limits how far the controller can look ahead in selecting an optimal control policy. It

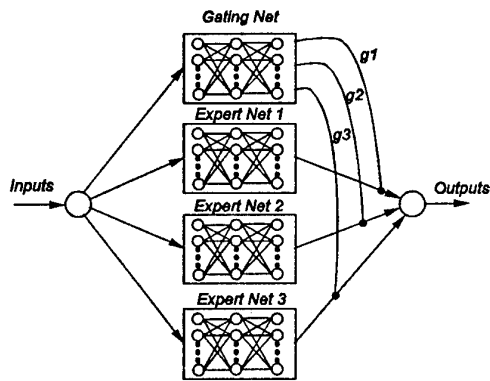


Figure 10. Competitive Net Architecture

should be emphasized that the controller of interest here is for a nonlinear system whose dynamics is approximated by the neural net, and there is no accurate analytical model to provide an infinite horizon.

The computation speed of a neural net is an important factor in a neurocontroller which requires on-line learning and real-time optimization. The speed is very much related to the size of the network. It is necessary to choose a network as small as possible while achieving desirable accuracy.

A network with some redundancy built in is generally more robust in the face of a changing environment. Redundancy helps to increase the stability or the memory retention of the network. During on-line learning it is essential the network be able to learn new dynamics in one region of the state space without compromising accuracy at another region.

To address the issues of accuracy, speed, and redundancy NeuroDyne is considering alternative neural network architectures. Two of these architectures, a hierarchical mixture expert (HME) network [5] or competitive net, and the use of global and local neural network models in tandem are discussed below.

Hierarchical Mixture Expert (HME) Network

Figure 10 shows an HME network or a competitive network. It consists of a gating network and multiple expert networks. The input space is made up of several local regions separated by soft boundaries where data points may lie in multiple regions simultaneously. Individual expert nets provide accurate modeling at particular local regions throughout the input space. The gating net, whose output is a function of the input that goes into the individual expert nets, determines the

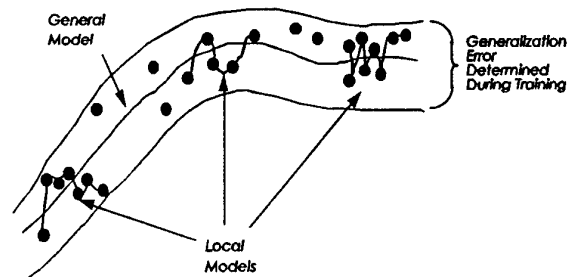


Figure 11. Global and Local Models

contribution of each of the expert nets to the overall output. Initial evaluation by NeuroDyne has shown that this architecture exhibits increased accuracy and converges (learns) about an order of magnitude faster than a conventional feedforward net. When undergoing on-line learning at a particular region in the state space, one of the expert networks can be trained while the other networks remain relatively unmodified. This will allow the network to maintain accuracy in a local region without compromising accuracy throughout the rest of the state space. Another advantage is the parallel nature of the architecture. Each of the expert nets and gating nets can be assigned to a separate processor and work in parallel. A disadvantage of this architecture is that it increases the complexity of the mathematics necessary in computing the Jacobians used by the optimization routine that were shown in equations (8) and (9).

Global and Local Models

Another approach being considered is maintaining both global and local versions of the neural networks on-line. The use of a global model and a local model in tandem is designed to maintain both good generalization and model accuracy [6]. The global model and local model are identical in terms of architecture but are updated and maintained differently. The global model is valid throughout the state space while the local model can depict localized phenomena more accurately than the global model, but can not be used anywhere else except in a local region. Figure 11 illustrates the difference between the general model and its many local models.

The local models are used by the neural controller to produce accurate control commands on-line. Since the local models can not be applied to input-output pairs in different parts of the state space they must be able to

learn on-line very quickly to track the system dynamics through varying local regions. If a new trajectory is to be tracked, the localized model representing the end point of a previous trajectory is most likely a poor starting guess for the first point of the new trajectory. The search for the network weight parameters generally does not converge if we start with this local model. Therefore, when a task is changed or when a trajectory discontinuity occurs, the general model must be used to start the evolution of the local model. Because of the fast on-line learning and accuracy requirements, the local model neural networks have a faster learning rate and a lower generalization error threshold.

The global models are initially trained off-line using simulation data collected from operating points throughout the state-space. On-line the global model will still be allowed to update but at a much slower learning rate and a higher generalization error threshold than that of the local model.

NEURAL NETWORK HARDWARE

To take full advantage of the inherently parallel nature of neural networks, they need to be implemented in hardware designed specifically for their implementation. Doing so will yield significant increases in execution speed over traditional sequential computing techniques. NeuroDyne has established a subcontract to develop the neural network hardware which will run the neural network algorithm. This task will be accomplished through the use of a commercially available digital neural network processor. Although both analog and digital neural network hardware is commercially available, it was determined that a digital solution would best meet the needs of this program. Analog implementations tend to be more susceptible to temperature variations and also tend to have lower resolution than digital implementations. Although analog neural network chips are faster than their digital counterparts, they suffer from the need to communicate with the digital world. Because of the additional delays induced by the D/A and A/D convertors required for I/O, an analog implementation only presents a speed advantage when a large network of 100 to 1000 nodes is used. A digital implementation also has the advantage of being similar to current approved flight hardware. Verification therefore would be more straightforward. The digital neural network chip which has been selected is the CNAPS chip from Adaptive Solutions. This hardware contains 64 nodes on a single chip and has 16 bit resolution. The developed architecture has been purposely designed with this limit in mind to insure implementation on a single chip would be possible. For a neural network with about 60 nodes a feedforward pass requires approximately 1 microsecond. The chip is provided on a processor board which is PC bus compatible. The development

environment for the CNAPS processor is very similar to the C language which should allow for easy algorithm conversion.

Future plans call for implementing the neural network algorithm in the CNAPS hardware housed in a PC chassis. This hardware/software prototype, running the optimal neural control algorithm, will be interfaced to a real time implementation of the PW 1128 state variable model. The performance of the neural network implementation in controlling the 1128 simulation will be evaluated.

SUMMARY

The Performance Seeking Control (PSC) program has demonstrated the benefits of model-based adaptive control algorithms. Implementing such an algorithm using neural networks offers the advantage of a faster implementation and the ability to learn on-line. Preliminary work has begun on the use of neural networks for adaptive optimization of aircraft engine performance. Future plans call for the refinement of the optimization algorithm and for the implementation of the software algorithm in a hardware prototype consisting of specialized neural network hardware. Capabilities which need to be demonstrated include the algorithm's ability to adaptively optimize the control for expected conditions of deterioration or off-nominal behavior. The speed at which the algorithm can accommodate these conditions also needs to be adequately demonstrated.

REFERENCES

- [1] Orme, J. and Gilyard, G., "Subsonic Flight Test Evaluation of a Propulsion System Parameter Estimation Process for the F100 Engine", AIAA 92-3745, 1992.
- [2] Nobbs, S.G., Jacobs, S.W., and Donahue, D.J., "Development of the Full-Envelope Performance Seeking Control Algorithm", AIAA 92-3748, 1992.
- [3] Mueller, F.D., Nobbs, S.G., Stewart, J.F., "Dual Engine Application of the Performance Seeking Control Algorithm", AIAA 93-1822, 1993.
- [4] Chisholm, J.D., "In-Flight Optimization of the Total Propulsion System," AIAA 93-3744, 1992.
- [5] Jordan, M.I., Jacobs, R.A., "Hierarchical Mixtures of Experts and the EM Algorithm", *Neurocomputation*, vol. 2, issue 2, March 1994.
- [6] Long, T.W., "A Learning Controller for Decentralized Nonlinear Systems", *American Control Conference*, June 2-4, 1993, San Francisco.

Paper 34: Discussion

Question from L Larkin, Pratt and Whitney Aircraft, USA

It was stated that the network had not been trained on transient data. The transient data shown was nearly a perfect match. How was that so?

Author's reply

It was inaccurately stated during the presentation that the neural networks had not been trained using transient data. Actually, a small number of transient conditions were used. Of the transient data available, half were randomly sampled for training and the rest were reserved for testing. So in the results shown, the neural networks had previous knowledge of half the data (randomly chosen), but the other half of the data were new to the networks. The fact that the available transient data for training were limited poses two limitations on our interpretation of the results. First, the state-space covered is very small. Although we could estimate the output under the operating conditions represented by the test data, we could not infer the generalisation ability of the network for conditions in other parts of the state-space. Also, because of the limited transient data available, we did not have the luxury to put aside an entire sequence of transient data for a testing set. Consequently, the transient estimation outputs shown contain half of the data already in the data base of the neural networks. Plans call for training and testing on more transient engine data in the future, to evaluate sufficiently the transient performance of the neural networks. It should also be noted that the Propulsion System Model (NN1) response essentially shows how well the Propulsion System Model is able to estimate future engine outputs one time stage ahead, given the engine outputs and the applied control command. Since each time stage is only 0.02 seconds, this plot is somewhat misleading and is not the best illustration of the neural network's capabilities. Figure 6 showing the output of the Controller Model (NN2) is a better illustration of the neural network's capabilities, since this network's outputs are totally different from the applied inputs. Perhaps a better plot would have been to compare the closed loop response of the two network models to the engine simulation response, while undergoing the same transient in thrust.

Question from K Chung, GE Aircraft Engines, USA

Are you addressing potential issues with certification/qualification of adaptive (self-adjusting) software?

Author's reply

This is an issue which definitely needs to be addressed and one we are presently struggling with. To date we have been concentrating on demonstrating the ability of neural networks to adaptively model aircraft engine dynamics on-line and therefore to be used for on-line optimisation. There are several considerations which may make flight certification more

straightforward. First of all, using neural networks for outer loop control tuning (adjusting control trims) seems much more feasible than using them for closed loop control. In this case, higher level supervisory logic could be used to insure that no control or operating constraints are compromised. If a failure were to occur, or if the network was not able to converge in time, the engine would in the worst case still have its baseline control to run on. Another consideration would be to use digital neural network processors, which are more similar to existing flight certified microprocessors than analogue neural network hardware is. Another thought might be to limit the permissible range of neural network weights, within certain bounds, so that all possible input/output scenarios might be checked.

DISTRIBUTED ARCHITECTURES FOR ADVANCED ENGINE CONTROL SYSTEMS

T.J. Lewis
 WL/POTA, Building 18
 1950 Fifth Street
 Wright-Patterson Air Force Base, Ohio, USA 45433-7251

SUMMARY

Controls and accessories (C&A) contribute significantly to the cost and weight of modern gas turbine engines. On average, the C&A subsystem accounts for approximately 15-20% of both engine weight and acquisition cost, and is the dominant cause of unscheduled maintenance. The goals of the Integrated High Performance Turbine Engine Technology (IHPTET) initiative demand that C&A weight, acquisition cost, and support cost be significantly reduced. The IHPTET C&A team is pursuing multiple approaches to achieving these reductions. Distributed control technology is one of the few that has the potential to effect reductions in all three categories. Weight can be decreased by replacing the traditionally complex full authority digital electronic control (FADEC) and heavy harness assembly with light-weight distributed processing elements interconnected via a simple communication and power distribution bus. Simplification of FADEC interfaces makes off-engine mounting feasible, enabling an acquisition cost reduction that is greater than the cost increase incurred by adding electronics to engine sensors and actuators. Distributing intelligence throughout the engine will improve the control system's ability to isolate faults. The resulting reductions in time to troubleshoot and unnecessary component removals will decrease maintenance costs. High temperature electronics are the key to the viability of the distributed control concept. Recent developments in this area will be reviewed.

LIST OF SYMBOLS

A/D	analog to digital
Ag	exhaust or jet area
ARPA	Advanced Research Projects Agency
BIT	built-in test
C&A	controls and accessories
CLC	control law computer
CVV	compressor variable vanes
D/A	digital to analog
DCS	distributed control system
DEC	digital engine controller
DECU	digital electronic control unit

DEEC	digital electronic engine control
ECU	engine control unit
EEC	electronic engine control
EHSV	electro-hydraulic servo valve
EMA	electromechanical actuator
EPR	engine pressure ratio
FADEC	full authority digital electronic control
FVV	fan variable vanes
HPT	high pressure turbine
I/O	inputs and outputs
IHPTET	Integrated High Performance Turbine Engine Technology
LOD	light-off detector
LVDT	linear variable differential transformer
MCM	multi-chip module
N ₁	fan rotor speed
NASA	National Aeronautics and Space Administration
PWB	printed wiring board
RTD	resistance temperature detector
RVDT	rotary variable differential transformer
SOI	silicon on insulator
WF	fuel flow rate
XTE	experimental technology engine

1. INTRODUCTION

Air Force-sponsored propulsion-related research and development is guided by the goals of the Integrated High Performance Turbine Engine Technology (IHPTET) initiative. The goals of IHPTET (Figure 1) have been defined to provide a doubling of turbopropulsion capability around the turn of the century.

	TF/TJ			Expendables		TP/TS	
	F _n /W _t	Cost	T ₃	F _n /W _a	Cost	HP/WT	SFC
PHASE I	+30%	-	+100°F	+35%	-30%	+40%	-20%
PHASE II	+60%	-20%	+200°F	+70%	-45%	+80%	-30%
PHASE III	+100%	-35%	+300°F	+100%	-60%	+120%	-40%

Figure 1. IHPTET Goals

Participants in this initiative include the United States Army, Air Force, Navy, the National

Aeronautics and Space Administration (NASA), and the Advanced Research Projects Agency (ARPA). These agencies have developed a joint approach to meeting IHPTET goals by flowing down requirements for improved performance to each major engine component area. This process involves defining component figures of merit and setting quantitative objectives for improvements. As Figure 1 shows, the pursuit of IHPTET goals is taking place in incremental steps, referred to as phases, in order to manage risk and facilitate transition of high payoff technologies to fielded weapon systems as they mature.

Controls and accessories (C&A) contribute significantly to the weight, acquisition cost, and maintenance cost of modern turbofan engines. The component weight breakout for an advanced turbofan engine with a thrust vectoring nozzle is illustrated in Figure 2. Experience with a variety of engine types, ranging from turboshaft/prop engines like the T700 and T406 to large turbofans of the F100/F110 class, indicates that C&A consistently accounts for 15-20% of total engine weight. Recent cost studies [1] show that the contribution of C&A to engine acquisition cost falls in the same range. Average cost projections for IHPTET Phase II engines are shown by component in Figure 3. Finally, Figure 4 shows that C&A are responsible for most unscheduled maintenance on modern turbofans (an F100 in this case) and are, therefore, a significant contributor to engine maintenance costs.

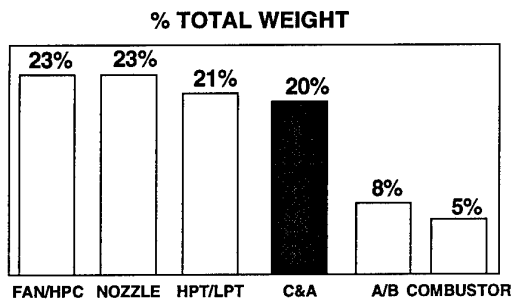


Figure 2. Turbofan Component Weights

COMPONENT ACQUISITION COST (250TH UNIT)

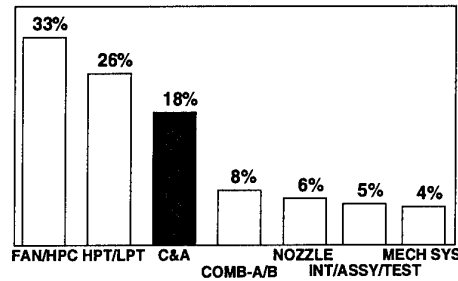


Figure 3. IHPTET Phase II Component Costs

% TOTAL MAINTENANCE ACTIONS

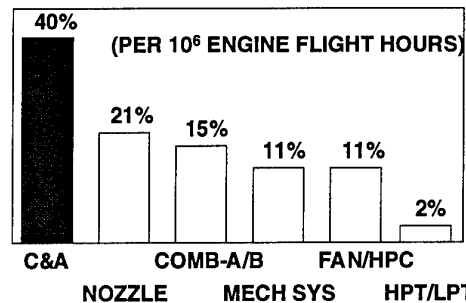


Figure 4. Sources of Unscheduled Maintenance

These factors have resulted in the identification of C&A as a separate component area within IHPTET, i.e., there are C&A technology development objectives (Figure 5) that must be met if IHPTET's overall goals are to be achieved.

CONTROL SYSTEM	TF/TJ		Expendables		TP/TS	
	Weight	Design Margin Reduction	Vol(Wt)	Cost	Weight	Design Margin Reduction
PHASE I	-20%	-20%	-20%	-30%	-20%	-20%
PHASE II	-35%	-35%	-35%	-45%	-35%	-35%
PHASE III	-50%	-50%	-50%	-60%	-50%	-50%

Figure 5. IHPTET Controls Objectives

The distributed engine control architecture described in this paper was defined and analyzed in the Air Force-sponsored Distributed Control Systems (DCS) program with GE Aircraft Engines (Air Force Contract F33615-92-C-2220). The preliminary design task in this program identified potential cost and weight advantages of distributed controls over conventional implementations. These characteristics have convinced the IHPTET controls team to make it a key part of our technology plan. The goals of this paper are to define a distributed engine control system, compare it to a centralized control, and identify

the key enabling technologies for the cost and weight reductions required by our IHPTET technology objectives.

2. BACKGROUND

Achieving IHPTET C&A technology objectives requires advances in both hardware and software. Referring again to Figure 5, the margin reduction objective is mostly concerned with the latter. Margin reduction means decreasing the safety factors typically used in the design of new compressors and turbines. This involves the exploitation of the additional process information provided by an embedded adaptive engine model. Compression system stall margin and high pressure turbine temperature margin are typically set at conservative levels to protect the turbomachinery from unsafe operating conditions in the presence of plant uncertainty. These design margins incur performance penalties in the form of reduced component efficiencies or added weight. An embedded model can be configured to accurately track stall pressure ratios and HPT inlet temperature in real-time, thus providing the control with information needed to keep the engine out of unsafe modes of operation. Engine component designers can capitalize on this by reducing their safety factors used to account for plant uncertainty. These reductions in design margin can be used to reduce weight, improve performance, or increase life, depending on the requirements of a particular application.

Control system weight reduction is of primary importance within IHPTET, especially as other component areas pursue technologies driving toward an overall 50% engine weight reduction (for a given maximum thrust rating). For example, advanced aerodynamic designs will reduce the number of compressor stages required to achieve a given pressure ratio. Counter-rotating spools enable the elimination of a complete turbine vane cascade. Revolutionary structures made from advanced organic matrix composite (OMC), metal matrix composite (MMC), and intermetallic materials will reduce weight throughout the engine. In the absence of developments aimed at weight reduction, the C&A portion of engine weight would grow from the current 15-20% to 30-35%. To further aggravate this situation, control system complexity continues to grow with time. Figure 6 shows this trend in

terms of total control system inputs and outputs (I/O). More I/O means more wires, connectors, switches, valves, actuators, or sensors, i.e., more weight.

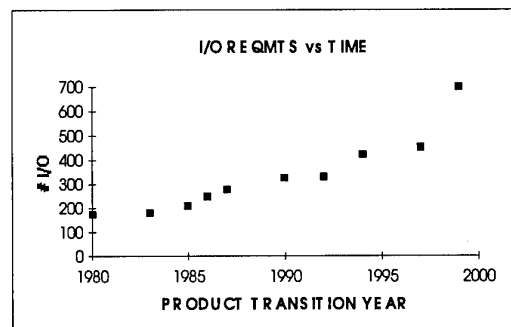


Figure 6. Growth in Input/Output Requirements

Approaches to weight reduction address the challenge at both the component and control subsystem level. The engine control subsystem is an integrated set of components, the responsibilities of which are to create the conditions required to produce requested thrust while protecting the turbomachinery from damage. Engine C&A includes the gearbox, lubrication system, actuation system, fuel delivery system, sensing system, and electrical system. On modern engines, the latter includes one or more digital control computers, depending on the level of redundancy. A typical weight distribution of these subsystems is shown in Figure 7.

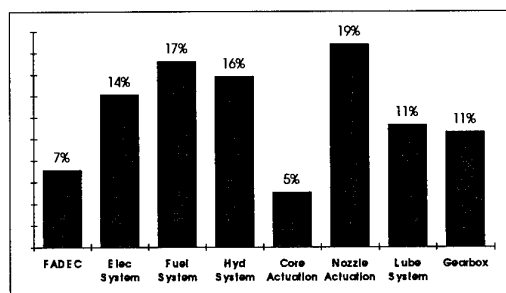


Figure 7. C&A Weight Distribution

Component weight reduction approaches include the application of advanced IHPTET-developed materials to pumps and actuators, which have historically been manufactured primarily from stainless steel. In addition to simple materials substitution, pump suppliers are investigating higher speed designs to minimize size and

variable geometry concepts to eliminate or simplify associated fuel metering hardware. Continued advances in electronic device integration and packaging have resulted in significant FADEC volume and weight reductions. Finally, distributed control technologies are of interest because of their potential to significantly reduce the cost and weight of engine electrical systems.

3. CONTROL SYSTEM FUNCTIONS

A detailed description of control system functions is required to provide a basis for comparing distributed and centralized architectures. The responsibilities of an engine control system are basically the same, whether a distributed or centralized architecture is employed. Figure 8 provides a functional description of control system operation.

To achieve a requested power setting, the control computer must first characterize the current state of the engine. It then compares this information to the desired state and generates an error vector. The result is next input to control algorithms that compute a vector of outputs required to bring the engine to the requested state, i.e., drive the error vector to zero. Typical outputs are gas generator fuel flow, augmentor fuel flow, jet area, and variable stator vane position. The solution space is constrained by the thermodynamical (compression system stall margin), chemical (minimum combustor fuel-air ratio to maintain flame) and mechanical (rotor speed, temperature) limits of the engine.

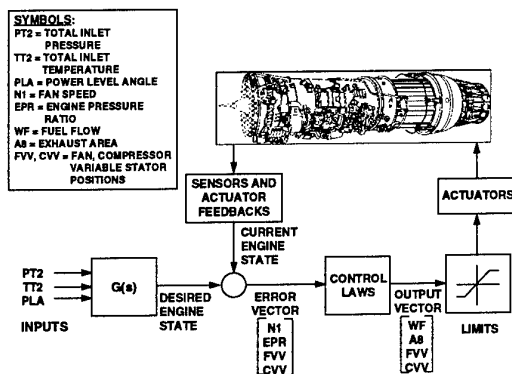


Figure 8. Control system functional schematic

Inputs. System characterization is accomplished with a standard suite of process, diagnostic, and

actuator position feedback sensors. Thermocouples, resistance-temperature detectors (RTDs) and, on some engines, optical pyrometers measure temperature. Capacitance- and vibrating cylinder-based sensors measure pressures. Inductive sensors measure rotor speeds. Linear or rotary variable differential transformers (LVDTs, RVDTs) sense actuator positions. Accelerometers measure vibrations at various engine locations for diagnostic purposes.

Outputs. Motors form the link between actuators and the rest of the control system, regardless of whether the power source is electric or hydraulic. The most common engine actuator type uses an electro-hydraulic servovalve (EHSV) to control power piston position. An EHSV features a force motor (alternatively called a torque motor) that, via an electrical current-driven armature displacement, ports high pressure hydraulic fluid to the side of the power piston required to move it the commanded position. Torque motor power requirements are in the milliwatt range; actuator motive force comes from the hydraulic system. Future engines may employ electromechanical actuation. A typical electromechanical actuator (EMA) linearly translates its piston with a motor-driven ballscrew. The motive force in this case is electrical and the power required is in kilowatts as opposed to milliwatts.

Computations. Analog input signals are scaled, linearized, and converted to digital words (typically 12 bits in length). Once data is in a digital format, it is written to a computer memory location. The control computer's central processing unit then retrieves the appropriate values and performs the necessary mathematical operations to compute control law outputs. These outputs are initially in physically meaningful units, e.g., fuel in pounds per hour or jet area in square inches. A straightforward calculation converts these figures into required actuator positions and, finally, the torque motor currents needed to move the actuator pistons to these positions. Digital devices include one or more microprocessors, memory chips, perhaps some programmable logic devices to control data flow, and some custom chips to control reading and writing from a communication bus, e.g., MIL-STD-1553B. Analog circuits consist of operational amplifier-based signal conditioning circuits to interface with process and actuator feedback sensors and to

generate the currents required to move the actuators. The analog and digital sections are interconnected by A/D and D/A converters. The primary difference between conventional digital control architectures and the proposed distributed control configuration is in the location of these integrated circuits.

4. CENTRALIZED ARCHITECTURE

A control architecture is said to be centralized when all signal conditioning and computational electronics, i.e., those devices that perform the digital control functions shown in Figure 8, are grouped in close proximity. Modern gas turbines have a ruggedized process control computer that contains all of these electronics in a single line replaceable unit (LRU). This LRU goes by many names, e.g., digital engine controller (DEC), digital engine control unit (DECU), engine control unit (ECU), electronic engine control (EEC), digital electronic engine control (DEEC), or full authority digital electronic control (FADEC). The state-of-the-art in digital control is best described by the latter name. Full authority controllers manage the engine from start to shutdown. An example of an advanced FADEC is shown in Figure 9.

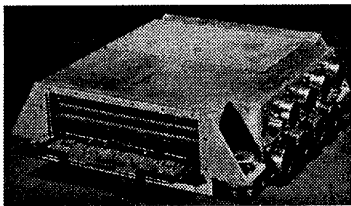


Figure 9. XTE-45 FADEC

This unit was developed for the XTE-45 IHPTET technology demonstrator engine. This FADEC features triplex redundancy to make it suitable for applications with a high degree of engine and flight control integration, e.g., a short take-off and vertical landing (STOVL) aircraft. It has three independent Motorola 68020-based processing channels, input signal conditioning circuitry for a fully triplex suite of sensors, and output drivers for actuators with triply redundant motor coils. Double-sided modules with surface mounted devices were required to fit this functionality into a reasonably sized box. As with all digital engine controls, the electrical system layout is only one

aspect of the overall design. Because FADECs are mounted directly on the engine case, mechanical and thermal management designs are of equal importance. The internal circuit board support structure is carefully designed so that excitation of resonant frequencies is avoided. Vibration isolators are used at each FADEC mounting point. It is fuel-cooled to keep electronic device junction temperatures low enough (typically below 100°C) to maintain component failure rates at acceptable levels. Pressure sensors are mounted in the FADEC to take advantage of its fuel coolant. The XTE-45 FADEC occupies about 1 ft³ of volume and weighs approximately 42 pounds. Although this was a one-of-a-kind technology unit, cost estimates for production units with similar technology indicate that this unit would cost in excess of \$200,000 when manufactured in quantities associated with typical military engine procurement programs.

Referring again to Figure 9, the large number of connectors on the FADEC enclosure gives an idea of the huge quantity of information that is processed. In fact, the minimum size of an advanced FADEC tends to be limited by the number of connectors required to interface it to the engine and aircraft. Harnessing in a dual redundant (duplex) engine control system typically exceeds 50 pounds in weight. This weight is a summation of the contributions from the signal wires, shielding, and harness overbraiding for strength. The number of conductors connecting an electrically redundant LRU to a FADEC is surprisingly large. Consider the duplex actuator interface shown in Figure 10.

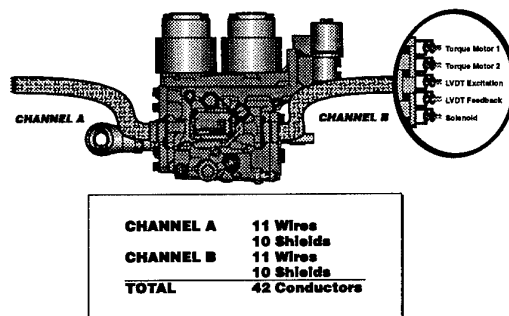


Figure 10. Dual-Redundant Actuator

It includes dual torque motors, each with redundant coils windings, and a dual LVDT interface.

With shielding, there is a total of 42 conductors extending from this actuator back to the FADEC. Sensor interfaces typically have 3 to 6 wires plus shielding for each redundant channel. There are numerous requirements for discrete inputs and outputs. Ignitor relays, switches to initiate various built-in tests (BIT), and switches to transfer from one mode of operation to another are just a few examples. A total of fifty discretes is a reasonable number for a FADEC-controlled engine. An advanced engine may have 10 or more actuators, a like number of sensors (if diagnostic sensors are included), plus discrete inputs and outputs. This means that a dual redundant control system requires in excess of 500 conductors to connect a FADEC to an engine, in addition to pressure lines between measurement points and the FADEC-mounted pressure transducers. This interface complexity is the principal reason that a FADEC is mounted on the engine case, as opposed to an environmentally friendlier location like the aircraft avionics bay.

Redundancy management in a centralized system is handled by the FADEC. A typical FADEC software package includes input signal management logic to select a value from redundant sensor readings to supply to the control laws. As long as some form of channel synchronization is used, such an approach keeps redundant channels operating on the same data. This eliminates the need for sophisticated algorithms for exchanging and comparing control law outputs before sending them to torque motor driver circuits.

5. DISTRIBUTED ARCHITECTURE

Increases in I/O requirements and new, high bandwidth control applications, e.g., active stability control and active structural control, are driving FADEC computational requirements so high that multiple processors will be mandatory in future systems. The key architectural issues are where these processors are located and what level of functionality they need. Using the approach described above involves housing multiple expensive, high performance processors in a FADEC, protecting them with an expensive package, and bringing all process information to them via (in modern applications) 10 or more connectors.

The distributed architecture described here differs from that centralized configuration in that low-level functions like input signal conditioning and output device driver circuits are physically located in the sensors and actuators. Each sensor and actuator also has processing capability and a communication bus interface. A generic, microcontroller-based smart module schematic is shown in Figure 11 (for the remainder of this paper, sensors and actuators with these characteristics will be referred to with adjective smart to differentiate them from their counterparts in conventional control systems).

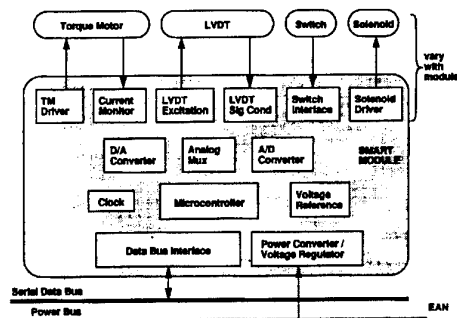


Figure 11. Generic smart module

The complex FADEC discussed previously is replaced by a simple control law computer (CLC) with a communication bus interface compatible with those found on the smart sensors and actuators. Heavy, multiconductor harnesses are replaced by 2 (in a duplex system) simple buses, each consisting of 2 wires to carry power to the remote smart modules and a twisted wire pair or fiber optic cable for digital communication. One could even envision a scheme in which communication takes place over the power wires [2]. The interface between the CLC and the smart sensors and actuators is so simple that off-engine mounting of the controller becomes an attractive alternative with respect to both cost and weight.

Smart sensors consist of a sensing element, an operational amplifier-based signal conditioning circuit, an A/D converter, and a simple processor to convert the reading to engineering units, a small amount of memory, and a bus interface to format the reading and send it to the CLC when requested. The processor also enables the unit to perform periodic or commanded BIT when diagnostics are required.

Smart actuators require additional complexity so that they may perform local loop closure in response to a position command from the CLC. Key smart actuator components include an LVDT interface circuit (excitation and decoding), an A/D converter to digitize the measured position, a processor, memory devices, a D/A converter, a torque motor driver circuit (if EHSV's are used), and a bus interface. Built-in test would consist of the self-diagnostic capability found in smart sensors and current wraparound checks on the associated EHSV torque motor. In the case of both smart sensors and smart actuators, all digital functions could be accomplished by a single integrated device called a microcontroller. Compare the smart actuator shown below in Figure 12 to the equivalent conventional actuator in Figure 10. The reduction in interface complexity is significant.

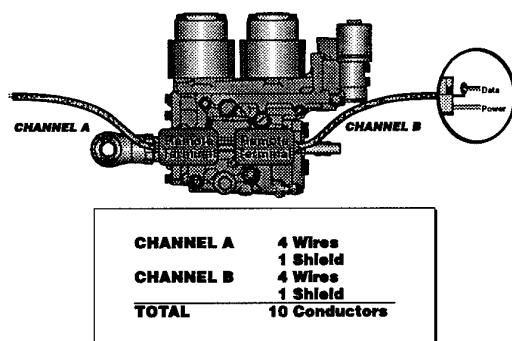


Figure 12. Dual-redundant smart actuator

Distributed processing complicates redundancy management. Redundant sensor values can still be handled by the CLC with the same input signal management schemes used in current systems. However, local loop closure requires that redundant LVDT feedbacks be exchanged between smart actuator channels. Actuator position commands from the CLC will probably also have to be exchanged. These exchanges could be accomplished over the engine control data bus, but this solution greatly increases message traffic and may unnecessarily drive required bus bandwidth. An alternative solution is to include a cross channel data link in each smart actuator module to enable communication with its redundant complement.

Clearly, the CLC and power/data bus are much lighter and less expensive than the FADEC and harness combination in the centralized control system. This is particularly true if the CLC is mounted in the aircraft avionics bay, eliminating the complex packaging requirements associated with engine mounting. The distributed control system's extensive BIT capability makes it superior to a centralized architecture from a maintainability standpoint. Distributed BIT provides the capability to isolate a fault to the control computer, a smart module, or the cable and connectors between them. A centralized system can do little more than determine whether a particular fault has occurred inside or outside the FADEC. Control system modifications are much less costly and time consuming with distributed architecture. Change can be accomplished by merely plugging the new sensor or actuator into the engine communication bus and updating the CLC software. In a centralized system, such a change would require at least a new harness. If the FADEC has no spare capability, it too would have to be modified.

The foregoing discussion ignores a few obvious problems. For instance, the cost payoff from mounting the CLC away from the engine would appear to be offset by the addition of electronics at every sensor and actuator and the need to actively cool each smart module. Similarly, the weight reductions in the control computer and harnessing would be mitigated by the addition of a control electronics and cooling system hardware to every sensor and actuator. However, these penalties assume no new technology. In fact, there are developments underway in high temperature electronics and high density electronics packaging that address these apparent shortcomings of distributed control. The combination of these technologies offers a way to get the benefits of distributed control while eliminating the cost and weight penalties.

6. ELECTRONICS MINIATURIZATION

Multi-chip module (MCM) technology [3] can minimize the size and weight impact of adding electronics to sensors and actuators. An MCM consists of several IC chips mounted on a substrate, typically 2 to 4 inches on a side. The chips are interconnected with conductive paths (traces) that are much finer than those found on printed

wiring boards (PWBs). The resulting package typically requires less than half the area and power of a PWB. Two or three MCMs would probably be required to implement the functions shown in Figure 11. These MCMs can be stacked so that the smart module that has only a minimal impact on the weight and size of a typical engine sensor or actuator. Figure 13 shows the projected impact of adding MCM-packaged smart electronics to a speed sensor housing.

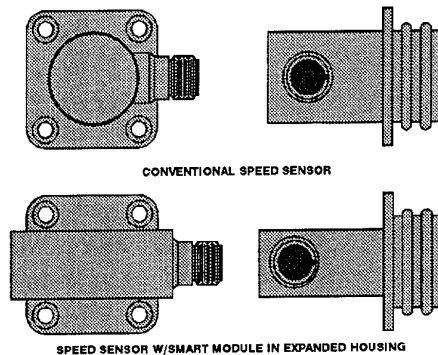


Figure 13. Conventional vs smart speed sensor

The cost impact of making sensors and actuators smart can be minimized by developing a standard set of MCMs applicable to multiple engines. All engines require speed sensors, RTDs, thermocouples, and pressure transducers. The vast majority of current engines use hydraulic actuators with torque motor-driven servovalves. There is no technical reason that a company, or for that matter the entire gas turbine industry, can not define standard interface electronics for commonly used sensors and actuator torque motors. Large volume purchases of MCMs are the surest way to drive down their cost. A cost analysis performed in the DCS program projected electrical system acquisition cost reductions from \$100,000 (on-engine FADEC) to \$150,000 (off-engine FADEC).

7. HIGH-TEMPERATURE ELECTRONICS

The real key to realizing the full benefits of distributed processing on an advanced gas turbine engine is the elimination of the temperature limitations of silicon-based electronics. A requirement to actively cool smart module electronics would likely turn the cost and weight benefits of

distributed control into penalties. The maximum temperature rating for silicon signal electronics is 125 °C (257 °F). External ambient engine temperatures range from two to three times that value (Figure 14), while case temperatures can be even higher (Figure 15). Device junction temperatures of 85 °C, 200 °C, and 300 °C are shown in Figure 14. Their placement assumes a 50 °F difference between junction temperature and nacelle air due to internal heat generation during a typical mission and shielding to protect aft-mounted components from the hot engine case.

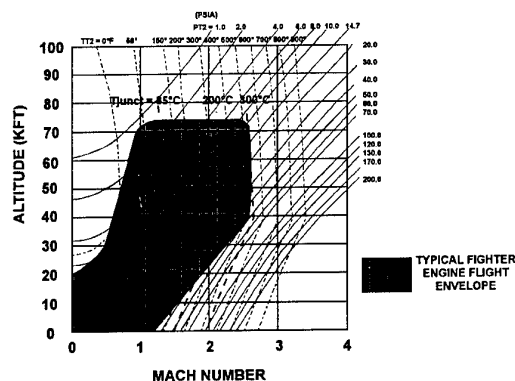


Figure 14. Nacelle hot-day stagnation temperatures

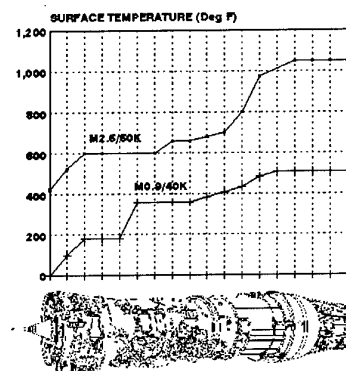


Figure 15. Engine external case temperatures

Commercial engine FADECs are mounted on a relatively cool fan case, well away from the hot case surrounding the engine core. The subsonic speed of passenger aircraft makes convective air cooling adequate for maintaining electronic device junction temperatures at acceptable levels. This thermal management scheme is not acceptable for a distributed control system. Smart

modules would be mounted on the core engine case. If these modules used silicon electronics, some form of active cooling would be required.

Installation and mission differences make active cooling of engine FADECs necessary on military fighter aircraft. Convective cooling is not effective in such applications due to low nacelle air velocity and excessive air and engine case temperatures during certain mission legs. Current military FADEC enclosures are designed so that heat is conducted away from the electronics to fuel-cooled plates. Because fuel delivered to the engine fuel pump has already been used as a heat sink for various aircraft heat loads, a separate cooling circuit using fuel directly from the tank is usually required (Figure 16).

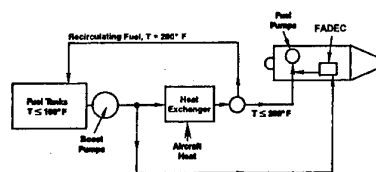


Figure 16. Fighter Engine FADEC Cooling

Using a separate cooling circuit adds cost, complexity, and weight, but it is necessary to keep electronic device junction temperatures at the level required for a full service life design.

A semiconductor technology with a continuous operating temperature capability in the 250 °C - 300 °C range would satisfy all smart module requirements except for nozzle actuation. Silicon-on-insulator (SOI) technology, commonly used in space applications due to its radiation hardness, also has high temperature capability [4]. Further investment in this technology could provide 300°C smart modules in the near term. However, there remains some question about the reliability of SOI when operated at its maximum temperature capability. Silicon electronics are derated from the specified 125 °C maximum to less than 100 °C when used in engine control applications. Reliability modeling shows such derating is required for full service life designs. Also, a smart module located on or near the nozzle may require electronics with a temperature capability in excess of 500°C. In anticipation of this future

need, the IHPTET C&A team began investigating potential high temperature semiconductors in 1986. The Future Advanced Control Technology Study (FACTS) [5] included an assessment of candidate high temperature semiconductors. In 1987, the Air Force awarded a small contract to Cree Research for the development of a high temperature transistor manufactured from silicon carbide (SiC). The success of this program made SiC the focus of Air Force-sponsored research and development in high temperature electronics technology.

Property	Si	GaAs	AlGaAs	SiC
Melting Point (°C)	1412	1238	1304	2830
Bandgap (eV)	1.12	1.43	1.92	2.86
Thermal Conductivity (W/cm °C)	1.5	0.5	0.1	5.0
Breakdown Electric Field (kV/cm)	300	400	500	4000
Electron Mobility (cm ² /VA)	1400	8500	3000	1000
Drift Velocity (cm/sec)	1x10 ⁷	1x10 ⁷	1x10 ⁷	2x10 ⁷

Figure 17. Physical Properties of Semiconductors

The high temperature properties of SiC have been well known for over thirty years [6]. Its physical properties make it attractive for a wide variety of applications (Figure 17).

Melting point and bandgap correlate with high temperature capability. High thermal conductivity and breakdown electric field are important attributes for power electronics. Electron mobility and drift velocity relate to switching speed, important in high frequency applications like radar. Silicon carbide is superior to silicon (Si), gallium arsenide (GaAs), and aluminum gallium arsenide (AlGaAs) for all applications except those requiring extremely high speed operation. However, interest waned in SiC in the 1970's, primarily due to difficulties in producing high quality wafers. Poor wafer quality translates into poor device yields and high cost, a fatal drawback in the electronics business. Cree Research made breakthroughs in wafer processing technology that led to the resurgence of interest in SiC described above.

Significant progress has been made since the initial discrete device demonstrations in the late 1980's. The Air Force Wright Laboratory and NASA Lewis Research Center have sponsored both in-house and contracted work aimed at making further improvements in SiC wafer quality and size, developing SiC power devices and integrated circuits, and applying them to gas turbine engine sensing applications. Westinghouse and General Electric (both the Aircraft Engine and Corporate Research and Development Groups) have been the primary contractors in this series of programs. Recent accomplishments include the development of an operational amplifier integrated circuit and an afterburner light-off detector (SiC also has optoelectronic properties that make it an excellent flame sensor). Figure 18 shows a conventional vacuum tube-based light-off detector (LOD) next to the SiC sensor.

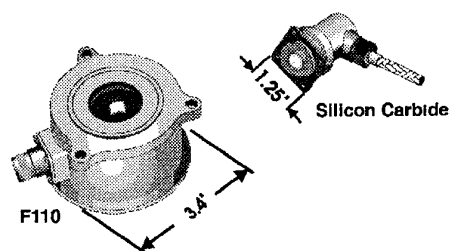


Figure 18. LOD Comparison

An IHPTET-sponsored program to develop a pressure sensor with SiC electronics was initiated in late 1994. The high temperature capability of this sensor will allow it to be close-coupled to the measurement point, instead of being mounted in the FADEC as in current systems. This program is the first step in high temperature smart module development. The next step is to expand current SiC developments into the realm of digital electronics. Silicon carbide processors, memory devices, and bus interfaces will be required if the smart module is to have the worst-case 500 °C temperature capability. Smart module functions in the proposed distributed system have purposely been kept at a basic level to minimize the sophistication required in these digital devices. It is easier to envision an 8-bit SiC microcontroller than a 32-bit, multimillion transistor microprocessor like those found in the current generation of desktop computers. The development of this device is a critical milestone in the IHPTET Phase

III C&A technology plan. One or more SiC smart modules will be demonstrated on an experimental technology engine around 2003.

8. CONCLUSION

The overall objective of the IHPTET initiative is to provide revolutionary improvements in gas turbine engine performance and cost. These seemingly contradictory goals have caused the IHPTET controls community to rethink traditional approaches to engine control system development. The search for improved engine performance requires increased control system capability. Adding functions to the currently-used centralized control architecture has resulted in a complex, expensive FADEC and heavy harnessing to interface it to the rest of the engine. A distributed architecture with advanced technology features has distinct cost and weight advantages over a centralized configuration for many complex control applications. The distribution of processing capability throughout the engine eases the computational burden, eliminates extensive I/O circuitry, and simplifies interfaces in the FADEC. Off-engine mounting becomes a viable alternative. Multi-chip module packaging offers a way to minimize the adverse size, cost, and weight impact associated with adding intelligence to sensors and actuators. High temperature electronics remove the requirement to actively cool the distributed electronics. Silicon-on-insulator electronics can be matured in the near term for this application; SOI temperature capability is adequate for most smart modules. Silicon carbide electronics are being developed because they satisfy all engine smart sensing and actuation needs and will be more reliable at any given operating temperature.

Distributed control is already making positive performance and cost reduction contributions to the many industries in which process control is critical to product development. It is showing up in a wide variety of products, most notably automobiles. Advances in electronics packaging and temperature capability will bring these benefits to advanced gas turbines, in both military and commercial applications.

9. ACKNOWLEDGMENTS

The Author wishes to express his gratitude for the contributions to this paper made by Dr. Phillip L. Shaffer of GE Aircraft Engines and Mr. Stephen J. Przybylko of Wright Laboratory. Dr. Shaffer is the Principal Investigator for the DCS program. He performed the analyses that support some of the contentions in this paper and created some of the figures that appear above. Mr. Przybylko has been the champion of high temperature electronics for engine controls since the FACTS program and provided materials that were of great help in the preparation of this manuscript.

10. REFERENCES

- [1] Skira, C.A., "Cost Reduction of Advanced Turbine Engines," AIAA-95-3024, 31st AIAA/ASME/SAE/ASEE Joint Propulsion Conference, San Diego CA, July 1995
- [2] Heath, S., "Echelon: Networking Control," IEE Review, October 1992
- [3] Tummala, R.R., et. al., "Multichip Packaging - A Tutorial," Proceedings of the IEEE, Volume 80, Number 12, December 1992
- [4] Grzybowski, R.R., Tyson, S.M., "High Temperature Testing of SOI Devices to 400 °C," 1993 International SOI Conference Proceedings, pp. 176-177
- [5] Przybylko, S.J., "Future Advanced Control Technology Study (FACTS) -- A Look at Emerging Technologies," AIAA-87-1930, 23rd AIAA/ASME/SAE/ASEE Joint Propulsion Conference, San Diego CA, July 1987

SAFETY CRITICAL SOFTWARE DEVELOPMENT FOR ADVANCED FULL AUTHORITY CONTROL SYSTEMS

Franco Tortarolo, Guido Crosetti, Carmine Difilippo

FiatAvio, Control Design
C.so Ferrucci 112 - 10138 Torino ITALY
Phone: +39-11-6858624
Fax: +39-11-6858486

Summary

The Full Authority Digital Engine Controls (FADEC's) have evolved to become one of the key element enabling improvements in engine performance, lifetime, reliability, testability and maintainability. In parallel the role of the software has evolved to the point where software has become the "soul" of the current generation of FADEC's.

Software has become, and will continue to be, one of the key safety critical elements of an engine, due to the ever increasing reliance on software to enhance engine safety, performance, reliability, testability, flexibility and maintainability.

The FADEC for the European Fighter Aircraft (Eurofighter 2000) has been developed by a four nations consortium. The software for the Eurofighter 2000 engine (EJ200) FADEC has been developed on a workshare basis under MTU responsibility. The multinational team, comprising of personnel from the four nations, has operated partly co-located at MTU and partly geographically distributed in the four nations.

This paper focuses on the experience gained during the specification and development of the System Development Environment and its subsequent use in the development of the safety critical software for the EJ200 FADEC where performance, reliability, testability and maintainability have equal priority. It concentrates on the methodologies and tools employed during each software development

phase with particular emphasis on safety related techniques.

The major lessons gained from the experience along with areas for future enhancement are summarized.

1. Introduction

DECU, ECU, FADEC are all commonly used synonyms, in the aerospace industries, to refer to a box jam-packed with electronics, the size of a couple shoe boxes, with the power consumption of a conventional light bulb and an equivalent mass of a portable television set, responsible for ensuring that the engine provides the corresponding thrust for each flight condition with the minimum pilot workload.

Engine control theories are well understood and have been applied on jet engines with mechanical and hydraulic system for many decades. However, the almost recent application of microelectronics has lead to a Copernican revolution. The rapid evolution in the field of microelectronics (increased performance and reliability and decreased cost, size and power consumption) has been the key factor during the last 20 years in the design of "more intelligent" and "true fault tolerant" 'Full Authority Digital Engine Control', without any need for mechanical back-up systems.

In parallel, microelectronics have revolutionized the application of software in FADEC's to improve engine performance, safety, lifetime, reliability, testability and maintainability.

Despite the fact that software is universally considered flexible and easy to change, engine companies have discovered that software has become one of the challenging elements in a FADEC due to its high performance and safety critical nature. In fact engine companies have discovered, from experience, that development of safety critical software is expensive, extremely time consuming and requires specialized teams working with strict disciplines and state-of-the-art System Development Environments (SDE).

A brief overview of the EJ200 FADEC architecture will be provided to give some idea of the degree of complexity of the hardware.

This will be followed by a look at the approach utilized to define the SDE used in the development of the EJ200 FADEC safety critical software. The approach to tailoring the varying customer and different partner company requirements and all the constraints imposed by the available or imposed tools will be presented, followed by details of the method and tools employed by the four nations for the system and software development.

A significant example, the Coding and Unit Testing Phase, will be magnified in order to provide a better understanding of the entire process.

At the end problems and winning points of the Eurojet experience will be summarized.

2. The EJ200

EJ200 is a two spool turbofan with variable inlet guide vanes and a convergent-divergent exhaust gas nozzle. Two of these engines equip the Eurofighter 2000.

The engine is under development by an European Consortium, Eurojet, composed by four partner companies: FiatAvio (Italy), ITP/SENER (Spain), MTU (Germany) and Rolls Royce (UK).

Each EJ200 is controlled by an engine mounted FADEC, called DECU (Digital Electronic Control Unit).

The first successful flight of the Eurofighter 2000 with EJ200 engines was achieved in June 1995.

3. DECU Hardware and Software

Every time a new engine is designed the requirements on the Control System become more and more stringent:

- ◆ higher reliability, testability and safety
- ◆ lower power consumption
- ◆ less mass and volume
- ◆ higher immunity to EMC and lightning
- ◆ more severe operational environmental conditions
- ◆ increased functionality and Input/Output
- ◆ lower maintenance cost

This is a natural evolution and mirrors the advances in microelectronics (increased performance and reliability and decreased cost, size and power consumption). The combination of increased complexity of FADEC functionality and advances in microelectronics have lead to more and more complex hardware and software.

Figure 1 spots the growth of the internal memory size of some ECU's of the last decades, as an approximate indication of the increase in complexity.

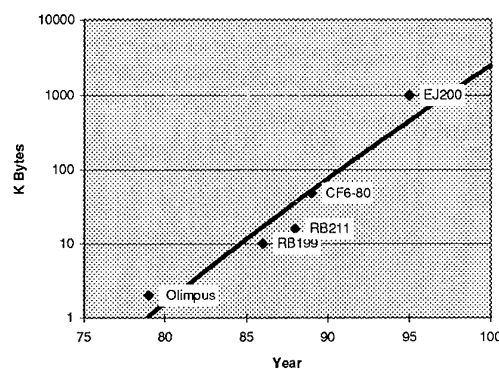


Figure 1: Increase of ECU's Program Memory from the 70's to 90's

The EJ200 DECU resident software implements all the control laws and schedules in order to provide the air flow system and fuel system with command signals required for the EJ200 engine control function and to provide all functions to detect and compensate

for control system defects and to provide monitoring data.

In line with common practice during the last two decades, the EJ200 DECU is designed as a dual lane fault tolerant system (Figure 2). The hardware and the software in each lane is identical.

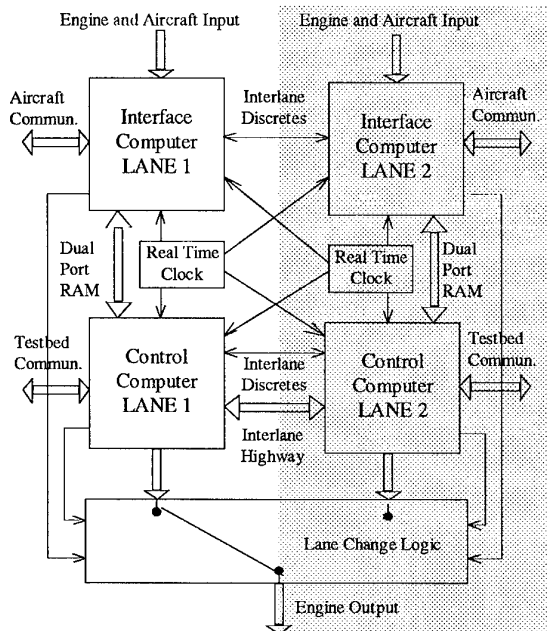


Figure 2: DECU Hardware Block Diagram

The DECU resident software executes in both lanes in parallel and is capable of operating in Master or Slave mode. The mode of operation in each lane is determined by the lane in control information provided by the lane change logic, which also permits control outputs to the engine only from the Master lane. The DECU resident software is capable of performing a lane deselection at any time on any lane to disable the lanes outputs to the engine.

Synchronization between the two lanes is provided by the Master lane real time clock.

The Interlane Highway permits the transfer of both performance and status information between the two lanes at fixed synchronization points. This permits supervision of input signals, used in the engine control logic, processing both the own lane and other lane data on each lane.

Identical input signals are available at each lane. In addition, the Interlane Highway permits the transfer of the Master lane data to enable the Slave lane to track the Master lane, ensuring a smooth transfer of lane control in case of a lane change.

Each lane comprises two Motorola 32 bit MC68020 processor in order to deliver the required performance.

The DECU resident software architecture permits the distribution of the software across the two processor and the degree of distribution is limited only by the interfaces (data inputs) available at each processor (Figure 3).

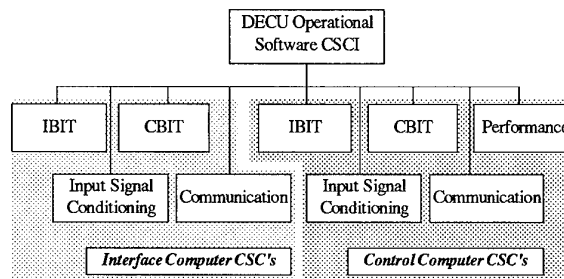


Figure 3: DECU Software Structure

Communication of data between the two processor of the same lane is achieved via dual port memory.

This concept has already permitted the hardware architecture to evolve from that illustrated in Figure 4a to Figure 4b without adverse effect on the software.

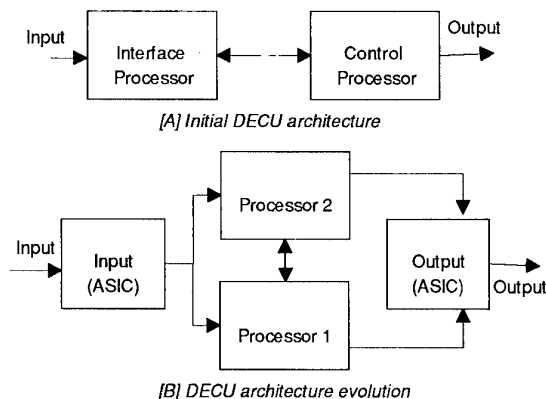


Figure 4: Lane Data Flow in the two DECU architectures (one lane)

The essential lesson learned is that a rigid hardware structure leads to a rigid software structure with little degree of freedom for the

software designs. A flexible hardware structure permits a far more freedom to the software designers in terms of architecture and degree of distribution of software to achieve a fine load balance and data throughput.

As a consequence the original DECU, oriented to allocate the input functions to one processor and the control laws to the other, was modified. A new architecture (Figure 5), more modular and multipoint, has been designed and the restrictions overcome.

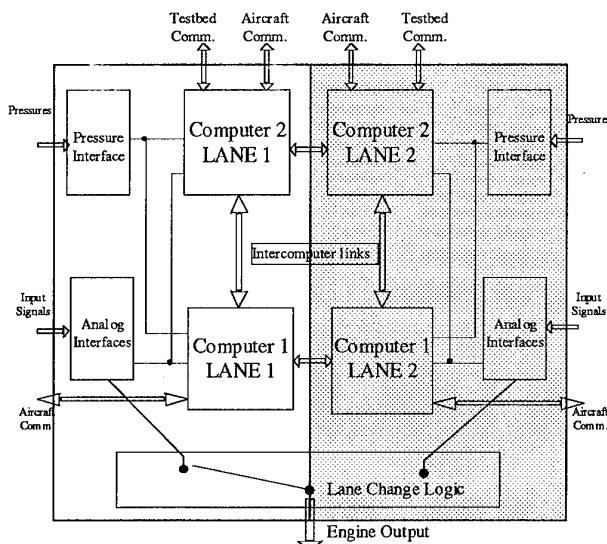


Figure 5: New DECU Block Diagram

It is based on higher confidence in complex ASIC¹s which perform Input/Output functions of the different signal types (frequency, analogue, thermocouples etc.).

ASIC's can be addressed indifferently by the two processors and the information can go from one source to almost everywhere inside the DECU. This configuration guarantees the maximum flexibility reducing hardware development and maintenance costs since the electronic cards are identical.

The software of the DECU, about 34000 line of Ada source code, has been categorized and developed as Risk Class I² in accordance with RTCA-DO178A³). It has been jointly developed by the four Partners under MTU

responsibility. The multinational team has operated partly co-located in MTU and partly geographically distributed.

To develop the DECU software and other on/off board engine electronic equipments (Engine Monitoring Unit, and Test Equipments) the Eurojet SDE was created.

4. System Development Environment

The use of integrated SDE's is common in aerospace software projects. However, the EJ200 SDE is peculiar in that it has been influenced not by only technical factors but also by national and political constraints particular to this military project.

These can be grouped into three categories:

- **Contractual Customer Requirements**

- ⇒ compliance with: RTCA-DO178A, DoD2167⁴, AQAP13⁵
- ⇒ equal importance for software Maintainability, Testability, Reliability and Performance
- ⇒ Ada Language for MC68020 target with a common Ada Compilation System with the aircraft supplier
- ⇒ Vax/VMS environment
- ⇒ maintainable during the aircraft life

- **Characteristics required by the Products**

- ⇒ complex functionality to be performed in short cycle times
- ⇒ complex hardware architectures
- ⇒ high integrity
- ⇒ years to be developed, with large teams and sometimes resource turnover

- **Internal Consortium Targets**

- ⇒ capability to integrate four Partner Companies geographically isolated
- ⇒ common environment for all the software products and uniform approach to share the know-how
- ⇒ proven and well integrated environment to reduce risks and costs

These requirements and constraints led to the definition and development of an SDE

¹ ASIC: Application Specific Integrated Circuit

² Risk Class I: "Functions for which the occurrence of any failure condition or design error would prevent the continued safe flight and landing of the aircraft."

³ RTCA-DO178A: Software Considerations in Airborne Systems and Equipment Certification

⁴ DoD2167: Defence System Software Development

⁵ AQAP-13: NATO Software Quality Control System

composed of a set of commercial and Eurojet proprietary system and software development tools and a set of development standards. The development standards include Standards for both system and software development.

The Standards define the methodologies to be applied (Configuration Control, Quality Assurance, System and Software Development, Verification and Validation) and the application of the tools.

The Eurojet Consortium made a lot of effort in order to have a successful SDE.

A special working group was dedicated to define, maintain and agree the SDE with the Customer, working in parallel with the development teams.

The tailoring of these requirements involved the study of the process, the evaluation of the best methodology for each discipline involved (QA, System and Software Engineering, Configuration Control, Project Management etc.), the selection and integration of the tools.

Approaching the SDE creation, the ideal solution is to integrate tools and methods at the state-of-the-art, but generally this is not always possible. The Eurojet approach was to give a strong emphasis to the appropriate method, in order to guarantee safety, and to balance new tools and their maturity (Figure 6) with an eye to the long SDE life.

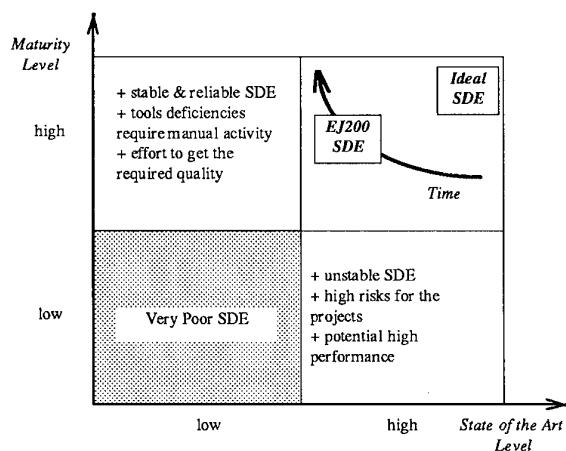


Figure 6: EJ200 SDE Maturity and State-of-the-art Evolution

In fact during the tailoring process the following guidelines were taken into account:

- ◆ method is more important than tool
- ◆ compromise advanced tools and their maturity
- ◆ reduce as possible the number of tools
- ◆ safety is achieved by an overall engineering approach
- ◆ safety is achieved through simplicity
- ◆ avoid the 'tools phobia'

The final product was a set of Standards and Tools.

The harmonization of all these aspects has proved to be a very complex and difficult task. The SDE is still evolving and lesson learned towards achieving the first successful flight and on-going suggestions from development teams are currently under implementation.

In the following paragraphs an overview of the SDE methodologies employed in the EJ200 DECU development lifecycle is presented.

4.1 System Development

System Development is covered by a set of three standards defining the system level methods:

- ♣ *System Development Standards*
- ♣ *System Configuration Management Plan*
- ♣ *Methods and Tools Application*

A formal system development is carried out through five phases: System Requirement Analysis, System Design, System Implementation, System Test and Integration, System Qualification (Figure 7).

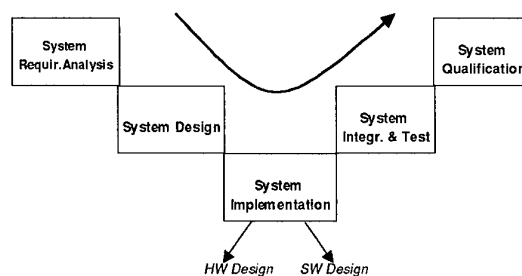


Figure 7: System Development Lifecycle

All phases are based on a top-down approach. Requirements traceability is performed during each phase using the SDE tool Epos.

During the first phase all requirements of the Contractual Specification are formally identified and categorized with the use of a tool (Epos) and then integrated with requirements coming from the engine and aircraft design.

In order to guarantee a complete requirement capture, the SDE requires different points of view (maintainability, safety etc.).

The requirements are allocated, through a multi-step top-down design process, to the various sub-systems of the Engine Control and Monitoring System (ECMS), including the DECU (Figure 8).

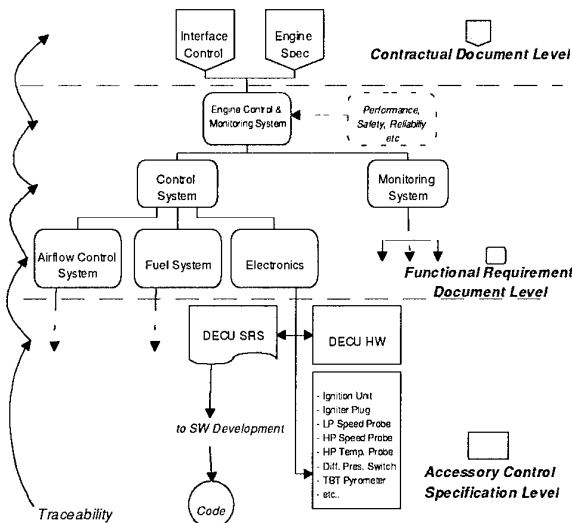


Figure 8: ECMS Documentation Tree

Data flow analysis is performed among the different (sub-)sub-systems in order to verify the correctness of the data communication.

During the third phase each (sub-)sub-system is designed (hardware/software development) and then integrated and tested (phase four).

This methodology allows the complete traceability of Customer's requirements through each phase of system development and subsequently each phase of the software development lifecycle.

The SDE tool Epos supports both the requirements traceability and categorization. Thus requirements can be not only traced but also analyzed to ensure their eventual implementation within the correct sub-system. The Epos tools also supports data flow analysis at each phase to check for both

correctness and consistency. Hazard Analysis and Fault Tree Analysis, up to Software Requirements level, are performed in parallel.

At the end of the System Development Lifecycle, Qualification activities are performed through the Development Rig Testing, the Bench Engine Testing and Flight Development Trials. The methods need functional level requirements to be categorized in terms of:

- 'degree of compliance' (i.e. the level to which compliance will satisfy the Airworthiness Authorities),
- 'activity configuration' (i.e. the build standard required to prove compliance)
- 'method of compliance' (i.e. how compliance is achieved).

Then the conformance is verified and declared by analysis, demonstration, inspection or test.

During each phase all documents are kept under configuration control. All modifications are configured and tracked using a sophisticated problem report/design change and build-control mechanism.

4.2 Software Development

The EJ200 SDE requires a classical waterfall software life cycle (Figure 9) with a formal review at the end of each phase.

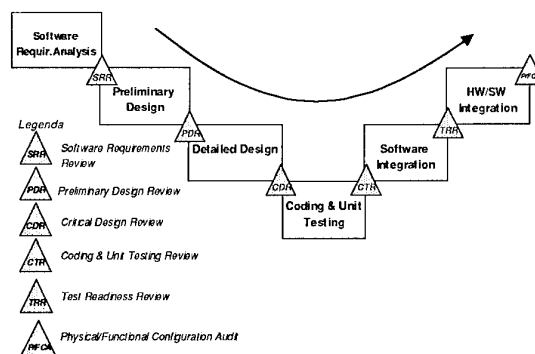


Figure 9: Software Development Lifecycle

Five Standards define the software methods:

- ♣ *Software Quality Evaluation Plan*
- ♣ *Software Development Standard*
- ♣ *Software Configuration Management Plan*

♣ *Methods and Tools Application*

♣ *Documentation Standards and Model Text*

The strong sequentiality, imposed by the classical waterfall with formal review at the end of each phase prior commencing with the next phase, was modified to permit phase overlapping and prototyping.

Phase overlapping reduces the overall timescales and allows better employment of available resources.

Prototyping introduces such benefits as early system/software requirements validation, experimental design solution and early critical software components realization and test (timing, algorithms, etc.). Both modifications increase the control and management activities but lead to a long term risk reduction through early identification of problems.

The methodology focuses on the 'what to do' at the Software Requirements Level and on 'how to do it' at design level.

Despite the general tendency to use 'object oriented' methods for the software design, a classic Yourdon Data Flow Design approach is recommended, with a degree of freedom for the project dependent features.

Test requirements are requested at different level of details as early as possible, in parallel at each phase.

As for the System development, from the Software Requirement Specification down to the code, strong traceability is requested, supported by the same tool, Epos.

Although the software safety is reached by an overall approach, the next section presents in detail the "Coding and Unit Testing Phase" in order to illustrate some of the specific activities required by the Standards.

4.2.1 Coding and Unit Testing Phase

In this phase the code is produced and tested at module level (i.e. Ada compilation unit).

As in any other phase Performance, Reliability Maintainability, Safety and Testability are the quality goals to reach.

They are reached through Analysis and Test activities which in turn are measured and assessed (Figure 10)

A lot of effort was dedicated in order to have this phase automated as much as possible. However some of the activities are still performed manually with very expensive manpower involved.

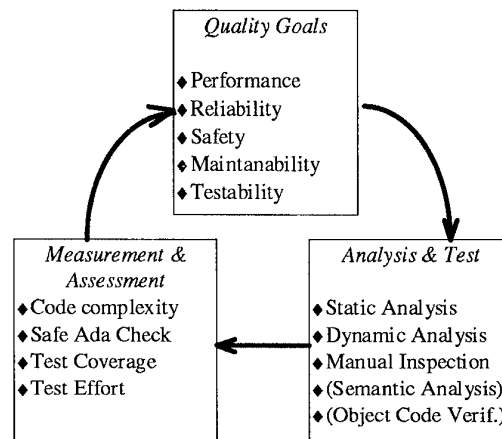


Figure 10: Code Goals, Analysis and Measurements

The principles used to define Analysis and Test strategy were:

- 1) use strategies which efficiently combine techniques
- 2) define test techniques to minimize the variable performance of testers
- 3) provide additional automated support for testers
- 4) emphasize guideline and training

Driven by the above rules, Eurojet code testing methodology is an integrated sequence of two macro steps:

Static Analysis & Dynamic Analysis

The SDE tool Ada Compiler, Testbed, Test Harness and the Emulator support the two analysis.

Static Analysis

The Ada code is analyzed both manually and by tools without executing it. There are five categories of checks (Figure 11):

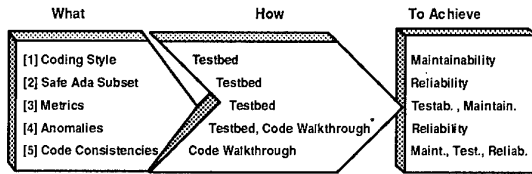


Figure 11: Static Analysis

[1] Coding Style (\Rightarrow Maintainability)

Code pretty printing is performed to have a common quality layout to aid readability. A detailed data naming convention is specified by the Standards and checked against all data, compilation units, filenames etc.

[2] Safe Ada subset (\Rightarrow Safety, Reliability)

Due to the safety critical nature of the DECU software, the use of all features of the Ada language is not permitted. Following an extensive EFA project study, an Ada language subset, called "Safe Ada" was specified. The use of Safe Ada subset is mandatory to the project and varies depending on the risk class of the software to be developed (Figure 12).

Ada Feature	LRM Ref.	Risk Class		
		I	II	III
Task	9.	C	B	B
Access Type	3.8	C	C	B
Generic	12.	C	B	B
Go To	5.9	C	C	C
User Exception	11.	C	B	B

Figure 12: Example of Ada Subset

There are three classes of construct:

Class A: there are no constraints on the use of this language feature

Class B: this language feature may be used, but its use shall to be justified and recorded during the Code Walkthrough

Class C: this feature shall not be used

An automatic checker verifies the correct employment of the Safe Ada constructs against the corresponding software risk class and reports any detected violations.

[3] Metrics (\Rightarrow Testability, Maintainability)

A good set of metrics indicates the complexity of the code under test. No errors are

discovered, but indications are presented on the complexity, the degree of nesting and the reducibility of the code structure.

Limits, depending on the class of software have been fixed. Any violation must be manually verified and officially approved during the review (Figure 13).

Type	Description	Limit
McCabe	Complexity of the code graph	< 10
Essential McCabe	Code Structure	0
Up-Up Knots	Non standard language constructs	0
LCSAJ Density	Number of paths that flow into the same point	< 10
Comment Density	Comment (Comment+Ada Statement)	>60%

Figure 13: Complexity Metrics for Risk Class I

[4] Data, Control, Information Flow Anomalies (\Rightarrow Safety, Reliability)

This check allows the discovery of anomalies in the code. Some of them can be errors. Possible anomalies are related to the Data Flow (sequence of actions on variables suspected to be erroneous), Control Flow (anomalies in program's control structure) and Information Flow (anomalies on variables interdependencies).

[5] Code Consistencies (\Rightarrow Safety, Reliability, Maintainability, Testability)

The code consistency means to verify that the code performs what the specification requires in a complete way. It is performed manually during Codewalkthrough (Figure 14).

Points of View:
Usage of types
Clear and legible code
Spelling errors
Meaningful comments
Code completeness versus design documents
No known compiler bugs affect the code
Improvement of testability
...

Figure 14: Code Consistency - example of points to be considered during the Codewalkthrough

Dynamic Analysis

The Ada code is executed on a limited (and validated) set of input values and its output correctness checked. Test cases are developed using two classical methodology: white box and black box.

The '**white box**' concerns the program's internal structure of the code and test cases are based on the logic or control flow.

The '**black box**' concerns the external (functional) behavior of the program as prescribed in the specifications. They are defined during the previous design phases.

The design of test cases is performed by independent people from coders.

The following methods drive the testers during the test cases design:

White Box:

- > Statement Coverage: every statement of the program must be executed
- > Branch Coverage: each decision must be set true and false at least once
- > Decision Condition Coverage: each condition in a decision must be set true and false at least once and the decision must be true and false at least once
- > Path Coverage: all possible paths must be executed

Black Box:

- > Range Coverage: each input variable is set to the particular boundary values (min., max., above max. etc.)
- > Error Guessing: tester experience and intuition is used in the test cases definition
- > Functional Coverage: the functionality is tested as much as possible against the requirements

The designed test cases must be proven to have an adequate coverage (Figure 15). This is performed automatically using Testbed tool. Once the coverage has reached the appropriate value the code is executed with all test cases (on host and target) and the results compared with the expected ones.

A support tool, Test Harness, helps the tester during this phase in order to extract the code from configuration control, to compile and

link the source, to execute it and to report the results.

<i>Method</i>	<i>RC I</i>	<i>RC II</i>	<i>RC III</i>
White Box			(recommended)
Statement	100%	100%	100%
Branch	100%	100%	100%
Path (LCSAJ)	100%	50%	20%
Decision/Condition	100%	100%	0%
Black Box			(recommended)
Above Range	Yes	Yes	Yes
On Range	Yes	Yes	Yes
Below Range	Yes	Yes	Yes
Out of Range	Yes	Yes	No
In Range	Yes	Yes	No
Error Guessing	Yes	Yes	No
Functional	Yes	Yes	Yes

Figure 15: Risk Class I, II, III Test Cases Coverage

Semantic Analysis & Object Code Verification

Two additional testing activities are still under evaluation with the Customer. These should be applied to DECU software in order to achieve the qualification for the production phase.

Semantic Analysis

It is a method to automatically verify the correctness of the code versus the design to establish that the code will do exactly what is intended to do and nothing else. This activity requires code annotation as part of the normal software development activities.

Object Code Verification

The Ada compiler translates the high level code into machine code.

This process may introduce different code structures and paths of the real executable code. This means that the coverage reached with dynamic testing in Ada may not be enough. The idea is to move the path coverage from the Ada source to the real assembler code produced by the compiler.

Unfortunately tools are still immature, complex and of questionable value. The evaluation is still ongoing.

4.3 The Tools

All EJ200 SDE tools are the result of a requirement analysis, a commercial evaluation

and subjected to an Eurojet Acceptance Test prior the official delivery. Moreover the long term support is taken into account.

The selection was particularly exhaustive in tools which can have some impact in terms of safety of the code, like the Ada Compilation System. In this case benchmarking of all available Ada compilers was carried out.

A special EFA contract with the Supplier was stipulated in order to implement some special features, and submit the compiler to a strong testing before the release. Moreover a detailed study about the compiler translation mechanisms from Ada to assembly was carried out to gain confidence that safety is guaranteed.

As far as possible immature tools have been rejected to avoid developing the application software in parallel with the tool itself.

The number of tools in the SDE has been kept to an absolute minimum to minimize the user learning phase and to avoid the problems with tools integration and continuous migration to new versions (and additional problems).

Despite employing this simple philosophy, a great deal of effort has gone in setting up the EJ200 SDE. Tools limitation and bugs have resulted in several extensive reviews of the development methodologies and practices.

All tools are based on Vax/VMS⁶ (Figure 16):

Epos⁷ and Interleaf⁸

Epos is the core design and documentation tool.

It supports requirements analysis (system and software), software design, project management and it supports automatically the traceability analysis.

In order to gain the benefits of modern desktop publishing tools and have a better quality documentation, Epos has been integrated with Interleaf;

Lifespan⁹

Tool for performing Configuration Control of all documentation and software;

Ada Compilation System¹⁰

Ada Compiler and Cross-Compiler with debuggers, Language Sensitive Editor, Source Code Analyzer, Performance Code Analyzer;

Testbed¹¹

A suite of software analysis tools, comprising Static Analysis and Dynamic Analysis, used during the software testing phase.

It checks the Ada subset, performs metrics and the Data/Control/Information Flow and the test cases coverage for the dynamic analysis;

Emulator¹²

The HP 64000UX development system with probes for hardware debug, software testing on the real DECU, timing measurements and integration;

Test Harness¹³

Suite of tools developed by the Eurojet Consortium to integrate the software testing environment and to help automatic unit testing so as to avoid repetitive user operations.

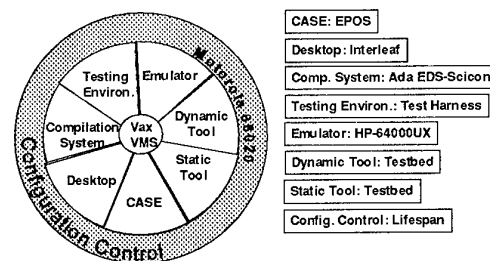


Figure 16: Tools

5. Lesson Learned

The SDE has been used to produce high integrity software. The first flight was

⁶ by Digital Equipment Corporation

⁷ by GPP

⁸ by Interleaf

⁹ by BAeSEMA

¹⁰ by EDS-Scicon

¹¹ by LDRA

¹² by Hewlett Packard

¹³ Eurojet Tool

successfully achieved in June 1995. Despite the fact that the EJ200 project is not yet finished, two of the three classes of requirements on the SDE (identified in para 4.) can be considered successfully reached:

- Customer Requirements have been fulfilled
- EJ200 SDE has allowed to produce code with features required by the products, such as high integrity

Certain SDE requirements, particularly those related to the Consortium have been only partly fulfilled.

The SDE has been able to integrate technicians from different Partners even on the development of the same software product but probably with higher costs and in a different way from that planned.

The experience leads to the following considerations.

What could be better

<Set up time>

Setting up the SDE took quite a long time, sometimes causing severe problems to the development teams.

SDE must be ready and properly tested before the development of products.

<Immaturity>

Despite the careful tool selection their immaturity, bugs and not well proven features induced extra cost and delay.

The tool selection effort must be very high, but problems will occur anyway and the risk shall be taken into account.

<Instability>

The alignment of methods to tools was not always easy and many cases the methods had to be modified resulting in an unstable SDE.

Methods are more important than tools but sometimes tools impeach the methods.

What is missing

<Metrics>

Besides some metrics related to the Coding and Unit Testing Phase, no other metrics have been developed in the SDE. No reliability

models or design complexity metrics or data collection or quality measurement have been developed, loosing an opportunity to have a better project quality and management control.

<Technical justification>

The SDE requires a strong documentation effort during all phases, but does not compel the designer to justify the design in detail.

Metrics must be present and the SDE must force the user to better document the technical choices.

What about the psychological impact

<SDE-phobia>

Some tools and part of the Standards of the SDE were not so easy to use as designers expected.

In some cases the design tools prevented the designers from designing what they wanted. Sometimes this caused 'psychological reactions' damaging the quality of the product.

The SDE should be organized in such a way that user's creativity is allowed where it is important (such as design) and constrained in more bureaucratic activities (problem reports, testing etc.). Moreover training is essential to avoid any adverse psychological impact.

<Paper invasion>

The SDE (and in particular the international standards) required the production of tons of paper to document the project.

The first flight certificated version of the DECU software required about 17000 pages, which means about half a page per line of Ada source code produced (Figure 17).

DECUSOFTWARE (V1.2.1)	
Ada Line of Code (LOC)	33800
Ada Unit	728
Code Comment Lines	86800
Epos SRS Requirements	486
Ada LOC per Unit (average)	46
Ada LOC per SRS req.'s	69
Total Documentation Pages	≈17500

Figure 17: Metrics on DECU software

Paper is often hard to be produced and always much harder to be maintained. A great deal of engineering effort had to be dedicated to this task, sometime inducing hostility in people.

Paper is essential but the quantity must be appropriate. It must be at the service of the engineers, not vice versa.

<Communication rules>

If the Standards are 'minimalist' then designers will have too much freedom and product quality could be jeopardized. If too detailed and prescriptive, with too many steps, they annoy the reader and create a negative attitude. In this case designers will try to deviate as much as possible and the quality of the product will go down as well.

The latter was sometimes the EJ200 case. Standards are a communication media and must have attributes of good communication (clarity, consistency, userfriendliness, effectiveness, appropriateness etc.).

Concerning this problem, during the Eurojet SDE experience a special questionnaire was distributed among the users. The Standards were interpreted as a communication media and the questionnaire constructed around the communication rules.

Clear indication of the weak points were highlighted and used as a feedback to improve the Standards.

Standards must respect the 'communication rules'.

<"I'm the best" syndrome>

In this multinational project, different teams and cultures were requested to work to the same rules.

Each development team criticized the SDE, proposing their own tools and methods as the best. This created centrifugal forces very difficult to be minimized.

Management must understand the importance of the SDE and control centrifugal forces.

In all aspects management is a critical point.

6. Conclusion

Despite some internal turbulence, the EJ200 SDE has been a great experience, with a

strong contribution from all Partners and an important occasion for technological share.

It has fulfilled most of the original goals even if its set up has been expensive, not without problems and some work remain incomplete.

In particular it has been possible to produce the design of the DECU software to the required high integrity.

It has also proven its key role in the production of safety critical software and its contribution to determine the risk and the cost of software development.

An SDE definition, especially for a multinational project, must be carefully thought and carried out with deep knowledge in many disciplines and with a strong 'common sense'.

Training, integration and rapid feedback from the working groups are also important.

The future SDE shall probably be less prescriptive in the phases where the designer creativity is important and formal when really necessary, and it shall pay particular attention to the psychological aspects.

7. Acknowledgments

A special thank:

to A2B members (present and past)

F. Waibel, N. Kagerer, R. Davis - MTU

P. Dix, S. Green, E. Roberts - RR

G. Walsh, A.S. Villegas - Sener

P. Busti - FiatAvio

for their technical battles

to M. S. Khan - Sener

for reengineering the paper in a more understandable English

to K. Mountford - MTU

for his constructive criticism against the SDE

to the Nefma/Nation members of the SISG for stimulating A2B

and

to MTU and all the other Partners for the successful collaboration in the DECU development.

REVIEW OF PHOTONIC SYSTEM DEVELOPMENT FOR PROPULSION CONTROLS

J.C. Birdsall
C.V. Fields
Pratt & Whitney
Government Engines And Space Propulsion
West Palm Beach, Florida 33410-9600

M. Agnello
Naval Air Warfare Center Aircraft Division (M5-3)
Patuxent River, MD 20670-5304
USA

1. ABSTRACT

The use of Photonics on aircraft gas turbine engines offer weight savings, Electromagnetic Interference (EMI) immunity and performance benefits for engine control systems. For these reasons, fly-by-light technology is being developed for use in future aircraft control systems. Full Authority Digital Electronic Control (FADEC) systems that are compatible with fly-by-light aircraft and that use fiber optics on the engine for sensing and control are under development at United Technologies Corporation. Pratt & Whitney has made progress in transitioning fiber optic sensors, harnesses and OEF (OEF) interfaces to engine demonstration programs. This paper will discuss the benefits of photonic propulsion control systems, describe the components of an optoelectronic engine control system, provide results from on-engine testing, present lessons learned and discuss areas that require additional development to achieve technology readiness for product transition.

2. INTRODUCTION

The next generation of gas turbine engines will have electronic propulsion control systems which make use of fiber optic technology. The benefits of fiber optic technology are weight savings, EMI immunity and performance improvements. Commercial and military aircraft will have tremendous weight savings when a large number of heavy copper wires are

replaced by fewer and lighter optic fibers. All aircraft are exposed to a range of EMI such as lightning and radar transmitters. The use of fiber optic technology for control systems provides inherent immunity to these EMI threats unlike electrical signal transmission methods, which require shielding that adds weight and complexity to the system. The FAA is very concerned about the possible EMI threat from passenger electronic devices and has issued a ban on their use during takeoff and landing. Another concern is the EMI threats from the multitude of aircraft electronic systems, (recently as one aircraft's wing tip strobe lights were switched on, the electrically sensed engine speed cockpit indicator fluctuated by 400 RPM due to EMI being input to the engine control system). Another benefit is improved control system performance from extended range optic sensors and higher speed optic data buses.

The benefits of optic technology are EMI immunity weight savings and performance improvements. For these reasons, fly-by-light aircraft are being designed for the near future. FADEC systems that are compatible with fly-by-light aircraft and that use fiber optics on the engine for sensing and control are being developed to realize the full improvement potential fiber optics offer for future flight vehicles. Progress has been made in transitioning fiber optic sensors, harnesses and OEF interfaces to engine demonstration programs. This paper will describe the components of an optoelectronic engine control

system, present lessons learned and provide results from on-engine testing.

3. OPTOELECTRONIC FADEC CONTROL SYSTEM COMPONENTS

The OEF propulsion control system designed for future fly-by-light aircraft consists of three component areas: OEF, optic sensors and fiber optic harnesses. The OEF control system is shown in Figure 1. The features of these OEF control system components and the status of bench and engine testing are discussed below.

OPTOELECTRONIC FADEC (OEF)

The design of the OEF is based on the advanced all electronic FADEC. To implement an optic system the input/output (I/O) circuitry in the control is replaced with optic components, such as light emitting diodes and photo detectors which convert the optic to electric signals. The basic computer architecture, processors, memory, internal data bus and power supply remain unchanged. Since the optic components are immune to EMI, most of the electromagnetic protection devices currently in the FADEC can be removed. These devices include tranzorbs, connector filter pins, filters and protection diodes.

The evolution of OEFs is shown in Figure 2. The first step was to mount optoelectronic interface components on large plug in circuit boards. The next step was to repack the optoelectronic components on small modules for insertion into the FADEC. The last step will be to mount miniaturized optoelectronic components directly on the FADEC circuit boards. This evolution will transition optoelectronic interfaces to full-scale development programs.

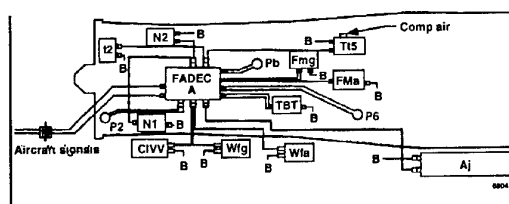


Figure 1

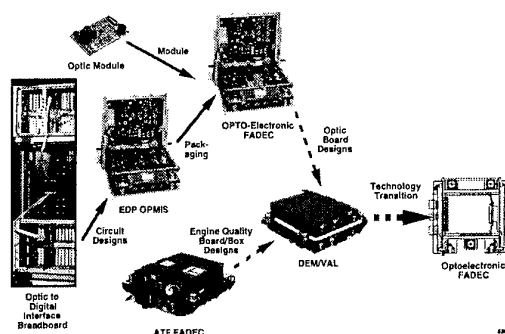


Figure 2

This evolutionary process began when the combined expertise of Pratt & Whitney, Hamilton Standard and United Technologies Research Center (UTRC) was used to enhance the technology transfer of advanced optical techniques toward the development of the first OEF system. To accomplish this, an optoelectronic interface system was developed for a brassboard FADEC. This system consisted of a card cage cabinet that accepted large plug-in optoelectronic interface boards. The optoelectronic interface boards converted the optic sensor signals to digital values and a processor in the card cage passed the sensor values to the FADEC through a data link. Optoelectronic interface boards were designed and fabricated for four optic sensors: speed, high temperature, analog code plate position, and wave length division multiplexed position. The speed and high temperature optic interface boards were installed in the optoelectronic interface cabinet and sent simulated optic sensor data to the FADEC during system bench tests. Actual optic engine sensors were successfully demonstrated using the optoelectronic interface system during engine tests in 1992 and 1993. An optic low temperature sensor was also demonstrated during the engine tests.

In 1992, the U.S. Navy awarded the OEF contract to Pratt & Whitney with a planned optic control system engine demonstration, as shown in Figure 3. The OEF used in the Navy program is an engine mounted control that contains two optoelectronic interfaces modules which are much smaller than the interfaces used in the plug-in card cage cabinet. The OEF will be the engine mounted test housing used for ongoing development of optic interface modules.

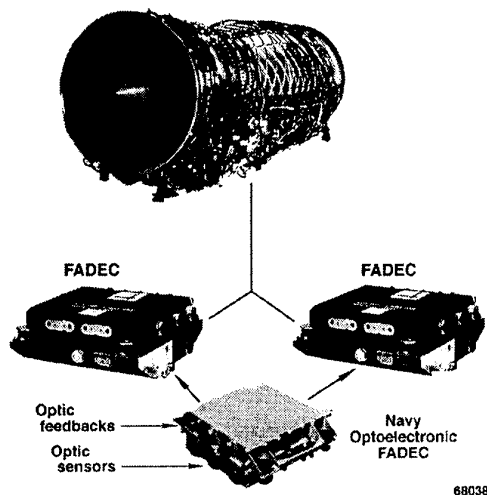


Figure 3

Optoelectronic interface lessons learned include the realization that each optic sensor type has a unique interface method and circuit for converting the optic signal to electronic data and that each interface is relatively large compared to the equivalent electronic interface. For these reasons, a common interface which decodes dissimilar optic sensors is desirable. Also, optic sensor multiplexing techniques and surface mounted optic components are required to prevent the OEF from growing in size compared to the current all electronic FADEC.

Optic Engine Sensors

A wide range of optic engine control sensors have been procured and evaluated. The optic sensors must have measurement accuracy and replaceability equal to or better than current electrical sensors and be survivable in the harsh engine environment. P&W has evaluated many optic sensors including speed, flow, temperature, fill, linear position, and rotary position using the optoelectronic interface cabinet. The optic sensors include a magneto-optic fan speed sensor from Simmonds Precision, a time rate of decay inlet air temperature sensor from Rosemount Aerospace, a black body exhaust gas temperature (EGT) sensor from Conax Buffalo, and a Microbend gearbox vibration sensor from Babcock & Wilcox. The optical inlet and exhaust temperature probes were tested in the gas path using proven electric probe housings to ensure engine safety. All the optical systems included 200 feet of fiber cable to connect the engine

mounted probes to remote optoelectronic interfaces located in the engine control room.

The optic speed probe and optic EGT probe were connected to the optoelectronic control system and the optical sensor data was compared to the conventional electric sensors during engine testing. The optic speed sensor data tracked the electric speed sensor closely. The optic EGT sensor data also tracked the electric EGT sensor closely, but during planned engine stall testing the optic data spiked higher than the electric data. The probable cause was that during the stall, the combustor flame extended to the engine exhaust area where the optic sensor picked up light from the combustor flame and interpreted it as a sharp temperature rise. The optic inlet air temperature probe data showed that the optical sensor had about a 5° F error compared to conventional electric reference sensor. Rosemount Aerospace, the optical system supplier, attributed this to substitution of a new 200 foot optic cable, which was necessary after the original cable was damaged during installation. When the OEF is engine mounted the 200 foot optic cables will be eliminated. Additional optic sensors are being procured and evaluated as they become available. The flexible modular design of the OEF allows the incorporation of new sensors and interfaces without the high cost of retrofitting control hardware.

On engine testing of optic sensors produced a few lessons learned. The most important lesson was the realization that air bubbles on an optic WDM position sensor code plate will prevent proper reading of the code plate. The actuator position sensor was designed to have the code plate immersed in fuel, but a problem was noticed when the actuator was removed from the engine and later reinstalled. The optic position sensor read incorrectly for a short time when the engine was restarted. It was determined that while the actuator was being stored, air entered the position sensor as fuel leaked out. This air became trapped when the actuator was reinstalled on the engine and caused an incorrect reading until the actuator cycled a few times which forced the air from the position sensor. This experience showed that an actuator should be designed so that the optic position sensor always contains either fuel or air, but not both.

Another lesson is that optic sensor interface power budget problems were solved by using two fibers per sensor instead of one. This scheme used one fiber for illumination and the second fiber for returned light, which effectively increased the amount of light falling on the photo detector.

Fiber Optic Engine Harnesses

The final component required to bring together an optic based engine control system is the optic harness. The optic harnesses and connectors must be designed to operate in the same thermal and vibration environment as the sensors, actuators and FADEC. Three flight quality fiber optic harnesses were procured from different manufacturers and tested. The harness used MIL-STD-38999 optic connectors and 100/140 optic fiber. Many optic test stand harnesses were also procured to support sensor testing. The connectors used included MIL-C-38999 with MIL-T-29504/4 and MIL-T-29504/5 termini, Hughes V-Lock, ITT FOMC, and SMA.

The optic connectors are perceived to be the least developed component in an OEF engine control system even though the optic harnesses have performed well during engine testing. For this reason, a Fiber Optic Reliability/Maintainability (FORM) Program has been started to reduce the risk of new technology fiber optic interconnections between the sensors and interface circuits. The scope of the FORM program is to conduct environmental testing of optic harnesses suitable for military and commercial engines. The test program will consist of optical, environmental, and mechanical tests. The goal of this program is to uncover possible reliability and performance issues associated with fiber optic harnesses before they are used in flight engine test programs. It is expected that the information generated by this testing program will be used for a number of purposes that will include providing feedback to harness suppliers to enable them to improve their designs and selection of connectors and fiber optic cable which are key components of harness design.

Environmental testing of six types of severe environment optic connectors has been completed. This program tested eighteen optic connector pairs from six manufacturers. The

environmental tests included durability, thermal shock, vibration, temperature/humidity, salt spray, fluid immersion, and impact. The test results are under review, but the preliminary observations indicate that in most of the tests the optic signal strength was not degraded by the connectors even though many of the mechanical features of the connector shells were damaged.

The comprehensive fiber optic harness testing has generated many lessons learned. There are two types of optic connector contacts, butt and lensed. The butt contacts have low initial insertion loss, but the loss increases slowly with time in a high vibration environment. The lensed contacts start with a higher initial insertion loss, but the loss remains constant over time. Another lesson is smaller connector back shell designs tailored for optic fibers are required to survive the high level of engine vibration. The back shells must also have a strain relief feature where the fibers exit the backshell to prevent the fibers from bending too sharply during handling.

Additional Optoelectronic Development Planned

Additional development in all three component areas is planned to further evolve the OEF control system. Further consolidation and miniaturization of optoelectronic interface circuit components is required. Optic engine sensor designs need to be optimized and additional sensor types such as pressure and linear position need to transition from the laboratory to the engine. Robust optic connectors and fiber harness designs must be developed to be as reliable as existing wire harnesses.

In order for a new technology to be accepted by the production aerospace community, it needs to have an established track record. For example, in the 1970's, Digital Electronics for engine controls was an unproved technology. Pratt & Whitney, Boeing and the airlines conducted a test program using commercial aircraft to flight test digital electronic engine controls in a passive mode and logged over 300,000 flight hours. This program established that digital electronic controls operated reliably in the jet engine environment. The reliability of OEFs will be established by flight testing four

units on 757 commercial aircraft which began in 1994. This program will accumulate 250,000 fleet hours of experience on optoelectronic interfaces in the In-Service flight environment. The reliability database generated will be instrumental in transitioning optoelectronics to full-scale development programs. To date, over 9000 powered hours have been accumulated on the In-Service OEFs.

4. Summary

Future fly-by-light aircraft will use photonics for the flight and propulsion control system. Propulsion control system components are being developed to use fiber optic technologies for engine control system sensing and control. Navy, Air Force, NASA and IRAD programs have developed and engine tested optic sensors, fiber optic engine harnesses and OEF interfaces. A flight test of OEFs on commercial aircraft will demonstrate the reliability of photonics for fly-by-light aircraft. Ongoing photonic programs are in place to achieve technology readiness for product transition.

Fl 33410, Phone: 407-796-4677, Fax: 407-796-4988.

Mark Agnello, NAWC AD Pax River, Program Manager, Advanced Controls and Integrated Systems - Mark Agnello has over 8 years experience managing control systems development programs and troubleshooting existing systems in fleet service. He has managed advanced technology programs that include fiber optic control system component development and active surge/stall control investigations. He has served as the Chairman of the Integrated High Performance Turbine Engine Technology (IHPTET) Controls Committee since 1991. He has extensive in-service experience with the propulsion controls on the SH-60, V-22, F/A-18, and AV8-B aircraft. Mr. Agnello received his BS in Electrical Engineering from the New Jersey Institute of Technology in 1987. Address: Naval Air Warfare Center Aircraft Division, Propulsion & Power Engineering (MS-3), 22119 James Rd., Patuxent River, MD, Phone: 301-342-7850 x257, Fax 301-342-1868.

RESUMES OF AUTHORS

Christopher V. Fields, Pratt & Whitney, Optoelectronic FADEC Demonstration Program Manager (Navy Contract) - Chris Fields has over 20 year's experience at the design and development of FADEC Control components and systems for military gas turbine engines. He has been involved with fiber optic technologies for five years and has two pending patents for a linear optic position sensor. Mr. Fields received his BS in Electrical Engineering at the University of Vermont in 1973. Address: Pratt & Whitney, P. O. Box 109600, West Palm Beach, Fl 33410, Phone: 407-796-4677, Fax 407-796-4988.

James C. Birdsall, Pratt & Whitney Optoelectronic FADEC Program Manager - Jim Birdsall has over 22 years experience in Military Engine Control System Development. He has managed P&W Internal Research and Development, and several other government technology contracts. He received his BS in Electrical Engineering from the University of South Florida in 1973. Address: Pratt & Whitney, P. O. Box 109600, West Palm Beach,

Paper 37: Discussion

Question from B Leroudier, Dassault Aviation, France

Is “throttle by light” cheaper than “throttle by wire”?

Author’s reply

At present it is much more expensive and this is likely to remain the case for a long time.

MODELLING OF A FUEL CONTROL UNIT FOR SMALL GAS TURBINE ENGINES FEATURING INTERACTING ELECTRONIC LINEAR ACTUATORS

A.I. Georgantas

National Research Council
Institute for Aerospace Research
Structures, Materials and Propulsion Laboratory
Montreal Road, Building M-7, Ottawa, Ontario, Canada, K1A 0R6

T. Krepec

R.M.H. Cheng

Concordia University
Mechanical Engineering Departement
Centre for Industrial Control
1455 de Maisonneuve Bl. W., Montreal, Quebec, Canada, H3G 1M8

ABSTRACT

This paper investigates an electronic fuel control unit for small gas turbine engines, with valves operated by linear digital actuators. The unit is based on the modified metering section of a conventional hydromechanical fuel control unit. A mathematical model of the system is first developed, and validated by experimentation; it is subsequently used for simulation and further study of the system dynamics. It has been demonstrated that this new system features greater functional flexibility and faster transient response than the conventional system. The possibility for back-up, in case of failure of one valve, is also discussed.

NOMENCLATURE

A	- flow area
A_0	- diaphragm area
A_{0e}	- effective diaphragm area
A_1	- pressurizing valve downstream pressure area
A_2	- pressurizing valve upstream pressure area
A_3	- pressurizing valve return line pressure area
B	- damping coefficient
C_d	- flow coefficient
F	- force
k	- spring rate
K_p	- pump displacement
K_Q	- pump leakage coefficient
W_f	- fuel mass flow rate
M	- valve mass
N	- pump speed
Q	- fuel volumetric flow rate
t	- time
T	- sampling time interval
V	- volume
x	- metering valve position
y	- by-pass valve position
z	- pressurizing valve position
β	- effective bulk modulus of elasticity of the fuel
ρ	- fuel density

Subscripts

b	- by-pass valve
c	- combustor
n	- fuel manifold
o	- preload
p	- pump, pressurizing valve
s	- spring
w	- valve stop
0	- return line
1	- metering valve upstream side
$2b$	- by-pass valve low pressure side
$2m$	- metering valve downstream side

INTRODUCTION

Fuel control systems for gas turbine engines have undergone revolutionary changes in recent years owing to the introduction of the microprocessor technology. The aircraft industry has a special interest in electronic controls because of their flexibility and potential to meet the fuel demands of more sophisticated modern engines. However, the transition from conventional to electronic systems is hampered by the lack of a satisfactory record on the reliability of electronic components and circuits. Consequently, two backup schemes of fuel electronic controls have emerged recently.

In the first backup scheme, a multi-channel electronic controller is interfaced with a metering servo valve (1). It is favoured by the bigger airliners and by military aircraft. If one of the channels fails to function properly, another takes over. Up to four channels may be incorporated into the system. The higher cost is compensated by the permanent readiness of the aircraft. In the event of failure, there is no need to interrupt the flight schedule and run into high cost penalties. A second channel simply takes over and repair can wait until the next scheduled overhaul.

The second backup scheme is more commonly used in smaller gas turbine engines, in which a conventional fuel control unit is equipped with electronic computation for

more accurate fuel scheduling (2). In case of electronic control failure, the unit operates in its conventional mode, thus providing the aircraft with "limp-home" capability.

This paper proposes a new concept which could lead to the development of a light and inexpensive electronic fuel control unit with back-up capability. Two versions are considered in this development. In the first version, a digital linear actuator operates a metering valve while a conventional pressure-diaphragm actuator operates a by-pass valve. In the second version, an additional digital actuator is incorporated in the design to operate the by-pass valve as well. A versatile back-up capability becomes possible in the second case. If one valve fails, the other one simply takes over completely. Preliminary tests performed on a modified conventional fuel control unit with the metering valve under electronic control have demonstrated the feasibility of this concept (3).

OPERATING PRINCIPLES

The schematic of the Bendix DP-F2 hydromechanical fuel control unit is shown in Fig. 1. The by-pass valve maintains a constant pressure difference across the metering valve by releasing excess fuel back to the pump. The fuel flow to the nozzles is a function of the metering valve position. The actuating mechanism consists of a "computing" bellows which receives signals from the compressor pressure and the mechanical speed governor.

The first version of the proposed electronic control system is obtained by removing the pneumatic bellows and the mechanical governor, and by bringing the metering valve under digital control (see Fig. 2). The second version is obtained by introducing digital control also to the by-pass valve (Fig. 3). In the latter case, the fuel flow rate can be controlled independently by either valve. If the by-pass valve fails to operate properly, the flow to the valve is cut-off automatically by a solenoid operated valve (Fig. 4). As a result, the pump delivery pressure increases and opens the relief valve. The metering valve controls the fuel flow rate based on the essentially constant fuel pressure created by the relief valve. If the metering valve fails, the flow through it is cut-off and a parallel path through a fixed orifice is opened. The fuel flow rate to the nozzles is determined by the pressure difference across the orifice which is controlled by the by-pass valve. To reduce the hazard of malfunction due to possible failure of the electronics, each valve is under a separate control management. In both modes of failure, the fuel control unit will not operate at its maximum capability.

Electronic fuel control has the advantage of being more flexible while employing

fewer mechanical components. A fuel schedule can be preprogrammed and stored in the EPROM (erasable programmable read-only memory module) of the microcontroller.

MATHEMATICAL MODEL OF FUEL CONTROL UNIT

A mathematical model of the control unit is developed so as to describe its response to a change of fuel-flow demand. The model can be used to optimize the interaction between the two valves and to design a fuel controller which best satisfies the requirements of a given gas turbine engine.

The fuel flow delivered by the fuel pump is a function of the rotational speed and the pressure difference across the pump:

$$Q_p = K_p N + K_c (P_1 - P_0) \quad (1)$$

The metered fuel flow rate is:

$$Q_{12m} = (C_d)_{12m} A_{12m} [2/\rho (P_1 - P_{2m})]^{1/2} \quad (2)$$

The excess fuel flow, which is returned to the pump through the by-pass valve, is:

$$Q_{10} = (C_d)_{10} A_{10} [2/\rho (P_1 - P_0)]^{1/2} \quad (3)$$

The flow through the damping orifice in the by-pass valve is:

$$Q_{2b2m} = (C_d)_{2b2m} A_{2b2m} \operatorname{sgn}(P_{2b}, P_{2m}) [2/\rho (P_{2b} - P_{2m})]^{1/2} \quad (4)$$

where $\operatorname{sgn}(P_{2b}, P_{2m})$ is included to take into consideration the direction of flow.

The flow through the minimum pressurizing valve is given by:

$$Q_{2mn} = (C_d)_{2mn} A_{2mn} [2/\rho (P_{2m} - P_n)]^{1/2} \quad (5)$$

and the fuel flow through the nozzles is:

$$Q_{nc} = (C_d)_{nc} A_{nc} [2/\rho (P_n - P_c)]^{1/2} \quad (6)$$

The rate of change of the pressure upstream of the metering valve is a function of volume and net fuel influx:

$$dP_1/dt = \beta/V_1 (Q_p - A_p(dy/dt) - Q_{12m} - Q_{10}) \quad (7)$$

The change of volume, V_1 , due to the by-pass valve diaphragm movement is very small and can be neglected.

Similarly, the rate of change of the pressure in the upper volume of the by-pass valve is given by:

$$dP_{2b}/dt = \beta/V_{2b} (A_p(dy/dt) - Q_{2m2b}) \quad (8)$$

As in the case of Eq. 7, V_{2b} is not significantly affected by the diaphragm movement.

The pressure downstream of the metering valve is described by:

$$dP_{2m}/dt = \beta/V_{2m} (Q_{12} + Q_{2b2m} - Q_{2mn}) \quad (9)$$

and the pressure in the fuel manifold by:

$$dP_n/dt = \beta/V_n (Q_{2m} - Q_{nc}) \quad (10)$$

The motion of the metering valve is quantized, being dictated by the resolution of the linear actuator. The number of steps and stepping rate command are issued by the electronic controller. Forces acting on the by-pass valve are created by the pressure difference across the diaphragm, the diaphragm spring and the change of momentum of the fuel flowing across the valve. The dynamic force balance of the by-pass valve is described by the following equation:

$$d^2y/dt^2 = 1/M_b [A_{p0}(P_1 - P_2b) - 2C_d A_b (P_1 - P_0) - K_{bs}y + F_{bs0}] \quad (11)$$

where the flow force coefficient A_b is a function of the flow area and the flow angles. An accurate prediction of the flow angles based on the geometry such as that of the by-pass valve is very difficult. Therefore, A_b was determined experimentally.

In the case of the double-actuator system, the estimation of the flow forces is not necessary. The by-pass valve follows the motion of the actuator as commanded by the electronic controller. This implies that the stepping rate is not very high and the actuator force is well above the valve unbalanced pressure force.

The dynamic force balance of the minimum pressurizing valve is described by the following equation:

$$d^2z/dt^2 = 1/M_p [A_1 P_{2m} + A_2 P_n - A_3 P_0 - K_{ps}z - K_{vps}(z - z_{max}) - F_{ps0} - B_p(dz/dt)] \quad (12)$$

At high flow rates the minimum pressurizing valve is fully opened and is thus treated as a fixed orifice. This case is implemented by modelling the valve stop as a spring with infinite constant.

MODEL VALIDATION

The steady state model was obtained from the dynamic model by setting all the transitory terms equal to zero (i.e. $d/dt = d^2/dt^2 = 0$). The static model describes the steady state behavior of the system for the complete travel of the metering valve at different pump speeds. It also provides the initial conditions for the dynamic model. Newton's first-order method was used to solve the set of non-linear equations. Error correction was applied to avoid divergence of the solution. Experimental and simulation results for metered fuel flow, pump pressure, minimum pressurizing valve travel, by-pass valve travel and pressure difference across the metering valve are shown in Fig. 5 as functions of the metering valve travel.

The dynamic model was implemented on a digital computer using the TUTSIM system simulation package. This package employs the Euler and Adams Bashforth rules of

integration. Discrete time blocks for sampled data processing are also available. Model parameters are changed interactively for rapid examination of their effect. The program can also be used in a batch processing mode to interact with user codes. This makes the optimization of the model parameters possible.

Experimental and simulation results for an approximated pulse actuation of the metering valve are shown in Fig. 6. It can be observed that the mathematical model describes the actual system extremely well. This observation establishes the validity of using the model for further investigation of the electronic system.

CONTROLLER STRUCTURES

The block diagram of the first version of the electronic system is shown in Fig. 7. The fuel flow rate is the feedback signal of the control loop. However, the engine speed may be used instead in case the engine is included in the loop. As yet another option, both feedback signals can be used in a cascade control configuration. The fuel flow rate signal will control the fuel control unit while the engine speed signal will control the engine process by setting the fuel flow demand. The fuel flow can be measured directly with a turbine flowmeter, or alternatively be derived from the position and pressure difference across the metering valve. The error signal is processed by the digital controller to produce the triggering signal TRG via the pulse-generation circuitry. The triggering signal then drives the actuator via the driver circuit. A direction control signal is provided by the digital controller directly. The controller output is purposely limited to ensure that the actuator force is always sufficient to drive the valve.

The block diagram of the second version of the electronic fuel control unit is shown in Fig. 8. The second actuator which operates the by-pass valve is under separate control to maintain a constant pressure difference across the metering valve. The actuator of the metering valve is controlled to meet changes in the fuel flow demand. This control strategy is similar to the previous one where the by-pass valve was under conventional control. An alternative and better control strategy is shown in Fig. 9, in which the two digital controllers operate simultaneously on the fuel flow error. The two valves assist each other to provide the required fuel flow rate.

SIMULATION RESULTS AND DISCUSSION

Simulation of the dynamic response of the electronic system with one actuator is shown in Fig. 10. Results are shown for an abrupt change in the fuel flow demand. A digital proportional-derivative (PD) controller is used. An integral term is not included since the actuator acts as an

integrator and sums up the executed steps. To ensure synchronous operation of the actuator (i.e. no lost steps), the maximum triggering frequency is limited to about 200 steps/sec, as dictated by the load-frequency characteristics of the actuator.

The discrete movement of the metering valve is reflected on the fuel flow rate, the differential pressure and the movement of the by-pass (see Fig. 10). The step size used (0.05 mm) is quite large and consequently the final fuel flow rate cannot be achieved accurately. The actuator is "hunting" about the final position, in an effort to reach the scheduled fuel flow. The hunting frequency depends on the controller gains. If the engine is included in the control loop, equilibrium between the fuel flow and engine load will not be reached and the system will remain in a continuous transient state. The hunting problem can be eliminated electronically by using a monostable multivibrator downstream of the pulse generation circuitry. The pulse train of the feedback signal must be used to trigger the monostable and the delay time must be adjusted to be slightly shorter than the period of the hunting pulses (4). This assumes that the hunting period is known "a priori". A simpler remedy to this problem is to use an actuator with a smaller stepping resolution. Results with a step size of 0.0125 mm are shown in Fig. 11. There it is observed that the undesirable hunting phenomenon has been eliminated without sacrificing the speed of response. However, it is not advisable to reduce the step size indefinitely, lest the response may become sluggish. There exists therefore an optimal actuator step size for a given desired speed of response.

Figure 12 shows some simulation results for the double-actuator electronic fuel control unit with the pressure difference maintained constant across the metering valve. The step size of the actuator operating the metering valve is 0.0125 mm and that of the actuator operating the by-pass valve is 0.00625 mm. A smaller step size is used in the by-pass valve because of the larger flow area gain of the valve (dA_{10}/dy). Every step of the actuator corresponds to a substantial change of the pressure difference. The by-pass valve responds to the metering valve movement in a way that is similar to the conventional system. One notices the existence of hunting in Fig 11. To correct the problem, one can reduce either the actuator step size, or the flow area gain of the valve. The latter solution is adopted simply because the actuator step size is already quite small. The by-pass valve flow area gain should not be reduced indiscriminately, since it can also slow down the response of the system. In general, a trade-off between the valve flow gain and the actuator step size should be worked out for the design of the control unit.

Figure 13 shows simulation results obtained when both actuators respond to a fuel flow change. The response is significantly faster as compared to the single-actuator unit, as well as to the double-actuator unit when the pressure difference is maintained constant. In the initial portion of the transient, the controller output is at its maximum due to a large fuel flow error. That results in both valves moving at their highest speed. Owing to its larger flow area gain, the by-pass valve causes a rapid increase of the pressure difference. This provides an initial "boost" to the change in the fuel flow rate. When the error signal is reduced below the value causing controller saturation, the metering valve moves more rapidly than the by-pass valve owing to its higher controller gain. By making the metering valve more sensitive to the flow error, its control prevails and eventually it becomes dominantly responsible for the final fuel flow adjustment. As a result, the amplitude and the frequency of hunting are greatly reduced (compare Fig. 12 to Fig. 13). In some applications where hunting can be tolerated, the transient response can be made faster by increasing the proportional gain of the by-pass valve controller.

Fig. 14 compares the fuel flow rate transient response achieved with the two versions of the electronic control unit to the fastest flow rate transient possible which occurs when the metering valve is actuated instantaneously. The response obtained, using the second control strategy of the double actuator unit, is closer to the best performance. A proper choice of a combination of the step sizes of the two actuators, the flow gains of the two valves and the gains of the controllers can further improve the system response. This requires the solution of an optimization problem involving all the above parameters and objectives simultaneously, and is outside the present scope.

SUMMARY

A dynamic mathematical model of an electronic fuel control unit has been developed and used to simulate the transient response of the unit to abrupt fuel flow demands. Two versions of the electronic fuel control unit have been investigated and the results documented in the paper. It has been demonstrated that some distinct advantages are obtainable as compared with the hydromechanical design. Some problems have been located, which are primarily due to the finite step size of the electronically actuated valves. The paper has also presented some viable solutions to counteract these problems. The second version of the electronic control unit has been found to be able to provide for a unique back-up capability, involving the interaction of two independently controlled digital actuators. This concept is very promising, warranting further investigation to establish its full potential. It is envisaged that a

systematic optimization effort will lead to the proper design parameters of the control unit for a given desired system response.

ACKNOWLEDGEMENTS

The authors wish to thank the Natural Sciences and Engineering Research Council of Canada and Bendix Avelex Inc. for their continued support of this research project.

REFERENCES

1. Kuhlberg, J. F., Newirth, M. J., and Kniat, J., "Integration of the PW2039 Engine Electronic Control System in the Boeing 757 Airplane," SAE paper, Nr. 841554, 1984.
2. Frew, J. S. and Keck, C. F., "Electronic Control System for Modern Turboprop Engine," SAE Paper, Nr. 810620, 1981.
3. Georgantas, A.I., Krepec, T., and Cheng, R.M.H., "Investigations on Electronically Actuated Metering Valve in a Fuel Control Unit for Small Gas Turbine Engines," Proceedings of the 1987 ASME International Computers in Engineering Conference and Exhibition, ASME, New York, August 19-13, 1987.
4. Cadzow, J.A., and Martens, H.R., "The Stepper Motor in Control Applications," Discrete-Time and Computer Control Systems, Prentice-Hall, Englewood Cliffs, New Jersey, 1970, pp. 365-367.

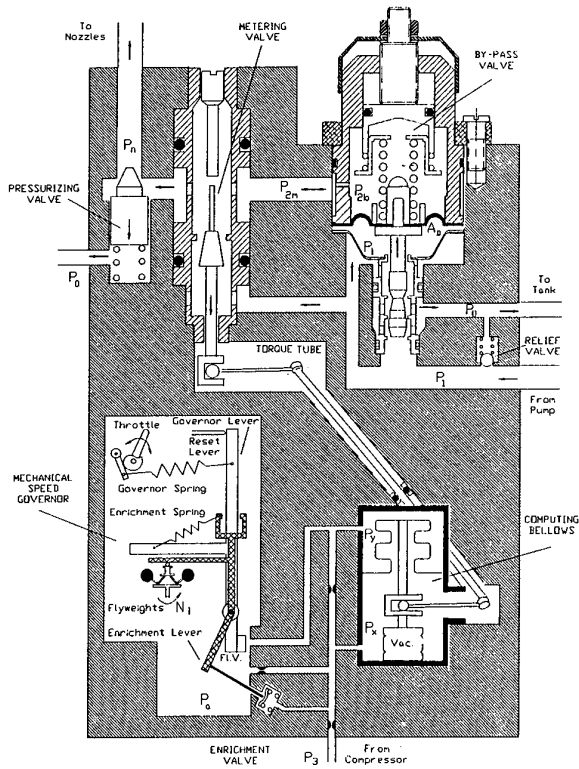


Fig. 1 Main components of the Bendix DP-F2 fuel control unit

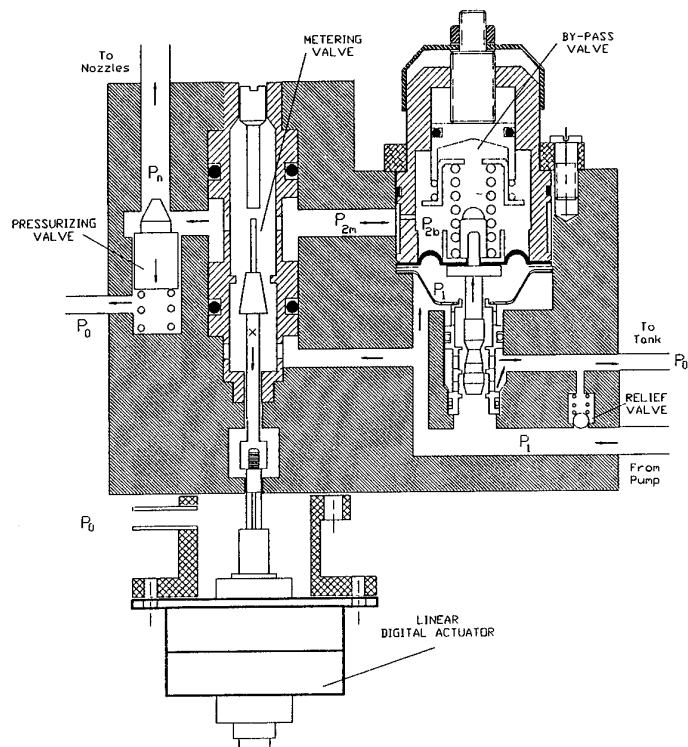


Fig. 2 Schematic of the first version of the electronic fuel control unit

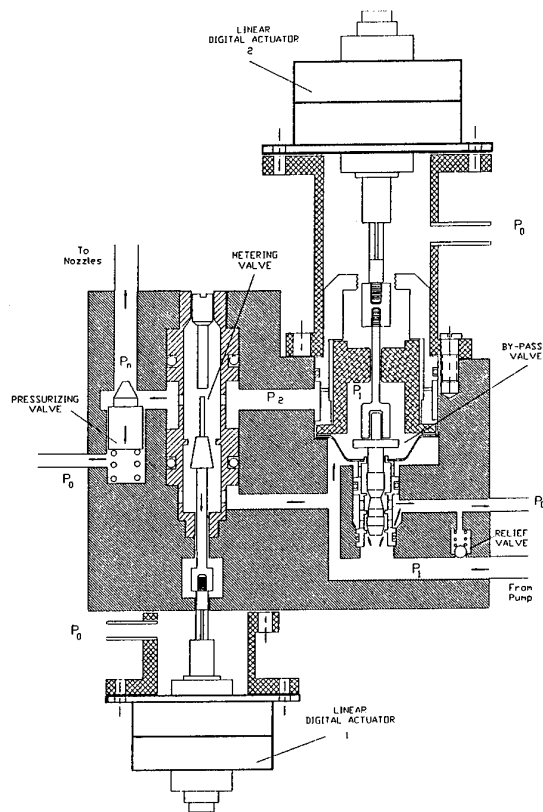


Fig. 3 Schematic of the second version of the electronic fuel control unit

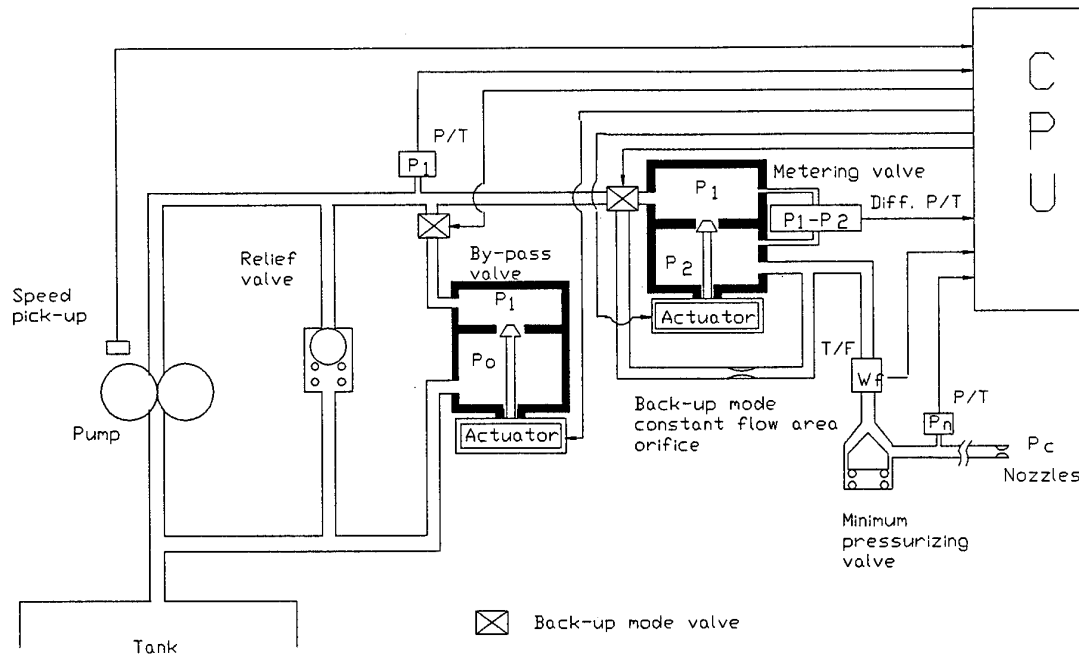


Fig. 4 Proposed concept of electronically controlled fuel metering system with two actuators

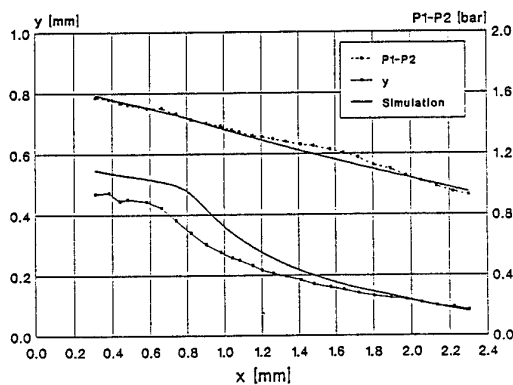
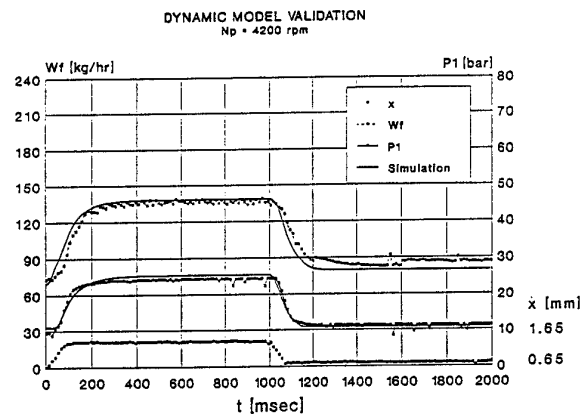
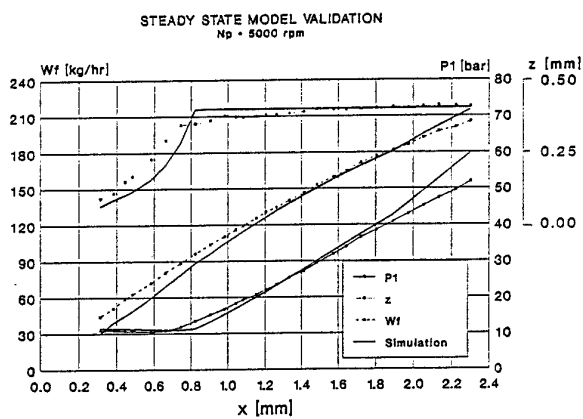


Fig. 5 Experimental and simulation results for steady state

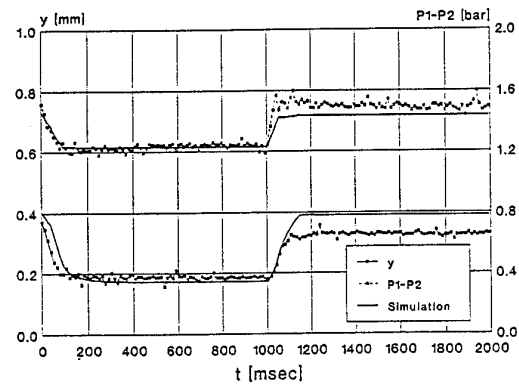


Fig. 6 Experimental and simulation transient response results

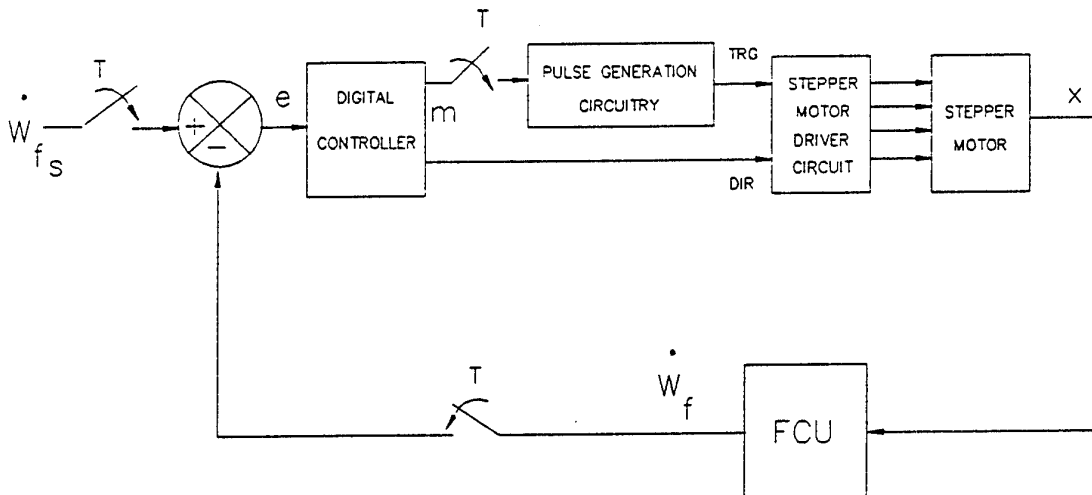


Fig. 7 Fuel flow control loop

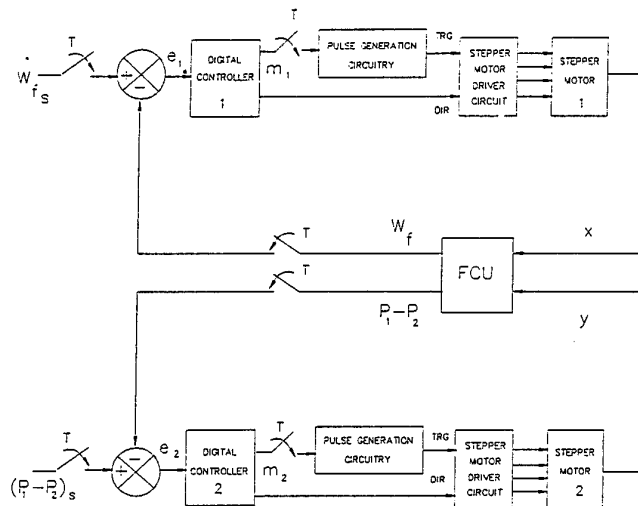


Fig. 8 First control strategy of the two-actuator electronic fuel control unit

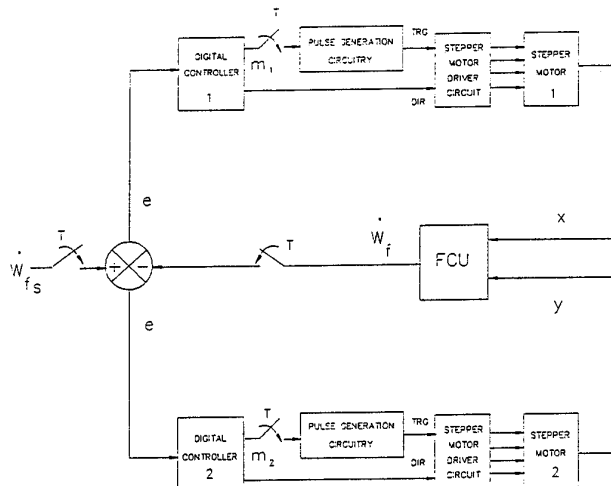


Fig. 9 Second control strategy of the two-actuator electronic fuel control unit

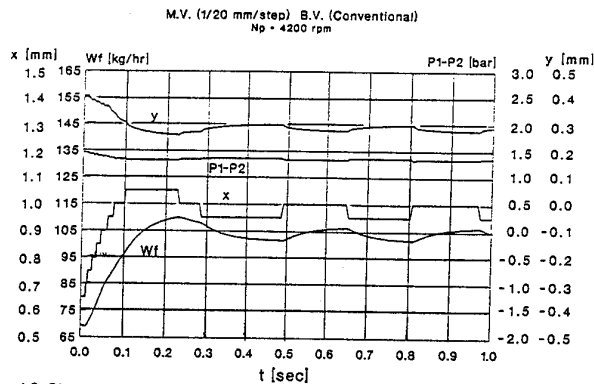


Fig.10 Simulation of dynamic response of electronic fuel control unit to a step fuel flow demand

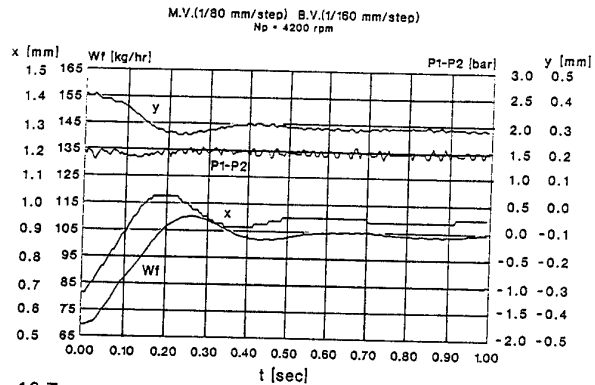


Fig.12 Two-actuator electronic unit dynamic response (first control strategy)

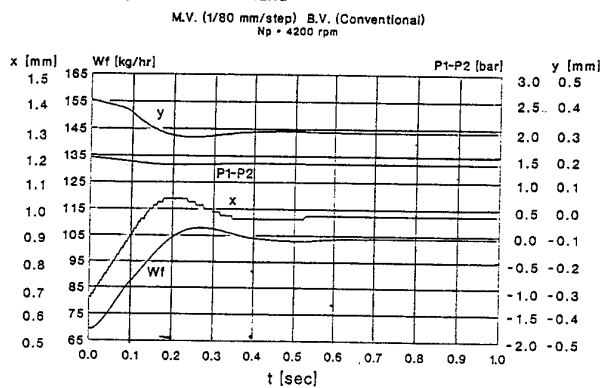


Fig.11 Simulation of dynamic response of electronic fuel control unit with the metering valve actuator step size reduced

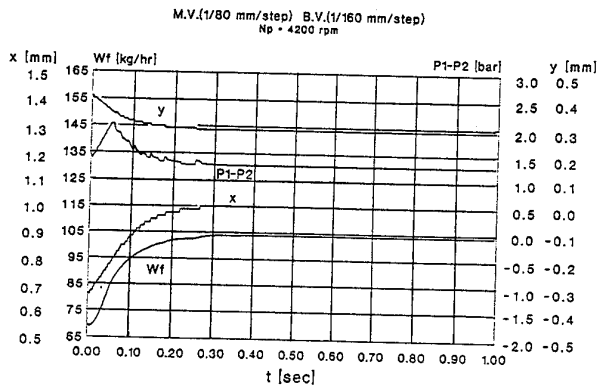


Fig.13 Two-actuator electronic unit dynamic response (second control strategy)

METERED FUEL FLOW RATE Np = 4200 rpm

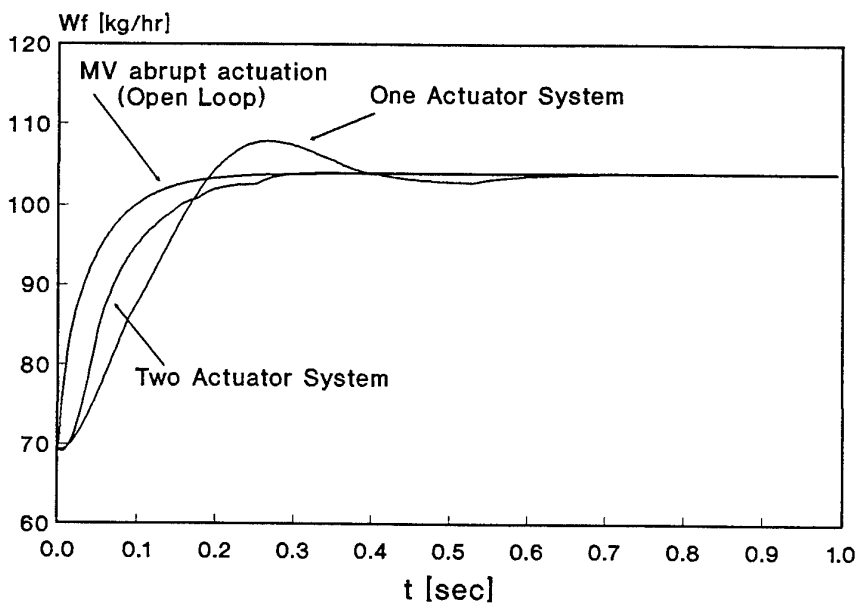


Fig.14 Metered fuel flow response

Paper 38: DiscussionQuestion from J Frealle, Turbomeca SA, France

For the back-up mode you require two solenoid actuators. Please could you comment on the cost and the failure analysis for such a system.

Author's reply

This paper presents the functional concept of the prototype of an electronic fuel control unit employing two linear actuators and two back-up mode solenoids. The design can be further optimised by reducing the number of components and therefore the cost. That in turn will simplify the failure analysis. For example, in a final configuration, two plunger type hydraulic valves can be incorporated inside a single-barrel housing to be operated by the two linear actuators from opposite ends of the barrel. At back-up mode, the function of the two solenoids is dependent. Therefore, only one double-stroke solenoid is required to operate both failure modes. When energised, the positive stroke will rotate both valves clockwise to block the flow in the failed valve and to align the second valve to an auxiliary passage. The negative stroke will rotate the valves counterclockwise to perform a similar function in case of failure of the second valve.

The VAAC Harrier Programme: Flying STOVL with 1- Inceptor Control

by G T Shanks and F J Scorer
Flight Dynamics and Simulation Department
Defence Research Agency, Bedford, MK41 6AE, UK

Summary

Active Control Technology, as applied to modern conventional take-off and landing aircraft, has been extended to integrate the flight and propulsion control systems of a Harrier aircraft. This extension allows the direct control of all the forces generated on the aircraft but it is the control concepts, and management options, that are under investigation. An experimental IFPC system has completed the Phase 1 flight trials programme and has demonstrated consistent pilot workload reduction for the recovery task. Comparisons between different methods of controlling the aircraft, including a 1- inceptor option, are presented and the implications of the technology on the engine power off-take for hover control is discussed.

1. Introduction

Future STOVL aircraft designs will have the potential to provide significantly more ways of generating and applying forces and moments at low airspeed. Such forces and moments will be generated by aerodynamic means and by a complex powerplant. Although the aerodynamic control effectors may be similar to present aircraft the number of actuators needed to control the powerplant may increase tenfold from the Harrier GR5/AV8B configuration. To ensure that the future pilot's task will have an acceptably low workload it will be necessary to manage the vehicle through integration of the flight and propulsion control (IFPC). This design approach builds on the application of Active Control Technology (ACT) to STOVL configurations, but to be effective and acceptable, will necessitate research to establish confidence and the appropriate design guidelines.

The VAAC Harrier aircraft is a DRA flight research vehicle which is studying the benefits that ACT extended to IFPC offers in terms of handling and control improvements when applied to current STOVL vehicles with the specific objective of minimising pilot workload in all weather recovery conditions. Concepts are evolving, through alternative options, which will provide the confidence to apply these techniques to future STOVL procurement and ensure an affordable product.

The Phase 1 flight test programme demonstrated the ability to control and manoeuvre a Harrier from wing-borne flight to the hover in jet-borne flight and land with Level 1 handling and control of the vehicle. The pilot recovery task was demonstrated with 2- inceptors and with all the control functionality on just 1- inceptor. Both inceptor solutions were implemented to control the longitudinal axis in such a way that the pilot was unaware of how the forces were being generated i.e. the implementation was transparent to him because the effector application was determined by the IFPC vehicle management system.

The paper describes the unique flight test facility, a summary of the IFPC vehicle management system, the current and future programme, some results of the Phase 1 flight test programme, and the potential implications of the design concepts on the propulsion system. The implications of this work are projected to future STOVL designs to ensure that the maximum advantage, with minimum risk, is taken of the technology thus providing the UK with an affordable, efficient and capable product.

2. Aircraft facility description and the unique features

A detailed description of the VAAC research aircraft facility, Fig 1, a Harrier I two-cockpit trainer, is given in ref 1 and 2. The

front cockpit has a near-standard production fit and is occupied by the safety pilot. The rear cockpit has been extensively modified with an experimental, digital, fly-by-wire flight control system (FCS) and ACT, Fig 2. The rear cockpit's longitudinal inceptors, i.e. the stick, throttle, nozzle lever, and flap selector, have been disconnected from the basic aircraft's mechanical circuits. Their positions are measured by electrical transducers and used as inputs to the experimental FCS, which has full-authority control of the tailplane, pitch reaction control valves, flaps, throttle and nozzle channels. The Phase 1 aircraft FCS standard controls the roll and yaw axes to the auto-stabiliser authority limits.

The FCS back-drives the front cockpit's pitch inceptors (pitch stick, throttle and nozzle) through clutch mechanisms to the standard aircraft mechanical circuits. This feature assists the safety pilot when the experimental FCS is engaged. Control reverts to the safety pilot through several forms of force override of the clutch mechanisms and discrete disconnects. The overall safety requirement for the aircraft is achieved by several independent protection features. These features cover the possibility of FCS failures, flight mechanics associated with the IFPC system and structural induced modes resulting from aeroservoelasticity effects. The FCS architecture has a mixture of duplex- and simplex-monitored systems. The control law software, which determines the aircraft's modified handling and control characteristics, is simplex-monitored by what is referred to as the Independent Monitor (IM). The IM is separate software executed on a separate processor and operates on the dissimilar redundancy principle. Once flight cleared this system provides an FCS and flight mechanics safety shell. The combination of protection provided by the safety pilot, the FCS architecture features and the IM, allows the control law software to be declared as non-safety critical. Thus experimental flight control laws can be installed and assessed, in flight, without significant clearance or flight safety implications.

A fully programmable head-up display (HUD) system serves both cockpits. Changes can be made to the rear cockpit HUD format, as required by the task objectives.

The design standard was originally driven by the anticipation that, for future advanced STOVL aircraft, the major handling and control questions would be associated with the longitudinal/pitch axes (because of the potential for additional rotational forces from a variety of sources, including the powerplant). Therefore, the VAAC programme has initially addressed the longitudinal plane, where the integrated management of the thrust vector and aerodynamic forces, to provide decoupled aircraft responses, was believed to offer significant potential to reduce pilot workload during low-speed flight. This assumption has since been confirmed, however the full recovery solution can only be specified when the handling requirements in all three axes has been determined. Following the achievements demonstrated by the Phase 1 standard, agreement was obtained to modify the aircraft to provide a full three-axes vehicle management system, which will be referred to as the Phase 2 standard.

3 Research Programme Objectives

To address the design of future STOVL aircraft, work is required to provide confidence in the technology application and to determine achievable guidelines that are appropriate to the customer need. The challenge to the future STOVL designer, Fig 3, is to merge the three main design disciplines of control, including stability, displays (information communications), and handling (manoeuvrability). Any weakness in any one of these three items will have an impact on the pilot workload rating. Thus harmonisation is essential to guarantee a product with Level 1 handling qualities. But to take full advantage of the benefits of current technology, application guidelines are required. The existing STOVL handling qualities data base, ref 3 and 4, do not provide adequate guidance for design purposes for future STOVL aircraft. Hence, an objective of the VAAC programme is to determine appropriate guidelines.

The research programme is now pursuing several directions, Fig 4, as follows:

- (i) Alternatives for the number of pilot's inceptors needed for the operational task.
- (ii) Alternative response types appropriate to task and the pilot's inceptor strategy.
- (iii) Alternative flight control law design methodologies.
- (iv) Control power requirements.
- (v) Control power management.
- (vi) Specification for alternative design of pilot's inceptors.
- (vii) HUD display formats.
- (viii) Harmonisation issues.
- (ix) Impact of IFPC on the powerplant.

For the purposes of this paper the discussion will be limited to items (i), (ii), (iv), and (ix). Discussion on the other topics has been included in ref 5.

3.1 Alternatives for pilot's inceptors

The application of ACT to future STOVL aircraft with a complex airframe-propulsion configuration having many motivators with force and moment redundancy where attitude, speed and flightpath control can be determined by several piloting techniques, raises the same question illustrated by the Harrier; how many inceptors are needed, independent of the rudder pedals, for effective operational use and how should they be distributed between the pilot's left-hand and right-hand? This concept is referred to as the inceptor strategy and is illustrated by Fig 5.

The options are summarised as follows and illustrated in Fig 6:

- (i) To retain the Harrier standard with three primary inceptors controlling pitch, thrust magnitude and thrust direction,
- (ii) Two primary inceptors, i.e. the left-hand ('throttle') and right-hand ('stick') controlling the orthogonal forces. This option will allow the HOTAS principle to be introduced.
- (iii) To combine the pilot control functionality onto 1- inceptor with a thumb-controller on the right-hand inceptor for specific tasks or as an alternative option if stick force requirements between low speed and high speed flight are incompatible.

- (iv) An adaptation of the above strategies to allow Translational Rate Command (TRC) during very slow speed flight. TRC allows direct command manoeuvres in the x- and y- horizontal plane (inertial axes) for the final landing task in the z-axis.

3.2 Alternative Response Types appropriate to Inceptor Strategy

The next question to address, on the basis that the vehicle has been adequately stabilised, is the allocation of the force components or the assignment of a response type to each inceptor. Fig 7 illustrates the possible command assignments in terms of the three orthogonal axes x, y, and z. The standard Harrier aircraft requires a change to the command assignment between wing-borne and jet-borne flight. IFPC technology however offers alternatives. With the 2- inceptor option the wing-borne case is as before, but the jet-borne case can be mechanised in three ways:

- (i) as now, but with only one left-hand inceptor. This option provides the plan positioning task in x and y to the right-hand. However a mode change to the command assignment of each hand is still required.
- (ii) maintain a consistent command assignment between flight regimes and thus achieve a unified control strategy. This option splits the plan positioning task between inceptors.
- (iii) provide the plan positioning task on the left-hand inceptor and the vertical task on the right hand inceptor.
- (iv) incorporate all functionality onto 1- inceptor.

The response types, in any control axis, are determined by the command path of the IFPC system from a choice of acceleration, velocity, and position or translation. There is as yet no agreement on a definitive standard for STOVL neither is there guidance available on the assignment of response types to the individual inceptors although preferences are now emerging, ref 7. Results from the Phase 1 programme, and manned simulation experiments in support of the Phase 2 programme, will be illustrated further in sections 5 and 7.

3.3 Control Power Management

The total control power requirement, generated by the reaction control system (RCS), can be separated into three components, trim, stability, both configuration dependent, and manoeuvrability. Control power, as illustrated by the Harrier aircraft in transition and hover, is recognised as a satisfactory standard. The definition of appropriate control power standards for future STOVL aircraft has been the subject of a recent study, ref 6. This activity, based on simulation experiments, quantified, with trim removed, acceptable values in representative conditions for a specific STOVL configuration. The results illustrated that the existing standards are appropriate with the exception of ;

- (i) using TRC for the x-force with deflected thrust, the pitch control power needed is considerably less.
- (ii) using TRC for the y-force introduced by bank angle, the control power needed is greater than with direct attitude control but the difference can be minimised with appropriate bandwidth selection.
- (iii) Yaw control power can be less than specified.

Section 7 describes an assessment of roll control power needed for manoeuvrability for the hover positioning task based on a generic STOVL model.

3.4 Impact of IFPC on the Powerplant

The Phase 1 control laws were specified and designed to provide a stable platform with the objective of providing Level 1 handling qualities for task dependent manoeuvres. The impact of this design goal on the powerplant, in particular the control power off-take from the engine by the RCS, was not considered directly as a design driver provided that the standard operating conditions were met. It is therefore appropriate to examine the impact, if any, of the technology application on the powerplant. Section 6 describes some analysis of the Phase 1 results.

4. Applications Software

A range of inceptor strategies, with different response types, can be programmed with the control law design processes, refs 2 and 7. The 3- inceptor strategy is the most straightforward implementation and is equivalent to the Harrier GR5 or AV8-B. This design provides attitude stabilisation including the elimination of the attitude cross-coupling terms introduced with nozzle movement and power variations. The right-hand inceptor demands pitch rate with attitude hold and the two left-hand inceptors control the thrust magnitude and nozzle angle as in the standard Harrier. This standard has been demonstrated in flight as the baseline standard for VAAC Phase 1. The option provides the Harrier pilot with a significant workload reduction as is evident in current Harrier types. i.e. GR5 and AV8-B.

For the 2- inceptor strategy the general principle adopted is to avoid mode changes between wing-borne and jet-borne flight although the option remains open particularly for the hover/landing task if a wave-off is required.

In a typical 2- inceptor strategy the right-hand inceptor demands pitch rate as the baseline standard for wing-borne flight. To avoid the need for mode changes, as the aircraft decelerates to the hover, the response type with the right-hand inceptor maintains a normal force command. This principle leads to the implementation of vertical acceleration or height rate demand as the response type appropriate to low speed and the hover. A blend region to earth referenced axes, transparent to the pilot, is used to transition from pitch rate to height rate demand. Thus an unconventional way of controlling the aircraft, to Harrier pilots, results in jet-borne flight although the aircraft flare during landing is conventional. To descend the pilot must push the right-hand inceptor forward, to decrease the rate of descent or flare or to climb back pressure is applied.

The same principle applies to the left-hand inceptor. The baseline standard is the Harrier throttle control for wing-borne speeds which blends to a closed-loop acceleration or speed

control at low speed and the hover. A change is required from airspeed to ground speed at low speed through a blend region to earth referenced axes. Thus to accelerate from the hover the pilot simply advances the left-hand inceptor. The acceptability of this principle has been assessed in flight trials and will be illustrated further in section 5.

Further refinements to the 2- inceptor solution, with flight path rate command on the right-hand inceptor in wing-borne flight, have been made to achieve the unified control solution.

5. Summary of results from the Phase 1 flight trials

5.1 Trial Scope

The Phase 1 development programme was completed with a comparative assessment of two control laws with different inceptor strategies as described in section 4, and ref 7. The control laws under test included both the 2- and 1- inceptor forms, and the 3- inceptor strategy representing the equivalent of the present generation of Harrier GR5 aircraft. Six pilots, a mixture of fixed-wing test pilots with and without STOVL experience, performed back to back handling and workload assessments of the control laws.

The assessment task was a level decelerating transition from wing-borne flight at 200 knots to a static hover, followed by a lateral translation to the landing spot and a vertical landing, Fig 8. Ratings were awarded separately for the deceleration, translation and vertical landing phases.

5.2 Results

The wide range of piloting experience levels caused some scatter in the individual ratings. However in all cases both the 2- and 1- inceptor strategies were rated significantly better than the 3- inceptor strategy. Fig 9 shows an example of the spread of ratings obtained. These results are expressed as Cooper-Harper ratings awarded by all pilots for the deceleration to hover phase (the first part of the assessment). Plotting the frequency of occurrence for a particular rating shows that a good range of Level 2 results were obtained for the 3- inceptor strategy. Both the 2-

and 1- inceptor options achieved overall Level 1 ratings. The Level 2 rating for the 1- inceptor option reflect the particular implementation of the single inceptor by a non-Harrier trained pilot. The fore/aft control with the single inceptor scheme was not ideal as commands were implemented via a non-proportional thumb switch. All the pilots felt that it would be possible to improve the handling qualities with an adequately engineered inceptor.

The results for the deceleration phase highlight that workload reduction is effected through the use of a task-tailored control law with unambiguous control over flightpath and speed. This implementation is significant to workload reduction because the pilot has independent control of these parameters through a single input. As pitch attitude, incidence, nozzle angle and thrust magnitude are determined by the IFPC system, and, if they are not of direct interest to the pilot in this flight phase, automatic management of these parameters will result in a significantly reduced pilot workload. Otherwise a control solution which relies on mode switching will be necessary with implications on pilot workload.

Although the aircraft is well stabilised with the 3- inceptor option, the pilot does not have direct control over either the flightpath or speed, the two key parameters that affect the task performance. To control those parameters the pilot must manipulate 3- inceptors to achieve the desired result whilst also manually keeping within other parameter limits. Thus the workload is higher than for the integrated approach used in the 2- or 1- inceptor options. For the second and third phases of the test, the results also show significant handling qualities improvements for both 2- inceptor variants over the 3- inceptor law. The key features of the 2- inceptor results are the decoupling of pitch attitude from fore/aft positioning and the use of a velocity command response for the vertical and longitudinal axes. All the trial pilots found the fore/aft position and height control tasks much easier with both 2- and 1- inceptors. The lateral control task remained the same for both control laws since the control scheme was common, but the overall task was made easier with the 2- and 1- inceptor variants. Fig 10 shows the distribution of handling qualities ratings for the vertical landing task. The results

of the 3- inceptor strategy show predominately Level 2 ratings whilst the 2- and 1- inceptor strategies have mainly Level 1 ratings.

An adverse factor raised in this particular 2- inceptor strategy was the split of the horizontal position control, as a plan position task, between left and right hands. This led to some tendency for the pilot to revert to type and confuse fore/aft demands with height control. The tendency was also present for the single inceptor variant, but reduced because the left hand inceptor had no function.

In summary, Fig 11 shows a composite graph of all the handling qualities results for all task elements. It shows clearly that a significant handling qualities and workload improvement was achieved by the use of the advanced control strategies. The inceptor assignments and characteristics were not ideal for the handling fidelity provided by the control law and require further development. However the way in which pilot workload can be significantly reduced was clearly demonstrated.

6 Impact of IFPC on the powerplant

The STOVL powerplant has to provide vehicle control and stabilisation at low speeds, when aerodynamic controls are not effective. As the Harrier pitch, roll and yaw controls are provided by the RCS, the bleed air causes an overall loss of thrust from the main engine nozzles and therefore reduces the weight at which the aircraft can hover. One potential concern is whether a highly augmented system would require more overall reaction control and thus air bleed from the core engine than is used by a less augmented or manual system.

6.1 Flight Data Analysis

Although not a programme factor during Phase 1 development, flight data has been analysed to compare the usage of reaction control air bleed between the basic aircraft and different advanced control laws. Air bleed usage is a direct function of control activity and so the contributions of each control channel to the overall bleed figure can be estimated. The flight data analysed related to non-maneuvring flight and therefore only provided insight into the control power usage for trimming and

stabilisation. Control power usage for manoeuvring alone was not addressed in this analysis.

The results of the analysis did not show any clear differences in bleed usage between the control laws and that used by the basic aircraft. The dominating factor in the air bleed taken from the engine was the need to trim the aircraft in pitch. Typically trim accounts for 80% of the hover bleed figure for a stationary hover. Since the trim requirements did not depend on the control law in use (at low speeds) this portion of the air bleed figure is not control law dependant. As the amount of air bleed for roll and yaw control was also similar the result from this analysis was that there was no evidence of increased air bleed requirements for stabilisation.

6.2 Simulation Data Analysis

Relaxation of the control power needed for trim, by configuration design, will emphasise that needed for stability and manoeuvrability. The impact of IFPC for manoeuvring, using the TRC response type in the lateral axis, has been assessed through a study of the control power expressed as body angular accelerations. The simulation task was to translate from a hover position alongside a ship to a defined landing spot and land vertically in the minimum time possible. Data was recorded for three pilots using control laws with varying response types and bandwidths. For example the TRC lateral velocity bandwidth was reduced from the baseline of 1 rad/s to less than 0.5 rad/s. Probability distributions of control power usage were then evaluated and matched to Cooper-Harper handling qualities ratings awarded by the pilots for the task difficulty.

Fig 12 shows the 95th percentile of roll control power used for each translation and landing run. The plot distinguishes between runs in which the control systems were awarded Level 1 and Level 2 ratings. Whilst there is scatter in these results, the trend is that the control systems giving Level 2 ratings used more control power to complete the task than those given Level 1 ratings.

This result shows that improvements to the vehicle handling qualities brought about by effective implementation of IFPC need not be at

the expense of an increase in control power and therefore powerplant requirements. It is projected, based on the findings from the Phase 1 flight data and the simulation trial, that overall the impact of IFPC would be to reduce the levels of control power required relative to that needed for a manually controlled aircraft. This projection will be tested in future flight trials with the Phase 2 system.

7. Concept study preparation for Phase 2 programme

In support of the control law development for Phase 2, the acceptability of different inceptor and response-type combinations have been assessed further in simulation. Many of the elements of the control laws used in Phase 1 were proven to be beneficial, so future control laws will incorporate these features. The Phase 1 non-optimal 2- and 1- inceptor physical implementations have been part of this work.

7.1 Hover control options investigation.

In an attempt to obtain a consensus for a control solution, a simulation trial focused on control in hovering flight. The basic piloting task was a hover translation and vertical landing on an 'Illustrious' class aircraft carrier. The questions previously discussed were reiterated i.e.

- (i) which aircraft inceptor and response type provide the best handling qualities, and
- (ii) what types and locations of inceptors are most suitable for the task?

The selection including left and right-hand sidesticks, centre-sticks and thumb controllers. The response types investigated included attitude, acceleration and velocity controllers. For the horizontal positioning task, all trial pilots rated translational rate control in x- and y- the best response-type from a minimum workload. Ideally this would be implemented using direct force control rather than indirectly through aircraft attitude. Since the Harrier does not have direct lateral thrust vectoring capability, lateral or y-translational control was implemented via aircraft bank attitude. Thrust vectoring was used for longitudinal or x-translational control, allowing constant pitch attitude. This combination was highly rated by the trials pilots and no benefit could be found

from indirect implementation of longitudinal or x-translational control through pitch attitude. The use of bank attitude to control lateral velocity was initially unsettling to some of the pilots, but rapidly gained acceptance as the pilots' confidence in the control system increased.

The height or z-axis control was implemented in either acceleration or velocity demand forms as in Phase 1 control laws. For this option all the pilots preferred to use a height rate demand system with a height hold mode. The height rate response had a baseline bandwidth of 1 rad/s which was judged to be the lower limit for acceptability, although this was not fully explored. Using an acceleration response-type, pilots had to concentrate more when setting up a particular height rate or acquiring a particular altitude.

Having established velocity control as the preferred response-types in all three axes, the pilots then tried different inceptor locations and axis assignments. The overall results were consistent with other flight phases. None of the pilots reported significant differences in workload with any inceptor combination that put the x and y horizontal velocity components on two axes of one inceptor and height rate separately or on a second inceptor. The Harrier and helicopter layouts are examples of this, but so is a layout in which left hand and right hand assignments are interchanged. For example using the left hand for positioning in x and y and the right hand for z control only also gave Level 1 handling qualities. The same result was obtained for a 1- inceptor option which assigned x- and y- position control to a stick-top thumb controller. These options are summarised in Fig 13. There were some issues associated with the exact inceptor type, such as force and displacement levels, but these were all secondary to the main findings and will be explored further once an inceptor layout decision had been taken.

7.2 Full flight envelope control development

The results of the hover control trial are being extended to provide the full flight envelope control strategy. The FCS Phase 2 developments will provide a flexible command path software structure so that response types

can be switched between inceptors without alteration of the software. Inceptor force characteristics between low speed and high speed will also be addressed. The Phase 2 control laws will also include the RCS power requirements as a design parameter.

8. Conclusions

Several options for control strategies and response types are being explored for application to future STOVL configurations. The development of vehicle management through IFPC systems has gained momentum, has increased confidence, and through application with the VAAC Harrier aircraft, advanced control strategies have been shown to significantly reduce pilot workload throughout the flight envelope. The approach allows innovative, but practical, design possibilities with 3-, 2- and 1- inceptor control strategies including various response types, to be achievable.

Flight trials results have demonstrated that the 2- inceptor and its 1- inceptor variant control strategies compared with a conventional 3- inceptor Harrier control strategy, introduces a significant reduction in pilot workload. A sample of pilots rated both the 2- and 1- inceptor system as predominantly Level 1, while Harrier pilots gave entirely Level 1 ratings for the 1- inceptor variant.

A large reduction in pilot workload has been achieved by eliminating all conscious mode changes and only introducing changes which are either natural or transparent to the pilot. These results provide the confidence to influence the way in which future STOVL aircraft are controlled.

An analysis of the impact of the technology on the powerplant has shown that the IFPC design implementations which provide Level 1 handling qualities ratings also used less control power than those which provide Level 2 ratings. Thus, with appropriate design guidelines, the impact of the technology on the powerplant will be consistently less than cases where pilot workload is higher, as is the situation with less augmented solutions or basic manual control. Future designs must ensure that no adverse effects are introduced by the technology.

The aircraft experimental IFPC system, modified to the Phase 2 standard, will allow the full 3- axes

control solution to be explored with several design options for control strategies and response types. Simulation trials with generic models have identified three combinations of response types, which when combined with the 2- and 1- inceptor strategies, are predicted to provide Level 1 handling qualities for hover manoeuvring over a ship deck and land.

The technology can provide major benefits but the assessment process and the recommended solution will need vision to determine the expectations of the next generation of operational pilots.

Acknowledgements

The VAAC Harrier programme is sponsored by the UK Ministry of Defence.

References

1. Shanks, G. T., The VAAC Harrier In-Flight Simulation Facility. International Symposium, In-Flight Simulation for the 90'S, Conference Proceedings DGLR-91-05, 1991.
2. Shanks, G.T., Fielding, C., Andrews, S.J., Hyde, R.A, Flight Control and Handling Research with the VAAC Harrier, International Journal of Control, Vol 59, No 1, 291-31, 1994.
3. MOD(UK) Defence Standard 00-970., Design and Airworthiness Requirements for Service Aircraft.
4. Mil-F-83300, Flying Qualities of piloted V/STOL Aircraft.
5. Shanks, G. T., Griffith D. V., Hawkins R. C., The Role of the VAAC Harrier Aircraft Programme in the Definition of Future STOVL Requirements, AIAA-93-4831-CP, International Powered Lift Conference.
6. Franklin, J. A., Criteria for Design of Integrated Flight/Propulsion Control Systems for STOVL Fighter aircraft, NASA TP 3356.
7. Fielding, C., Gale, S.L., Griffith, D.V., Flight Demonstration of an Advanced Pitch Control Law in the VAAC Harrier, Paper presented at the AGARD Flight Mechanics Symposium, Turin, Italy, 9-12 May 1994.

(c) British Crown Copyright 1995/DERA
Published with the permission of the controller
of Her Britannic Majesty's Stationary Office.

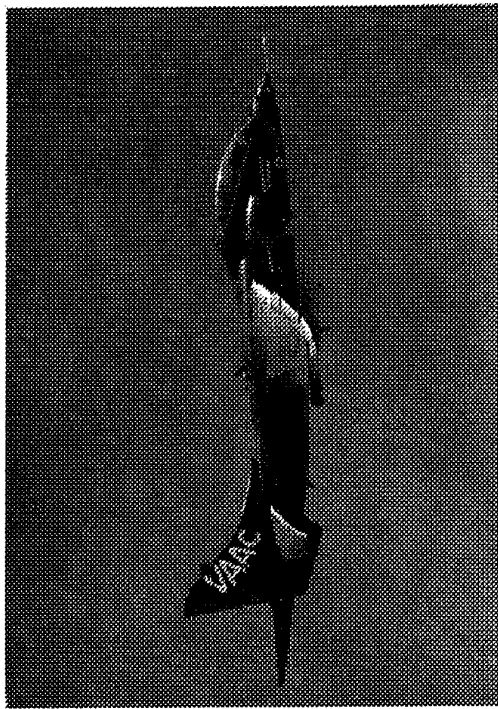


Figure 1: The VAAC Harrier Aircraft

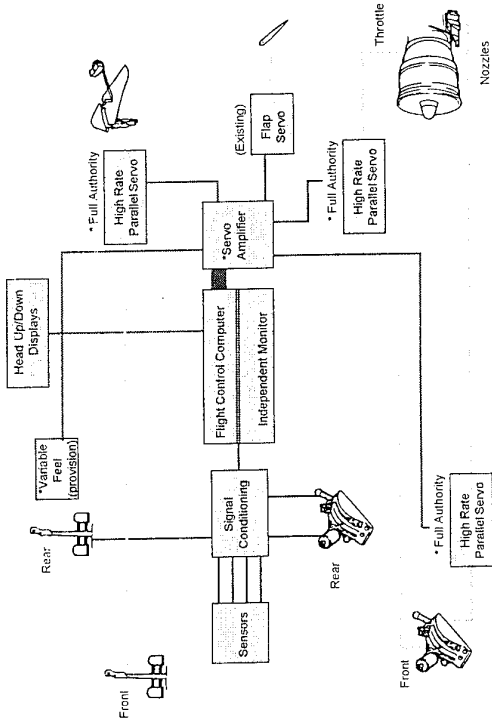
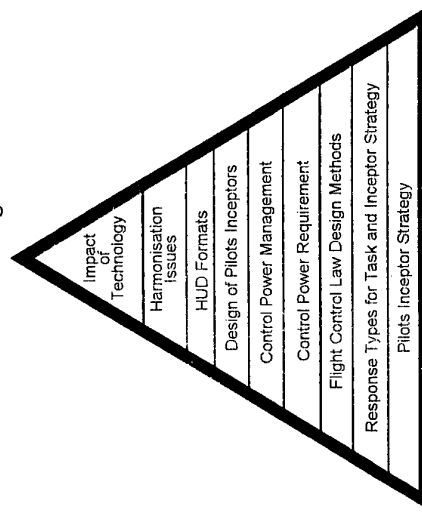


Figure 2: Harrier XW175 VAAC Longitudinal Control System

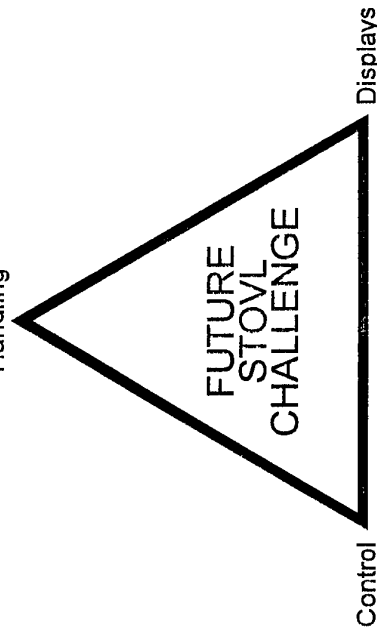
Handling



Displays

Figure 3: The STOVL Challenge to Guidelines Expression

Handling



Displays

Figure 4: Key Items Required for Guidelines Expression

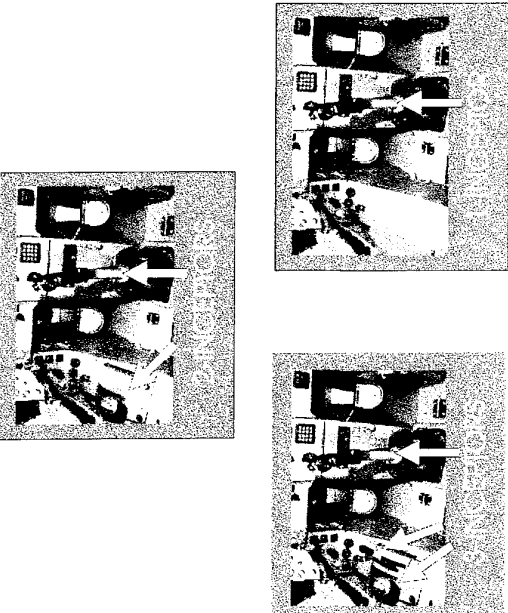


Figure 5: VAAC Harrier Inceptor Options

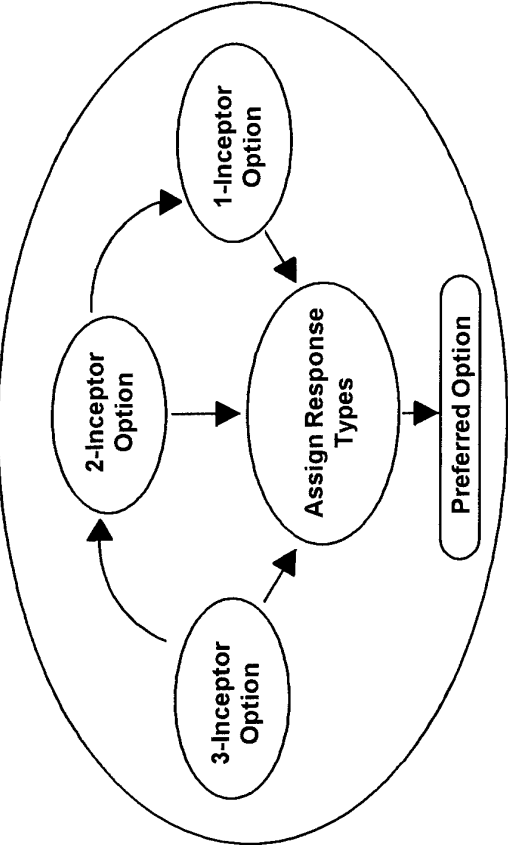


Figure 6: Alternative Pilot Inceptor Options

CONFIGURATION	LEFT - HAND	RIGHT - HAND
Standard Harrier or 3-Inceptor (CTOL) (STOVL)	X (1-inceptor) Z (2-inceptors)	Z and Y X and Y
2-inceptor <i>Either</i> (CTOL) (STOVL) <i>Or</i> (STOVL) <i>Or</i> (STOVL)	X (1-inceptor) Z (1-inceptor) X (1-inceptor) X and Y (1-inceptor)	Z and Y X and Y Z and Y Z
1-inceptor (CTOL) or (STOVL)	Not Used	Z with X and Y on 'Thumb'

Figure 7: Force Assignment to Inceptors

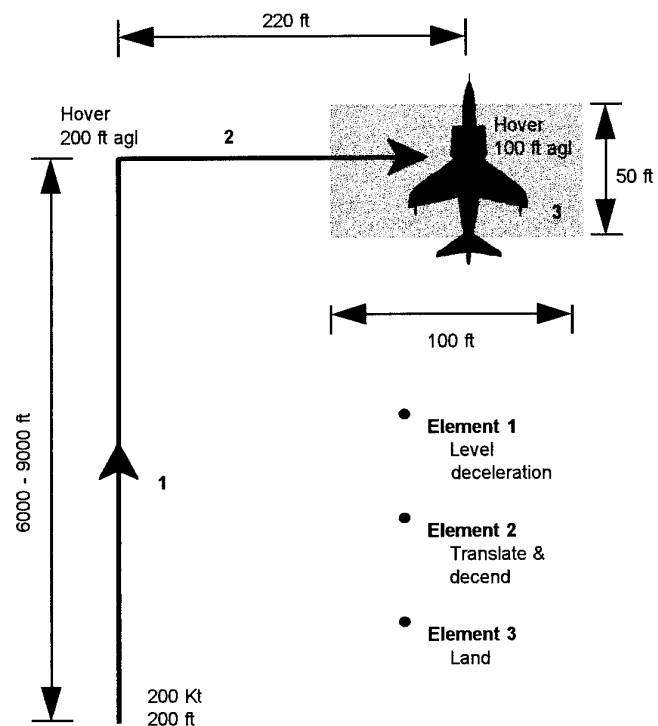


Figure 8: The Assessment Task

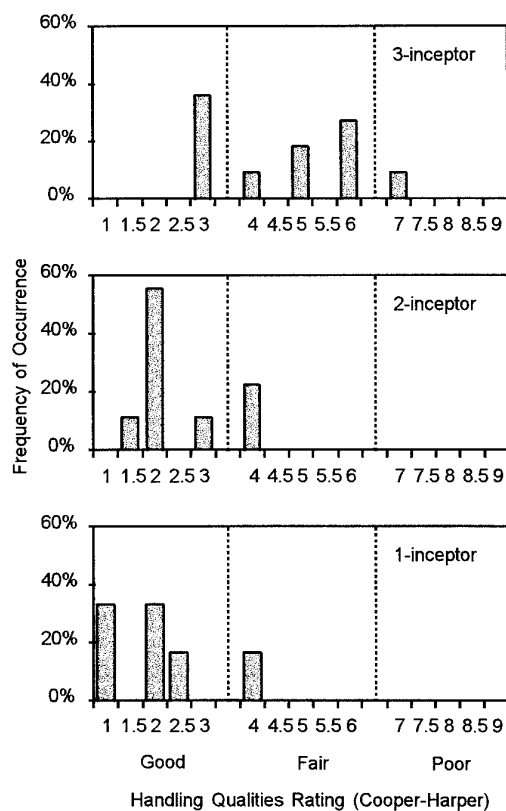
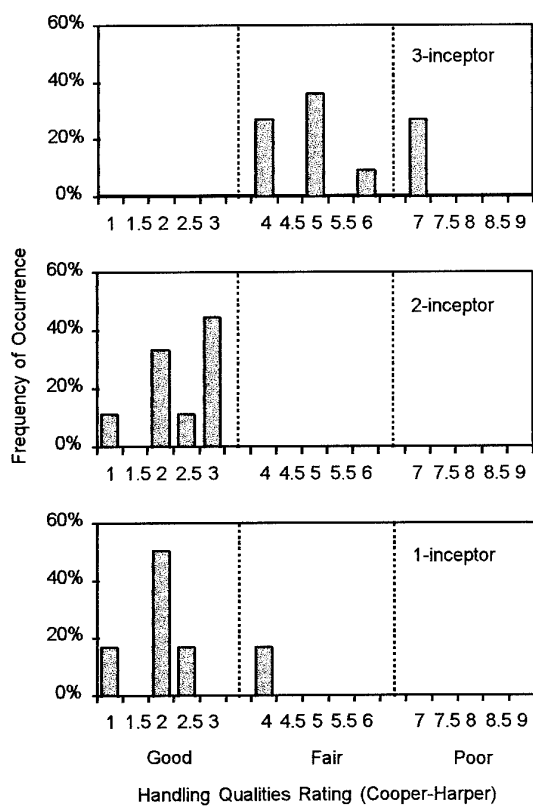


Figure 9: Task Element 1 - Handling Qualities Ratings Figure 10: Task Element 3 - Handling Qualities Ratings

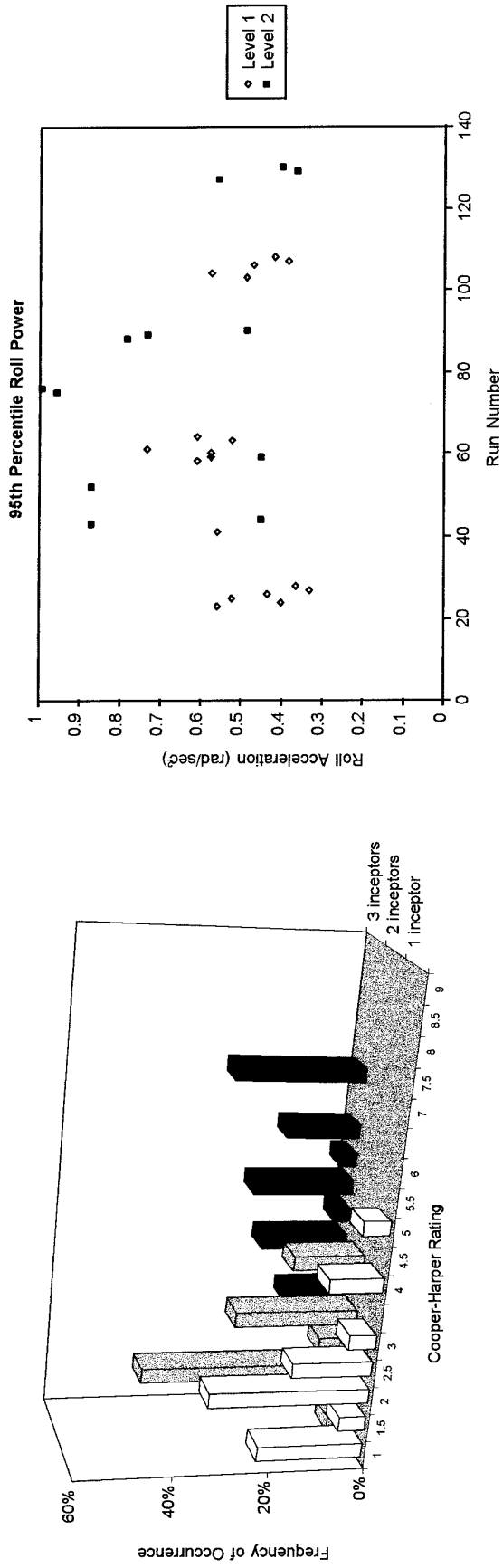


Figure 11: Combined Results - Handling Qualities

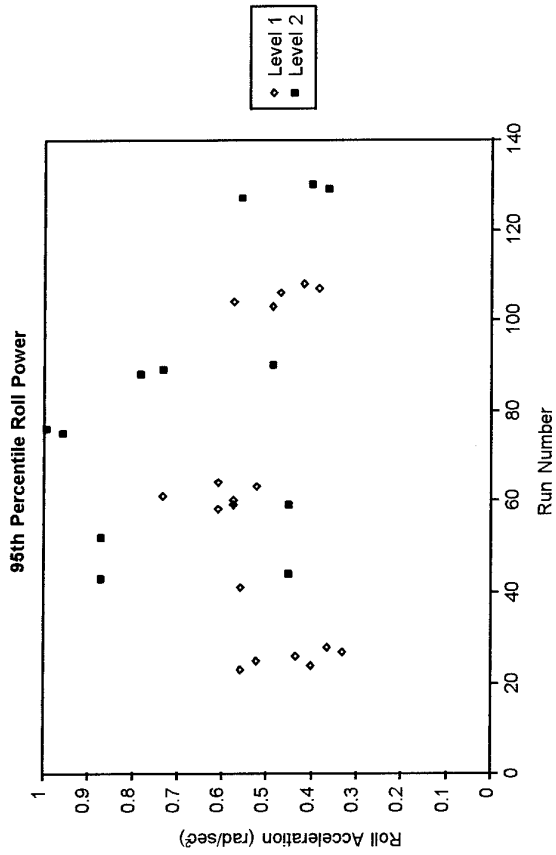


Figure 12: Roll Control Power with TRC Response Types

LEFT - HAND		RIGHT - HAND			
Longitudinal	Lateral	Longitudinal	Lateral	Thumb Longitudinal	Thumb Lateral
TRC 'X'	TRC 'Y'	Height Rate	-----	-----	-----
Height Rate	-----	TRC 'X'	TRC 'Y'	-----	-----
-----	-----	Height Rate	-----	TRC 'X'	TRC 'Y'

Key: TRC Translational Rate Control
'X' Aircraft longitudinal axis component of groundspeed
'Y' Aircraft lateral axis component of groundspeed

Figure 13: Inceptor Strategies Giving Level 1 Handling Qualities for Hover

INTEGRATED FLIGHT AND PROPULSION CONTROL SIMULATION TOOLS FOR ADVANCED AIRCRAFT AND PROPULSION SYSTEMS

Kurt J. Sobanski
Irfan Khalid
Pratt & Whitney
P.O. Box 109600
West Palm Beach, FL 33410-9600

SUMMARY

Pratt & Whitney and McDonnell Douglas Aerospace teamed together, under the Air Force Wright Laboratory sponsored Propulsion Critical Integrated Control (PROLIFIC) program, to develop and demonstrate an Integrated Flight and Propulsion Control (IFPC) system for flight critical applications. The team implemented the PROLIFIC IFPC in real-time hardware using state-of-the-art digital electronic computer boards. The system included simulations of the engine and aircraft as well as propulsion and flight controls, executing closed loop in a piloted flight simulation environment. Advanced control modes and logic including a Multi-Variable Control (MVC), an On-Board engine Model (OBM), and Nozzle Control logic for a Spherical Convergent Flap Nozzle (SCFN), were developed and demonstrated. Additional technical accomplishments of the PROLIFIC program included the development and demonstration of: quad redundant propulsion controls, distributed processing control architecture, a high speed optic data bus, floating point software for engine controls and piloted flight simulation. This paper discusses these accomplishments as well as the benefits of the PROLIFIC real-time system as a cost effective development tool for advanced control technologies. In addition, the paper recommends improvements to IFPC tools in order to meet the demanding requirements of future military tactical aircraft.

INTRODUCTION

The material presented focuses on IFPC development tools for present and future military tactical aircraft. These tools are required to develop and thoroughly verify all propulsion system components prior to flight. Propulsion control systems become flight critical elements for aircraft configurations such as Short Take-Off and Vertical Landing (STOVL) and reduced tail area aircraft with thrust vectoring engine nozzles (Ref 1). In STOVL applications, the propulsion system becomes a flight critical element during jetborne operation when the propulsion system is solely responsible for maintaining hover position. With reduced tail aircraft, the propulsion and nozzle system, in conjunction with the flight control surfaces, become responsible for controlling the aircraft. Throughout the envelope, the flight control maintains stable flight by

using continuous nozzle vector adjustments to supplement flight control surfaces.

As aircraft flight control systems become more coupled with propulsion systems, so does the need for highly integrated control laws and the associated development tools. In the PROLIFIC program, a tool set for development and evaluation of IFPC systems was established in order to meet these needs. Many of the tools used in the program proved very effective and will be used in future developments. The future holds additional challenges for today's tools. This paper discusses these challenges and offers some candidate tools and methods to be pursued for the next generation of advanced fighter aircraft.

IMPORTANCE TO THE AEROSPACE INDUSTRY

Increasing complexity. The aerospace community faces a host of reasons for taking interest in improving existing tools and processes for IFPC development. The growth in complexity of electronic control systems over the years has been paralleled by a similar growth in the tools required to design, build and verify weapon system hardware and software elements. Growth in the future is expected to stretch the capability of today's tools.

Cost and development time closely follow complexity. Economic scrutiny and government pressure continuously focus on affordability to determine whether or not to invest the necessary resources to produce new systems. Future simulation tools must not only enhance the technical development of advanced systems, but must also improve the weapons system affordability.

An opportunity exists for aircraft and propulsion system manufacturers to examine current capability and plan for future requirements. Today's military customers demand affordability in addition to the traditional high performance, low weight, high reliability and maintainability. Processes that were developed in previous years when weapons systems performance and weight dominated customer requirements placed little emphasis on affordability. Key opportunities exist in the refinement of IFPC tools and integration of product development activities.

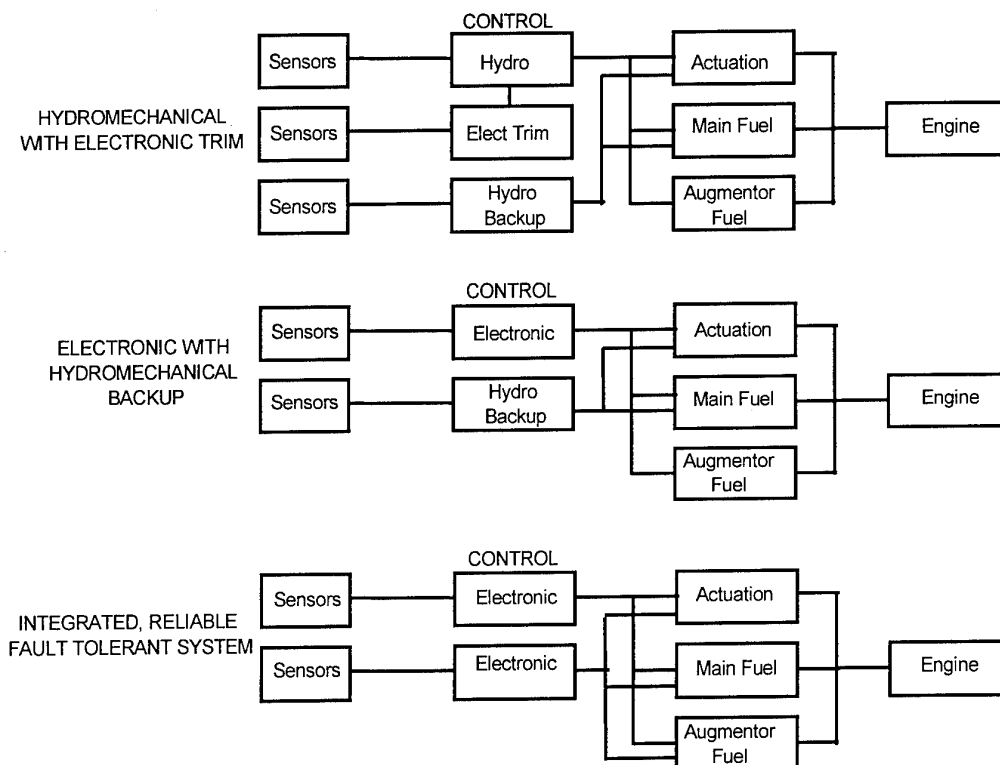


Figure 1. Control Technology Evolution

ELECTRONIC ENGINE CONTROL SYSTEMS HISTORY

Early Electronic Controls

In the 1960's, gas turbine manufacturers incorporated the first electronic controllers in gas turbine engines. The controls used single sensors for input and drove trimming motors attached to hydromechanical control units. With the trimmers, engine manufacturers gained additional performance around the envelope by operating engines closer to turbine temperature limits.

As electronics became more sophisticated, controllers with multiple inputs and outputs were developed. Some manufacturers produced multi-loop analog controls while others implemented digital computer based control systems. Controls built during this time period were somewhat limited in authority and usually had hydromechanical backups. Integration with flight controls was limited to a mechanical or analog power setting and several discrete switches to communicate commands to the engine control or information to the aircraft.

Redundant Full Authority Controls

With recent advances in electronics and associated packaging technologies, engine control systems have

progressed to full authority, redundant systems many times more capable than their hydromechanical predecessors. Along with the capability followed added complexity in hardware design, software design, verification, systems integration and propulsion system testing. To facilitate the development and verification of control hardware and software, real-time simulation tools were developed which realistically emulated the electro-mechanical interfaces, hydromechanical control components, jet engine processes and flight control interfaces (Ref 2). The full authority control systems required an increased level of integration. MIL-STD-1553 data busses carried an array of commands, feedback and engine operating parameters between the aircraft and engine controls. Figure 1 depicts the progression of electronic control development over the last several decades.

PROLIFIC PROGRAM OVERVIEW

To address the complexity of advanced aircraft and flight criticality of propulsion control systems, Pratt & Whitney and McDonnell Douglas developed models that consisted of:

- Mixed Flow Vectored Thrust aircraft model (Figure 2)
- STOVL STF952 Engine Model (Figure 3)
- Quad-Redundant Engine Control
- Pilot Interface

The aircraft is a supersonic, single engine, blended body STOVL configuration. The inlet system consists of twin, side mounted inlets for up and away operation and two top mounted inlets for STOVL operation. In hover mode, lift, trim and Reaction Control System (RCS) nozzles use a combination of compressor bleed air and turbine exhaust to control the aircraft (Ref 3).

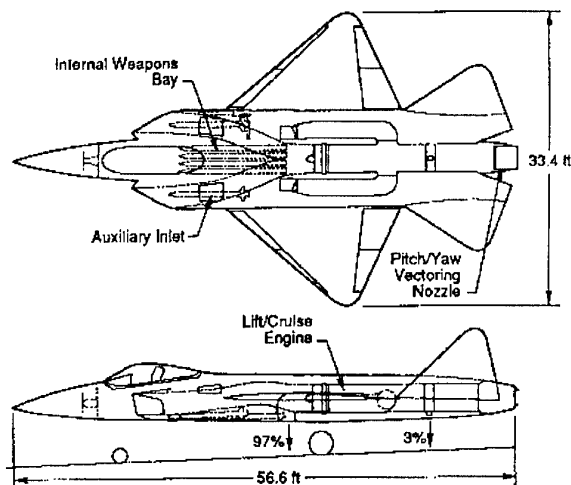


Figure 2. McDonnell Douglas Aerospace Mixed Flow Vectored Thrust STOVL Aircraft (Ref 3)

The P&W STF952 engine is a twin spool, augmented turbofan engine with a Spherical Convergent Flap (SCF) Nozzle (Figure 3). In the up and away mode, the engine operates as a conventional takeoff and landing mixed flow turbofan engine with all thrust exiting the engine through the SCF nozzle. In the transition and hover modes, the lift and RCS ducts are pressurized so that thrust may be ported out through combinations of the lift, trim, RCS or SCF nozzles (Ref 4).

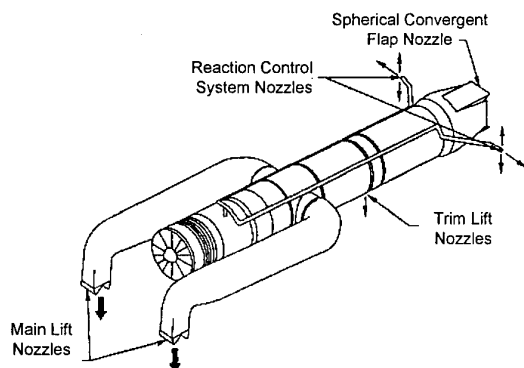


Figure 3. P&W STF952 STOVL Mixed Flow Vectored Thrust Engine (Ref 4)

Simulations of the aircraft and propulsion system components were configured to provide a piloted,

closed loop simulation environment (Figure 4). Commercially available state-of-the-art computer hardware was employed for real-time IFPC implementation. Communication between individual IFPC elements was accomplished through a fiber optic data bus (Ref 5).

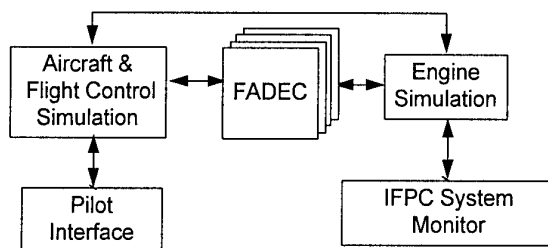


Figure 4. PROLIFIC IFPC Development System

Since one of the primary objectives of the PROLIFIC program was to develop a highly fault tolerant IFPC, the system was designed with multiple-redundant Full Authority Digital Electronic Controls. A quad redundancy level was established in the early phase of the program through a reliability requirements assessment performed based on the PROLIFIC vehicle's mission (Ref 6). The propulsion control software was functionally partitioned into four tasks, each of which executed on its own processor.

PROLIFIC FADEC Processor Architecture

The FADEC contained 4 processors per channel, designated as the Input Output Processor (IOP), the Control Laws Processor (CLP), the Nozzle Control (NC) and the On-Board engine Model (OBM) (Figure 5). The IOP was responsible for all engine control input & output functions, including reading of sensor and actuator feedbacks, performing actuator loop closures, and providing current requests to drive effectors. In addition, the IOP detected, isolated, and accommodated failures in sensors, actuators, and flight control inputs. The CLP utilized a Multi-Variable Control (MVC) approach to provide control of engine thrust, while minimizing loss in compressor stall margin. The CLP accomplished this through modulation of fuel flow, compressor vanes, and total exhaust area. The NC was responsible for controlling the lift, trim and Spherical Convergent Flap Nozzle (SCFN) areas based on the CLP requests, as well as mode transitions between conventional and hover modes. The OBM was responsible for calculating engine gross thrust to be used by the CLP for closed loop control of thrust. Calculated values of unmeasured engine parameters were also provided to the CLP for engine limit protection. In addition, the OBM calculated values of engine sensors, providing a means to check actual sensor validity in the IOP (Ref 5).

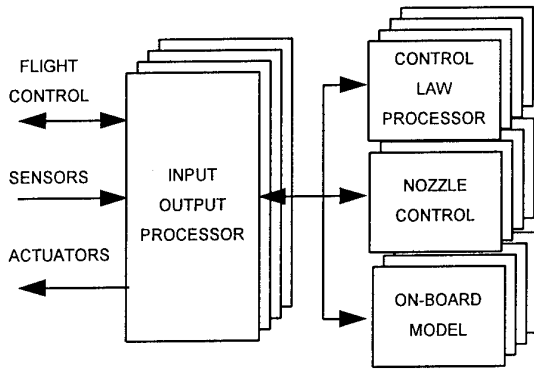


Figure 5. Quad-Redundant Full Authority Digital Electronic Control

PROLIFIC Simulations

The development of the real-time engine simulation followed a typical modeling design process which initially focused on formulation of a detailed, non-linear, aero-thermal representation. Linear representations of this model were then developed for different engine operating points to create the engine State Variable Model (SVM) (Ref 5). The NASA/P&W developed Rocket Engine Transient Simulation System (ROCETS) was used for developing the simulation. The ROCETS tool was used for its capability in modeling high frequency aerodynamic effects unique to the STOVL configuration. In addition, this tool provided a library of engine component modules for convenient model interfacing, and provided automatic linearization capability to generate the state space matrices of partial derivatives for SVM development (Ref 7). A SVM of the McAir six degree of freedom aircraft model was also developed, and was integrated with the engine simulation using ROCETS.

PROLIFIC IFPC Development Tools & Techniques

The PROLIFIC program made several contributions to Integrated Flight and Propulsion Control (IFPC) development that transitioned to P&W's present day propulsion system design and verification methodology. Some of the tools and techniques were used at P&W under PROLIFIC for the first time, while others have been used in previous programs. Each of the following tools and techniques made significant contributions to the success of the program.

PROLIFIC Real-Time Implementation

The PROLIFIC IFPC was implemented using commercially available Motorola 68040 microprocessor boards housed in VME card cages. (VME defines a standard backplane bus into which numerous electronic devices can be inserted to assemble flexible computing power) (Ref 5). Each FADEC software package executed within its own 68040 processor board and

parameters were transferred between processors within a FADEC via the VME bus. Engine simulation software elements such as actuator/sensor models and the engine SVM were also distributed on separate boards for real-time implementation, as were the flight control and aircraft software elements (Ref 5). The PROLIFIC real-time system configuration demonstrated a low cost method for implementation and evaluation of IFPC hardware and software. For a production program, this methodology provides significant insight into the system operation and control issues, prior to investment of development time or funds for flight hardware.

Pilot-in-the-Loop Flight Simulator

A "pilot-in-the-loop" interface and cockpit display were also developed for the PROLIFIC IFPC. Cockpit commands such as Power Lever Angle (PLA), pitch, roll, and yaw requests were transmitted to the aircraft/flight simulation card cage from conventional stick and throttle hardware. A Silicon Graphics Onyx workstation received aircraft position information from the simulation to create the cockpit displays (Ref 5). Use of the interface simplified system testing and set the stage for automated verification methodologies transitioned to existing engine programs.

Pictures-to-Code Software and Configuration Control

The PROLIFIC real-time FADEC software was generated using the P&W Pictures to Code tool, which automatically generates ADA floating point code from electronically drawn pictures. This tool provided a significant level of automation and engineering time savings through establishing a direct link from software design to generation of executable code.

IFPC Monitor System

A MicroVAX computer monitor system was used for PROLIFIC IFPC development and testing. The monitor system provided capabilities such as software downloading, real-time displaying of system parameters, static and transient data recording and graphing. In addition, the monitor provided function generator capability for synthesizing inputs to simulate sensor and actuator faults (Ref 5). More advanced features of the system include the ability to perform frequency analysis of control system parameters.

Floating Point Software for Engine Controls

One of the most significant contributions from the PROLIFIC program to P&W engine programs is the demonstration of floating point software for engine control. Prior to this demonstration, P&W engine controls were programmed in fixed point format, which resulted in the value of calculated control parameters being limited to a numerical scale value. Floating point

does not limit calculations to a scaling, and results in significant benefits including:

- Increased parameter resolution
- Less potential for numeric overflow
- Decreased design time
- Decreased compile time
- Decreased troubleshooting time

The above mentioned benefits have resulted in significant cost savings for engine control software development and verification (Ref 5).

FUTURE REQUIREMENTS

STOVL Aircraft

Advanced aircraft tend to increase coupling between flight control surfaces and propulsion system dynamics. STOVL applications are a prime example of the coupling effects between systems. Transitions from wingborne to jetborne and back again require a high degree of coordination to effectively alter flight control surfaces while maintaining propulsion system thrust. During the transitions, the IFPC system must maintain effective engine nozzle area while aft thrust is being translated downward. Real-time IFPC simulation tools are critical to enhancing the development of STOVL technologies.

Subsystem Integration Technology (SUIT)

Under the Air Force sponsored SUIT program, McAir, P&W, and Allied Signal developed concepts for integrating all aircraft and engine subsystems responsible for power generation and cooling, in order to reduce vehicle weight (Ref 8). Implementation of the SUIT concepts is dependent upon power extraction from the engine system through engine compressor bleed. The effects of this bleed on the engine system are inherently nonlinear, and result in a non trivial computational error when modeled in real-time with traditional engine State Variable Models. Improved real-time simulation tools are required for accurate modeling of these bleed effects, which is critical to enhancing the development of SUIT concepts.

Real-Time Simulations For High Response Systems

Control systems technologies have recently been evolving to accommodate higher response aircraft applications such as vibration and noise control, magnetic bearings, Internal Starter Generator, and aerodynamic control for high speed rotating machinery. The control approaches for these applications typically require the capability of high speed digital signal processors (DSP) to execute the Fourier Transform based algorithms necessary to process high frequency input signals. In addition, higher response actuation and sensing are critical for successful implementation of these techniques. To enhance the development of these

control approaches, further developments are required in real-time modeling of high response systems.

The advantages of employing real-time models for control system development have been clearly demonstrated in the case of the jet engine control. Although initial control design and development are performed using a detailed non-real-time aero-thermodynamic model of the engine, final verification is performed with a real-time engine model to closely replicate actual operation. The same methodology is desired for higher response systems. The challenging aspect of higher response real-time model development is producing real-time software which will execute fast enough to ensure accurate representation of actual system response. In addition, importance must be given to the selection of appropriate high speed processors which will meet the update rate requirements.

Magnetic Bearings

An example of a high response control technology which would benefit from real-time model development is magnetic bearings for jet engine rotor support (Ref 9). Magnetic bearings operate by creating an electromagnetic field which attracts the rotor toward the stator. The rotor position is detected by sensors which provide a signal to the bearing digital controller. The controller commands electromagnet coil currents through power amplifiers for positioning the rotor at the desired location. Presently, digital controller development and verification for magnetic bearings are accomplished through off-line analysis and extensive, time consuming rig testing. A preferred approach is to enhance the development and verification of the controller using a real-time model of the rotor and magnetic bearing system, to replace the actual rig. The simulation software must execute fast enough to approximate a system response on the order of the engine rotor frequency which may be as high as 400 Hz. This system response is significantly higher than that simulated by present day real-time engine models which typically simulate actuator responses of under 10 Hz. With the advancements made in microprocessor technology and real-time software techniques, the required increase in computational capability may be achievable.

Control of Rotating Stall and Surge

Another high response control application that will benefit from real-time modeling is active control of rotating stall and surge in gas turbine engines. This control approach operates by sensing pressure instabilities in the engine compressor flowpath and processing this information in a DSP based control that commands a high response bleed valve system to remove the instability (Ref 10). Although compressor rig testing is presently required for control development and verification, significant benefits could be achieved

through integration testing with a real-time model that simulates the aerodynamic characteristics of the instability, bleed valves and sensors. System response rates for this application are at least on the order of the engine rotor speed, making this another challenging real-time modeling application.

Distributed Controls

Distributed control moves FADEC processing from a central location to smart sensors and actuators. This control architecture will affect our future approach to system design and verification and should be considered when developing tools for future aircraft and propulsion systems.

ENABLING IFPC TECHNOLOGIES

After the PROLIFIC program was completed several additional needs were identified for future IFPC development efforts:

- High fidelity real-time non-linear engine models
- Low cost, flight capable equivalent version of the high speed data bus
- Integrated Product Development Approach

High Fidelity Models

As mentioned previously, a State Variable Model (SVM) was used to simulate the PROLIFIC engine. Engine manufacturers typically use SVMs or simplified aero-thermodynamic models for gas turbine engine software verification and real-time simulation of IFPC systems. If engine developers had enough computing power, the detailed aero-thermodynamic model would be chosen for tasks that require simulation accuracy. In the past ten to fifteen years, real-time control system modelers have been limited in capability due to processing speed. In the near future, engineers may have the capability to run the non-linear models in real-time. Advances in processor technology and innovative ways of handling conventionally non-deterministic convergence solutions may become enablers for the new modeling technique. The advantages of implementing high fidelity aero-thermodynamic engine models on a real-time system are discussed in the following paragraphs.

Multi-Function Models. One potential benefit is that the high fidelity models are more capable of handling tomorrow's engine designs than a typical State Variable Model. New systems designs that include STOVL operation, integrated subsystems and electrically powered actuators and bearings will require engine models that accurately model bleed extraction and other off nominal operating conditions. Existing models could be modified by adding more inputs, states and outputs. However, it would be time consuming and costly to use

a specialized SVMs for multiple purposes. The number of states and outputs would become large enough to significantly slow down the computation cycle. With the real-time high fidelity model, a number of off-nominal cases could be simulated without modifying the model to suit specific needs.

Single Model Analysis. A significant issue that arises during engine control system development is that detailed aero-thermodynamic models are used for performance analysis and the SVM is used for real-time testing and verification. With SVMs, a 5 percent error is acceptable for steady state and transient operation. The percentage error does not seem significant alone, but becomes significant when the models do not produce the same results. For example, a 5 % offset in turbine operating temperature can cause a control system to behave differently if the offset causes the control to operate against the turbine temperature limit. The result is that the verification process forces an analyst to determine the source of the discrepancy. The investigation is usually time consuming and often adds no real value to the system development. High fidelity models have the potential to eliminate the costs associated with bookkeeping two models for the same engine.

Enhanced Failure Mode Analysis. An aero-thermodynamic model inherently has better fault accommodation testing capability than less detailed models. More accurate representations of component failures can be simulated because the more detailed model is not operating point sensitive. Fault injection due to system failures, flow path leaks or efficiency changes would be fairly straight forward.

Reduced Model Development Time and Cost. Use of high fidelity models has potential to reduce engine model development time and cost and deliver a higher quality product. If the models could be made to run in real-time, the steps involving generation, retargeting and checking out scaled down models could be eliminated.

Flight Critical Communication Networks

The PROLIFIC data bus used off-the-shelf VME boards to implement the IFPC communication network. Demonstration of the data bus helped provide a set of requirements for the next generation propulsion control systems. Features of the data bus architecture have potential to reduce cost and increase performance in future systems:

- high speed
- low latency
- software transparent, memory mapped transfers
- error detection and correction

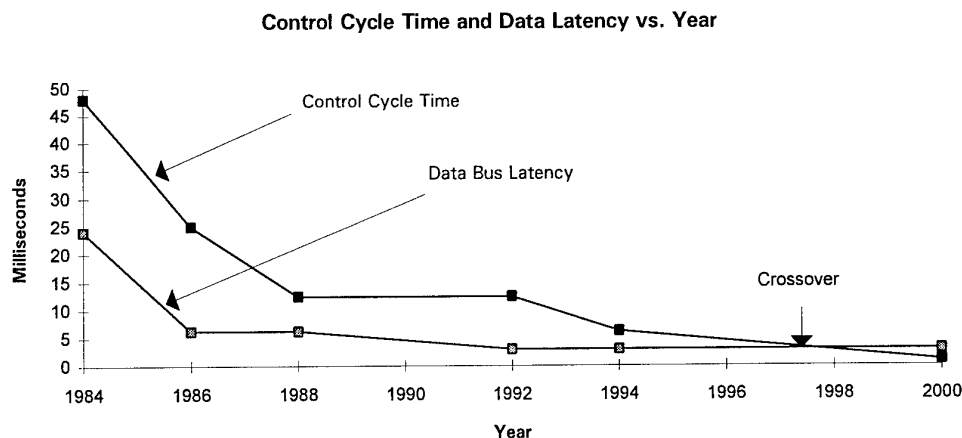


Figure 6. IFPC Control Cycle Time and Data Bus Latency

The PROLIFIC optic data bus utilized a token ring method for communication between all nodes in the network. Nodes communicated with other nodes by calculating parameters located in a global memory space on each data bus board. As parameters were calculated, the data bus hardware automatically updated all nodes on the ring network within a few microseconds. Software designers were able to set up communication between nodes by locating parameters in particular sections of memory. This feature allowed the compiler to automate the process of assigning memory locations to specific parameters.

Performance advantages of the data bus include low latency and reduced processor overhead. In traditional systems, latency is a key factor in data bus software design. The goal is to minimize message transport delay in order to maintain system response. The measured node to node latency of 6 microseconds relieved latency concerns due to data bus transport delays. Processor overhead with the optic data bus was significantly reduced since the FADEC was able to communicate with other nodes without the overhead of the usual interrupt service routines.

In advanced aircraft, latency between subsystems can result in decreased control loop phase margin. IFPC designs that require bandwidths greater than a few hertz can benefit from the described approach. As control systems become more capable, the frame execution time of control algorithms is approaching the latency associated with conventional data buses. Data bus latency will soon become the limiting factor in high bandwidth control systems. (Figure 6, Ref 5).

The PROLIFIC program derived a significant benefit from the data bus during the integration and test phase of the program. No communication anomalies were detected. The trouble--free integration process can be attributed to the speed and simplicity of the interfaces.

Communication anomalies typically account for over half of the IFPC integration anomalies. An alternate approach allows systems integrators to focus efforts elsewhere.

The predominant data bus currently used for flight propulsion control communication in military aircraft is the MIL-STD-1553B bus. A comparison of this bus with the data bus used in PROLIFIC is provided in Table 1. The listed characteristics of the PROLIFIC bus are desirable for future IFPC implementations.

Table 1. Data Bus Specification Comparison

	1553	PROLIFIC	Units
Media	Electrical	Fiber Optic	
Structure	Linear Command/Response	Token Passing Ring	
Data Rate	1	170	Mbits/sec
Effective Throughput	50	6200	KBytes/sec
Latency (Best)	2000*	6	micro sec
Latency (Worst)	25000*	10	micro sec
Max # of Nodes	31	256	

* Latency is dependent on control system update rate

The benefits discussed were realized by using available commercial hardware. For production engines and aircraft, a fiber optic or electrical flight quality version of the communication network is needed.

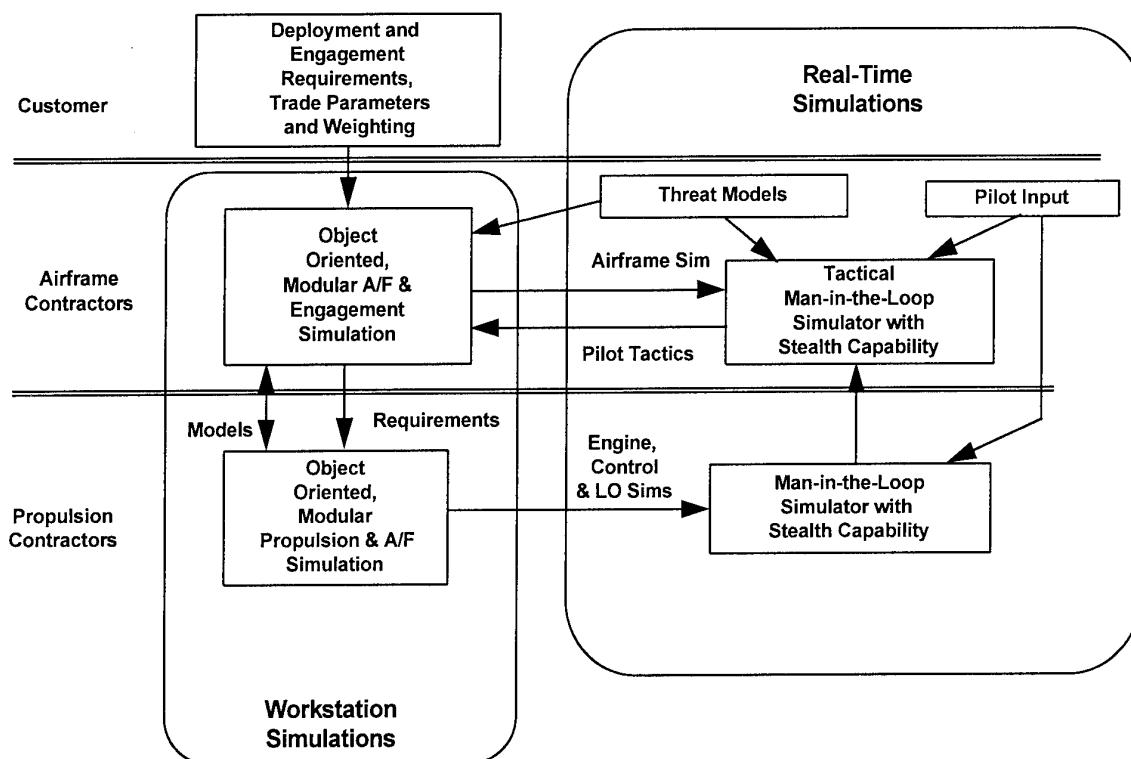


Figure 7. IFPC System Development Tools

Integrated Product Development

One important aspect of the aircraft system development process is the integration of all functions and subsystems to provide an optimum design. As weapons systems become more complex, the need intensifies to closely coordinate requirements, design, fabrication and testing efforts from the customer to the lowest tier supplier.

An example IFPC development tool set is shown in Figure 7. The tools include functions at the customer, airframe and subsystem level. The tools focus on:

- Customer requirements
- User involvement
- Complete system integration and optimization
- Simulation based, progressive development approach
- Air combat simulation capability
- Standard interfaces and tools

Success of future development programs will depend on the ability of team members to effectively use IFPC development tools to provide high quality systems. In an ideal development process, requirements from customers would be incorporated into simplified simulations at each level of the supply chain. After established and acceptable, detailed simulations could be implemented in the entire system by suppliers at each level.

From the start of the conceptual design process through flight test, the user involvement is critical. Pilot interfaces, workload and tactics need to be evaluated as early in the development process as practical to ensure a successful design. Integration of all aircraft systems is necessary to meet mission requirements.

Air combat simulation and evaluation of weapon system models are also critical throughout the development process. Technologies incorporated into an aircraft affect pilot tactics. Through the use of advanced simulations, pilots can develop these tactics and evaluate effectiveness of low observable technologies on mission success rates.

In the IFPC development process, it is important that each team member works a predetermined plan to complete the entire system and that no effort is duplicated. Prime contractors and suppliers must coordinate effort to ensure tool and simulation compatibility. In an ideal situation, one simulation of each component would be provided to a systems integrator with overall responsibility. In the case of propulsion systems, suppliers could use the integrated simulations to evaluate engine performance throughout the flight envelope. The ability of system developers to integrate these functions into high fidelity real-time systems will enhance the capability of tactical aircraft manufacturers.

CONCLUSIONS

Flight and propulsion control systems have become more complex as weapons system requirements have increased over the past two decades. Tools that support the development process have followed a parallel path in complexity and integration. The PROLIFIC program demonstrated several key development tools and methodologies that address this growth in complexity. These tools and methodologies will be used to support future propulsion system development programs at Pratt & Whitney and include:

- Real-time engine and aircraft simulations
- Piloted flight simulators
- Floating point engine control software
- Pictures-to-code software development
- High speed, low latency communication networks
- Integrated IFPC monitor system
- Integrated Product Development approach to simulation development and evaluation

In the future, attention will be focused on a few key items to improve the capability of reducing system development cost and time while providing more advanced systems. These items include:

- High fidelity simulations
- Continued pursuit of a flight quality, cost effective, high performance IFPC communication network
- Continued pursuit of Integrated Product Development approaches to IFPC simulations and real-time evaluation tools.

REFERENCES

1. Doane, P., Gay, C., Fligg, J., Multi-System Integrated Control (MuSIC) Program Final Report, Contract F33615-84-C-3015, WRDC-TR-90-6001, June 1990
2. Roth, S., Celiberti, L., "Micro-Computer/Parallel Processing for Real Time Testing of Gas Turbine Control Systems", in "AIAA/SAE/ASME/ASEE 23rd Joint Propulsion Conference", June 29-July 2, 1987, AIAA-87-1926.
3. McDowell, P., "Users Manual for the Six Degree of Freedom Simulation of the Model 4636 Mixed flow Vectored Thrust ASTOVL Aircraft", McDonnell Douglas, October 1992.
4. Rosson, R., "User's Manual for PROLIFIC Transient Aircraft/Engine Simulation", Pratt & Whitney, AF Contract F33657-85-C-2130.
5. Glickstein, M., Hill, B., Kerr, L., Khalid, I., Larkin, L., Mills, J., Phillipot, J., Rosson, R., Sobanski, K., Wood, B., "Propulsion Critical Integrated Control (PROLIFIC) Final Report - Book 1", AF Program Manager: Timothy J. Lewis, Contract F33657-85-C-2130, WL-TR-94-2093, September 1994.
6. Tillman, K., Ikeler, T., Peck, R., McDowell, P., "PROLIFIC Task 1 Design, Development, and Demonstration Plan", Contract F33615-84-C-3015, WL-TR-91-2114, January 1992.
7. Mason, J., Byrd C., Parham R., Roadinger, T., "Rocket Engine Transient Simulation System",
8. Carter III, H., Matulich, D., Weiss C., "A Subsystem Integration Technology Concept", in "SAE Aerospace Atlantic", April 1993, Paper 931382.
9. Weiss, C., "The More Electric Engine", Pratt and Whitney, May 1993.
10. Eveker, K., Gysling, D., Nett, C., "Integrated Control of Rotating Stall and Surge in Aeroengines", in "Sensing, Actuation, and Control in Aeropropulsion", SPIE, 1995.

Paper 40: Discussion

Question from A T Webb, Edwards AFB, USA

Do you feel that the simulation methods you have described have applicability to in-flight validation and flight testing of the integrated control system and engines?

Author's reply

Yes, it is clear that simulation will be extremely useful during flight test, both at the test site and at the contractor's facility. This is already being seen in the F22/F119 programme.

Question from G Tanner, Rolls-Royce, UK

Do you have any views about the possible need for a quadruplex architecture for a future integrated control system?

Author's reply

The level of redundancy is highly dependent on the application. For the programme discussed in the paper, the reliability study done early in the programme established a requirement for a quadruplex approach. Pratt and Whitney's current level of redundancy is dual for a conventional aircraft. For a future flight critical application, I believe a dual or possibly triplex system is more realistic.

Question from G T Shanks, Defence Research Agency, UK

In terms of the modelling fidelity you discussed in the paper, have you identified any metrics appropriate to the application, or are we faced with the need for ever more capable hardware to run the systems?

Author's reply

If we are successful at implementing a non-linear aerothermal model in real time, using advanced techniques (eg neural networks and fuzzy logic), we should expect a good match between the results of non-real-time analysis and real-time integration test results. There is commercially available neural network hardware that may make this approach possible.

Integrated Flight and Propulsion Controls For Advanced Aircraft Configurations

Dr. Walter Merrill and Dr. Sanjay Garg
National Aeronautics and Space Administration
Lewis Research Center, M/S 77-1
21000 Brookpark Rd, Cleveland, Ohio 44135
USA

Abstract

The research vision of the NASA Lewis Research Center in the area of integrated flight and propulsion controls technologies is described. In particular the Integrated Method for Propulsion and Airframe Controls developed at the Lewis Research Center is described including its application to an advanced aircraft configuration. Additionally, future research directions in integrated controls are described.

Introduction

The research vision at the NASA Lewis Research Center in the area of integrated flight and propulsion controls (IFPC) technologies is to perform high-payoff research that is focused on the critical needs of our customers, is collaborative with our industry and university partners and includes mechanisms for effective technology transfer. The technology of integrated flight/propulsion controls is required when aircraft configurations exhibit significant levels of coupling between the airframe and propulsion systems. Recognizing that advanced configurations, such as high performance military aircraft, Single Stage to Orbit vehicles, the High Speed Civil Transport, and powered lift vehicles, would exhibit significant coupling, researchers began to develop methods for designing controls that would adequately address this coupling. Coupling can be addressed by looking at either the "inner loop" of the IFPC, generally associated with basic airframe and engine stability and limit protection, and the "outer loop" of the IFPC, generally associated with the distribution of effector power to achieve desired aircraft characteristics and capabilities.

The first significant attempt at an advanced method for designing integrated controls was the USAF Design Methods for Integrated Controls (DMICS) Program. Two separate approaches, one based upon centralized design¹, and one based upon a partitioned design approach², were developed and applied to an F18 configuration. Subsequently, the partitioned DMICS approach was applied in the US/UK joint powered lift program. Here the target application aircraft was a modified F16, called the E7D, for short takeoff and vertical landing (STOVL)

capability. The modifications included a delta wing configuration, an ejector thrust system, a ventral nozzle, and a reaction control system (RCS). Designs were completed for a hover task and evaluated by fixed based, piloted simulation with good results³. A second application of the partitioned DMICS approach, with some modification, was applied to a mixed-flow vectored thrust STOVL configuration. Again fixed-based piloted simulations were accomplished⁴.

NASA Lewis has taken the first generation DMICS technology and extracted the benefits of the centralized design and the partitioned approaches and combined them into an advanced, or second generation approach for integrated control design, improving upon the limitations of the DMICS approaches. The technology is called Integrated Methodology for Propulsion/Airframe Control⁵ (IMPAC). This paper will describe the IMPAC method and other research conducted in support of the development of this technology. Secondly, this paper will discuss the vision of the IFPC team at NASA Lewis for future research in integrated controls.

IMPAC

A flowchart of the IMPAC design approach is shown in Figure 1. The major IMPAC design steps are (1) Generation of integrated airframe/engine models for control design; (2) Centralized control design considering the airframe and engine system as an integrated system; (3) Partitioning of the centralized controller into separate airframe and engine subcontrollers; (4) Operational flight envelope expansion through scheduling of the partitioned subcontrollers; (5) Nonlinear design such as incorporation of limit logic for operational safety; and (6) Full system controller assembly and evaluation. These design steps are briefly described in the following. A detailed description of the methodology is available in Ref. [5].

Given that integrated, nonlinear dynamic models for the system are available, the first task in the IMPAC design methodology involves generation of dynamic models to be used for control law

synthesis (Block 1). These control design models are, in general, traditional linear perturbation models of the system taken at various operating points. An important issue in a centralized linear IFPC design approach is how nonlinearities of subsystems (e.g., propulsion system) will effect the validity of the centralized linear control law synthesis. Therefore, some "conditioning" of the control design models, based on nonlinear effects and control design requirements, will be required to obtain state-space dynamic models of the integrated system that will allow a "realistic" centralized control design.

The centralized control design process (Block 2) uses the full system state-space linear control design models previously developed and is based on available multivariable linear control design techniques that have the capability to meet the IFPC requirements, for example H_∞ based control synthesis techniques [6]. Design criteria formulated from system performance requirements and system open-loop dynamic studies provide the necessary control design specifications (e.g., frequency or time dependent weighting factors) for the chosen linear design technique. Because the linear control law synthesis tool may result in a high order centralized controller, controller order reduction may be performed at this point in the method. The result of this process is an operating point specific, centralized linear feedback controller for the integrated system.

Once an acceptable centralized controller is designed, it is partitioned into decentralized subcontrollers (Block 3) using mathematical techniques that have been developed, see for example Ref. [7]. The controller partitioning task requires that a candidate control structure for the partitioned system be specified. For example, for the IFPC problem the assumed control structure is hierarchical with the airframe (flight) control partition exercising some authority over the propulsion control partition. Comparisons between the centralized and partitioned linear controllers are made to validate the partitioning results as well as acceptability of the chosen decentralized control structure. The result of the controller partitioning task is a set of linear subcontrollers which match the performance and robustness characteristics of the centralized controller to a specified tolerance.

After completion of the operating point specific linear partitioned subsystem control design, detailed individual subsystem nonlinear control design must be performed. The first step in the nonlinear control design involves extension of the individual subsystem controllers to full envelope operation (Block 4) as defined by the system requirements. Typically this would involve gain scheduling of

individual operating point subcontrollers to account for parameter variations due to change in operating conditions. It is envisioned that use of modern robust control synthesis tools to perform the linear control design tasks will reduce the complexity of controller scheduling.

The second subsystem nonlinear control design task (Block 5) involves accounting for the effects of any additional subsystem nonlinearities such as propulsion system safety limits. For example, the propulsion system would require exhaust nozzle area control limit logic to ensure that engine surge margins are maintained. After the appropriate nonlinear control loops have been designed, the subcontrollers can be validated using the subsystem dynamic models. The result of this task is the nonlinear limit and accommodation logic to be added to the full envelope subsystem controllers.

The final task in the IMPAC design approach is reassembly of the full envelope, nonlinear subsystem controllers to form the closed-loop integrated system. Evaluations of the final IFPC design can then be performed using nonrealtime simulations as well as pilot-in-the-loop (PITL) simulations. These evaluations would test the actual system performance (e.g., handling qualities) against the desired system performance specifications.

As with any design process, achieving acceptable control design using the IMPAC methodology will involve iterations through the various design steps. However, the strength of the IMPAC approach is that it considers the complete integrated system at each design step and provides the designer the means to systematically assess the level of integrated system performance degradation in going from one step to the other. The control designer can then make some "intelligent" trade-offs between controller complexity and achieved performance at each design step, thus reducing the number and severity of the design iterations.

STOVL IFPC Design

IMPAC has been applied to the design of an IFPC for the E7D STOVL configuration⁸. This configuration is shown in Figure 2. The emphasis has been a design for the transition mode of flight with a piloted, fixed based evaluation of the approach.

Figure 3 is a block diagram of the full integrated flight and propulsion control system. The main elements of the IFPC system are briefly described in the following. The airframe control

subsystem consists of the following four main sections: the pilot gradients and command limiting, the lateral controller and limit logic blocks, the longitudinal measurement blending, controller and limit logic blocks, and the airframe trim schedules. The pilot gradient and command limiting block provides rate and range limits and scales the pilot effectors to appropriately sized commands. The resulting commands are then passed to both the lateral and longitudinal controllers. The lateral control system maintains closed-loop control of roll rate, yaw rate and the sideslip angle using the ailerons, rudder, and roll and yaw RCS. The longitudinal control system maintains closed-loop control of pitch angle and rate, forward velocity and acceleration, and the flight path angle using the elevons, aft nozzle angle, ventral nozzle angle, pitch RCS, and thrust from the aft and ventral nozzles and the ejectors. The trim schedules provide the nominal steady state operating point information for all of the actuators, including the nominal thrust values. The limit protection scheme bounds the hard actuator limits for both the lateral and longitudinal controllers and provides limit information back to the nominal controllers to prevent integrator windup and to maintain closed-loop stability while trying to maintain closed-loop performance.

The engine control subsystem acts on thrust commands from the longitudinal control system. The airframe trim schedules also provide thrust trim commands and gain scheduling variables to the engine subcontroller. The engine subcontroller consists of the following four main sections: the fan speed schedule, the nominal engine controller, the safety and actuator limit logic, and the thrust estimator. The fan speed is scheduled as a function of the total commanded thrust. The nominal engine controller maintains closed-loop control over fan speed and the three estimated engine thrusts (aft and ventral nozzles and ejectors). While fan speed is measured directly, a measure of actual engine thrust is not available, so a nonlinear static model of the engine provides estimates of the engine thrusts given the available engine information. The engine achieves the closed-loop control by manipulating the fuel flow, the ejector butterfly valve position, and the aft and ventral nozzle areas. The engine limit logic contains actuator rate and range bounds and operational limits for the engine, consisting of the accel/decel fuel flow limits, the fan stall margin, minimum burner pressure, and fan rotor overspeed. Limit information is fed back to the nominal control system to maintain stability during limit conditions. A second version of the thrust estimator is used to calculate thrust bounds based on the engine accel/decel schedule. These thrust bounds are fed back to the longitudinal controller actuator limit block

to provide thrust command limits for the longitudinal controller.

In order to evaluate the performance of the integrated control design, a piloted simulation was performed on the fixed base flight simulator⁹. The major objectives of the piloted evaluation were to assess controllability, performance and workload during a series of four flight scenarios. The four scenarios included a vertical tracking task, a combined longitudinal and lateral tracking task, an abort sequence, and a general maneuverability sequence. For the tracking tasks the pilot's objective was to maintain precise control of the flight path symbol by overlaying it on a ghost guidance symbol which is programmed to fly an optimal trajectory to a simulated landing. For the abort sequence and general maneuverability tasks, the pilot's objective was to assess the controllability and predictability of the aircraft response during excessive excursions from the nominal flight path.

Two pilots, one with V/STOL and powered-lift aircraft experience, and the other with extensive fighter aircraft experience, performed piloted, fixed-based simulation evaluations of the IMPAC design. Example aircraft response time histories for the vertical and combined tracking tasks are shown in figures 4 and 5, respectively. As seen from Figure 4, the IFPC design tightly follows acceleration and velocity commands. The flightpath command is also tracked well, although there is some delay in response due to control communication delays. There is some initial pitch deviation due to deceleration commands which the pilots felt could be bothersome in instrument flight. The results in Figure 5 also show tight tracking of the velocity command as well as the bank angle and heading commands. The very small sideslip response indicates good turn coordination which will result in significant reduction in pilot workload.

The pilot comments revealed good vertical flightpath tracking with excellent decoupling from velocity and lateral response. Also, the comments reflected a good capability to maintain steady deceleration while tracking the ghost symbol to a simulated landing. The pilots could successfully perform abort sequences and large maneuverability changes without loss of control predictability or excessive workload. There did exist, however, uncommanded pitch deviations due to coupling with flightpath and acceleration commands. These pitch deviations could become objectionable in moving base simulation and indicated a need for better pitch regulation in the integrated control design. Some pitch deviations occurred due to coupling of pitch and deceleration commands caused by actuator saturations

from the engine control. Overall, the integrated control design gave successful performance in its first piloted simulation of the STOVL maneuvers, and this study assisted in revealing improvements for an integrated control redesign.

Current and Future Directions

Currently, the NASA Lewis IFPC program is progressing on three fronts. First, we are continuing to develop the IMPAC method by additional research into the application of genetic search algorithms to integrated control. Here the idea is to apply genetic approaches to improve the partitioning phase of the design by improving the optimization approach.

Second, we are emphasizing transfer of the basic technologies demonstrated in the IMPAC STOVL application to the private sector. These specifically include the H Infinity design experience gained, some new and effective ways to handle integrator windup and actuator saturation in multivariable systems, and the IMPAC method itself.

Third, we are beginning a program to develop a software based tool that will embody the IMPAC philosophy for integrated controls design. It is the vision that this software package will establish an architecture that will not only encompass the IMPAC approach but also will include other design methods that have been proposed for application to integrated controls design. For example, NASA Langley has developed excellent tools for the automated design of flight control systems. These tools are based upon several years of research in areas such as Direct Eigenvalue assignment¹⁰, and Stochastic Optimization Feedback/Feedforward Technology (SOFFT)¹¹. These technologies, particularly SOFFT, could be used within the IMPAC framework to perform the centralized design and potentially the partitioning phases, or in a stand alone mode for flight controls. Finally, it is believed that a careful architecture definition and the availability of embedded expert design advice would make such a software design tool a powerful and extremely useful capability. This would establish a de facto standard to help focus future integrated controls tools and methods development for maximum impact at minimum investment.

In the future, we see three important needs in the area of integrated controls. The first, as already discussed, would be the completion of a prototype software design capability for integrated controls. It is obviously highly desirable that this

design capability reduce design process time and yield much more robust control designs. Additionally, and perhaps more importantly in the long run, such a design capability should enable a new level of interaction between advanced configuration designers and flight/propulsion subsystem specialists. In the future, advanced configurations could begin to emerge that exploit high degrees of coupling, enabled by robust IFPC. It is the opinion of the authors that the past practice in advanced designs resulted in compromised designs that avoided coupling. This was an admission that in the past it was too difficult or too complex to perform successful integrated designs. Such a new capability would free the advanced designer to look for and achieve potentially radical designs that would represent significant improvements in performance.

Second, there is a need for a successful, full scale, flight demonstration of the payoff of an integrated controls design on an advanced configuration. Such a demonstration is an expensive proposition and will undoubtedly require the resources of more than a single organization resulting in a cooperative program of national or international scope.

Thirdly, the IMPAC method has been successfully applied to the "inner loop" control design problem. The next step will be to modify the approach to enable highly successful "outer loop" control system designs. This will enable the designer to attack both aspects of a complete integrated flight/propulsion control system.

Concluding Remarks

NASA Lewis Research Center (LeRC) researchers have developed a second generation integrated controls design methodology and demonstrated the methodology through integrated flight/propulsion control design for a complex Short Take-Off and Vertical Landing aircraft configuration. Current integrated controls activities at LeRC include transfer of the integrated controls technologies to the aerospace industry through contracted programs, further development of the methodology through in-house and sponsored research at universities, and development of a computer aided software design tool for integrated control system design. It is envisioned that these activities will result in industry acceptance of the advanced integrated control design techniques and will allow for radical new aerospace vehicle designs that represent significant performance improvements over current configurations.

References

1. Smith, K.L., "Design Methods for Integrated Control Systems," AFWAL-TR-86-2103, Wright Patterson AFB, OH, December 1986.
2. Shaw, P.D., Rock, S.M., and Fisk, W.S., "Design Methods for Integrated Control Systems," AFWAL-TR-88-2061, Wright Patterson AFB, OH, June 1988.
3. Adibhatla, S., et al., "STOVL Controls Technology," final report for NASA contract No. NAS3-25193, General Electric Aircraft Engines, Evendale, OH, March 1994.
4. Weiss, C. et al., "STOVL Controls Integration Program," final report for NASA contract No. NAS3-25194, Pratt & Whitney, West Palm Beach, FL, October 1993.
5. Garg, S., Ouzts, P., Lorenzo, C.F., and Mattern, D.L., "IMPAC - an Integrated Methodology for Propulsion and Airframe Control," 1991 American Control Conference, Boston, MA, June 1991.
6. Garg, S., "Robust Integrated Flight/Propulsion Control Design for a STOVL Aircraft Using H-Infinity Control Design Techniques," *Automatica*, Vol. 29, No. 1, pp. 129-145, 1993.
7. Garg, S., "Partitioning of Centralized Integrated Flight/Propulsion Control Design for Decentralized Implementation," *IEEE Trans. on Control Systems Technology*, Vol. 1, No. 2, pp. 93-100, 1993.
8. Garg, S., Mattern, D., "Application of an Integrated Methodology for Propulsion and Airframe Control Design to a STOVL Aircraft," AIAA 1994.
9. Bright, M., Simon, D., Garg, S., Mattern, D., Ranaudo, R., O'Donoghue, D., "Piloted Evaluation of an Integrated Methodology for Propulsion and Airframe Control Design."
10. Ostroff, Aaron J.; and Proffitt, Melissa S.: Longitudinal-Control Design Approach for High-Angle-of-Attack Aircraft. NASA TP 3302, Feb. '93.
11. Halyo, Nesim; Direskeneli, Haldun; and Taylor, Deborah B.: A Stochastic Optimal Feedforward and Feedback Control Methodology for Superagility. NASA CR-4471, Nov. 1992.

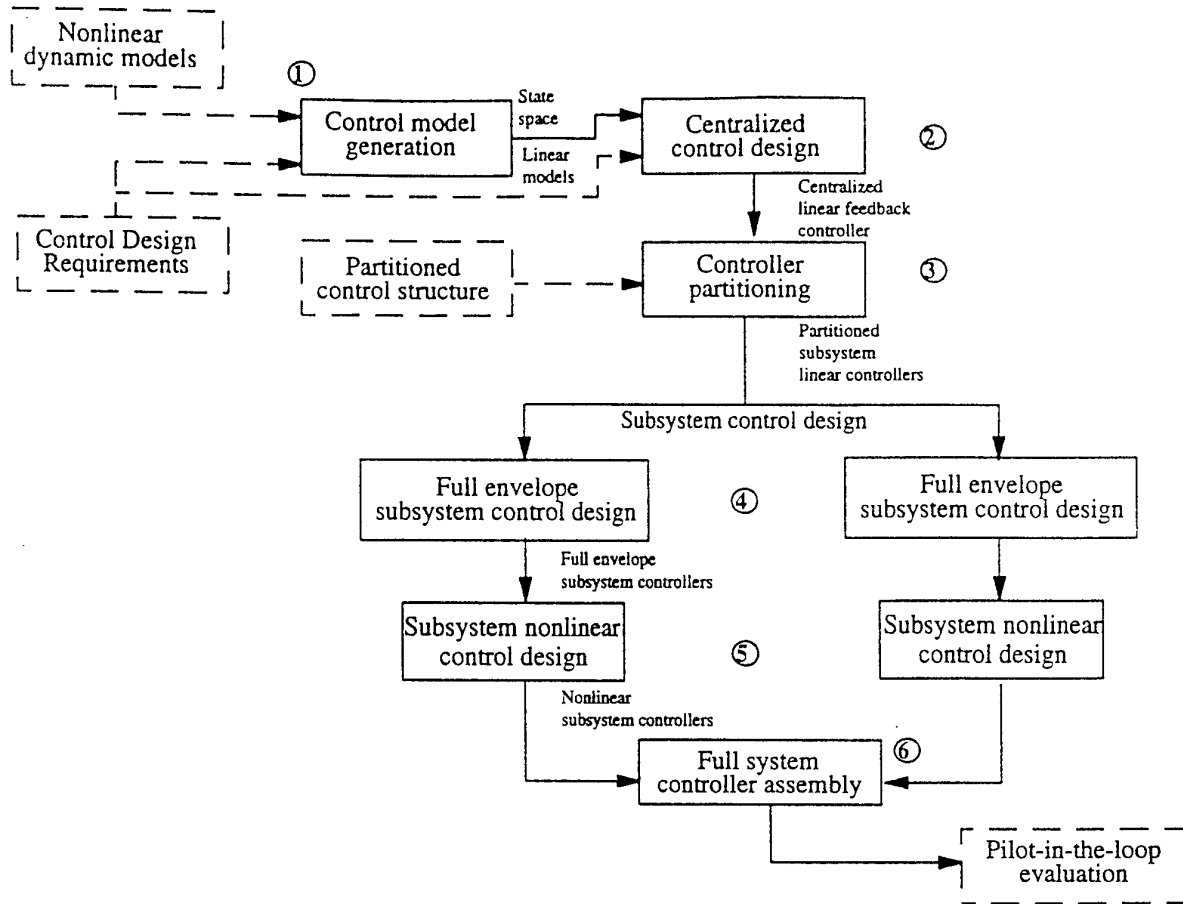


Figure 1. IMPAC Flowchart

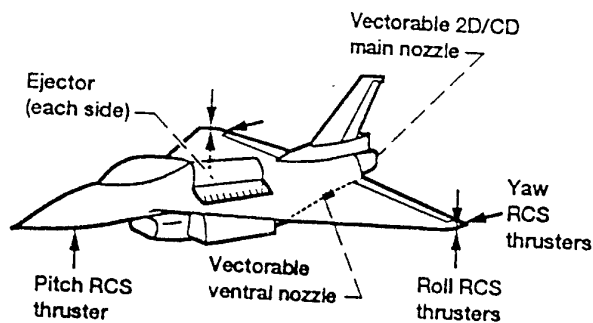


Figure 2. E7D Aircraft Configuration

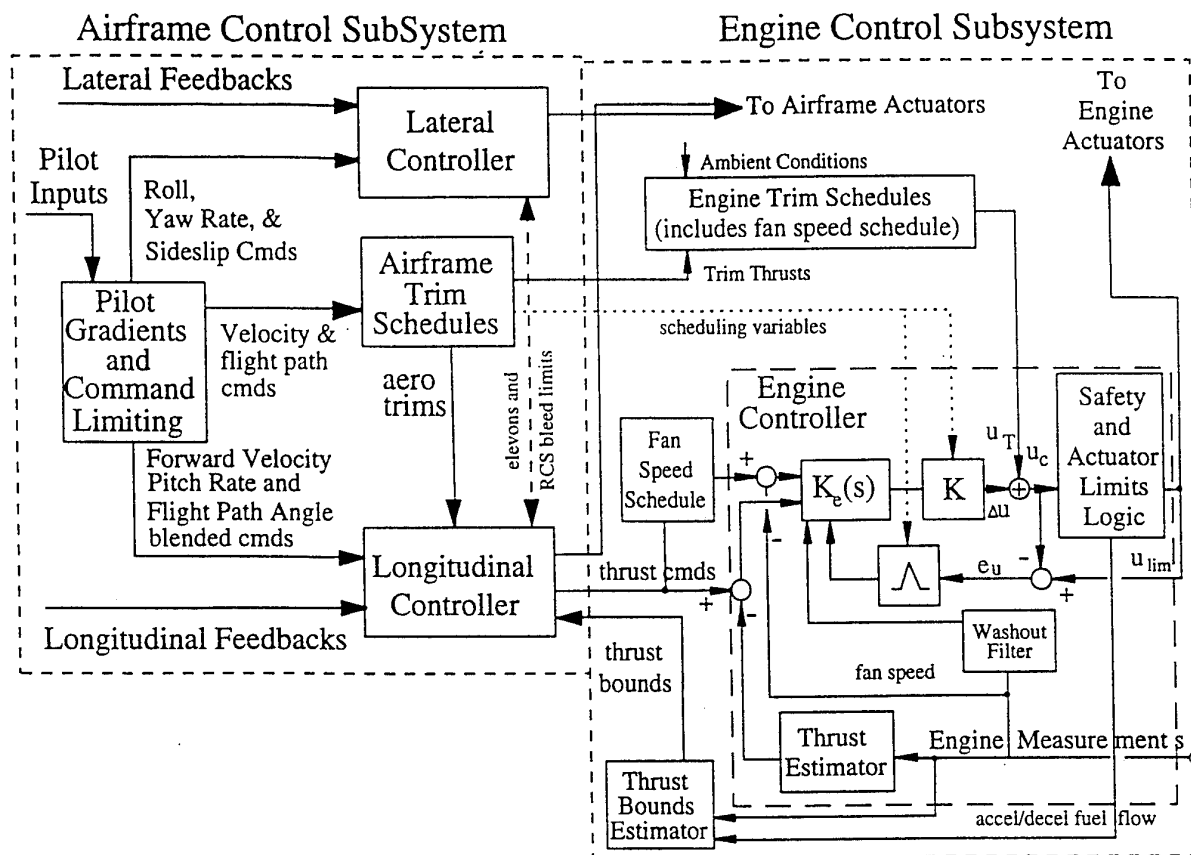


Figure 3. Partitioned, Integrated Controller with Details of Engine Controller

• Vertical Tracking Task

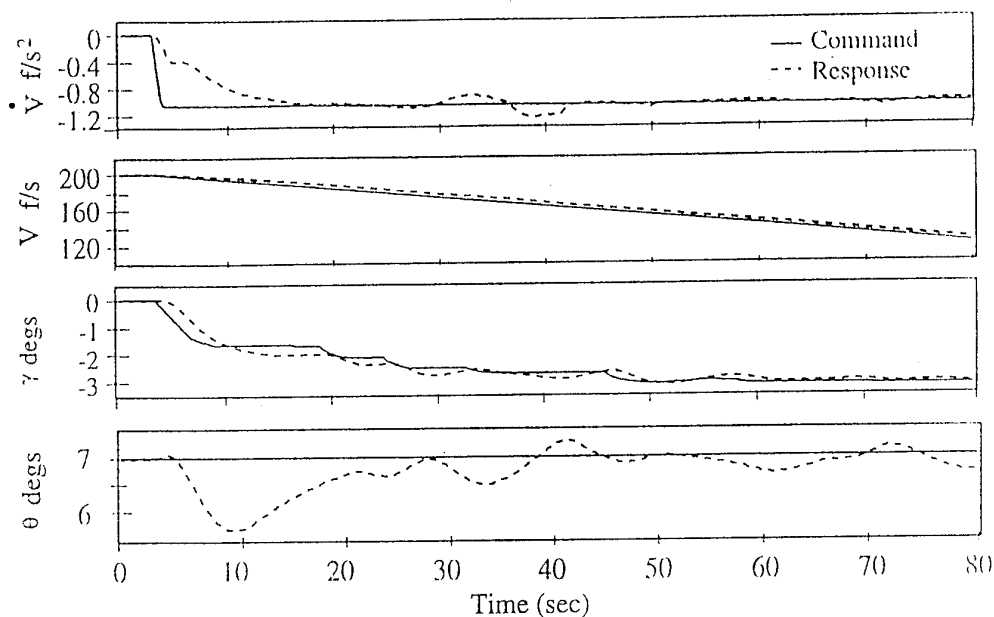


Figure 4. Example Time Histories for Vertical Tracking Task

• Combined Vertical and Lateral Tracking Task

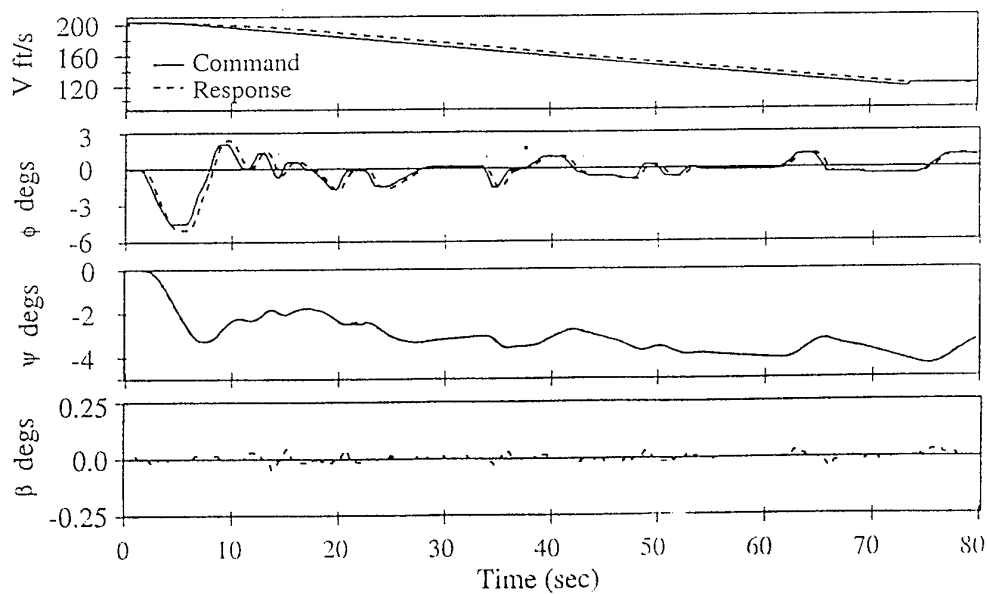


Figure 5. Example Time Histories for Combined Tracking Task

Paper 41: Discussion

Question from G T Shanks, Defence Research Agency, UK

In the processes described, particularly the centralised/decentralised design options, did you consider the impact of flight clearance issues associated with certification?

Author

Since the IMPAC approach results in control implementations (by design) comparable to today's implementations, no special consideration was given to flight clearance in this research. It is recognised that multivariable controls designs generally present many challenges to successful flight/propulsion controls certification.

Question from Prof N Munro, UMIST, UK

Although your initial centralised control sets the benchmark for your subsequent decentralised designs, it represents a much more difficult design task than the latter. If the subsystem performance target could be exceeded, could the subsequent integrated decentralised control give a better overall performance?

Author's reply

For the size and complexity of aircraft systems studied, highly optimised centralised designs have been achieved. Better performance than these will not be possible with the decentralised, partitioned controller. However, if the system complexity is such as to disallow highly optional centralised designs, decentralised designs may well lead to superior overall designs.

Propulsion Integration Issues for Advanced Fighter Aircraft

Marvin C. Gridley
 Steven H. Walker
 Wright Laboratory
 WL/FIMA Bldg 450
 2645 Fifth Street Suite 7
 Wright-Patterson AFB, OH 45433-7913
 USA

1. SUMMARY

Twenty-first century aircraft will require the integration of a multitude of complex component technologies to provide the highest levels of performance and maintainability at the lowest cost. The main focus of research will be weapons system effectiveness rather than a concentration on individual component performance. Two propulsion integration issues that need to be addressed for any future fighter are advanced short duct inlets and lighter weight, lower cost nozzles.

2. INTRODUCTION

Historically, the threat to USAF aircraft has dictated that technology advances in propulsion integration be oriented towards increasing performance. Changes in the global political climate and the resulting impact on national economic priorities have shifted the emphasis away from performance to economy. Next generation aircraft must have lower life cycle cost, be more reliable, perform more and varied missions, and have longer life. Further, multi-service variants will be encouraged as a way to cut costs.

Propulsion integration technologies are keys to attaining goals of lower cost, RM&S, and increased utility. Simplicity in integration should lead to lower cost through greater configuration freedom and internal aircraft packaging flexibility, satisfying multi-service requirements.

Performance remains an important issue. Global technology development will mean more and more potential threats with technologically advanced weapons systems. Therefore, the next generation aircraft will, at a minimum, be required to perform at current systems levels. Additionally, future aircraft systems must be more flexible, to perform a variety of missions to counter changing threats.

Propulsion integration technologies also address performance issues. For inlets, large performance payoffs come from increased configuration freedom with smaller inlets allowing a configurator to put more fuel on board an aircraft to increase its range, or to package an aircraft for lower weight and volume. Fluidically controlled nozzles will allow throat area variation and vectoring with fixed geometries.

3. INLET SYSTEM INTEGRATION

3.1 Inlet Technology Goals

Traditionally, the figure of merit for aircraft inlet systems has been performance. Previous operational inlet designs maximized total pressure recovery and minimized distortion at

the engine face, and minimized overall frontal observables. Current budgetary realities have caused a shift in the technology development approach to center around maintaining current levels of inlet system aerodynamic performance at a reduced life cycle cost and/or increased aircraft utility.

Current USAF inlet technology development has the following goals for the year 2000:

- decrease inlet weight by 50% from current baseline
- decrease inlet volume by 50% from current baseline
- maintain or increase current inlet performance levels

The baseline inlet system is the current state-of-the-art in inlet system technology: a caret inlet aperture with a long, serpentine subsonic diffuser, similar to the design pictured in Figure 1. This design provides for high aerodynamic performance and survivability throughout the tactical fighter envelope.

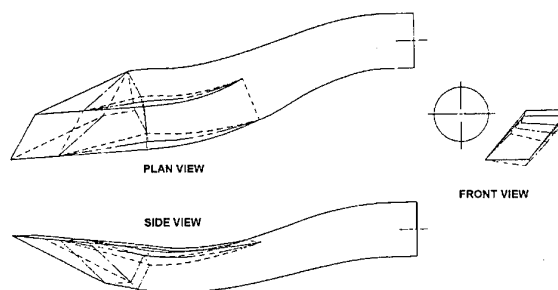


Figure 1 - Caret Inlet System

3.2 Background

Historically, inlet complexity has increased with the maximum Mach capability of the aircraft, Figure 2. Traditional inlet performance enhancement techniques such as variable geometry, boundary layer diverters, bypass systems, and bleed have been incorporated to achieve the levels of performance required for high performance aircraft.

Recent advances in inlet design methodology, namely computational fluid dynamics (CFD) techniques, have allowed inlet designers more insight into inlet and diffuser flowfields. This alleviates some traditional geometric constraints and allows inlet designers (and aircraft configurators) greater flexibility. For example, inlets for certain applications may now

be designed without diverters or bleed systems along with much more compact subsonic diffusers.

	B.L. Diverter	Side or Splitter Plate	Comp Surface	B.L. Bleed	Variable Geom	Bypass System	
F-89							Subsonic
F-5A							
F-101							
F-102							Mach
F-16							1.2-2.0
F-18							
F-104							
ACIS Target							
F-105							
F-106							
F-4							Mach
F-14							2.0-2.2
F-15							
YF-23							
F-22							
F-111							Mach 2.5

Figure 2 - Inlet Complexity with Max Mach Number

One of the most promising techniques for inlet design is illustrated in Figure 3. A bump shaped, waverider compression surface is defined by streamlines emanating from the intersection of a plane which passes through the shock wave resulting off a cone placed in a supersonic flow field. The resulting pressure gradient on the bump surface pushes the low energy boundary layer outboard. By combining this type of compression surface with a properly designed cowl, an inlet can be made "diverterless" for Mach numbers up to ≈ 2.0 .

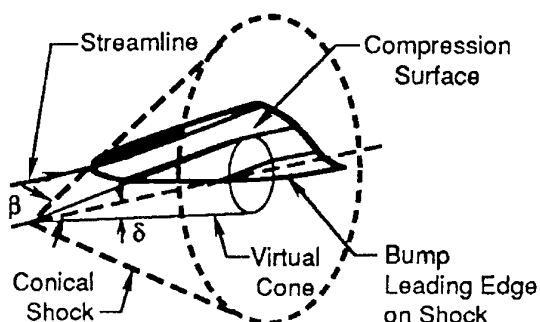


Figure 3 - Bump Compression Surface¹

This methodology was used to design inlets in the USAF Wright Laboratory Management of Advanced Inlet Boundary Layers¹ (MAIBL) program. The objective of MAIBL was to develop design criteria for LO inlet boundary layer control (BLC) systems. Several different boundary layer control techniques were tested in the MAIBL program, including shaping (e.g., the bump compression surface), flush and pitot boundary layer diverters, wall jets, and porous and slot bleed systems. Aerodynamic performance was determined using CFD

and subscale testing. Results shown in Figure 4 indicate that LO inlet BLC methods could provide adequate aerodynamic performance for advanced fighter applications.

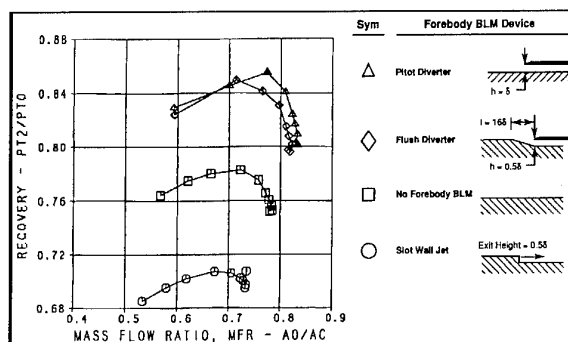


Figure 4 - MAIBL Performance Results, $M = 1.9$, $\alpha = 0^\circ$

In the NASA/McDonnell Douglas Performance Study for Inlet Installations² (PSII) program, a conceptual design trade study was performed to determine the impact of inlets incorporating design features for low observables on inlet performance, weight, and cost for fighter and attack aircraft. The trade studies used Quality Function Deployment (QFD) techniques to prioritize issues and select the optimum air induction system configuration for each of two notional aircraft: a multi-role lightweight fighter and an advanced medium attack bomber. The QFD scores were driven by performance, observables, weight, and cost. Figure 5 shows the aircraft and air induction system configurations for the selected optimum multi-role lightweight fighter. Figure 6 illustrates trade study results which led to the selection of this configuration as optimum. The multi-role lightweight fighter air induction system chosen received the highest QFD ranking, and also resulted in the lowest cost air induction system with the lowest increase in air vehicle TOGW.

Deficiencies in parametric aerodynamic databases for generic LO inlets were identified in the PSII study and a roadmap outlining programs to generate applicable and generic RCS databases was created. Integrated inlet models and test plans were developed for follow-on wind tunnel studies.

3.3 Advanced Compact Inlet Systems

The next step in inlet configuration work was to integrate the various component technologies into a complete inlet system. Insufficient research dollars led to a somewhat new approach for USAF technology development. The Advanced Compact Inlet Systems (ACIS) cooperative program, with combined government and industry investment and participation was formed to develop integrated inlet systems designed to meet the new technology emphasis of affordability. The specific objective of ACIS is to develop integrated inlet systems designed to be low cost, lightweight, and highly survivable.

ACIS was organized as a cooperative program, coordinated by the USAF Wright Laboratory, with partners NASA Langley Research Center, Boeing Military Aircraft, Lockheed Martin Tactical Aircraft Systems, McDonnell Douglas Corporation, and Northrop-Grumman Corporation. Additionally, Allison

Advanced Development Company, General Electric, and Pratt & Whitney are partners representing engine technology development. This arrangement allows all partners to leverage the resources of others to meet program goals.

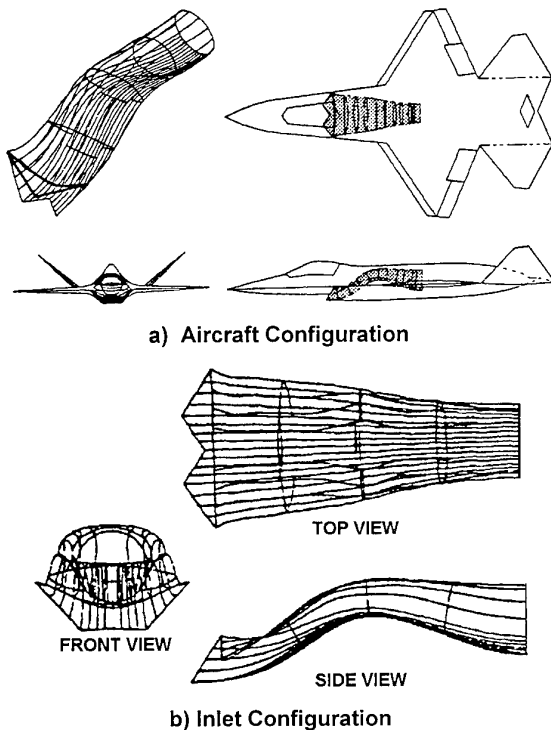


Figure 5 - Selected Multi-role Lightweight Fighter²

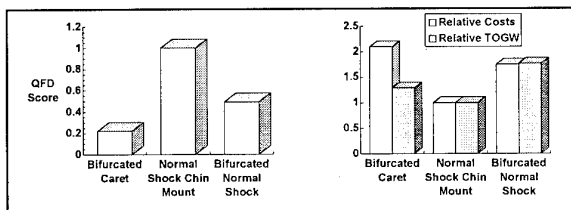


Figure 6 - Air Induction System Trade Study Results²

Because technology development is being focused on affordability, the priorities for ACIS inlet design are as follows:

- life cycle cost
- weight
- aircraft system performance
- survivability
- aerodynamic performance

With these priorities set, the technical groundrules for the ACIS program are as follows:

- 1) The inlet system must be fixed geometry. As seen in Figure 7, an inlet with no moving parts offers a reduction in inlet weight percent, with a corresponding reduction in aircraft TOGW.
- 2) The diffuser must be compact, with diffuser $L/D < 3.5$. Less diffuser volume allows for greater configuration flexibility. Shorter diffusers decrease total inlet volume.
- 3) The inlet system must use zero or minimal and low observable boundary layer control. Boundary layer control subsystems (diverters, bleed systems, etc.) and other inlet systems (bypass, auxiliary inlets, etc.) can have a large impact on overall aircraft system life cycle cost, weight, range/payload performance, and RM&S.
- 4) The inlet system must maintain or increase current levels of aerodynamic and low observable performance. For example, a desired pressure recovery at $M = 1.6$ is 95%, with acceptable engine face flow distortion.

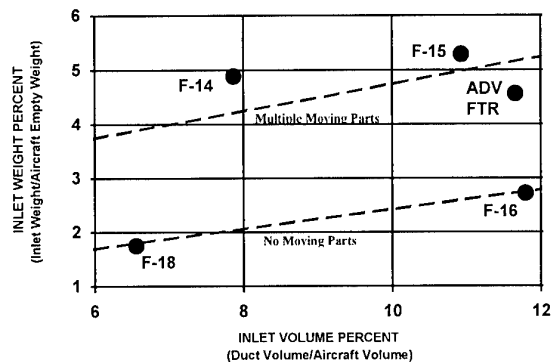


Figure 7 - Inlet Weight/Volume Impact

Additionally, ACIS partners function as a team. All data generated under the ACIS program will be shared with ACIS participants as the program progresses. Reviews are held quarterly to chart progress and provide technical feedback to all partners. Each partner also has invested company resources towards meeting ACIS objective. For example, some participants are providing internal resources for model design, with the model built using USAF funding. Others are doing vehicle trade studies under internal funding and providing portions of the results to ACIS partners. This "buy-in", combined with the shared data agreements, allows each partner to achieve an excellent cost/benefit ratio.

Air induction system configurations within ACIS are highlighted as follows:

- A very simple underslung integration with minimal boundary layer control and a maximum Mach capability of 1.8, with a very compact diffuser ($L/D = 1.44-2.0$).
- A diverterless inlet in a twin inlet, bifurcated duct integration. The diverterless inlet provides the required boundary layer control and compression at higher Mach numbers. None of the traditional boundary layer control mechanisms (diverters, bleed) or bypass system (for airflow

matching at higher speeds) is utilized. This design is therefore very simple, lightweight, and easier to design and produce.

- An inlet concept which utilizes a bump to provide boundary layer control and compression in a single underslung integration. Aircraft sensitivity to air induction system design is another component of the effort.
- An inlet concept which uses a "blended" caret type design in a twin inlet, bifurcated duct integration. The focus is to verify integrated aerodynamic performance of several engine face front frame devices. This will also provide data used to help trade simple duct combined with a front frame versus long serpentine duct approaches to survivability.

4. EXHAUST SYSTEM INTEGRATION

4.1 Nozzle Technology Goals

The overall goal for Airframe-Propulsion Integration in the 1990s is the reduction of weight, cost, and signature levels in propulsion systems while maintaining the current levels of aircraft performance. Current state-of-the-art exhaust systems account for 30% of the overall propulsion system weight compared to exhaust systems of 20 years ago. Past systems were between 5% and 8% of the total engine system cost (Figure 8). Today's exhaust systems must withstand higher temperatures and pressures generated by advanced engines. More aggressive signature requirements force the exhaust system to use materials and manufacturing processes that add weight and cost to these systems. Requirements for thrust vectoring increase the weight, cost, and parts count of current exhaust systems.

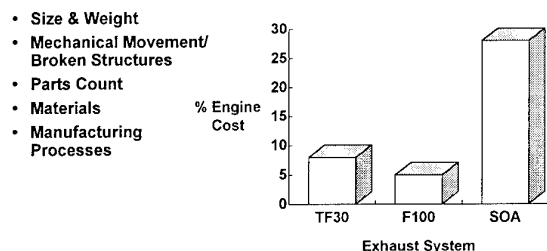


Figure 8 - Historical Nozzle Cost Drivers

Current USAF nozzle technology development has the following goals for the year 2000:

- reduce nozzle acquisition cost by 25% over baseline
- reduce nozzle weight by 50% over baseline
- increase survivability over baseline

A representative example of an exhaust system capable of meeting today's requirements is the Pratt & Whitney Spherical Convergent Flap (SCF) nozzle shown in Figure 9. This nozzle concept was one of six different nozzle designs studied in detail under the USAF Wright Laboratory Exhaust Nozzles for Aerocontrol³ (ENAC) program in the late 1980s. This concept incorporates thrust reversing as well as thrust vectoring. It is capable of at least 20° of pitch vectoring at 60°/sec and 20° of

yaw vectoring at 40°/sec. The SCF nozzle achieves pitch vectoring by simultaneously deflecting the upper and lower divergent flaps. Yaw plane vectoring is obtained by rotating the aft portion of the nozzle, which requires a rotation of the aftbody as well.

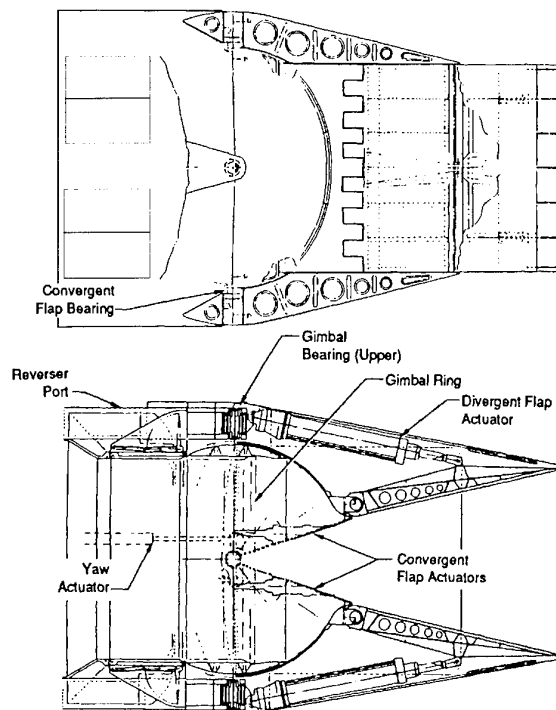


Figure 9 - Spherical Convergent Flap Nozzle³

The SCF nozzle transitions from a round cross section to a rectangular cross section at the throat location while a traditional nozzle transitions starting at the turbine exit. A substantial weight savings over a rectangular-to-rectangular baseline nozzle was achieved by using the round-to-rectangular throat transition. The SCF nozzle including thrust reverser and pitch/yaw thrust vectoring weighs 627 pounds when sized for 241 lbm/sec engine airflow⁴.

In Figure 9, one can see the actuators required to move the large pitch vectoring flaps, and imagine the actuators required to move the nozzle/aftbody structure to achieve yaw vectoring. The number of mechanical actuators, seals, and parts required for the SCF nozzle are similar to the number of parts used in state-of-the-art exhaust systems. This approach, while successful in achieving the required nozzle performance goals, leads to heavy and costly systems that are high maintenance and require specialized manufacturing processes.

The elimination of parts within a nozzle while maintaining current levels of performance will lead to reductions in weight, signature, and cost. One of the enabling technologies for parts elimination is innovative fluidic control technology. Fluidic control of the nozzle area ratio and of the thrust vectoring

function would reduce substantially the required number of exhaust system parts.

4.2 Background

Historically, fluidic control was first used in rocket nozzle systems. As rocket engines increased in size and weight, secondary air injection methods for controlling the primary rocket nozzle flow were investigated as alternatives to heavier gimbal systems. In classical experimental and theoretical studies reported by Blaszak and Fahrenholz⁵ and Gunter and Fahrenholz⁶, symmetric secondary air injection for throttling control and asymmetric secondary air injection for thrust vector control were investigated at the exit of an axisymmetric, convergent nozzle. Secondary air injection angles of 90°, 60°, and 45° to the upstream primary flow direction were used. The symmetric injection results showed that the reduction in the primary flow varied almost in direct proportion to the secondary flow rate. Also, as the primary nozzle pressure ratio, p_o/p_{atm} , was increased, more secondary air flow was required to achieve the same reduction in the primary flow (Figure 10). Some variation in primary flow reduction was also measured versus variation in injection slot width. In all cases of symmetric injection, the thrust coefficient varied between 0.94 and 0.98.

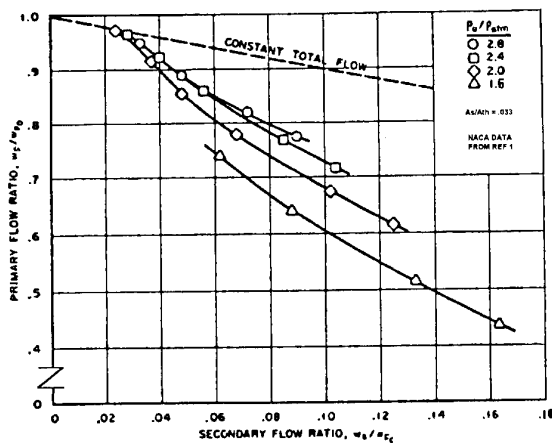


Figure 10 - Symmetric Injection Experimental Data⁵

For the cases of asymmetric blowing, similar primary flow reductions were measured as in the symmetric blowing cases with the smaller secondary area ratios, A_s/A_n . A side force coefficient was used to quantify the amount of thrust vectoring achieved by the asymmetric blowing. The trend for this measurement was a nearly linear side force increase with a secondary flow ratio, w_s/w_{p0} , increase (Figure 11). The side force coefficient also decreased with increasing p_o/p_{atm} for the same w_s/w_{p0} .

A theoretical analysis of secondary injection for area control was also completed. An isentropic, 1-D vortex sheet model and secondary expansion model were used to model the experimental setup of Blaszak and Fahrenholz⁵ (Figure 12a, b). Figure 13 shows the good agreement obtained between the theoretical calculations and experimental data. In general, this level of agreement was found between the experimental data

and theoretical calculations for all of the configurations tested. Blaszak and Fahrenholz⁵ state that this only makes sense since the vortex sheet model and secondary flow expansion model are "extremes" or boundary conditions of the real flow field.

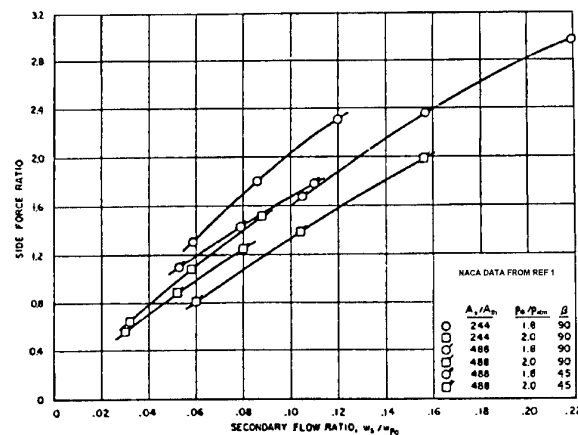
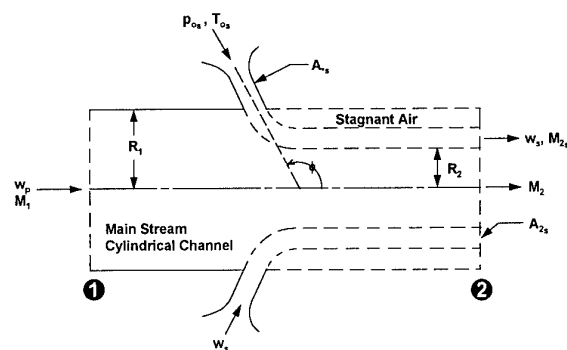
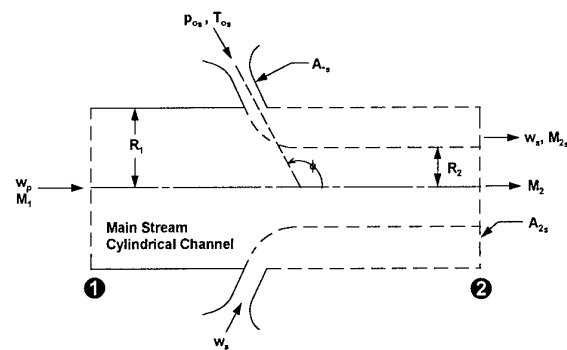


Figure 11 - Asymmetric Injection Experimental Data⁵



a) Vortex Sheet Model



b) Secondary Expansion Model

Figure 12 - Area Control Models⁶

Some of the overall conclusions of Blaszak and Fahrenholz⁵ on fluidic area control were the following:

- 1) The reduction in the primary flow is about 2.5 times the injected secondary mass flow.
- 2) Flow throttling is insensitive to injection orifice arrangement (slots versus holes) in symmetric and asymmetric injection.
- 3) Flow throttling varies significantly with injection angle.
- 4) The effect of primary nozzle geometry is attenuated by increasing p_o/p_{atm} .
- 5) The thrust is directly proportional to the total nozzle flow.

Some of the overall conclusions of Gunter and Fahrenholz⁶ on fluidic control for thrust vectoring were the following:

- 1) The asymmetric injection position for maximum side force is in the supersonic portion of the nozzle far enough downstream to avoid an oblique shock reflection off the opposing wall that would create a counter-force to oppose the desired side force.
- 2) Side force varies in direct proportion to secondary injection mass flow.
- 3) Injection ports shaped to produce supersonic flow will produce more side force.
- 4) The optimum gas injection configuration will be specific to every primary nozzle geometry.

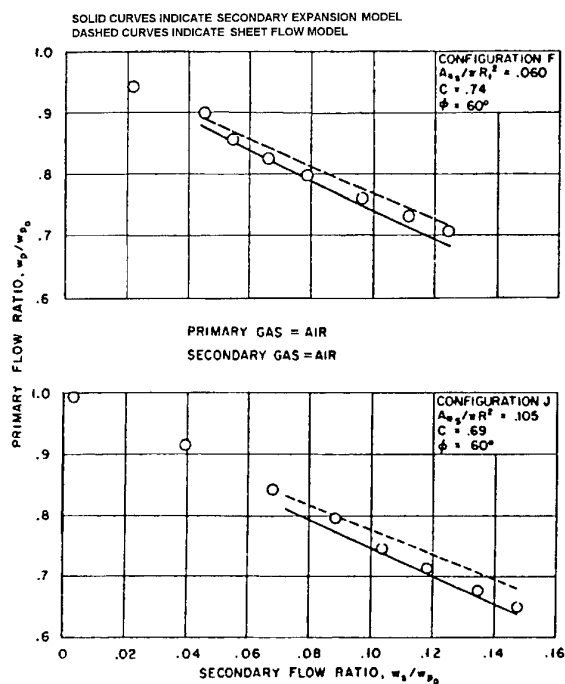
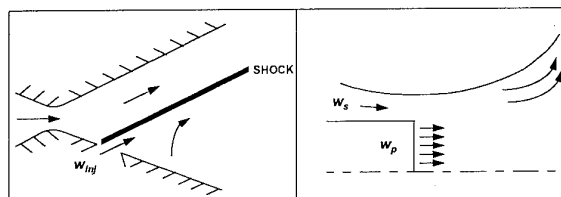


Figure 13 - Theoretical/Experimental Comparison⁶

4.3 Recent Work

Recent investigations have concentrated on using similar secondary injection schemes for jet engine exhaust nozzle

applications. A static nozzle test by Chiarelli, Johnson, Shieh, and Wing⁷ investigated two methods for fluidic thrust vectoring in a rectangular nozzle: shock thrust vector control and Coanda surface blowing (Figure 14a, b). Pitch deflection is achieved by injecting secondary flow into the primary nozzle through a spanwise slot in the divergent flap. The secondary injected air creates an oblique shock wave that turns the flow through an angle based on 2D shock theory. Secondary weight flow ratios of more than 10% were required to achieve adequate pitch deflection levels in the range of 15° to 20° using the oblique shock turning method (Figure 15a). Yaw deflection is achieved by secondary air delivered tangentially to the Coanda flaps at the nozzle exit which are offset laterally. The primary jet will attach to one side based on the Coanda effect along the flap. Yaw vectoring angles achieved using the Coanda surface blowing were small, typically 5° or lower (Figure 15b). Both pitch and yaw vectoring decreased substantially with increasing nozzle pressure ratio. The approach taken in this effort is representative of several ongoing advanced configuration research efforts. Many of these advanced efforts have achieved larger vectoring angles with smaller amounts of secondary air.



a) Shock Thrust Vector Control

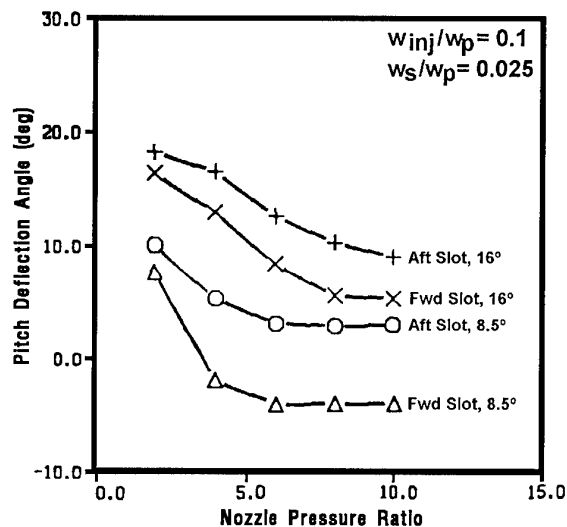
b) Coanda Surface Blowing

Figure 14 - Fluidic Thrust Vectoring Concepts⁷

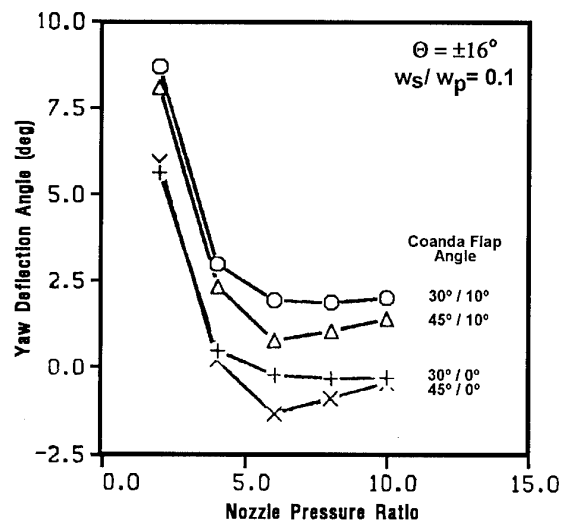
A recent internal study completed by Pratt & Whitney included a static test at NASA Langley Research Center of a fluidic yaw vectoring nozzle concept. A parametric matrix of secondary injection hole patterns and locations was investigated within advanced, three-dimensional primary flowpath contours (Figure 16a). Yaw vectoring was achieved by the introduction of secondary injection air to enhance asymmetric surface pressurization of the primary flowpath. Secondary weight flow ratios of as little as 7.5% yielded yaw deflection levels of up to 21° (Figure 16b). Of particular note is the sustained level of vectoring effectiveness with increasing nozzle pressure ratio, which is a substantial improvement over the typical effectiveness drop off evidenced in previous studies.

A recent internal study completed by Lockheed Martin Tactical Aircraft Systems Company and Pratt & Whitney was the Aerodynamically Controlled Exhaust Nozzle (ACE) program⁸. This program expanded on the earlier rocket fluidic control work using CFD methods to address the effect of nozzle geometry on throttling effectiveness. An optimum nozzle configuration and injection scheme were designed based on sensitivities in nozzle contour, injection slot number, location, and angle, nozzle divergence angle, and injection air properties, among others. Once an optimum on-design nozzle geometry was designed, the off-design performance was measured on a static thrust stand. Figure 17 compares the percentage of throat

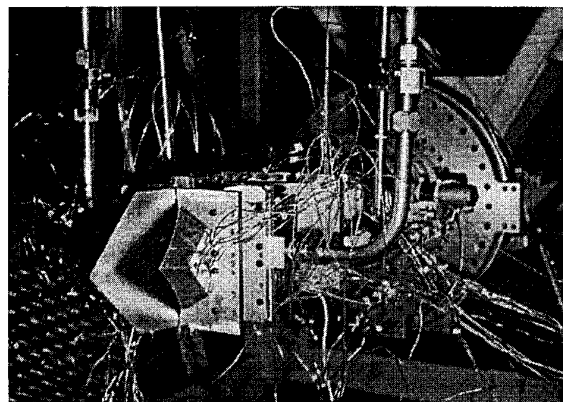
area control versus the secondary flow rate ratio for the ACE nozzle to several past fluidic area control studies. Essentially, the ACE nozzle achieved 40% more throat area control than the earlier rocket nozzle concepts for the same secondary flow rate ratio. The ACE nozzle used a very shallow injection angle of 15° and a secondary air pressure ratio of 2.0 to achieve the extra control at the same secondary flow rate ratio. A 50% reduction of A8 suggests that fluidic area control may someday be feasible for a fixed cycle engine.



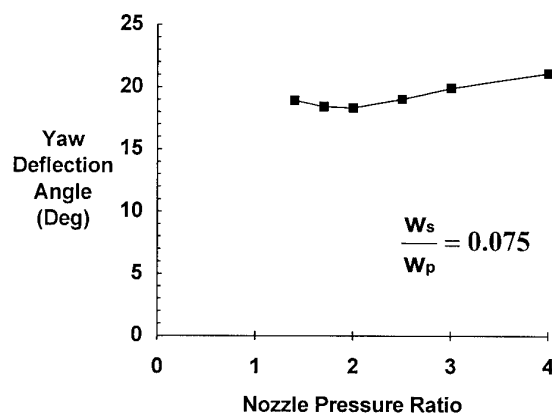
a) Pitch Vectoring



a) Yaw Vectoring

Figure 15 - Fluidic Thrust Vectoring Results⁷

a) Nozzle Test Rig



b) Nozzle Test Results

Figure 16 - Fluidic Thrust Vectoring Nozzle Test

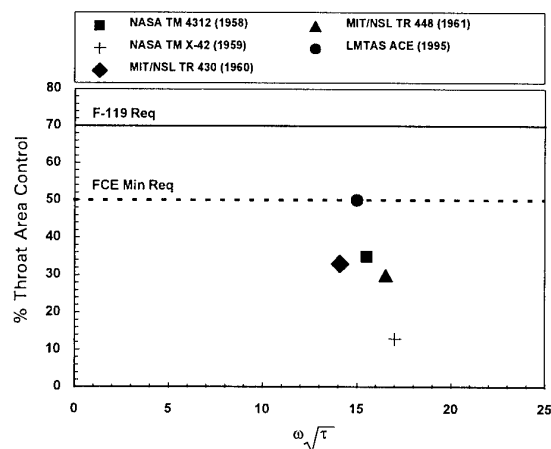


Figure 17 - ACE Nozzle Test Result Comparison

4.4 Fluidic Injection Nozzle Technology (FLINT) Program

Past and current work in fluidic area control and thrust vectoring has produced many successes. However, the pace of the technical progress has been evolutionary due to small efforts funded with "left over" resources. Future work in fluidic control must be organized and coordinated in order to obtain the support required to produce revolutionary, innovative fluidic concepts that are capable of maximum control with minimum secondary air requirements. A national effort has been initiated to provide that organization and coordination. The program is called Fluidic Injection Nozzle Technology (FLINT).

The objective of the FLINT program is to develop and mature innovative fluidic concepts that control a jet without large numbers of moving parts. Jet control may include nozzle area control, thrust vectoring, mixing enhancement, or noise reduction. The initial approach is to explore a broad range of fluidic concepts in a cooperative program composed of government, industry, and academia. This national approach will focus the fluidic technologies involved in the various concepts, insure that duplication is minimized through regular coordination, and most importantly, insure that adequate resources are invested and maintained.

Three technology thrust areas have been identified as requiring development and maturation under the FLINT program: fluidic thrust vectoring, fluidic area control, and active control. Three initiative teams corresponding to the three thrust areas will explore a broad range of innovative fluidic concepts using USAF/NASA contract funding as well as company IRAD investments. Figure 18 shows the initiative thrust areas and current team members.

Thrust Vectoring	Area Control	Active Control
Pratt & Whitney	Lockheed Martin Tactical Aircraft Systems	McDonnell Douglas - East
Florida State University	General Electric Aircraft Engines	McDonnell Douglas - West
University of Minnesota	Pratt & Whitney	Georgia Tech
Rockwell International	Wright Laboratory	Pratt & Whitney
Boeing	NASA Langley Research Center	Air Force Office of Scientific Research
Northrop Grumman		Wright Laboratory
Wright Laboratory		NASA Langley Research Center
NASA Langley Research Center		

Figure 18 - FLINT Initiative Teams

The thrust vectoring initiative is structured into two sub-initiatives: counterflow and an advanced fluidic thrust vectoring (AFTV) concept. The counterflow concept is shown in Figure 19. Collars are placed on either side of the primary flow nozzle creating gaps between the exhausting jet and the collar surfaces, which are curved away from the jet axis in the streamwise direction⁹. To achieve upward thrust vectoring as shown in the

figure, a secondary reverse flow is established in the upper shear layer of the jet by activating a vacuum pump connected to the cavity between the primary nozzle and the upper collar. This concept has been tested in the laboratory and on the static thrust stand at NASA Langley Research Center in early 1995. The suction flow rate required to vector the jet up to a maximum angle of 16° is relatively small. Under the FLINT thrust vectoring initiative, the flow attachment process of the primary jet to the collar geometry will be investigated in more detail. The effective vector angle based on geometric parameters such as gap height and collar length as well as flow parameters such as suction flow rate and primary pressure ratio will also be examined.

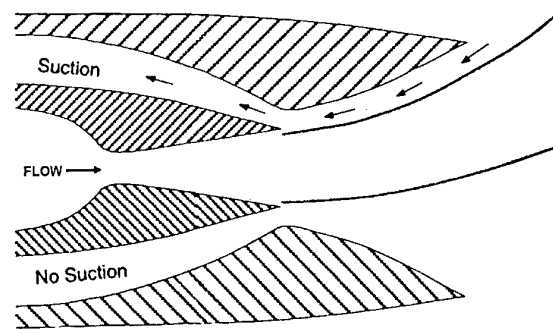


Figure 19 - Counterflow Concept⁹

The AFTV concept work will be a hybrid fluidic-mechanical concept tested at NASA Langley Research Center. Airframe industry members will use CFD to screen various 3D candidate concepts. The concept with the highest potential payoff will be built by Pratt & Whitney and tested.

The fluidic area control initiative will concentrate on secondary air injection approaches similar in scope to the Aerodynamically Controlled Exhaust Nozzle research. The main focus of the work under the FLINT program, however, is to obtain more A8 area control using less secondary air. A highly shaped 3D nozzle configuration will be investigated using a CFD Taguchi matrix to determine an optimized configuration. A static test at Lockheed Martin will determine the off-design performance of the nozzle. A follow-on task will investigate a combined fluidic-mechanical device for A8 area control using a similar Taguchi matrix approach leading to a second test.

The third initiative will use fluidic actuation devices at the nozzle lip to control the primary jet. This is a departure from steady-state injection and is thus given the name active control. This initiative will develop and mature a device known as the zero-mass flux jet or synthetic jet (Figure 20a). According to Allen and Glezer¹⁰, zero-mass flux jets are synthesized by a train of vortices generated at the sharp orifice lip as a result of the time-harmonic motion of a small diaphragm driven by a piezoceramic disc mounted at the bottom of a sealed cavity. In order to produce thrust vectoring in a primary jet, the zero-mass flux jet is integrated in a streamwise fashion and activated at a certain frequency (Figure 20b). The vectoring is the result of a Coanda effect resulting from strong entrainment and a low pressure region that are introduced by the control jet. Vector

angles up to 30° have been obtained for low speed jets with essentially no secondary air required.

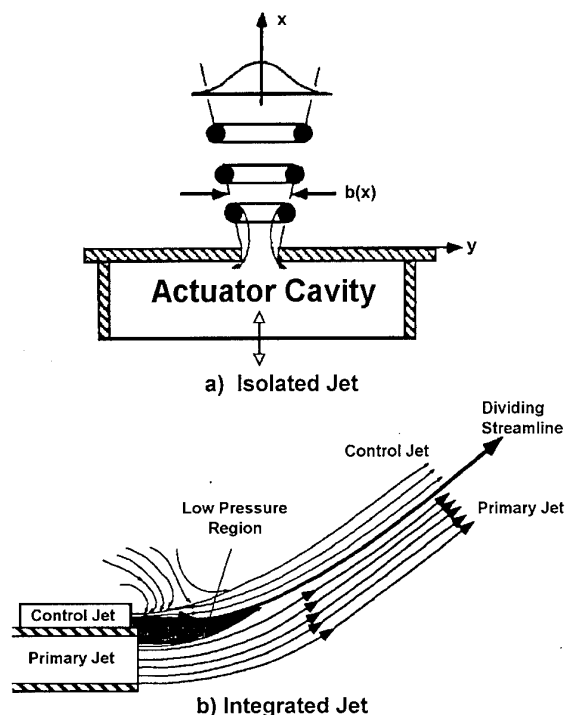


Figure 20 - Synthetic Jet Concept¹⁰

One application for the synthetic jet concept is a redesign for the C-17 engine nacelle. If an active control device such as the synthetic jet can be used to mix or deflect the plume in order to significantly reduce the temperature, the reverser can be removed, and significant savings realized. Under FLINT, the synthetic jet concept will be integrated into a C-17 nozzle model and tested to quantify the benefits of active control in a real system.

5. CONCLUSIONS

Propulsion integration issues for advanced fighter aircraft have been identified. Integration of fixed geometry, short and highly offset subsonic diffuser, and minimal BLC inlets has been presented as the main focus of current USAF inlet research. Recently developed design criteria and tools have opened the inlet design space to help realize these new configurations. Potential payoffs of 50% reduced inlet weight and 50% reduced inlet volume by the year 2000 will lead to reduced cost and increased aircraft utility. Inlet system aerodynamic and signature performance will be maintained or increased.

Fluidically controlled nozzles promise to be a high payoff technology area. Current technology emphasis is on fluidic thrust vectoring, fluidic area control, and active control. The focus is on applying fluidic advances to practical nozzle geometries. Potential payoffs of 25% reduced nozzle acquisition cost, 50% reduced nozzle weight, and signature

reduction by the year 2000 will lead to reduced LCC cost and increased aircraft utility.

6. ACKNOWLEDGEMENTS

The authors would like to acknowledge the contributions and helpful discussions with the cooperative partners of the Advanced Compact Inlet Systems and Fluidic Injection Nozzle Technology programs.

7. REFERENCES

1. McDonnell Douglas, "Management of Advanced Inlet Boundary Layers", WL-TR-94-3005, January 1994.
2. Bingaman, D.C., "Performance Study for Inlet Installations", NASA CR 189714, November 1992.
3. Smereczniak, P., "Exhaust Nozzles for Aerocontrol, Vol. 1, Summary of Nozzle Static Test and Thrust Vectoring Utilization Results", WRDC-TR-89-3068, 1989.
4. Mace, J., Smereczniak, P., Krekeler, G., Bowers, D., MacLean, M., and Thayer, E., "Advanced Thrust Vectoring Nozzles for Supersonic Fighter Aircraft", AIAA-89-2816, 1989.
5. Blaszk, J. and Fahrenholz, F., "Rocket Thrust Control By Gas Injection", Massachusetts Institute of Technology Naval Supersonic Laboratory, Technical Report 430, 1960.
6. Gunter, F. and Fahrenholz, F., "Final Report On A Study Of Rocket Thrust Control By Gas Injection", Massachusetts Institute of Technology Naval Supersonic Laboratory, Technical Report 448, 1961.
7. Chiarelli, C., Johnson, R., Shieh, C. and Wing, D., "Fluidic Scale Model Multi-Plane Thrust Vector Control Test Results", 29th Joint Propulsion Conference, AIAA-93-2433, 1993.
8. Catt, J., Miller, D., and Giuliano, V., "A Static Investigation of Fixed Geometry Nozzles Using Fluidic Injection for Throat Area Control", AIAA-95-2604, 1995.
9. Strykowski, P. and Krothapalli, A., "Thrust Vector Control of Rectangular Jets Using Counterflow", AFOSR Contractor's Meeting Abstract, St. Louis, MO, 1994.
10. Allen, M. and Glezer, A., "Jet Vectoring Using Zero-Mass Flux Control Jets", AFOSR Contractor's Meeting Abstract, WPAFB, OH, 1995.

Paper 42: Discussion

Question from B Leroudier, Dassault Aviation, France

Could you clarify whether or not the future nozzle described in your paper will have moving parts? If there are moving parts, there will be permanent bleed to vary A_8 . Have you considered the effects of this bleed on fuel flow and weight?

Author's reply

Yes, small devices are required for vectoring. The effects of bleed have been taken into account in estimating the net benefits.

Question from Dr W Merrill, NASA Lewis, USA

Have you considered the potential of advanced controls to modify adaptively the tolerance of an engine to increased distortion? This could give freedom to design the inlet to give even greater improvements in inlet weight and length, utilising integrated engine/thrust control.

Authors' reply

No. We think we can keep distortion within allowable limits through greater use of improved tools such as computational fluid dynamics to identify and correct aerodynamic problems earlier in the design process.

Question from Dr F Heitmeir, MTU, Germany

Can you give a view on how soon the fluidic nozzle control technique might be seen in operational engines?

Author's reply

We could see a flight test of the system in about 10 years, with full application after that.

Question from K Bradbrook, BAe Defence, UK

Can you say what is the operating frequency of the diaphragm in the isolated jet used for thrust vector control?

Author's reply

The tests conducted so far were for subsonic jets, and the frequency used was approximately 60 Hz. This is not true for other jet Mach numbers. So, the frequency of the diaphragm is dependent on the speed of the jet (among other parameters). Future exploration in the FLINT program (discussed in the paper) will expand the application to supersonic jets, with changes in the frequency. The FLINT program will address these issues further to determine application requirements for the synthetic jet concept.

PROPULSION INTEGRATION ASPECTS IN ADVANCED MILITARY AIRCRAFT

E Hienz

L Illuzzi

Eurofighter Jagdflugzeug GmbH
Am Soeldnermoos 17
85399 Hallbergmoos Germany

P Herrmann

Eurojet Turbo GmbH
Inselkammerstr. 5
82008 Unterhaching Germany

SUMMARY

Going back in history, airframe/engine integration was mainly related to physical aspects requiring only a low degree of sophistication.

With the advent of more complicated technology and more overall system performance consciousness, propulsion integration has become a major task split between airframe and engine engineers. It now includes performance, functional and physical aspects all needing to be integrated to meet specific requirements.

The aircraft and engine configurations are therefore optionised simultaneously at a very early stage of development. Some of the major interfaces influencing configuration, performance and operability will be discussed, ie. Intake/Engine/Afterbody; Electronic Controls Integration including monitoring; Performance optimisation; Systems; Installation.

LIST OF SYMBOLS

2D	Two Dimensional
ABCP	Afterburner Core Pump
ABFMU	Afterburner Fuel Metering Unit
ACA	Advanced Combat Aircraft
ACAC	Air Cooled Air Cooler
ACFC	Air Cooled Fuel Cooler
ATF	Altitude Test Facility
AVS	Avionic System
BME	Basic Mass Empty
BPR	Bypass Ratio
BSD	Bulk Storage Device
CFC	Carbon Fibre Composite
CFD	Computational Fluid Dynamics
CIU	Cockpit Interface Unit
CSMU	Crash Survivable Memory Unit
DDL	Direct Digital Link
DECU	Digital Electronic Control Unit
EAP	Experimental Aircraft Programme
ECS	Environmental Control System
EF	Eurofighter
EFA	European Fighter Aircraft
EJ	Eurojet
EMU	Engine Monitoring Unit
FADEC	Full Authority Digital Engine Control
FCS	Flight Control System
FF	Fuel Flow
FSCP	First Stage Core Pump
FSP	First Stage Pump
GFE	Government Furnished Equipment
HE	Heat Exchanger
HP	High Pressure
HW	Hard Wired
IGV	Inlet Guide Vanes
IPU	Interface Processing Unit
IMRS	Integrated Monitoring & Recording System
ITP	Industrias des Turbo Propulsores
KN	KiloNewton
LP	Low Pressure

MFMU	Main Fuel Metering Unit
MHDD	Multifunction Head Down Display
MDP	Maintenance Data Panel
NEFMA	Nato European Fighter Management Agency
SDR-D	European Staff Requirement for Dev.
SFC	Specific Fuel Consumption
SPS	Secondary Power System
SSICA	Stick Sensor & Interface Control Assembly
SSGP	Second Stage Gear Pump
TU	Turbo Union
TV	Thrust Vectoring
UCS	Utility Control System

1. INTRODUCTION

By the late 1990s the life expectancy of the current inservice aircraft in the UK, Germany, Italy and Spain tasked with air superiority - Phantoms, F104s and Mirage F1s - will be over and replacements needed. EF2000 has been thoroughly evaluated against the alternatives and has been identified as the most cost effective aircraft capable of meeting the air defence requirement of the four Nations well into the next century.

The European Staff Requirement for Development (ESR-D) was initiated in December 1985 and reached its final definitive form in 1987. The ESR-D defined in detail the key parameters relating to the combat performance of the aircraft, the equipment it must carry and the ease with which it can be operated in all weathers, with minimum support, from short runways.

To meet the ESR-D, EF2000 (Fig. 1) must be extremely agile and capable of air combat manoeuvres not possible in previous fighters. Special emphasis has therefore been placed on low wing loading, high thrust to weight ratio, excellent all-round vision and 'carefree handling'. The aircraft's high performance must be matched by the attack identification and defence systems which include the long range radar and air-to-air missiles, plus comprehensive electronic warfare capabilities further to increase weapon system effectiveness and survivability. High reliability, high component life and ease of maintenance are all vitally important design features of EF2000 with the aim of greatly reducing the life cycle costs of the aircraft and minimising support requirements and cost.

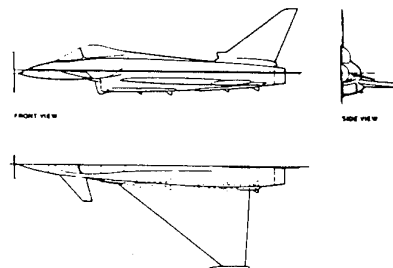


Fig. 1 EF2000 Configuration

The EJ200 engine is specifically tailored to match EF2000's mission requirements, in particular, offering a combination of very high thrust - around 90 kN in full reheat and 60 kN in full dry power - and low fuel consumption. Great emphasis is put on reliability, maintainability and low cost of ownership.

The Eurofighter and Eurojet management structure is modelled on that of three-nation Tornado programme, with Spain now joining the United Kingdom, Germany and Italy for the four nation EF2000 programme.

NEFMA, the NATO European Fighter Management Agency, represents the interests of the four Governments.

Eurofighter is the industrially owned management company which coordinates the activities of its four partners - British Aerospace, Daimler-Benz Aerospace, Alenia and CASA. This consortium is responsible for the complete weapons system, but not the EJ200 engine. Final assembly of the aircraft will take place in all four countries.

Eurojet, comprising Rolls-Royce, Motoren und Turbinen Union (DASA), Fiat and Industrias des Turbo Propulsores is the industrial company responsible for the development and manufacture of the EJ200 engine for EF2000.

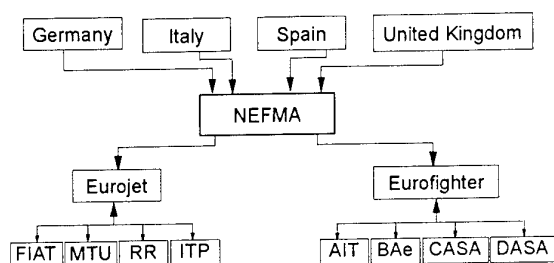


Fig. 2 Project Organisation

2. PROJECT HISTORY

The EF2000 configuration (Fig. 1) was developed over a period of years primarily from DASA (then MBB) and BAe project studies of the late 70's which cumulated in the ACA/EAP project in the early 80's.

On the engine side, technology programmes in the UK (demo engine), Germany (LP Compressor/HP Compressor), Italy and Spain had ensured that the necessary know-how on critical components was available to support EJ200. The engine programme benefited heavily from collaboration experience of the Tornado/RB 199 project earlier.

3. ENGINE INTEGRATION

The subject of engine/airframe integration is probably as old as powered flight. It has gone through many stages of development, always posing problems no smaller than the level of sophistication current with the two components to be integrated and the operational requirements.

Looking at today's state of development of military systems and requirements (like in the past always at the forefront of technology) we indeed find ourselves confronted with highly complicated machines requiring enormous consolidated effort on the part of both engine and airframe engineers.

For this type of aircraft the engines represent roughly one fourth to one third of the total aircraft effort (mass, cost

etc.). It is obvious that the propulsion system and the quality of its integration strongly influences overall aircraft flying performance, cost of ownership and programme success. This requires a very close collaboration from the initial project stages between engine companies and propulsion integration engineers of the airframe companies. The framework within which this collaboration takes place is dependent on the contractual relationship between engine and airframe contractors, however, in technical terms the job is the same.

Indeed it is interesting to note that on EF2000 two different engines and contracts are used. The two first prototypes (aircraft) use the proven RB 199 (customised) to facilitate early flight testing with the fewest possible restrictions. These engines were procured on a separate contract by Eurofighter directly from Turbo Union. From third prototype onward, EJ200s are being installed as GFE (Government Furnished Equipment).

The technical task of integration must be laid down very early in the Programme in an Interface Control Document, ensuring optimal compatibility in all aspects. This allows tailoring of the engine design specifically for the design missions (very numerous in a four-nation project). This contractual document between customer, aircraft and engine manufacturer defines the "Functional", "Performance" and "Physical" requirements for the propulsion system and its integration and must be met by the engine specification, which in turn is contractual between Customer and engine manufacturer only.

The key integration parameters and their effect on the aircraft are shown below (Fig. 3).

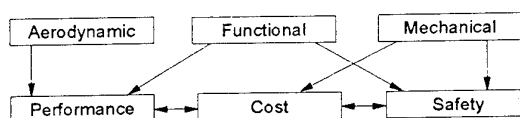


Fig. 3 Main Interfaces

Developing the engine and aircraft concurrently leaves, of course, ample room for overall interface optimisation provided all parties acknowledge the priority for total system efficiency.

4. PROPULSION SYSTEM REQUIREMENTS

The European Staff Requirement put priority on the air-to-air role so that a fair compromise for all other missions had to be considered.

The aircraft configuration dictated a very compact lightweight engine configuration to fit into a closely cowled duct.

Because of the specific mission and performance requirements, a low reheat SFC and relatively high pressure ratio was envisaged as desirable. By comparison the RB199 was optimised for low level interdiction requiring low dry SFC's resulting in an intermediate BPR layout not really suitable for EF2000.

4.1 Cycle Choice

Due to the numerous and different missions to be considered for all 4 Services, a tremendous amount of engine/aircraft optimisation loops had to be performed. Engine and aircraft size were optimised for missions driving the design. The final key diagram is shown in Fig. A2 giving an indication of the amount of effort spent.

On the engine side a similar optimisation process was being conducted simultaneously. To arrive at the lowest total A/C BME (basic mass empty) the engine cycle was varied within limits as shown in Fig. A1.

The overall compression pressure ratio was set to the highest level possible within the constraints of engine and airframe materials which dictate the maximum acceptable level of compression exit temperatures within the EFA flight envelope. The benefits of this on cruise sfc are shown in Fig. 4.

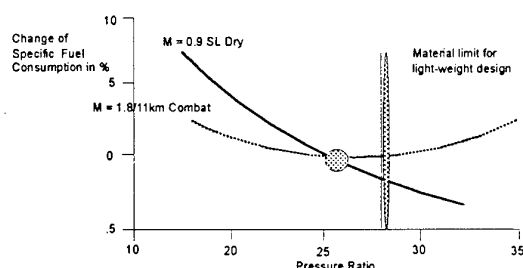


Fig. 4 Effective of Overall Pressure Ratio on Fuel Consumption

The resulting engine parameters are described in Fig. 5. The points of note are that the engine is running at some 200° C higher Turbine Entry Temperature than current fighter engines but despite this has a longer life and is to have a thrust/weight ratio of 10 to 1 compared with 8 to 1 for the previous generation of engines. The reheat boost is lower than on earlier engines because the lower by-pass ratio has been used and reheat has been limited for the best possible fuel consumption. The engine is fitted with a convergent/divergent nozzle for the first time on a design for the involved countries.

■ By-Pass Ratio	0.4
■ Fan Pressure Ratio	4.2
■ Overall Pressure Ratio	26
■ Max Reheat Thrust Class	90 kN
■ Max Dry Thrust Class	60 kN
■ Turbine Temperatures	~ 200° C higher than current fighter engines
■ Thrust-Weight Ratio Approx.	10

Fig. 5 EJ200 Cycle Parameters

■ By-Pass Ratio	- High core power to cover off-takes
■ Fan Pressure Ratio	- High specific thrust (dry and reheat) - Low reheated fuel consumption
■ Overall Pressure Ratio	- Low fuel consumption in dry cruise operation
■ Turbine Temperatures	- High growth potential - Long life turbines - Small turbine sizes (low weight)
■ Convergent Divergent	- High thrust and low specific fuel consumption at high mach no's (high nozzle pressure ratios) - No penalty on long loiter missions

Fig. 6 EJ200 Cycle Choice Benefits

Fig. 6 summarises the choice of various cycle parameters. The convergent/divergent nozzle was chosen because a higher reheated thrust at supersonic Mach numbers can be obtained due to the better nozzle expansion. Of more importance, this higher thrust at a given fuel flow improves the reheat sfc even more and is a very important parameter for maintaining combat at supersonic speeds. The detailed study shows that the nozzle can be designed for negligible loss at sub-sonic missions and in particular for ferry and low speed loiter missions. The performance of a convergent divergent nozzle relative to the simpler convergent nozzle is compared on Fig. 7/8 to emphasise better thrust and even subsonic SFC in reheat operation.

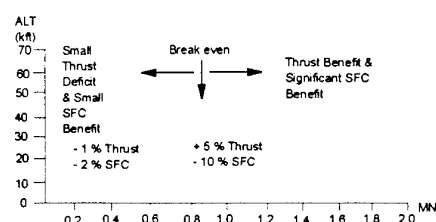


Fig. 7 Convergent-Divergent vs Convergent Nozzle Reheat Operation

- Effects - Significant improvements in aerodynamic performance particularly at high nozzle pressure ratios
- Benefits - Significant thrust increases and specific fuel consumption reductions during supersonic flight
- Considerable resultant increase in combat duration capability
- Virtually no loss in subsonic cruise/loiter performance
- No resultant penalty on long loiter missions

Fig. 8 Convergent-Divergent Nozzle Choice

5. AERODYNAMIC INTERFACE

The Aerodynamic interface between engine and airframe remains as one of the most critical and difficult to establish with complete confidence. However, the experience of the EF2000 partner companies from the Tornado programme did indicate the importance of having a well defined aerodynamic interface even if it was accepted that some elements of the interface requirement would have to remain only loosely defined until the flight test phase.

5.1 Intake/Engine Compatibility

The basic requirement for the integrated EF2000 Weapon System as far as intake/engine compatibility is concerned is for carefree handling ie. surge free operation with unrestricted use of the throttle throughout the flight envelope. This applies even with weapon firing.

The basic requirement for the intake was therefore to achieve a minimum of flow distortion even at very high angles of attack. This dictated a 2D chin intake arrangement with the aircraft forward fuselage providing a pre-turning effect on the intake flow. To cope with high and low speed conditions where distortion can be induced by mismatch of intake area and streamtube flow area, a variable cowl was provided. Finally, to avoid interference with armament firing, the gun was located some 1.8m behind the intake entry plain to avoid blast wave and gun gas ingestion problems. Fig. A3 shows the final

configuration resulting from several models tested in the wind tunnel and experience gained from EAP.

On the engine, stringent basic design aims were set for basic surge margin on the compressors.

5.1.1 Surge Interaction

In addition to the performance optimisation, a special model (Fig. A4) was built that could simulate a surge pressure pulse in one intake allowing us to evaluate the effect in the other (receiving) intake/engine. This was considered necessary due to the proximity of the intakes and the surge interaction experienced by Concord which has a similar configuration. Fig. A5 shows one of the surge wave generators used which provided initial results and the confidence. This was then substantiated and extended using a CFD model by BAe. The final test was done on the aircraft at static conditions by deliberately surging both the RB199 interim engine and the EJ200 on one side while checking the receiving intake/engine. As no measurable effect was recorded it is concluded that the assessment for the (more critical) low speed regime was correct.

In the supersonic area, where interaction may occur, quick recovery as demonstrated in the Concord cases avoids a possible problem. This has been substantiated in part during surges in the ATF.

5.1.2 Distortion Swirl

The descriptors were defined based largely on Tornado/RB199 experience where even a full size rake was used in one intake to analyse compatibility problems.

Instantaneous distortion and bulk swirl were considered the main parameters and were defined in a way also to account for any planar wave effect that may occur. With no IGV's on the engine, swirl and its effect on distortion tolerance were thoroughly analysed for both counter and counter-rotating swirl.

Finally, aeromechanical interference was extensively analysed where it was found that excitation in the 2nd32 engine order required some special analysis and testing. As it turned out the real engine when tested exhibited more than adequate tolerance.

Reduced sensitivity to intake flow distortion was brought about through the application of wide chord blading to the fan. This is backed up by a full authority digital control system which is provided with high integrity air data. With control over fuel, nozzle and HP compressor first stage guide vanes, the control system provides considerable flexibility to counter any problems including any armament firing interactions.

5.2 Afterbody/Nozzle Interface

Fig. A6 shows areas requiring specific attention for the configuration selected. Before overall optimisation could be achieved, several models were tested in wind tunnels in order to find the best compromise between drag, nozzle cooling and unsteady pressure effects on the outer nozzle flaps. Convergent/divergent, convergent and ejector nozzle configurations were analysed.

5.2.1 Drag Considerations

A minimum rear fuselage cross-section and con-di nozzle configuration showed the best results for the given missions.

5.2.2 Unsteady Pressures

Jet-screach-caused excitation of (air) cavities in the aft body area between nozzles and fin can lead to pressure

fluctuations (unsteady, peak to peak pressure) which act on the nozzle flaps reducing their life tremendously. This is a well-known phenomena peculiar to engines installed closely together.

Fig. A7/8 show several options tested in the tunnel resulting in a configuration that partly filled the void thereby lowering unsteady pressures to acceptable levels.

5.2.3 Nozzle Cooling

To facilitate nozzle flap cooling, V-slots were introduced in a way not adversely to affect aft body drag. A final review after some flight experience will determine the requirement of more refinement.

6. PHYSICAL INSTALLATION

For the engine manufacturer the aircraft is usually looked at as a "necessary test bed" to fly its wonderful product. For the airframers the engine is a throttle box excrescent "the smaller the better".

With these assumptions the job to install the engine is not exactly a bed of roses for the people who do it. The result is that, no matter how large a space is left for the engine, the rear fuse is in the end "tailored" onto it, and on the other side engine accessories, cables and pipes continuously "escape" from the envelope originally assigned to it, so that finally seeing an engine going in and out of the engine bay appears like a miracle.

In this programme great care was exercised on the engine physical installation, this being a very cost sensitive matter for the maintainability implications it has.

The integration of a new engine in a new aircraft is a job which requires a lot of work from both parties involved, but it offers a big advantage: the optimisation of all interfaces so that the final result is the benefit of the overall performance of the weapon system.

As a result of the customer requirements placed on the two contracts, the engine's physical installation is being carried out by both Eurofighter and Eurojet.

The result is quite satisfactory as it is possible to install the engine as a self-contained change unit in a very limited room satisfying stringent integration, maintainability and accessibility requirements.

The configuration of the engine installation into the aircraft is similar to that adopted for the Tornado, based on the experience gained and the good results achieved from that project.

Each engine is connected to the airframe by two side links on the front and two links with an hanger type adaptor on the rear (Fig. A9).

The thrust is transmitted by means of a single top thrust spigot in the same station as the front links.

The connection between the aircraft intake duct and the engine intake is by means of a metallic adaptor ring fitted on the duct sealed by a piston ring which is part of the engine.

The other physical interfaces between the engine and the airframe are:

- o the low pressure (LP) bleed for the fuel tanks pressurisation
- o the high pressure (HP) bleed for the Secondary Power System (SPS) and the Environmental Control System (ECS)
- o the fuel feed
- o the power off take shaft

- o the witness drain
- o the gearbox breather exhaust
- o electrical interfaces

The engine bay ventilation is ensured by two NACA intakes (one per bay) located on the engine bay door on the bottom of the fuselage. The ventilation air is discharged through the internozzle base area, protected by two flame arrester grids.

Due to CFC (Carbon Fibre Composite) structure of the aircraft and to the proximity of the fuel tanks in the centre fuselage to the engine bays, special attention was paid to the overheat/fire protection system. The engine bays are completely fire proof and an additional insulation blanket on the front side of them prevents fire from causing a dangerous increase in temperature in the adjacent fuel tanks.

One problem not experienced in the Tornado experience, arose when a detail evaluation of the engine/aircraft relative movements, as a result of combined deflections in flight, was carried out. It was found that, under the combined effects of inertia and aeroloads, the aircraft and the engine were deflecting closing the free gap between them. This was attributed to the peculiar aircraft configuration. A thorough investigation pointed out the critical areas, leading to local redesign of engine and airframe parts and to a "tailored" engine envelope.

The power off-take sliding device, incorporated in the engine gearbox to allow the combined axial deflections, was revised and the aircraft/engine intake interface was redesigned in combination with the DECU position and mounting on the engine. The effects of them on the aerodynamic path were also checked and found to be negligible.

A good example of integration for the sake of overall aircraft benefit in terms of mass saving and safety is represented by the decision to incorporate the HP bleed Air Cooled Air Cooler (ACAC) in the engine despite a slightly more complex design of the engine. For safety reasons (to avoid leakage of hot air in case of failure of piping, with possible damage to the aircraft CFC structure) a shut off valve was installed directly onto the engine as an aircraft supply item.

Another area that requested a lot of work from both engine and aircraft manufacturers is the afterbody/nozzle interface. From the mechanical integration point of view the task was to find a design solution that, within the aerodynamic constraints, allowed a quick engine change with minimum mass and respecting the maintainability requirements. The final decision was to install a fairing on the engine part of the afterbody skin (rear fairing) and to manufacture the final part of the engine reheat adjacent to the nozzle following the aircraft lines.

The maintainability requirements that play a major role in the life cycle cost of the aircraft are very stringent for EF2000 and have been taken into consideration in all aspects of engine installation design. Much effort was made to keep to a minimum the engine change time.

The electrical connectors were reduced to two on the aircraft side of the harness and to three on the engine side (two onto the DECU and 1 onto the electrical service connector). For this the electrical harness for the engine mounted HP bleed shut off valve was integrated in the engine harness and special connectors were developed.

The fuel duct has a quick disconnection joint on the aircraft side and the LP bleed has a plug-in connection. For safety reasons (high pressure and temperature) a "V" clamp joint was adopted for the HP bleed connection (between the valve and the rest of the aircraft piping),

which is easily accessible from the top of the aircraft. The power off-take shaft has three bolt flanges on both sides.

The thrust spigot, the rear mounting interface and the associated ground equipment, basically taken from Tornado design, were developed to allow an engine change under normal conditions without the need of jacking the aircraft or using any other special tool.

The engine mounted rear fairing is removable with the engine installed (gaining free access to the nozzle actuators) as well as the other engine accessories.

7. MECHANICAL SYSTEMS INTERFACES

7.1 Fuel System

In addition to its main purpose, which is to feed the engine, fuel is used to dissipate heat from the aircraft gearboxes. On the engine side the heat sources are represented by the oil system, the hydraulic system and the DECU (Fig. A10).

On the aircraft side, fuel is circulated back to the collector tank picking up heat from the aircraft systems as shown in Fig. A10. This allows the engine to be used as an ideal heat sink without heating up the other aircraft fuel tanks.

Following the philosophy to have a self contained engine installation, between the engine and the aircraft there is a single point fuel interface, which requires the fuel interface temperature to be sufficiently low to allow the engine heat to be dissipated within the maximum fuel temperature limit.

This solution simplifies the overall fuel system design (no fuel recirculation line), with clear benefit in terms of mass and complexity.

The fuel demand ratio and air cooled fuel coolers are used on the aircraft side to keep the interface temperature below the maximum value agreed at the interface to the engine. An aircraft supplied fuel flowmeter is mounted on the engine to measure the fuel flow in dry settings. This is due to the high precision measurement required by the fuel management system to supply precise input to the flight control system.

There are two independent fuel feed lines to the two engines. To allow a safe engine operation even in case of the aircraft boost pumps failure, the aircraft feed line and the engine fuel system architecture have been designed to minimise the pressure losses. The fuel system integration is being widely checked on an integration rig at the engine companies where all the feed line from the aircraft collector tank to the engine, together with the engine, are being tested paying particular attention to the assessment of the pressure hammershock.

7.2 SPS (Secondary Power System)

The engine and the aircraft gearboxes are connected with a power off take shaft at very high speed. The right and left hand sides are pneumatically linked with air tapped off the HP bleed of the engine. Compared with the Tornado, where there was a mechanical link between the engine gearboxes, this system offers more flexibility and reliability. It allows drive to both aircraft gearboxes with only one engine or to assist in flight engine relight. A dog clutch is incorporated in the aircraft gearbox to allow this gearbox to be activated/ deactivated depending on the corresponding engine speed. The shear neck and the sliding device are incorporated in the engine gearbox (Fig. A11).

8. CONTROL AND MONITORING SYSTEM INTEGRATION

8.1 General

Under this heading we include all interfaces covering electric/ electronic communication between engine and airframe ie. actual control of the engine from the cockpit/autopilot, monitoring and warnings (pilot), inflight monitoring (maintenance) and crash recording.

The overall aircraft communication architecture is of course established and optimised for all the different systems present in a sophisticated aircraft like the one under consideration. For practical reasons therefore, the propulsion system is integrated into this overall communication system leaving only few possibilities for exclusive direct link communication.

As a result, there are signals that have to trespass several links between source and user, thus requiring a close watch on signal harmonisation and documentation. Also, a lot of thought had to be given to hardwired vs. software transmission as well as to the class of software to be used.

The result is shown in Fig. A12 [electrical and electronic interface] which contains all propulsion relevant communication links within the overall aircraft architecture.

8.3 System Description

The engine system comprises the DECU (FADEC) which is engine mounted and the EMU (aircraft mounted) and of course the engine proper. The following are aircraft integration interfaces:

- o between DECU and FCS (bus)
- o between EMU and IPU (direct digital link)
- o between DECU and throttle box/display (HW/dig.)
- o between intake and DECU (HW)

As can be seen there are basically two methods of inter-systems communication used, namely bus links and hardwired links. Ideally, all data transfer should be done via a bus system but since both engine systems are identical, common mode software failures could cause problems. Common sense and practical considerations therefore require that certain links are kept hardwired.

Whereas it was easy to put the less critical parameters on the bus links, the question what to do with the throttle demand signal caused considerable discussion. The classic method of hardwiring, as used on Tornado, was first considered essential for integrity reasons and there was positive experience available. In Tornado it was also possible to have a mechanical link between throttles of the twin seater. In the autopilot/throttle mode, the demand signal is transmitted mechanically to the throttle through a servo-actuator. The performance of that system is quite satisfactory for Tornado and could also cope well with a linear throttle for RPM characteristic in auto throttle. As requirements for mass reduction, quicker response times and lower dead bands became essential, we had to opt for a bus link between the throttle box and the DECU and also between the two cockpits of the twin-seaters. Not only was mass and space minimised, the bus-linked throttle signal response is now fast enough to meet all auto-pilot demands since it is routed directly (bus) to the DECU from the flight control system avoiding any mechanical interface in the loop. There is still a mechanical actuator used that moves the throttle lever to the auto-demanded position but this is merely a follow-up function outside the main loop and fully satisfies the requirement for identical power level on engine and throttle box.

All other display/warning and control information is transmitted via the FCS bus to the cockpit and utility system since the FCS bus is connected directly to all other buses on the aircraft ie. avionic bus, cockpit bus and utility system bus. In this case the FCS bus acts merely as a link between the different users.

9. EFA/EJ200 POTENTIAL

In order to meet the stringent initial requirements, growth potentials are often consumed ahead of time. It is therefore essential to preserve at least those provisions where physics or physical limits dominate ie. inlet size etc. Conversely, specific performance through advanced technology are normally achievable within the given physical constraints.

Interface provisions in EF2000/EJ200 will allow an overall growth of at least 15%. This will be achieved partly by technology improvements.

In addition, inherent flexibility in the control concept will enable a shift in emphasis (optimisation) to other missions if so required.

Envelope extensions as shown in Fig. A13 would be a case in point.

Provisions to accommodate modification to achieve these improvements are provided and would include:

- o introduction of thrust vectoring nozzles on the engines
- o expanding the flight control system (FCS) to cover thrust vectoring (TV)
- o integrating FCS and DECU (TV)
- o adjust engine performance in left part of flight envelope to meet aircraft performance requirements.

Since the engine control (DECU) is bus-compatible and communicates directly with the FCS bus, integration of thrust vectoring is greatly facilitated.

10. CONCLUSION

Our experience, we believe, led to an excellent standard of collaboration between aircraft and engine companies throughout the feasibility study, definition phase and programme development phase. It illustrates confidence in the ability of engine and aircraft companies to meet their design targets within a given programme and under separate contracts, provided interface requirements are adequately defined and harmonised at an early stage and are also contractually agreed. The early interface and integration agreements also enabled both engine and aircraft manufacturer to arrive at the same technology base prior to project launch.

All this is happening successfully because of the spirit of cooperation of the many companies involved on both sides.

ACKNOWLEDGEMENTS

The authors wish to thank their companies and NEFMA for permission to publish this paper. They also wish to thank their colleagues from the 8 Partner Companies who, in the course of the development, were involved in the propulsion integration area. They all, directly or indirectly, contributed to the substance of this paper.

REFERENCES

1. R. Mishler & T. Wilkinson:
"Emerging Airframe/Propulsion Integration Technologies at General Electric".
AIAA 92-3335
2. R. J. Lane (†) & J.. Behenna:
"EJ200 - The Engine for the New European Fighter Aircraft."
ASME 90-GT-119
3. Dr. Rauh, W. Anders:
"Aircraft Engine Integration for an Advanced Fighter."
MBB-LKE 129-S-PUB-225
4. J. M. Seiner, J. C. Manning:
"Dynamic Pressure Loads Associated with Twin Supersonic Plume Resonance."
AIAA-86-1539
5. H. Fichter, E. Hienz:
"Airframe/Engine Integration Deriving some Future Requirements."
AIAA-83-1125
6. E. Hienz, R. Vedova:
"Requirements, Definition and Preliminary Design for an Axisymmetric Vectoring Nozzle, to Enhance Aircraft Manoeuvrability."
AAIAA-84-1212
7. W. Schreiber, E. Hienz:
"A look at Comprehensive Engine/Airframe Integration for High Performance Aircraft."
5th ISABE Conference 1981
8. K. Lotter:
"Aerodynamische Probleme der Integration von Triebwerk und Zelle bei Kampfflugzeugen."
MBB-UFE-1359 Ö

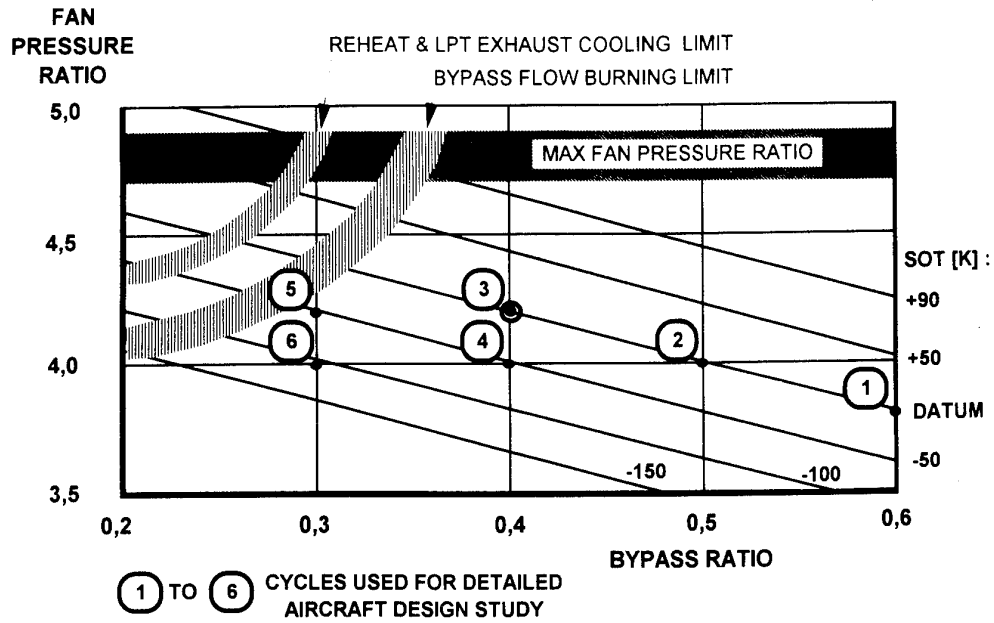


Fig. A1 ENGINE CYCLE PARAMETERS

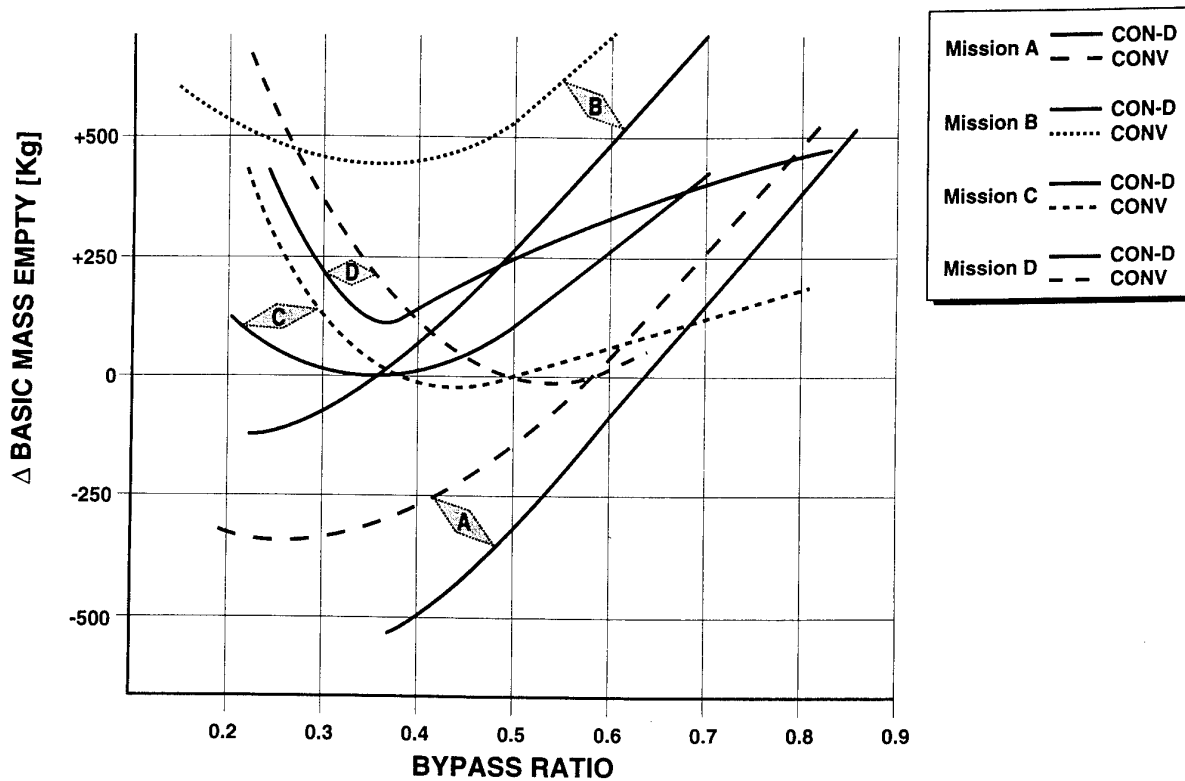


Fig. A2 CYCLE STUDY

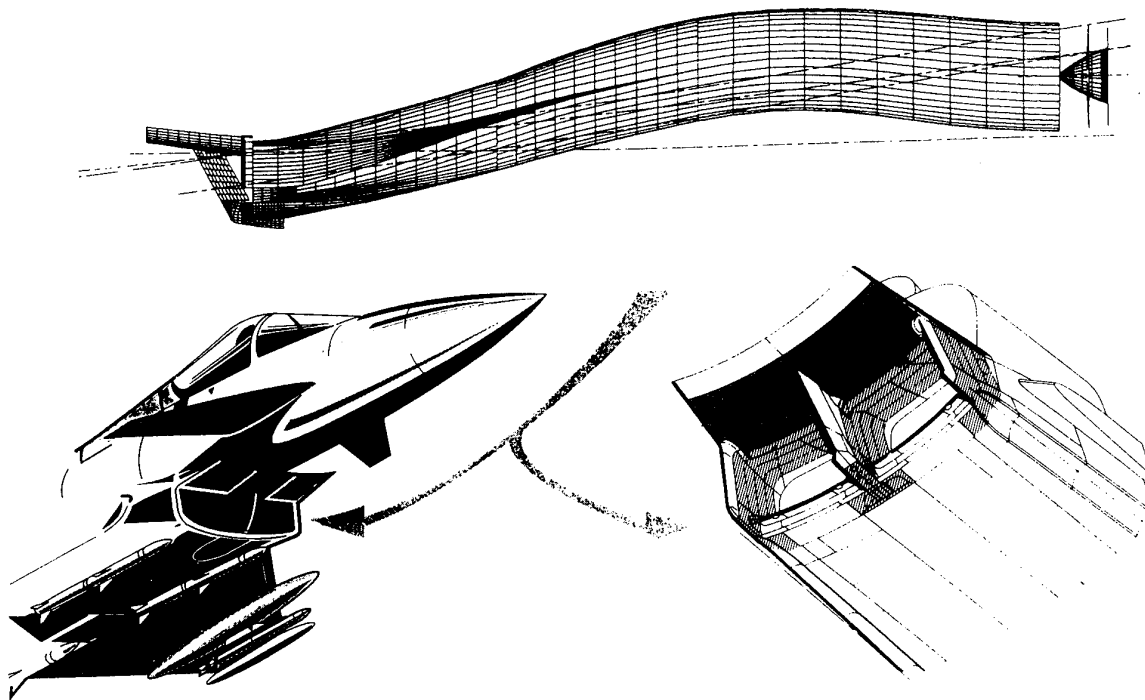


Fig. A3 INTAKE CONFIGURATION

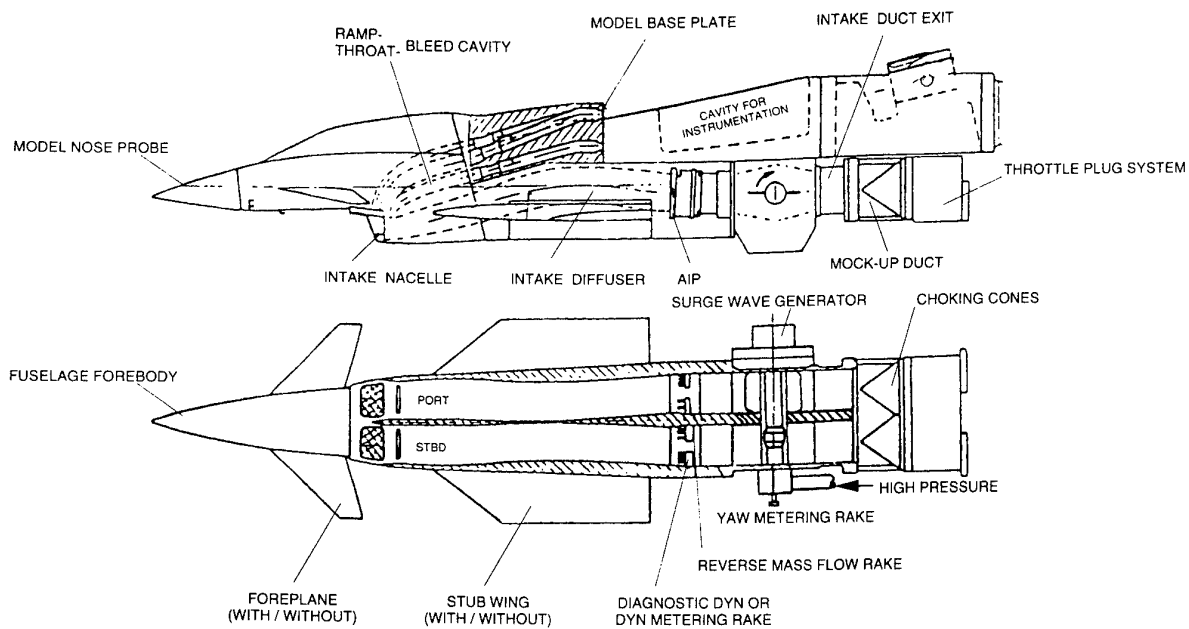


Fig. A4 INTAKE MODEL

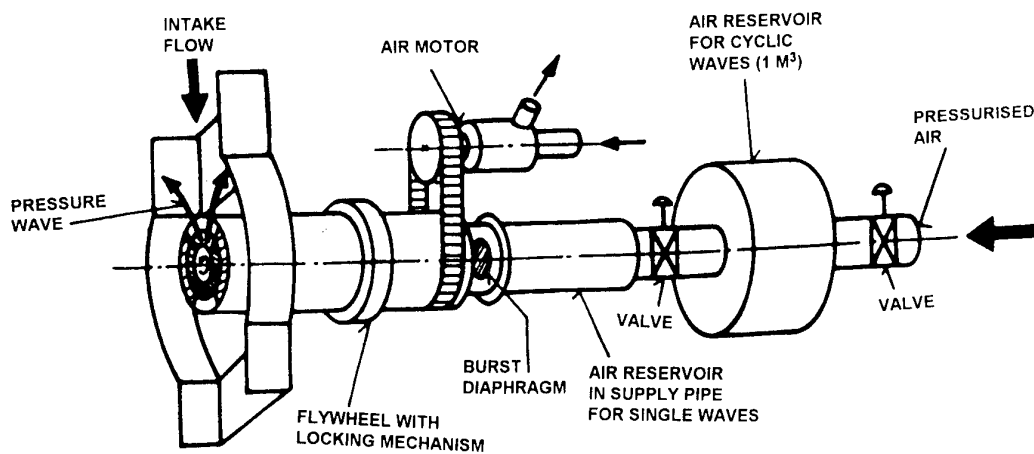


Fig. A5 SURGE WAVE GENERATOR

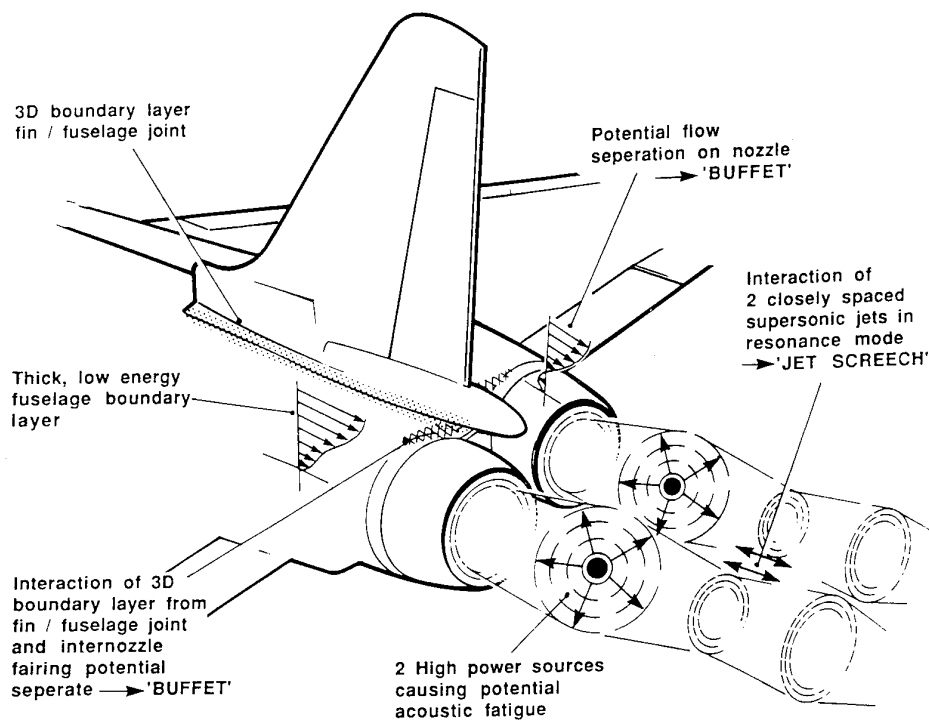
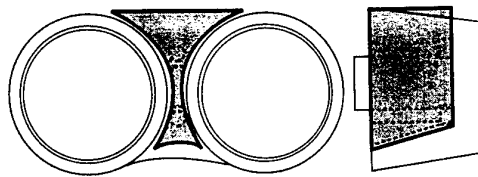
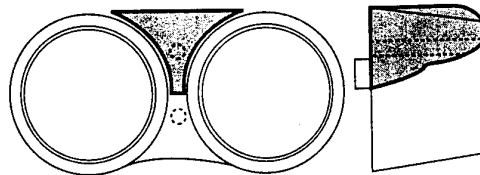


Fig. A6 NOZZLE AFTERBODY PHENOMENA

INTERNOZZLE FAIRING (INF)



PEN - NIB - FAIRING (PNF)



SPLITTER

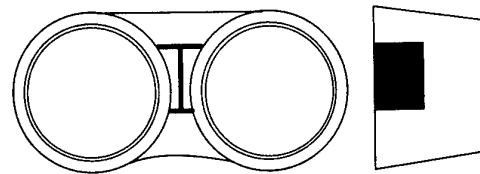


Fig. A7 AFTERBODY CONFIGURAITONS

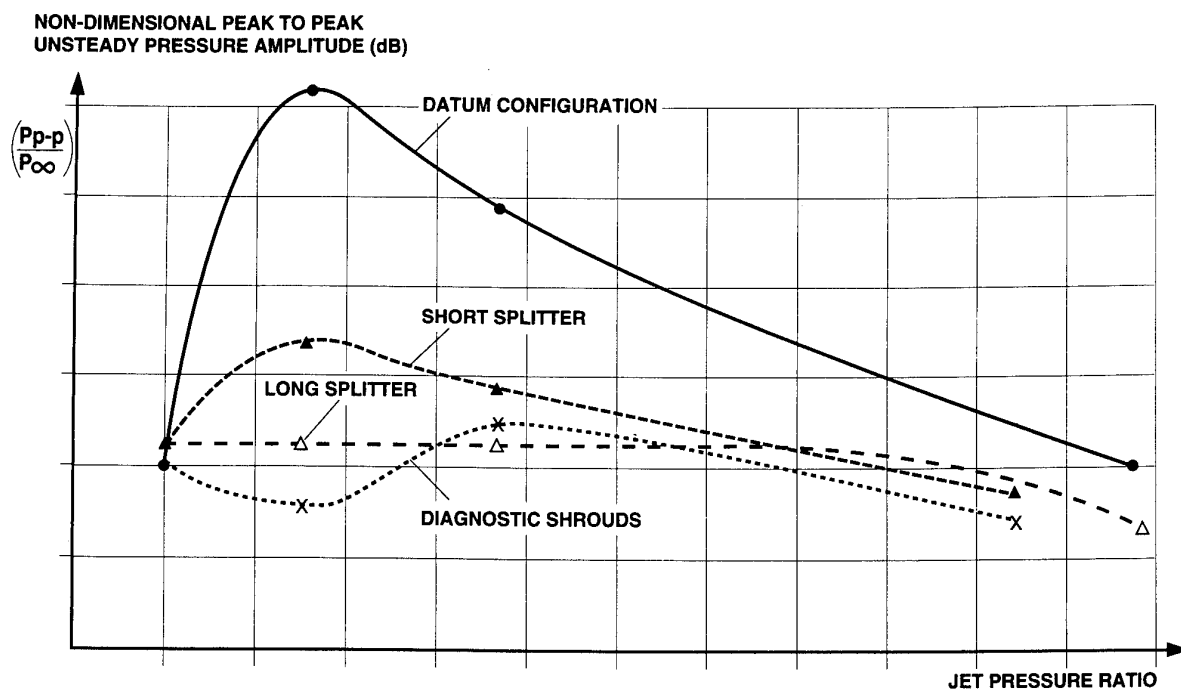


Fig. A8 MAXIMUM UNSTEADY PRESSURE

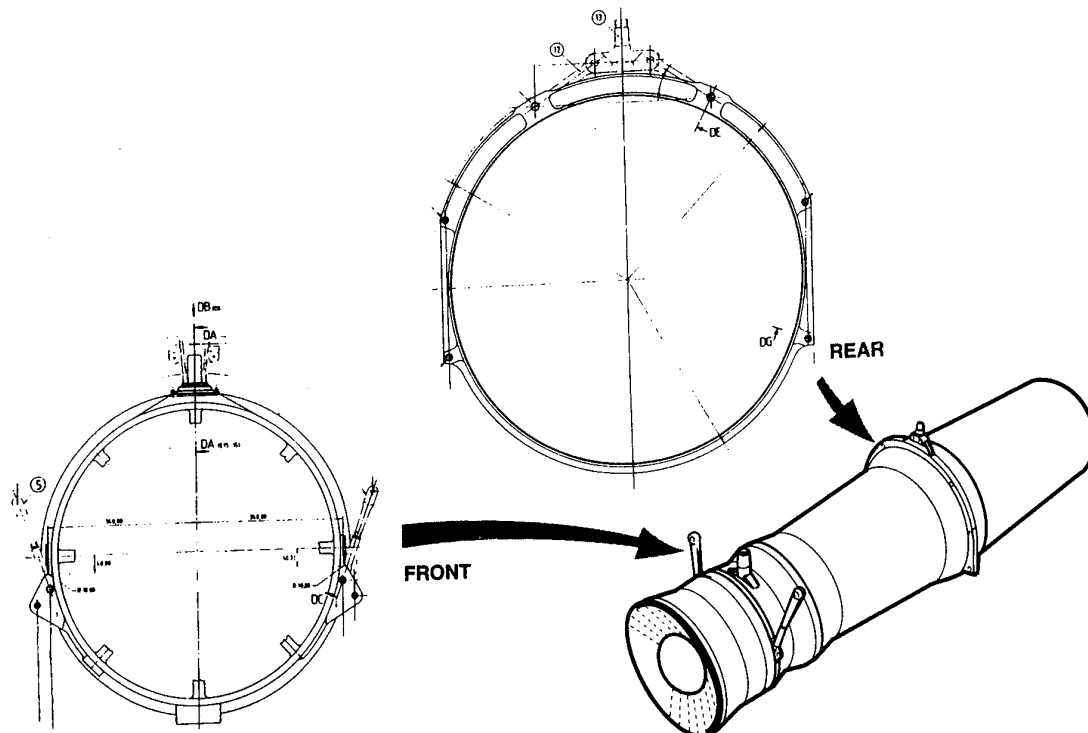


Fig. A9 ENGINE MOUNTING

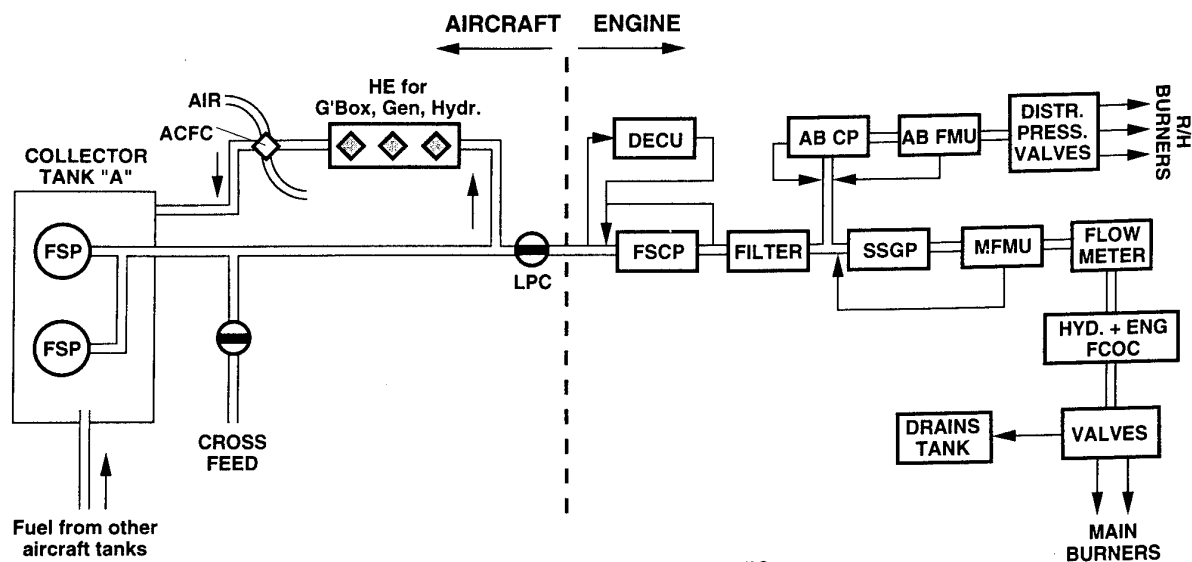


Fig. A10 FUEL SYSTEM SCHEMATIC

- 1 MAIN ENGINE
- 2 FLEXIBLE PTO SHAFT
- 3 FREE WHEEL/DOG CLUTCH
- 4 GEARBOX
- 5 AIR TURBINE STARTER MOTOR
- 6 CONSTANT FREQUENCY GENERATOR
- 7 DC GENERATOR
- 8 HYDRAULIC PUMP
- 9 FUEL COOLED OIL COOLER
- 10 ATSM CONTROL & SHUT-OFF VALVE
- 11 PROOV (CROSS BLEED)
- 12 SPS PRESSURE SENSOR
- 13 SPS PRESSURE REDUCING & SHUT-OFF VALVE
- 14 GROUND CONNECTION
- 15 APU STARTER
- 16 APU SHUT-OFF VALVE
- 17 ENGINE BLEED SHUT-OFF VALVE
- 18 APU
- 19 APU CONTROL UNIT
- 20 APU GENERATOR
- 21 FUEL SHUT-OFF VALVE
- 22 SPS COMPUTER (LEFT UCS)
- 23 SPS COMPUTER (RIGHT UCS)
- 24 COCKPIT CONTROL
- 25 NON-RETURN VALVE
- 26 INTAKE ACTUATOR
- 27 APU CONTACTOR

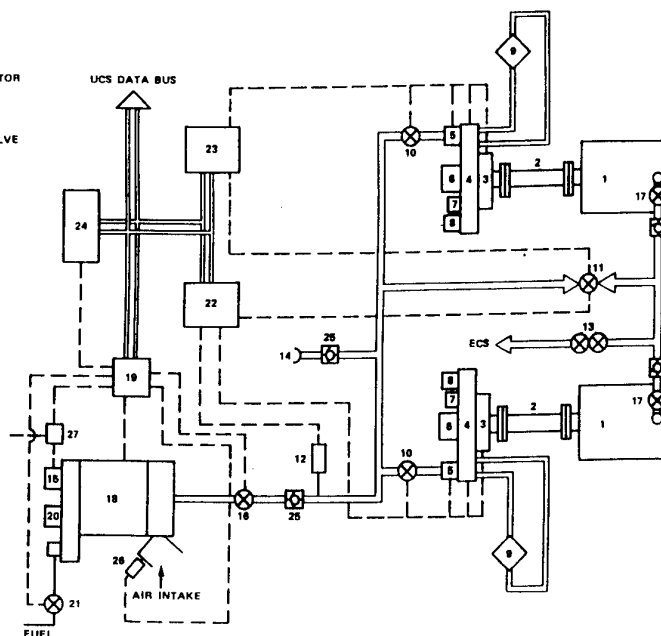


Fig. A11 SPS SCHEMATIC

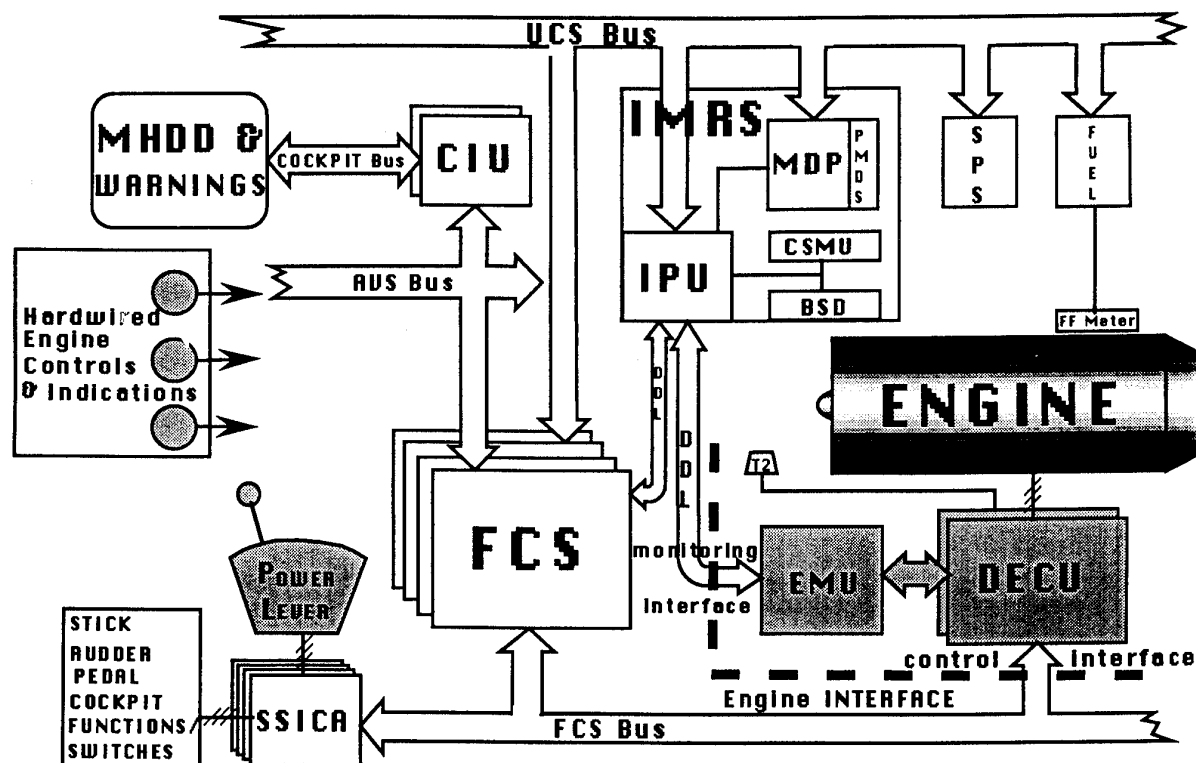


Fig. A12 CONTROL AND MONITORING ARCHITECTURE

Flight Envelope Extension

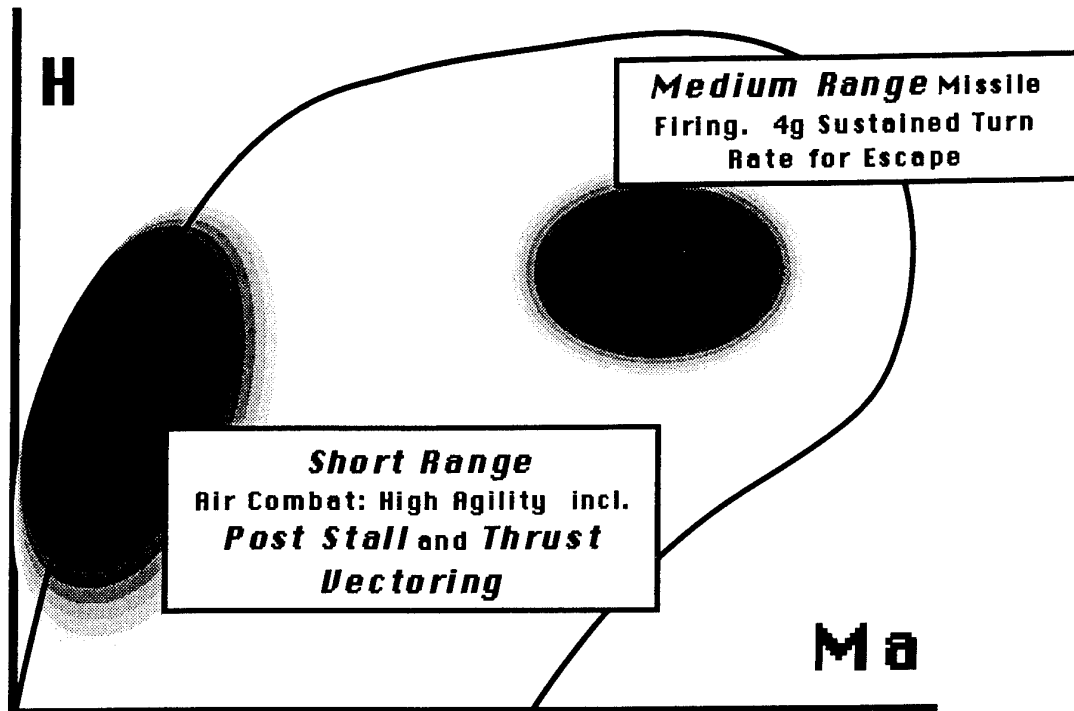


Fig. A13 FLIGHT ENVELOPE EXTENSION

REPORT DOCUMENTATION PAGE

1. Recipient's Reference	2. Originator's Reference AGARD-CP-572	3. Further Reference ISBN 92-836-0025-8	4. Security Classification of Document UNCLASSIFIED/ UNLIMITED												
5. Originator Advisory Group for Aerospace Research and Development North Atlantic Treaty Organization 7 rue Ancelle, 92200 Neuilly-sur-Seine, France															
6. Title Advanced Aero-Engine Concepts and Controls															
7. Presented at/sponsored by The Propulsion and Energetics Panel 86th Symposium held in Seattle, USA, 25-29 September 1995															
8. Author(s)/Editor(s) Multiple			9. Date June 1996												
10. Author's/Editor's Address Multiple			11. Pages 428												
12. Distribution Statement There are no restrictions on the distribution of this document. Information about the availability of this and other AGARD unclassified publications is given on the back cover.															
13. Keywords/Descriptors <table><tbody><tr><td>Military aircraft</td><td>Design</td></tr><tr><td>Fighter aircraft</td><td>Gas turbine engines</td></tr><tr><td>Aircraft engines</td><td>Jet engines</td></tr><tr><td>Propulsion</td><td>Integrated systems</td></tr><tr><td>Flight control</td><td>Control equipment</td></tr><tr><td>Thrust vector control</td><td></td></tr></tbody></table>				Military aircraft	Design	Fighter aircraft	Gas turbine engines	Aircraft engines	Jet engines	Propulsion	Integrated systems	Flight control	Control equipment	Thrust vector control	
Military aircraft	Design														
Fighter aircraft	Gas turbine engines														
Aircraft engines	Jet engines														
Propulsion	Integrated systems														
Flight control	Control equipment														
Thrust vector control															
14. Abstract <p>The Propulsion and Energetics Panel Symposium on Advanced Aero-Engine Concepts and Controls was held from 25-29 September 1995 in Seattle, USA. It dealt with propulsion, including thrust vectoring, for future combat aircraft, vertical landing aircraft and transport aircraft. Better fuel efficiency, longer range and higher operational flexibility will be gained from aero engines with advanced cycles which require improvements in fluid dynamics, materials and cooling. Five Sessions (37 papers including the keynote): Engine research and demonstration, requirements and programmes (3); Aircraft engine integration (5); Propulsion system and component technology (10); Engine control systems (13); Integrated flight and propulsion control (5). Dual use application of results is intended.</p>															

Aucun stock de publications n'a existé à AGARD. A partir de 1993, AGARD détiendra un stock limité des publications associées aux cycles de conférences et cours spéciaux ainsi que les AGARDographies et les rapports des groupes de travail, organisés et publiés à partir de 1993 inclus. Les demandes de renseignements doivent être adressées à AGARD par lettre ou par fax à l'adresse indiquée ci-dessus. *Veuillez ne pas téléphoner.* La diffusion initiale de toutes les publications de l'AGARD est effectuée auprès des pays membres de l'OTAN par l'intermédiaire des centres de distribution nationaux indiqués ci-dessous. Des exemplaires supplémentaires peuvent parfois être obtenus auprès de ces centres (à l'exception des Etats-Unis). Si vous souhaitez recevoir toutes les publications de l'AGARD, ou simplement celles qui concernent certains Panels, vous pouvez demander à être inclu sur la liste d'envoi de l'un de ces centres. Les publications de l'AGARD sont en vente auprès des agences indiquées ci-dessous, sous forme de photocopie ou de microfiche.

CENTRES DE DIFFUSION NATIONAUX

ALLEMAGNE

Fachinformationszentrum Karlsruhe
D-76344 Eggenstein-Leopoldshafen 2

BELGIQUE

Coordonnateur AGARD-VSL
Etat-major de la Force aérienne
Quartier Reine Elisabeth
Rue d'Evere, 1140 Bruxelles

CANADA

Directeur, Services d'information scientifique
Ministère de la Défense nationale
Ottawa, Ontario K1A 0K2

DANEMARK

Danish Defence Research Establishment
Ryvangs Allé 1
P.O. Box 2715
DK-2100 Copenhagen Ø

ESPAGNE

INTA (AGARD Publications)
Pintor Rosales 34
28008 Madrid

ETATS-UNIS

NASA Headquarters
Code JOB-1
Washington, D.C. 20546

FRANCE

O.N.E.R.A. (Direction)
29, Avenue de la Division Leclerc
92322 Châtillon Cedex

GRECE

Hellenic Air Force
Air War College
Scientific and Technical Library
Dekelia Air Force Base
Dekelia, Athens TGA 1010

ISLANDE

Director of Aviation
c/o Flugrad
Reykjavik

ITALIE

Aeronautica Militare
Ufficio del Delegato Nazionale all'AGARD
Aeroporto Pratica di Mare
00040 Pomezia (Roma)

LUXEMBOURG

Voir Belgique

NORVEGE

Norwegian Defence Research Establishment
Attn: Biblioteket
P.O. Box 25
N-2007 Kjeller

PAYS-BAS

Netherlands Delegation to AGARD
National Aerospace Laboratory NLR
P.O. Box 90502
1006 BM Amsterdam

PORTUGAL

Estado Maior da Força Aérea
SDFA - Centro de Documentação
Alfragide
2700 Amadora

ROYAUME-UNI

Defence Research Information Centre
Kentigern House
65 Brown Street
Glasgow G2 8EX

TURQUIE

Millî Savunma Başkanlığı (MSB)
ARGE Dairesi Başkanlığı (MSB)
06650 Bakanlıklar-Ankara

Le centre de distribution national des Etats-Unis ne détient PAS de stocks des publications de l'AGARD.

D'éventuelles demandes de photocopies doivent être formulées directement auprès du NASA Center for AeroSpace Information (CASI) à l'adresse ci-dessous. Toute notification de changement d'adresse doit être fait également auprès de CASI.

AGENCES DE VENTE

NASA Center for
AeroSpace Information (CASI)
800 Elkridge Landing Road
Linthicum Heights, MD 21090-2934
Etats-Unis

ESA/Information Retrieval Service
European Space Agency
10, rue Mario Nikis
75015 Paris
France

The British Library
Document Supply Division
Boston Spa, Wetherby
West Yorkshire LS23 7BQ
Royaume-Uni

Les demandes de microfiches ou de photocopies de documents AGARD (y compris les demandes faites auprès du CASI) doivent comporter la dénomination AGARD, ainsi que le numéro de série d'AGARD (par exemple AGARD-AG-315). Des informations analogues, telles que le titre et la date de publication sont souhaitables. Veuillez noter qu'il y a lieu de spécifier AGARD-R-nnn et AGARD-AR-nnn lors de la commande des rapports AGARD et des rapports consultatifs AGARD respectivement. Des références bibliographiques complètes ainsi que des résumés des publications AGARD figurent dans les journaux suivants:

Scientific and Technical Aerospace Reports (STAR)
publié par la NASA Scientific and Technical
Information Division
NASA Headquarters (JTT)
Washington D.C. 20546
Etats-Unis

Government Reports Announcements and Index (GRA&I)
publié par le National Technical Information Service
Springfield
Virginia 22161
Etats-Unis
(accessible également en mode interactif dans la base de
données bibliographiques en ligne du NTIS, et sur CD-ROM)



AGARD holds limited quantities of the publications that accompanied Lecture Series and Special Courses held in 1993 or later, and of AGARDographs and Working Group reports published from 1993 onward. For details, write or send a telefax to the address given above. *Please do not telephone.*

AGARD does not hold stocks of publications that accompanied earlier Lecture Series or Courses or of any other publications. Initial distribution of all AGARD publications is made to NATO nations through the National Distribution Centres listed below. Further copies are sometimes available from these centres (except in the United States). If you have a need to receive all AGARD publications, or just those relating to one or more specific AGARD Panels, they may be willing to include you (or your organisation) on their distribution list. AGARD publications may be purchased from the Sales Agencies listed below, in photocopy or microfiche form.

NATIONAL DISTRIBUTION CENTRES

BELGIUM

Coordonnateur AGARD — VSL
Etat-major de la Force aérienne
Quartier Reine Elisabeth
Rue d'Evere, 1140 Bruxelles

CANADA

Director Scientific Information Services
Dept of National Defence
Ottawa, Ontario K1A 0K2

DENMARK

Danish Defence Research Establishment
Ryvangs Allé 1
P.O. Box 2715
DK-2100 Copenhagen Ø

FRANCE

O.N.E.R.A. (Direction)
29 Avenue de la Division Leclerc
92322 Châtillon Cedex

GERMANY

Fachinformationszentrum Karlsruhe
D-76344 Eggenstein-Leopoldshafen 2

GREECE

Hellenic Air Force
Air War College
Scientific and Technical Library
Dekelia Air Force Base
Dekelia, Athens TGA 1010

ICELAND

Director of Aviation
c/o Flugrad
Reykjavik

ITALY

Aeronautica Militare
Ufficio del Delegato Nazionale all'AGARD
Aeroporto Pratica di Mare
00040 Pomezia (Roma)

LUXEMBOURG

See Belgium

NETHERLANDS

Netherlands Delegation to AGARD
National Aerospace Laboratory, NLR
P.O. Box 90502
1006 BM Amsterdam

NORWAY

Norwegian Defence Research Establishment
Attn: Biblioteket
P.O. Box 25
N-2007 Kjeller

PORTUGAL

Estado Maior da Força Aérea
SDFA - Centro de Documentação
Alfragide
2700 Amadora

SPAIN

INTA (AGARD Publications)
Pintor Rosales 34
28008 Madrid

TURKEY

Millî Savunma Başkanlığı (MSB)
ARGE Dairesi Başkanlığı (MSB)
06650 Bakanlıklar-Ankara

UNITED KINGDOM

Defence Research Information Centre
Kentigern House
65 Brown Street
Glasgow G2 8EX

UNITED STATES

NASA Headquarters
Code JOB-1
Washington, D.C. 20546

The United States National Distribution Centre does NOT hold stocks of AGARD publications.

Applications for copies should be made direct to the NASA Center for AeroSpace Information (CASI) at the address below.

Change of address requests should also go to CASI.

SALES AGENCIES

NASA Center for
AeroSpace Information (CASI)
800 Elkridge Landing Road
Linthicum Heights, MD 21090-2934
United States

ESA/Information Retrieval Service
European Space Agency
10, rue Mario Nikis
75015 Paris
France

The British Library
Document Supply Centre
Boston Spa, Wetherby
West Yorkshire LS23 7BQ
United Kingdom

Requests for microfiches or photocopies of AGARD documents (including requests to CASI) should include the word 'AGARD' and the AGARD serial number (for example AGARD-AG-315). Collateral information such as title and publication date is desirable. Note that AGARD Reports and Advisory Reports should be specified as AGARD-R-*nnn* and AGARD-AR-*nnn*, respectively. Full bibliographical references and abstracts of AGARD publications are given in the following journals:

Scientific and Technical Aerospace Reports (STAR)
published by NASA Scientific and Technical
Information Division
NASA Headquarters (JTT)
Washington D.C. 20546
United States

Government Reports Announcements and Index (GRA&I)
published by the National Technical Information Service
Springfield
Virginia 22161
United States
(also available online in the NTIS Bibliographic
Database or on CD-ROM)

